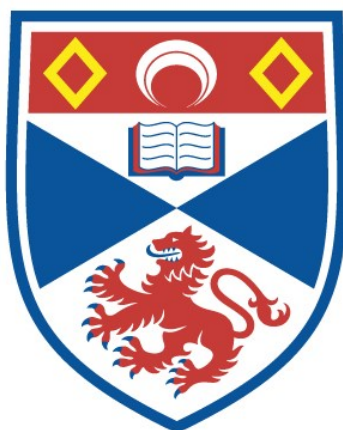


Enantioselective palladium and isothiourea dual catalysis

Jacqueline Bitai

A thesis submitted for the degree of PhD
at the
University of St Andrews



2022

Full metadata for this thesis is available in
St Andrews Research Repository
at:

<https://research-repository.st-andrews.ac.uk/>

Identifier to use to cite or link to this thesis:

DOI: <https://doi.org/10.17630/sta/169>

This item is protected by original copyright

This item is licensed under a
Creative Commons License

<https://creativecommons.org/licenses/by-nc-nd/4.0>

Declarations

Candidate's declaration

I, Jacqueline Bitai, do hereby certify that this thesis, submitted for the degree of PhD, which is approximately 67,000 words in length, has been written by me, and that it is the record of work carried out by me, or principally by myself in collaboration with others as acknowledged, and that it has not been submitted in any previous application for any degree. I confirm that any appendices included in my thesis contain only material permitted by the 'Assessment of Postgraduate Research Students' policy.

I was admitted as a research student at the University of St Andrews in September 2017.

I received funding from an organisation or institution and have acknowledged the funder(s) in the full text of my thesis.

Date 07.10.2021

Signature of candidate

Supervisor's declaration

I hereby certify that the candidate has fulfilled the conditions of the Resolution and Regulations appropriate for the degree of PhD in the University of St Andrews and that the candidate is qualified to submit this thesis in application for that degree. I confirm that any appendices included in the thesis contain only material permitted by the 'Assessment of Postgraduate Research Students' policy.

Date 07.10.2021

Signature of supervisor

Permission for publication

In submitting this thesis to the University of St Andrews we understand that we are giving permission for it to be made available for use in accordance with the regulations of the University Library for the time being in force, subject to any copyright vested in the work not being affected thereby. We also understand, unless exempt by an award of an embargo as requested below, that the title and the abstract will be published, and that a copy of the work may be made and supplied to any bona fide library or research worker, that this thesis will be electronically accessible for personal or research use and that the library has the right to migrate this thesis into new electronic forms as required to ensure continued access to the thesis.

I, Jacqueline Bitai, confirm that my thesis does not contain any third-party material that requires copyright clearance.

The following is an agreed request by candidate and supervisor regarding the publication of this thesis:

Printed copy

Embargo on all of print copy for a period of 2 years on the following ground(s):

- Publication would preclude future publication

Supporting statement for printed embargo request

The work contained within this thesis will be part of a manuscript we are preparing to submit to a peer-reviewed journal.

Electronic copy

Embargo on all of electronic copy for a period of 2 years on the following ground(s):

- Publication would preclude future publication

Supporting statement for electronic embargo request

The work contained within this thesis will be part of a manuscript we are preparing to submit to a peer-reviewed journal.

Title and Abstract

- I require an embargo on the abstract only.

Date 07.10.2021

Signature of candidate

Date 07.10.2021

Signature of supervisor

Underpinning Research Data or Digital Outputs

Candidate's declaration

I, Jacqueline Bitai, understand that by declaring that I have original research data or digital outputs, I should make every effort in meeting the University's and research funders' requirements on the deposit and sharing of research data or research digital outputs.

Date 07.10.2021

Signature of candidate

Permission for publication of underpinning research data or digital outputs

We understand that for any original research data or digital outputs which are deposited, we are giving permission for them to be made available for use in accordance with the requirements of the University and research funders, for the time being in force.

We also understand that the title and the description will be published, and that the underpinning research data or digital outputs will be electronically accessible for use in accordance with the license specified at the point of deposit, unless exempt by award of an embargo as requested below.

The following is an agreed request by candidate and supervisor regarding the publication of underpinning research data or digital outputs:

Embargo on all of electronic files for a period of 2 years on the following ground(s):

- Publication would preclude future publication

Supporting statement for embargo request

The work contained within this thesis will be part of a manuscript we are preparing to submit to a peer-reviewed journal.

Title and Description

- I require an embargo on the description only

Date 07.10.2021

Signature of candidate

Date 07.10.2021

Signature of supervisor

Acknowledgements

Throughout the four years of my PhD studies, I was fortunate to receive a lot of support and encouragement from colleagues, friends and family. I want to thank my supervisor, Andy Smith, for giving me the opportunity to carry out this PhD work in his group, for his support and guidance and the freedom to explore when Chemistry has taken unexpected turns. Special thanks go to Claire for all the help over the years and the patience for proof-reading this thesis, and all the other pieces of work I've sent your way.

I also want to thank all the members of the ADS group, past and present, and our intermediate lab buddies from the CPJ group for making the lab an enjoyable place to work in. I am especially grateful to Stephi, for taking care of me when I first started, inside and outside the lab. I also want to thank Ally for being an incredibly pleasant fellow, his appreciation and his continued effort - working with you is a treat and I wish you all the best for the future!

A very special thank you goes to my dinner buddies Jason and Calum. Thanks for all the fun nights, the good food and the great company. Going through the troubles of a PhD together already makes it so much easier.

A very big thank you to all my pole gals I had the pleasure of meeting over the years! Especially Jenny and Ashley - thank you for all the fun hours of practice, for being incredibly enthusiastic and simply amazing friends.

Although being far away, I cannot say how grateful I am for all my friends and family back home. I especially want to thank my parents for their continued support and for always believing in me.

Finally, I want to thank my boyfriend Daniel for simply everything. Thank you for going with me wherever chance takes us, for being there through good and bad. It's been a truly interesting journey and I am excited for the next chapter in our lives.

Funding

This work was supported by the University of St Andrews (School of Chemistry).

Research Data/Digital Outputs access statement

Research data underpinning this thesis are available at <https://doi.org/10.17630/da9d96a3-9199-41a5-a06b-20a9686ed96d>

Abstract

This thesis details the development of dual catalytic processes involving achiral palladium and enantiopure isothioureia catalysts for the synthesis of enantioenriched and highly functionalised products. Taking inspiration from related literature examples demonstrating the compatibility of palladium and isothioureia catalysis, the extension of existing methodologies as well as the development of novel processes were investigated.

Based on the relay catalytic allylic amination/[2,3]-rearrangement protocol, previously developed in our group for the synthesis of enantioenriched α -amino ester derivatives, the scope and limitations of this process were probed. Initial studies aimed at identifying functional groups that could be tolerated in the relay catalysis. Electron-withdrawing amide substituents proved most promising and were explored in more depth to furnish enantioenriched α -amino ester derivatives featuring a 1,4-dicarbonyl motif.

As processes reported so far had focused on ammonium enolates as reaction partners, the range of reactivity modes accessible by isothioureia catalysis had not been fully exploited in dual catalytic methodologies. As such, the development of a cooperative palladium and isothioureia catalysis process employing α,β -unsaturated acyl ammonium intermediates was explored. This process furnishes enantioenriched cyclopentane products with up to four contiguous stereogenic centres with high stereoselectivity (up to 99:1 dr, up to 97:3 er). The scope and limitations of this process were probed, with subsequent derivatisation reactions demonstrating the synthetic utility of the products. In addition, a range of control experiments provided insight into the mechanism of this cooperative palladium and isothioureia catalysis.

PhD Publications

The work described in this thesis has formed the basis for the following peer-reviewed publications:

- *Exploring the scope of tandem palladium and isothiourea relay catalysis for the synthesis of amino acid derivatives.* [Jacqueline Bitai](#), Alexandra M. Z. Slawin, David B. Cordes and Andrew D. Smith, *Molecules* **2020**, 25, 2463.
- *α,β -Unsaturated acyl ammonium species as reactive intermediates in organocatalysis: an update.* [Jacqueline Bitai](#), Matthew T. Westwood and Andrew D. Smith, *Org. Biomol. Chem.*, **2021**, 19, 2366.
- *Cooperative palladium/isothiourea-catalyzed enantioselective formal (3+2) cycloaddition of vinylcyclopropanes and α,β -unsaturated esters.* [Jacqueline Bitai](#), Alastair J. Nimmo, Alexandra M. Z. Slawin and Andrew D. Smith, *Manuscript in preparation*.

Abbreviations

Å	Ångström (1×10^{-10} m)	DCE	Dichloroethane
A	Acceptor	DHPB	3,4-Dihydro-2 <i>H</i> -benzo[4,5] thiazolo[3,2- <i>a</i>]pyrimidine
Ac	Acetyl	DIBAL	Diisobutylaluminium hydride
AcOH	Acetic acid	DiPAMP	Ethane-1,2-diylbis[(2- methoxyphenyl) phenylphosphane]
anhydr.	Anhydrous	DMAP	4-Dimethylaminopyridine
aq.	Aqueous	DME	Dimethoxyethane
Ar	Aryl	DMF	Dimethylformamide
BINAP	2,2'-Bis(diphenylphosphino)- 1,1'-binaphthalene	DMSO	Dimethyl sulfoxide
Bn	Benzyl	DOPA	3,4-Dihydroxyphenylalanine
Boc	<i>N</i> - <i>t</i> -Butoxycarbonyl	DPEN	1,2-Diphenylethylenediamine
b.p.	Boiling point	dppe	1,2-Bis(diphenylphosphino) ethane
BPhen	Bathophenanthroline	dr	Diastereoisomeric ratio
BTM	Benzotetramisole	<i>E</i>	Entgegen (in context of alkene bond geometry)
Bu	Butyl	<i>E</i>	Electrophile
<i>c</i>	Concentration	EDCI	1-Ethyl-3-(3-dimethyl aminopropyl)carbodiimide
Cbz	Carboxybenzyl	EDG	Electron-donating group
CDI	1,1'-Carbonyldiimidazole	EI	Electron impact
COD	1,5-Cyclooctadiene	eq	Equivalent(s)
conc.	Concentrated	er	Enantiomeric ratio
CPA	Chiral phosphoric acid	ESI	Electrospray ionisation
Cy	Cyclohexyl	Et	Ethyl
D	Donor	Et ₂ O	Diethyl ether
DABCO	1,4-Diazabicyclo[2.2.2]octan		
DACH-Ph	1,2-Diaminocyclohexane- <i>N,N'</i> -bis(2- diphenylphosphinobenzoyl		
dba	Dibenzylideneacetone		
DCC	Dicyclohexylcarbodiimide		

EtOAc	Ethyl acetate	MeOH	Methanol
EWG	Electron-withdrawing group	mol%	Molar percentage
FG	Functional group	m.p.	Melting point
G	Gibbs free energy	Ms	Methane sulfonyl
GC	Gas chromatography	MS	Molecular sieves
Hal	Halogen	NBS	<i>N</i> -Bromosuccinimide
HBTM	HomoBTM	<i>n</i> -BuLi	<i>n</i> -Butyllithium
HG II	Hoveyda-Grubbs Catalyst® 2 nd Generation	n.d.	not determined
HMDS	Hexamethyldisilazane	NHC	<i>N</i> -Heterocyclic carbene
HMPA	Hexamethylphosphoramide	NMR	Nuclear magnetic resonance
HOBt	Hydroxybenzotriazole	NOE	Nuclear Overhauser effect
HPLC	High performance liquid chromatography	NSI	Nanospray ionisation
HRMS	High resolution mass spectrometry	Nu	Nucleophile
<i>i</i> -	Iso	P	Product
Ipc ₂ B(allyl)	<i>B</i> -Allyldiisopinocampheyl- borane	PdFurCat	<i>cis</i> -Bromobis(tri(2-furyl) phosphine)(<i>N</i> -succinimide) palladium(II)
IR	Infrared spectroscopy	PFP	Pentafluorophenyl
ITU	Isothiourea	Ph	Phenyl
kcal	Kilocalorie	PNP	4-Nitrophenyl
KR	Kinetic resolution	Pr	Propyl
L	Ligand	PS-BEMP	Polymer-supported 2- <i>t</i> - butylimino-2-diethylamino- 1,3-dimethylperhydro-1,3,2- diazaphosphorine
LA	Lewis acid	quant.	quantitative
LB	Lewis base	R	General substituent
LG	Leaving group	RAMP	(<i>R</i>)-1-Amino-2-methoxy- methylpyrrolidine
Lit.	Literature	rt	Room temperature
M	Molar (mol/L)	S	Solvent
M	Metal	sat.	Saturated
Me	Methyl		
MeCN	Acetonitrile		

SM	Starting material	TLC	Thin layer chromatography
t	Time	TM	Tetramisole
T	Temperature	TMS	Trimethylsilyl
<i>t</i> -	Tertiary	Ts	Tosyl
TBAF	Tetra- <i>n</i> -butylammonium fluoride	TS	Transition state
TBME	<i>t</i> -Butyl methyl ether	wt%	Weight percentage
TBS	<i>t</i> -Butyldimethylsilyl	XantPhos	4,5-Bis(diphenylphosphino)- 9,9-dimethylxanthene
TCP	Trichlorophenyl	Z	Zusammen (in context of alkene geometry)
Tf	Trifluoromethane sulfonyl		
TFA	Trifluoroacetic acid		
THF	Tetrahydrofuran		

Table of Contents

Chapter 1: Introduction	1
1.1 Chirality and asymmetric synthesis	1
1.2 Asymmetric Catalysis	4
1.3 Enantioselective organocatalysis using tertiary amine Lewis bases	5
1.3.1 The advancement of chiral isothiourea catalysts	6
1.3.2 Catalyst turnover strategies	9
1.4 Palladium catalysed allylic substitution reactions	10
1.4.1 Potential isomerisation processes for Pd η^3 -allyl intermediates	12
1.4.2 Nucleophiles in allylic substitution reactions	15
1.5 Dual catalytic processes	16
1.5.1 Combining transition metal and organocatalysis	17
1.5.2 Combining transition metal and isothiourea catalysis	21
1.6 Aims and Objectives	24
Chapter 2: Relay palladium and isothiourea catalysis	25
2.1 Project Overview	25
2.2 Introduction	26
2.2.1 Sigmatropic Rearrangements	26
2.2.2 [2,3]-Sigmatropic Rearrangements	29
2.2.3 [2,3]-Sigmatropic rearrangement of ammonium ylids	33
2.3 Concept and Aims	39
2.4 Results and Discussion	41
2.4.1 Initial functional group assessment	41
2.4.2 Reaction optimisation for ethyl ester containing allylic phosphate	43
2.4.3 Amide containing allylic phosphates	46
2.5 Conclusion	62
Chapter 3: Cooperative palladium and isothiourea catalysis	63
3.1 Project Overview	63
3.2 Introduction	64
3.2.1 Formal (3+2) cycloadditions using vinylcyclopropane substrates	64

3.2.2	α,β -Unsaturated acyl ammonium intermediates in cycloaddition and annulation processes.....	71
3.3	Concept and Aims	74
3.4	Results and Discussion.....	76
3.4.1	Initial Assessment	76
3.4.2	Optimisation of reaction conditions	76
3.4.3	Mechanistic control experiments	83
3.4.4	Investigation of salt effect	86
3.4.5	Re-optimisation of reaction parameters.....	89
3.4.6	Key insights from optimisation studies	93
3.4.7	Scope and Limitations	94
3.4.8	Scalability and product derivatisations.....	103
3.4.9	Proposed mechanism and stereochemical rationale	105
3.5	Conclusion	108
Chapter 4: Summary and Outlook		109
Chapter 5: Experimental Details.....		112
5.1	General Information	112
5.2	General Procedures.....	115
5.2.1	General Procedure A: Synthesis of allylic phosphates	115
5.2.2	General Procedure B: Amide coupling	115
5.2.3	General Procedure C: Basic ester hydrolysis with LiOH.....	116
5.2.4	General Procedure D: Reduction of unsaturated acids.....	116
5.2.5	General Procedure E: Relay Pd/ITU catalysis	117
5.2.6	General Procedure F: Preparation of vinyl cyclopropanes	117
5.2.7	General Procedure G: Preparation of α,β -unsaturated aryl oxide esters..	118
5.2.8	General Procedure H: Acidic ester hydrolysis.....	118
5.2.9	General Procedure I: Optimisation of cooperative catalysis conditions ...	118
5.2.10	General Procedure J: Cooperative Pd/ITU formal (3+2) cycloaddition	119
5.3	Synthesis of Catalysts.....	120
5.4	Experimental details for Chapter 2.....	124
5.4.1	Preparation of <i>p</i> -nitrophenyl amino esters.....	124
5.4.2	Preparation of allylic phosphate starting materials	125

5.4.3	Relay Pd and ITU catalysis products.....	150
5.4.4	Identified side-products	168
5.5	Experimental details for Chapter 3.....	170
5.5.1	Preparation of vinylcyclopropanes.....	170
5.5.2	Preparation of Michael acceptors.....	176
5.5.3	Cooperative Pd and ITU catalysis products.....	195
5.5.4	Gram scale catalytic reaction	217
5.5.5	Product Derivatisations.....	217
5.6	NOE Experiment.....	226
5.7	Single crystal X-ray diffraction analysis	228
References.....		234
Appendix I: Example NMR spectra		244
	Example spectra from Chapter 2.....	244
	Calculation of ¹ H NMR yield and dr for Chapter 3.....	248
	Example spectra from Chapter 3.....	251
Appendix II: Example HPLC and GC traces		253
	Example HPLC traces from Chapter 2	253
	Example HPLC and GC traces from Chapter 3	255

Chapter 1: Introduction

1.1 Chirality and asymmetric synthesis

The landscape of synthetic organic chemistry has seen major advancements over the last century. The way in which we think about organic transformations has changed, by considering their efficiency and impact in terms of atom economy, waste prevention, or reagent toxicity following the principles of green chemistry.^{1,2} Similarly, the bond forming events accessible have also expanded dramatically, with modern methods allowing for excellent levels of control over chemo-, regio- and stereoselectivity. The latter has gained considerable importance as pharmaceuticals,³ agrochemicals,⁴ or odour and flavour compounds⁵ contain an increasing number of chirality elements, which often requires their accessibility in enantiopure form.

Chirality is a symmetry property that renders a molecule non-superimposable upon its mirror image, resulting in a pair of enantiomers. One of the most common forms of chirality is point chirality, describing a tetrahedral atom, usually carbon, but also sulfur, phosphorus or nitrogen, with four different substituents. Thus, opposite enantiomers differ in their spatial arrangement. As a consequence, even though a pair of enantiomers has the same physicochemical properties, by placing them in a chiral environment, they can be distinguished based on their differing spatial requirements, potentially resulting in different effects for each enantiomer. For example, the smell of lemons and oranges is caused by the same molecule limonene, with the only difference being the configuration of the C(4)-stereogenic centre (Figure 1, left).⁶ By coming in contact with the chiral environment in our receptors, (*R*)-limonene conveys the smell of oranges, whereas (*S*)-limonene is associated with the smell of lemons. The choice of enantiomer can have even greater consequences than a change in smell. The drug (*S*)-DOPA is used for the treatment of Parkinson's disease, but its enantiomer (*R*)-DOPA is toxic to humans (Figure 1, right).⁷

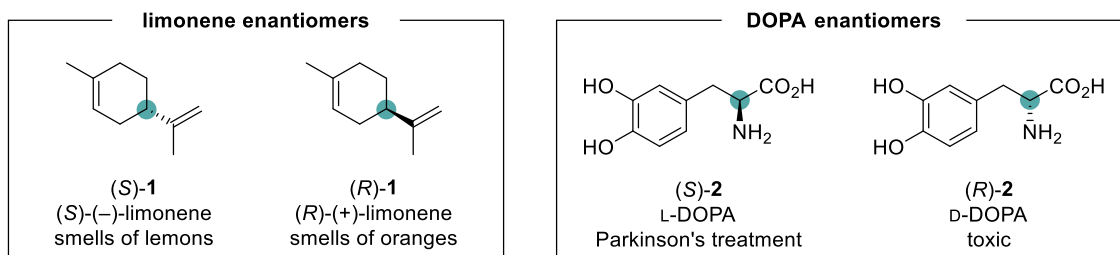
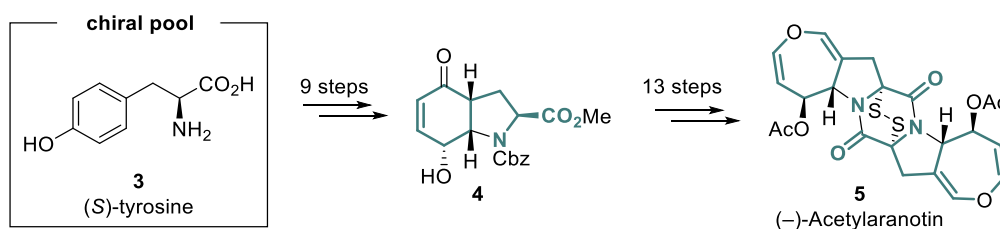


Figure 1 Examples of pairs of enantiomers with different biological effects.

In order to assess the effect of the individual enantiomers it is crucial to have access to each in enantiopure form. A number of strategies have been developed to achieve this goal. Of particular interest are those creating new stereogenic centres with control of the relative and absolute configuration, generalised as asymmetric synthesis. The following methods can be distinguished:

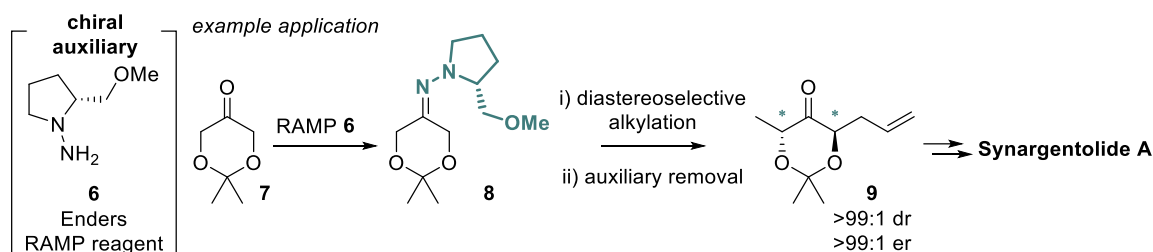
(i) chiral pool synthesis: This approach uses naturally occurring enantiopure compounds, such as amino acids or carbohydrates (Scheme 1, left).^{8,9} The stereochemical information from the starting material is usually preserved in the product and used to direct the relative stereochemistry of diastereoselective transformations *en route*. This has been elegantly demonstrated by Tokuyama and co-workers in the total synthesis of (-)-Acetylaranotin **5** (Scheme 1, right).¹⁰ The atoms and stereochemistry of the starting (*S*)-tyrosine **3** are preserved in the product and used to direct the formation of new stereogenic centres. Although the starting materials for a chiral pool synthesis are usually cheap and available in enantiopure form, this approach is inherently limited to the formation of products that fit the natural precursors.



Scheme 1 Box: chiral pool compound; right: application in total synthesis.

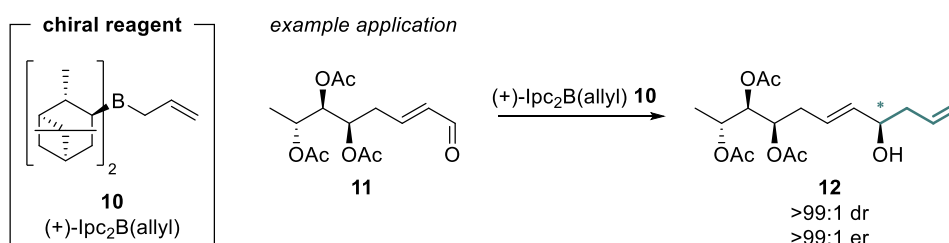
(ii) chiral auxiliaries: An enantiopure molecule is covalently attached to the substrate and used to direct the stereoselectivity of subsequent transformations. After the reaction, the auxiliary is removed to reveal the enantiopure product. This approach has been extensively used over the last decades, with a range of different auxiliaries available.¹¹ An example by Enders and Reichenbach demonstrates the use of RAMP

auxiliary **6** in the asymmetric synthesis of Synargentolide A, which enabled the installation of the first two stereogenic centres in excellent diastereo- and enantioselectivity (**9**) (Scheme 2).¹² Although auxiliaries reliably and predictably facilitate stereoselective transformations, a major drawback is the requirement for stoichiometric amounts of auxiliary and additional synthetic steps for incorporation and removal.



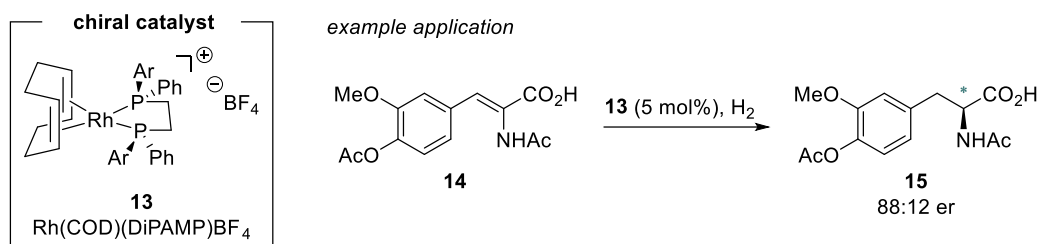
Scheme 2 Box: chiral auxiliary; right: application in stereoselective synthesis.

(iii) chiral reagents: The stereoiducing element resides on the chiral reagent and is transferred onto the substrate in a stereoselective reaction. Within this class, a range of boron reagents have been demonstrated to be particularly useful, as exemplified by the asymmetric allylation of aldehyde **11** using (+)-Ipc₂B(allyl) reagent **10** (Scheme 3).¹² This approach circumvents the need for additional synthetic steps, however the chiral reagent is still required in stoichiometric amounts and can often be expensive.



Scheme 3 Box: chiral reagent; right: application in stereoselective synthesis.

(iv) asymmetric catalysis: A very small amount of a chiral molecule, the catalyst, is used to facilitate the desired, stereoselective transformation. In this approach, the catalyst is regenerated after each cycle and no additional synthetic steps are required. One of the very first examples reported by Knowles and co-workers demonstrated the asymmetric hydrogenation of enamine **14** in the presence of a rhodium catalyst and a chiral phosphine ligand to generate L-DOPA precursor **15** with high enantioselectivity (Scheme 4).¹³



Scheme 4 Box: chiral catalysts; right: application in stereoselective synthesis.

Each of the above approaches has proven useful many times in the pursuit of enantiopure compounds. By far the most attractive, however in terms of atom economy and range of transformations accessible, is asymmetric catalysis, which will be considered in more detail in the following sections.

1.2 Asymmetric Catalysis

A catalyst is a substance that provides a lower energy (activation energy ΔG^\ddagger) pathway for a given transformation without changing the reaction outcome and without being consumed in the reaction (Figure 2a). Two potential modes of catalysis can be envisioned to achieve an overall reduction of ΔG^\ddagger . The catalyst can either lead to a lower energy transition state (green curve) or raise the ground state energy of the starting material (orange curve). For either scenario, the catalyst facilitates the intended transformation under milder reaction conditions. In asymmetric catalysis, the catalyst also leads to the preferred formation of one enantiomer over the other. This is achieved by employing a chiral catalyst which induces enantioselectivity by forming diastereomeric transition state assemblies with the substrate on the way to either enantiomer (Figure 2b).¹⁴ In order to obtain useful levels of enantioselectivity in the product, two criteria have to be met:

(i) the uncatalyzed, hence unselective reaction pathway should energetically not be accessible under the reaction conditions. This means that no reaction should be observed in the absence of catalyst. In cases when the reaction still proceeds even without catalyst, the rate of the catalysed process should be much higher than for the uncatalysed one to avoid an unselective racemic background reaction.

(ii) the difference in energy of the diastereomeric transition states ($\Delta\Delta G^\ddagger$) needs to be sufficiently large to significantly favour the formation of one enantiomer over the other. The numbers depicted in Figure 2b highlight the required energy differences at

room temperature in order to achieve certain levels of enantioselectivity.¹⁵ For comparison, the rotational barrier of ethane at room temperature is 3.0 kcal/mol.

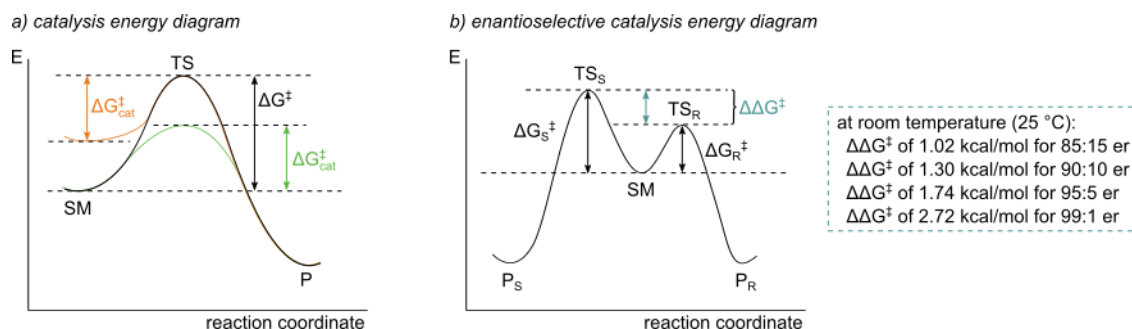


Figure 2 Energy diagrams for a) a catalyzed reaction; b) an enantioselective catalysis reaction and required energy differences for certain selectivity levels.

These numbers indicate that large changes in product enantioselectivity can be brought about by very small variations in transition state energies. The factors influencing the respective transition state energies are manifold and often the result of a combination of different interactions, including hydrogen bonding, van der Waals interactions or electrostatic interactions. Today, a variety of chiral catalysts with different modes of activation are well established, enabling the stereoselective transformation of a broad range of substrates. They can generally be assigned to one of three categories (Figure 3): transition metal catalysts, organocatalysts, or biocatalysts, with examples including Noyori-Ikariya catalyst **16**,¹⁶ MacMillan's imidazolidinone catalyst **17**¹⁷ and hydrolase enzyme 3bl7 **18**,¹⁸ respectively. Of particular relevance to this work is the use of chiral, Lewis base organocatalysts, which will be introduced in the next section.

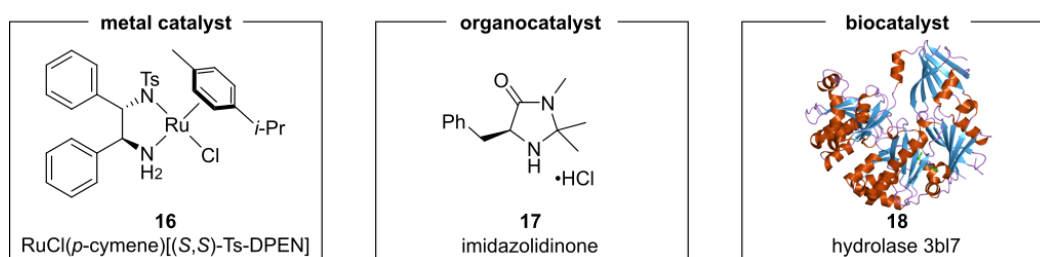


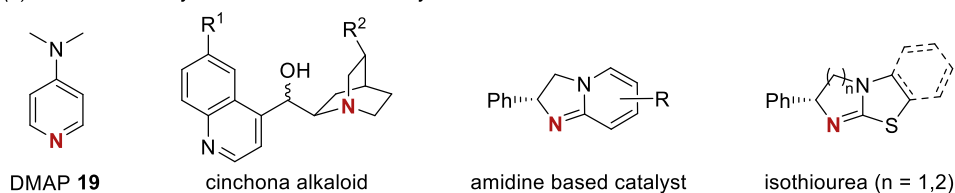
Figure 3 Examples for different types of catalysts.

1.3 Enantioselective organocatalysis using tertiary amine Lewis bases

Lewis basic organocatalysts based on a tertiary amine scaffold have seen widespread application in the transformation of substrates at the carboxylic acid oxidation level. Common catalysts include DMAP **19**, cinchona alkaloids, amidine based catalysts as well

as isothioureas (Figure 4a). Substrates amenable to this type of catalysis require a carboxylic acid derivative bearing a good leaving group, such as acid chlorides, acid anhydrides, thioesters and electron deficient aryl esters (Figure 4b). Activation of these substrates is achieved through nucleophilic addition of the catalyst, forming a covalent acyl ammonium adduct. This mode of activation is classified as a $n \rightarrow \pi^*$ interaction, as the Lewis base catalyst donates electron density through its lone pair into the π^* orbital of the substrate. The reactive species accessible include acyl ammonium, ammonium enolate and α,β -unsaturated acyl ammonium intermediates. Depending on the nature of the intermediate, different reactivities can be observed. For an ammonium enolate intermediate, the binding of the Lewis base catalyst leads to an increase in acidity of the C(2)-protons, resulting in an enhanced nucleophilicity. In acyl ammonium and α,β -unsaturated acyl ammonium intermediates, on the other hand, an increase in electrophilicity at the C(1) and C(3) position is observed, respectively.

(a) Common tertiary amine Lewis base catalysts



(b) Common precursors and reactive intermediates accessible

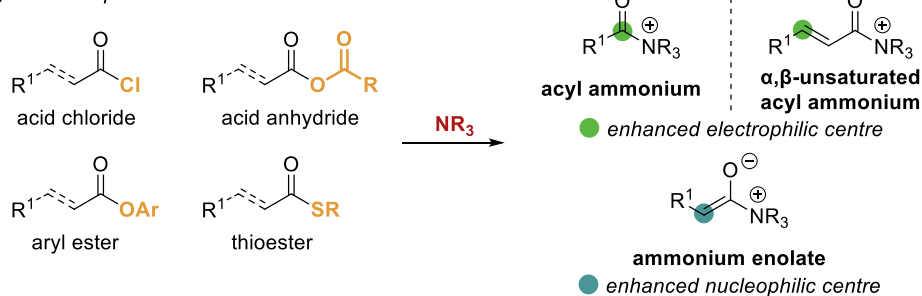
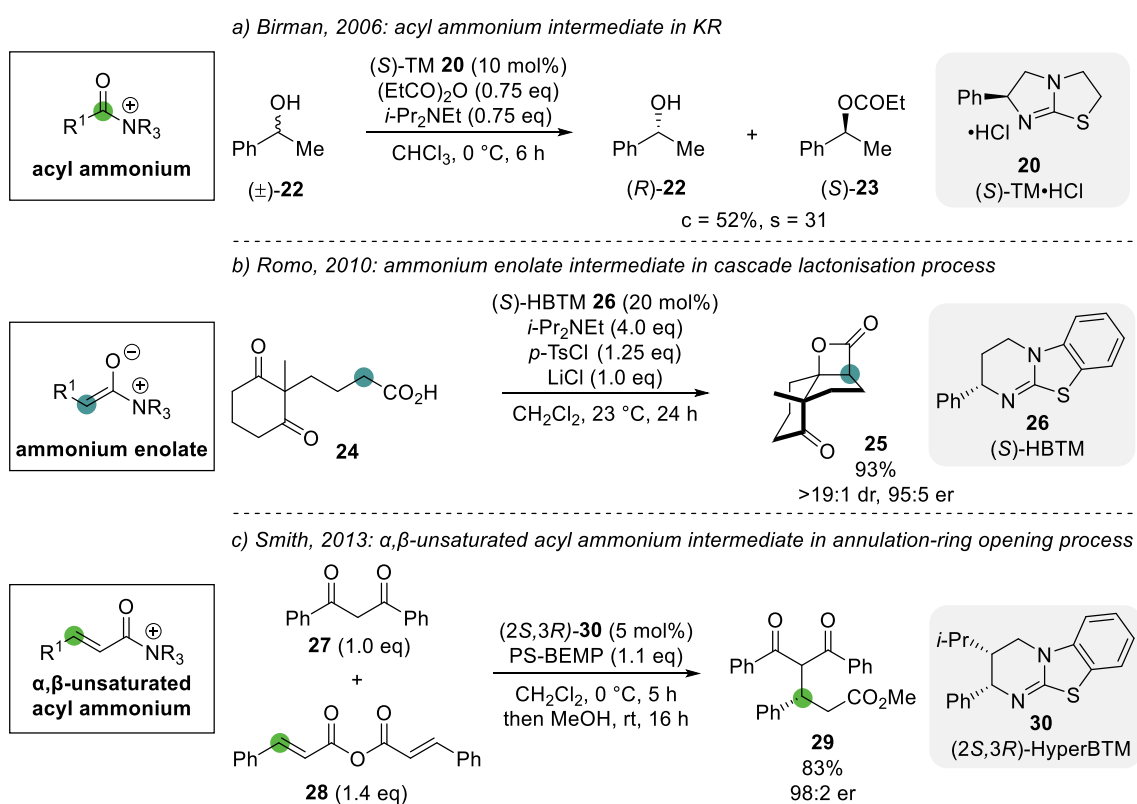


Figure 4a) Common tertiary amine Lewis base catalysts; b) common carboxylic acid precursors and reactive intermediates accessible.

1.3.1 The advancement of chiral isothiourea catalysts

In 2006, Birman and co-workers reported the first use of a chiral isothiourea Lewis base as organocatalyst.¹⁹ The commercially available drug molecule tetramisole (TM) **20** and its benzannulated derivative benzotetramisole (BTM) **21** (see Figure 5) were shown to be efficient acyl transfer catalysts for the kinetic resolution of secondary benzylic and allylic alcohols (Scheme 5a). In 2010, Romo and co-workers demonstrated the first application of

an isothiurea catalyst in the generation of ammonium enolates (Scheme 5b).²⁰ *In situ* derivatization of the carboxylic acid starting material **24** followed by treatment with base to generate an ammonium enolate enabled the formation of tricyclic β -lactones **25** in excellent yield, diastereo- and enantioselectivity. Three years later, the first catalytic generation of α,β -unsaturated acyl ammonium intermediates using isothiurea catalysis was reported by Smith and co-workers (Scheme 5c).²¹ Employing 1,3-bisnucleophiles **27** in a Michael addition-annulation process allowed the formation of lactone or lactam products in high yield and with excellent enantioselectivity. Addition of methanol also gave access to the ring opened analogues **29** without erosion of enantiopurity.



Scheme 5 Examples of the first use of isothiurea catalysts in: a) acyl ammonium catalysis; b) ammonium enolate catalysis; c) α,β -unsaturated acyl ammonium catalysis.

The continued interest in isothiureas as Lewis base catalysts spurred further catalyst development by the groups of Okamoto,²² Birman,²³ Shiina²⁴ and Smith,²⁵ resulting in a small library of structural analogues (Figure 5), capable of furnishing excellent yields and selectivities for a variety of transformations featuring acyl ammonium,²⁶ C(1)-ammonium enolate²⁷ and α,β -unsaturated acyl ammonium intermediates.²⁸

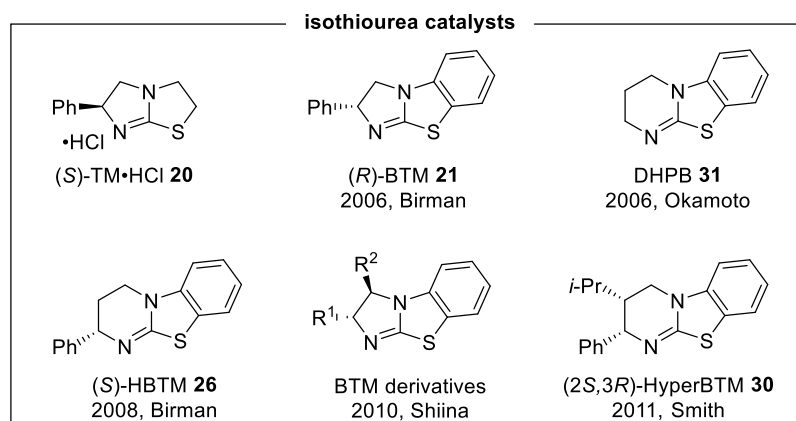


Figure 5 Common isothiourea catalysts

Although the individual reactions might be quite different, the success of the isothiourea catalysts can be rationalised through common principles applicable to all reactive intermediates. In general, a non-bonding 1,5-O \cdots S interaction between the carbonyl oxygen and the sulfur atom of the catalyst is invoked for the catalyst bound intermediate (Figure 6). A combination of computational and experimental studies have shown that this results from an intramolecular orbital interaction between the oxygen lone pair and the antibonding S-C orbital ($n_{\text{O}} \rightarrow \sigma^*_{\text{S-C}}$).²⁹ This contact is significantly shorter than the sum of the relevant van der Waals radii and is energetically favourable, as suggested by crystallographic³⁰ and computational studies.^{31–33} As a result, the conformational freedom of the substrate is restricted. This, in combination with the stereodirecting phenyl group of the catalyst effectively blocking the *si* face, forces any reaction to take place on the *re* face, resulting in excellent facial selectivity.

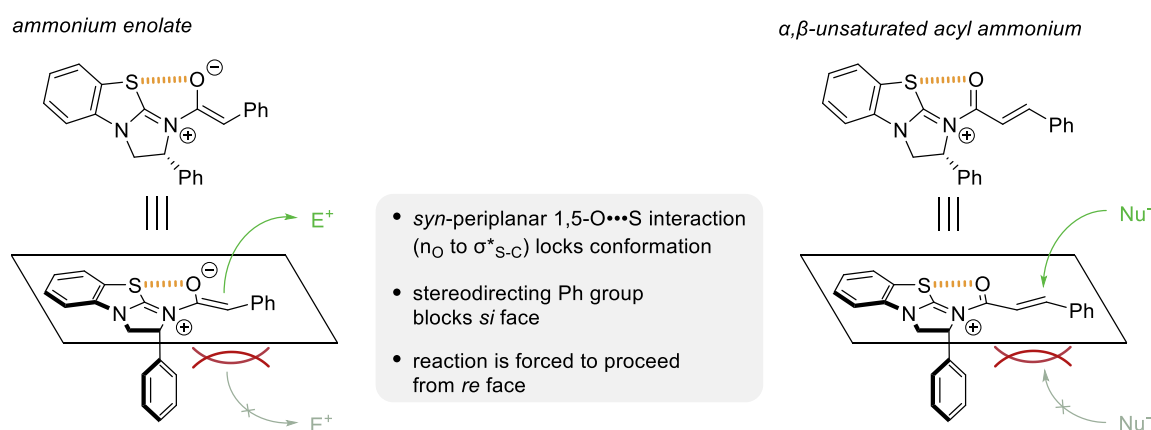
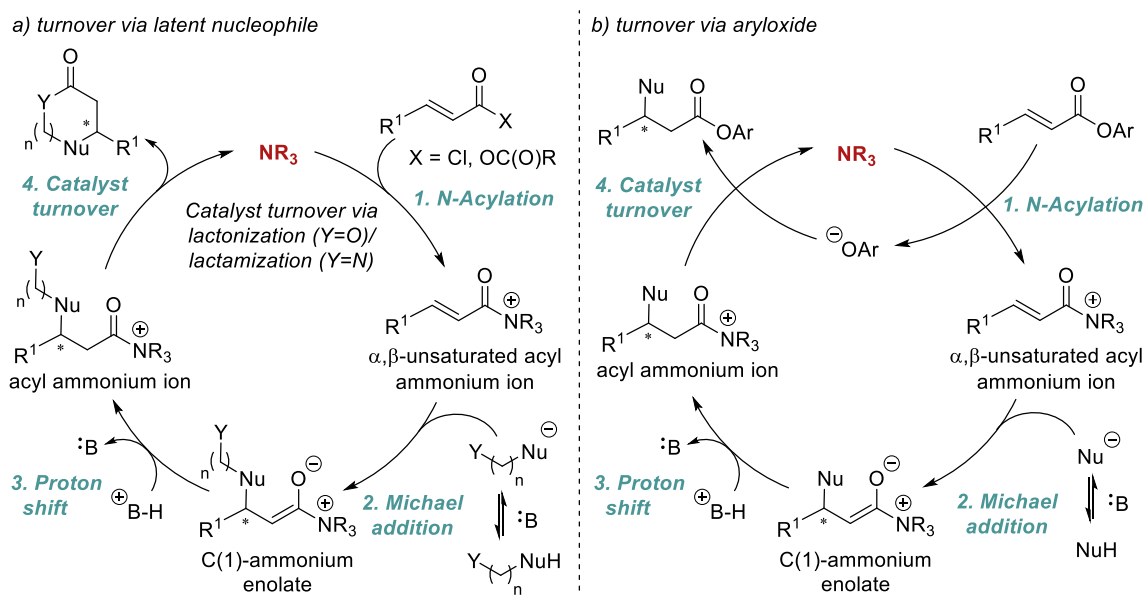


Figure 6 Stereochemical rationale in isothiourea catalysis.

1.3.2 Catalyst turnover strategies

The catalytic cycle in isothiourea catalysis typically begins with acylation of the catalyst by the corresponding carboxylic acid derivative, forming an acyl ammonium ion pair. Depending on the leaving group of the acylating starting material, two distinct catalyst turnover strategies are possible, exemplified on a catalytic cycle featuring an α,β -unsaturated acyl ammonium intermediate (Scheme 6), but equally applicable to ammonium enolate catalysis. Traditional approaches rely on acid chlorides and acid anhydrides as starting material, as they are often commercially available and provide good reactivity. Upon catalyst acylation, these substrates liberate weakly nucleophilic chloride and carboxylate counterions. As these are not able to displace the catalyst at the end of the transformation, an additional reaction partner is required to facilitate catalyst turnover. In the case of α,β -unsaturated acyl ammonium catalysis, this can be achieved by employing bis-(pro)nucleophiles (e.g. 1,3-diketones, acylbenzothiazoles) (Scheme 6a). The reactive nucleophile (Nu^-) can be generated *in situ* to undergo Michael addition with the α,β -unsaturated acyl ammonium ion pair, forming an intermediate C(1)-ammonium enolate. Subsequent proton transfer gives an acyl ammonium ion. Finally, the second, latent nucleophile (Y) can facilitate intramolecular catalyst turnover via lactonization or lactamization. Though powerful, this approach is inherently limited to producing cyclic products. To overcome this limitation, the carboxylic acid starting material needs to have a good enough leaving group to facilitate catalyst acylation, generating a counterion that is also nucleophilic enough to turn over the catalyst at the end of the reaction, while not interfering in any other steps in the catalytic cycle. One possibility for such counterions are the aryloxides liberated from electron deficient aryl esters, as pioneered by Scheidt and co-workers in 2009.^{34,35} In this scenario, the aryloxide (ArO^-) released upon *N*-acylation of the catalyst, can react with the post reaction acyl ammonium ion to generate the corresponding aryl ester product and promote catalyst turnover (Scheme 6b). This strategy represents a complementary approach to using bis-(pro)nucleophiles as it enables the use of simple, monofunctional nucleophiles to generate linear products, broadening the scope of isothiourea catalysis.

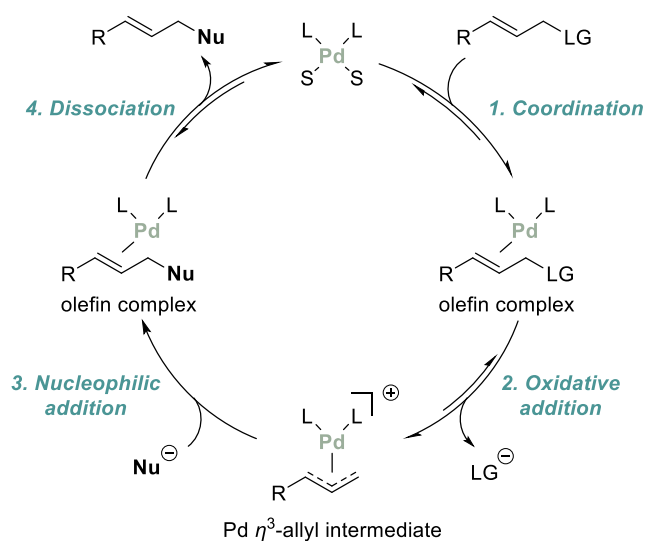


Scheme 6 Catalyst turnover strategies in isothiurea catalysis via a) latent nucleophile or b) aryloxide.

1.4 Palladium catalysed allylic substitution reactions

Over the last 50 years, transition metal catalysed allylic substitution reactions have been intensively investigated and developed into a common tool in today's synthetic chemistry. In particular asymmetric allylic substitution reactions have been used as key steps in numerous syntheses of natural products.^{36,37} Although a variety of transition metals have shown activity for this transformation, methodologies relying on palladium³⁸ and iridium³⁹ are the most developed and understood.

A generalised catalytic cycle for a palladium catalysed allylic substitution reaction shown in Scheme 7 starts with coordination of the palladium catalyst to the π -bond of the allylic substrate bearing a leaving group (LG), forming an olefin complex.⁴⁰ Oxidative addition expels the leaving group and gives the key cationic palladium η^3 -allyl intermediate. Nucleophilic attack at the less substituted allylic terminus of the electrophilic π -allyl moiety, followed by dissociation of the resulting olefin complex, releases the substituted product and regenerates the catalyst. Importantly, formation of the η^3 -allyl intermediate is a reversible process, with the equilibrium position dependent on the nature of the substrate, the leaving group and the ligands around Pd. Subsequent nucleophilic addition is usually considered irreversible, biasing the overall process toward product formation. The rate limiting step in this catalytic process can be either oxidative addition or nucleophilic substitution, depending on the involved transition states.



L = ligand; S = solvent or vacant; LG = leaving group; Nu = nucleophile

Scheme 7 General catalytic cycle for palladium catalysed allylic substitution reactions.

The following paragraphs highlight some general considerations that can be made for palladium catalysed allylic substitution reactions, with a more detailed discussion on allyl palladium intermediates and nucleophiles thereafter.

To tune the activity of the palladium catalyst, electron donating phosphine ligands are usually employed to facilitate oxidative addition. As such, simple monodentate phosphines like triphenylphosphine (PPh_3) or other trialkylphosphines (P(alk)_3) are commonly used. Depending on the exact transformation, the use of moderately electron-withdrawing phosphine ligands might also be applicable, which render the π -allyl intermediate more electrophilic and hence facilitate nucleophilic attack.⁴¹

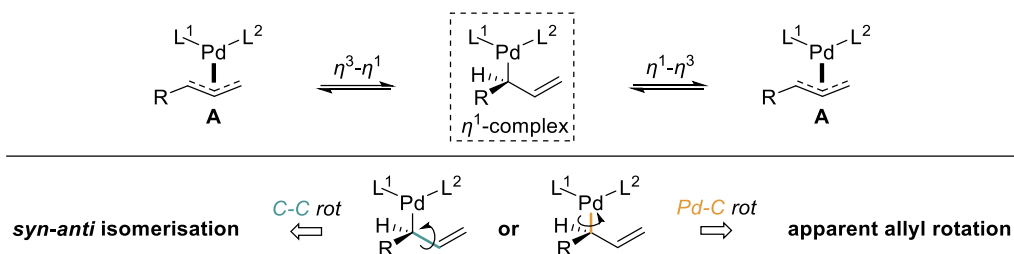
With unsymmetrical allylic substrates, regioselectivity becomes an important consideration. As a general rule, palladium catalysed allylic substitution reactions will give the linear product with nucleophilic attack occurring at the less hindered allylic terminus. In contrast, when iridium is employed as the catalytically active metal, nucleophilic attack usually takes place at the more substituted allylic terminus, resulting in the branched product.⁴²

A variety of leaving groups can be employed for the allylic substrate. Most commonly alcohol derivatives such as acetates ($-\text{OCOR}$), carbonates ($-\text{OCO}_2\text{R}$) or phosphates ($-\text{OP(O)(OR)}_2$) are used, but other examples based on sulfur (e.g. sulfones),

nitrogen (e.g. nitro groups) or halides have also been reported. More elaborate precursors such as cyclopropanes and epoxides can also be used. As a general rule, a better leaving group will shift the equilibrium towards the Pd η^3 -allyl intermediate as ion-pair return will be less favoured, resulting in a faster catalytic turnover.⁴¹

1.4.1 Potential isomerisation processes for Pd η^3 -allyl intermediates

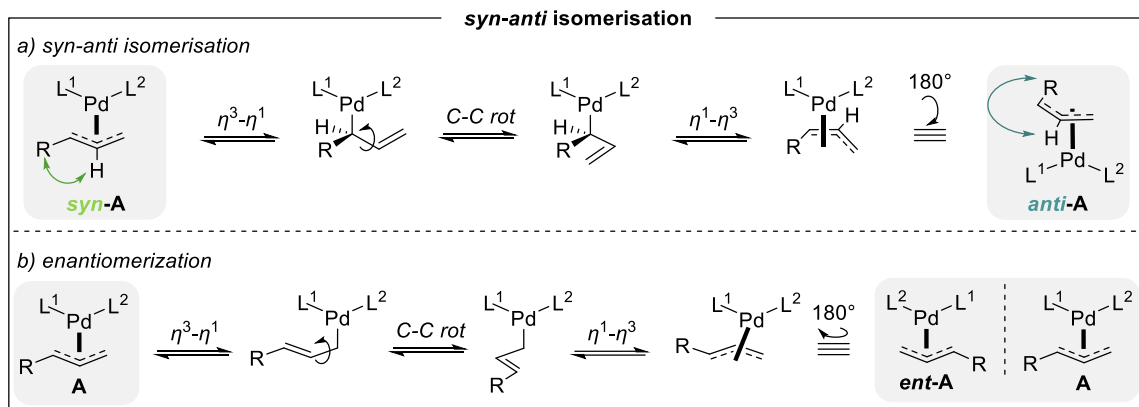
The key Pd η^3 -allyl intermediate can be subject to isomerisation processes, especially when the equilibria involved are faster than subsequent nucleophilic attack, which can have a significant influence on the regio- and stereoselectivity of the overall process. Two major types of isomerisation have to be considered: *syn-anti* isomerisation and apparent allyl rotation. Both processes occur via η^3 - η^1 - η^3 isomerisation, also known as π - σ - π isomerisation (Scheme 8, top). However, the allyl fragment in the intermediate tetracoordinate η^1 -complex can undergo different σ -bond rotations. Isomerisation processes that occur via C-C bond rotation are classified as *syn-anti* isomerisation, whereas rotation around the Pd-C bond is characteristic for apparent allyl rotation (Scheme 8, bottom). Depending on the nature of the allyl fragment, these processes can have different consequences for the overall Pd π -allyl complex.⁴⁰



Scheme 8 Isomerisation processes: generalised mechanism (top); classification based on σ -bond rotation (bottom).

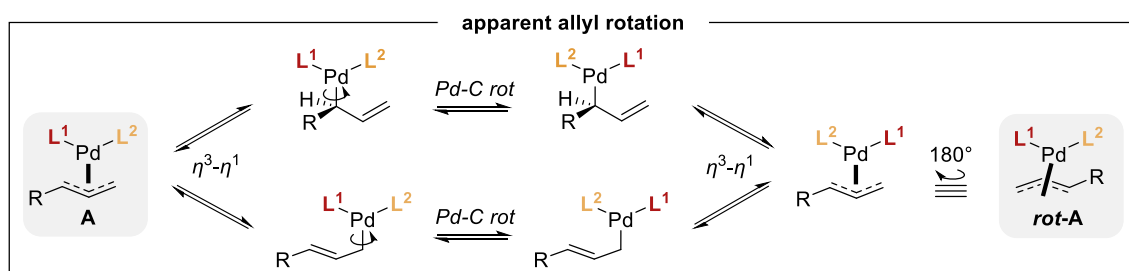
For *syn-anti* isomerisation one such consequence becomes apparent when considering the position of the allylic substituent R with regards to the C(2)-H, which can be either *syn* or *anti* (Scheme 9a). Interconversion of the *syn-anti* isomers occurs via η^3 - η^1 - η^3 isomerisation, with the *syn*-isomer being generally more energetically favourable. Starting from the *syn*-isomer, η^3 - η^1 isomerisation leads to the formation of the tetracoordinate η^1 -complex, with excess ligand or solvent usually filling the vacant coordination site (not shown for simplicity). Rotation around the C-C σ -bond followed by η^1 - η^3 isomerisation gives the Pd η^3 -allyl complex with the allylic substituent R in the *anti*-position. This isomerisation process also results in an exchange of the complexed allyl face, but does not change the

relative position of the allyl carbons and the ligands towards each other. In case of a monosubstituted allyl fragment, an alternative isomerisation pathway is also possible, as the allylic termini are not identical. If coordination to the palladium centre occurs through the less substituted allylic carbon, *syn-anti* isomerisation results only in an exchange of the complexed allyl face without changing the allyl geometry, which leads to the formation of the enantiomeric Pd η^3 -allyl complex (*ent-A*) (Scheme 9b).



Scheme 9 *Syn-anti* isomerisation processes via an η^1 -intermediate.

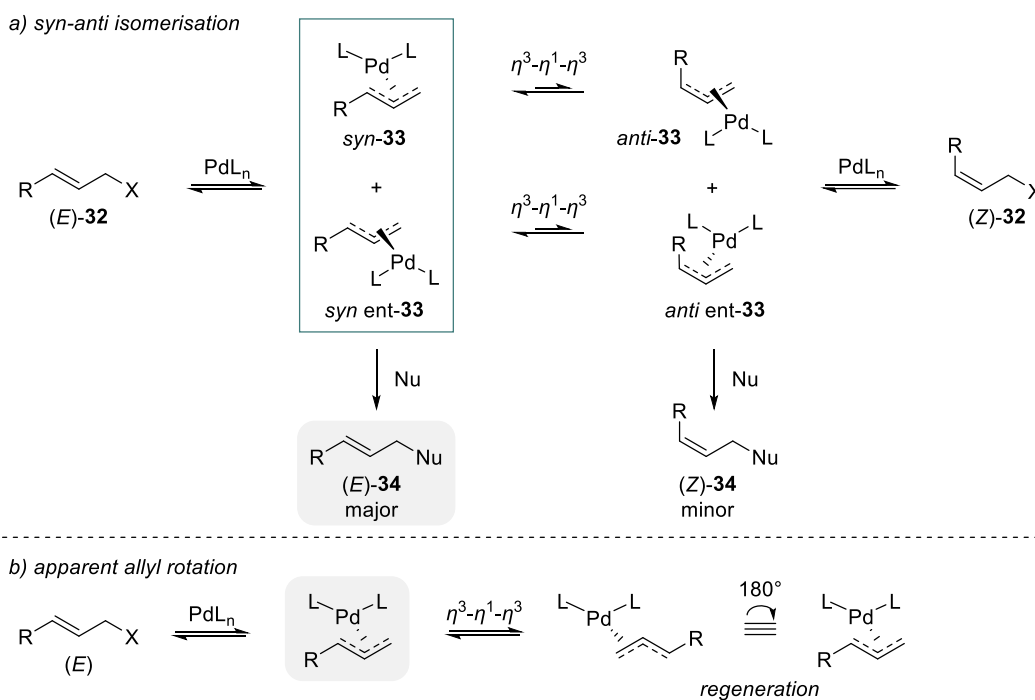
As for the second isomerisation process, apparent allyl rotation describes the formal rotation of the allyl fragment around the hypothetical palladium-allyl bond. In analogy to *syn-anti* isomerisation processes, η^3 - η^1 isomerisation can result in two different tetracoordinate η^1 -intermediates (Scheme 10). Rotation around the Pd-C σ -bond followed by η^1 - η^3 isomerisation, results in a Pd π -allyl complex with a rotated allyl fragment. In this scenario, the outcome of the overall process is the same for both potential intermediates. In contrast to a *syn-anti* isomerisation process, apparent allyl rotation changes the relative position of the allyl carbons and the coordinated ligands, but does not exchange the allyl face complexed to the palladium centre.



Scheme 10 *Apparent allyl rotation* via η^1 -allyl intermediate.

The implications of these isomerisation processes depend on the nature of the substrate, nucleophile and ligands involved, potentially resulting in different regio- and

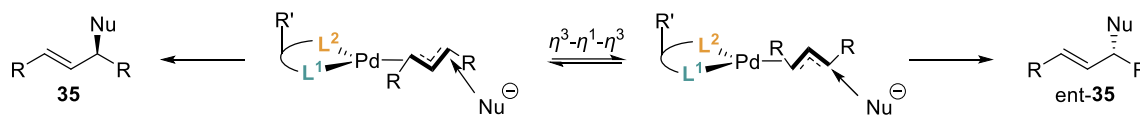
stereochemical outcomes. In the simplest case, using monodentate PR_3 ligands and linear, monosubstituted allylic substrates, the above-described isomerisation processes will only influence the alkene geometry in the product. Starting from either (*E*)-**32** or (*Z*)-**32** initially generates the corresponding *syn*- and *anti*-Pd π -allyl complexes (**33**), as oxidative addition occurs with retention of the alkene geometry (Scheme 11a). Subsequent *syn-anti* isomerisation processes facilitate the equilibration towards a common, energetically more favourable *syn*- η^3 -allyl intermediate, which exists as a pair of enantiomers (Scheme 11a, box). Attack of a nucleophile at the less substituted carbon gives the corresponding (*E*)-isomer **34** as the major product. As the molecule is not chiral, enantiomerization processes of the intermediate complex **33** are inconsequential. Hence, starting from either (*E*)- or (*Z*)-allyl precursor will result in the same product, as long as nucleophilic substitution is slow compared to *syn-anti* isomerisation. In this scenario, given that the ligands L are identical, apparent allyl rotation has no influence on the reaction outcome, as the Pd η^3 -allyl complex is regenerated in this process (Scheme 11b).



Scheme 11 Exemplified implications of *syn-anti* isomerisation (a) and *apparent allyl rotation* (b).

In the case of unsymmetrical ligands however, *apparent allyl rotation* can result in the formation of different product enantiomers, as exemplified in Scheme 12. A bulky, bidentate ligand with different donor atoms (e.g. $\text{L}^1 = \text{P}$, $\text{L}^2 = \text{N}$) can direct the approach of the nucleophile along a certain trajectory. *Apparent allyl rotation* changes the

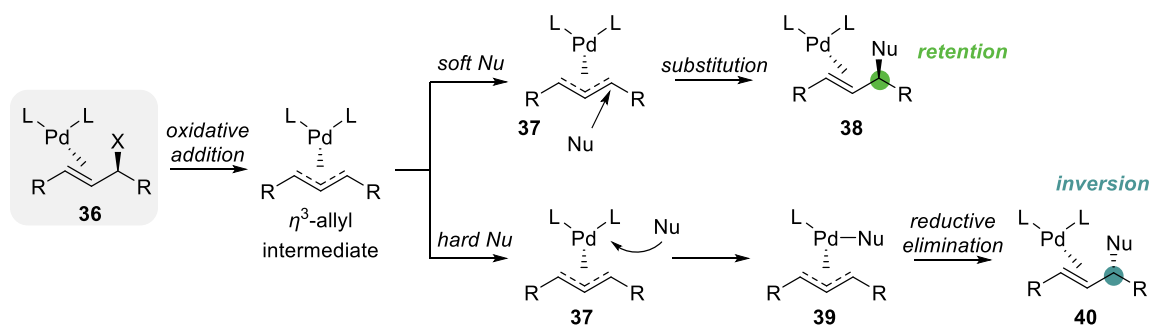
orientation of the allyl fragment along this trajectory, potentially resulting in different enantiomers being formed.



Scheme 12 Enantiomerization as a consequence of apparent allyl rotation.

1.4.2 Nucleophiles in allylic substitution reactions

Nucleophiles are usually simplistically categorised as soft or hard, depending on the pK_a of their conjugate acid.⁴³ Hence, soft nucleophiles are defined as those derived from conjugate acids with a $pK_a < 25$ (such as stabilised carbanions, alcohols or amines), whereas hard nucleophiles are derived from conjugate acids with a $pK_a > 25$ (such as organometallic reagents). Depending on the nature of the nucleophile, two mechanistic pathways for nucleophilic attack on the π -allyl intermediate can be differentiated (Scheme 13). Starting from enantiopure allylic substrate **36**, coordination of the palladium catalyst and subsequent oxidative addition occurs on the opposite face to the leaving group, giving symmetrical η^3 -allyl intermediate **37** with formal inversion of configuration. Subsequently, two outcomes are possible, depending on the nucleophile. Use of soft nucleophiles will result in direct substitution on the allylic terminus from the opposite side of the palladium centre. This again takes place with inversion of stereochemistry, which results in overall retention of configuration in the substituted product **38**. Hard nucleophiles, on the other hand, first coordinate to the palladium centre (**39**), with subsequent reductive elimination giving the product. In this case, the nucleophile is transferred from the same face as the palladium centre, which proceeds with retention of configuration for this step, but results in an overall inversion of stereochemistry in the substituted product **40**.



Scheme 13 Nucleophile dependent stereochemical outcome in Pd catalysed allylic substitution reactions.

Allylic substitution reactions can be used to form a variety of carbon-carbon and carbon-heteroatom bonds, with soft nucleophiles making up the majority of reaction partners used in the literature. Soft carbon nucleophiles, stabilised by two electron-withdrawing groups and generated through deprotonation of the corresponding C-H acidic compound (e.g. diesters, ketoesters, nitrile-esters, etc) are most commonly used to form new C-C bonds. The allylic substitution reaction involving soft carbon nucleophiles is also commonly called the Tsuji-Trost reaction, based on the pioneering works of Jiru Tsuji⁴⁴ and Barry Trost⁴⁵. Heteroatom nucleophiles are also classified as soft and have been successfully employed in the formation of C-N, C-O and C-S bonds, amongst others.⁴⁶

1.5 Dual catalytic processes

Catalytic transformations are of great importance to modern chemistry in enabling more efficient, economical and environmentally friendly processes. Of particular interest are protocols that allow the combination of multiple catalytic transformations within a single synthetic step run as a one-pot setup. This strategy is attractive as it minimizes work-up and purification steps, thereby circumventing yield losses and generation of waste. It also shortens the overall synthetic sequence, saving time and energy as well as maximizing synthetic efficiency. Compared to traditional synthesis methods, multi-catalysis strategies also avoid the handling of unstable or toxic intermediates, as they will only be generated in small amounts and converted promptly to more stable compounds. In addition, new reaction pathways might be accessible by exploiting highly reactive but fleeting intermediates, which would not be stable enough for isolation under classical synthesis conditions. Moreover, the combination of multiple catalytic reactions in a single synthetic step could also have beneficial effects on the overall reactivity, selectivity and efficiency of the process. Despite numerous potential advantages, designing a multi-catalytic process poses several challenges. The most profound is the compatibility of all the different components – catalysts, substrates, formed intermediates and products, or additional reagents. As the growing number of reports on dual- or multi-catalytic processes highlights, researchers have been successful in overcoming these challenges.^{47,48}

1.5.1 Combining transition metal and organocatalysis

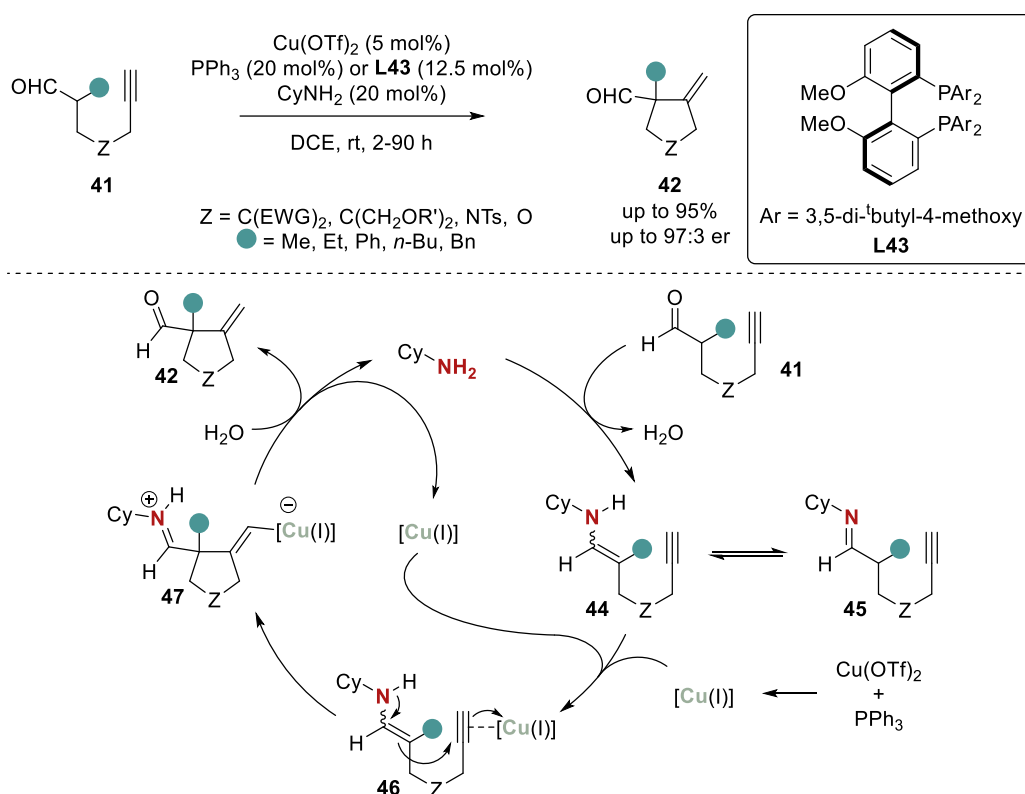
Of particular significance for the work presented herein is the combination of transition metal catalysis with organocatalysis. Both are well established methodologies with broad applicability, with their combination bearing the potential for opening new reaction pathways and new opportunities for stereocontrol. The challenge associated with this pairing is to avoid the deactivation of the catalysts by strong Lewis acid-base interactions, which would lead to catalytically inactive Lewis adducts. Within the multitude of dual transition metal and organocatalytic processes,^{49,50} distinctions can be made based upon the different modes of activation used to transform the substrates. Unfortunately, there is no generally accepted taxonomy within the chemistry community, resulting in various categories being suggested to classify and differentiate these processes. In recent reports,^{51,52} up to seven such categories were proposed, however only two of those – cooperative catalysis and relay catalysis – are relevant for the current work and will be discussed in more detail.

1.5.1.1 Cooperative catalysis

In cooperative catalysis both catalysts work together simultaneously to activate two distinct functionalities within the substrates. This sets up the reactive intermediates generated by each catalyst to react with each other and form the product. This catalytic method can be operative in an intra- and intermolecular fashion, with examples for each shown below. It should be noted that cooperative catalysis is often used interchangeably with the term synergistic catalysis,⁵³ with no apparent preference for either within the organic chemistry community.

An intramolecular cooperative organo- and transition metal catalysis strategy was employed by Ratovelomanana-Vidal and Michelet in 2011 for the synthesis of a variety of five-membered carbocycles.⁵⁴ The methodology employed CyNH₂ (20 mol%) and a combination of Cu(OTf)₂ (5 mol%) and PPh₃ (20 mol%) for the simultaneous activation of an aldehyde and an alkyne functionality within substrate **41** (Scheme 14). In their mechanistic proposal the amine catalyst reacts with **41** to form an enamine intermediate **44**. The copper catalyst coordinates to the alkyne, promoting an intramolecular ring closure by nucleophilic attack from the enamine to form the corresponding five-membered ring **47**. Subsequent hydrolysis of the formed imine and protodemetalation of

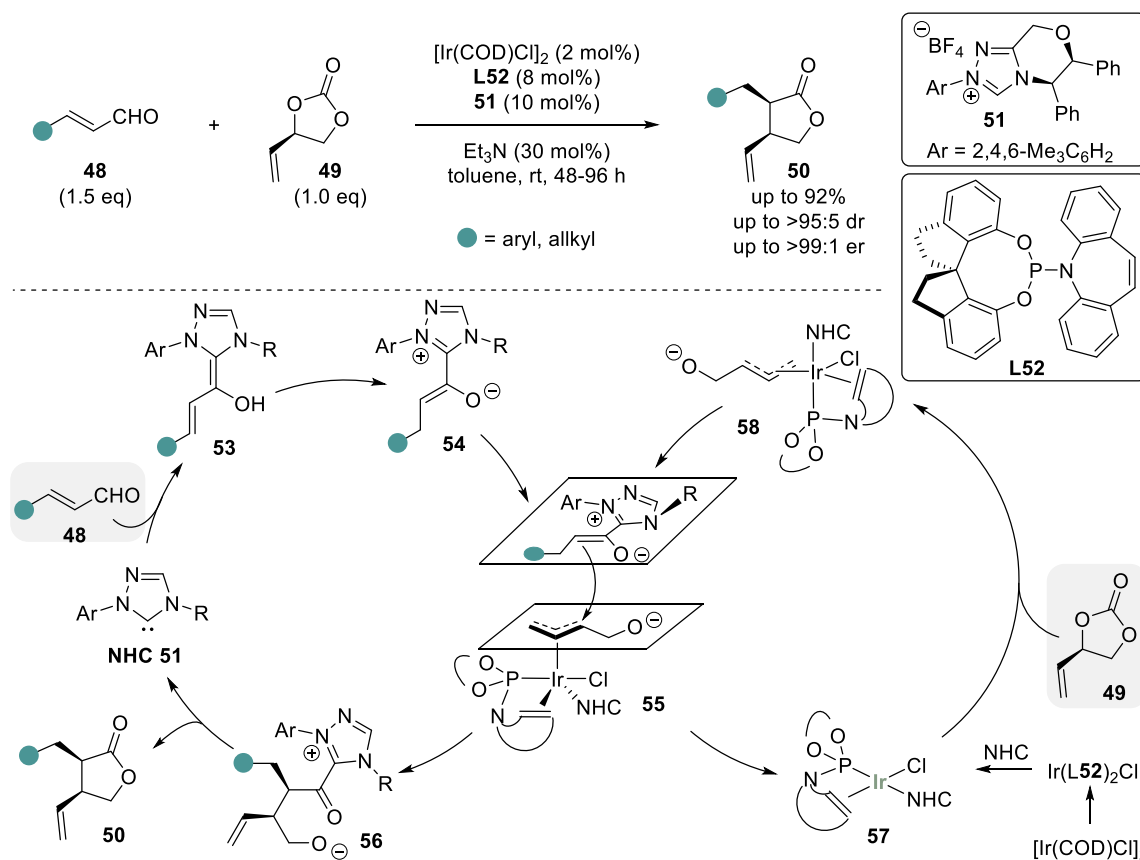
the vinylcopper complex liberates the cyclic product **42** and regenerates the catalysts. This methodology was subsequently expanded to include starting materials with a broad range of carbon and heteroatom tethers, furnishing various carbo- and heterocycles including cyclopentanes, indanes, pyrrolidines and tetrahydrofurans in high yields.⁵⁵ In control experiments the authors demonstrated the necessity of both catalysts for the carbocyclization to take place. Following on from their initial reports, they also developed an enantioselective variant of this cooperative catalysis.⁵⁶ By using C₂-symmetrical phosphine **L43** as chiral ligand for copper in place of PPh₃, it was possible to synthesise chiral cyclopentanes with an all-carbon quaternary stereogenic centre in good yields and up to 97:3 er.



Scheme 14 Cooperative primary amine and copper catalysis.

In 2019, Glorius and co-workers showcased an intermolecular, cooperative organo- and transition metal catalysis using *N*-heterocyclic carbene (NHC) and iridium catalysts.⁵⁷ Starting from readily available α,β -unsaturated aldehydes **48** and vinyl carbonate **49**, highly enantioenriched α,β -disubstituted γ -lactones **50** could be obtained under mild conditions (Scheme 15). Key to this transformation was the simultaneous activation of the substrates by the organocatalyst **51** (10 mol%) and the catalytically active iridium complex **57**, formed *in situ* from $[\text{Ir}(\text{COD})\text{Cl}]_2$ (2 mol%) and spinol-derived phosphoramidite ligand

L52 (8 mol%). In their mechanistic proposal the NHC catalyst reacts with aldehyde **48** to form the corresponding Breslow intermediate (homoenol **53**), followed by proton transfer to give enolate **54**. At the same time, the iridium catalyst undergoes oxidative addition to vinyl carbonate **49**, which after decarboxylation gives Ir π -allyl intermediate **58**. The chiral elements of the catalysts dictate the facial selectivity in the subsequent nucleophilic addition between the enolate and allyl intermediate (**55**). Preferential attack at the branched position followed by lactonization of the acyl azolium species **56** delivers γ -lactone **50** and regenerates the catalysts. Employing this methodology, lactones bearing various aryl and heteroaryl moieties could be obtained in good yields with excellent stereocontrol. A particular feature of this methodology is the potential for a diastereodivergent synthesis to obtain all four stereoisomers of the product by choosing the appropriate NHC/ligand enantiomer combination. In control experiments the authors demonstrated the necessity for an excess of NHC catalyst compared to the amount of iridium catalyst for the reaction to take place. Additionally, a striking counter-anion effect was seen, with the presence of chloride ions proving essential for catalytic activity.

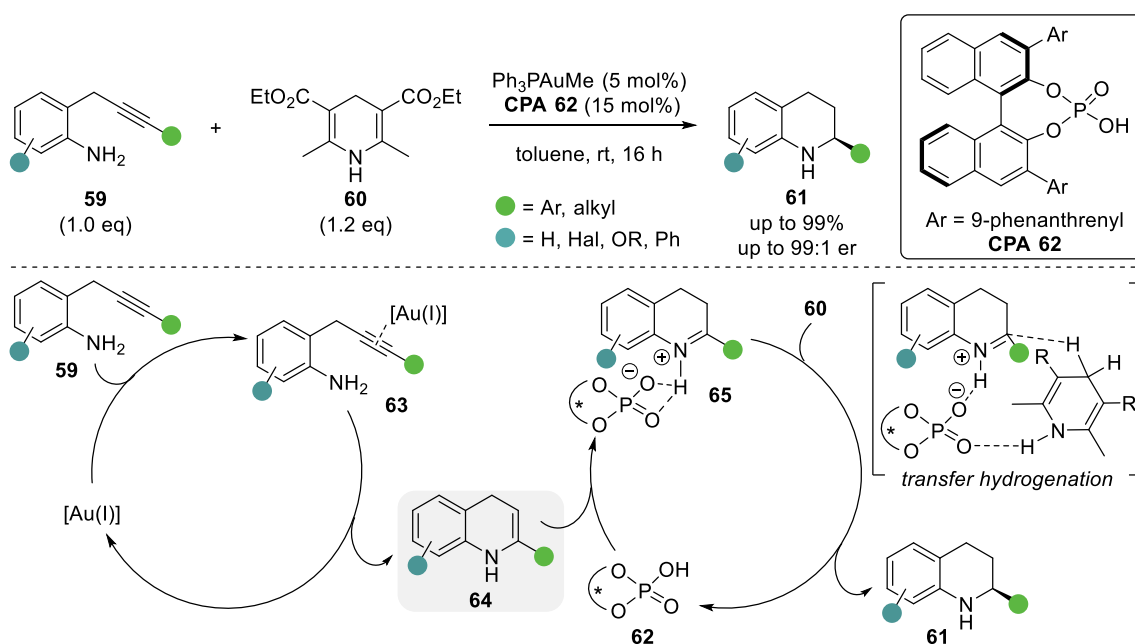


Scheme 15 Cooperative NHC and Ir catalysis

1.5.1.2 Relay (sequential) catalysis

In relay or sequential catalysis, both catalysts operate simultaneously but transformation of the substrates takes place in two discrete catalytic cycles in a sequential fashion. Hence, the substrates are transformed to an intermediate by the first catalyst, which in turn acts as the substrate for the second catalyst to form the final product.

In 2009, this strategy was applied by Gong and co-workers in the synthesis of enantioenriched tetrahydroquinolines using sequential gold and Brønsted acid catalysis.⁵⁸ Employing alkyne **59** and Hantzsch ester **60** in the presence of Ph_3PAuMe (5 mol%) and chiral phosphoric acid (CPA) **62** furnished the desired products in high yields and excellent enantioselectivities (Scheme 16). The catalysis is initiated by coordination of the gold catalyst to alkyne **59**, activating the triple bond for intramolecular hydroamination. The resulting 1,4-dihydroquinoline intermediate **64** serves as substrate for the second catalytic cycle facilitated by the chiral phosphoric acid. Isomerisation in the presence of CPA **62** gives chiral ion pair **65**, which undergoes asymmetric transfer hydrogenation with Hantzsch ester **60** to yield enantioenriched tetrahydroquinoline **61**.

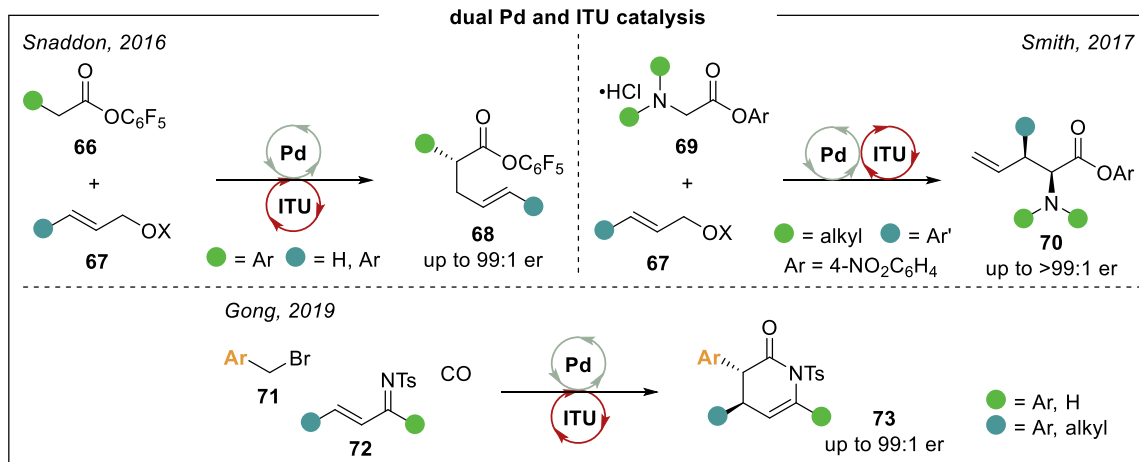


Scheme 16 Gold and chiral phosphoric acid relay catalysis.

1.5.2 Combining transition metal and isothioureia catalysis

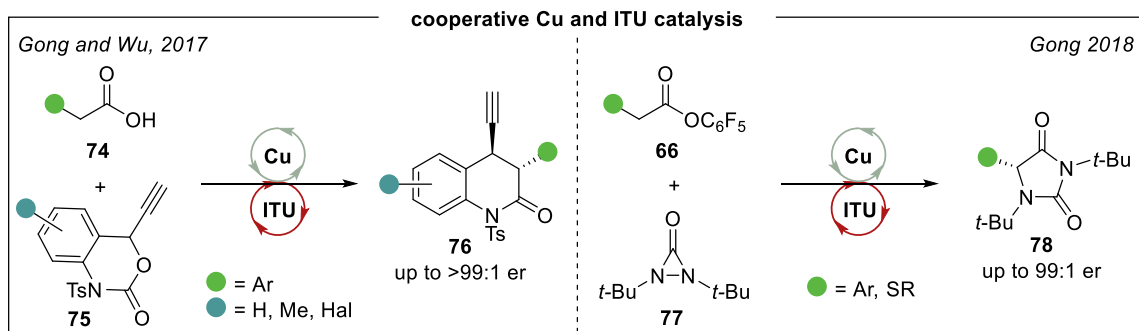
The combination of various transition metal and isothioureia catalysts poses an attractive expansion to transformations traditionally facilitated by these catalysts, as it would greatly widen the pool of potential reaction partners and the possibilities for stereocontrol. With isothioureias being Lewis bases and transition metals generally considered as Lewis acids, Lewis adduct formation represents an area of concern as it could prove detrimental to any intended dual catalytic process. However, numerous methodologies relying on a combination of a transition metal and an isothioureia catalyst have been reported, showcasing the compatibility of these catalytic systems.

In 2016, Snaddon and co-workers reported the first combination of isothioureia (ITU) and transition metal catalysis using (*R*)-BTM and a Pd-Xantphos complex for the stereoselective α -allylation of aryl acetic acid esters (Scheme 17, left).⁵⁹ The same group subsequently expanded this methodology to incorporate various functional groups within the allylic fragment (**67**), including, amongst others aryl,^{60,61} boron,⁶² silicon,⁶³ and electron-withdrawing groups.⁶⁴ In 2017, Smith and co-workers showcased a palladium and isothioureia relay catalysis methodology for the stereoselective synthesis of functionalised α -amino acid derivatives **70** (Scheme 17, right).⁶⁵ Gong and co-workers employed a dual catalytic palladium and isothioureia approach in the formation of dihydropyridones **73** (Scheme 17, bottom).⁶⁶ Use of the simple feedstock chemicals alkyl halides (**71**) and carbon monoxide (CO) in the presence of a palladium catalyst allowed the *in situ* formation of ammonium enolate species, which underwent isothioureia controlled Michael addition-lactamization with unsaturated imines **72**. Notably, these methodologies rely solely on the isothioureia catalyst for enantioinduction, with product selectivities reaching up to 99:1 er in all examples.



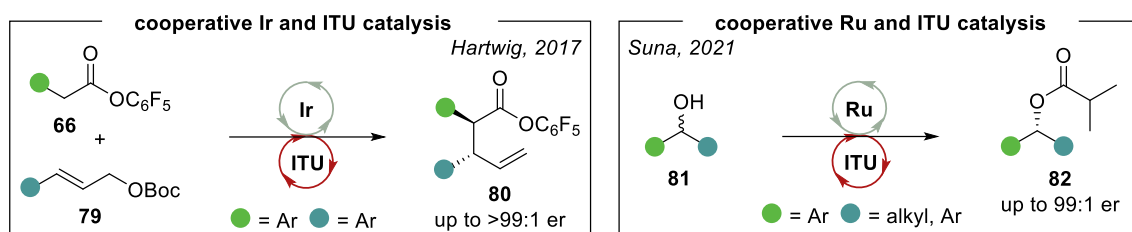
Scheme 17 Examples of dual palladium and isothioureia catalysis.

In 2017, the groups of Gong⁶⁷ and Wu⁶⁸ independently reported the successful combination of copper and isothioureia catalysis. The generation of electrophilic copper-allenylidene complexes from benzoxazinones **75** and trapping with ammonium enolate species generated from carboxylic acid **74** allowed the formation of dihydroquinolinone products **76** with excellent stereoselectivity (Scheme 18, left). Subsequently, Gong and co-workers also employed a dual catalytic copper/isothioureia methodology for the synthesis of highly enantioenriched diaziridinones **78** (Scheme 18, right).⁶⁹



Scheme 18 Examples of cooperative copper and isothioureia catalysis.

In 2017, Hartwig and co-workers used a combination of a chiral iridium catalyst and chiral isothioureia BTM to obtain α -allylated aryl acetic acid esters **80**.⁷⁰ Compared to Snaddon's work, the use of an iridium catalyst rather than a palladium catalyst resulted in the selective formation of the corresponding branched products (Scheme 19, left). Recently, Suna and co-workers reported a combination of ruthenium and isothioureia catalysis in the dynamic kinetic resolution of secondary alcohols (Scheme 19, right).⁷¹ Again, excellent levels of enantioselectivity (up to 99:1 er) were observed in both methodologies.



Scheme 19 Examples of iridium (left) or ruthenium (right) and isothioureia catalysis.

Although these examples clearly highlight the compatibility of isothioureia catalysts with various transition metals, some limitations have also been encountered. When the groups of Nolan and Smith attempted to combine isothioureia and gold catalysis, the intended transformations proved unsuccessful, with only starting materials returned.⁷² Instead, irreversible binding of the Lewis basic isothioureia to the Lewis acidic gold centre was observed, resulting in the formation of isolable, chiral Au^I- and Au^{III}-isothioureia complexes (Figure 7).

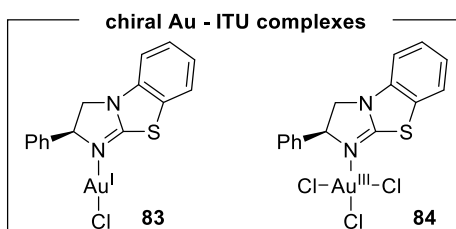


Figure 7 Isolated, chiral Au - isothioureia complexes.

This example highlights the need to gain a deeper understanding of the behaviour of isothioureias in the presence of transition metals to further expand the scope of compatible catalytic partners. In addition, the range of reactivity modes accessible by isothioureia catalysis has not yet been fully exploited in dual catalytic processes. Methodologies so far have been focused on ammonium enolates as reactive intermediates, with only the most recent example by Suna also utilising acyl ammonium intermediates. Notably, no methodologies featuring α,β -unsaturated acyl ammonium intermediates in combination with a transition metal catalyst have been reported to date.

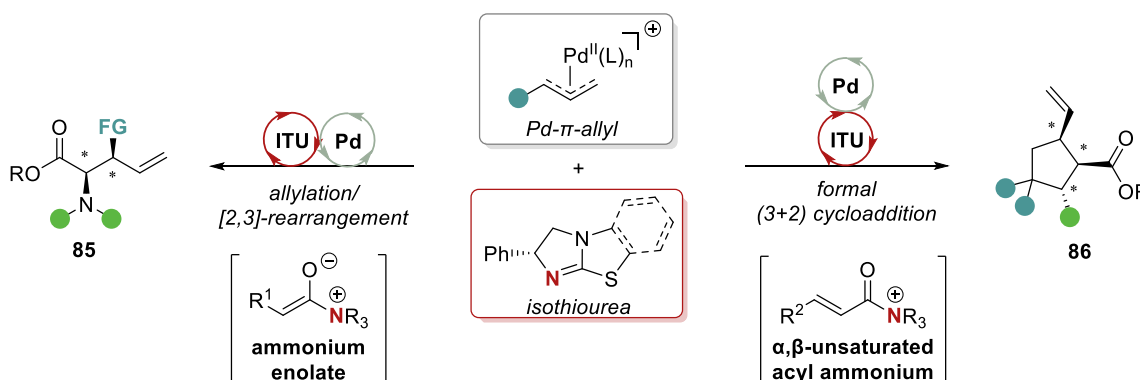
1.6 Aims and Objectives

The dual catalytic processes featuring transition metal catalysts and Lewis basic isothioureia catalysts showcased in this chapter highlight the potential of such catalyst combinations for accessing new reaction pathways. These methodologies also represent a versatile way of broadening the scope of potential reaction partners for the individual catalytic transformations, thereby allowing access to novel product scaffolds. As the use of isothioureia catalysts in dual catalytic methodologies has emerged as a fairly recent area of research, more potential combinations are yet to be identified.

As such, this thesis aims at exploring new avenues to engage isothioureia catalysts in dual catalytic processes, focusing on palladium as the transition metal catalyst. In particular, the use of Pd π -allyl intermediates as reaction partner in combination with different isothioureia bound intermediates is examined.

Chapter 2 investigates the combination of Pd π -allyl intermediates and ammonium enolate intermediates in a relay catalytic process featuring a palladium catalysed allylic amination followed by an isothioureia controlled [2,3]-rearrangement to furnish enantioenriched amino esters **85**. Based on previous work, the potential for broadening the scope of this process is evaluated by incorporating various functional groups (FG) within the allylic reaction partner.

Chapter 3 demonstrates the first use of α,β -unsaturated acyl ammonium intermediates in a dual catalytic process. By engaging these reactive species with zwitterionic Pd π -allyl intermediates, a stereoselective formal (3+2) cycloaddition process to generate highly substituted cyclopentane products **86** is developed.

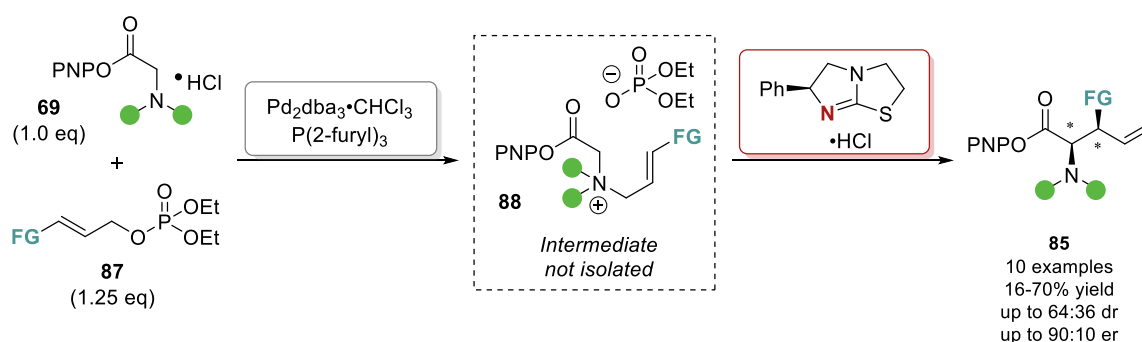


Scheme 20 Proposed work on dual catalytic palladium and isothioureia catalysis.

Chapter 2: Relay palladium and isothiourea catalysis

2.1 Project Overview

This chapter describes the extension of a dual palladium and isothiourea catalysed allylic amination / [2,3]-sigmatropic rearrangement process previously developed in our group. In this methodology, an allylic ammonium salt **88** is generated *in situ* by a palladium catalysed allylic substitution of allylic phosphate **87** with glycine ester **69**. Subsequent acylation of this salt with the isothiourea, followed by generation of an ammonium ylid in the presence of base, promotes [2,3]-sigmatropic rearrangement to yield functionalised amino acid derivatives with high diastereo- and enantioselectivity. Limitations within the previous work required allylic phosphates derived from cinnamyl alcohols, while in this work allylic phosphates containing ester, amide, silyl and protected alcohol functional groups (FG), as well as a branched substrate, have been investigated. Application of these functionalised allylic phosphates **87** in the relay palladium and isothiourea catalysis resulted in the formation of highly functionalised *syn*- α -amino acid derivatives **85** in good yield (up to 70%) and moderate to high stereocontrol (up to 60:40 dr and 90:10 er).

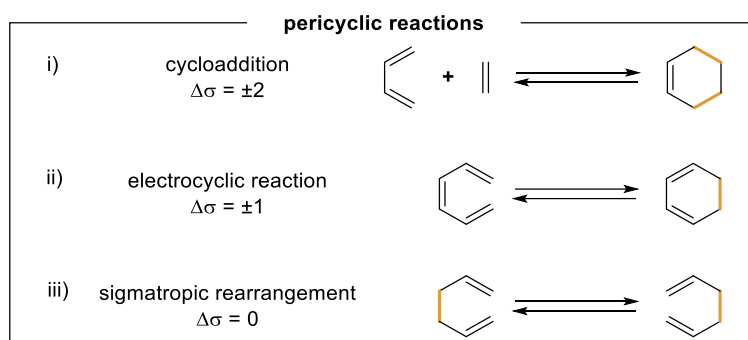


Scheme 21 Relay palladium and isothiourea catalysis.

2.2 Introduction

2.2.1 Sigmatropic Rearrangements

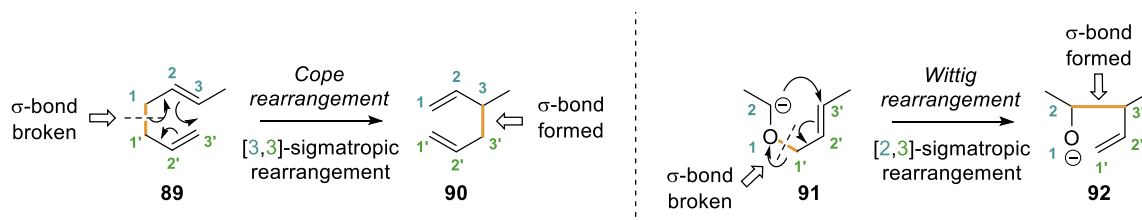
Sigmatropic rearrangements have proven to be a useful tool in organic synthesis, especially in the formation of complex molecules in a stereoselective fashion.³⁷ Together with cycloadditions and electrocyclic reactions, sigmatropic rearrangements are categorised as pericyclic reactions (Scheme 22). These types of reactions are characterised by a concerted, cyclic transition state, in which bonds are formed and broken without the involvement of intermediates. Each of these shows a characteristic change in the number of σ -bonds (highlighted in Scheme 22 in orange). In cycloadditions, cyclic molecules are either formed or broken with an overall change in the number of σ -bonds of ± 2 (Scheme 22(i)). The most famous example from this class is the Diels-Alder reaction.⁷³ Electrocyclic reactions also involve the formation or opening of cyclic structures (Scheme 22(ii)). However, only one σ -bond is formed or broken in the process and only one conjugated π -system is involved, rather than the two non-conjugated π -systems that characterise cycloadditions. The third class, sigmatropic rearrangements, are defined by the migration of a σ -bond with the redistribution of one or more adjacent π -bonds so that the overall number of σ -bonds stays unchanged (Scheme 22(iii)).



Scheme 22 Types of pericyclic reactions.

To further distinguish between different reactions within each category, Woodward and Hoffmann developed an unambiguous numbering system to classify these types of processes. Illustrated using an example of a sigmatropic rearrangement, their numbering system counts the atoms between the broken and newly formed σ -bond (Scheme 23).⁷⁴ Starting on the σ -bond to be broken, the involved atoms are numbered with 1 and 1'. Continuing the numbering in opposite directions towards the atoms between which the

new σ -bond will be formed gives the specific class of sigmatropic rearrangement. Hence, the illustrated Cope and Wittig rearrangements are examples of [3,3]- and [2,3]-sigmatropic rearrangements, respectively. The sum of this number label also implies the total number of atoms involved in the cyclic transition state, which are six for a [3,3]-rearrangement and five for a [2,3]-rearrangement.



Scheme 23 Nomenclature and examples for sigmatropic rearrangements.

In 1965, Woodward and Hoffmann also introduced a set of rules in order to assess whether pericyclic reactions are thermally or photochemically allowed, based on orbital symmetry considerations for the desired transformations.⁷⁵⁻⁷⁷ For each of these reactions the components taking part in the transformation have to be identified – where a component is a bond or orbital directly involved in the reaction. For example, a double bond is a π^2 component ('2' indicating the number of electrons and ' π ' indicating the type of orbital), a single bond is a σ^2 component and an orbital located on a single atom is an ω component (ω^0 indicating an empty orbital, for example in a carbocation, and ω^2 indicating a filled orbital, for example in a carbanion or a lone pair). Furthermore, it must be indicated whether a component forms new bonds on the same face at both ends (suprafacial component, suffix *s*) or on opposite faces (antarafacial component, suffix *a*) as depicted in Figure 8 for π -components.

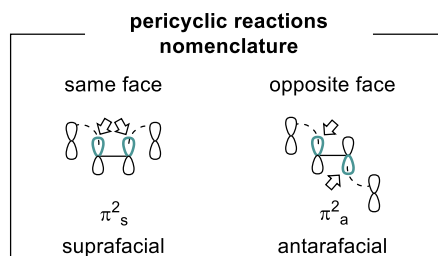


Figure 8 Suprafacial vs. antarafacial bond formation.

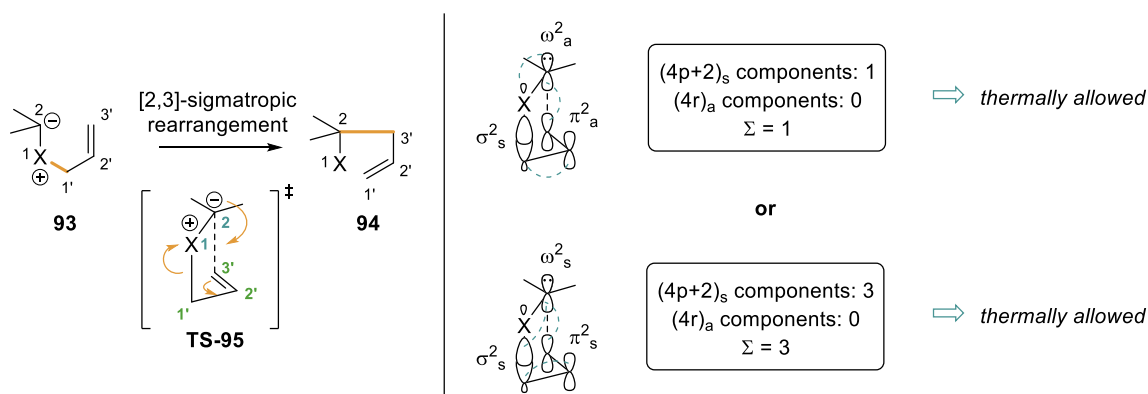
Based on this classification and the number of electrons, the components involved in the reaction can be categorised in one of four categories: $(4p + 2)_s$, $(4p + 2)_a$, $(4q)_s$, $(4q)_a$, where p and q are integral numbers. Woodward and Hoffmann then developed Equation

1, where only $(4p + 2)_s$ and $(4q)_a$ components have to be considered. According to their approach, a pericyclic reaction will be thermally allowed if the sum of the components in Equation 1 is odd. If the sum is an even number, the transformation will only be allowed photochemically. The application of these rules will be illustrated for an example of a [2,3]-sigmatropic rearrangement.

$$\Sigma (4p + 2)_s + (4q)_a$$

Equation 1 Woodward Hoffmann equation for pericyclic reactions.

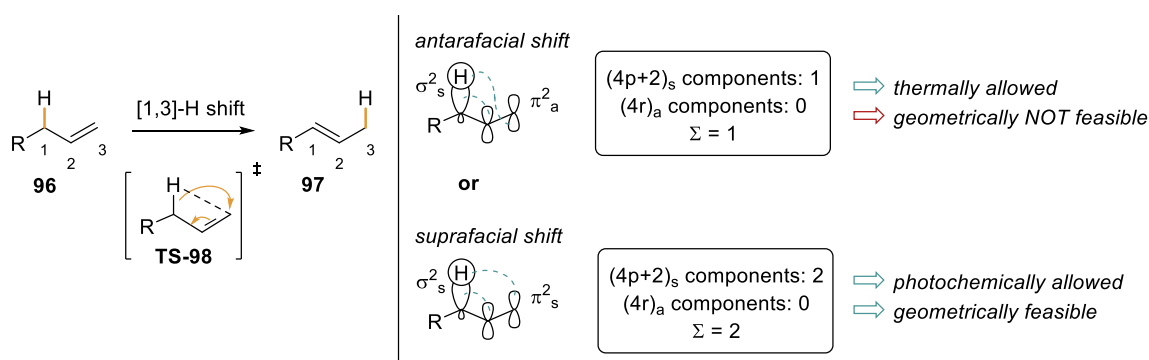
As shown in Scheme 24 the components involved in a [2,3]-sigmatropic rearrangement are the carbanion at C(2) (ω^2 component), the σ -bond being broken (σ^2 component) and the migrating π -bond (π^2 component). Each of these components can be classified as a $(4p + 2)$ component for $p = 0$. In order to use Equation 1, the faces from which the new bonds are formed must be determined. In fact, there are two equally correct ways to consider the formation of the new bonds, as demonstrated in Scheme 24 (right). One possibility is to draw the σ^2 component reacting in a suprafacial fashion with the other two reacting in an antarafacial fashion, yielding one $(4p + 2)_s$ component. Another possibility is to draw all three components reacting suprafacially, yielding three $(4p + 2)_s$ components overall. In each case, the sum for Equation 1 is an odd number, demonstrating that a [2,3]-sigmatropic rearrangement is a thermally allowed process.



Scheme 24 Woodward-Hoffmann rules as exemplified on a [2,3]-sigmatropic rearrangement.

In addition to the generalisations Woodward and Hoffmann made based on orbital symmetry considerations resulting in Equation 1, the geometrical feasibility of a transformation must also be taken into account. As a consequence, even though a reaction might be symmetry allowed according to the Woodward-Hoffmann rules, it might not be geometrically feasible and therefore will not proceed. This can be exemplified on another

type of sigmatropic rearrangements, a [1,3]-hydrogen shift. A [1,3]-H shift describes the migration of a H-atom from its current position (1) to its new position (3) with simultaneous shift of a double bond (Scheme 25). The components involved are the C-H σ -bond (σ^2 component) and the double bond (π^2 component). When the H-shift proceeds in an antarafacial fashion, the reaction is thermally allowed, however it is not geometrically feasible, as the transition state structure would be very distorted, preventing sufficient orbital overlap. A suprafacial H-shift, on the other hand, is geometrically feasible and according to Woodward-Hoffmann rules allowed under photochemical conditions.



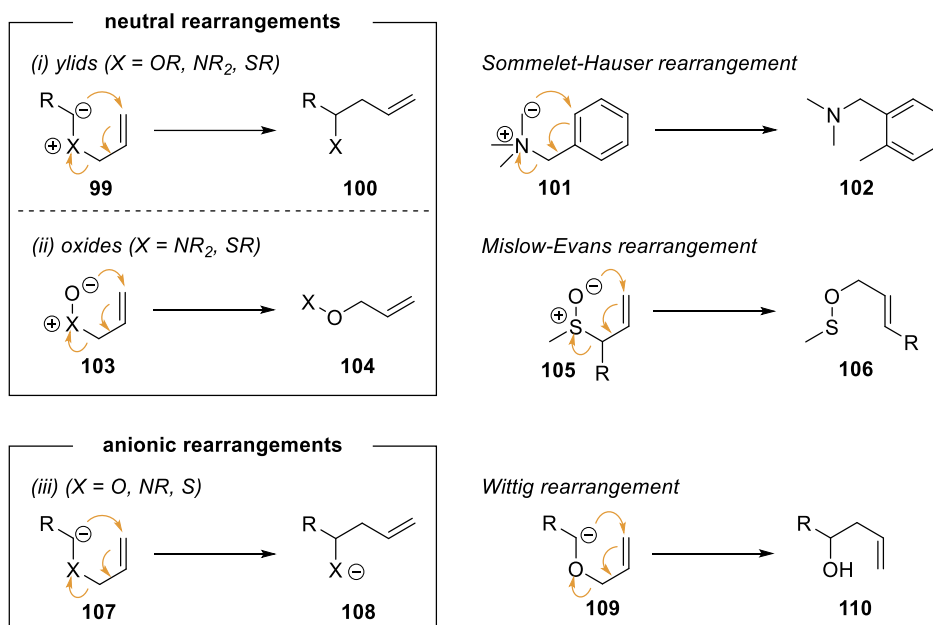
Scheme 25 Geometrical considerations in sigmatropic rearrangements.

Within the class of sigmatropic rearrangements, [3,3]-sigmatropic rearrangements have been extensively studied and used in total synthesis.³⁷ This can be ascribed to their predictable and reliable outcome for the synthesis of olefins and stereocentres owing to the rigid six-membered cyclic transition state. [2,3]-Sigmatropic rearrangements are less well studied and their stereochemical outcome is often more difficult to control. Nonetheless, they are very useful reactions as they allow for easy access to functionalised molecules, the installation of up to two new stereogenic centres and a new π -bond. The following section will provide a more detailed discussion of the characteristics of [2,3]-sigmatropic rearrangements and highlight significant developments in this area.

2.2.2 [2,3]-Sigmatropic Rearrangements

Based on the nature of the reactive species in [2,3]-sigmatropic rearrangements, the reactions can be categorised as neutral: employing either onium ylids **99** (Scheme 26(i)), or heteroatom-oxides **103** (Scheme 26(ii)); or anionic: featuring heteroatom-stabilised carbanions **107** (Scheme 26(iii)). Examples for each type of rearrangement include the

Sommelet-Hauser rearrangement,⁷⁸ the Mislow-Evans rearrangement,^{79,80} or the Wittig rearrangement,⁸¹ respectively. The main focus of this discussion will be on [2,3]-sigmatropic rearrangements of onium ylids, which will be explored in more detail in section 2.2.3.



Scheme 26 Categories of [2,3]-sigmatropic rearrangements and examples.

2.2.2.1 Stereochemical considerations for [2,3]-sigmatropic rearrangements

[2,3]-Sigmatropic rearrangements proceed via a cyclic five-membered, six-electron transition state with an envelope conformation. Compared to [3,3]-sigmatropic rearrangements, this transition state is less rigid and hence more susceptible to substituent effects.⁸² Thus, the preferred conformation in the transition state will be dependent on the steric and electronic properties of the substituents around the new σ - and π -bond as well as the involved heteroatom. Although [2,3]-sigmatropic rearrangements have great synthetic potential, their widespread application has been hampered by the lack of theoretical and mechanistic investigations, which makes it more difficult to reliably predict the stereochemical outcome compared to [3,3]-sigmatropic rearrangements. Hence, further fundamental studies are necessary to gain a deeper understanding of this process. The following paragraphs introduce general considerations which affect the relative and absolute configuration around the new σ -bond as well as the π -bond geometry in the product.

In order to rationalise any observed stereoselectivities for a given reaction, possible pre-transition state assemblies have to be considered. In a [2,3]-sigmatropic rearrangement, two conformations are possible depending on the orientation of the substituents opposite the envelope 'apex' (R^1 and H) (Figure 9). If R^1 is situated on the same side as the 'apex', the conformer will be referred to as *endo*. If R^1 is on the opposite side to the 'apex', the conformer will be labelled *exo*. The same holds true in cases where another substituent instead of hydrogen is present, with R^1 being the substituent of higher priority according to Cahn-Ingold-Prelog rules.

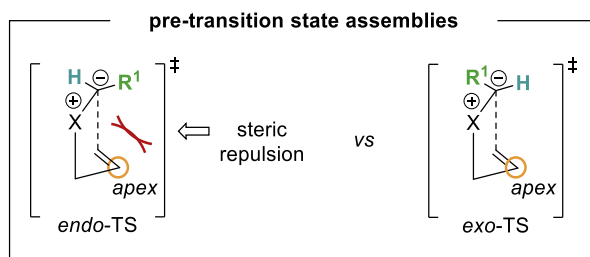
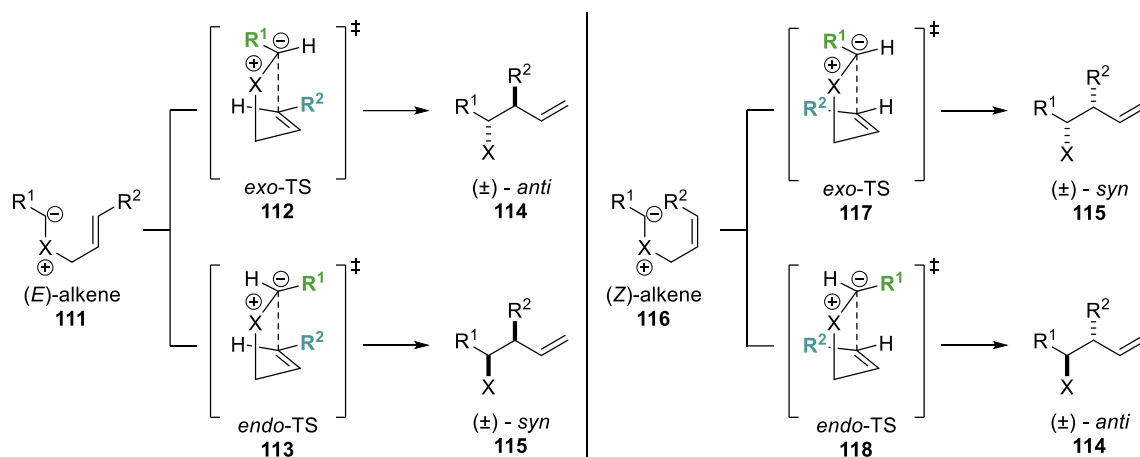


Figure 9 Pre-transition state assemblies.

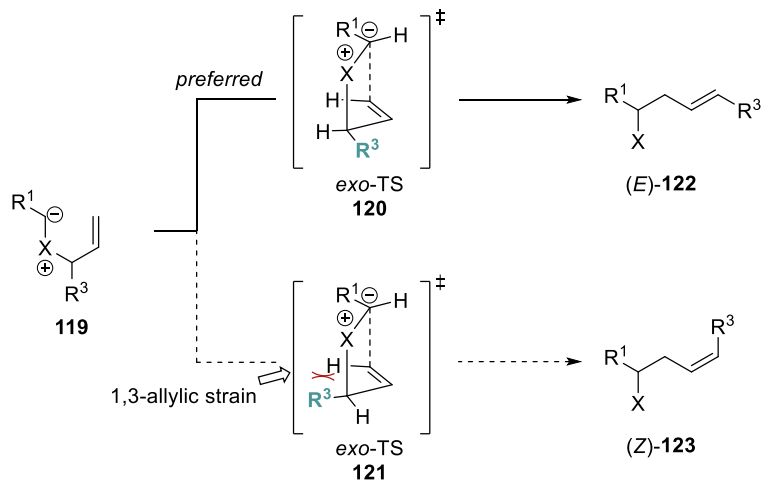
The observed diastereoselectivity of a given [2,3]-sigmatropic rearrangement is dependent on the relative energies of the respective *endo* and *exo* transition states as demonstrated by Houk and Marshall for the [2,3]-Wittig rearrangement.⁸³ An *exo* transition state is often more favourable as the steric repulsion between R^1 and the substituents on the 'apex' is reduced in this conformation. As shown in Scheme 27, opposite diastereomers of the product are accessible when starting with either (*E*)- or (*Z*)-alkene, as the double bond geometry determines the orientation of R^2 . Proceeding through an *exo*-TS will lead to *anti*-product **114** when starting from an (*E*)-alkene **111**, whereas starting from a (*Z*)-alkene **116** will give the corresponding *syn*-product **115**. Hence, [2,3]-sigmatropic rearrangements are often stereospecific with regard to the relative product configuration and allow for control of the desired diastereoselectivity by selecting the double bond geometry in the starting material.



Scheme 27 Diastereoselectivity determining transition states in [2,3]-sigmatropic rearrangements.

Control of the absolute stereochemistry is in many cases more difficult and less well understood than the relative configuration. Many synthetic methods rely either on chirality transfer from existing stereogenic centres in the starting molecule or the use of stoichiometric reagents such as chiral auxiliaries or ligands. Current examples for these methods will be presented in section 2.2.3.2.

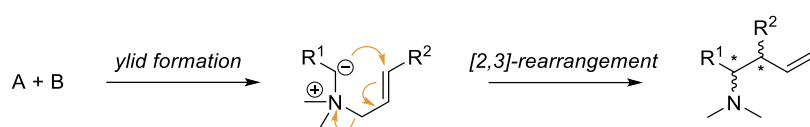
Consideration of the geometry of the newly formed π -bond becomes important if the onium ylid bears a substituent R^3 at the allylic position next to X (Scheme 28). In these cases, the newly formed double bond can have either (*E*)- or (*Z*)-geometry. Assuming that an *exo*-transition state is again more favourable, the transition states **120** and **121** have to be considered. As 1,3-allylic strain is minimized in TS **120**, it is energetically more favourable and results in the formation of the corresponding (*E*)-alkene **122**. However, depending on the configuration of the starting material, the reaction might have to proceed via TS **121**, which would result in the corresponding (*Z*)-alkene **123**.



Scheme 28 Factors controlling the geometry of the new π -bond.

2.2.3 [2,3]-Sigmatropic rearrangement of ammonium ylids

The [2,3]-sigmatropic rearrangement of ammonium ylids offers great synthetic utility as an efficient and potentially stereoselective route to α -functionalised amino acid derivatives, which are widely used as chiral catalysts or building blocks in peptide chemistry and total synthesis.⁸⁴ For widespread application, control over the stereochemical outcome of the rearrangement is critical. In addition, the accessibility of the starting ammonium ylid is equally important but has proven non-trivial in the past. Hence, ylid formation and subsequent [2,3]-rearrangement form the overall process depicted in Scheme 29, leading from simple starting materials to chiral molecules with high molecular complexity.



Scheme 29 General reaction sequence: ammonium ylid formation – [2,3]-rearrangement.

In the following sections, common methods for the preparation of the intermediate ammonium ylid and strategies for efficient stereocontrol in the following rearrangement step will be presented.

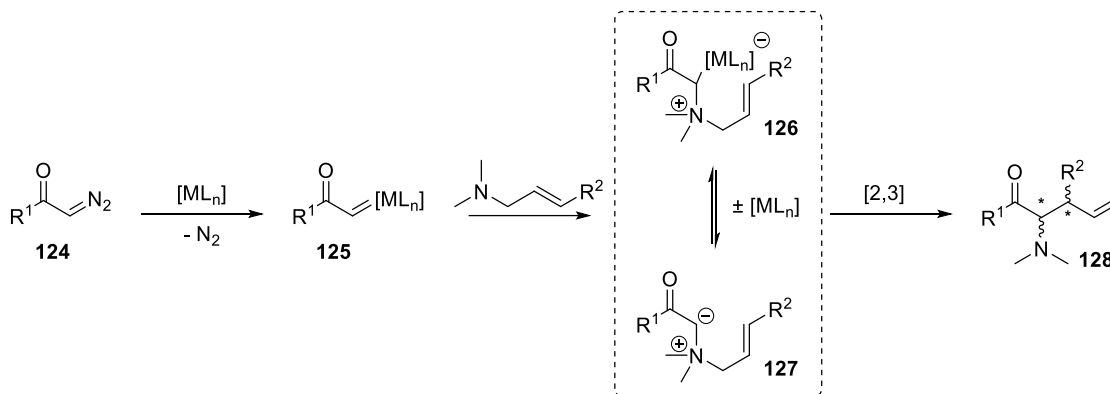
2.2.3.1 Preparation of ammonium ylids

Ammonium ylids can be prepared from a number of different precursors. However, only the two most common methods will be discussed here: (i) preparation from diazo compounds in the presence of a metal catalyst and (ii) deprotonation of allylic ammonium salts.

(i) Preparation from diazo compounds

The use of diazo compounds as allylic ammonium ylid precursors has been extensively studied.⁸⁵ In the presence of a suitable metal catalyst (usually based on rhodium or copper) the corresponding diazo compound **124** can react with the metal centre to form a metal carbenoid **125** with loss of nitrogen (Scheme 30). This species is now highly reactive towards nucleophilic attack by a suitable tertiary allylic amine. Subsequent formation of the ammonium ylid **127** regenerates the metal complex, rendering this approach catalytic. Although this method has been widely used, it is partially hampered by the challenging synthesis of diazo compounds and their relative instability. Moreover, the generation of

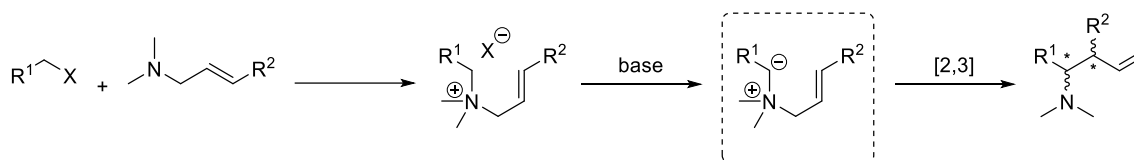
ammonium ylids usually requires elevated temperatures, which can have a detrimental effect on the stereoselectivity of the subsequent rearrangement.⁸⁶



Scheme 30 Ammonium ylid formation from diazo compounds.

(ii) Deprotonation of Ammonium Salts

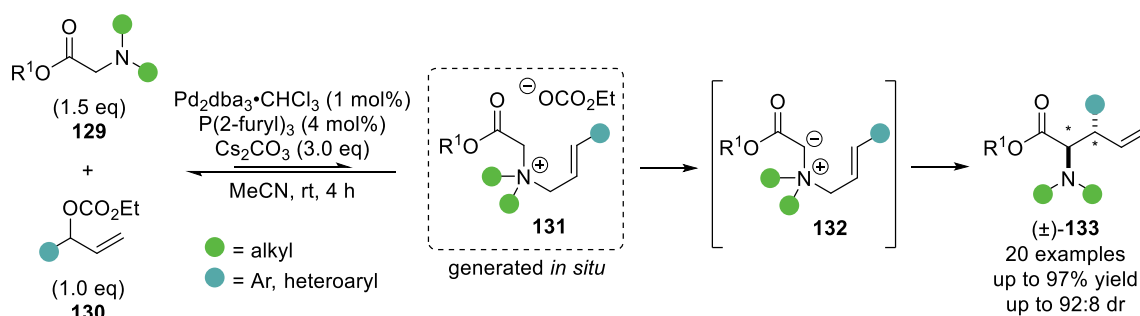
A popular method for the generation of ammonium ylids is via the deprotonation of the corresponding ammonium salt (Scheme 31). Quaternary ammonium salts can be easily prepared by alkylation of a tertiary amine with an alkyl halide. Depending on the nature of the ammonium salt, different bases can be used for deprotonation next to the positively charged nitrogen.⁸⁶ Hydroxides or alkoxides are a common choice for the formation of stabilised ylids (e.g. bearing a carbonyl substituent (R^1)), whereas stronger bases such as metal amides or alkyl lithium bases are needed for the deprotonation of simple alkyl salts.



Scheme 31 Ammonium ylid formation via deprotonation of ammonium salts.

Although this method is popular for the generation of allylic ammonium ylids, it has some drawbacks associated with it. First, the isolation of the intermediate ammonium salt is often challenging, limiting the scope of this methodology. To circumvent this problem, methodologies allowing its *in situ* generation are highly desirable. Moreover, under the basic reaction conditions of the rearrangement, dealkylation of the ammonium salt can also occur as the tertiary amine is a good leaving group which can be displaced in an S_N2 reaction. By generating the ammonium salt *in situ*, only small amounts of it would be present as subsequent [2,3]-rearrangement could continuously take place, lowering the chance of dealkylation.

In 2011, Tambar and co-workers reported the use of a palladium catalysed allylic substitution reaction to generate quaternary ammonium salts *in situ* from the intermolecular reaction of α -amino esters and allylic carbonates (Scheme 32).⁸⁷ In their methodology, amino ester **129** and allylic carbonate **130** form the desired ammonium salt **131** employing $\text{Pd}_2(\text{dba})_3 \cdot \text{CHCl}_3$, $\text{P}(2\text{-furyl})_3$ and Cs_2CO_3 in acetonitrile. Subsequent deprotonation of the intermediate salt to form ylid **132** followed by [2,3]-sigmatropic rearrangement furnished α -alkylated amino esters **133** in excellent yield and *anti*-diastereoselectivity. This methodology is tolerant of a variety of substituents. Branched as well as linear carbonates featuring aromatic substituents with electron-withdrawing and -donating groups as well as heterocycles could be employed. Different tertiary amines could also be applied, including cyclohexyl and dimethyl amino esters and a variety of aliphatic and aromatic ester groups (R^1). The observed diastereoselectivity was attributed to the [2,3]-rearrangement proceeding via an *exo* transition state, leading to the observed racemic *anti*-product **133**. However, it was difficult to gain mechanistic insight as the authors could not observe the intermediate ammonium salt. This was attributed to two factors: firstly, a high rate of deprotonation of the ammonium salt to form ylid **132** and subsequent rearrangement leading to only transient existence of the ammonium salt. Secondly, it was proposed that the formation of ammonium salt **131** via palladium catalysis is reversible, with the equilibrium disfavoring salt formation. This could be demonstrated in crossover experiments and might account for the absence of tertiary amines as nucleophiles in catalytic allylic substitutions.^{46,88}

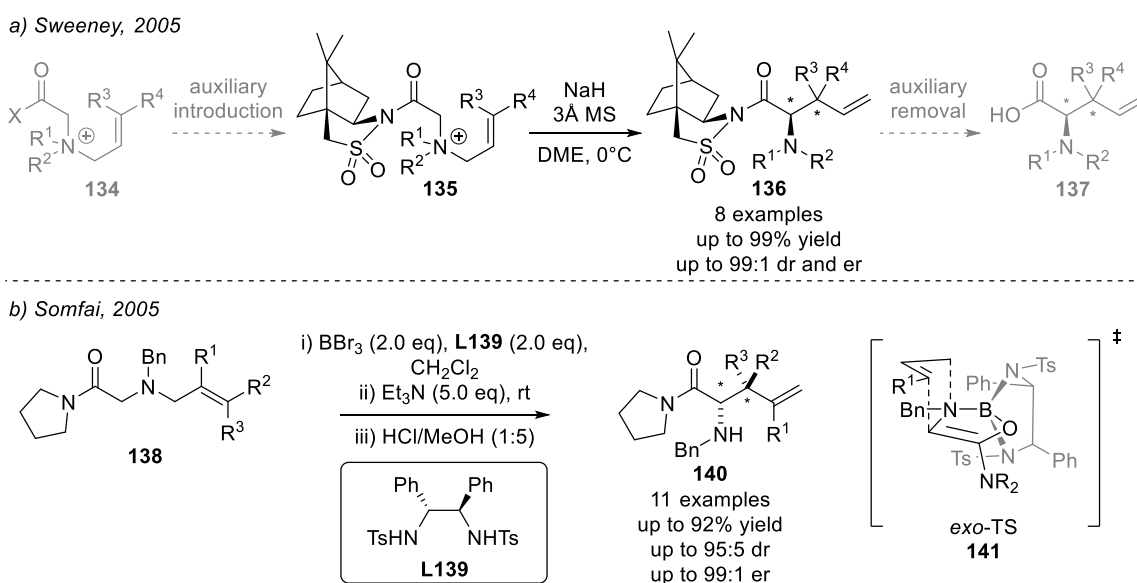


Scheme 32 Pd-catalysed *in situ* formation of ammonium salts followed by base-promoted [2,3]-rearrangement.

2.2.3.2 Stereocontrol in [2,3]-rearrangements of ammonium ylids

Whilst diastereoselective [2,3]-rearrangements of ammonium ylids are well represented in the literature,⁸⁵ enantioselective variants are less common. Asymmetric [2,3]-rearrangements usually rely on the use of stoichiometric amounts of chiral auxiliaries or chiral ligands. In 2005, Sweeney and co-workers reported the [2,3]-rearrangement of acyclic, allylic ammonium ylids with high stereocontrol employing Oppolzer's camphorsultam auxiliary (Scheme 33a).⁸⁹ In this methodology, the preformed *N',N',N'*-allyldimethyl glycinoyl (1*S*,2*R*)-sultam **135** underwent diastereoselective [2,3]-rearrangement in the presence of base giving excellent yields and diastereoselectivity. By choosing the opposite enantiomer of the auxiliary, both enantiomers of the product were accessible. Although this method demonstrates the feasibility of stereoselective [2,3]-rearrangements, it produces stoichiometric waste and two additional steps for introducing and removing the auxiliary are necessary.

Also in 2005, Somfai and co-workers demonstrated the use of superstoichiometric amounts of a chiral Lewis acid to promote the enantioselective [2,3]-rearrangement of allylic ammonium ylids (Scheme 33b).⁹⁰ In their methodology, the chiral Lewis acid is generated *in situ* from BBr₃ and sulphonamide **L139**, which can react with the substrate to give the corresponding oxazaborolidine (see *exo*-TS **141**). In the presence of base, the ammonium ylid is generated and undergoes [2,3]-sigmatropic rearrangement to give product **140** in good yields and with good diastereo- and enantioselectivity.

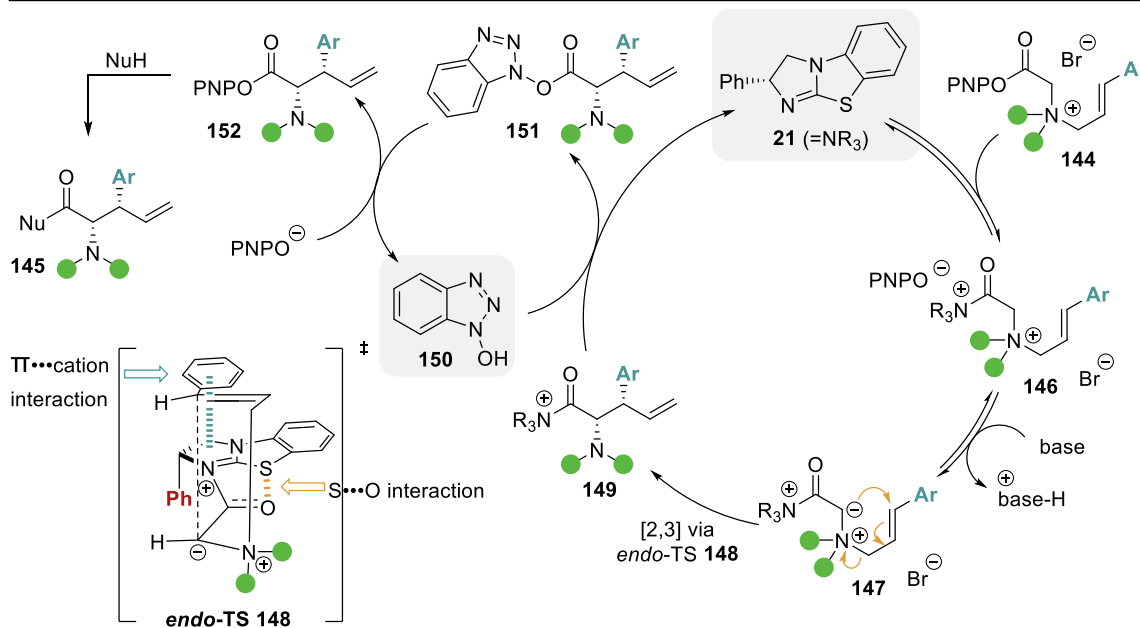
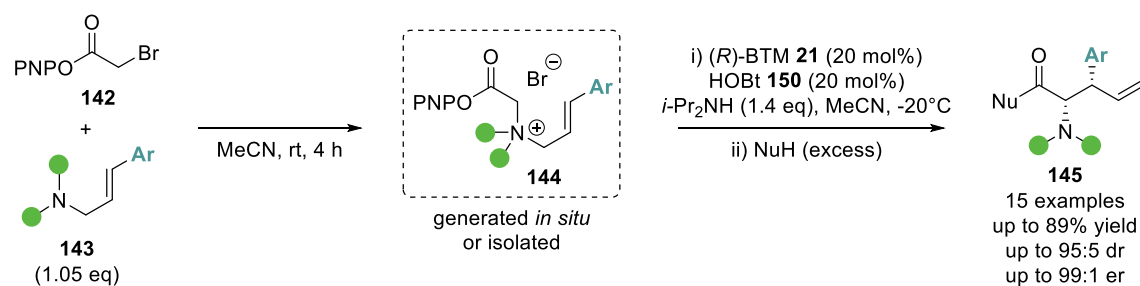


Scheme 33 Enantioselective [2,3]-rearrangement of ammonium ylids.

These approaches demonstrate that excellent stereoinduction in [2,3]-sigmatropic rearrangements is possible. However, they rely on (super)stoichiometric amounts of chiral reagents, making catalytic variants highly desirable. Whilst catalytic methodologies have been employed for the generation of the intermediate ammonium salt, they are extremely rare in enantioselective [2,3]-rearrangements. To date only one approach of a catalytic enantioselective [2,3]-sigmatropic rearrangement of allylic ammonium ylids has been reported by Smith and co-workers (Scheme 34),⁹¹ with an extension to propargylic ammonium ylids described by Song and co-workers.⁹² Starting from *p*-nitrophenyl (PNP) bromoacetate **142** and an allylic amine **143**, the intermediate ammonium salt **144** was either isolated or formed *in situ*, before reacting with (*R*)-BTM **21** and *i*-Pr₂NH as base to promote the formation of ammonium ylid **147** and subsequent [2,3]-rearrangement. Use of HOBt **150** and addition of an external nucleophile (Nu) gave *syn*- α -amino acid derivatives **145** in good yield with excellent diastereo- and enantioselectivity. A range of aromatic substituents (Ar) were tolerated, bearing electron-donating and -withdrawing groups as well as cyclic and acyclic substituents on the amine functionality. Variation of the external nucleophile allowed access to different amino acid derivatives, including alcohols, amides or unactivated esters. The proposed catalytic cycle starts with acylation of the isothiourea catalyst **21** by ammonium salt **144**. Subsequent deprotonation with base leads to the formation of ammonium ylid **147**, which rearranges via *endo*-TS **148** to yield **149**. Final catalyst turnover is facilitated by the co-catalyst HOBt **150**, which itself is regenerated by previously displaced *p*-nitrophenoxide. Upon completion of the catalysis, an external nucleophile was added to generate amino acid derivatives **145**. The methodology relies on the use of activated amino esters for two reasons: firstly, *p*-nitrophenoxide is an excellent nucleofuge that can be easily displaced by the Lewis basic catalyst, and secondly, it is nucleophilic enough to displace the co-catalyst HOBt at a later stage in the catalytic cycle in a so called “rebound” fashion, which enables the regeneration of the catalyst. To rationalise the observed stereoselectivity and gain a deeper understanding of the reaction mechanism, a mechanistic and computational study was subsequently published by Smith and co-workers.⁹³ This work confirms the proposed mechanism depicted in Scheme 34 and suggests that the [2,3]-sigmatropic rearrangement is the rate- and product determining step. In addition, transition state **148** was identified as the stereodetermining step, displaying the following key interactions:

i) A stabilising 1,5-S...O interaction between the S atom of the catalyst and the carbonyl O of the substrate, resulting from a π to σ^*_{C-S} delocalisation. This rigidification of the transition state in combination with the facial selectivity imparted by the phenyl directing group of the catalyst gives a rationale for the high enantioselectivity observed.

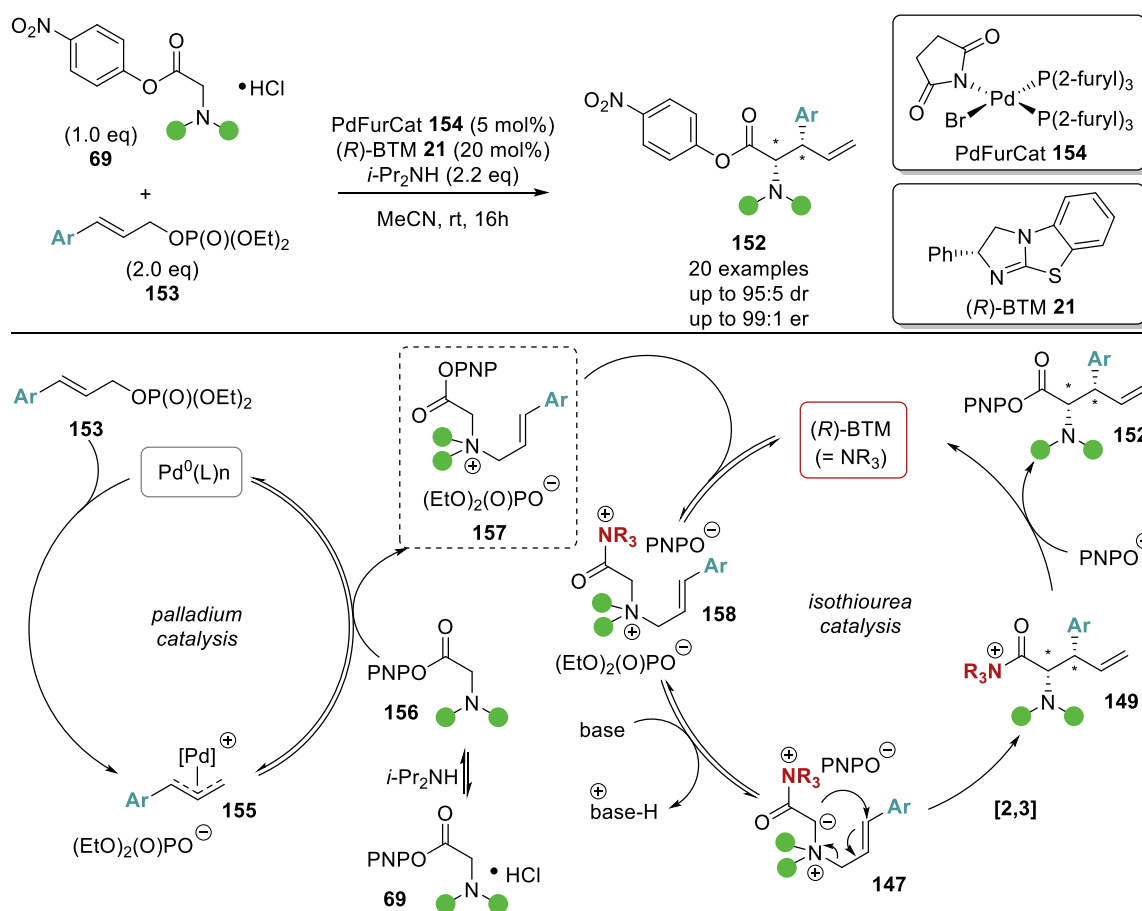
ii) The preference for the formation of *syn* product via *endo*-TS **148** compared to the observed *anti* selectivity in Tambar's report (see 2.2.3.1(ii)) can be explained by a favourable π -cation interaction between the positively charged catalyst and the aromatic substituent (Ar) of the substrate.



Scheme 34 Organocatalysed enantioselective [2,3]-rearrangement of ammonium ylids.

2.3 Concept and Aims

Following on from this work, Smith and co-workers described the successful combination of Tambar's allylation strategy with isothiurea controlled [2,3]-rearrangement, resulting in a dual palladium and isothiurea relay catalysis to obtain chiral α -amino acid derivatives.⁶⁵ Their methodology relied on a sequential transformation of the initial substrates via an *in situ* generated ammonium salt to give the desired product (Scheme 35). In the first catalytic cycle, the active palladium catalyst, generated *in situ* from the precatalyst PdFurCat **154**, facilitates the intermolecular allylic substitution of allylic phosphate **153** with the tertiary amine functionality of free base **156**. The resulting ammonium salt **157** can acylate the chiral isothiurea catalyst **21** to form activated acyl ammonium **158**. Subsequent formation of ammonium ylid **147** in the presence of base enables [2,3]-rearrangement. In this step, two new stereogenic centres are formed which are controlled by the chiral isothiurea catalyst. Subsequent displacement of the catalyst by the aryloxide (PNPO⁻) regenerates the catalyst and releases the final product **152**, which could be obtained in good yields and excellent diastereo- and enantioselectivity.



Scheme 35 Relay palladium and isothiurea catalysis.

Although this methodology demonstrated great improvements to the previously reported isothiourea catalysed [2,3]-rearrangement of isolated ammonium salts (see section 2.2.3.2), some limitations still remain. Most notably, the requirement of having an aromatic substituent within the allylic phosphate, as this seems crucial for obtaining good stereoselectivity.

The current work investigates the potential for expanding the scope beyond cinnamyl derived allylic phosphates to accommodate more diverse substituents in this dual palladium and isothiourea catalysis. Considering the current mechanistic understanding for this process, the following questions arise: (i) what effects on reactivity will be observed by having functional groups other than aryl within the allylic phosphate? (ii) will it still be possible to obtain high levels of stereocontrol without the stabilising effect of a π -cation interaction?

2.4 Results and Discussion

2.4.1 Initial functional group assessment

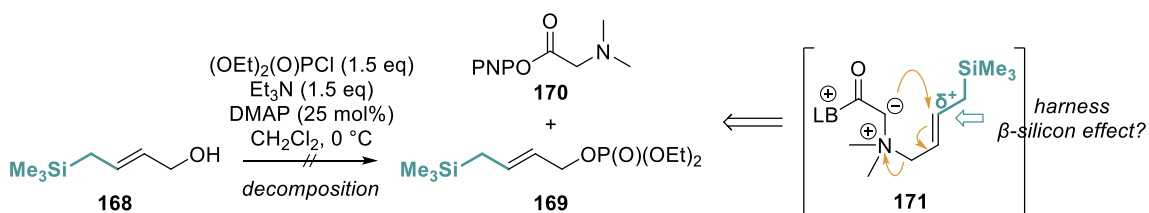
Initial investigations aimed to identify functional groups other than aryl substituents that could be tolerated in the dual *N*-allylation/[2,3]-rearrangement protocol. Readily accessible allylic alcohols containing an electron-withdrawing C(3)-ester substituent, an electron-donating C(3)-silyl substituent, a silyl protected homoallylic alcohol and a C(2)-phenyl branched allylic substrate were chosen to probe the electronic and steric limitations within the allylic fragment. Their feasibility was tested under the previously established relay catalysis conditions, subjecting the corresponding allylic phosphates **160-163** and *N,N*-dimethyl 4-nitrophenyl ester hydrochloride salt **159** to PdFurCat **154** (5 mol%) as stable palladium catalyst precursor, (\pm)-BTM **21** as Lewis base catalyst and *i*-Pr₂NH as external base in MeCN at room temperature (Table 1). Pleasingly, ester containing phosphate **160** gave the desired product in promising 70% yield as determined by ¹H NMR analysis of the crude reaction mixture. Trimethylsilyl (Me₃Si) containing phosphate **161**, on the other hand, showed no reactivity, with only starting materials returned. This observation is in agreement with the expected electronic requirements in the [2,3]-rearrangement step, where an electron-withdrawing group would enhance the electrophilicity at C(3) and hence facilitate the rearrangement, whereas an electron-donating group would have the opposite effect. It was speculated that having a silyl substituent in the β -position rather than the α -position would suit the electronic requirements, potentially harnessing the β -silicon effect to stabilise the transition state (Scheme 36). Unfortunately, attempts to synthesise the desired β -silyl allylic phosphate **169** failed, resulting in decomposition upon phosphorylation of the corresponding allylic alcohol (**168**). Gratifyingly, phosphate **162** bearing a silyl protected alcohol and sterically demanding C(2)-phenyl mesylate **163** also furnished the desired products, albeit in lower yields as determined by ¹H NMR analysis (33% and 32%, respectively). Notably, the use of mesylate as leaving group rather than phosphate was crucial for the formation of rearranged product **167**, as the latter showed no reactivity. This result is consistent with observations by Snaddon and co-workers, who demonstrated the requirement for reactive mesylate substrates in a related dual catalytic process.⁶⁰ Unfortunately, PNP ester **167** could not be isolated as it proved unstable to column chromatography. Products

containing an ethyl ester substituent (**164**) and a silyl protected alcohol (**166**) could be isolated in 61% and 30% yield with modest diastereoselectivities of 60:40 dr and 55:45 dr, respectively. As ethyl ester **160** gave better results in this initial assessment, it was taken for further optimisation.

Table 1 Initial functional group assessment in relay palladium/isothiourea catalysis.

entry ^a	allyl precursor	product	yield [%] ^b	dr ^c
1			70 (61)	60:40
2			-	-
3			33 (30)	55:45
4			32 (-)	-

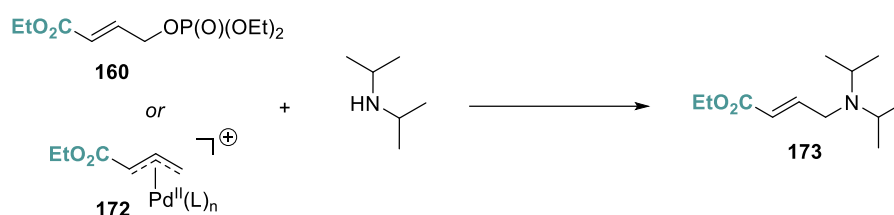
^a Reactions performed on a 0.25 mmol scale. ^b Combined NMR yield of diastereoisomers determined by ¹H NMR analysis using 1,4-dinitrobenzene as internal standard. Values in parenthesis are isolated yields. ^c Determined by ¹H NMR analysis of the crude material.



Scheme 36 Attempted synthesis and proposed application of β -silyl containing allylic phosphate.

2.4.2 Reaction optimisation for ethyl ester containing allylic phosphate

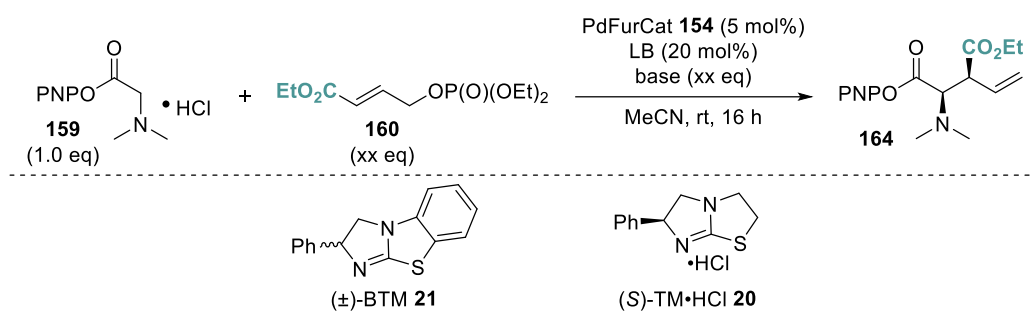
During the isolation of PNP ester product **164**, several issues were encountered. The desired product contained varying amounts of unreacted phosphate **160**, isothioureia catalyst (\pm)-BTM **21** and an unknown side-product, which proved difficult to remove via column chromatography. The side product was identified as amine **173**, presumably resulting from a competing allylic substitution with the amine base *i*-Pr₂NH acting as the nucleophile (Scheme 37).



Scheme 37 Side-product formation observed in unoptimized relay catalysis.

To mitigate these problems and increase the isolated yield of PNP ester **164**, the adjustments outlined in Table 2 were made. The formation of side product **173** was completely suppressed by changing to the tertiary amine base *i*-Pr₂NEt without effecting the catalytic transformation (Table 2, entry 2). In addition, changing the catalyst from (\pm)-BTM **21** to (\pm)-TM·HCl **20** further simplified the purification, allowing the desired product to be isolated in 56% yield without altering the observed reactivity or stereoselectivity (entry 3). Finally, the amount of phosphate **160** could be reduced to 1.25 eq without any effects on the reaction outcome (entry 4). With these optimised conditions in hand, PNP ester **164** could be isolated in 70% yield as an inseparable mixture of diastereoisomers in 60:40 dr with good enantioselectivity using (*S*)-TM·HCl (90:10 *er*_{maj}, 70:30 *er*_{min}) (entry 5). The relative and absolute configuration within the major diastereoisomer were assigned by analogy to related isothioureia catalysed [2,3]-rearrangement reactions and further confirmed by single crystal X-ray diffraction analysis of a related derivative (**186**_{maj}, see 2.4.3.1, Figure 10).

Table 2 Optimisation of relay catalysis for ethyl ester containing allylic phosphate.



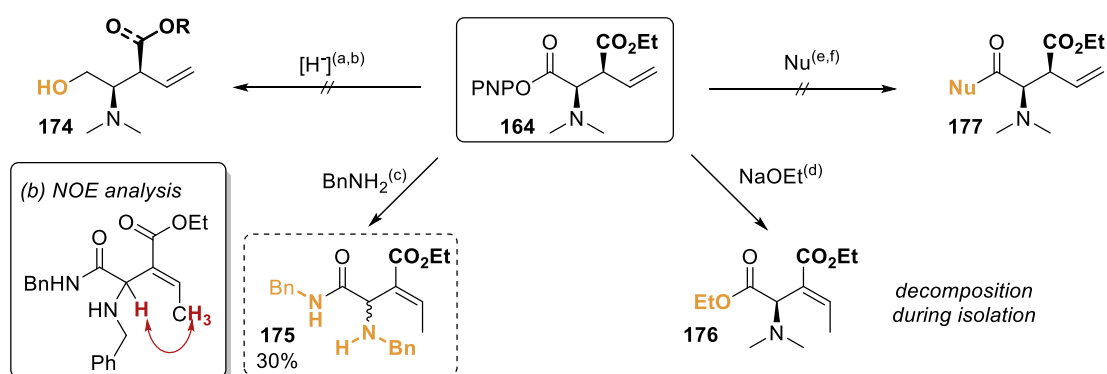
entry ^a	LB catalyst	base	phosphate	yield [%] ^b	dr ^c
1	(±)-BTM	<i>i</i> -Pr ₂ NH (2.2 eq)	2.0 eq	70	60:40
2	(±)-BTM	<i>i</i> -Pr ₂ NEt (2.2 eq)	2.0 eq	65 (17)	56:44
3	(±)-TM·HCl	<i>i</i> -Pr ₂ NEt (2.4 eq)	2.0 eq	87 (56)	67:33
4	(±)-TM·HCl	<i>i</i> -Pr ₂ NEt (2.4 eq)	1.25 eq	(62)	55:45
5	(S)-TM·HCl	<i>i</i> -Pr ₂ NEt (2.4 eq)	1.25 eq	(70)	60:40 ^d

^a Reactions performed on a 0.25 mmol scale. ^b Combined NMR yield of diastereoisomers determined by ¹H NMR analysis using 1,4-dinitrobenzene as internal standard. Values in parentheses are isolated yields.

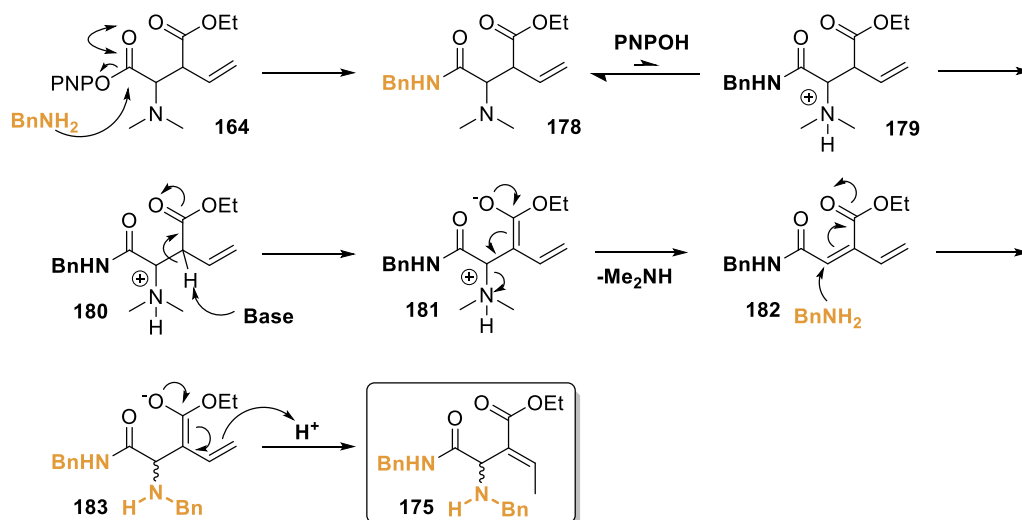
^c Determined by ¹H NMR analysis of the crude material. ^d 90:10 *er*_{major}, 70:30 *er*_{minor}; enantiomeric ratios determined by chiral stationary phase HPLC analysis.

With a simplified protocol in place, a closer look was taken at the variation in isolated yield compared with the yield expected based on ¹H NMR analysis of the crude reaction mixture (Table 2). This discrepancy is indicative of the PNP ester product being unstable to purification by column chromatography, which is a recognised problem in the literature, often circumvented by converting the initial PNP ester product into more stable derivatives *in situ*.^{65,91} Based on established methods within the group, a range of nucleophiles was explored to achieve the desired derivatisations (Scheme 38a). Unfortunately, none of the reductive or nucleophilic reagents led to the desired derivatised product, but resulted in decomposition instead, with no material isolated in most cases. For the derivatisation with benzylamine (BnNH₂), compound **175** was the only product isolated, and its identity was confirmed by ¹H NMR, ¹³C NMR and mass spectrometry analysis. The alkene configuration was assigned through NOE experiments, with reciprocal NOE enhancement observed for the protons highlighted in Scheme 38b. A plausible mechanism for the formation of side-product **175** is proposed in Scheme 38c, starting with the intended amide formation to give derivative **178** and free phenol PNPOH. The released phenol can act as Brønsted acid, protonating the NMe₂ group,

transforming it into a good leaving group (**179**). Proton abstraction, either by phenoxide or BnNH_2 , leads to the elimination of dimethylamine (Me_2NH) and the formation of diene **182**. As BnNH_2 is present in excess, another molecule can add via Michael addition to give **183**, which, after protonation of the dienolate, yields side-product **175** with the double bond having migrated into conjugation. A similar migration of the double bond has also been observed by ^1H NMR analysis of the crude material upon derivatisation with NaOEt (**176**, Scheme 38a). However, as no material could be isolated after column chromatography, the identity of product **176** could not be confirmed.

(a) Attempted derivatisation of PNP ester **164**

Reaction Conditions: a) DIBAL (4.0 eq), CH_2Cl_2 , -78°C to rt, 2 h; b) LiBH_4 (1.2 eq), THF, rt, 1 h; c) BnNH_2 (5.0 eq), CH_2Cl_2 , rt, 16 h; d) NaOEt (1.5 eq), EtOH, 0°C to rt, 2 h; e) pyrrolidine (1.5 eq), CH_2Cl_2 , rt, 16 h; f) EtOH, DMAP (0.25 eq), rt, 16 h.

(c) Proposed mechanism for the formation of side product **175**

Scheme 38 Derivatisation of PNP ester **164** (a) with different reagents; (b) assignment of alkene geometry via ^1H NOE correlations; (c) proposed mechanism for side-product formation.

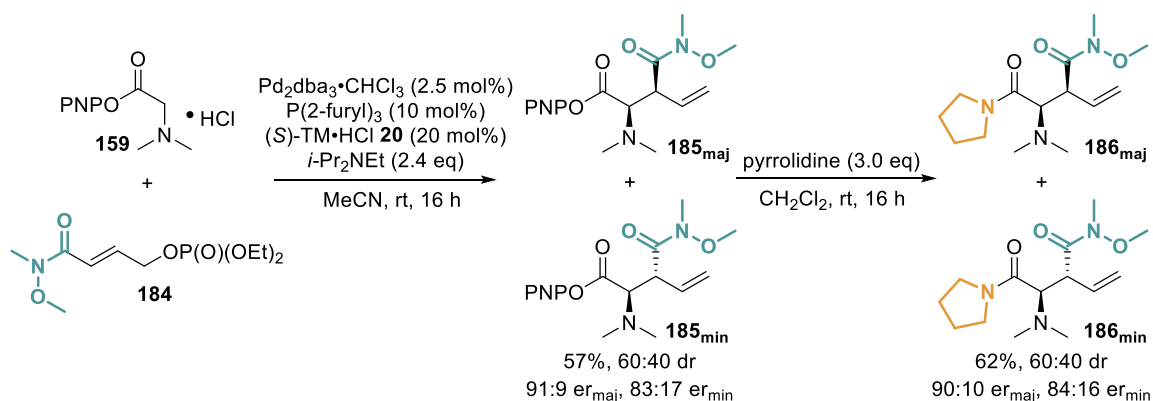
The observed difficulties in the derivatisation of PNP ester **164** can likely be attributed to the acidity of the C(3)-H, which seems to be readily deprotonated under the investigated reaction conditions, enabling unwanted side reactions. It was hypothesised that a less

electron-withdrawing amide substituent could minimize these undesired reaction pathways as the corresponding C(3)-H should be less acidic. Hence, amide-containing allylic phosphates were next investigated.

2.4.3 Amide containing allylic phosphates

2.4.3.1 Initial assessment

First, the validity of our hypothesis was tested by subjecting Weinreb amide containing allylic phosphate **184** to the above optimised catalysis conditions. (The development of a synthetic strategy to access these substrates will be discussed in 2.4.3.3.) Gratifyingly, good reactivity could be observed, furnishing the desired PNP ester **185** as separable diastereoisomers in 57% combined, isolated yield in 60:40 dr and promising enantioselectivity (91:9 $e_{r_{maj}}$, 83:17 $e_{r_{min}}$) (Scheme 39). Importantly, subsequent derivatisation of the separate diastereoisomers with pyrrolidine gave the corresponding amide products **186_{maj}** and **186_{min}** without loss of enantiointegrity or the formation of side products. This result served as proof of concept that by reducing the acidity of the C(3)-H, derivatisation and isolation of the allylation/[2,3]-rearrangement product is feasible. In addition, single crystal X-ray diffraction analysis allowed the unambiguous assignment of the relative *syn*-configuration of the major diastereoisomer **186_{maj}** (Figure 10).



Scheme 39 Initial assessment of amide containing allylic phosphate

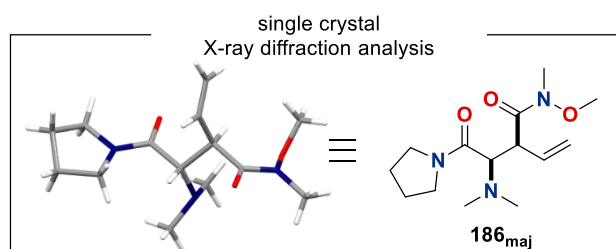
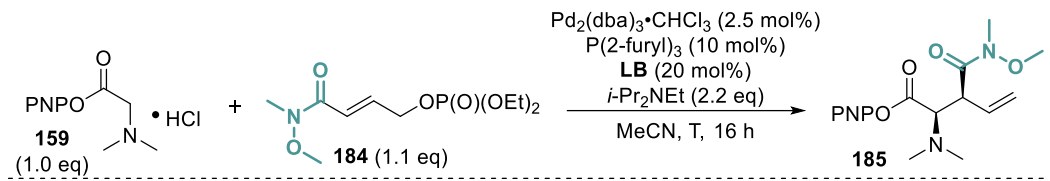


Figure 10 Determination of relative configuration for **186_{maj}**.

2.4.3.2 Optimisation of catalysis conditions, product isolation and derivatisation

To further improve the observed stereoselectivity, a selection of Lewis base catalysts as well as variation of the reaction temperature were investigated (Table 3). Interestingly, all catalysts tested gave the product in a similar ^1H NMR yield (60-68%) and even a slight improvement in diastereoselectivity (up to 68:32 dr) compared with (*S*)-TM·HCl (Table 3, entries 2-4). Unfortunately, no improvement in enantioselectivity was observed, with Tetramisole still performing best. Lowering the reaction temperature to 0 °C resulted in a slightly improved diastereoselectivity with no change in enantioselectivity, but led to a dramatic drop in reactivity, giving only 10% ^1H NMR yield after 24 h (Table 3, entry 5). Hence, the already established conditions using (*S*)-TM·HCl **20** as Lewis base catalyst at room temperature were kept as optimal.

Table 3 Catalysis optimisation for amide containing phosphate.



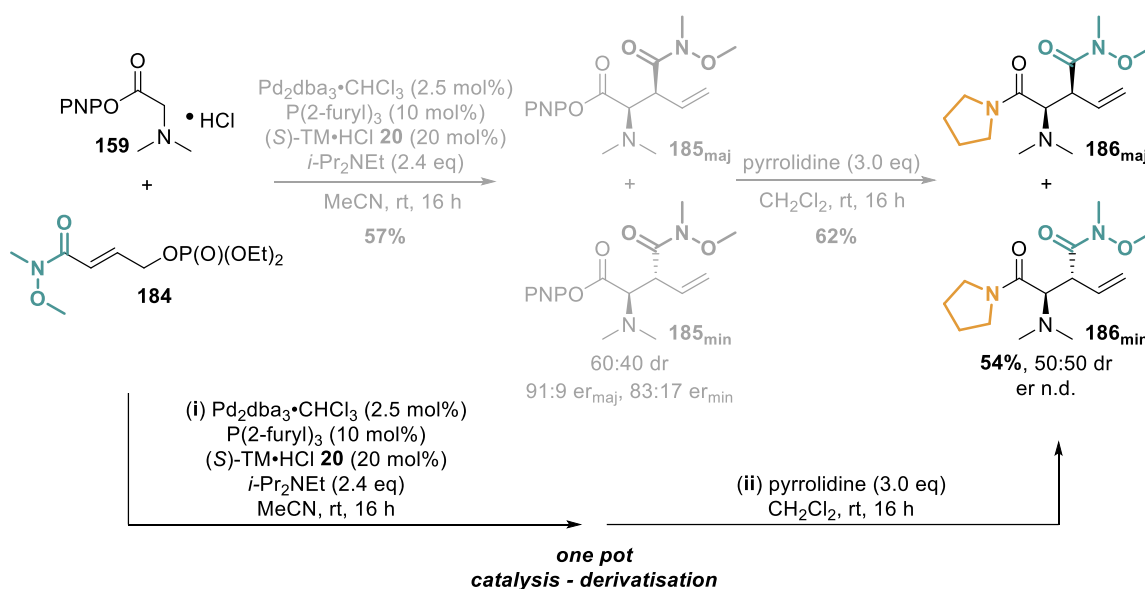
Chemical structures of Lewis base catalysts are shown below the reaction scheme:

- (*S*)-TM·HCl **20**
- (*R*)-BTM **21**
- (2*S*,3*R*)-HyperBTM **30**
- Quinidine **187**

entry ^a	LB catalyst	T [°C]	^1H NMR yield [%] ^b	dr ^c	er ^d
1	(<i>S</i>)-TM·HCl ^f	rt	62	54:46	91:9 (maj) 83:17 (min)
2	(<i>R</i>)-BTM	rt	61	68:32	13:87 (maj) 28:72 (min)
3	(2 <i>S</i> ,3 <i>R</i>)-HyperBTM	rt	68	63:37	40:60 (maj) 46:54 (min)
4	Quinidine	rt	60	60:40	50:50 (maj) 50:50 (min)
5 ^e	(<i>S</i>)-TM·HCl ^f	0	10	68:32	91:9 (maj) 83:17 (min)

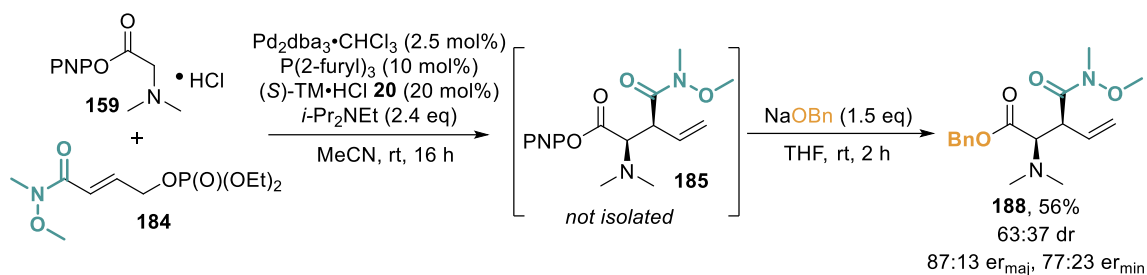
^a Reactions performed on a 0.25 mmol scale. ^b Combined NMR yield of diastereoisomers determined by ^1H NMR analysis using 1,4-dinitrobenzene as internal standard. ^c Determined by ^1H NMR analysis of the crude material. ^d Determined by chiral stationary phase HPLC analysis. ^e Reaction run for 24 h. ^f 2.4 eq *i*-Pr₂NEt used.

Next, attention was shifted towards optimising the isolation and derivatisation protocol. Although PNP ester **185** could be isolated in good yield, variation in the diastereomeric ratio compared to the crude mixture was observed (50:50 dr_{cr} vs 60:40 $dr_{isolated}$). In addition, the two-step isolation-derivatisation protocol resulted in a low overall yield of only 35% for the combined diastereoisomers of the final amide product **186**. To avoid these issues, an alternative one-pot catalysis-derivatisation procedure was investigated. Direct addition of the pyrrolidine nucleophile to the catalysis reaction mixture after 16 h resulted in an improved 54% isolated yield of the amide product, without altering the diastereomeric ratio (Scheme 40). Unfortunately, the diastereoisomers of the final amide product were no longer separable, thus the enantiomeric ratio of the product could not be unambiguously determined.



Scheme 40 One pot relay catalysis-derivatisation protocol with a pyrrolidine nucleophile.

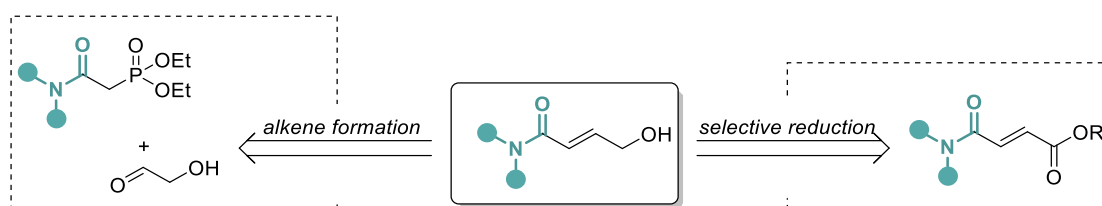
To improve the separation of the derivatised diastereoisomers, an alternative protocol using benzyl alcohol (BnOH) as the nucleophile was investigated. Importantly, this strategy required use of activated sodium benzyolate (NaOBn) and the removal of the palladium catalyst from the crude reaction mixture prior to addition of the nucleophile, as no reaction was observed with BnOH in the presence of catalytic DMAP or residual palladium catalyst. Therefore, the crude reaction mixture was filtered through silica before addition of NaOBn in THF, generating the desired benzyl ester **188** in 56% isolated yield with 63:37 dr and without loss of enantiopurity (87:13 er_{maj} , 77:23 er_{min}) (Scheme 41). Notably, each diastereoisomer could be isolated in >95:5 dr after purification.



Scheme 41 Optimised one-pot derivatisation protocol using sodium benzylate.

2.4.3.3 Synthesis of amide containing allylic phosphates

At the onset of synthesising amide containing allylic alcohols as effective precursors for the desired allylic phosphates, no general protocol for their synthesis had been established. Therefore, two conceptually different strategies were considered to access the desired allylic alcohol (Scheme 42): (i) installation of the alkene, for example in a Horner-Wadsworth-Emmons (HWE) reaction, or (ii) selective reduction of the corresponding 1,4-dicarbonyl compound.



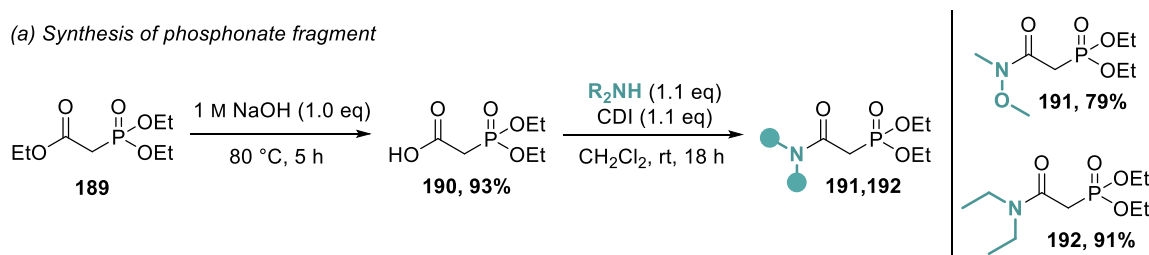
Scheme 42 Potential synthetic routes for the synthesis of amide containing allylic alcohols.

2.4.3.3.i. Horner-Wadsworth-Emmons strategy

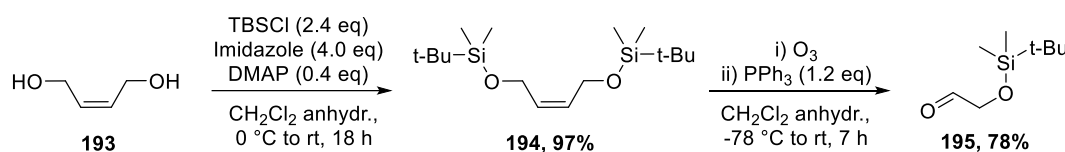
Accessing the desired allylic alcohol via installation of the alkene (Scheme 42, path (a)) is an attractive strategy as it would allow a modular approach towards the desired amide target. The synthesis of the required phosphonate and aldehyde fragments is well precedented and could be achieved in two steps each following literature procedures.^{94,95} Weinreb amide containing phosphonate **184** was synthesised from commercially available ethyl ester **189** via hydrolysis and subsequent amide coupling to yield the desired phosphonate **191** in 73% yield over two steps (Scheme 43a). Importantly, this route tolerated the incorporation of various amines, as the corresponding diethyl amide **192** could also be synthesised in 85% overall yield. The aldehyde fragment was synthesised starting from readily available 1,4-butanediol **193**. Double protection of the alcohol functionality with TBSCl followed by ozonolysis of the alkene under mildly reducing conditions gave the desired aldehyde **195** in 75% overall yield (Scheme 43b). The

key coupling reaction of both fragments furnished the desired α,β -unsaturated amide **196** in good 53% yield with excellent (>95:5) (*E*)-selectivity. Subsequent deprotection followed by phosphorylation of the allylic alcohol allowed a first entry towards the desired amide containing allylic phosphate **184**, albeit in only modest 43% yield. The comparatively low yields of the last two steps might be a result of difficulties during isolation and purification of the intermediate allylic alcohol **197**, with remaining impurities affecting the final phosphorylation step.

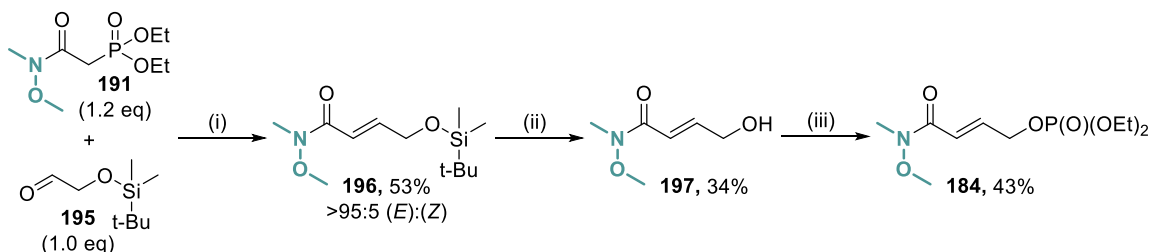
(a) Synthesis of phosphonate fragment



(b) Synthesis of aldehyde fragment



(c) Fragment coupling via HWE reaction

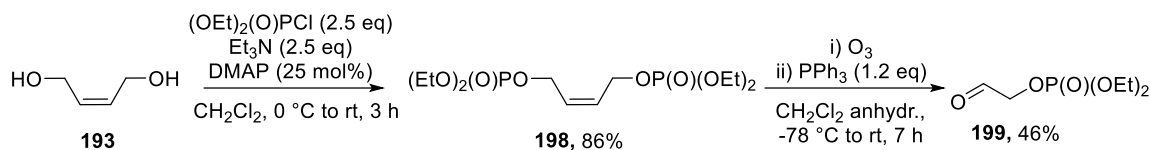


Conditions: i) $i\text{-Pr}_2\text{NEt}$ (1.1 eq), LiCl (6.7 eq), MeCN, rt, 48 h; ii) TBAF (3.0 eq), THF anhydrous, 0 °C to rt, 16 h; iii) $(\text{OEt})_2(\text{O})\text{PCl}$ (2.5 eq), DMAP (25 mol%), Et_3N (2.5 eq), CH_2Cl_2 , 0 °C to rt, 16 h.

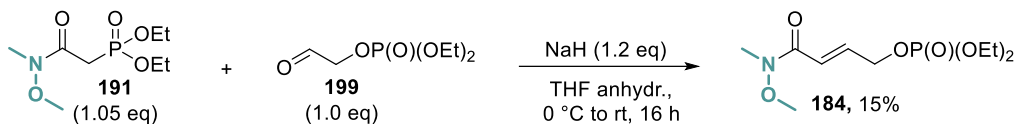
Scheme 43 HWE strategy to synthesise amide containing allylic phosphates.

It was also possible to generate the aldehyde fragment with the phosphate group already in place, albeit in lower HWE yield compared to the silylated diol route (Scheme 44a). However, subjecting the corresponding aldehyde **199** to HWE conditions resulted in a mixture of products, which were difficult to separate, resulting in only 15% isolated yield of the desired allylic phosphate **184**.

(a) Synthesis of phosphate containing aldehyde fragment



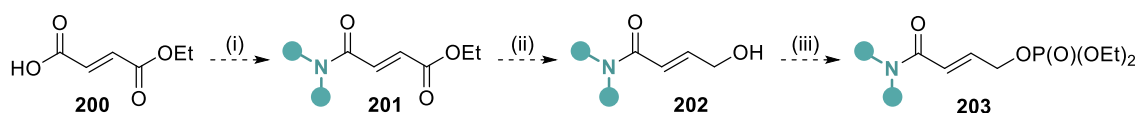
(b) Fragment coupling via HWE reaction



Scheme 44 Preparation of phosphate containing aldehyde fragment and subsequent HWE coupling.

2.4.3.3.ii. Selective reduction strategy

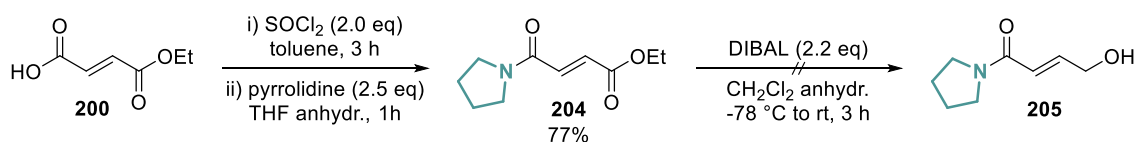
As an alternative route, the synthesis of an amide containing allylic phosphate was designed in analogy to the synthesis of ester containing allylic phosphate **160**, as depicted in Scheme 45. Starting from commercially available monoethyl fumarate **200**, derivatisation of the carboxylic acid into the desired amides furnishes the necessary amide esters **201**. By variation of the amine, amides with varying substituents are readily accessible. Subsequently, a selective reduction of the ester is required to yield the desired allylic alcohol, which, following phosphorylation, would yield the targeted amide containing allylic phosphate **203** in a straight-forward, three step synthesis. The key challenge in this strategy is selectively reducing the ester functionality without reducing the amide or the alkene.



Intended transformations: (i) amide coupling; (ii) selective reduction; (iii) phosphorylation

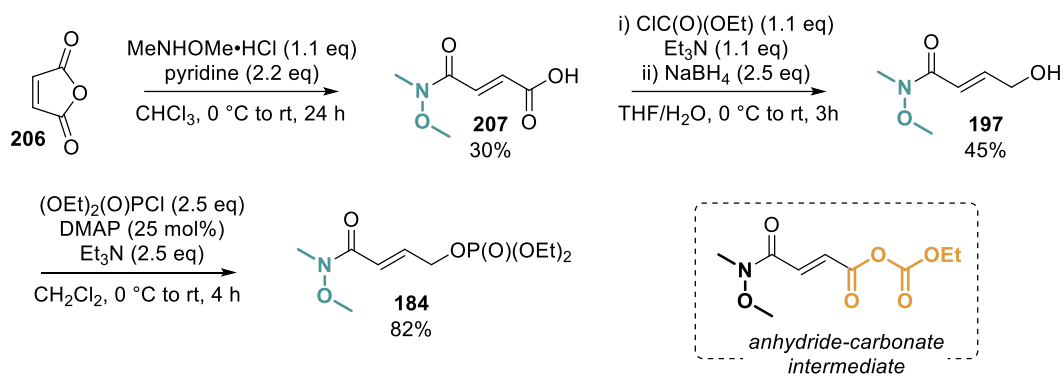
Scheme 45 Proposed synthetic route towards amide containing allylic phosphates via selective reduction.

To test this strategy, pyrrolidine containing amide **204** was selected as model substrate with DIBAL as the reducing agent, as it is commonly employed for the reduction of α,β -unsaturated esters and should be mild enough to leave the amide untouched (Scheme 46). Unfortunately, it was not possible to isolate any material after the reaction, presumably due to decomposition.



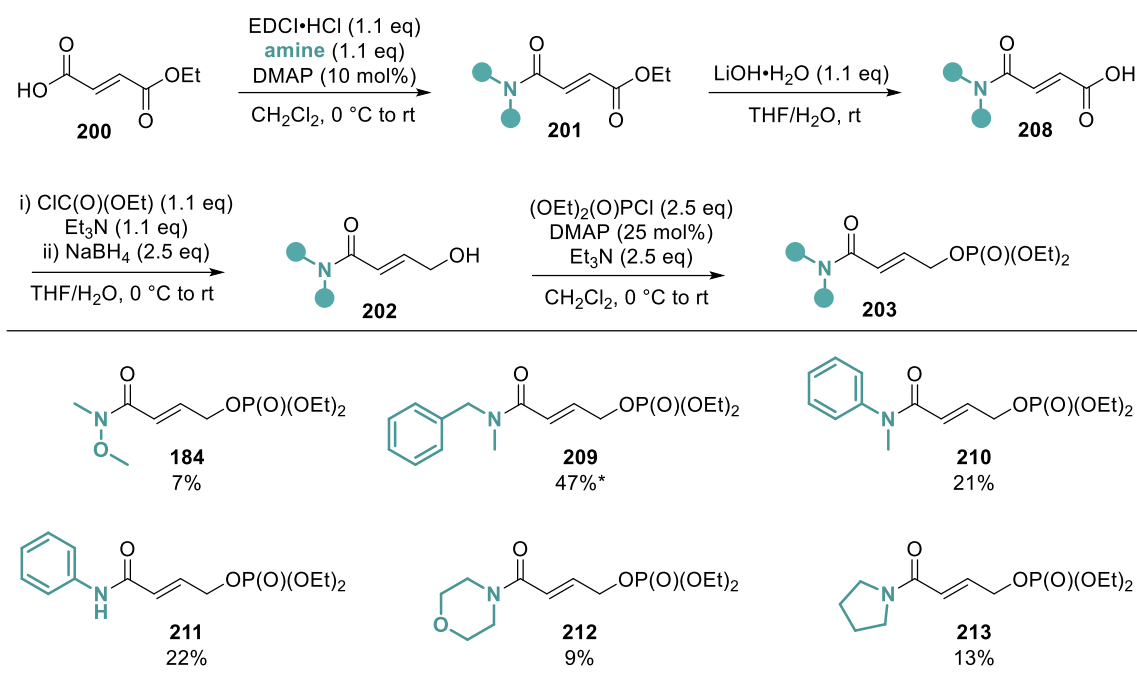
Scheme 46 Attempted selective reduction using DIBAL.

At this point, an extended search in the literature brought another route, first reported by Jacobi and co-workers,⁹⁶ to our attention. Weinreb amide containing allylic alcohol **197** was synthesised in two steps from readily available maleic anhydride by ring opening with *N,O*-dimethyl hydroxyl amine followed by reduction of *in situ* generated anhydride carbonate to yield the desired allylic alcohol **197** in 14% over two steps (Scheme 47). Importantly, subsequent phosphorylation gave the desired allylic phosphate in much higher yield compared to the HWE strategy (82% vs. 43%), indicative that no reactivity inhibiting impurities were formed in this route. The key step in this sequence is the *in situ* generation of the reactive anhydride-carbonate intermediate, which can be reduced with NaBH₄ as a mild reductant, giving the desired allylic alcohol without unwanted side reactions or decomposition.



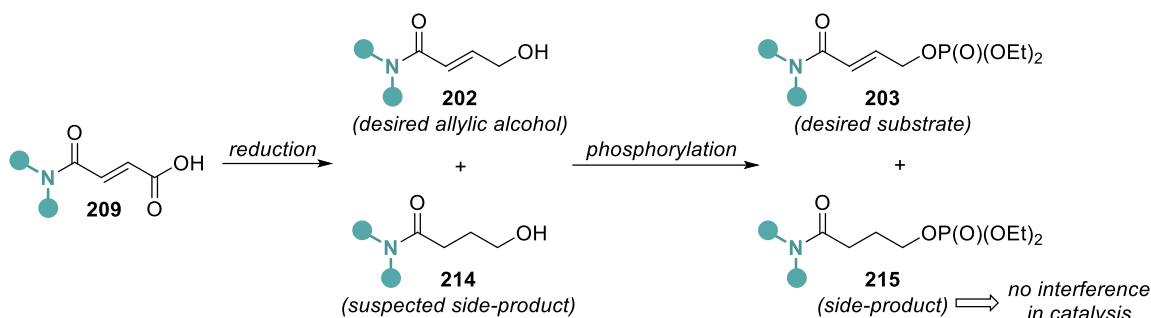
Scheme 47 Synthesis of Weinreb amide containing allylic phosphate via selective reduction.

Unfortunately, opening of maleic anhydride with different amines did not prove generally applicable, requiring a slightly modified route towards the intermediate amide acid for different amide groups. At the same time, Snaddon and co-workers reported a cooperative Pd/ITU dual catalysis employing allylic phosphates containing carboxylic acid derivatives.⁶⁴ Their synthesis also featured the reduction strategy first reported by Jacobi to access the required substrates. Inspired by this and Jacobi's work, as well as previously established methods within the group to access amide acids, the following general synthesis strategy was developed (Scheme 48, top). Following amide coupling on monoethyl fumarate and hydrolysis, the obtained amide acid **208** could be subjected to the previously established reduction conditions, affording the desired allylic alcohols **202**. Subsequent phosphorylation yields the final amide containing allylic phosphate, allowing access to a selection of secondary and tertiary amides featuring aliphatic and aromatic substituents (Scheme 48, bottom).



Scheme 48 General synthesis strategy and library of amide containing allylic phosphates. Quoted yields represent the overall isolated yield starting from monoethyl fumarate. *Overall yield for a mixture of desired phosphate and inseparable by-product.

Although this strategy seemed rather general and straightforward, over the course of synthesising differently substituted amide containing allylic alcohols, several issues were encountered that resulted in low isolated yields for the reduction step. Different side-products were present in the crude reaction mixture post-reduction, necessitating meticulous purification of these alcohols in order to obtain good yields in the following phosphorylation step and to avoid the formation of inseparable side-products. From crude ¹H NMR analyses, the major impurity was suspected to be the fully reduced amide alcohol **214** (Scheme 49) however, it could not be isolated and characterised unambiguously. Moreover, its formation was difficult to control, resulting in varying amounts of side-product generated for each synthesis. Where a full separation of both alcohols **202** and **214** was not possible, the corresponding phosphates **203** and **215** were generated in the subsequent phosphorylation step, again proving difficult to separate. However, as the reduced phosphate **215** could not act as an electrophile in the palladium catalysis, it was hypothesised that its presence should not result in unwanted side-reactions in the relay catalytic process. Moreover, the rearrangement product should be of sufficiently different polarity to allow efficient separation from unreacted phosphates **215** post-catalysis.



Scheme 49 Suspected side-products in reduction and phosphorylation steps.

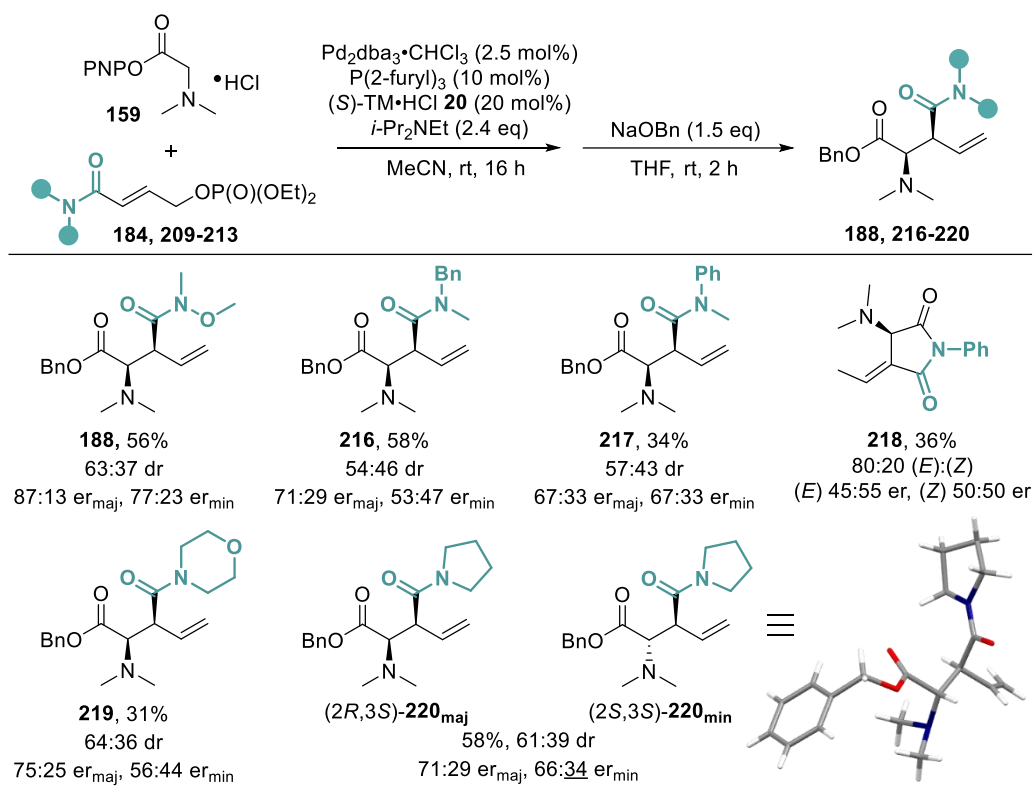
It should be noted that considering these findings, further optimisation of the reduction protocol would be necessary for future applications. Alternatively, the HWE strategy could also be revisited. Optimisation of either the deprotection step using silyl protected aldehyde **195** or the coupling conditions using phosphate substituted aldehyde **199** might result in a feasible alternative. Nonetheless, the current synthetic route allowed access to sufficient material to probe the scope of the desired dual catalytic process.

2.4.3.4 Scope of relay allylation/[2,3]-rearrangement using amide substrates

The range of phosphates synthesised was next applied in the relay allylation/[2,3]-rearrangement catalysis using the previously optimised conditions (Table 4). The model Weinreb amide **184** gave the corresponding product **188** in 56% isolated yield in 63:37 dr in favour of the *syn*-diastereoisomer with good enantioselectivity (87:13 $e_{\text{r}}^{\text{maj}}$, 77:23 $e_{\text{r}}^{\text{min}}$). Differently substituted acyclic and cyclic tertiary amides were also well tolerated, resulting in similar diastereomeric ratios between 54:46 and 67:33, but generally lower enantioselectivities (67:33 – 75:25 $e_{\text{r}}^{\text{maj}}$, 53:47 – 67:33 $e_{\text{r}}^{\text{min}}$) than the model substrate. Amides bearing a *N*-Ph (**210**) or *N*-morpholinyl (**212**) substituents also gave the corresponding products **217** and **219** in a diminished yield (34% and 31%, respectively). All products could be isolated as separable diastereoisomers with the relative configuration assigned by analogy to **186** (Figure 10). The absolute configuration was assigned by analogy to that previously reported for related isothioureia catalysed [2,3]-rearrangement reactions based on the catalyst enantiomer used in the current process.^{65,93} In addition, a crystal structure was obtained for the minor diastereoisomer **220**_{min}, confirming its relative configuration to be *anti*. Notably, the absolute configuration was determined to be (2*S*,3*S*)-**220**_{min}. Based on the mechanistic understanding of the catalytic process and the low enantiopurity (66:34 er) of the sample, the obtained crystal structure

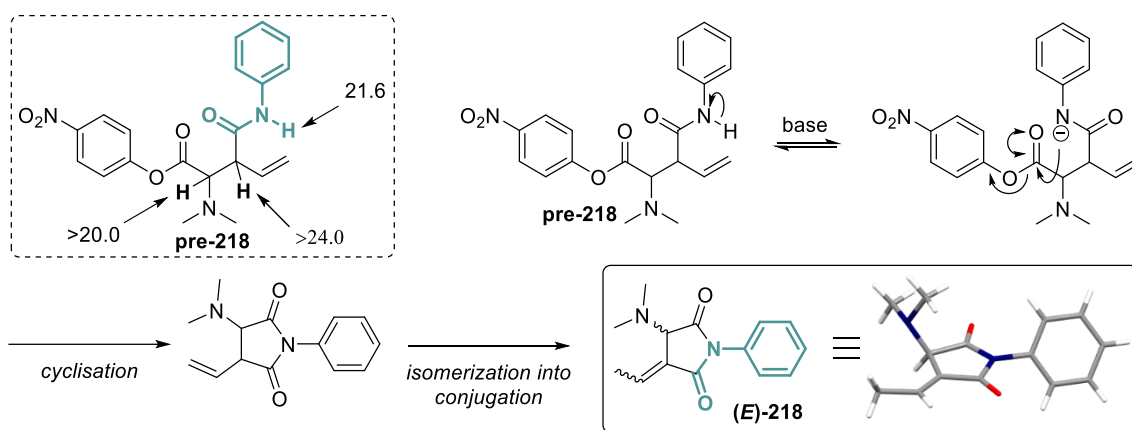
is assumed to correspond to the minor enantiomer. So far, this assumption could not be unequivocally verified by additional analysis.

Table 4 Scope of amide containing allylic phosphates ^{a-d}



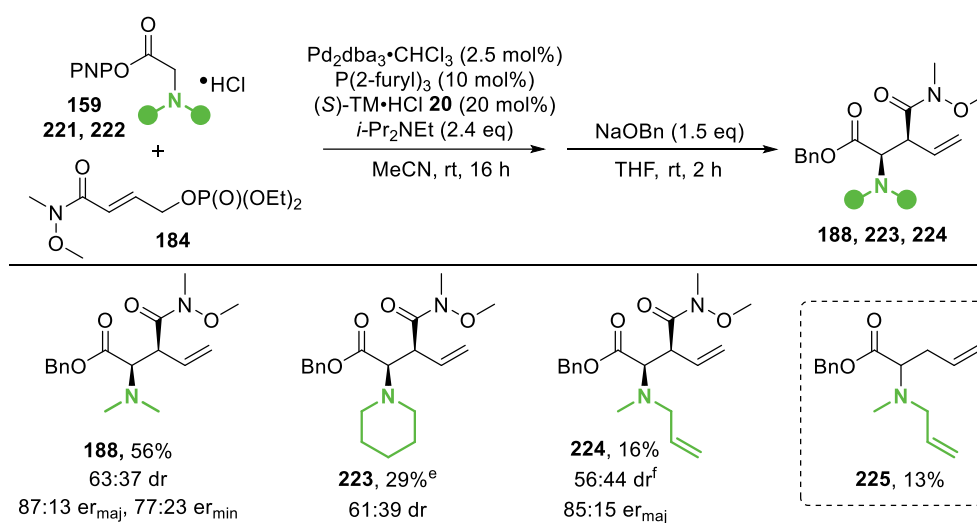
^a Reactions performed on a 0.3 mmol scale. ^b Combined yields of isolated diastereoisomers. ^c dr determined by ¹H NMR analysis of the crude reaction mixture. ^d er determined by chiral stationary phase HPLC analysis.

Interestingly, use of a secondary amide **211** did not yield the anticipated product, but resulted in the formation of cyclic imide **218** instead. The product was isolated in 36% combined yield of fully separable (*E*)- and (*Z*)-isomers ((*E*):(*Z*) 80:20). Unfortunately, both isomers were obtained as racemic mixtures. The formation of cyclic imide **218** is proposed to occur after the allylation/[2,3]-rearrangement sequence, which initially yields the expected, linear product **pre-218** (Scheme 50). Rough estimations of pK_a values taken from Evans pK_a table⁹⁷ suggest that deprotonation of N-*H* is feasible under the basic reaction conditions, and would facilitate intramolecular cyclisation, either by displacing *p*-nitrophenoxide (as shown) or the catalyst directly. Subsequent isomerisation of the alkene into conjugation would furnish cyclic imide **218**. The absence of enantiopurity could either arise from the [2,3]-rearrangement with the catalyst failing to induce any enantioselectivity, or from racemisation post-catalysis. The structure of the (*E*)-isomer was unambiguously identified by single crystal X-ray diffraction analysis.



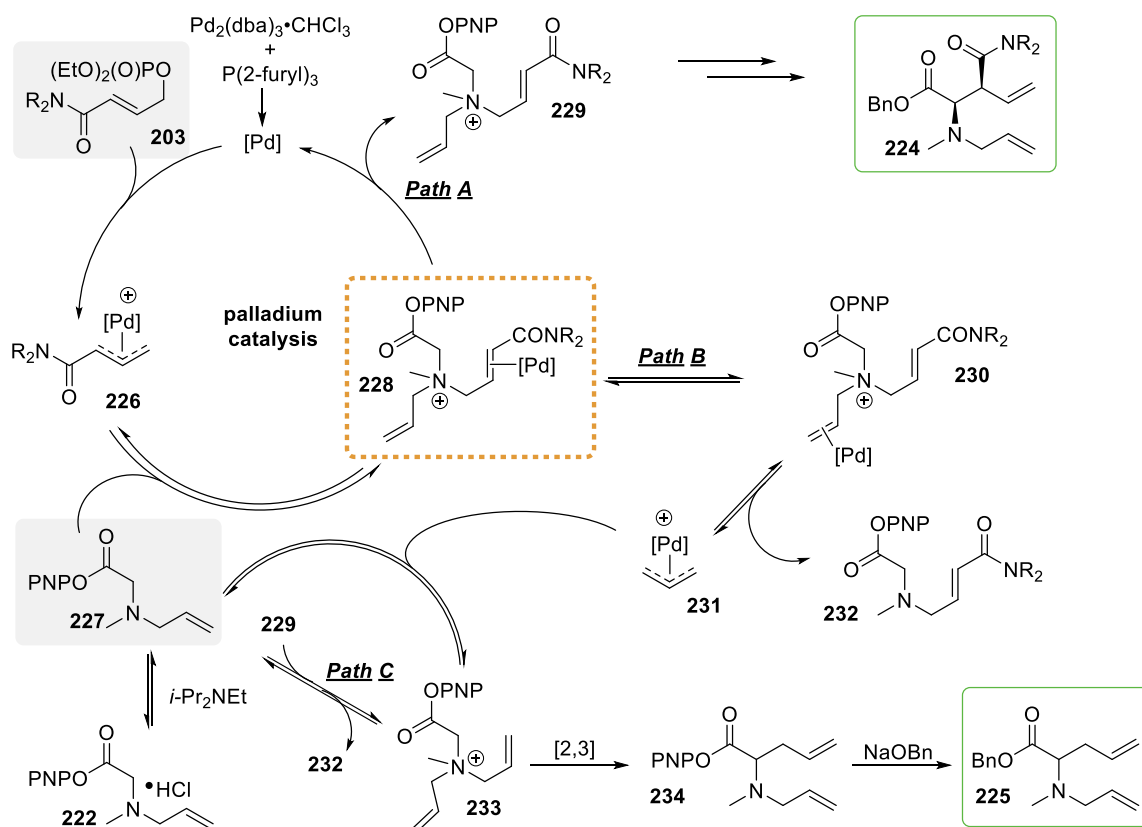
Scheme 50 Proposed mechanism for the formation of cyclic imide 218.

Next, variation of the *N*-substituent within the glycine ester substrate was investigated (Table 5). Changing to a cyclic *N*-piperidinyl substituent (**221**) resulted in a dramatically reduced reactivity, consistent with previous work.⁶⁵ Thus, product **223** was obtained in only 29% isolated yield, even after a prolonged reaction time of 84 h, with 61:39 dr as an inseparable mixture of diastereoisomers. Unfortunately, the enantiomeric ratios could not be determined. Use of an unsymmetrical *N*-allyl-*N*-methylglycine ester **222** gave the desired product **224** in only 16% yield, with low diastereoselectivity (56:44 dr), but good enantioselectivity (85:15 *er*_{major}). Surprisingly, compound **225** was also isolated from the reaction in 13% yield, indicative of competing reaction pathways as a consequence of an additional *N*-allyl unit.

Table 5 Scope of glycine esters ^{a-d}

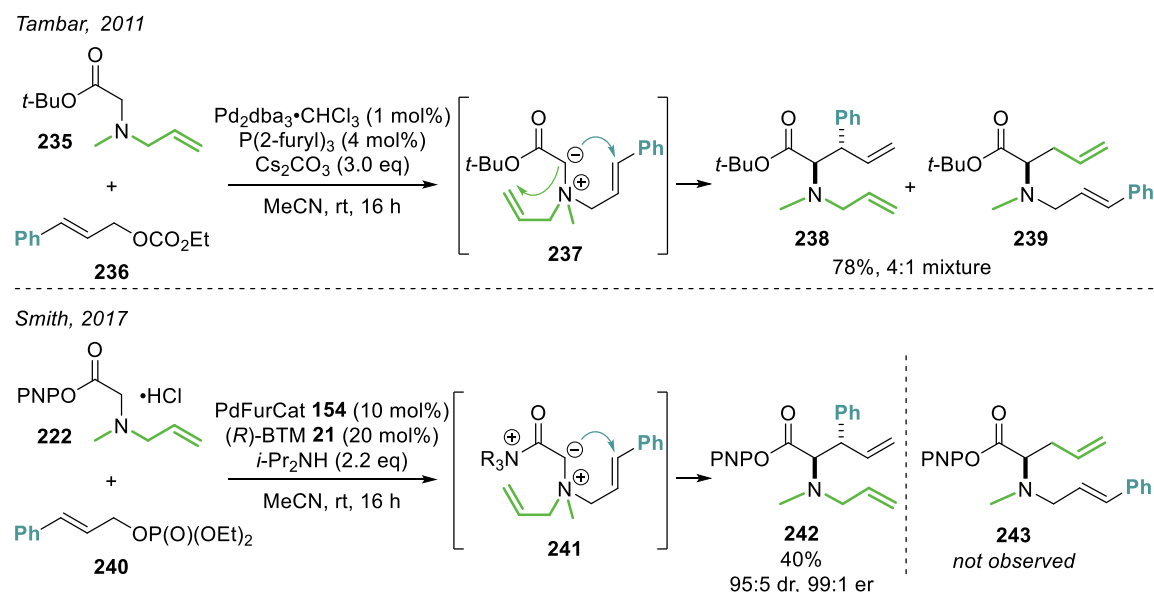
^a Reactions performed on a 0.3 mmol scale. ^b Combined yields of isolated diastereoisomers. ^c *dr* determined by ¹H NMR analysis of the crude reaction mixture. ^d *er* determined by chiral stationary phase HPLC analysis. ^e Reaction run for 84 h. diastereoisomers could not be separated, *er* could not be determined. ^f *er* for minor diastereoisomer could not be determined.

A proposed mechanism for the formation of **225** is depicted in Scheme 51. The catalysis starts with the active palladium catalyst undergoing oxidative addition with allylic phosphate **203** to give allyl intermediate **226**. After nucleophilic substitution with *N*-allyl-*N*-methylglycine ester **227** to give the intermediate ammonium salt **228**, different pathways are conceivable. **Path A** follows the anticipated pathway for the allylation/[2,3]-rearrangement sequence, yielding intermediate ammonium salt **229**, which upon rearrangement gives the desired product **224**. Alternatively, dissociation of the palladium catalyst from intermediate **228** and re-coordination to the unsubstituted allyl fragment would enable **Path B**. As the formation of the intermediate ammonium salt is a reversible process, oxidative addition from intermediate **230** would give unsubstituted Pd- π -allyl intermediate **231** and modified glycine ester **232** as side-product, however, this could not be isolated. The unsubstituted Pd- π -allyl complex **231** can react with another molecule of PNP ester **227**, giving ammonium salt **233** bearing two unsubstituted allyl fragments. The formation of **233** from an uncatalyzed nucleophilic substitution of ammonium salt **229** with PNP ester **227** (**Path C**) cannot be ruled out. [2,3]-Rearrangement of the ylid formed from ammonium salt **233** will lead to PNP ester **234**, which upon derivatization with NaOBn gives the observed side product **225**.



Scheme 51 Possible pathways for the formation of side-product **225**.

The exchange of *N*-allyl units observed in this work has not been reported previously for an *N*-allylation/rearrangement protocol. Earlier work from our group^{65,98,99} as well as Tambar and co-workers⁸⁷ showed that the use of *N*-allyl-*N*-methyl esters or *N,N*-diallyl esters was well tolerated, resulting in exclusive, or at least favoured rearrangement via the *N*-cinnamyl unit (Scheme 52). In agreement with the results obtained for an isothioureia catalysed protocol, the product resulting from rearrangement via the *N*-allyl substituent from unsymmetrically substituted ammonium salt **241** was also not observed in the current work.



Scheme 52 Use of *N*-allyl units in allylation/[2,3]-rearrangement protocols.

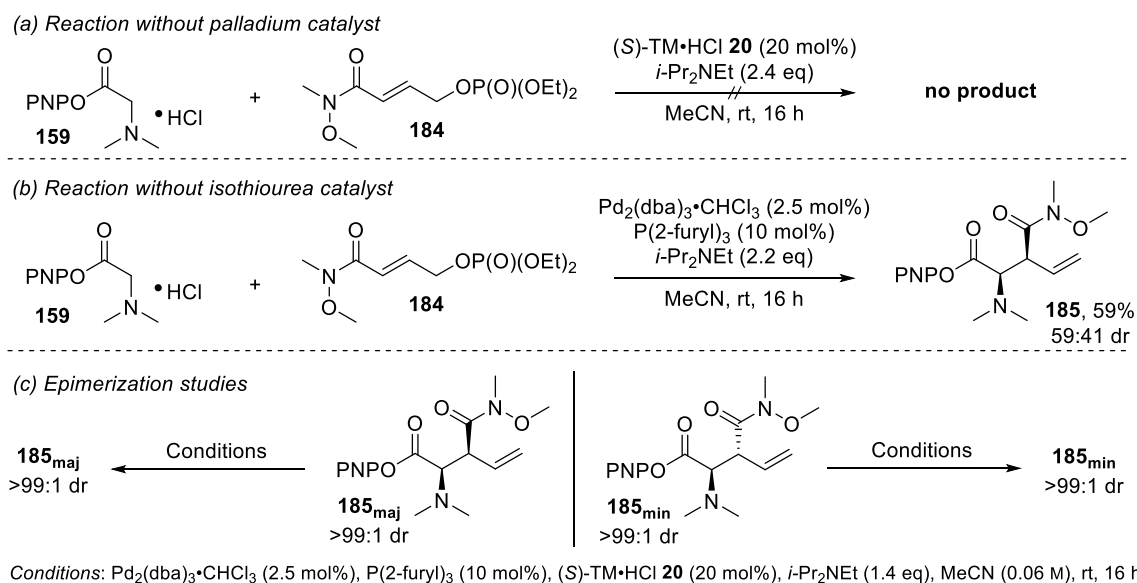
These results indicate that the developed *N*-allylation/[2,3]-rearrangement method is highly susceptible to changes in *N*-substitution as well as the allylic fragment, requiring a fine balance to obtain the desired products in high yield and with high stereocontrol, and to suppress undesired side-reactions.

2.4.3.5 Mechanistic control experiments

To gain further mechanistic insight, a series of control experiments was performed. At first, the significance of each catalyst was investigated. In the absence of palladium catalyst, no reaction occurred with only starting materials returned (Scheme 53a). In the absence of isothioureia catalyst however, a significant background reaction was observed, giving the product in 59% yield as a racemic mixture (Scheme 53b). This result indicates a Brønsted base-catalysed reaction pathway, which was not observed for cinnamate

derived phosphates⁶⁵ and might account for the comparatively lower enantioselectivities observed in this work. Interestingly, even without the isothioureia catalyst the reaction still proceeded in favour of the *syn*-diastereoisomer. This is in contrast to previous observations by our group and Tambar and co-workers,⁸⁷ who reported preferred formation of the *anti*-diastereoisomer under Brønsted basic conditions. The only other report describing a bias to generate *syn*-amino acid derivatives involves a *N*-allylation/[2,3]-rearrangement sequence between proline derivatives and cinnamyl alcohol derivatives bearing *ortho*-substituents on the aryl ring.¹⁰⁰ These findings indicate the preference for either *exo* or *endo* transition state in the [2,3]-rearrangement is highly susceptible to changes in substituents and that further investigations are necessary to gain a deeper understanding of the influencing parameters.

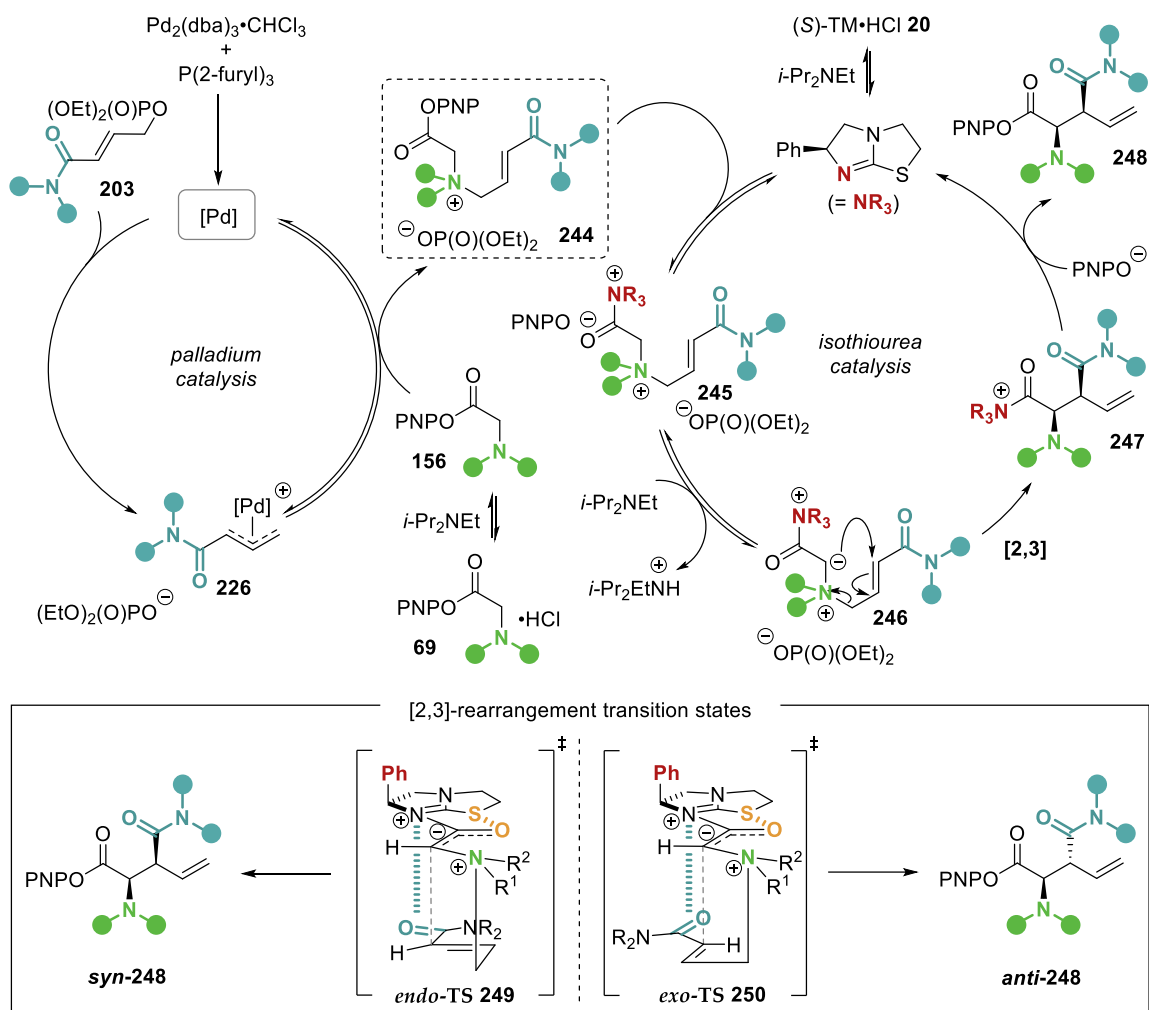
Additional control experiments looked at the potential for product epimerization under the reaction conditions (Scheme 53c). PNP ester **185** was isolated as separate diastereoisomers and each re-subjected to standard catalysis conditions. After 16 h, no change in diastereomeric ratio was observed for either, indicating that epimerization of the PNP ester product does not occur under these conditions. However, epimerization of the acyl ammonium species post-rearrangement and prior to catalyst turnover cannot be ruled out, as displacement of the catalyst by the aryloxy is assumed to be irreversible based upon previous work.⁹³



Scheme 53 Mechanistic control experiments.

The mechanism for this relay palladium and isothioureia *N*-allylation/[2,3]-rearrangement catalysis is proposed in analogy to related, previous work (Scheme 54).^{65,93} The catalytic cycle starts with the generation of the active palladium catalyst [Pd] from the catalyst precursor Pd₂(dba)₃·CHCl₃ and the P(2-furyl)₃ ligand. Oxidative addition of allylic phosphate **203** gives Pd- π -allyl species **226**, which undergoes reversible nucleophilic substitution with free-based glycine ester **156**. This generates ammonium salt **244** as the key intermediate. Upon acylation of the free-based isothioureia catalyst TM and deprotonation, ammonium ylid **246** is generated. Subsequent [2,3]-rearrangement followed by aryloxide facilitated catalyst turnover yields product **248**. The stereochemical outcome of the reaction can be rationalised by considering the following key interactions in the transition state of the stereodetermining [2,3]-rearrangement:

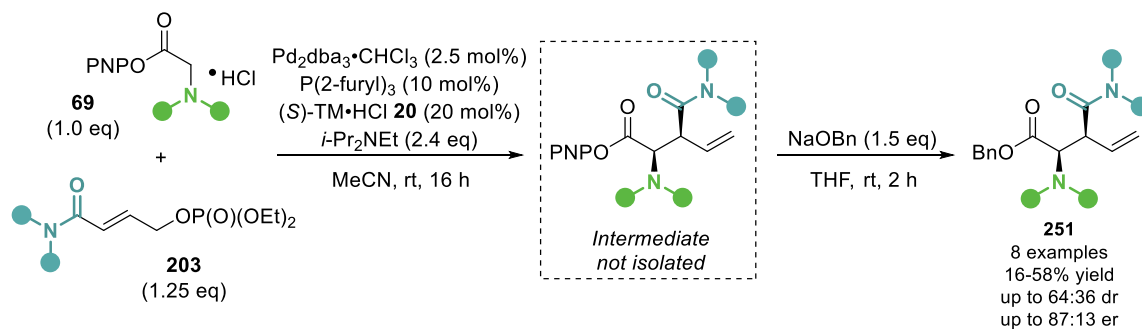
A stabilising 1,5-S \cdots O interaction between the carbonyl oxygen and the isothioureia sulfur atom (no to σ^*_{C-S}) locks the ylid in its position, restricting its conformational freedom. With the stereodirecting Ph group of the catalyst adopting a pseudoaxial position to minimise 1,2-strain, the allylic fragment is forced onto the opposite face, resulting in excellent stereocontrol over the C(2) centre in the subsequent [2,3]-rearrangement. The configuration of the C(3) centre is then determined by the preferential rearrangement through *endo* transition state **249**, leading to the major *syn*-diastereoisomer. This is thought to be the result of a favourable electrostatic C=O \cdots cation interaction between the amide carbonyl and the positively charged catalyst. Similar interactions have been proposed for isothioureia catalysed kinetic resolutions.^{101–103} The observed diastereoselectivities in this work are lower compared to the ones obtained for aryl substituted allylic fragments displaying a stabilising $\pi\cdots$ cation interaction, indicating that the preferential rearrangement through either *endo* or *exo* transition state is very susceptible to steric and electronic changes within the allylic fragment.



Scheme 54 Proposed relay catalytic cycle and rearrangement transition states.

2.5 Conclusion

The current work demonstrates the potential for expanding the functional group tolerance beyond aryl substituents in the dual palladium and isothioureia catalysed *N*-allylation/[2,3]-rearrangement protocol previously established. Successful incorporation of electron-withdrawing ester and amide functionalities as well as a silyl protected homoallylic alcohol and C(2)-branched substituent was demonstrated. However, product instability during isolation and derivatisation limited further investigations to amide containing allylic phosphates. Thus, highly functionalised α -amino acid derivatives bearing an amide substituent were pursued and could be isolated in good yield and stereoselectivity following a relay allylation/[2,3]rearrangement and subsequent derivatisation protocol (Scheme 55).



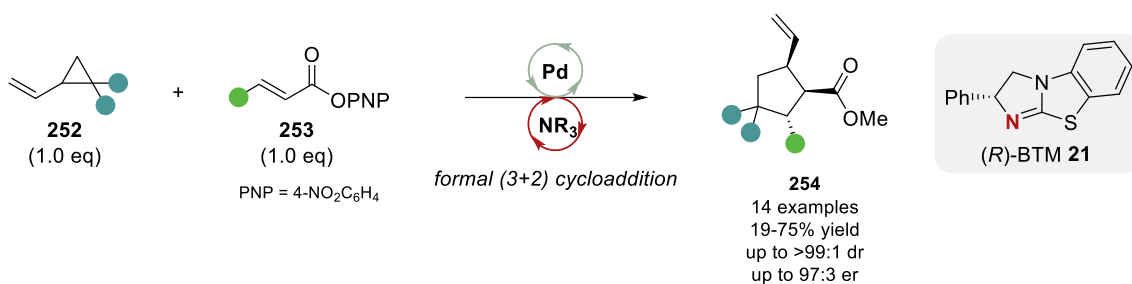
Scheme 55 Relay palladium and isothioureia catalysis using amide containing allylic phosphates.

Mechanistic experiments revealed a Brønsted base catalysed background reaction to be operative in the absence of isothioureia catalyst, potentially resulting in the lower enantioselectivities observed compared to previous work. In addition, the low diastereoselectivities obtained in the current work highlight the need for further investigations to gain a deeper understanding of the factors influencing the transition state in the [2,3]-rearrangement step.

Chapter 3: Cooperative palladium and isothiourea catalysis

3.1 Project Overview

This chapter describes the development of a cooperative catalysis process employing palladium π -allyl chemistry and α,β -unsaturated acyl ammonium catalysis. Simultaneous activation of vinylcyclopropanes **252** and α,β -unsaturated *p*-nitrophenyl esters **253** in the presence of Pd(PPh₃)₄ and the enantiopure isothiourea (*R*)-BTM **21** promotes an intermolecular formal (3+2) cycloaddition to generate highly functionalised cyclopentane products **254** with up to 4 contiguous stereogenic centres. The products were obtained in generally high yields and excellent diastereo- and enantioselectivity. Notably, this is the first report of a dual catalytic process involving α,β -unsaturated acyl ammonium intermediates, providing a versatile methodology for the synthesis of densely substituted vinylcyclopentanes.



Scheme 56 Cooperative palladium and isothiourea catalysis.

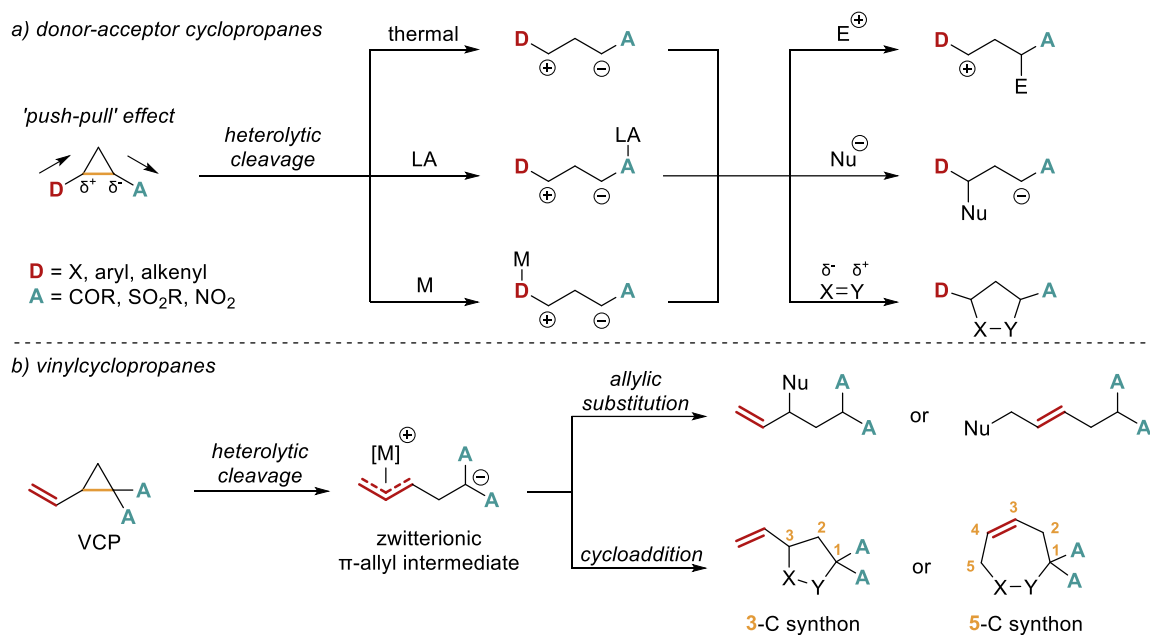
3.2 Introduction

The cyclopentane core is an important structural motif as it is found in many natural products¹⁰⁴ and pharmaceuticals.¹⁰⁵ Compared to six-membered carbocycles, which can be easily accessed via Diels-Alder cyclisation or Robinson annulation, five-membered carbocycles are more difficult to synthesise. Potential strategies via cycloaddition or annulation processes are often less generally applicable and control over relative and absolute stereochemistry is usually more challenging. Therefore, approaches that generate highly functionalised cyclopentane scaffolds from simple starting materials with excellent stereocontrol are highly desirable. Important strategies for the construction of substituted cyclopentanes include the Pauson-Khand reaction¹⁰⁶ or (3+2) dipolar cycloadditions. The latter has proven particularly versatile in recent years, with the development of numerous all-carbon 1,3-dipoles allowing access to a variety of cyclopentane structures. Among the potential dipole precursors, vinylcyclopropanes have been extensively used as three carbon synthons and will be explored in more detail in the following section.

3.2.1 Formal (3+2) cycloadditions using vinylcyclopropane substrates

Cyclopropanes have become attractive precursors for the stereoselective preparation of functionalised building blocks by ring-opening reactions.¹⁰⁷ Although the cyclopropane ring is highly strained, the C-C bonds are kinetically stable and typically rather sluggish to react unless “activated”. Ring activation can be achieved by placing electron-donating groups (donor, D) and electron-withdrawing groups (acceptor, A) on vicinal ring carbons, giving so-called donor-acceptor (D-A) cyclopropanes (Scheme 57a). Common donor substituents include electron rich heteroatoms, as well as aryl and alkenyl groups, whereas electron-withdrawing functionalities, such as carbonyl, sulfonyl or nitro substituents are commonly found as acceptors. These units create a so-called 'push-pull' effect, which renders the C-C bond between the donor and acceptor group highly polarised and susceptible to bond cleavage. The main methods for initiating heterolytic ring opening include thermal activation, Lewis acid (LA) coordination to the acceptor groups or low valent metal (M) coordination to the donor groups. In each case, a zwitterion intermediate in the form of a 1,3-dipole is generated, which can engage in

reactions with electrophiles, nucleophiles and dipolarophiles. This versatility renders D-A cyclopropanes powerful building blocks in organic synthesis.^{108,109} In particular vinylcyclopropanes (VCPs), a sub-class of D-A cyclopropanes bearing a vinyl donor group (Scheme 57b), have become privileged reaction partners as they can be engaged in a multitude of transformations.¹¹⁰ VCPs can be readily ring-opened in the presence of transition metals, forming zwitterionic π -allyl intermediates. These intermediates can engage in allylic substitution type processes, giving the corresponding alicyclic products. Particularly attractive, however, is the application of these zwitterions as all-carbon dipoles in formal dipolar cycloaddition reactions. Traditionally, they have been used as a three-carbon synthon for the synthesis of functionalised cyclopentanes.¹¹¹ Although less exploited, they can also be engaged as a five-carbon synthon in (5+x) cycloadditions, enabling the formation of seven-, eight-, or nine-membered rings.¹¹²

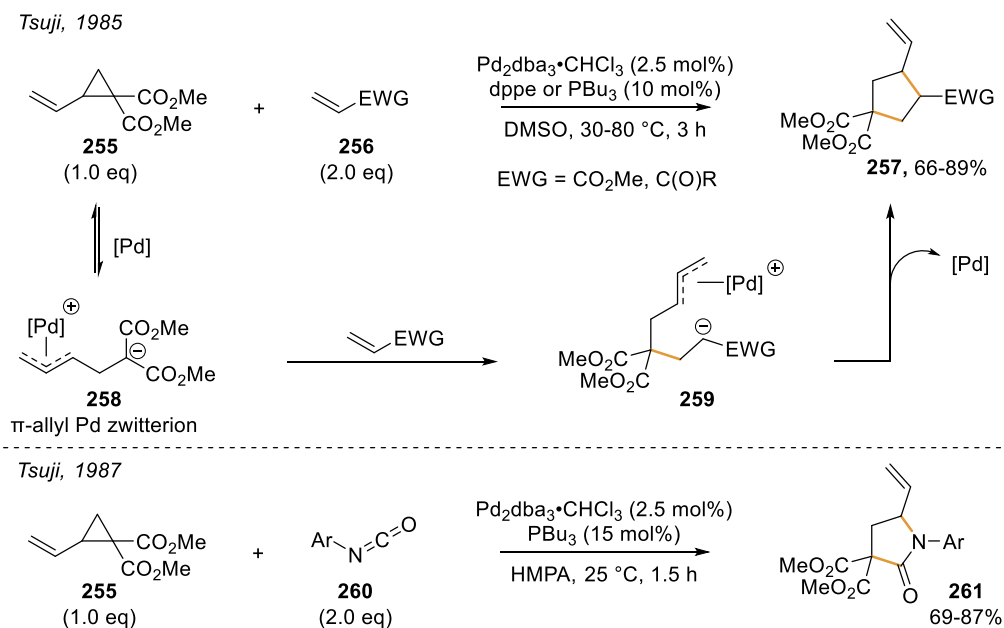


Scheme 57 General reactivity profile for a) donor-acceptor cyclopropanes; b) vinylcyclopropanes.

3.2.1.1 Palladium catalysed VCP opening in formal (3+2) cycloadditions

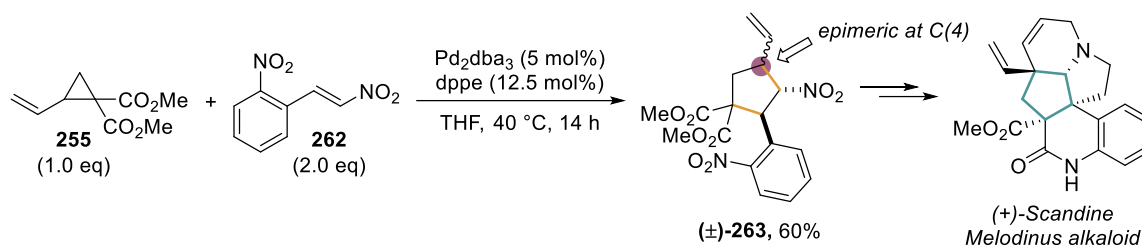
The opening of VCPs can be accomplished by a number of transition metals, with palladium being one of the most explored. In 1985, Tsuji and co-workers first demonstrated the potential of catalytically generated palladium π -allyl zwitterions to engage in formal (3+2) cycloadditions with α,β -unsaturated ketones or esters to generate vinyl-substituted cyclopentane products (Scheme 58, top).¹¹³ Using diester substituted VCP **255** and Michael acceptors **256** in the presence of $\text{Pd}_2\text{dba}_3 \cdot \text{CHCl}_3$ and either dppe or

PBu₃ as ligand furnished the corresponding cyclopentane products **257** in good yields and short reaction times. The authors proposed a stepwise mechanism, starting with the generation of a palladium π -allyl zwitterion **258** followed by Michael addition to give intermediate **259**. Subsequent attack of the formed enolate onto the π -allyl moiety liberates the product and regenerates the catalyst. The same group also demonstrated the expansion of this methodology to aryl isocyanates **260** as dipolarophiles, furnishing vinyl substituted butyrolactams **261** in good yield (Scheme 58, bottom).¹¹⁴



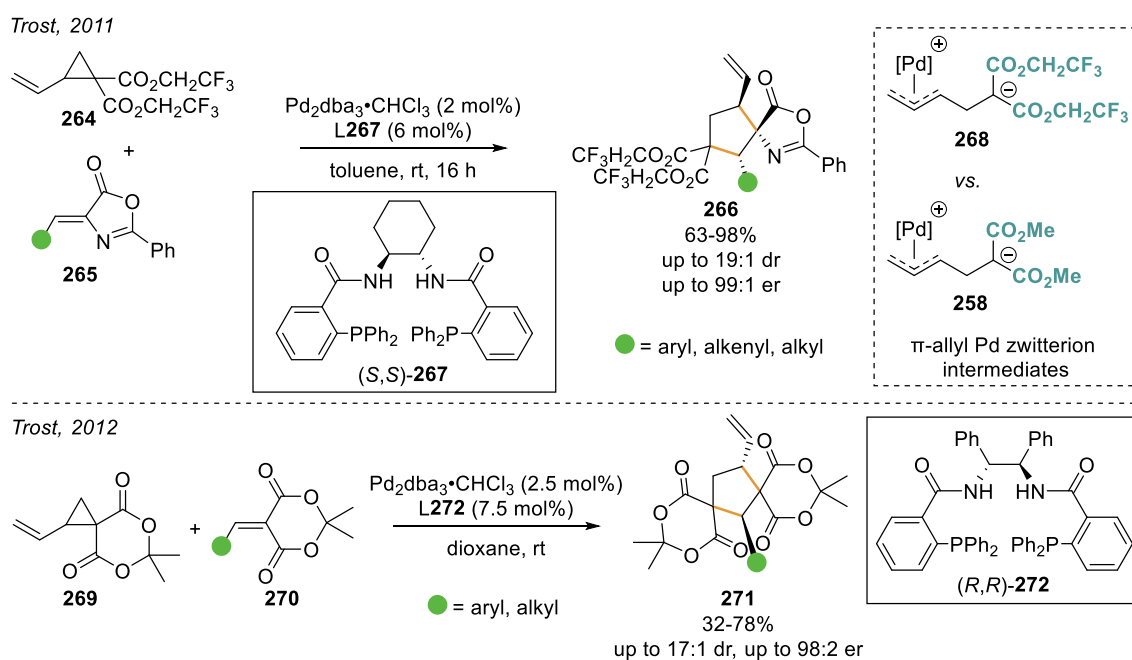
Scheme 58 Seminal work by Tsuji on Pd catalysed (3+2) cycloadditions using VCPs.

Although this methodology offered great potential for the synthesis of functionalised cyclopentanes, it remained largely unexplored for more than 20 years. In 2011, Stoltz and co-workers reported the first application of a similar (3+2) cycloaddition strategy for the construction of the highly substituted cyclopentane core in the Melodinus alkaloid family (Scheme 59).¹¹⁵ Employing VCP **255** and commercially available nitroolefin **262** in the presence of Pd₂dba₃ (5 mol%) and dppe ligand (12.5 mol%) furnished the desired cyclopentane **263** as an inseparable mixture of two diastereoisomers in 60% yield. Importantly, single crystal X-ray diffraction analysis at a later stage revealed that i) the cycloaddition proceeds stereospecifically with regard to the alkene geometry, retaining the *trans*-relationship in the product; ii) the products are epimeric only at C(4).



Scheme 59 Application of Pd catalysed (3+2) cycloaddition in the synthesis of Melodinus alkaloids.

In the same year, Trost and Morris reported the first enantioselective formal (3+2) cycloaddition exploiting palladium catalysed VCP opening (Scheme 60, top).¹¹⁶ Using VCP **264** and azlactone Michael acceptor **265** in the presence of Pd₂dba₃·CHCl₃ (6 mol%) and chiral Trost ligand **267** gave the desired cyclopentane products in high yields and with excellent stereocontrol (up to 19:1 dr, up to 99:1 er). Notably, only two of four possible diastereoisomers were observed, with the major diastereoisomer displaying a *syn-anti* relationship between the three contiguous stereogenic centres. Interestingly, employing a VCP with methyl ester groups (**255**) instead of trifluoroethanol ester groups resulted in dramatically reduced reactivity (16% yield). This was attributed to the methyl ester derived intermediate **258** being less stable, resulting in a shorter lifetime compared to the trifluoroethanol ester intermediate **268**. Subsequently, Trost and co-workers expanded this enantioselective methodology to incorporate Meldrum's acid derived VCP **269** and Michael acceptors **270** (Scheme 60, bottom).¹¹⁷



Scheme 60 First examples of enantioselective palladium catalysed formal (3+2) cycloadditions.

Following on from these pioneering works, numerous examples have been reported showcasing the diastereo- and enantioselective formation of highly functionalised cyclopentane structures through a palladium catalysed formal (3+2) cycloaddition approach. Based on these examples, the following general observations can be made:

- The reaction tolerates a range of temperatures and a variety of solvents, with toluene and ethereal solvents being most prominent.
- Palladium-dba complexes are commonly used as catalyst precursors in combination with phosphine ligands (usually bidentate).
- Induction of enantioselectivity is controlled by the palladium catalyst by employing chiral, bidentate ligands.
- VCPs based on diester or dinitrile acceptor groups are most commonly used, with more elaborate examples such as 1,3-indanedione or *N*-protected oxindole acceptors also reported.
- A variety of Michael acceptors has been successfully applied in this formal (3+2) cycloaddition methodology, including nitroolefins, α,β -unsaturated keto esters and imines, activated indoles and benzofurans, and unsubstituted acrylic esters (Figure 11). Importantly, substitution in the β -position is usually limited to aryl-, heteroaryl or (less commonly) alkyl substituents. In addition, potent activating groups, such as a nitro or imine functionality are required for good reactivity, with simple α,β -unsaturated esters traditionally proving unreactive.

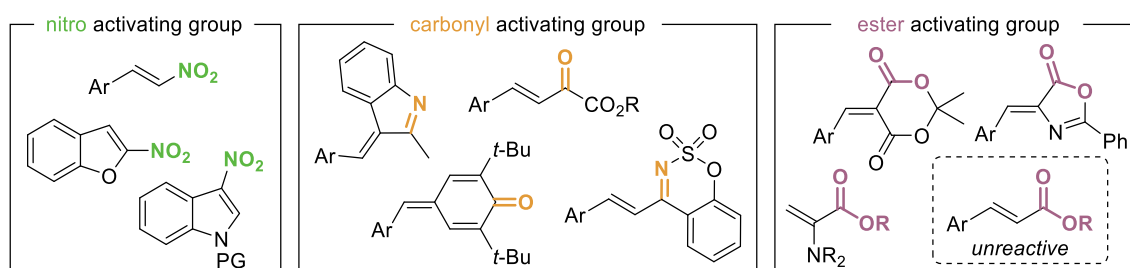


Figure 11 Michael acceptors explored in palladium catalysed formal (3+2) cycloadditions.

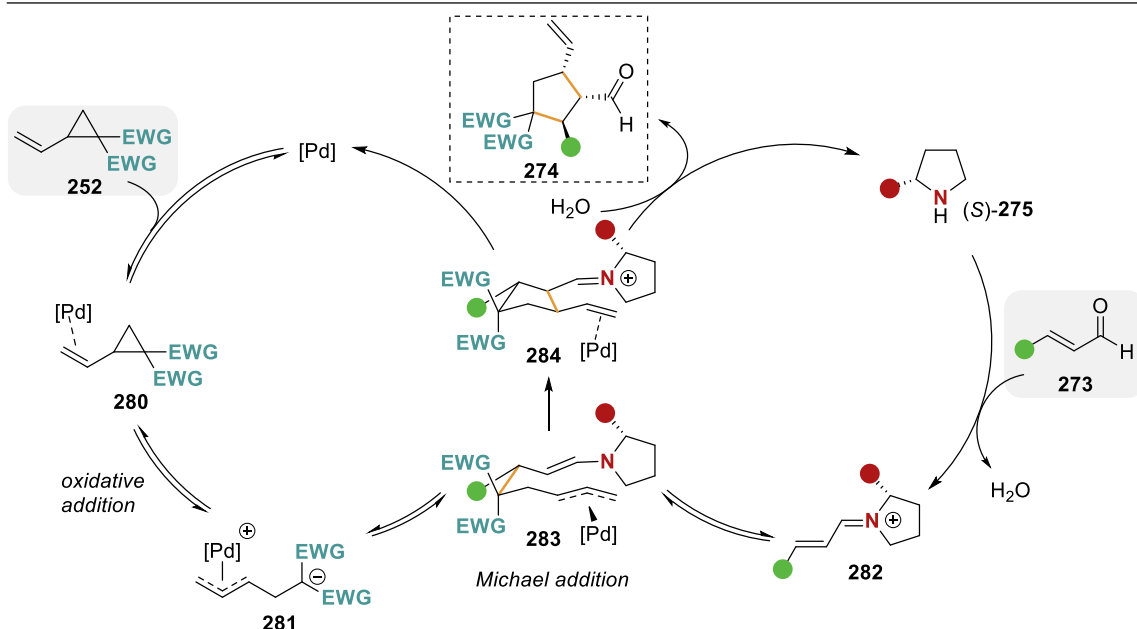
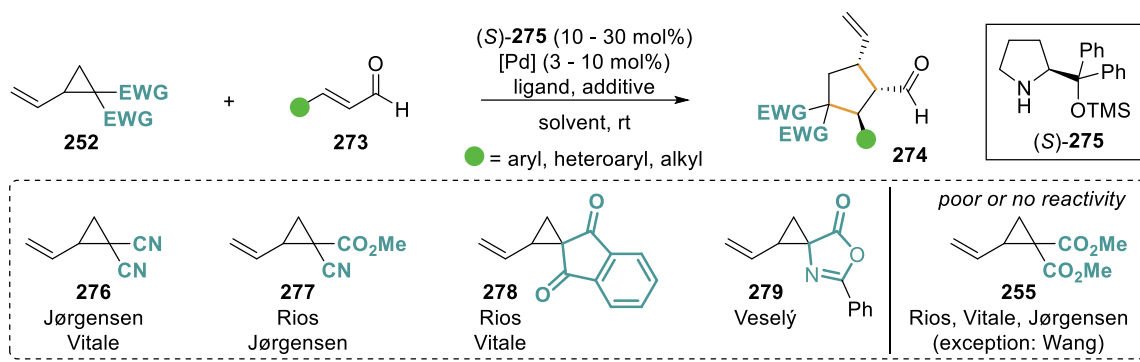
The developed methodologies are usually specific to certain combinations of VCP and Michael acceptor, with variation of either often leading to poor reactivity or selectivity. This highlights that the palladium catalysed formal (3+2) cycloaddition has a narrow reactivity window. To further broaden the scope of this process, alternative catalytic strategies to activate the substrates and induce stereoselectivity need to be explored. One

possibility is a combined palladium and organocatalysed approach, which will be discussed in more detail in the following section.

3.2.1.2 Cooperative palladium and 2nd amine catalysis

In 2016, the groups of Vitale,¹¹⁸ Jørgensen,¹¹⁹ Wang¹²⁰ and Rios^{121,122} independently reported a cooperative palladium and secondary amine catalysis to facilitate VCP ring opening and formal (3+2) cycloaddition with α,β -unsaturated aldehydes. This methodology requires the simultaneous activation of both substrates by the respective catalysts and relies solely on the chiral organocatalyst for enantioinduction. Generally, these protocols use 10 – 30 mol% of chiral secondary amine **275** and up to 10 mol% palladium catalyst, generated from either Pd(dba)₂ or Pd₂dba₃ (Scheme 61, top). Interestingly, the transformation proceeds with or without phosphine ligands or Brønsted acid additive (depending on the exact conditions) and in a variety of solvents. Control experiments also showed that in the absence of either catalyst, no product is formed. In general, the developed processes gave the products in high yields, with high diastereocontrol (up to three diastereoisomers, generally >85:10:5 dr) and with excellent enantiocontrol (>90:10 er). Different aryl substituents on the α,β -unsaturated aldehyde (**273**) were well tolerated, with alkyl substituents also giving good yields in some cases. A variety of electron-withdrawing groups on the VCP could be applied in this process, including dinitrile (**276**), mixed nitrile and ester (**277**) and indanedione (**278**). In 2019, Veselý and co-workers also demonstrated the compatibility of azlactone derived VCP **279** with this transformation, yielding the corresponding spirocyclic product.¹²³ It should be noted, however that the VCP scope within any process was rather limited, as a change in electron-withdrawing groups often led to diminished reactivity and selectivity. This was particularly noticeable when moving to diester substituted VCPs **255**. With the exception of Wang's work, diester substituents generally led to poor reactivity or no conversion at all. These results highlight the sensitivity of the optimised process to steric and electronic changes within the substrates. The proposed mechanism for this cooperative palladium and secondary amine catalysis is depicted in Scheme 61 (bottom). Palladium catalysed oxidative addition of VCP **252** yields zwitterionic π -allyl intermediate **281**. At the same time, α,β -unsaturated aldehyde **273** reacts with the chiral secondary amine catalyst **275**, forming iminium ion **282**. Subsequent Michael addition between the stabilised carbanion

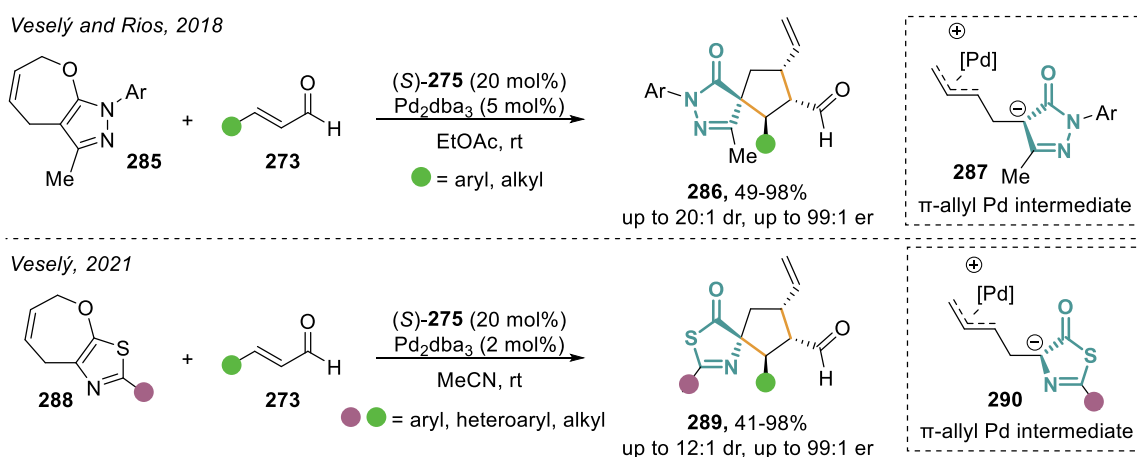
and the α,β -unsaturated iminium ion yields enamine intermediate **283**. Intramolecular ring closure, dissociation of the palladium catalyst, and subsequent hydrolysis of the iminium ion liberates the final cyclopentane product **274**. Importantly, Michael addition is presumed to be reversible, with facial selectivity being controlled by the chiral organocatalyst.



Scheme 61 Cooperative palladium and secondary amine catalysis using VCPs.

This cooperative catalysis strategy was later expanded to heterocyclic precursors instead of VCPs to generate a zwitterionic π -allyl intermediate for the synthesis of spirocyclic cyclopentane products. In 2018, the groups of Veselý and Rios reported the use of bicyclic pyrazolone derivatives **285** in combination with unsaturated aldehydes **273** for the synthesis of spirocyclic products **286** (Scheme 62, top).¹²⁴ The simultaneous activation of the substrates by the secondary amine organocatalyst **275** (20 mol%) and Pd₂dba₃ (5 mol%) allowed the formation of cyclopentane products in generally high yields with good diastereoselectivity and with excellent enantioselectivity (>96:4 er). Recently, Veselý and

co-workers applied this concept to the synthesis of spirothiazolones (Scheme 62, bottom).¹²⁵ Using bicyclic thiazole derivative **288** and α,β -unsaturated aldehydes **273** in the presence of organocatalyst **275** (20 mol%) and Pd₂dba₃ (5 mol%) furnished the desired spirocycles in high yields with high diastereo- and excellent enantiocontrol. Although these protocols don't use VCPs, the zwitterionic π -allyl intermediates **287** and **290** generated from the bicyclic precursors are identical to the ones obtained by using VCPs. In the case of bicyclic thiazole derivatives, the corresponding VCP was obtained as by-product during the starting material synthesis. Hence, these precursors represent an expansion of the electron-withdrawing groups tolerated in this formal (3+2) cycloaddition methodology, allowing the construction of highly substituted spirocyclic compounds.

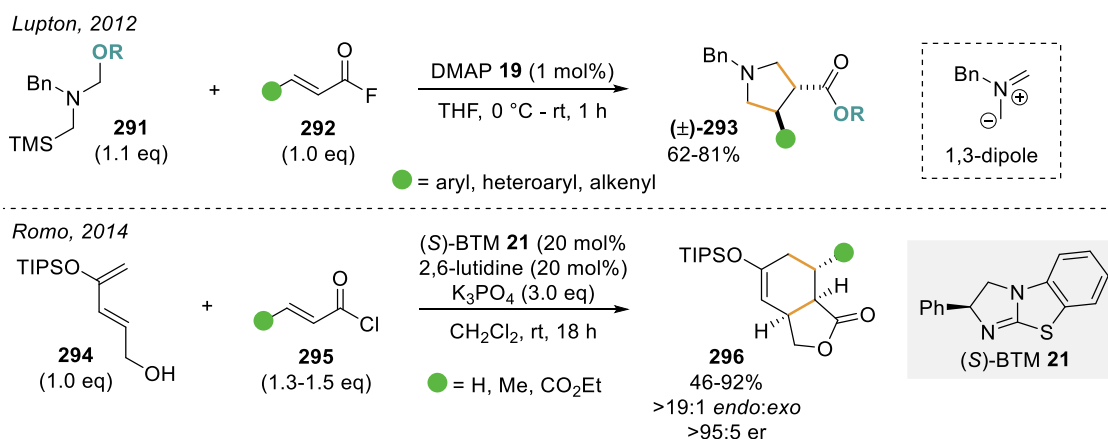


Scheme 62 Dual palladium and 2° amine catalysis using heterocyclic 1,3-dipole precursors.

3.2.2 α,β -Unsaturated acyl ammonium intermediates in cycloaddition and annulation processes

α,β -Unsaturated carboxylic acid derivatives are versatile reaction partners in a variety of transformations and are often commercially available. Their potential to engage in cycloaddition reactions or Michael addition cascade processes to generate highly substituted cyclic products is particularly attractive. Chiral tertiary amine Lewis base catalysts are commonly employed to activate these substrates and control the stereoselectivity of these cyclisation processes. In 2012, Lupton and co-workers reported the first Lewis base catalysed 1,3-dipolar cycloaddition of unstabilised azomethine ylids to generate substituted pyrrolidines (Scheme 63, top).¹²⁶ Using α,β -unsaturated acyl fluorides **292** and ylid precursor **291** in the presence of DMAP **19** as catalyst furnished the corresponding pyrrolidine products **293** in high yields and as single diastereoisomers.

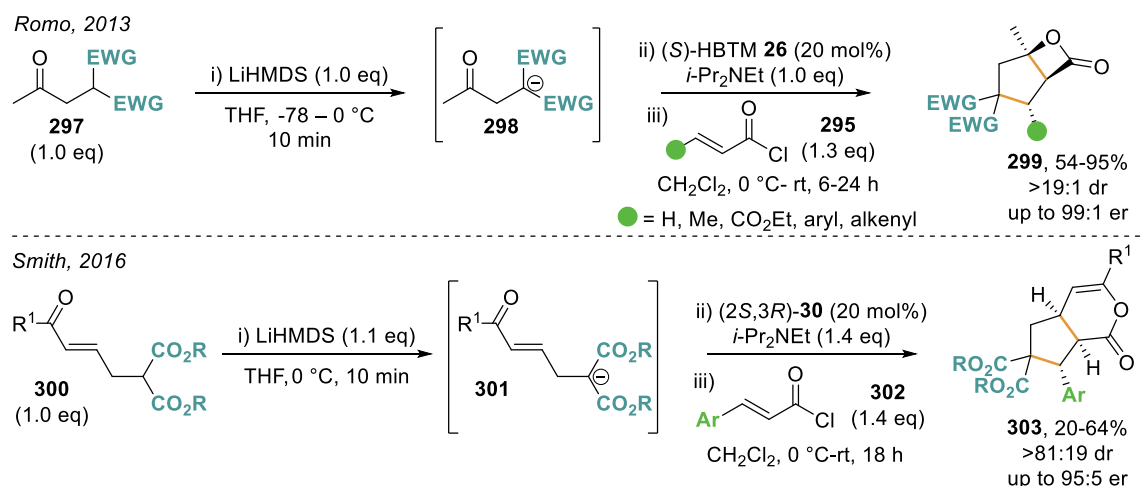
Unfortunately, use of chiral Lewis base catalysts resulted in only low levels of enantioselectivity, with only isothiourea catalyst HyperBTM **30** providing any (but still modest) enantioenrichment at catalytic loadings (10 mol%, 57:43 er). This was attributed to the 1,3-dipole preferentially reacting with the acyl fluoride, and the catalyst only becoming involved in post-cycloaddition esterification. The first successful application of α,β -unsaturated acyl ammonium intermediates in enantioselective cycloadditions was reported by Romo and co-workers in 2014 (Scheme 63, bottom).³² Using α,β -unsaturated acid chlorides **295** and dienes **294** in the presence of (*S*)-BTM **21** and auxiliary base, Diels-Alder cycloaddition furnished bicyclic lactones **296** in good yields and high enantioselectivities (up to 99:1 er). Importantly, an alcohol-tether on the diene was required to facilitate catalyst turnover post-cycloaddition via intramolecular lactonization.



Scheme 63 α,β -Unsaturated acyl ammonium intermediates in cycloaddition reactions.

α,β -Unsaturated acyl ammonium intermediates have also been shown to be viable reaction partners in stepwise cycloadditions, proceeding via a Michael addition – annulation cascade. A range of cyclic motifs are accessible through this strategy, with examples showcasing the formation of cyclopentanes detailed below. In 2013, Romo and co-workers reported the synthesis of highly substituted cyclopentanes employing unsaturated acid chlorides and keto malonates in a one-pot, multistep procedure (Scheme 64, top).¹²⁷ Lithium enolate formation from keto malonate **297** followed by the addition of Lewis base catalyst (*S*)-HBTM **26** and acid chloride **295** furnished the desired cyclopentane products **299** in good yields and excellent diastereo- and enantioselectivity (>19:1 dr, >95:5 er). This process is proposed to proceed via Michael addition of the lithium enolate onto α,β -unsaturated acyl ammonium followed by intramolecular ring closure and lactonization to facilitate catalyst turnover. In 2016, Smith and co-workers employed

malonate tethered enones in a related Michael addition annulation process to generate cyclopentane annulated δ -lactones (Scheme 64, bottom).¹²⁸ *In situ* formation of enolate **301** enables Michael addition onto acid chloride **302** in the presence of isothiurea catalyst (2*S*,3*R*)-HyperBTM **30**. Subsequent intramolecular Michael addition onto the tethered enone followed by lactonization generates the corresponding cyclopentane product **303** with high enantioselectivity.



Scheme 64 Michael addition - annulation cascades using α,β -unsaturated acyl ammonium intermediates.

3.2.2.1 Implications of α,β -unsaturated acyl ammonium formation on reactivity

The effect of acyl ammonium formation on the reactivity of the Michael acceptor can be viewed from two aspects. On the one hand, isothiurea-based ammonium salts are assumed to exhibit an increased steric hindrance at the carbonyl carbon, disfavoring 1,2-addition, making 1,4-addition the preferred pathway.¹²⁹ On the other hand, the positively charged nitrogen can inductively withdraw electron density from the Michael acceptor, which would lead to an increase in electrophilicity at the β -carbon, as well as the carbonyl carbon. However, ¹³C NMR studies have shown that this effect is relatively small (Figure 12).¹³⁰ Comparing the ¹³C shifts of the formed acyl ammonium to the parent acyl chloride or aryl ester reveals only a minimal deshielding of the β -carbon. In contrast to acyl ammonium formation, iminium ion formation exhibits a significant activation of the β -carbon through resonance effects. Hence, the influence of acyl ammonium formation on subsequent reactivity is dominated by steric hindrance at the carbonyl centre, with only minimal activation of the β -carbon for nucleophilic attack.

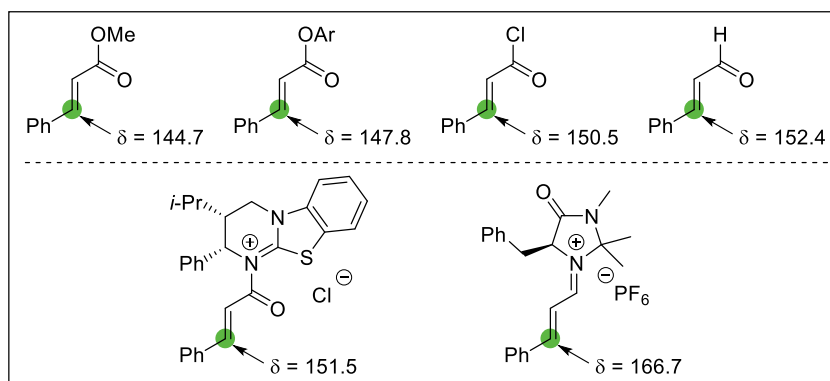
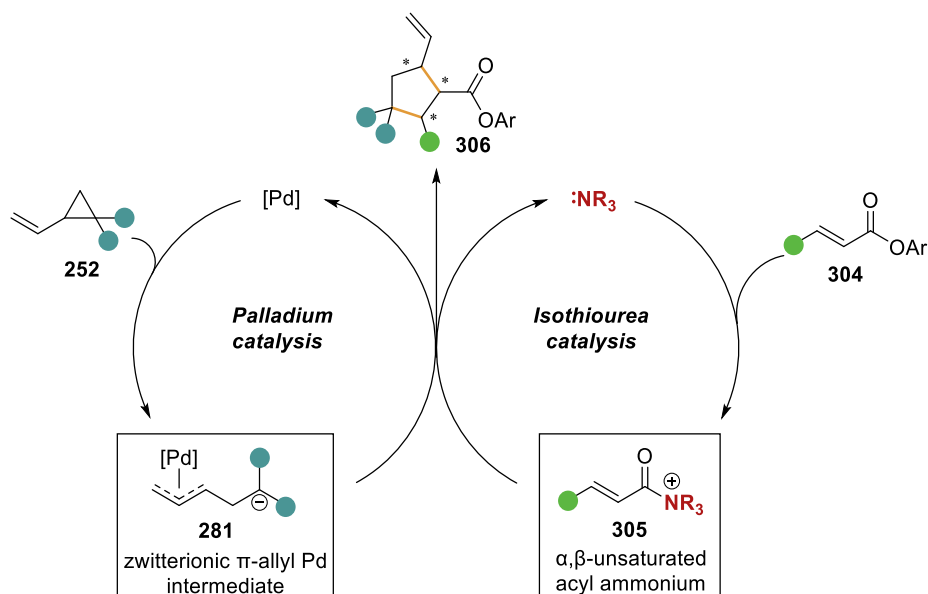


Figure 12 ^{13}C NMR shifts of β -carbons of β -phenyl substituted Michael acceptors; OAr = 4- $\text{NO}_2\text{C}_6\text{H}_4$.

3.3 Concept and Aims

At the onset of this work, the compatibility of isothioureia and transition metal catalysis had been demonstrated in numerous reactions employing ammonium enolate or acyl ammonium intermediates. However, no dual catalytic examples using α,β -unsaturated acyl ammonium species had been reported. Drawing from the reactivity these intermediates have demonstrated in isothioureia-catalysed cycloaddition and Michael addition-annulation processes, expanding the scope of reaction partners to access versatile product scaffolds is of great interest. Particularly attractive would be a strategy where the reactive nucleophile is catalytically generated *in situ* from readily available starting materials. Inspired by the work on dual palladium and secondary amine catalysis for the synthesis of highly substituted cyclopentanes, a related dual catalytic process employing α,β -unsaturated acyl ammonium intermediates and Pd π -allyl zwitterions was envisaged (Scheme 65). In this scenario, the palladium catalyst activates vinylcyclopropane **252** for ring-opening to form zwitterionic Pd π -allyl intermediate **281**. At the same time, the isothioureia catalyst engages α,β -unsaturated aryl ester **304**, forming α,β -unsaturated acyl ammonium **305**. Intermolecular reaction between these intermediates delivers the desired cyclopentane product with up to four contiguous stereogenic centres.



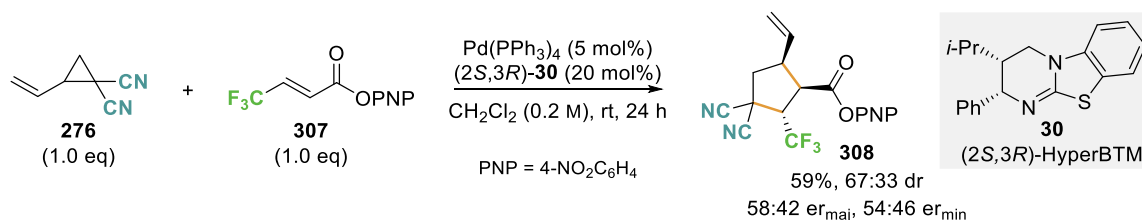
Scheme 65 Proposed dual palladium and isothioureia catalysis.

For this cooperative catalysis strategy to be successful, some major challenges have to be overcome. The palladium and isothioureia catalysts and respective intermediates need to be compatible to avoid catalyst poisoning. Moreover, activation of the substrates must occur simultaneously to allow the intermediates to react with each other. Importantly, the pathway leading to the product must be more favourable than backwards reaction to the starting materials or the formation of side products. Especially for VCPs, self-polymerisation in the absence of a suitable reaction partner is a recognised phenomenon.^{131,132} Finally, to achieve high levels of stereocontrol, the isothioureia catalysed reaction pathway has to be more facile than any uncatalysed racemic background reaction.

3.4 Results and Discussion

3.4.1 Initial Assessment

To assess the feasibility of the proposed cooperative palladium and isothioureia catalysis, dinitrile substituted vinylcyclopropane **276** and β -CF₃ substituted Michael acceptor **307** were treated with (2*S*,3*R*)-HyperBTM **30** and commercially available Pd(PPh₃)₄ in CH₂Cl₂ at room temperature (Scheme 66). Pleasingly, full conversion of starting materials was observed after 24 hours, giving the desired cyclopentane product **308** in 59% isolated yield as an inseparable mixture of two diastereoisomers (67:33 dr), but with low enantioselectivity (58:42 er_{maj}, 54:46 er_{min}). The relative and absolute configuration of the major diastereoisomer were assigned based on crystallographic data (see 3.4.7.2, Figure 15) and considering the catalyst enantiomer used. Interestingly, of the four potential diastereoisomers, only two were formed in the reaction. Importantly, degassing the solvent with argon before the reaction and conducting the transformation under an inert atmosphere were crucial for reactivity.



Scheme 66 Initial assessment of cooperative palladium and isothioureia catalysis.

3.4.2 Optimisation of reaction conditions

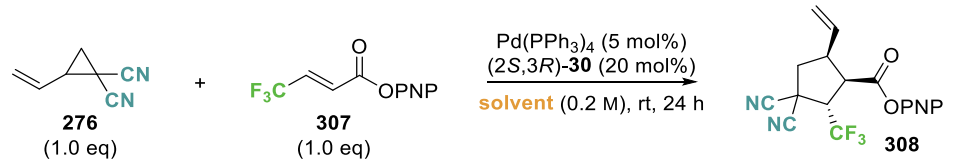
Based on this initial result, the conditions of the cooperative catalysis were modified to improve the yield and stereoselectivity of this transformation. The influence of the solvent, the isothioureia catalyst, the palladium source and ligand, the aryloxy leaving group as well as other parameters were investigated.

3.4.2.1 Solvent screen

First, a range of aprotic solvents with different polarities was trialled in this dual catalytic process. Interestingly, the reaction proceeded in all assessed solvents, albeit with varying ¹H NMR yield and stereoselectivity (Table 6). Performing the reaction in highly polar solvents MeCN and DMF gave the highest NMR yields (83% and 87%, respectively)

(entries 2,3). While MeCN gave the product in similar diastereo- and enantioselectivity to CH₂Cl₂, the use of DMF resulted in an increased stereoselectivity (81:19 dr, 78:22 er_{maj}). A selection of ethereal solvents generally furnished the product in moderate NMR yields and with low enantioselectivity (entries 4-7). The only exception in this series was THF (entry 4), which gave the product in 55% NMR yield, but with promising diastereo- and enantiocontrol (83:17 dr, 78:22 er_{maj}). A selection of preferable, greener solvents was also investigated. Acetone gave the product in good 72% NMR yield with promising diastereo- and enantioselectivity (81:19 dr, 75:25 er_{maj}) (entry 8). Performing the reaction in isopropyl acetate (*i*-PrOAc) resulted in 56% NMR yield with low enantioselectivity (59:41 er_{maj}) (entry 9). The use of 2-MeTHF furnished the product in diminished 35% NMR yield, albeit with promising diastereo- and enantioselectivity (77:23 dr, 71:29 er_{maj}) (entry 10). With DMF, THF and acetone showing similar reactivity and selectivity, acetone was chosen as the optimal solvent based on its classification as a preferred solvent in the solvent selection guide published by Pfizer scientists.¹³³

Table 6 Evaluation of reaction solvents in the cooperative Pd and ITU catalysis.



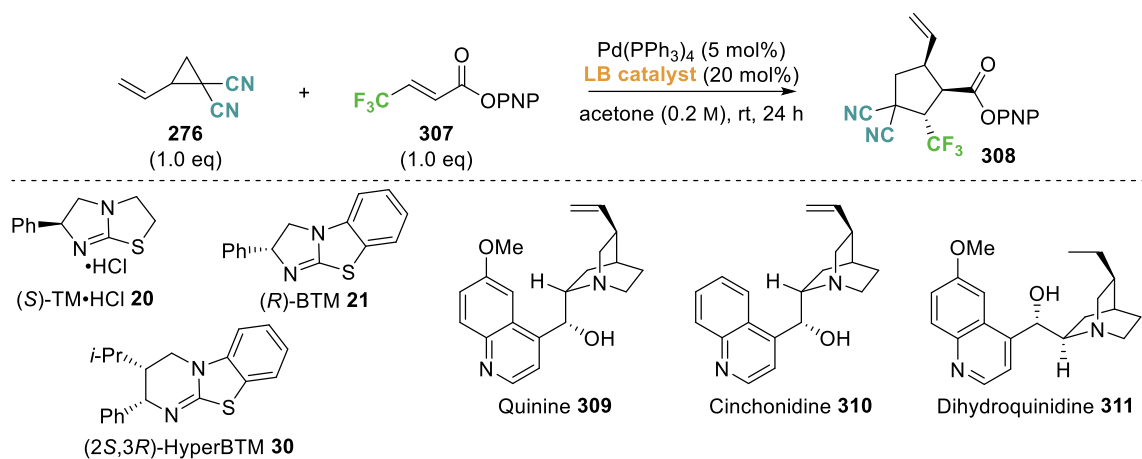
entry ^a	solvent	¹ H NMR yield [%] ^b	dr ^c	er _{maj} ^d	er _{min} ^d
1	CH ₂ Cl ₂	(59) ^e	67:33	58:42	54:46
2	MeCN	83	70:30	59:41	64:36
3	DMF	87	81:19	78:22	91:9
4	THF	55	83:17	78:22	76:24
5	1,4-dioxane	49	82:18	62:38	69:31
6	Et ₂ O	62	67:33	52:48	53:47
7	TBME	63	70:30	51:49	55:45
8	acetone	72	81:19	75:25	76:24
9	<i>i</i> -PrOAc	56	72:28	59:41	61:39
10	2-MeTHF	35	77:23	71:29	69:31

^a Reactions performed on a 0.1 mmol scale. ^b Combined NMR yield of diastereoisomers determined by ¹H NMR analysis using 1,3,5-trimethoxybenzene as internal standard. ^c Determined by ¹⁹F{¹H} NMR analysis of the crude material. ^d Determined by chiral stationary phase HPLC analysis. ^e Combined isolated yield of diastereoisomer.

3.4.2.2 Lewis base catalyst screen

The effect of varying the Lewis base catalyst was next investigated (Table 7). Performing the reaction with (*R*)-BTM **21** as the Lewis base catalyst did not lead to an improvement in ¹H NMR yield or stereoselectivity compared to HyperBTM (entry 2). Use of the isothiourea catalyst (*S*)-TM·HCl **20** resulted in a dramatic increase in diastereoselectivity (95:5 dr) and improved enantioselectivity (15:85 *er*_{maj}) (entry 3). As the minor diastereoisomer was only present in small amounts, its enantiomeric ratio could not be determined with confidence. Notably, as Tetramisole is commercially available as the HCl salt, addition of *i*-Pr₂NEt (20 mol%) to the reaction was necessary to generate the free base *in situ*.

Table 7 Evaluation of tertiary amine Lewis base catalysts.



entry ^a	LB catalyst	¹ H NMR yield [%] ^b	dr ^c	<i>er</i> _{maj} ^d	<i>er</i> _{min} ^d
1	(2 <i>S</i> ,3 <i>R</i>)-HyperBTM 30	93	77:23	72:28	69:31
2	(<i>R</i>)-BTM 21	83	65:35	73:27	92:8
3	(<i>S</i>)-TM·HCl 20 ^e	81	95:5	15:85	-
4	Quinine 309	82	57:43	50:50	48:52
5	Cinchonidine 310	91	55:45	51:49	50:50
6	Dihydroquinidine 311	54	60:40	51:49	50:50
7	(<i>S</i>)-TM·HCl 20 (10 mol%) ^e	88	93:7	18:82	9:91
8	(<i>S</i>)-TM·HCl 20 (5 mol%) ^e	91	83:17	29:71	41:59

^a Reactions performed on a 0.1 mmol scale. ^b Combined NMR yield of diastereoisomers determined by ¹H NMR analysis using 1,3,5-trimethoxybenzene as internal standard. ^c Determined by ¹⁹F{¹H} NMR analysis of the crude material. ^d Determined by chiral stationary phase HPLC analysis. ^e Equimolar amount *i*-Pr₂NEt to TM·HCl added to reaction mixture.

Alternative tertiary amine Lewis base catalysts from the cinchona alkaloid family were also investigated. Although the product was obtained in comparable NMR yields to isothioureia catalysts, only low diastereocontrol and no enantiocontrol was observed in these cases (entries 4-6). With isothioureia catalyst TM·HCl **20** providing the best results, the potential for lowering the Lewis base catalyst loading was also investigated. Performing the reaction with 10 mol% TM·HCl furnished the product in similar NMR yield and stereoselectivity (entry 7). However, a drop in diastereo- and enantioselectivity was observed when only 5 mol% isothioureia catalyst was used (entry 8). These results suggest that the isothioureia catalyst loading can be reduced, but for consistency it was kept at 20 mol% during the optimisation process.

3.4.2.3 Palladium source and ligand screen

As the nature of the palladium source and ligands employed in palladium catalysed processes are known to exert a significant influence on reactivity and selectivity, a selection of palladium precursors and ligands was evaluated (Table 8). Compared to the use of the preformed Pd(0)-complex Pd(PPh₃)₄ (entry 1), employing alternative Pd(0) precursors (Pd(dba)₂ and Pd₂dba₃·CHCl₃) in the absence of phosphine ligands did not result in any product formation with only starting materials returned (entries 2,3). To evaluate ligands other than PPh₃, Pd₂dba₃·CHCl₃ was used as a palladium source in combination with various ligands. Use of bidentate ligand dppe **312** also gave no conversion of starting materials to product (entry 4). Performing the reaction in the presence of Xantphos **313** furnished the product in similar ¹H NMR yield and enantioselectivity to the preformed complex Pd(PPh₃)₄, albeit in lower diastereoselectivity (entry 5). Use of electron-poor phosphine ligand P(2-furyl)₃ (**314**) resulted in a diminished NMR yield, presumably due to an increase in the polymerisation rate of VCP **276**, as only unreacted ester **307** remained. Phosphoramidite ligand **315** showed diminished reactivity, giving only 49% product as determined by ¹H NMR analysis after 24 hours with unreacted starting materials remaining. With Pd(PPh₃)₄ still providing the best result, a reduction in catalyst loading was next investigated. Unfortunately, performing the reaction with only 2.5 mol% Pd(PPh₃)₄ resulted in a reduced reaction rate, giving only 46% NMR yield after 24 hours with unreacted starting materials still remaining (entry 8). Hence, 5 mol% of Pd(PPh₃)₄ were kept as optimal.

Table 8 Evaluation of palladium precursors and ligands.

entry ^a	Pd source	ligand ^b	¹ H NMR yield [%] ^c	dr ^d	er _{major} ^e	er _{minor} ^e
1	Pd(PPh ₃) ₄	-	81	95:5	15:85	-
2	Pd(dba) ₂	-	0	-	-	-
3	Pd ₂ dba ₃ ·CHCl ₃	-	0	-	-	-
4	Pd ₂ dba ₃ ·CHCl ₃	dppe 312	0	-	-	-
5	Pd ₂ dba ₃ ·CHCl ₃	Xantphos 313	81	76:24	14:86	8:92
6	Pd ₂ dba ₃ ·CHCl ₃	P(2-furyl) ₃ 314	50	>95:5	17:83	-
7	Pd ₂ dba ₃ ·CHCl ₃	L 315	49	87:13	29:71	16:84
8	Pd(PPh ₃) ₄ ^f	-	46	95:5	17:83	-

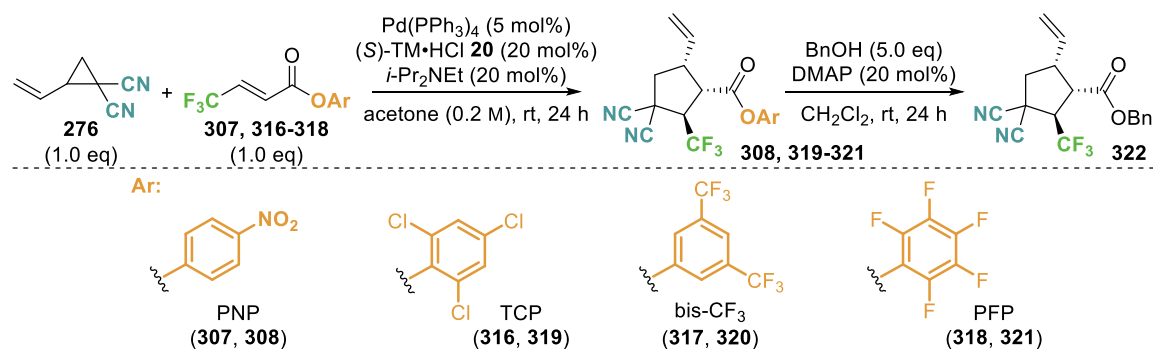
^a Reactions performed on a 0.1 mmol scale. ^b 20 mol% of monodentate ligands (314, 315) or 10 mol% of bidentate ligands (312, 313) used. ^c Combined NMR yield of diastereoisomers determined by ¹H NMR analysis using 1,3,5-trimethoxybenzene as internal standard. ^d Determined by ¹⁹F{¹H} NMR analysis of the crude material. ^e Determined by chiral stationary phase HPLC analysis. ^f 2.5 mol% Pd(PPh₃)₄ used.

3.4.2.4 Screening of aryloxy leaving groups

The aryloxy plays an important role in the dual catalytic process. It must be an effective leaving group to facilitate *N*-acylation of the isothioureia catalyst and also be nucleophilic enough to promote catalyst turnover at the end of the catalytic cycle. Hence, the effect on these properties by varying the steric and electronic nature of the aryloxy was examined (Table 9). In each case, the NMR yield and diastereomeric ratio were determined by ¹H NMR analysis after 24 hours of the crude reaction mixture, with product enantioselectivity determined from the corresponding benzyl ester product after derivatisation of the crude material with BnOH (5.0 eq). Unfortunately, none of the trialled aryloxides showed an improvement in enantioselectivity. 2,4,6-Trichlorophenyl (TCP) ester **316** gave the product with decreased dr (76:24) and in essentially racemic form (entry 2), consistent with *N*-acylation of the isothioureia catalyst being slower than a

competitive, racemic background reaction (see 3.4.3). In addition, derivatisation with BnOH failed to reach completion even after 72 hours, further indication that the steric demand of the *ortho*-chloro substituents limits the reactivity of the carbonyl group. A similar observation was made when using pentafluorophenyl (PFP) ester **318**. Although the reaction proceeded with high stereocontrol, the product was obtained in a drastically reduced NMR yield (45%, entry 4) and derivatisation to the benzyl ester required a prolonged reaction time of 48 hours. These results indicate that aryloxides bearing *ortho*-substituents seem to be less reactive in subsequent derivatisation reactions, limiting their applicability in this cooperative catalysis process. In comparison, 3,5-bis(trifluoromethyl) (bis-CF₃) ester **317** furnished the product in similar diastereo- and enantioselectivity to *para*-nitrophenyl ester **307** (entry 3 and 1, respectively), with full conversion to the benzyl ester after 24 hours. However, as the NMR yield was slightly lower, PNP ester **307** was kept as the most productive substrate.

Table 9 Evaluation of aryl oxide leaving groups.



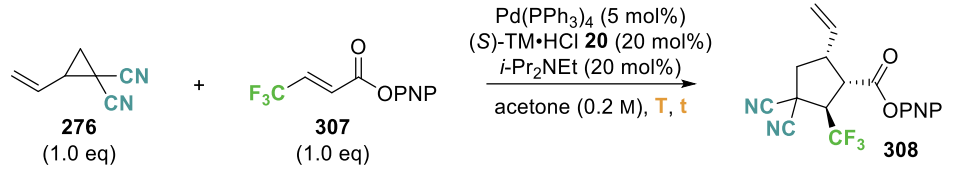
entry ^a	Ar	¹ H NMR yield [%] ^b	dr ^c	er _{maj} ^d	er _{min} ^d
1	PNP	81	95:5	15:85	-
2	TCP ^e	84	76:24	44:56	45:55
3	bis-CF ₃	72	94:6	13:87	-
4	PFP ^f	45	94:6	16:84	-

^a Reactions performed on a 0.1 mmol scale. ^b Combined NMR yield of diastereoisomers determined by ¹H NMR analysis of the crude material using 1,3,5-trimethoxybenzene as internal standard. ^c Determined by ¹⁹F{¹H} NMR analysis of the crude material. ^d Determined from the benzyl ester product by chiral stationary phase HPLC analysis. ^e 72 h reaction time with BnOH. ^f 48 h reaction time with BnOH.

3.4.2.5 Variation of reaction temperature and time

The influence of the reaction temperature and time on the ^1H NMR yield and stereoselectivity was also investigated (Table 10). Unfortunately, lowering the temperature did not lead to an improvement in enantioselectivity. Instead, a drastic decrease in reactivity was observed, resulting in a diminished NMR yield after 24 hours at 0°C (entry 2) or requiring four days to reach full conversion of starting materials (-22°C , entry 3). Performing the reaction at room temperature, the potential for decreasing the reaction time was investigated. Reducing the time to 16 hours still resulted in full conversion of starting materials, giving the product with similar NMR yield and stereoselectivity (entry 4). It is worth noting, however, that slight variations in conversion were observed depending on the current ambient conditions, with temperature in the laboratory varying up to $\pm 5^\circ\text{C}$. Hence, for consistency the reaction time was kept at 24 hours.

Table 10 Influence of reaction temperature and time on the cooperative catalysis.



entry ^a	T [$^\circ\text{C}$]	time [h]	^1H NMR yield [%] ^b	dr ^c	er _{maj} ^d
1	25	24	81	95:5	15:85
2	0	24	42	>95:5	16:84
3	-22	96	86	>95:5	18:82
4	25	16	78	>95:5	16:84

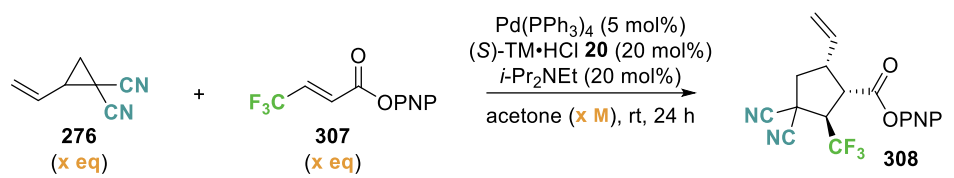
^a Reactions performed on a 0.1 mmol scale. ^b Combined NMR yield of diastereoisomers determined by ^1H NMR analysis using 1,3,5-trimethoxybenzene as internal standard. ^c Determined by $^{19}\text{F}\{^1\text{H}\}$ NMR analysis of the crude material. ^d Determined by chiral stationary phase HPLC analysis.

3.4.2.1 Variation of substrate stoichiometry and concentration

Finally, the influence of the substrate stoichiometry and concentration was also investigated (Table 11). Performing the reaction with an excess of either VCP **276** or PNP ester **307** did not lead to an improvement in ^1H NMR yield or stereoselectivity (entries 2,3). Variation of the reaction concentration had also no influence on the diastereo- and enantioselectivity, giving the product with consistent dr (~95:5) and er (~83:17) (entries 4-82 |

6). Deviation from a concentration of 0.2 M, however, led to a decrease in NMR yield. Hence, the previous conditions employing equimolar amounts of both substrates at 0.2 M concentration were kept as optimal (entry 1).

Table 11 Influence of reactant stoichiometry and concentration.



entry ^a	VCP : PNP	conc. [M]	¹ H NMR yield [%] ^b	dr ^c	er _{maj} ^d
1	1.0 : 1.0	0.2	81	95:5	15:85
2	1.5 : 1.0	0.2	88	>95:5	17:83
3	1.0 : 1.5	0.2	74	94:6	19:81
4	1.0 : 1.0	0.1	68	>95:5	16:84
5	1.0 : 1.0	0.4	70	>95:5	18:82
6	1.0 : 1.0	0.8	63	94:6	19:81

^a Reactions performed on a 0.1 mmol scale. ^b Combined NMR yield of diastereoisomers determined by ¹H NMR analysis of the crude material using 1,3,5-trimethoxybenzene as internal standard. ^c Determined by ¹⁹F{¹H} NMR analysis of the crude material. ^d Determined by chiral stationary phase HPLC analysis.

3.4.3 Mechanistic control experiments

Although the attempts to optimise the cooperative catalysis process resulted in conditions that gave the product in high NMR yield (81%) and with excellent 95:5 dr, the enantioselectivity could not be improved beyond 15:85 er. To gain further mechanistic insight and rule out epimerisation under reaction conditions, a series of control experiments was undertaken. In the absence of palladium catalyst, no reaction occurred with only starting materials returned (Table 12, entry 1). In contrast, in the absence of the isothioureia catalyst the reaction still proceeded but gave the product as a 1:1 mixture of diastereoisomers in racemic form (entry 2). This competitive, racemic background reaction might account for the difficulty in improving the enantioselectivity of the process. Further control experiments were aimed at investigating the effect of the salt *i*-Pr₂NEt·HCl, formed *in situ* upon deprotonation of the isothioureia catalyst TM·HCl **20** with tertiary amine base *i*-Pr₂NEt. Conducting the reaction with the free base TM in the absence of any salt led to a drastic decrease in diastereo- and enantioselectivity (entry 3). Similar

observations were made when the HCl salt of (2*S*,3*R*)-HyperBTM **30** was used compared to the free base (entries 4, 5), suggesting that the salt additive plays a significant role in this dual catalytic process. A more detailed investigation on the effect of different salts will be discussed in the next section (0).

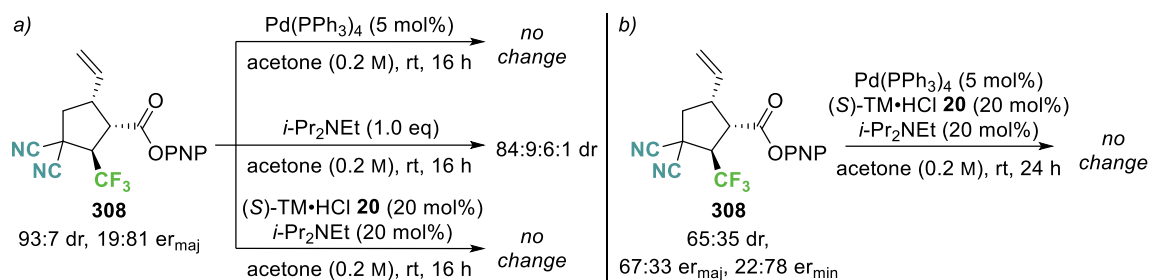
Table 12 Control experiments.

optimised conditions

entry ^a	variation	¹ H NMR yield [%] ^b	dr ^c	er _{maj} ^d	er _{min} ^d
1	no [Pd]	0	-	-	-
2	no ITU, no <i>i</i> -Pr ₂ NEt	95	50:50	50:50	50:50
3	(<i>S</i>)-TM (free base), no <i>i</i> -Pr ₂ NEt	99	67:33	32:68	19:81
4	30 ·HCl	78	>95:5	79:21	64:36
5	30 , no base	93	77:23	72:28	61:39

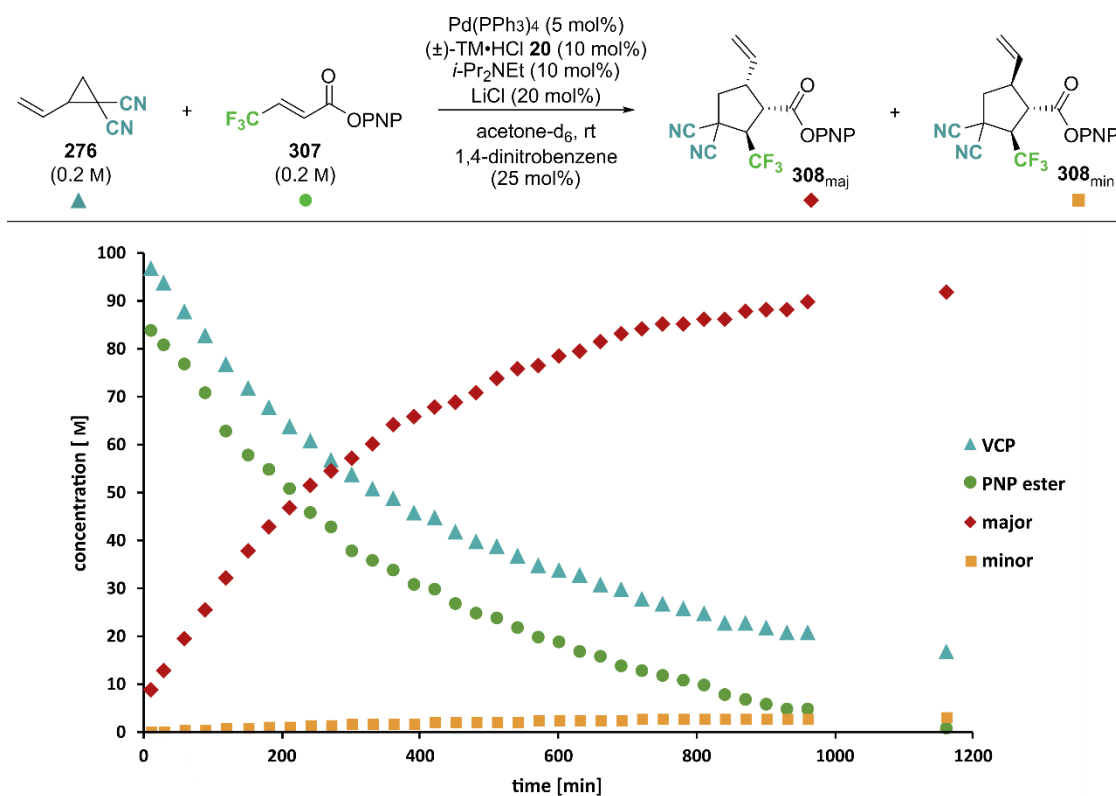
^a Reactions performed on a 0.1 mmol scale. ^b Combined NMR yield of diastereoisomers determined by ¹H NMR analysis of the crude material using 1,3,5-trimethoxybenzene as internal standard. ^c Determined by ¹⁹F{¹H} NMR analysis of the crude material. ^d Determined by chiral stationary phase HPLC analysis.

Next, the PNP ester product **308** was isolated with 93:7 dr and 81:19 er_{maj} and subjected to various conditions with the change in diastereo- and enantioselectivity measured (Scheme 67a). Treating the product with 5 mol% Pd(PPh₃)₄, no change in dr or er was observed. The presence of base (*i*-Pr₂NEt, 1.0 eq) resulted in additional signals detected by ¹⁹F NMR analysis, giving an overall ratio of 84:9:6:1 compared to 93:0:7:0 dr. When the product PNP ester was subjected to catalyst (*S*)-TM·HCl **20** (20 mol%) and *i*-Pr₂NEt (20 mol%), again no change in dr or er was observed. These results indicate that although epimerisation in the presence of an equimolar amount of base can occur, this seems unlikely under reaction conditions. Additionally, the product was synthesised and isolated with a lower diastereoselectivity (65:35 dr) and re-subjected to the standard catalysis conditions (Scheme 67b). No change in the diastereomeric ratio was observed in this case, suggesting that the dr is kinetically controlled and does not change over time.



Scheme 67 Mechanistic control experiments.

To confirm these findings, the reaction progress was monitored by *in situ* ^1H and $^{19}\text{F}\{^1\text{H}\}$ NMR analysis. Using slightly modified reaction conditions with 10 mol% TM·HCl, additional 20 mol% LiCl (see section 0) and 1,4-dinitrobenzene as internal standard, the consumption of starting materials and formation of product over time were analysed and are depicted in Figure 13. Notably, the product is formed with consistently high diastereoselectivity (>95:5 dr), with no erosion observed over the course of the reaction.

Figure 13 Reaction progress monitored by ^1H and $^{19}\text{F}\{^1\text{H}\}$ NMR analysis.

3.4.4 Investigation of salt effect

To further investigate the effect of salt additives on the stereoselectivity of the reaction, different anion – cation combinations were evaluated. For these experiments, (*R*)-BTM **21** was chosen as the isothiourea catalyst to avoid mixtures of different ions, which would have been present when using TM·HCl **20**. Initially, a selection of salts containing various organic and inorganic ions was tested in the cooperative catalysis process. As can be seen from Table 13, the presence of halide ions seemed to be crucial for obtaining high diastereoselectivity, irrespective of the nature of the cation (entries 2-4). Notably, a slight increase in enantioselectivity was also observed in these cases. In contrast, in the absence of a halide ion, the stereoselectivity was comparable to the results obtained without any salt additive (entries 5 and 1). Interestingly, performing the reaction without the isothiourea catalyst but in the presence of 20 mol% *i*-Pr₂NEt·HCl furnished the product with an improved 75:25 dr (entry 6) compared to no additive (50:50 dr, Table 12, entry 2), with both diastereoisomers obtained as racemic mixtures.

Table 13 Evaluation of different salt additives in the cooperative catalysis.

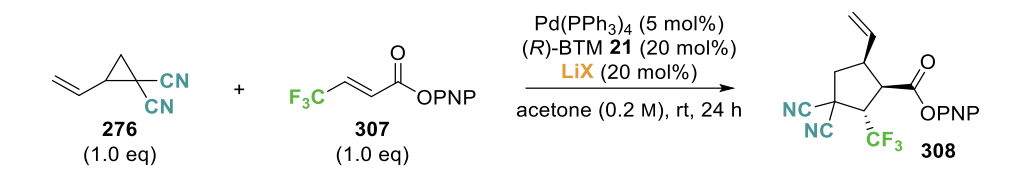
entry ^a	additive	¹ H NMR yield [%] ^b	dr ^c	er _{maj} ^d	er _{min} ^d
1	-	83	65:35	73:27	92:8
2	<i>i</i> -Pr ₂ NEt·HCl	90	>95:5	83:17	-
3	Bu ₄ NBr	85	>95:5	80:20	-
4	LiCl	92	>95:5	86:14	-
5	NaOAc	82	66:34	69:31	57:43
6	<i>i</i> -Pr ₂ NEt·HCl (no ITU)	99	75:25	-	-

^a Reactions performed on a 0.1 mmol scale. ^b Combined NMR yield of diastereoisomers determined by ¹H NMR analysis using 1,3,5-trimethoxybenzene as internal standard. ^c Determined by ¹⁹F{¹H} NMR analysis of the crude material. ^d Determined by chiral stationary phase HPLC analysis.

Next, the influence of different halide ions was further probed by using the corresponding LiX salts (Table 14). Notably, no difference in diastereo- or enantioselectivity was

observed for this series. However, a significant decrease in product ^1H NMR yield was found in the order $\text{Cl}^- > \text{Br}^- \gg \text{I}^-$. Hence, LiCl was selected as the optimal additive.

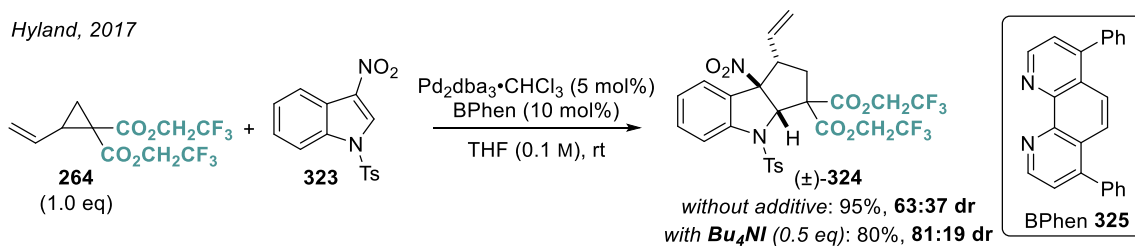
Table 14 Evaluation of LiX salts in the cooperative catalysis.



entry ^a	additive	^1H NMR yield [%] ^b	dr ^c	er _{major} ^d
1	LiCl	92	>95:5	86:14
2	LiBr	87	>95:5	84:16
3	LiI	44	>95:5	-

^a Reactions performed on a 0.1 mmol scale. ^b Combined NMR yield of diastereoisomers determined by ^1H NMR analysis using 1,3,5-trimethoxybenzene as internal standard. ^c Determined by $^{19}\text{F}\{^1\text{H}\}$ NMR analysis of the crude material. ^d Determined by chiral stationary phase HPLC analysis.

These beneficial effects of halide counterions have been previously observed in similar transformations. Hyland and co-workers reported a marked improvement in the diastereoselectivity of the formal (3+2) cycloaddition of VCP **264** to 3-nitroindole **323** in the presence of halide additives (Scheme 68).¹³⁴ In this case, 0.5 equivalents of Bu_4NI gave the best result, providing the product with an improved 81:19 dr compared to 63:37 dr in the absence of any additives.



Scheme 68: Importance of halide ions demonstrated by Hyland and co-workers.

In general, the effect of halide ions in transition metal catalysis is well documented,¹³⁵ and several experimental^{136,137} and computational^{138,139} studies have been undertaken to investigate the implications on Pd π -allyl chemistry in more detail. It was observed that the addition of Cl^- ions generally increases the rate of π - σ - π isomerisation, attributed to enhanced stability caused by Cl^- coordination to the intermediate, tetracoordinate η^1 -complex. This can be rationalised by considering the structural changes in the Pd-allyl complex during the isomerisation process (Figure 14, top). Transitioning from the

η^3 -complex to the η^1 -complex generates a vacant coordination site (yellow box), which can be occupied by access ligand or a solvent molecule to provide additional stabilisation for the η^1 -intermediate. In comparison to the η^3 -complex, the η^1 -complex is higher in energy (Figure 14, bottom). Therefore, the η^3 - η^1 - η^3 isomerisation process is associated with a certain energy barrier. Increased stabilisation of the η^1 -intermediate lowers its energy, which reduces the energy barrier to its formation, leading to an increase in rate for η^3 - η^1 - η^3 isomerisation. As Cl^- ions seem to provide particularly efficient stabilisation compared to excess ligand (e.g. PPh_3) or coordinating solvents (e.g. Et_2O), this simplified consideration can provide a rationale for the observed “halide effect”.

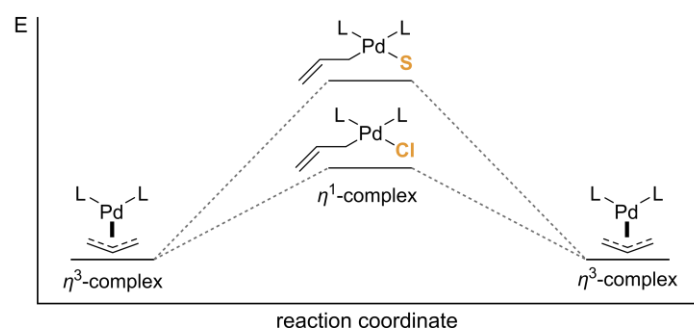
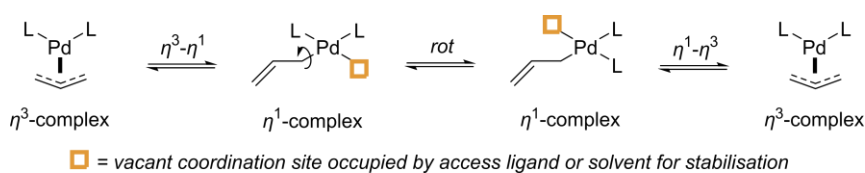
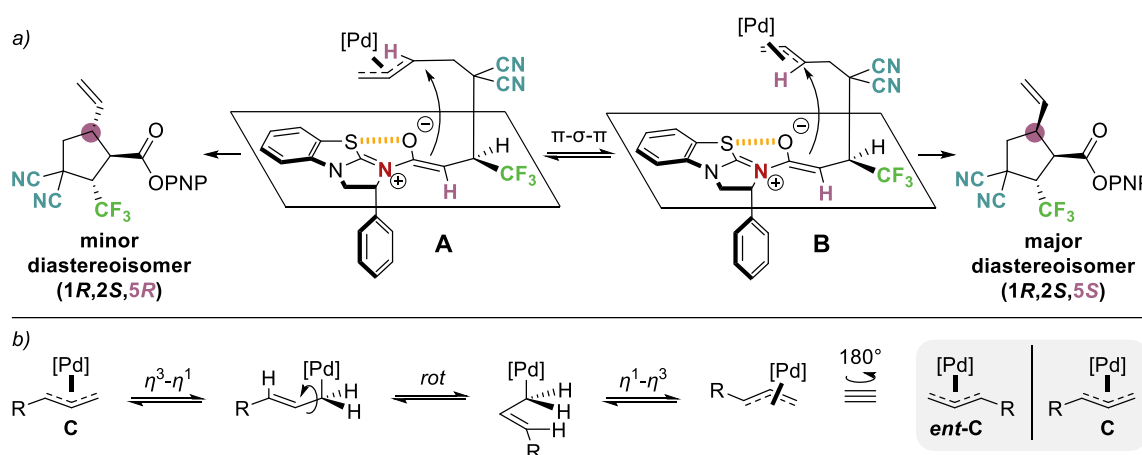


Figure 14 π - σ - π Isomerisation: top) general mechanism; bottom) relative energies of associated intermediates.

The implications of this effect for the current cooperative catalysis process are outlined below. Based on earlier mechanistic control experiments, it has been established that the dr does not change over time once the product had been formed, i.e., the ring-closing step is assumed to be irreversible (see section 3.4.3). For Cl^- ions to influence the diastereoselectivity of the reaction, any π - σ - π isomerisation process must occur faster than ring closure via enolate attack onto the π -allyl fragment. This would allow the formation of the more stable diastereoisomer through continued isomerisation of the different Pd π -allyl intermediates. The postulated intermediates leading to the major and minor diastereoisomers are depicted in Scheme 69a (**A** and **B**). Considering the relative position of the highlighted hydrogen atoms (**H**), intermediate **A** leads to the minor diastereoisomer, displaying an *anti*-relationship between the C(5)-vinyl substituent and the C(1)-ester substituent. Intermediate **B**, on the other hand, exhibits a *syn*-relationship

between the highlighted hydrogen atoms, forming the major diastereoisomer. As no stereocontrol is exerted over the initial π -allyl formation, both intermediates are equally likely to be formed. In the absence of Cl^- ions, the isomerisation process is not fast enough to allow full equilibration to the more favourable *syn*-intermediate **B**, resulting in a lower dr for the product. The addition of Cl^- ions increases the isomerisation rate sufficiently to allow the selective formation of the major diastereoisomer. A more detailed mechanism for this π - σ - π isomerisation process is proposed in Scheme 69b. Notably, this scenario leads to an enantiomerization at the internal allylic carbon, giving rise to the diastereomeric Pd π -allyl intermediates **A** and **B**.



Scheme 69 Effect of π - σ - π isomerisation on cooperative catalysis: a) formation of diastereoisomers. b) allyl isomerisation mechanism.

3.4.5 Re-optimisation of reaction parameters

Having established the beneficial effects of Cl^- ions on the stereoselectivity of the cooperative catalysis process, selected reaction parameters were re-evaluated.

3.4.5.1 Re-evaluation of isothiourea catalysts

At first, various isothiourea catalysts were re-investigated in the presence of 30 mol% LiCl as additive. As the earlier Lewis base catalyst screen showed that the catalyst loading could be reduced to 10 mol% without a decrease in stereoselectivity, this amount was chosen for the current evaluation. Gratifyingly, performing the reaction with 5 mol% $\text{Pd}(\text{PPh}_3)_4$, 10 mol% isothiourea catalyst and 30 mol% LiCl in acetone at room temperature furnished the desired product in high NMR yield and excellent diastereoselectivity (>95:5 dr) (Table 15), irrespective of the isothiourea used. Interestingly, product

enantioselectivity did not vary significantly between the different catalysts, with BTM derivatives generally performing better (entries 3,7,8). As no clear trend was deducible in the isothioureia evaluation and considering the commercial availability of TM·HCl, it was chosen as the catalyst for further evaluations.

Table 15 Evaluation of isothioureia catalysts in the presence of LiCl.

Reaction scheme showing the synthesis of 308 from 276 and 307 using Pd (5 mol%), ITU (10 mol%), and LiCl (30 mol%) in acetone (0.2 M) at room temperature for 24 h.

Reaction conditions: Pd] (5 mol%), ITU (10 mol%), LiCl (30 mol%), acetone (0.2 M), rt, 24 h.

Starting materials: 276 (1.0 eq) and 307 (1.0 eq).

Product: 308.

Chemical structures of ITU catalysts:

- R = Ph: (S)-**20**
- R = *i*-Pr: (S)-**326**
- R = H: (R)-**21**
- R = OMe: (R)-**327**
- (2*S*,3*R*)-**30**
- (2*R*,3*S*)-**328**
- (+)-**329**

entry ^a	ITU	¹ H NMR yield [%] ^b	dr ^c	er _{major} ^d
1	-	97	88:12	49:51
2	(<i>S</i>)-TM·HCl 20 ^e	80	>95:5	18:82
3	(<i>R</i>)-BTM 21	71	>95:5	84:16
4	(2 <i>S</i> ,3 <i>R</i>)-HyperBTM 30	80	95:5	75:25
5	(2 <i>R</i> ,3 <i>S</i>)-HyperSe 328	84	>95:5	17:83
6	(<i>S</i>)- <i>i</i> -PrBTM·HCl 326 ^e	89	>95:5	25:75
7	(+)-fused BTM 329	90	>95:5	84:16
8	(<i>R</i>)-OMeBTM 327	83	>95:5	85:15

^a Reactions performed on a 0.1 mmol scale. ^b Combined NMR yield of diastereoisomers determined by ¹H NMR analysis using 1,3,5-trimethoxybenzene as internal standard. ^c Determined by ¹⁹F{¹H} NMR analysis of the crude material. ^d Determined by chiral stationary phase HPLC analysis. ^e 10 mol% *i*-Pr₂NEt and 20 mol% LiCl used.

3.4.5.2 Evaluation of chiral palladium – isothioureia catalyst combinations

With enantioselectivities for this dual catalytic process still not exceeding 85:15 er_{major}, the potential for improvement by combining a chiral palladium catalyst with a chiral isothioureia was considered (Table 16). Initially, the reproducibility of the reaction conditions was evaluated by performing the reaction with Pd₂dba₃·CHCl₃ and PPh₃ as ligand instead of the preformed Pd(PPh₃)₄ complex in the presence of 10 mol% TM·HCl in acetone, but without additional LiCl (entry 1). However, no conversion of starting materials was observed under these conditions. This raised the question whether the

presence of salts in the reaction mixture could inhibit the formation or reactivity of the active Pd catalyst species. Therefore, the addition of LiCl was suspended for the ligand evaluation and (*R*)-BTM **21** was chosen as isothiourea catalyst. When the initial reaction was repeated using (*R*)-BTM instead of (*S*)-TM·HCl, the product was formed in comparable ¹H NMR yield and stereoselectivity to using preformed Pd(PPh₃)₄ (both in the absence of LiCl additive), but required a prolonged reaction time of 48 h (entry 2). Subsequently, chiral ligand **267** was trialled, as the Trost ligand family has been used on numerous occasions for related, enantioselective formal (3+2) cycloadditions. However, no conversion of starting materials was observed (entry 3). When the solvent was changed to the more commonly used toluene, still no formation of product occurred (entry 4). As a control, the reaction was performed in the absence of isothiourea catalyst, furnishing the product in moderate ¹H NMR yield and stereoselectivity (55%, 62:38 dr, 34:66 er_{major}, entry 5). This result had two important implications: First, it indicated an incompatibility between the Trost ligands and isothioureas. Secondly, it highlights the importance of the isothiourea catalyst for this cooperative catalysis, as the use of a chiral palladium catalyst resulted in inferior stereoinduction. To verify this observation, the reaction was also performed in THF, again in the absence of isothiourea catalyst (entry 6). Although the NMR yield and diastereoselectivity were improved in this case (99%, 79:21 dr), the product was obtained in essentially racemic form. Alternative chiral ligand (*S*)-BINAP **330** was also evaluated in the presence or absence of (*R*)-BTM (entries 7,8). Interestingly, the product was formed with similar levels of enantiocontrol, giving the same major enantiomer in both cases. However, the obtained NMR yield and diastereoselectivity was low (<29%, ~55:45 dr). Finally using (*S*)-BINAP, the reaction was also performed in the presence of 30 mol% LiCl (entry 9). Although a marked improvement in diastereoselectivity was observed, the NMR yield and enantioselectivity remained low. These results indicate that the stereoselectivity of this dual catalytic process is predominantly controlled by the isothiourea catalyst, with the correct choice of palladium – ligand combination being vital for good reactivity. As the trialled ligands performed worse than the preformed Pd(PPh₃)₄ catalyst, the latter was kept as the optimal choice.

Table 16 Evaluation of chiral ligands in the cooperative catalysis.

entry ^a	ligand (mol%)	solvent	¹ H NMR yield [%] ^b	dr ^c	er _{maj} ^d
1 ^e	PPh ₃ (15)	acetone	0	-	-
2 ^f	PPh ₃ (15)	acetone	77	75:25	70:30
3	(<i>R,R</i>)-DACH-Ph (10)	acetone	0	-	-
4	(<i>R,R</i>)-DACH-Ph (10)	toluene	0	-	-
5 ^g	(<i>R,R</i>)-DACH-Ph (10)	toluene	55	62:38	34:66
6 ^g	(<i>R,R</i>)-DACH-Ph (10)	THF	99	79:21	46:54
7	(<i>S</i>)-BINAP (10)	THF	15	56:44	83:17
8 ^g	(<i>S</i>)-BINAP (10)	THF	28	53:47	87:13
9 ^h	(<i>S</i>)-BINAP (10)	THF	17	89:11	65:35

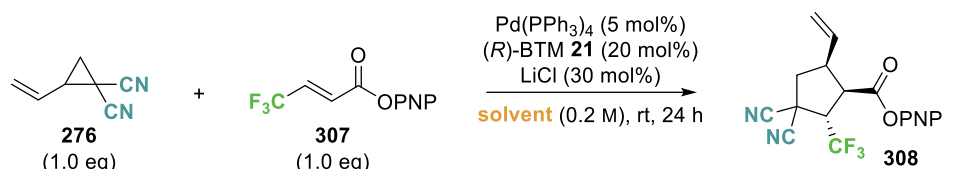
^a Reactions performed on a 0.15 mmol scale. ^b Combined NMR yield of diastereoisomers determined by ¹H NMR analysis using 1,3,5-trimethoxybenzene as internal standard. ^c Determined by ¹⁹F{¹H} NMR analysis of the crude material. ^d Determined by chiral stationary phase HPLC analysis. ^e 10 mol% (*S*)-TM·HCl and 10 mol% *i*-Pr₂NEt used. ^f 48 h. ^g Reaction performed without (*R*)-BTM. ^h 30 mol% LiCl used.

3.4.5.3 Re-evaluation of reaction solvents

At this point, the issues encountered when using TM·HCl **20** in the evaluation of chiral ligands prompted a change to (*R*)-BTM **21** as the preferred isothioureia catalyst in combination with preformed Pd(PPh₃)₄. Based on literature reports for related transformations, toluene, THF and EtOAc were selected for an extended solvent screen. Performing the reaction in the presence of 30 mol% LiCl furnished the desired product in high ¹H NMR yields with excellent diastereoselectivity, except for toluene (entry 2). Importantly, THF and EtOAc gave the product with improved enantioselectivity compared to acetone (>90:10 er_{maj} vs. 87:13 er_{maj}, entries 3,4 vs. 1). Attempts to lower the isothioureia catalyst loading to 10 mol% using EtOAc as the solvent resulted in a slight decrease in product dr and er (entry 5). Finally, a combination of EtOAc and THF in a 3:2

ratio proved optimal, furnishing the product in excellent 92% NMR yield, 95:5 dr and 94:6 er_{maj} .

Table 17 Evaluation of solvents in the presence of LiCl.

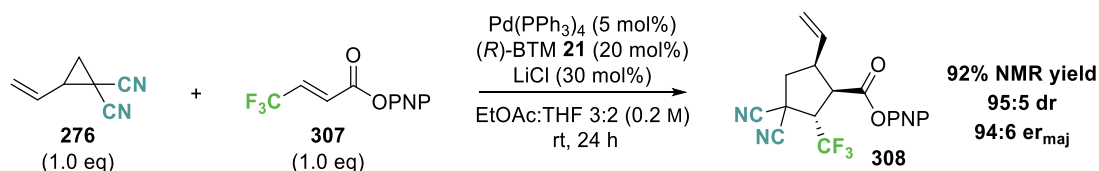


entry ^a	solvent	¹ H NMR yield [%] ^b	dr ^c	er_{maj} ^d
1	acetone	86	>95:5	87:13
2	toluene	77	72:27	69:31
3	THF	63	95:5	92:8
4	EtOAc	88	91:9	91:9
5 ^e	EtOAc	91	88:12	87:13
6	EtOAc:THF 3:2	92	95:5	94:6

^a Reactions performed on a 0.1 mmol scale. ^b Combined NMR yield of diastereoisomers determined by ¹H NMR analysis using 1,3,5-trimethoxybenzene as internal standard. ^c Determined by ¹⁹F{¹H} NMR analysis of the crude material. ^d Determined by chiral stationary phase HPLC analysis. ^e 10 mol% (R)-BTM used.

3.4.6 Key insights from optimisation studies

After performing an extensive evaluation of various reaction parameters, the optimal conditions for this cooperative palladium and isothioureia catalysis process have been established using 5 mol% Pd(PPh₃)₄, 20 mol% (R)-BTM **21** and 30 mol% LiCl in a mixed solvent system (EtOAc:THF 3:2) at room temperature for 24 hours (Scheme 70).



Scheme 70 Optimised reaction conditions for the cooperative palladium and isothioureia catalysis.

The following key points should be highlighted from the optimisation results:

- a suitable palladium catalyst was required for reactivity.
- a racemic background reaction occurred in the absence of isothioureia catalyst, resulting in a 1:1 mixture of diastereoisomers.

- the isothioureia catalyst was essential for obtaining high levels of stereocontrol, as inferior results were obtained when a chiral palladium catalyst was used instead.
- the addition of a sub-stoichiometric amount of Cl⁻ ions in the form of LiCl was crucial for excellent diastereocontrol (>95:5 dr) and resulted in improved levels of enantiocontrol.
- a wide range of reaction conditions allowed the formation of product in good yield. However, to achieve high levels of stereocontrol, a careful choice of the appropriate combination of catalysts, additives and solvent was pivotal.

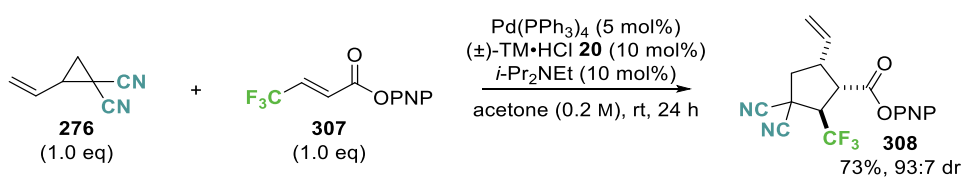
3.4.7 Scope and Limitations

Having established the optimal conditions for the synthesis of highly functionalised cyclopentane products via dual palladium and isothioureia catalysis, the scope and limitations of this process were next evaluated. Initially, different nucleophiles were trialled for post-catalysis transformations to ensure the reproducibility of the isolated product yields. Next, the nature of β-substituents tolerated within the Michael acceptor was investigated. Finally, the influence of various electron-withdrawing groups within the VCP was studied.

3.4.7.1 Evaluation of nucleophile addition post-catalysis

*Note: The following investigations were performed prior to the final optimisation of the catalysis reaction conditions. At this point, isothioureia catalyst TM·HCl 20 in combination with *i*-Pr₂NEt in acetone were used to generate the desired cyclopentane product. However, as the influence of the catalysis conditions on the subsequent nucleophilic derivatisation should be negligible, the results obtained from this study were considered as generally applicable.*

First, direct isolation of the product as the PNP ester was evaluated (Scheme 71). Purification of the crude reaction mixture via silica column chromatography allowed the isolation of the PNP ester product **308** in 73% yield as an inseparable mixture of diastereoisomers with high 93:7 dr.



Scheme 71 Direct isolation of cyclopentane PNP ester.

Although isolation of the PNP ester proved feasible, the yield seemed highly dependent on the speed with which the column chromatographic purification was performed. Prolonged time on the column led to reduced isolated yields, presumably due to hydrolysis of the PNP ester under these conditions. To simplify the isolation and purification procedure and to improve the reproducibility, independent of the practitioner, alternative nucleophilic derivatisations post-catalysis were investigated (Table 18). For this purpose, the respective nucleophiles were directly added to the catalysis reaction mixture after 24 hours. First, commonly used benzylamine (BnNH₂) and benzyl alcohol (BnOH) were selected. The addition of 5.0 eq BnNH₂ furnished the corresponding amide product **331** after 4 hours in 49% isolated yield (entry 1). In addition, bicyclic product **332** was also isolated from the reaction as an inseparable mixture of diastereoisomers (92:8 dr) in 24% yield (Scheme 72). Although this represents an interesting opportunity for further product derivatisation, specifically the desymmetrization of the C(3) nitrile groups, the existence of multiple product isomers was undesirable for a generally applicable, simple derivatisation protocol. In addition, close monitoring of the reaction progress was critical, as a prolonged reaction time led to a drastic decrease in yield and the formation of numerous side-products.

Table 18 Evaluation of nucleophiles for *in situ* post-catalysis derivatisation.

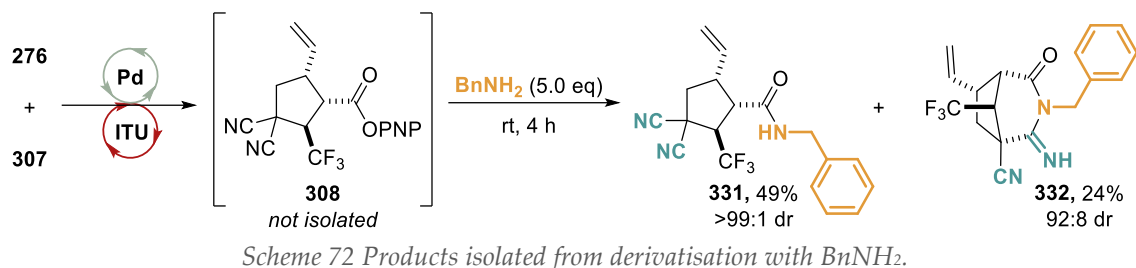
entry ^a	NuH (eq)	product	yield [%] ^b	dr ^c
1 ^d	BnNH ₂ (5.0)	331	49	>99:1
		332	24	92:8
2	BnOH ^e (5.0)	322	56	>95:5
3	MeOH ^e (25.0)	333	72	>95:5

^a Reactions performed on a 0.25 mmol scale. ^b Combined isolated yield of diastereoisomers.

^c Determined by ¹⁹F{¹H} NMR analysis of the crude material. ^d Reaction stopped after 4 h of BnNH₂ addition. ^e 20 mol% DMAP added.

Use of BnOH gave benzyl ester **322** in 56% isolated yield and in excellent >95:5 dr (entry 2), without the formation of side-products or decomposition. Alternatively, MeOH provided the corresponding methyl ester **333** in improved 72% isolated yield and similar

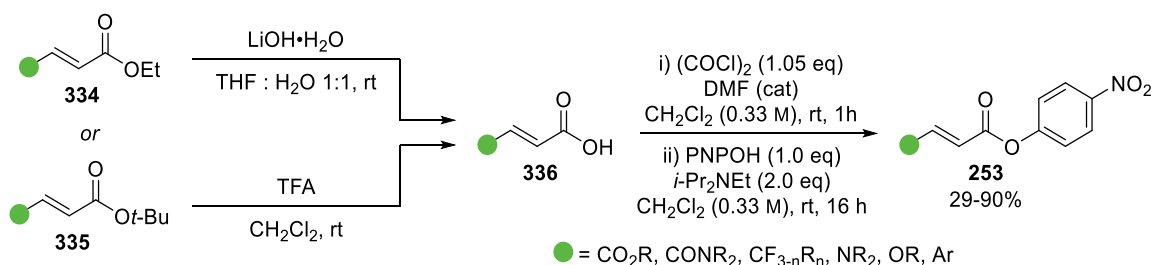
diastereoselectivity (>95:5 dr, entry 3), proving optimal for the intended *in situ* derivatisation. Notably, the addition of DMAP as catalyst in combination with simple alcohol nucleophiles BnOH and MeOH was necessary, as almost no conversion of the PNP ester was observed in its absence.



3.4.7.2 Variation of Michael acceptor

3.4.7.2.i. Synthesis of β -substituted Michael acceptors

To assess the generality of the cooperative catalysis, a range of differently substituted Michael acceptors was prepared. Considering that a common limitation in α,β -unsaturated acyl ammonium catalysis is the requirement for Michael acceptors bearing electron-withdrawing β -substituents, substrates containing ester, amide and polyfluorinated groups were targeted. In addition, Michael acceptors containing aryl and heteroatom substituents were also prepared. The synthesis of the target compounds followed the general route outlined below (Scheme 73). Starting from the corresponding ethyl (**334**) or *t*-butyl ester (**335**), which were either commercially available or prepared following literature procedures, hydrolysis under basic or acidic conditions furnished the desired carboxylic acid **336**. Conversion of the acid to the acid chloride using oxalyl chloride followed by esterification with *p*-nitrophenol (PNPOH) in a one-pot two-step procedure gave the corresponding PNP esters **253** in generally high yields (29-90%).



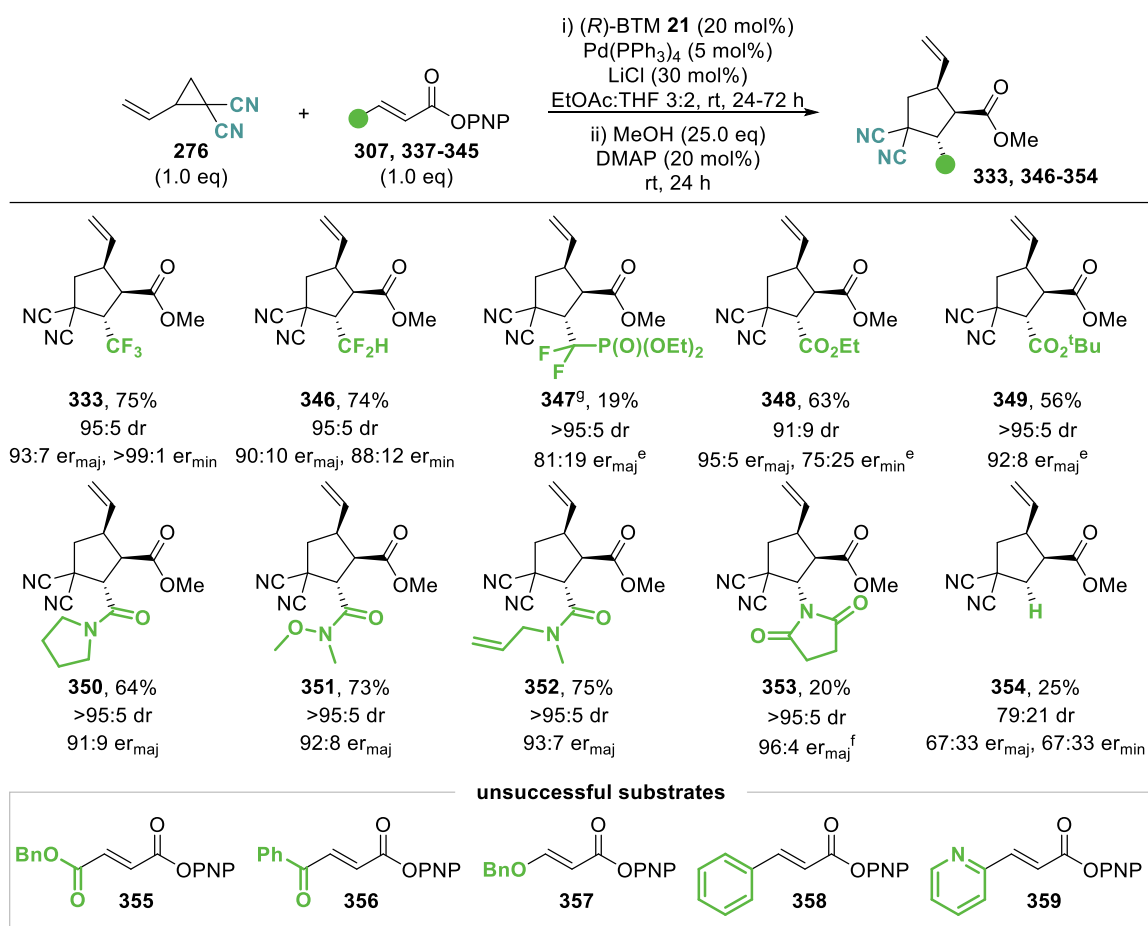
Scheme 73 General synthetic route towards β -substituted PNP esters.

3.4.7.2.ii. β -Substituted Michael acceptors in the cooperative catalysis

With a range of β -substituted Michael acceptors in hand, their applicability in this cooperative catalysis was investigated. Using the optimised conditions of 20 mol% (*R*)-BTM **21**, 5 mol% Pd(PPh₃)₄ and 30 mol% LiCl in EtOAc/THF furnished the CF₃ containing cyclopentane product **333** in 75% yield with 95:5 dr and high enantioselectivity (93:7 *er*_{major}, >99:1 *er*_{minor}). Moving to a CF₂H substituent gave the product **346** in similar yield and dr, but with slightly reduced enantioselectivity (90:10 *er*_{major}, 88:12 *er*_{minor}). Notably, the presence of the medicinally relevant difluorophosphonate group CF₂P(O)(OEt)₂¹⁴⁰ was also well tolerated in the catalysis, furnishing the PNP ester product within 24 hours in high dr, but slightly reduced 81:19 *er*_{major}. However, *in situ* derivatisation with MeOH proved troublesome, as the reaction stopped at around 50% conversion, ultimately requiring 1.0 eq of DMAP and a prolonged reaction time of 4 days to reach full conversion to the methyl ester product **347**. The observed difficulties are a likely explanation for the low isolated yield in this case (19%). Alternatively, direct isolation of the corresponding PNP ester proved equally fruitless, resulting in an even lower isolated yield, likely due to product decomposition during column chromatography. Other non-fluorinated electron-withdrawing β -substituents also led to product formation. Use of different ester groups as β -substituent gave the corresponding products **348** and **349** in slightly reduced yield, but with excellent diastereo- and enantioselectivity (\geq 91:9 dr, up to 95:5 *er*_{major}). Notably, *t*-butyl ester containing product **349** could be isolated as a single diastereoisomer in 56% yield after purification by column chromatography. Different amide substituents also provided good reactivity, giving the products **350-352** in high yields (64-75%) and with excellent dr and er (>95:5 dr, \geq 91:9 *er*_{major}). Notably, incorporation of an allyl unit within the amide substituent did not lead to any side reactions, with cyclopentane **352** isolated as a rotameric mixture (5:4) in 75% yield. Incorporation of *N*-succinimide as a heteroatom substituent gave the cyclopentane product **353** in a diminished 20% isolated yield, but with excellent stereoselectivity (>95:5 dr, 96:4 *er*_{major}). In this case, the corresponding Michael acceptor (**344**) showed significantly reduced reactivity, requiring 72 hours for the cooperative catalysis to reach full conversion. Additionally, an excess of VCP was necessary as VCP polymerisation occurred as a competing reaction pathway. The reduced reactivity observed might in part be due to the heterogeneity of the reaction mixture, as the incorporation of the succinimide substituent drastically decreased solubility. This was

also observed for the final methyl ester product **353**, complicating purification and contributing to the low isolated yield. Finally, acrylic acid derived Michael acceptor **345** was also probed, giving the cyclopentane product **354** in only 25% isolated yield after a prolonged reaction time (48 h) with drastically reduced diastereo- and enantioselectivity (79:21 dr, 67:33 er). Although no formation of side-products or decomposition of starting materials was observed, potential polymerisation of both starting materials as a rationale for the low product yield cannot be ruled out.

Table 19 Scope of Michael acceptors in the cooperative catalysis. ^{a-d}



^a Reactions performed on a 1.0 mmol scale. ^b Combined isolated yield of diastereoisomers. ^c dr of isolated product after purification by silica column chromatography determined by ¹⁹F{¹H} or ¹H NMR analysis. ^d er determined by chiral stationary phase GC or HPLC analysis. ^e er determined by chiral stationary phase HPLC analysis from the intermediate PNP ester product. ^f er determined by ¹⁹F{¹H} NMR analysis after derivatisation with (S)-1-(4'-Fluorophenyl)ethanol. ^g Derivatisation run with 1.0 eq DMAP for 96 h.

The use of benzyl ester containing Michael acceptor **355** resulted in partial conversion of starting materials, with slow decomposition of product observed, indicative of an incompatibility of the benzyl ester functionality with the current dual catalytic process. Incorporation of a β-ketone substituent (**356**) led to rapid conversion of starting materials,

but resulted in a messy reaction mixture with no product signals detectable. Benzyl ether and 2-pyridine containing Michael acceptors **357** and **359** proved insoluble under reaction conditions, with no product formation detected. Phenyl containing substrate **358** also showed no reactivity under the catalysis conditions. Notably, full consumption of VCP was observed in these three cases, indicating that VCP polymerisation will occur in the absence of a suitable reaction partner. These examples further highlight the importance of a sufficiently electron-withdrawing substituent in the β -position, with aryl substrates proving traditionally challenging in α,β -unsaturated acyl ammonium catalysis. The relative and absolute configuration of the major (1*R*,2*S*,5*S*)-diastereoisomer **349_{maj}** was determined by single crystal X-ray diffraction analysis with all other products assigned by analogy.

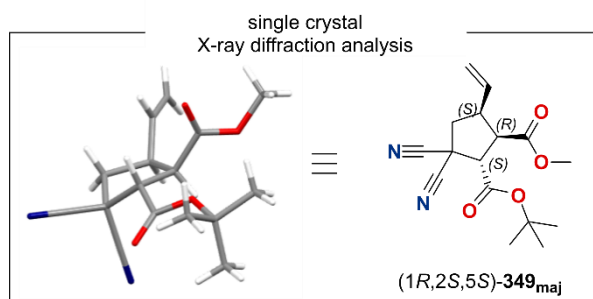


Figure 15 Crystal structure for major diastereoisomer **349_{maj}**.

The limitations of the cooperative catalysis process were further probed by employing β -disubstituted Michael acceptor **360** to furnish the corresponding cyclopentane product containing an all-carbon quaternary centre (Figure 16). Performing the reaction under standard conditions resulted in partial conversion of PNP ester **360** and full consumption of VCP **276** after 24 hours as determined by ^1H NMR monitoring of the reaction progress. Unfortunately, the addition of another equivalent VCP **276** to the reaction mixture did not lead to any further conversion of Michael acceptor, but again resulted in full consumption of VCP after another 24 hours. This indicates inhibition of the catalysis process after a certain amount of product had been formed. Interestingly, a change in product dr was detected between 24 and 48 hours, which has not been observed previously.

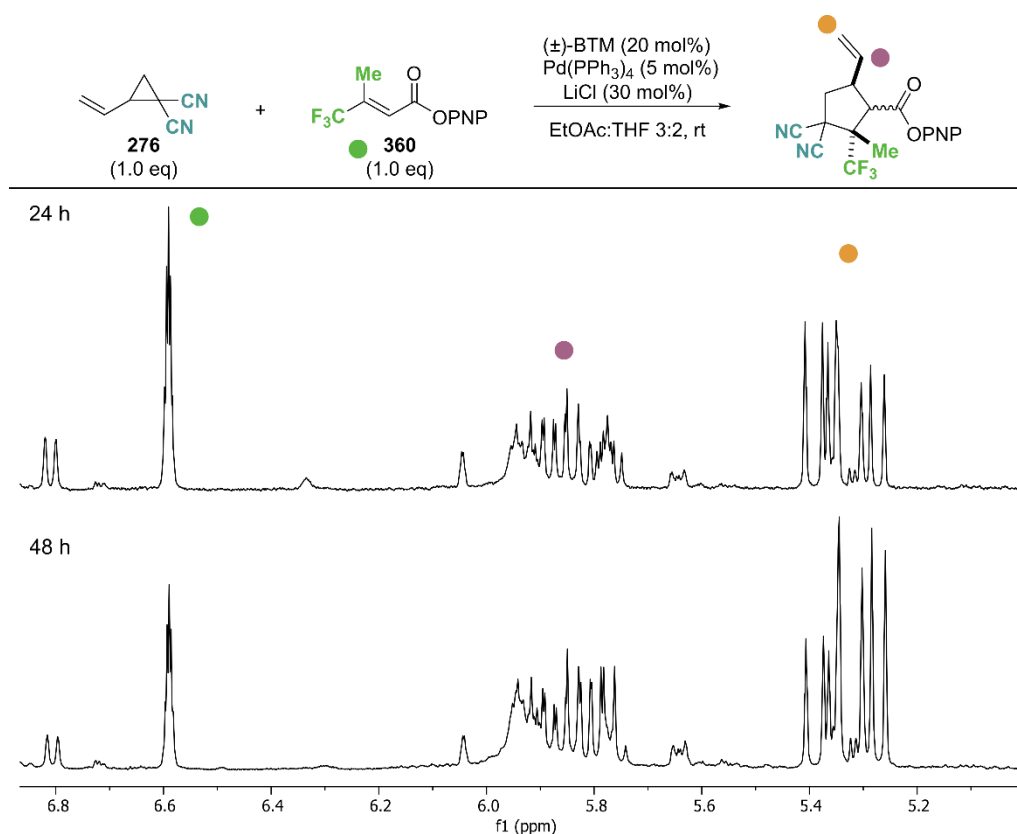
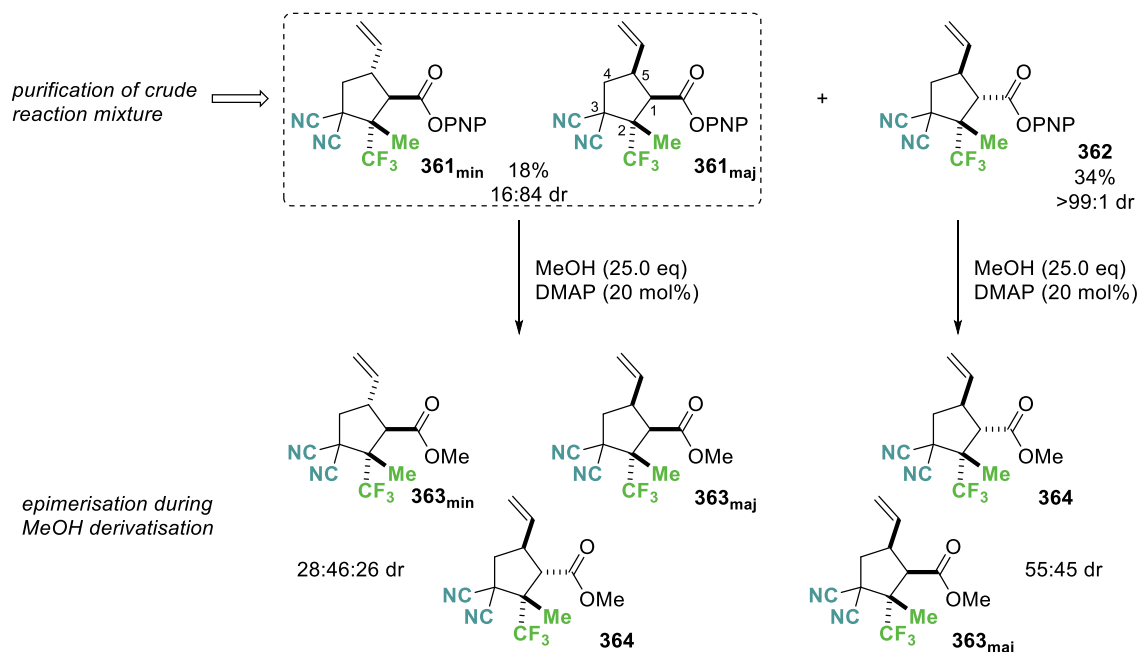


Figure 16 ^1H NMR monitoring of reaction progress using Michael acceptor **360**.

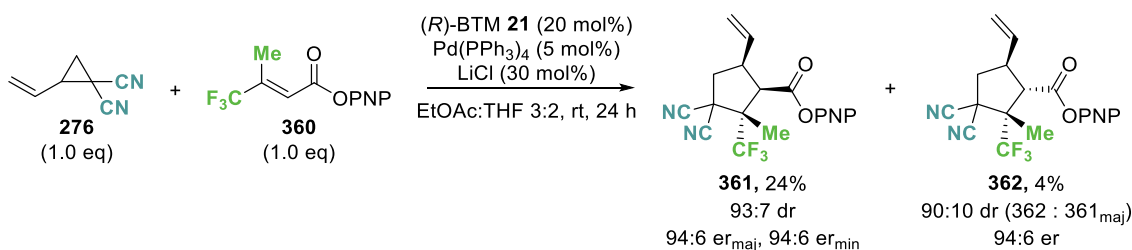
Purification of the crude reaction mixture at this point resulted in the isolation of three diastereoisomers (Scheme 74). Based on the mechanistic understanding of the cooperative catalysis process, the initially formed major diastereoisomer **361**_{maj} was assigned in analogy to the other cyclopentane products. In addition, minor diastereoisomer **361**_{min} was also formed in the process, being epimeric at C(5). As ^1H NMR analysis showed, diastereoisomer **361**_{maj} decreases over time, with a new, previously unobserved diastereoisomer **362** increasing at the same rate. This third diastereoisomer is proposed to arise from epimerisation at C(1) and was fully separable by column chromatography from **361**_{maj} and **361**_{min}, which were isolated as an inseparable mixture with 84:16 dr. Subsequent derivatisation of the isolated PNP esters with MeOH (25.0 eq) and DMAP (20 mol%) resulted in further interconversion of diastereoisomers. Unfortunately, the methyl ester derivatives were no longer separable by column chromatography. These observations suggest that an increase in steric congestion at the C(2) centre leads to an increased acidity of the C(1) hydrogen atom, facilitating epimerisation under the catalysis and derivatisation conditions. Moreover, with the methyl and CF_3 substituent being

comparable in size, there seems to be no preference for the relative orientation of the ester substituent, leading to a thermodynamic equilibrium.



Scheme 74 Observed epimerisation upon introduction of quaternary centre.

In light of these observations, the cyclopentane product was isolated as the PNP ester after 24 hours reaction time, giving the product in a total 28% yield as three diastereoisomers, all with high 94:6 er.



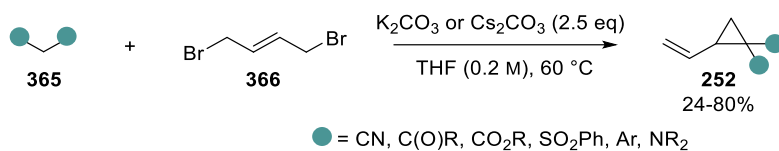
Scheme 75 Isolated cyclopentane products bearing an all-carbon quaternary centre.

3.4.7.3 Variation of vinylcyclopropane

3.4.7.3.i. Synthesis of vinylcyclopropanes

To probe the scope and limitations of the vinylcyclopropane starting material, the nature of the acceptor groups was varied. Based on literature examples of related processes, VCPs bearing nitrile, ester and sulfone groups as well as heterocyclic acceptor groups were targeted. The desired vinylcyclopropanes were synthesised in one step from (typically) commercially available starting materials following a literature procedure¹⁴¹ with slight modifications (Scheme 76). Reacting equimolar amounts of the corresponding

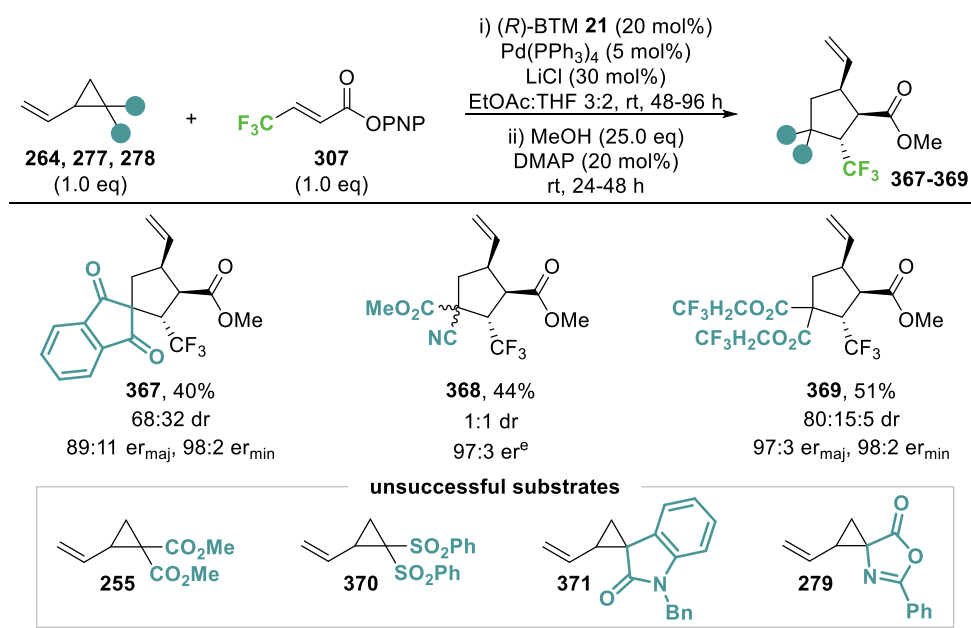
C-H acidic compound **365** bearing the desired electron-withdrawing groups and 1,4-dibromobutene **366** in the presence of base furnished the corresponding VCPs in generally high yields (24-80%).



Scheme 76 General synthesis strategy towards vinylcyclopropanes.

3.4.7.3.ii. Scope of vinylcyclopropanes in the cooperative catalysis

Next, variation of the electron-withdrawing groups within the VCP starting material was investigated. Use of 1,3-indanedione substituted VCP **278** gave the spirocyclic product **367** in 40% isolated yield with drastically reduced diastereoselectivity (68:32 dr), but good enantioselectivity (89:11 er_{maj}). Employing unsymmetrically substituted VCP **277** bearing a nitrile and an ester group furnished cyclopentane product **368** bearing four contiguous stereogenic centres in 44% yield and with excellent enantioselectivity (97:3 er). Unfortunately, Michael addition of the intermediate zwitterion was not selective, resulting in a 1:1 mixture of partially separable diastereoisomers epimeric at the quaternary carbon centre. Notably, the catalysis employing unsymmetrical VCP **277** or indanedione substituted VCP **278** required a prolonged 48 hours to reach full conversion. The decrease in reactivity was even more pronounced when moving to diester substituted VCPs. Use of di(trifluoroethyl) ester activated VCP **264** necessitated a reaction time of four days to reach full conversion, furnishing cyclopentane **369** in 51% isolated yield with moderate 80:15:5 dr, but excellent enantioselectivity (97:3 er_{maj}). When simple methyl ester substituted VCP **255** was used, no reactivity was observed at all. Employing disulfone containing VCP **370** was equally unsuccessful with only starting materials returned. In the case of oxindole substituted VCP **371**, which was employed as a single diastereoisomer, no reaction with Michael acceptor **307** was observed. Instead, epimerisation of the VCP in the presence of Pd(PPh₃)₄ occurred, resulting in a 60:40 diastereomeric mixture after 24 hours. Similar observations have been reported by Yang and co-workers.¹⁴² Finally, azlactone derived VCP **279** was trialled in the cooperative catalysis. Although good reactivity was observed, resulting in full consumption of starting materials within 24 hours, a complex mixture of products was obtained.

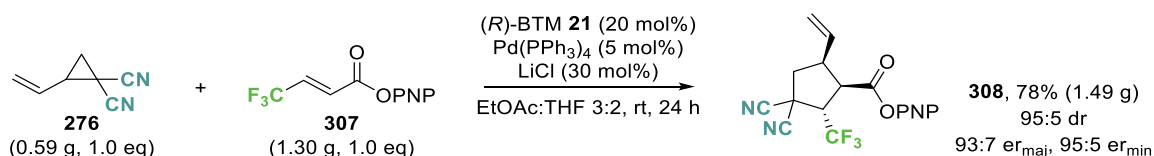
Table 20 Scope of vinylcyclopropanes in the cooperative catalysis. ^{a-d}

^a Reactions performed on a 1.0 mmol scale. ^b Combined isolated yield of diastereoisomers. ^c dr of isolated product after purification by silica column chromatography determined by ¹⁹F{¹H} NMR analysis. ^d *er* determined by chiral stationary phase GC or HPLC analysis. ^e *er* determined by chiral stationary phase HPLC analysis from the intermediate PNP ester. The *er* for the other diastereoisomer could not be determined.

These results highlight the requirement for sufficiently electron-withdrawing groups within the VCP substrate to facilitate reaction with the α,β -unsaturated acyl ammonium intermediate generated in the cooperative catalysis. Moreover, the reaction outcome with regards to product yield and dr seems very sensitive to the nature of the VCP partner. The decrease in reactivity upon variation of the VCP has been observed in related literature examples, and is one of the limitations of these processes, often requiring additional optimisation for each VCP substrate. However, enantioselectivities remain high throughout the scope of VCPs in this cooperative catalysis, indicative of the excellent stereocontrol exhibited by the isothiourea catalyst.

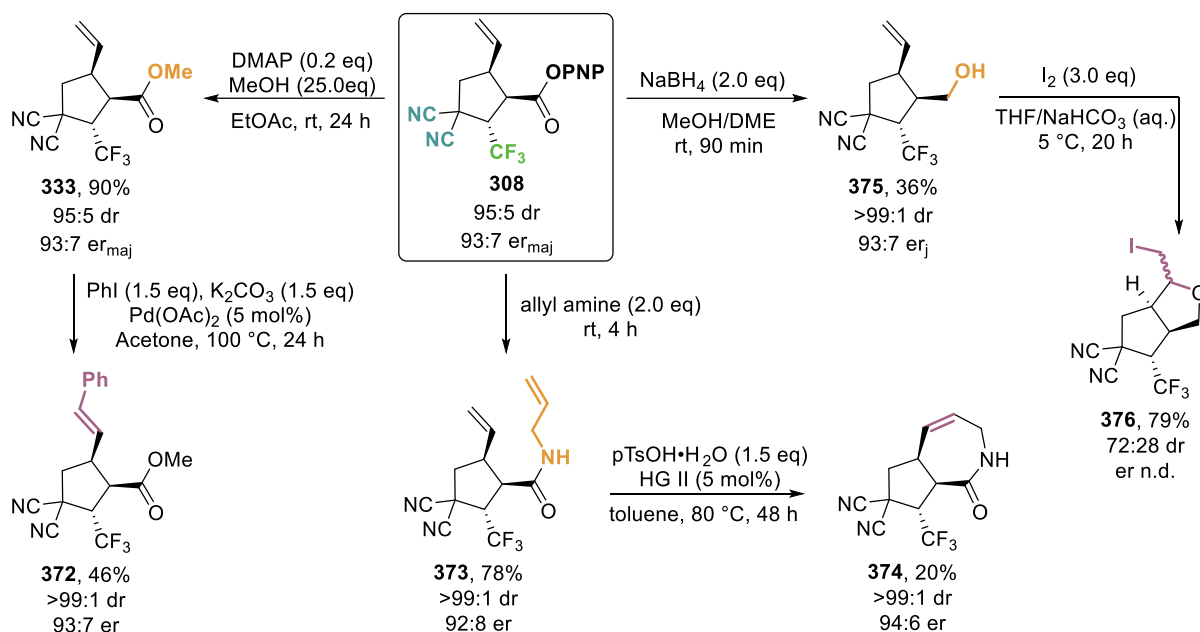
3.4.8 Scalability and product derivatisations

To demonstrate the practicality of the developed cooperative catalysis process, the reaction was performed at gram scale. Employing dinitrile substituted VCP **276** (0.59 g, 5.0 mmol) and Michael acceptor **307** (1.30 g, 5.0 mmol) under standard catalysis conditions furnished the desired cyclopentane product **308** after 24 hours in high 78% isolated yield (1.49 g) with excellent diastereo- and enantioselectivity (95:5 dr, 93:7 *er*_{maj}) identical to the small-scale reaction.

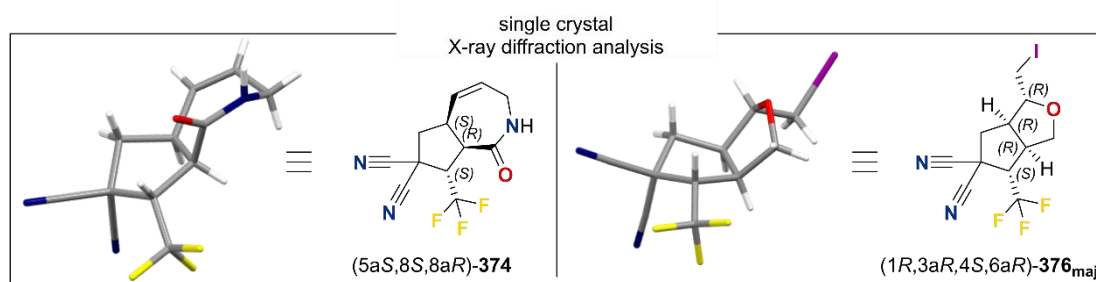


Scheme 77 Gram scale experiment.

To further showcase the synthetic utility of the cyclopentane products, PNP ester **308** was subjected to a range of derivatisation conditions, followed by additional transformations aimed at increasing molecular complexity. Treating the isolated PNP ester product **308** with MeOH and DMAP gave the corresponding methyl ester **333** in excellent 95% isolated yield and unchanged dr and er. Notably, the yield obtained for the stepwise isolation – esterification procedure is similar to the yield obtained following *in situ* MeOH derivatisation (74% vs 75%, respectively). A subsequent Heck coupling reaction on methyl ester **333** gave the desired (*E*)-alkene **372** in modest 46% yield without erosion of enantiopurity. Derivatisation of PNP ester **308** with allyl amine was also well tolerated, furnishing allyl amide **373** in 78% isolated yield as a single diastereoisomer after purification by column chromatography. Subsequent ring-closing metathesis employing Hoveyda-Grubbs second generation ruthenium catalyst (HG II) furnished bicyclic lactam **374**, albeit in only 20% yield. The structure and relative configuration of lactam **374** was further confirmed by single crystal X-ray diffraction analysis (Figure 17, left). Finally, reduction of the PNP ester was also attempted using NaBH₄ as the reducing agent. However, this reaction generally resulted in low yields and the formation of numerous side-products. Performing the reaction in a mixture of MeOH and DME proved optimal as side-product formation could be minimised. Nonetheless, alcohol **375** could only be isolated in 36% yield, but as a single diastereoisomer with excellent enantioselectivity (93:7 *er*). Treatment of the cyclopentane alcohol **375** with I₂ in the presence of base facilitated intramolecular iodocyclisation to yield bicyclic ether **376** in 78%. Notably, this transformation was not selective with regards to the newly formed stereogenic centre, yielding a separable mixture of diastereoisomers (72:28 dr). The relative and absolute configuration of the major diastereoisomer **376**_{maj} were also confirmed by single crystal X-ray diffraction analysis (Figure 17, right).

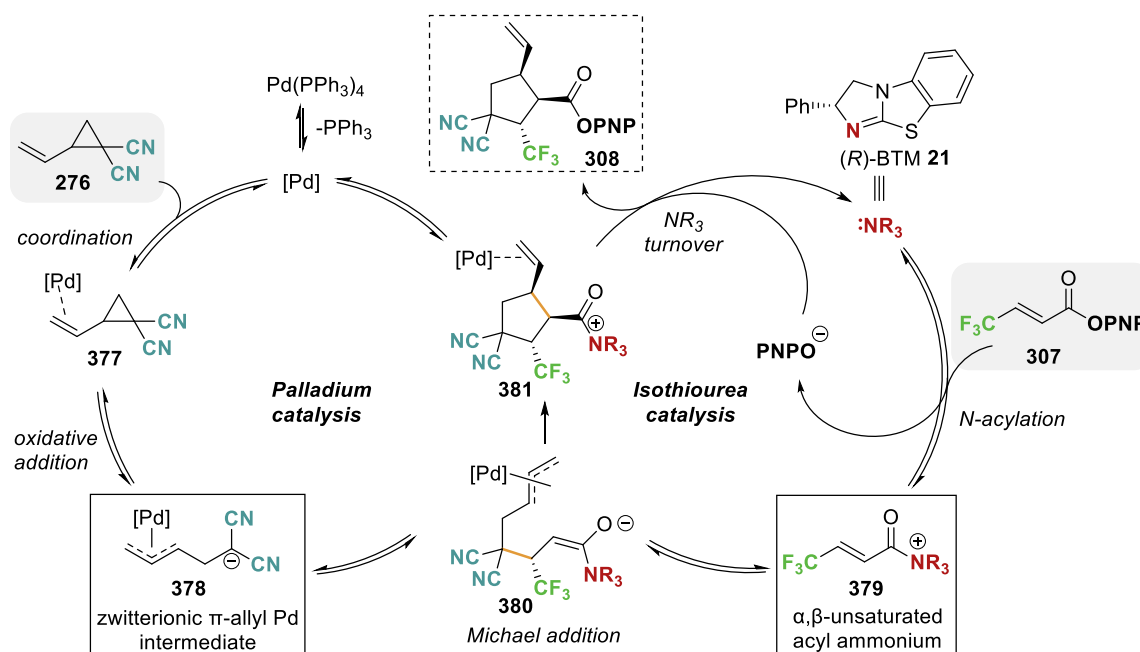


Scheme 78 Derivatization of cooperative catalysis products.

Figure 17 Crystal structures of lactam **374** (left) and ether **376_{maj}** (right).

3.4.9 Proposed mechanism and stereochemical rationale

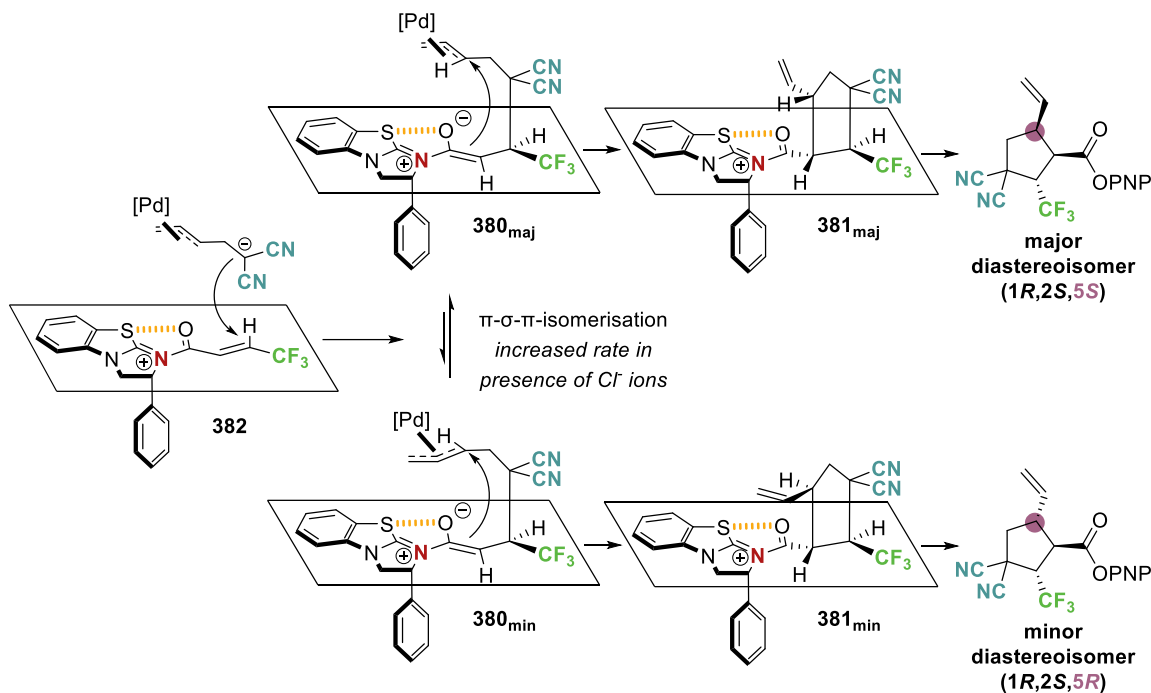
Considering the mechanistic information gained in earlier experiments and the general understanding of palladium π -allyl and α,β -unsaturated acyl ammonium catalysis, the following mechanism for the developed cooperative catalysis is proposed (Scheme 79). Starting from commercially available Pd(PPh₃)₄, ligand dissociation enables reversible coordination to VCP **276**. Subsequent oxidative addition generates zwitterionic Pd π -allyl intermediate **378**. At the same time, isothiourea catalyst (*R*)-BTM **21** undergoes reversible *N*-acylation with PNP ester **307**, generating α,β -unsaturated acyl ammonium **379**. The reactive intermediates **378** and **379** are set up to undergo reversible Michael addition, followed by intramolecular ring closure to generate cyclopentane **381**. Decomplexation of the palladium catalyst and irreversible turnover of the isothiourea catalyst by *p*-nitrophenoxide (PNPO) furnishes the final product **308**.



Scheme 79 Proposed mechanism for cooperative palladium and isothiourea catalysis.

With the isothiourea catalyst being the stereocontrolling element in the catalytic process, the stereochemical outcome can be rationalised by considering the following interactions (Scheme 80). A stabilising 1,5-S \cdots O interaction between the carbonyl oxygen and the isothiourea sulfur atom (no to σ^*_{C-S}) restricts the conformational freedom of the α,β -unsaturated acyl ammonium. With the stereodirecting phenyl group of the catalyst adopting a pseudoaxial position to minimise 1,2-strain, initial Michael addition is forced to proceed on the opposite face, resulting in excellent stereocontrol over the C(2) centre. The formed enolate intermediate 380 then undergoes intramolecular ring closure, which is assumed to be irreversible and sets the configuration at C(1) and C(5). The stereochemistry at C(1) is still controlled by the isothiourea catalyst, as the enolate intermediate exhibits the same conformational restrictions, which forces attack onto the π -allyl fragment to occur from the same face as initial Michael addition. Notably, the stereochemical information from the (*E*)-alkene is retained in the product, resulting in an *anti*-orientation of the C(1) and C(2) substituents. Lastly, the configuration of the π -allyl fragment determines the stereochemistry at C(5). Two orientations need to be considered for the π -allyl moiety (380_{major} and 380_{minor}), giving rise to two diastereoisomers which are epimeric at C(5). The major diastereoisomer is obtained from a *syn*-orientation of the π -allyl and the ammonium enolate (380_{major}), which seems to be more favourable than the corresponding *anti*-orientation (380_{minor}). As an achiral palladium catalyst is used, no facial

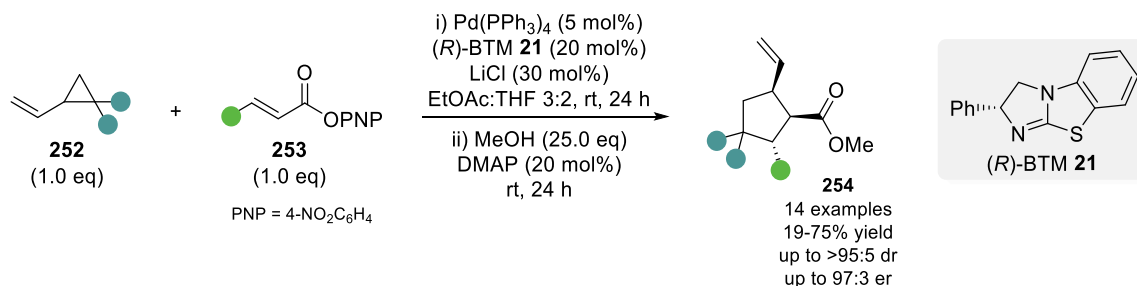
selectivity is observed for initial oxidative addition, which, in the absence of isothiourea catalyst gives rise to a 1:1 mixture of diastereoisomers (Table 12, entry 2). In the presence of isothiourea catalyst, the formation of *syn*-isomer **381_{maj}** is favoured, but as the rate of π - σ - π isomerisation is slow compared to nucleophilic attack onto the π -allyl, only low levels of diastereoselectivity are observed (65:35 dr, Table 7, entry 2). However, the rate of isomerisation can be sufficiently increased through the addition of Cl⁻ ions, leading to excellent diastereoselectivity in favour of the (1*R*,2*S*,5*S*)-isomer (95:5 dr).



Scheme 80 Stereochemical rationale for cooperative palladium and isothiourea catalysis.

3.5 Conclusion

The current work describes the first application of α,β -unsaturated acyl ammonium intermediates in a dual catalytic process. Combination of palladium π -allyl chemistry with isothioureia Lewis base organocatalysis enabled the stereoselective synthesis of highly functionalised cyclopentane products with up to four contiguous stereogenic centres. The simultaneous activation of vinylcyclopropane **252** and α,β -unsaturated *p*-nitrophenyl ester **253** in the presence of catalytic amounts of Pd(PPh₃)₄ (5 mol%) and (*R*)-BTM **21** (20 mol%) facilitates intermolecular, formal (3+2) cycloaddition. Performing the reaction with sub-stoichiometric amounts of LiCl (30 mol%) was crucial for obtaining high levels of diastereo- and enantioselectivity. While a range of electron-withdrawing substituents within the α,β -unsaturated ester was tolerated, aryl substituents proved unreactive. This result makes the current methodology complementary to existing processes for the generation of functionalised cyclopentane products. In addition, different acceptor groups on the VCP could be incorporated, albeit with a decrease in yield and diastereoselectivity. The synthetic utility of the cyclopentane products was showcased through various derivatisation reactions to generate functionalised molecules with increased molecular complexity and without erosion of enantiopurity.



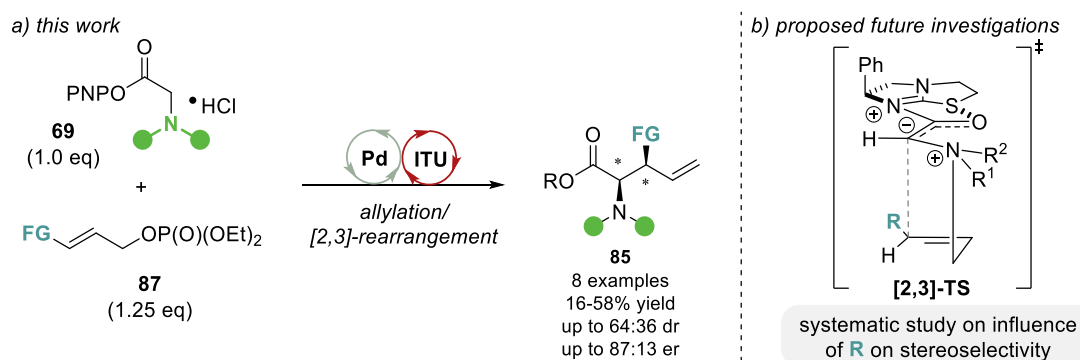
Scheme 81 Cooperative palladium and isothioureia catalysis for the stereoselective synthesis of cyclopentanes.

Mechanistic experiments highlighted the importance of both catalysts for the cooperative catalysis process. A racemic background reaction occurred in the absence of isothioureia catalyst, whereas in the absence of palladium catalyst, no reaction was observed. Further experiments revealed the necessity of a halide additive for a highly diastereoselective process by promoting π - σ - π isomerisation processes.

Chapter 4: Summary and Outlook

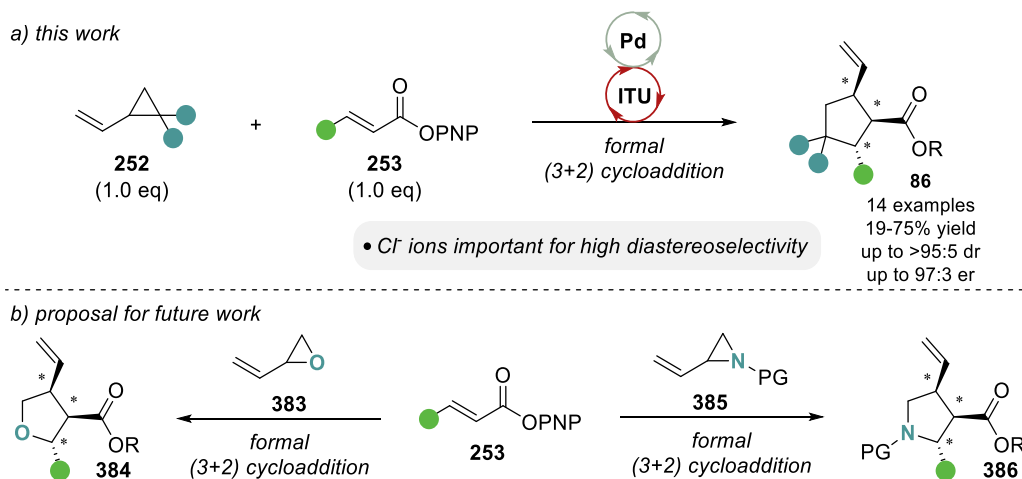
This thesis aimed to broaden the compatibility of isothioureas catalysed transformations in dual catalytic processes, expanding the pool of potential reaction partners and products obtainable. Focusing on intermediates accessible through palladium catalysis, the successful application of dual catalytic palladium and isothioureas methodologies in the synthesis of highly functionalised product scaffolds was demonstrated.

The first example investigated the potential to expand the substrate scope of the relay catalytic allylic amination/[2,3]-rearrangement process previously developed in our group (Chapter II). Employing glycine ester derivatives **69** and functionalised allylic phosphates **87** in the presence of catalytic amounts of palladium and isothiurea allowed the formation of enantioenriched *syn*- α -amino acid derivatives **85** (Scheme 82a). Although electron-withdrawing groups were successfully incorporated, this protocol resulted in decreased diastereo- and enantioselectivities compared to the previous work. These results highlight the sensitivity of this process to steric and electronic changes within the allylic substituent. To increase the applicability and predictability of enantioselective [2,3]-sigmatropic rearrangements of allylic ammonium ylids, further studies to gain a deeper mechanistic understanding are necessary (Scheme 82b). In particular, a systematic investigation on the influence of the allylic substituents (R) on the stereochemical outcome of the rearrangement would immensely aid future developments.



Scheme 82 Summary of relay catalytic process and proposed future investigations.

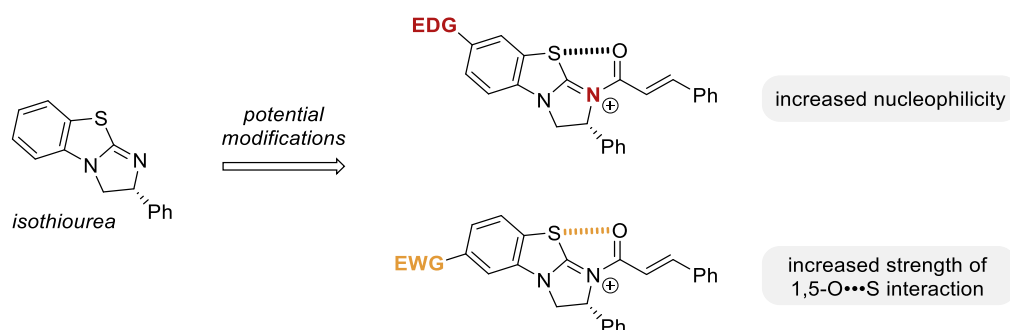
The compatibility of palladium and isothioureia catalysis was further demonstrated in the stereoselective synthesis of highly substituted cyclopentanes (Chapter III) (Scheme 83a). Notably, this is the first example of a dual catalytic process involving isothioureia bound α,β -unsaturated acyl ammonium intermediates. Control experiments revealed the importance of halide additives and the appropriate choice of isothioureia catalyst and reaction solvent for obtaining high levels of diastereo- and enantioselectivity. The synthetic utility of the developed methodology was further demonstrated by various post-catalysis transformations, increasing molecular complexity whilst maintaining stereointegrity. While currently limited to the synthesis of carbocycles, the exploitation of alternative dipoles, generated through palladium catalysis, would enable the formation of a diverse range of cyclic structures. The use of heteroatom containing allylic partners like vinyl epoxides **383** or vinyl aziridines **385**, for example would allow the formation of enantioenriched tetrahydrofurans **384** or pyrrolidines **386** in a related dual palladium and isothioureia catalysed formal (3+2) cycloaddition (Scheme 83b).¹⁴³



Scheme 83 Summary of cooperative palladium and isothioureia catalysis and proposed future work.

The scope of Michael acceptors in the developed process was limited to substrates bearing electron-withdrawing groups in the β -position, with simple aryl substituents proving unreactive. This is a limitation commonly found in α,β -unsaturated acyl ammonium catalysis. To address this shortcoming, further catalyst development could improve the widespread applicability of isothioureia catalysts. Introducing appropriate substituents within the catalyst backbone could alter the nucleophilicity of the catalyst and the strength of the 1,5-O \cdots S interaction found in the isothioureia bound intermediate (Scheme 84). As demonstrated by Birman and co-workers,¹⁴⁴ introduction of electron-donating

groups greatly improved the catalytic activity compared to the standard catalysts, which allowed the activation of substrates that proved extremely sluggish or entirely unreactive. Based on these findings, introducing electron-donating substituents *para* (or potentially *ortho*) to the nitrogen could enable the use of otherwise unreactive substrates. Alternatively, placing electron-withdrawing substituents *para* to sulfur could increase the strength of the 1,5-O \cdots S interaction which would lead to an increased stabilisation of the reactive intermediate, which in turn should lead to an increased catalytic activity. This effect was demonstrated in 2020 by our group, showcasing the increased activity of HyperSe **328** (the selenium analogue of HyperBTM **30**), rationalised by the increased strength of the 1,5-O \cdots Se interaction.³⁰



Scheme 84 Proposed catalyst modifications.

Finally, the application of isothiourea catalysis in dual catalytic processes more broadly is still in its infancy and will probably be an active area of research for many years to come. There is still huge potential for this to be exploited in combination with various transition metal catalysed transformations. In addition, combinations with catalysts operating by a different mode of activation would open new avenues for stereoselective transformations. Combinations of isothiourea catalysis with photocatalysis or Lewis/Brønsted acid catalysis are just a few examples of potential pairings that could be explored.

Chapter 5: Experimental Details

5.1 General Information

All reagents and solvents were obtained from commercial suppliers and were used without further purification unless otherwise stated. Purification was carried out according to standard laboratory methods. Tetramisole·HCl was obtained from Sigma-Aldrich. Pd₂dba₃·CHCl₃ was purchased from Strem Chemicals Inc. and recrystallized from CHCl₃/acetone following the procedure reported by Ananikov and co-workers.¹⁴⁵

Reactions involving moisture sensitive reagents were carried out in flame-dried glassware under an inert atmosphere (N₂ or Ar) using standard vacuum line techniques. Anhydrous solvents (Et₂O, CH₂Cl₂, THF and toluene) were obtained after passing through an alumina column (Mbraun SPS-800). Petrol is defined as petroleum ether 40–60 °C.

Room temperature (rt) refers to 20–25 °C. Temperatures of 0 °C and –78 °C were obtained using ice/water and CO₂(s)/acetone baths, respectively. Temperatures of 0 °C to –78 °C for overnight reactions were obtained using an immersion cooler (HAAKE EK 90) with EtOH or acetone as bath medium. Reactions involving heating were performed using DrySyn blocks and a contact thermocouple.

Under reduced pressure refers to the use of either a Büchi Rotavapor R-200 with a Büchi V-491 heating bath and Büchi V-800 vacuum controller, a Büchi Rotavapor R-210 with a Büchi V-491 heating bath and Büchi V-850 vacuum controller, a Heidolph Laborota 4001 with vacuum controller, an IKA RV10 rotary evaporator with a IKA HB10 heating bath and ILMVAC vacuum controller, or an IKA RV10 rotary evaporator with a IKA HB10 heating bath and Vacuubrand CVC3000 vacuum controller. Rotary evaporator condensers are fitted to Julabo FL601 Recirculating Coolers filled with ethylene glycol and set to –5 °C.

Analytical thin layer chromatography (TLC) was performed on pre-coated aluminium plates (Kieselgel 60 F254 silica) and visualisation was achieved using ultraviolet light

(254 nm) and/or staining with either aqueous KMnO_4 solution, ethanolic phosphomolybdic acid, or ethanolic Vanillin solution followed by heating. Manual column chromatography was performed in glass columns fitted with porosity 3 sintered discs over Kieselgel 60 silica or Millipore® Silica Gel 60 (for aryl ester compounds) using the solvent system stated. Automated chromatography was performed on a Biotage Isolera Four running Biotage OS578 with a UV/Vis detector using the method stated and cartridges filled with Kieselgel 60 silica or a Biotage Selekt running SELEKT 1.4.2-13403 with a UV/Vis detector using the method stated and Biotage Sfär Silica D 60 μm cartridges. Melting points were recorded on an Electrothermal 9100 melting point apparatus, (dec) refers to decomposition.

Optical rotations were measured on a Perkin Elmer Precisely/Model-341 polarimeter operating at the sodium D line with a 100 mm path cell at 20 °C. Concentrations (c) are stated in g/100 mL.

HPLC analyses were obtained on either a Shimadzu HPLC consisting of a DGU-20A5 degassing unit, LC-20AT liquid chromatography pump, SIL-20AHT autosampler, CMB-20A communications bus module, SPD-M20A diode array detector and a CTO-20A column oven or a Shimadzu HPLC consisting of a DGU-20A5R degassing unit, LC-20AD liquid chromatography pump, SIL-20AHT autosampler, SPD-20A UV/Vis detector and a CTO-20A column oven. Separation was achieved using either a DAICEL CHIRALCEL OD-H column or DAICEL CHIRALPAK AD-H, AS-H, IA and IC columns using the method stated. HPLC traces of enantiomerically enriched compounds were compared with authentic racemic spectra.

GC analyses were obtained on a Shimadzu GC consisting of a Shimadzu AOC-20i auto injector and a Shimadzu GC-2025 gas chromatograph. Analysis was performed using Shimadzu GCsolution v2.41 software and separation was achieved using a Restek Rt- β DEXcst column (length: 30 m, thickness: 0.25 mm, film thickness: 0.25 μm).

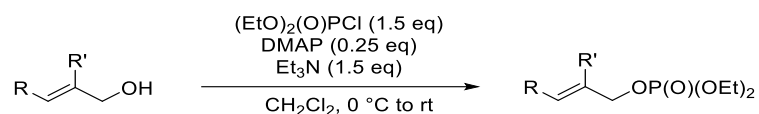
Infrared spectra were recorded on a Shimadzu IRAffinity-1 Fourier transform IR spectrophotometer fitted with a Specac Quest ATR accessory (diamond puck). Spectra were recorded of either thin films or solids, with characteristic absorption wavenumbers (ν_{max}) reported in cm^{-1} .

^1H , $^{13}\text{C}\{^1\text{H}\}$, $^{19}\text{F}\{^1\text{H}\}$ and $^{31}\text{P}\{^1\text{H}\}$ NMR spectra were acquired on either a Bruker AV400 with a BBFO probe (^1H 400 MHz; $^{19}\text{F}\{^1\text{H}\}$ 377 MHz, $^{31}\text{P}\{^1\text{H}\}$ 162 MHz), a Bruker AVII 400 with a BBFO probe (^1H 400 MHz; $^{19}\text{F}\{^1\text{H}\}$ 376 MHz, $^{31}\text{P}\{^1\text{H}\}$ 162 MHz), a Bruker AVIII-HD 500 with a SmartProbe BBFO+ probe (^1H 500 MHz, $^{13}\text{C}\{^1\text{H}\}$ 126 MHz, $^{31}\text{P}\{^1\text{H}\}$ 202 MHz) or a Bruker AVIII 500 with a CryoProbe Prodigy BBO probe (^1H 500 MHz, $^{13}\text{C}\{^1\text{H}\}$ 126 MHz, $^{31}\text{P}\{^1\text{H}\}$ 202 MHz) in the deuterated solvent stated. All chemical shifts are quoted in parts per million (ppm) relative to the residual solvent peak. All coupling constants, J , are quoted in Hz. Multiplicities are indicated as s (singlet), d (doublet), t (triplet), q (quartet), p (pentet), m (multiplet), and multiples thereof. The abbreviation Ar denotes aromatic, app denotes apparent and br denotes broad. NMR peak assignments were confirmed using 2D ^1H correlated spectroscopy (COSY), 2D ^1H nuclear Overhauser effect spectroscopy (NOESY), 2D ^1H - ^{13}C heteronuclear multiple-bond correlation spectroscopy (HMBC), and 2D ^1H - ^{13}C heteronuclear single quantum coherence (HSQC) where necessary.

Mass spectrometry (m/z) data were acquired by either electrospray ionisation (ESI), electron impact (EI), or nanospray ionisation (NSI) at either the University of St Andrews Mass Spectrometry Facility, the EPSRC UK National Mass Spectrometry Facility at Swansea University or SIRCAMS at University of Edinburgh.

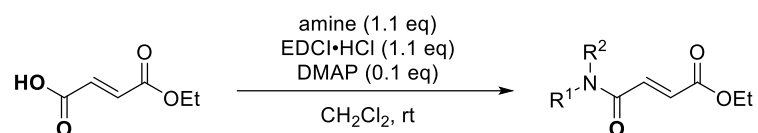
5.2 General Procedures

5.2.1 General Procedure A: Synthesis of allylic phosphates



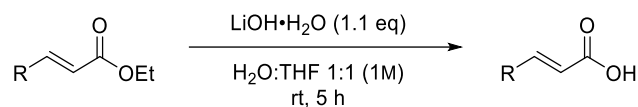
Following the procedure reported by Smith and co-workers⁶⁵, allylic alcohol (1.0 eq) was added to a flame dried round bottom flask and dissolved in anhydrous CH₂Cl₂ (0.1 M) under inert atmosphere. Et₃N (1.5 eq) and DMAP (0.25 eq) were added. The mixture was cooled to 0 °C and diethyl chlorophosphate (1.5 eq) was added dropwise. Stirring was continued at room temperature until TLC analysis indicated complete conversion. The reaction mixture was quenched with sat. aq. NaHCO₃ (equal volume), the phases were separated, and the aqueous phase was extracted with CH₂Cl₂ (3 × equal volume). The combined organic phases were dried over MgSO₄, filtered and the solvent was removed under reduced pressure. The crude residue was purified by silica column chromatography as specified.

5.2.2 General Procedure B: Amide coupling



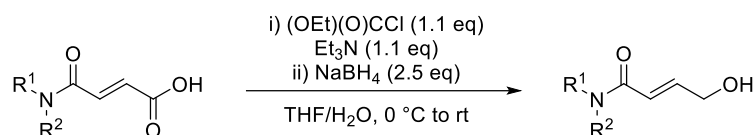
Adapting a procedure reported by Snaddon and co-workers,⁶⁴ monoethyl fumarate (1.0 eq) and amine (1.1 eq) were dissolved in CH₂Cl₂ (0.4 M), followed by the addition of EDCI·HCl (1.1 eq) and DMAP (0.1 eq) at 0 °C. The reaction mixture was allowed to warm to room temperature overnight and subsequently washed with 1 M HCl (2 × equal volume) and brine (2 × equal volume). The organic phase was dried over MgSO₄, filtered and the solvent was removed under reduced pressure to yield the corresponding amide ester, which was used without further purification.

5.2.3 General Procedure C: Basic ester hydrolysis with LiOH



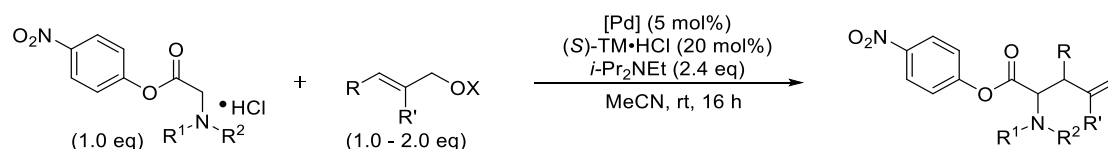
Adopting the procedure reported by Smith and co-workers¹⁴⁶, the corresponding ethyl ester (1.0 eq) was dissolved in a 1:1 mixture of H₂O : THF (1 M), followed by the addition of LiOH·H₂O (1.1 eq). The reaction mixture was stirred at room temperature for the time stated and subsequently adjusted to pH 2 with 2 M HCl. The aqueous phase was extracted with CH₂Cl₂ (3 × equal volume), the combined organic phases were dried over MgSO₄, filtered and the solvent removed under reduced pressure to afford the corresponding carboxylic acid, which was used without further purification.

5.2.4 General Procedure D: Reduction of unsaturated acids



Adapting the procedure reported by Jacobi and co-workers,¹⁴⁷ to a stirred solution of unsaturated acid (1.0 eq) and Et₃N (1.1 eq) in anhydrous THF (0.4 M) under inert atmosphere at 0 °C was added dropwise ethyl chloroformate (1.1 eq). The resulting suspension was stirred at 0 °C for 1 h, filtered and the solid was washed twice with anhydrous THF. The combined filtrates were added dropwise to a vigorously stirred solution of NaBH₄ (2.5 eq) in H₂O (0.7 M) at 0 °C. The reaction mixture was allowed to warm to room temperature and stirred until TLC indicated complete conversion. The mixture was adjusted to pH 5 with 1 M HCl and extracted with EtOAc (4 × equal volumes). The combined organic phases were dried over MgSO₄, filtered and the solvent was removed under reduced pressure. The crude product was purified by silica column chromatography as specified.

5.2.5 General Procedure E: Relay Pd/ITU catalysis



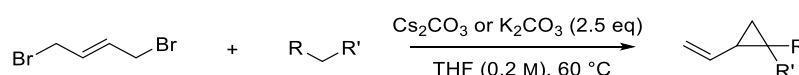
A Schlenk tube was charged with PdFurCat (5 mol%), or Pd₂(dba)₃·CHCl₃ (2.5 mol%) and P(2-furyl)₃ (10 mol%), (*S*)-TM·HCl (10 mol%) and PNP ester (1.0 eq). The tube was evacuated and flushed with argon three times. Degassed MeCN (0.06 M) was added and the mixture stirred for 10 min at room temperature. Subsequently, phosphate or mesylate (1.0 – 2.0 eq) and *i*-Pr₂NEt (2.4 eq) were added in this order and the reaction mixture stirred at room temperature for 16 h. An aliquot was taken and concentrated to dryness under reduced pressure. ¹H NMR spectroscopic analysis of the crude mixture was used to determine the dr. The reaction mixture was then filtered over a short plug of silica with MeCN and the filtrate concentrated under reduced pressure. The residue was purified by silica column chromatography as specified or directly derivatised with NaOBn.

Derivatisation with NaOBn:

The crude reaction mixture was dissolved in anhydrous THF (6.0 mL). Freshly prepared NaOBn (1 M in anhydrous THF, 0.45 mL, 0.45 mmol, 1.5 eq) was added dropwise at room temperature and the reaction monitored by TLC. After complete conversion (ca. 3h) the reaction was quenched with sat. aq. NaHCO₃ solution (equal volume) and diluted with EtOAc. The phases were separated and the aqueous phase was extracted with EtOAc (3 × equal volume). The combined organic phases were washed with sat. aq. NaHCO₃ (2 × equal volume) and brine (equal volume). The organic phase was dried over MgSO₄, filtered and the solvent was removed under reduced pressure to afford the crude product, which was purified by silica column chromatography as specified.

NaOBn (1 M in THF) was prepared by treating BnOH with NaH in anhydrous THF.

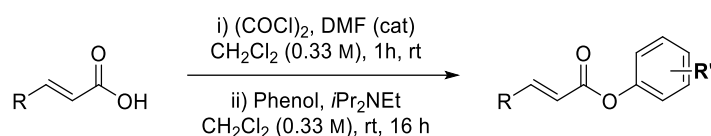
5.2.6 General Procedure F: Preparation of vinyl cyclopropanes



Adapting the procedure reported by Plietker and co-workers¹⁴¹, malonate derivative (1.0 eq) and 1,4-dibromobut-2-ene (1.0 eq) were dissolved in THF (0.2 M) under N₂

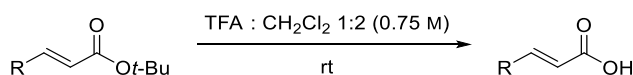
atmosphere, followed by the addition of Cs_2CO_3 or K_2CO_3 (2.5 eq). The mixture was heated at reflux until TLC indicated full conversion of starting materials, subsequently allowed to cool to room temperature and filtered over Celite with Et_2O (equal volume). The combined organic phases were washed with sat. aq. NaHCO_3 (equal volume), H_2O and brine, dried over MgSO_4 , filtered and the solvent removed under reduced pressure. The crude product was purified by silica column chromatography as specified.

5.2.7 General Procedure G: Preparation of α,β -unsaturated aryl oxide esters



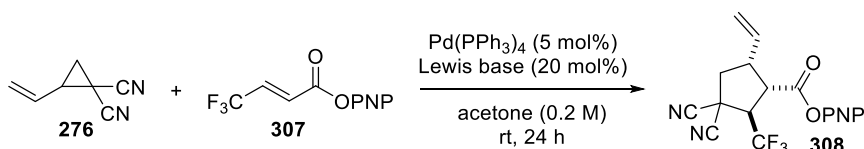
Following the procedure reported by Smith and co-workers¹⁴⁸, oxalyl chloride (1.05 eq) and DMF (cat.) were added to a stirred solution of α,β -unsaturated acid (1.0 eq) in anhydrous CH_2Cl_2 (0.33 M) at room temperature under N_2 atmosphere. The mixture was allowed to stir for 1 h, after which a solution of the corresponding phenol (1.0 eq) and *i*- Pr_2NEt (2.0 eq) in anhydrous CH_2Cl_2 (0.33 M) was added dropwise and the mixture allowed to stir overnight. The solvent was removed under reduced pressure and the crude product purified as specified.

5.2.8 General Procedure H: Acidic ester hydrolysis



Adopting the procedure reported by Smith and co-workers,¹⁴⁶ the corresponding *t*-butyl ester (1.0 eq) was dissolved in TFA : CH_2Cl_2 1:2 (0.75 M). The reaction mixture was stirred at room temperature overnight and the solvent was removed under reduced pressure to afford the corresponding carboxylic acid, which was used without further purification.

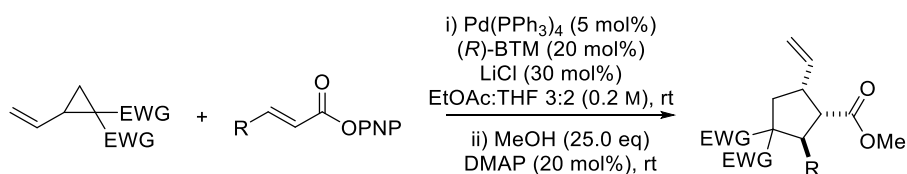
5.2.9 General Procedure I: Optimisation of cooperative catalysis conditions



An oven-dried 4 mL vial containing a magnetic stir bar and equipped with a Teflon septum insert screw cap was charged with $\text{Pd}(\text{PPh}_3)_4$ (5 mol%), isothiurea catalyst

(20 mol%) and (*E*)-4,4,4-trifluorobut-2-enoic acid, 4-nitrophenyl ester **307** (1.0 eq). The vial was evacuated and flushed with N₂ three times. Acetone (0.2 M), purged prior with Ar for 30 minutes, was added followed by the addition of 2-vinylcyclopropane-1,1-dicarbonitrile **276** (1.0 eq). The reaction vial was sealed and allowed to stir at room temperature for 24 h. 1,3,5-Trimethoxybenzene (0.33 eq, 0.33 M solution in acetone) was added at the end of the reaction and the reaction mixture filtered over a short plug of silica with EtOAc. The solvent was removed under reduced pressure and the crude mixture was analysed by ¹H and ¹⁹F-NMR and chiral stationary phase HPLC. An example for how the NMR yield and the dr based on ¹H and ¹⁹F NMR analysis were derived is demonstrated in Appendix I.

5.2.10 General Procedure J: Cooperative Pd/ITU formal (3+2) cycloaddition



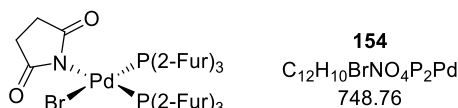
Prior to the reaction, EtOAc and anhydrous THF were purged with Ar for 30 min. An oven-dried Schlenk tube containing a magnetic stir bar was charged with Pd(PPh₃)₄ (5 mol%), (*R*)-BTM (20 mol%) and PNP ester (1.0 eq) and evacuated and flushed with N₂ three times. LiCl in THF (30 mol%, 0.5 M) was added followed by the remaining amount of THF. Vinylcyclopropane (1.0 eq) was added as a stock solution in EtOAc (118 mg/mL) followed by the addition of remaining EtOAc. The reaction was stirred at room temperature (25 °C) and the reaction progress monitored by ¹H NMR analysis. Once the starting materials had been consumed, anhydrous MeOH (25.0 eq) and DMAP (20 mol%) were added. No further precautions to exclude air or moisture were necessary at this point. The reaction mixture was stirred at room temperature until complete by ¹H NMR analysis (usually 24 h) and filtered over a short plug of silica with EtOAc. The EtOAc filtrate was washed with 1 M NaOH (2 × equal volume) and brine (1 × equal volume), dried over MgSO₄, filtered and the solvent removed under reduced pressure. The crude product was purified by silica column chromatography as specified.

Racemic samples were prepared using (±)-TM·HCl (10 mol%), *i*-Pr₂NEt (10 mol%) and LiCl (20 mol%) in acetone (0.2 M).

5.3 Synthesis of Catalysts

Isothiourea catalysts (*R*)-BTM¹⁴⁹ **21**, (*2S,3R*)-HyperBTM²⁵ **30**, (*2R,3S*)-HyperSe³⁰ **328** and (*R*)-OMe-BTM¹⁵⁰ **327** were available in the laboratory and were synthesised according to published procedures.

cis-Bromobis(tri(2-furyl)phosphine)(*N*-succinimide)palladium(II) (PdFurCat 154)

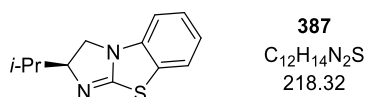


Following the procedure reported by Smith and co-workers,⁶⁵ a Schlenk flask was charged with Pd₂dba₃·CHCl₃ (172 mg, 0.17 mmol, 0.5 eq) and P(2-furyl)₃ (158 mg, 0.68 mmol, 2.0 eq) and evacuated and flushed with argon three times. Anhydrous CH₂Cl₂ (12 mL, freshly purged with argon) was added and the mixture stirred for 10 min at room temperature. Subsequently, NBS (61.0 mg, 0.34 mmol, 1.0 eq) was dissolved in 4.0 mL anhydrous CH₂Cl₂, added to the reaction mixture and stirred for 10 min. The mixture was diluted with *n*-hexane (20 mL) and poured onto additional *n*-hexane (150 mL). The resulting precipitate was washed with *n*-hexane (4 × 100 mL) and dried under reduced pressure to yield the title complex as a brown solid (249 mg, 97%) as a mixture of geometrical isomers (*cis* : *trans* ca. 9:1).

¹H NMR (400 MHz, CD₂Cl₂) δ_H: 1.96 (4H, s, (CH₂C(O))₂, *trans*), 2.12 – 2.21 (2H, m, CH₂C(O), *cis*), 2.37 – 2.46 (2H, m, CH₂C(O), *cis*), 6.46 (3H, dt, *J* 3.4, 1.6, 3 × ArH, *cis*), 6.51 (3H, dt, *J* 3.3, 1.6, 3 × ArH, *cis*), 6.59 – 6.63 (6H, m, 6 × ArH, *trans*), 7.02 – 7.08 (3H, m, 3 × ArH, *cis*), 7.14 – 7.17 (3H, m, 3 × ArH, *cis*), 7.32 – 7.36 (6H, m, 6 × ArH, *trans*), 7.52 – 7.57 (3H, m, 3 × ArH, *cis*), 7.69 (3H, td, *J* 1.9, 0.7, 3 × ArH, *cis*), 7.78 – 7.80 (6H, m, 6 × ArH, *trans*).

³¹P{¹H} NMR (162 MHz, CD₂Cl₂) δ_P: -26.3 (d, ²*J*_{PP} 13.5, P(2-Fur)₃, *cis*), -27.1 (d, ²*J*_{PP} 13.0, P(2-Fur)₃, *cis*), -32.5 (s, P(2-Fur)₃, *trans*).

Data in accordance with literature.¹⁵¹ (LB ref: JB-001)

(S)-2-Isopropyl-2,3-dihydrobenzo[d]imidazo[2,1-b]thiazole ((S)-*i*-Pr-BTM) (387)

Adapting the procedure from Shiina and co-workers,²⁴ a 50 mL pressure tube was charged with 2-chlorobenzothiazole (3.77 mL, 29.0 mmol, 1.0 eq), (*S*)-valinol (3.0 g, 29.0 mmol, 1.0 eq) and *i*-Pr₂N₂Et (7.4 mL, 43.5 mmol, 1.5 eq), sealed and the mixture stirred at 130 °C for 45 h. The reaction mixture was allowed to cool to room temperature, dissolved in 10 mL CH₂Cl₂ (gentle heating advantageous) and purified directly by silica column chromatography (2% *i*-PrOH to 6% *i*-PrOH in CH₂Cl₂, R_f 0.23 in 4% *i*-PrOH in CH₂Cl₂) to afford the intermediate (*S*)-2-(benzo[d]thiazol-2-ylamino)-3-methylbutan-1-ol as white solid (5.1 g, 74%).

¹H NMR (500 MHz, CDCl₃) δ_H: 0.92 (3H, d, *J* 6.8, C(3)H(CH₃)), 0.99 (3H, d, *J* 6.8, C(3)H(CH₃)), 1.88 – 1.99 (1H, m, C(3)H), 3.43 (1H, br s, C(2)H), 3.77 (1H, dd, *J* 11.7, 6.1, C(1)H^AH^B), 3.87 (1H, dd, *J* 11.7, 3.1, C(1)H^AH^B), 4.60 (1H, brs, NH), 6.59 (1H, brs, OH), 7.06 – 7.10 (1H, m, Ar(5)H or Ar(6)H), 7.26 – 7.31 (1H, m, Ar(5)H or Ar(6)H), 7.53 – 7.55 (1H, m, Ar(4)H or Ar(7)H), 7.55 – 7.57 (1H, m, Ar(4)H or Ar(7)H).

The intermediate alcohol (2.36 g, 10.0 mmol, 1.0 eq) was dissolved in anhydrous CH₂Cl₂ (100 mL). Et₃N (5.5 mL, 40.0 mmol, 4.0 eq) was added and the mixture cooled in an ice bath for 10 min. MsCl (1.0 mL, 13.0 mmol, 1.3 eq) was added dropwise, the reaction mixture warmed to room temperature and stirred until TLC (4% *i*-PrOH in CH₂Cl₂) indicated complete conversion (ca. 2 h). MeOH (0.6 mL) was added and the reaction mixture heated at reflux overnight. After cooling to room temperature, the mixture was washed with H₂O, dried over MgSO₄, filtered and the solvent removed under reduced pressure. The crude product was purified by silica column chromatography (hexane : *i*-PrOH : Et₃N 95:4:1, R_f 0.19) to afford (*S*)-*i*-Pr-BTM as pale yellow oil (2.1 g, 95%), which solidifies upon cooling.

[α]_D²⁰ –130.1 (c 1.05 in CHCl₃) {Lit.²⁴ [α]_D²³ –141.6 (c 0.35 in benzene)}.

chiral HPLC analysis Chiralcel AD-H (95:5 hexane : *i*-PrOH, flow rate 1.5 mlmin⁻¹, 211 nm, 40 °C) t_R(2*R*): 6.5 min, t_R(2*S*): 10.3 min, 0.1 : 99.9 er.

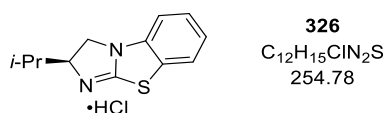
¹H NMR (500 MHz, CDCl₃) δ_H: 0.97 (3H, d, *J* 6.7, CH(CH₃)), 1.05 (3H, d, *J* 6.7, CH(CH₃)), 1.90 (1H, oct, *J* 6.7, CH(CH₃)₂), 3.49 (1H, app. t, *J* 8.7, C(3)H^AH^B), 3.87 (1H, dd, *J* 9.8, 8.9, C(3)H^AH^B), 4.38 (1H, ddd, *J* 9.8, 8.5, 6.5, C(2)H), 6.65 (1H, dd, *J* 7.7, 0.7, Ar(5)H or Ar(8)H),

6.93 (1H, td, J 7.7, 1.2, Ar(6) H or Ar(7) H), 7.17 (1H, td, J 7.7, 1.2, Ar(6) H or Ar(7) H), 7.24 – 7.27 (1H, m, Ar(5) H or Ar(8) H).

A racemic sample was prepared using (\pm)-valinol following the same procedure. Spectroscopic data in accordance with literature.²⁴ (LB ref: JB-554, JB-561 (\pm))

(S)-2-Isopropyl-2,3-dihydrobenzo[d]imidazo[2,1-b]thiazole hydrochloride

((S)-*i*-Pr-BTM·HCl) (326)



To a solution of (*S*)-*i*-Pr-BTM **387** (1.16 g, 5.3 mmol, 1.0 eq) in Et₂O (21 mL) was added HCl (2 M in Et₂O, 10.6 mmol, 2.0 eq) and the reaction mixture stirred for 5 min at room temperature. The solvent was removed under reduced pressure to yield the title compound as a white solid (1.34 g, 99%). **m.p.** (Et₂O) 229 – 230 °C.

$[\alpha]_D^{20}$ –85.5 (c 1.08 in MeCN).

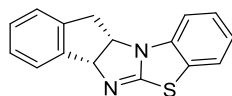
¹H NMR (500 MHz, DMSO-*d*₆) δ _H: 0.95 (3H, d, J 6.7, CH(CH₃)), 0.99 (3H, d, J 6.7, CH(CH₃)), 2.01 (1H, oct, J 6.7, CH(CH₃)₂), 4.28 – 4.34 (1H, m, C(3) $H^A H^B$), 4.55 – 4.66 (2H, m, C(2) H and C(3) $H^A H^B$), 7.37 (1H, ddd, J 8.4, 7.3, 1.3, Ar(7) H), 7.50 (1H, dd, J 8.1, 1.2, Ar(5) H), 7.53 – 7.58 (1H, m, Ar(6) H), 7.99 – 8.05 (1H, m, Ar(8) H), 11.68 (1H, s, NH).

¹³C{¹H} NMR (126 MHz, DMSO-*d*₆) δ _C: 18.0 (CH(CH₃)), 18.1 (CH(CH₃)), 32.4 (CH(CH₃)₂), 48.8 (C(3) H_2), 70.3 (C(2) H), 113.0 (ArC(5) H), 124.9 (ArC(7) H), 125.3 (ArC(8) H), 127.6 (ArC(8a)), 128.4 (ArC(6) H), 135.1 (ArC(4a)), 169.8 (C=N).

HRMS (ESI⁺) C₁₂H₁₅N₂S [M]⁺ found 219.0948, requires 219.0950 (–0.9 ppm).

ν_{\max} (film, cm⁻¹) 3003, 2960 (C-H), 2870, 2605 (N-H), 1600, 1589, 1577, 1504 (C=C), 1465, 1446, 1373, 1284, 1257, 756.

(LB ref: JB-570)

(4*b*R,11*a*S)-4*b*,11*a*-Dihydro-12*H*-benzo[*d*]indeno[1',2':4,5]imidazo[2,1-*b*]thiazole**((+)-(R,S)-fused-BTM) (329)**

329
C₁₆H₁₂N₂S
264.35

Adapting the procedure reported by Shiina and co-workers,²⁴ a 25 mL pressure tube was charged with 2-chlorobenzothiazole (0.65 mL, 5.0 mmol, 1.0 eq), (1*R*,2*R*)-*trans*-1-amino-2-indanol (746 mg, 5.0 mmol, 1.0 eq) and *i*-Pr₂NEt (1.3 mL, 7.5 mmol, 1.5 eq), sealed and the mixture stirred at 130 °C for 69 h. The reaction mixture was allowed to cool to room temperature, dissolved in 2.5 mL MeOH and purified directly by silica column chromatography (2% to 4% *i*-PrOH in CH₂Cl₂, R_f 0.25 in 2% *i*-PrOH in CH₂Cl₂) to afford the intermediate 1-(benzo[*d*]thiazol-2-ylamino)-2,3-dihydro-1*H*-inden-2-ol as a beige solid (871 mg, 62%).

¹H NMR (500 MHz, CD₃OD) δ_H: 2.89 (1H, dd, *J* 15.7, 6.6, C(3)*H*^A*H*^B), 3.27 – 3.34 (1H, m, C(3)*H*^A*H*^B), 4.45 (1H, td, *J* 6.8, 5.6, C(2)*H*), 5.22 (1H, d, *J* 5.6, C(1)*H*), 7.06 – 7.12 (1H, m, ArCH), 7.19 – 7.31 (4H, m, 4 × ArCH), 7.32 – 7.35 (1H, m, ArCH), 7.46 (1H, ddd, *J* 8.1, 1.2, 0.6, ArCH), 7.61 (1H, ddd, *J* 7.9, 1.2, 0.6, ArCH).

The intermediate alcohol (824 mg, 3.12 mmol, 1.0 eq) was suspended in anhydrous CH₂Cl₂ (32 mL). Et₃N (1.7 mL, 12.5 mmol, 4.0 eq) was added and the mixture cooled in an ice bath for 10 min. MsCl (0.31 mL, 4.05 mmol, 1.3 eq) was added dropwise, the reaction mixture warmed to room temperature and stirred until TLC (4% *i*-PrOH in CH₂Cl₂) indicated complete conversion (ca. 3 h; additional 0.1 mL MsCl added to reach full consumption of alcohol). MeOH (0.2 mL) was added and the reaction mixture heated at reflux overnight. After cooling to room temperature, the mixture was washed with H₂O, dried over MgSO₄, filtered and the solvent removed under reduced pressure. The crude product was purified by silica column chromatography (2% MeOH in CH₂Cl₂, R_f 0.24), followed by recrystallisation from CH₂Cl₂/hexane to afford (+)-(R,S)-fused-BTM as light brown needles (479 mg, 58%).

m.p. (CH₂Cl₂/hexane) 162 – 165 °C {Lit.²⁴ 161 – 163 °C (CH₂Cl₂/hexane)}.

[α]_D²⁰ +908 (*c* 1.0 in MeOH) {Lit.²⁴ [α]_D²³ +881.8 (*c* 1.0 in MeOH)}.

¹H NMR (500 MHz, CDCl₃) δ_H: 3.41 (1H, dd, *J* 17.0, 1.9, C(12)*H*^A*H*^B), 3.53 (1H, dd, *J* 17.0, 7.0, C(12)*H*^A*H*^B), 4.97 (1H, ddd, *J* 8.5, 7.0, 1.9, C(11*a*)*H*), 6.10 (1H, d, *J* 8.5, C(4*b*)*H*), 6.82 (1H,

dd, J 7.9, 1.6, ArC(10) H), 6.96 (1H, td, J 7.7, 1.1, Ar(8) H), 7.21 (1H, td, J 7.7, 1.2, Ar(9) H), 7.24 – 7.28 (3H, m, 3 \times Ar H), 7.28 – 7.33 (1H, m, Ar H), 7.54 – 7.57 (1H, m, ArC(7) H).

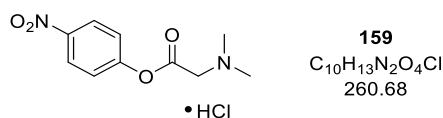
Spectroscopic data in accordance with literature.²⁴ (LB ref: JB-566)

5.4 Experimental details for Chapter 2

5.4.1 Preparation of *p*-nitrophenyl amino esters

p-Nitrophenyl amino esters **221** and **222** were prepared by Thomas H. West according to literature procedure.^{65,91}

N,N-Dimethylglycine, *p*-nitrophenyl ester, hydrochloride (**159**)



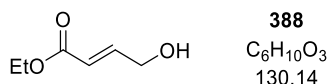
Following the procedure reported by Smith and co-workers,⁶⁵ *N,N*-dimethylglycine (3.00 g, 28.8 mmol, 2.0 eq), *p*-nitrophenol (2.00 g, 14.4 mmol, 1.0 eq) and EDCI·HCl (4.10 g, 21.4 mmol, 1.5 eq) in CH₂Cl₂ (45 mL) were stirred at room temperature overnight. The reaction was quenched by the addition of sat. aq. NaHCO₃ solution (50 mL) and the phases were separated. The aqueous phase was extracted with CH₂Cl₂ (3 \times 40 mL). The combined organic phases were washed with brine (2 \times 40 mL), dried over MgSO₄, and filtered. The solvent was removed under reduced pressure. The crude product was filtered over a short plug of silica with EtOAc until the filtrate was colourless and the solvent was removed under reduced pressure. The residue was dissolved in CH₂Cl₂ (15 mL) and HCl (2 M in anhydrous Et₂O, 14.4 mL, 28.8 mmol, 2.0 eq) was added to precipitate the product as its hydrochloric salt. The precipitate was filtered, washed with CH₂Cl₂ and dried to yield compound **159** as an off-white solid (2.52 g, 64%).

¹H NMR (400 MHz, DMSO-*d*₆) δ _H: 2.93 (6H, s, N(CH₃)₂), 4.54 (2H, s, CH₂-N), 7.54 – 7.62 (2H, m, Ar(2,6) H), 8.35 – 8.43 (2H, m, Ar(3,5) H).

Data in accordance with literature.⁶⁵ (LB ref: JB-035, JB-159)

5.4.2 Preparation of allylic phosphate starting materials

(E)-4-Hydroxy-2-butenoic acid, ethyl ester (388)

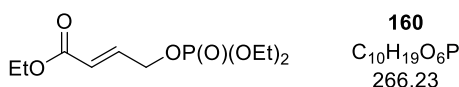


Following the procedure reported by Smith and co-workers,¹⁵² borane (1.0 M in THF, 14 mL, 14 mmol, 1.0 eq) was added dropwise to a stirred solution of monoethyl fumarate (2.02 g, 14 mmol, 1.0 eq) in anhydrous THF (10 mL) at 0 °C. After complete addition, the reaction mixture was allowed to warm to room temperature and stir for 12 h. The reaction was quenched with 50% aq. AcOH (10 mL) and then THF was removed under reduced pressure. The remaining solution was neutralized with sat. aq. NaHCO₃ solution and extracted with EtOAc (4 × 30 mL). The combined organic phases were dried over MgSO₄, filtered and the solvent removed under reduced pressure. Purification by silica column chromatography (petrol : EtOAc 4:1 to 1:1, R_f 0.47 in petrol : EtOAc 1:1) gave the title compound as a pale yellow liquid (905 mg, 49%).

¹H NMR (400 MHz, CDCl₃) δ_H: 1.28 (3H, t, *J* 7.1, OCH₂CH₃), 4.19 (2H, q, *J* 7.1, OCH₂CH₃), 4.34 (2H, dd, *J* 4.0, 2.1, C(4)H₂), 6.09 (1H, dt, *J* 15.7, 2.1, C(2)H), 7.02 (1H, dt, *J* 15.7, 4.0, C(3)H).

Data in accordance with literature.¹⁵³ (LB ref: JB-007, JB-008, JB-028)

(E)-4-[(Diethoxyphosphinyl)oxy]-2-butenoic acid, ethyl ester (160)



Following **General Procedure A** using allylic alcohol **388** (195 mg, 1.5 mmol, 1.0 eq), diethyl chlorophosphate (325 μL, 2.25 mmol, 1.5 eq), Et₃N (314 μL, 2.25 mmol, 1.5 eq) and DMAP (46.0 mg, 0.38 mmol, 0.25 eq) in anhydrous CH₂Cl₂ (10 mL) gave the title compound following purification by silica column chromatography (*n*-hexane : EtOAc 1:1 to 1:2, R_f 0.19 in *n*-hexane : EtOAc 1:1) as a pale yellow oil (283 mg, 71%).

¹H NMR (400 MHz, CDCl₃) δ_H: 1.28 (3H, t, *J* 7.1, CH₂CH₃), 1.34 (6H, td, *J* 7.0, 1.0, P(OCH₂CH₃)₂), 4.13 (4H, dq, *J* 8.1, 7.1, P(OCH₂CH₃)₂), 4.20 (2H, q, *J* 7.2, CH₂CH₃), 4.69 (2H, ddd, *J* 7.3, 4.2, 2.1, C(4)H₂), 6.11 (1H, dt, *J* 15.6, 2.0, C(2)H), 6.92 (1H, dtd, *J* 15.7, 4.3, 1.8, C(3)H).

^{13}C $\{^1\text{H}\}$ NMR (126 MHz, CDCl_3) δ_{C} : 14.2 (CH_2CH_3), 16.1 (d, $^3J_{\text{CP}}$ 6.7, $\text{P}(\text{OCH}_2\text{CH}_3)_2$), 60.6 (CH_2CH_3), 64.1 (d, $^2J_{\text{CP}}$ 5.9, $\text{P}(\text{OCH}_2\text{CH}_3)_2$), 65.3 (d, $^2J_{\text{CP}}$ 4.9, $\text{C}(4)\text{H}_2$), 122.0 ($\text{C}(2)\text{H}$), 141.2 (d, $^3J_{\text{CP}}$ 7.7, $\text{C}(3)\text{H}$), 165.8 ($\text{C}=\text{O}$).

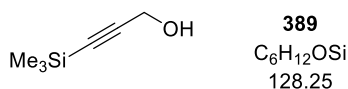
^{31}P $\{^1\text{H}\}$ NMR (162 MHz, CDCl_3) δ_{P} : -1.09 ($\text{P}(\text{O})(\text{OEt})_2$).

HRMS (NSI $^+$) $\text{C}_{10}\text{H}_{20}\text{O}_6\text{P}$ $[\text{M}+\text{H}]^+$ found 267.0992, requires 267.0992 (± 0.0 ppm).

ν_{max} (film, cm^{-1}) 2983 (C-H), 2935, 2910, 1718 ($\text{C}=\text{O}$), 1666 ($\text{C}=\text{C}$), 1446, 1392, 1367, 1303, 1263 ($\text{P}=\text{O}$), 1178, 1095, 1018 (P-OEt), 962.

(LB ref: JB-011, JB-015, JB-032)

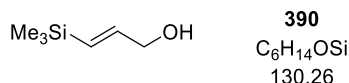
3-(Trimethylsilyl)prop-2-yn-1-ol (389)



Adapting a procedure reported by Hoveyda and co-workers¹⁵⁴, in a flame dried two-necked flask under inert atmosphere, propargylic alcohol (0.26 mL, 4.46 mmol, 1.0 eq) was dissolved in anhydrous THF (30 mL). The solution was cooled to -78 °C before *n*-BuLi (2.5 M in *n*-hexane, 3.8 mL, 9.37 mmol, 2.1 eq) was added slowly. After stirring the mixture for 45 min at -78 °C, TMSCl (1.24 mL, 9.81 mmol, 2.2 eq) was added dropwise. The reaction mixture was allowed to warm to room temperature over 3 h. The reaction was quenched by the addition of H_2O (5 mL) and 1 M HCl (15 mL) and stirred at room temperature until TLC (*n*-hexane : EtOAc 9:1) indicated complete conversion of the intermediate TMS protected alcohol. The phases were separated, and the aqueous phase extracted with Et_2O (3×15 mL). The combined organic phases were washed with brine (40 mL), dried over MgSO_4 , filtered and the solvent was removed under reduced pressure to afford the title compound as a yellow oil (529 mg, 92%).

^1H NMR (400 MHz, CDCl_3) δ_{H} : 0.19 (9H, s, $\text{Si}(\text{CH}_3)_3$), 1.98 (1H, br s, CH_2OH), 4.28 (2H, s, CH_2OH).

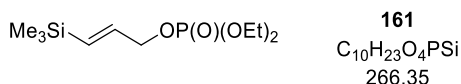
Data in accordance with literature.¹⁵⁵ (LB ref: JB-004, JB-005)

(E)-3-(Trimethylsilyl)prop-2-en-1-ol (390)

Following the procedure reported by Hoveyda and co-workers¹⁵⁴, in a flame dried flask, alcohol **389** (250 mg, 1.95 mmol, 1.0 eq) was dissolved in anhydrous Et₂O (5 mL) under an inert atmosphere and cooled to 0 °C. Red-Al® (65 wt% in toluene, 1.22 mL, 3.9 mmol, 2.0 eq) was diluted with anhydrous Et₂O (equal volume) and added slowly. After complete addition, the reaction mixture was allowed to warm to room temperature and stir until TLC (petrol : EtOAc 6:1) indicated complete conversion. The reaction mixture was quenched with H₂O (1 mL) and H₂SO₄ (3.6 M, 2 mL) and diluted by the addition of H₂O (10 mL) and Et₂O (10 mL). The phases were separated and the aqueous phase was extracted with Et₂O (3 × 10 mL). The combined organic phases were washed with brine (15 mL), dried over MgSO₄, filtered and the solvent was removed under reduced pressure to afford the title compound as a colourless oil (253 mg, 99%).

¹H NMR (400 MHz, CDCl₃) δ_H: 0.08 (9H, s, Si-(CH₃)₃), 4.18 (2H, dd, *J* 4.4, 1.8, C(1)H₂), 5.92 (1H, dt, *J* 18.8, 1.7, C(3)H), 6.19 (1H, dt, *J* 18.8, 4.4, C(2)H).

Data in accordance with literature.¹⁵⁶ (LB ref: JB-006, JB-009)

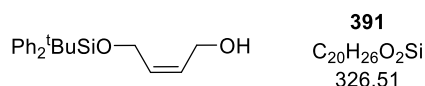
(E)-3-(Trimethylsilyl)prop-2-en-1-yl-phosphoric acid, diethyl ester (161)

The title compound was prepared following **General Procedure A** using allylic alcohol **390** (195 mg, 1.5 mmol, 1.0 eq), diethyl chlorophosphate (0.32 mL, 2.25 mmol, 1.5 eq), Et₃N (0.31 mL, 2.25 mmol, 1.5 eq) and DMAP (46.0 mg, 0.38 mmol, 0.25 eq) in anhydrous CH₂Cl₂ (15 mL). The crude mixture was purified by silica column chromatography (*n*-hexane/EtOAc 1:1) to yield **161** as a colourless oil (366 mg, 91%).

¹H NMR (400 MHz, CDCl₃) δ_H: 0.10 (9H, s, Si-(CH₃)₃), 1.36 (6H, td, *J* 7.0, 1.0, P(OCH₂CH₃)₂), 4.14 (4H, dq, *J* 7.9, 7.1, P(OCH₂CH₃)₂), 4.56 (2H, ddd, *J* 7.9, 4.4, 1.1, C(1)H₂), 6.02 (1H, dt, *J* 18.7, 1.1, C(3)H), 6.10 (1H, dtd, *J* 18.6, 4.4, 0.7, C(2)H).

³¹P {¹H} NMR (162 MHz, CDCl₃) δ_P: -0.80 (P(O)(OEt)₂).

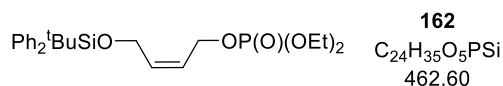
Data in accordance with literature.¹⁵⁷ (LB ref: JB-010)

(Z)-4-[[*t*-Butyldiphenylsilyloxy]-2-buten-1-ol (391)

Following the procedure reported by Takahata and co-workers,¹⁵⁸ a flame dried round bottom flask was charged with NaH (60 wt% suspension in oil, 240 mg, 6.0 mmol, 1.2 eq) under an inert atmosphere. The solid was washed twice with *n*-hexane, dried under reduced pressure and subsequently suspended in anhydrous THF (10 mL). *cis*-Butene-1,4-diol (0.41 mL, 5.0 mmol, 1.0 eq) was added slowly and the mixture was stirred for 1 h. *t*-Butyldiphenylsilylchloride (1.43 mL, 5.5 mmol, 1.1 eq) was added at 0 °C and the reaction was allowed to stir at room temperature until TLC (EtOAc) indicated complete conversion. The mixture was quenched with sat. aq. K₂CO₃ solution (10 mL), diluted with Et₂O (5 mL) and the phases were separated. The aqueous phase was extracted with Et₂O (3 × 10 mL), the combined organic phases were washed with brine, dried over MgSO₄, filtered and the solvent was removed under reduced pressure. The crude product was purified by silica column chromatography (petrol : EtOAc 5:1 to 2:1, R_f 0.26 in petrol : EtOAc 4:1) to yield the title compound as a colourless liquid (1.53 g, 94%).

¹H NMR (400 MHz, CDCl₃) δ_H: 1.11 (9H, s, C(CH₃)₃), 1.86 (1H, br s, OH), 4.02 – 4.09 (2H, m, CH₂-OSi), 4.29 – 4.34 (2H, m, CH₂-OH), 5.63 – 5.80 (2H, m, CH=CH), 7.41 – 7.49 (6H, m, 2 × Ar(2,4,6)H), 7.71 – 7.78 (4H, m, 2 × Ar(3,5)H).

Data in accordance with literature.¹⁵⁸ (LB ref: JB-061)

(Z)-4-[[1,1-Dimethylethyl)diphenylsilyloxy]-2-buten-1-yl-phosphoric acid, diethyl ester (162)

Following **General Procedure A**, allylic alcohol **391** (1.00 g, 3.06 mmol, 1.0 eq), diethyl chlorophosphate (0.66 mL, 4.6 mmol, 1.5 eq), Et₃N (0.64 mL, 4.6 mmol, 1.5 eq) and DMAP (93 mg, 0.7 mmol, 0.25 eq) in anhydrous CH₂Cl₂ (30 mL) gave the title compound after purification by silica column chromatography (*n*-hexane : EtOAc 3:1 to 1:1, R_f 0.33 in *n*-hexane : EtOAc 1:1) as a colourless liquid (1.01 g, 73%).

$^1\text{H NMR}$ (500 MHz, CDCl_3) δ_{H} : 1.07 (9H, s, $\text{C}(\text{CH}_3)_3$), 1.31 (6H, td, J 7.1, 1.0, $\text{P}(\text{OCH}_2\text{CH}_3)_2$), 4.08 (4H, dqd, J 8.5, 7.1, 1.5, $\text{P}(\text{OCH}_2\text{CH}_3)_2$), 4.30 (2H, ddt, J 5.9, 1.8, 0.9, $\text{C}(4)\text{H}_2$), 4.52 (2H, ddt, J 8.9, 6.4, 1.2, $\text{C}(1)\text{H}_2$), 5.64 (1H, dtt, J 11.2, 6.5, 1.7, $\text{C}(2)\text{H}$), 5.81 (1H, dtt, J 11.5, 5.8, 1.5, $\text{C}(3)\text{H}$), 7.39 – 7.46 (6H, m, $2 \times \text{Ar}(2,4,6)\text{H}$), 7.67 – 7.72 (4H, m, $2 \times \text{Ar}(3,5)\text{H}$).

$^{13}\text{C}\{^1\text{H}\}$ NMR (126 MHz, CDCl_3) δ_{C} : 16.1 (d, $^3J_{\text{CP}}$ 6.7, $\text{P}(\text{OCH}_2\text{CH}_3)_2$), 19.1 ($\text{C}(\text{CH}_3)_3$), 26.7 ($\text{C}(\text{CH}_3)_3$), 60.3 ($\text{C}(4)\text{H}_2$), 63.2 (d, $^2J_{\text{CP}}$ 5.5, $\text{C}(1)\text{H}_2$), 63.7 (d, $^2J_{\text{CP}}$ 5.8, $\text{P}(\text{OCH}_2\text{CH}_3)_2$), 125.1 (d, $^3J_{\text{CP}}$ 7.2, $\text{C}(2)\text{H}$), 127.7 ($2 \times \text{ArC}(2,6)\text{H}$), 129.8 ($2 \times \text{ArC}(4)\text{H}$), 133.1 ($\text{C}(3)\text{H}$), 133.3 ($2 \times \text{ArC}(1)$), 135.5 ($2 \times \text{ArC}(3,5)\text{H}$).

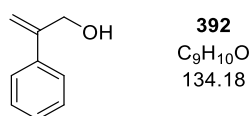
$^{31}\text{P}\{^1\text{H}\}$ NMR (162 MHz, CDCl_3) δ_{P} : -0.84 ($\text{P}(\text{O})(\text{OEt})_2$).

HRMS (NSI $^+$) $\text{C}_{24}\text{H}_{36}\text{O}_5\text{PSi}$ [$\text{M}+\text{H}$] $^+$ found 463.2057, requires 463.2064 (-1.5 ppm).

ν_{max} (film, cm^{-1}) 3070, 2980, 2931 (C-H), 2856 (C-H), 1737, 1473, 1427 (Si-Ph), 1390, 1369, 1263 (P=O), 1165, 1107 (Si-Ph), 1018 (P-OEt), 975.

(LB ref: JB-063)

2-Phenylprop-2-en-1-ol (392)



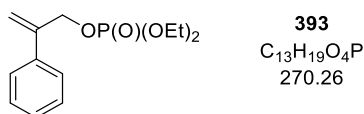
Following the procedure reported by Snaddon and co-workers,⁶⁰ in a flame dried three necked flask Mg turnings (1.46 g, 60.0 mmol, 3.0 eq) were covered with anhydrous Et_2O under an inert atmosphere. A small amount of iodine was added, followed by the dropwise addition of a solution of bromobenzene (5.32 mL, 50.0 mmol, 2.5 eq) in anhydrous Et_2O (40 mL). The rate of addition was adjusted to keep a constant reflux. After complete addition the reaction mixture was heated at reflux for 1 h and subsequently allowed to cool to room temperature. CuI (571 mg, 3.0 mmol, 0.15 eq) was added, the mixture stirred for 30 min, then propargylic alcohol (1.16 mL, 20.0 mmol, 1.0 eq) in anhydrous Et_2O (10 mL) was added slowly, and after complete addition the reaction mixture heated at reflux for 24 h. The reaction was quenched with sat. aq. NH_4Cl solution (25 mL) at 0 °C, allowed to warm to room temperature and stirred until all solids had dissolved (usually overnight). The phases were separated and the aqueous phase was extracted with Et_2O (3×30 mL). The combined organic phases were washed with brine, dried over MgSO_4 , filtered and the solvent was removed under reduced pressure. The

crude product was purified by silica column chromatography (petrol : EtOAc 6:1 to 4:1, R_f 0.26 in petrol : EtOAc 4:1) to yield the title compound as a yellow liquid (1.81 g, 68%).

$^1\text{H NMR}$ (400 MHz, CDCl_3) δ_{H} : 1.74 (1H, br s, OH), 4.57 (2H, s, CH_2OH), 5.37 – 5.40 (1H, m, $\text{C}=\text{CH}_2$), 5.49 – 5.52 (1H, m, $\text{C}=\text{CH}_2$), 7.30 – 7.43 (3H, m, $\text{Ar}(2,4,6)\text{H}$), 7.45 – 7.51 (2H, m, $\text{Ar}(3,5)\text{H}$).

Data in accordance with literature.⁶⁰ (LB ref: JB-060, JB-071)

2-Phenyl-2-propen-1-yl-phosphoric acid, diethyl ester (393)



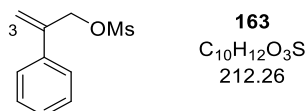
Following **General Procedure A**, allylic alcohol **393** (1.00 g, 7.45 mmol, 1.0 eq), diethyl chlorophosphate (1.61 mL, 11.2 mmol, 1.5 eq), Et_3N (1.56 mL, 11.2 mmol, 1.5 eq) and DMAP (228 mg, 1.86 mmol, 0.25 eq) in anhydrous CH_2Cl_2 (50 mL) gave the title compound after purification by silica column chromatography (*n*-hexane : EtOAc 1:1 to 1:3, R_f 0.24 in *n*-hexane : EtOAc 1:1) as a pale yellow liquid (1.75 g, 84%).

$^1\text{H NMR}$ (400 MHz, CDCl_3) δ_{H} : 1.24 – 1.32 (6H, m, $\text{P}(\text{OCH}_2\text{CH}_3)_2$), 4.00 – 4.10 (4H, m, $\text{P}(\text{OCH}_2\text{CH}_3)_2$), 4.89 – 4.94 (2H, m, $\text{C}(1)\text{H}_2$), 5.42 (1H, br s, $\text{C}(3)\text{H}^{\text{A}}\text{H}^{\text{B}}$), 5.55 (1H, br s, $\text{C}(3)\text{H}^{\text{A}}\text{H}^{\text{B}}$), 7.25 – 7.37 (3H, m, $\text{Ar}(2,4,6)\text{H}$), 7.40 – 7.47 (2H, m, $\text{Ar}(3,5)\text{H}$).

^{31}P $\{^1\text{H}\}$ NMR (162 MHz, CDCl_3) δ_{P} : -1.09 ($\text{P}(\text{O})(\text{OEt})_2$).

Data in accordance with literature.¹⁵⁹ (LB ref: JB-062)

2-Phenylallyl methanesulfonate (163)



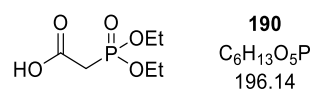
Following the procedure reported by Snaddon and co-workers,⁶⁰ in a flame dried round bottom flask, methanesulfonic anhydride (2.05 g, 11.8 mmol, 2.0 eq) was added to a stirred solution of alcohol **392** (5.88 mmol, 790 mg, 1.0 eq) in anhydrous CH_2Cl_2 (15 mL). The mixture was cooled to 0 °C and *i*- Pr_2NEt (2.05 mL, 11.8 mmol, 2.0 eq) was added dropwise. The reaction mixture was allowed to warm to room temperature and stir until TLC (petrol : EtOAc 4:1) indicated complete conversion. The solvent was removed under

reduced pressure and the crude product was purified by silica column chromatography (petrol : Et₂O 5:1 to 2:1) to yield the title compound as a yellow liquid (748 mg, 60%).

¹H NMR (400 MHz, CDCl₃) δ_H: 2.97 (3H, s, CH₃), 5.16 (2H, d, *J* 1.1, C(1)H₂), 5.52 – 5.55 (1H, m, C(3)H^AH^B), 5.72 (1H, s, C(3)H^AH^B), 7.34 – 7.44 (3H, m, Ar(2,4,6)H), 7.46 – 7.52 (2H, m, Ar(3,5)H).

Data in accordance with literature.⁶⁰ (LB ref: JB-077, JB-095)

2-(Diethoxyphosphinyl)acetic acid (190)



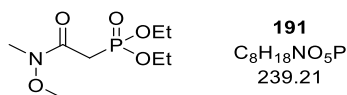
Following the procedure reported by Campagne and co-workers,⁹⁴ a solution of triethyl phosphonoacetate (5.0 g, 22.3 mmol, 1.0 eq) in 1 M NaOH (22.3 mL, 22.3 mmol, 1.0 eq) was heated to 80 °C for 5 h. After cooling to room temperature, the reaction mixture was acidified with conc. HCl (1.5 mL) and extracted with EtOAc (5 × 20 mL). The solvent was removed under reduced pressure to afford the title compound as a colourless oil (4.1 g, 93%).

¹H NMR (400 MHz, CDCl₃) δ_H: 1.35 (6H, t, *J* 7.1, P(OCH₂CH₃)₂), 2.98 (2H, d, *J* 21.5 Hz, CH₂), 4.15 – 4.25 (4H, m, P(OCH₂CH₃)₂).

³¹P{¹H} NMR (162 MHz, CDCl₃) δ_P: 21.4 (P(O)(OEt)₂).

Data in accordance with literature.¹⁶⁰ (LB ref: JB-113)

P-[2-(Methoxymethylamino)-2-oxoethyl]-phosphonic acid, diethyl ester (191)



Following the procedure reported by Campagne and co-workers,⁹⁴ CDI (1.09 g, 6.7 mmol, 1.1 eq) was added in portions to a stirred solution of **190** (1.2 g, 6.1 mmol, 1.0 eq) in CH₂Cl₂ (17 mL). After gas evolution had ceased, (*N,O*)-dimethylhydroxylamine hydrochloride (657 mg, 6.7 mmol, 1.1 eq) was added and the reaction was stirred at room temperature overnight. The reaction was quenched by the addition of H₂O (17 mL), the phases were separated, and the aqueous phase was extracted with CH₂Cl₂ (3 × 10 mL). The combined

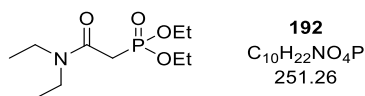
organic phases were washed with H₂O (2 × 15 mL) and the solvent was removed under reduced pressure to yield the title compound as a colourless oil (0.96 g, 79%).

¹H NMR (400 MHz, CDCl₃) δ_H: 1.34 (6H, t, *J* 7.1, P(OCH₂CH₃)₂), 3.16 (2H, d, ²*J*_{HP} 22.0, CH₂), 3.21 (3H, s, NCH₃), 3.77 (3H, s, OCH₃), 4.13 – 4.23 (4H, m, P(OCH₂CH₃)₂).

³¹P{¹H} NMR (162 MHz, CDCl₃) δ_P: 21.1 (P(O)(OEt)₂).

Data in accordance with literature.⁹⁴ (LB ref: JB-115, JB-121)

(2-(Diethylamino)-2-oxoethyl)phosphonic acid, diethyl ester (192)



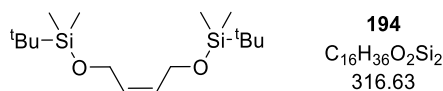
Following the procedure reported by Campagne and co-workers,⁹⁴ CDI (926 mg, 5.7 mmol, 1.1 eq) was added in portions to a stirred solution of **190** (1.0 g, 5.2 mmol, 1.0 eq) in CH₂Cl₂ (15 mL). After gas evolution had ceased, diethyl amine hydrochloride (625 mg, 5.7 mmol, 1.1 eq) was added and the reaction was stirred at room temperature overnight. The reaction was quenched by the addition of H₂O (15 mL), the phases were separated and the aqueous phase was extracted with CH₂Cl₂ (3 × 10 mL). The combined organic phases were washed with H₂O (2 × 15 mL) and the solvent was removed under reduced pressure to yield the title compound as a colourless oil (1.17 g, 91%) as a rotameric mixture (1:1).

¹H NMR (400 MHz, CDCl₃) δ_H: 1.12 (3H, t, *J* 7.1, N(CH₂CH₃)^A), 1.19 (3H, t, *J* 7.1, N(CH₂CH₃)^B), 1.32 (6H, t, *J* 7.1, P(OCH₂CH₃)₂), 3.01 (2H, d, ²*J*_{HP} 22.1, CH₂), 3.38 (2H, q, *J* 7.1, N(CH₂CH₃)^A), 3.42 (2H, *J* 7.1, N(CH₂CH₃)^B), 4.12 – 4.23 (4H, m, P(OCH₂CH₃)₂).

³¹P{¹H} NMR (162 MHz, CDCl₃) δ_P: 21.5 (P(O)(OEt)₂).

Data in accordance with literature.⁹⁴ (LB ref: JB-116)

(Z)-1,4-Bis(*t*-butyldimethylsilyloxy)-2-butene (194)



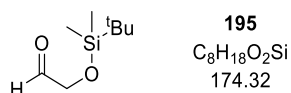
Following the procedure reported by Charette and co-workers,⁹⁵ in a flame dried round bottom flask under an inert atmosphere, a solution of *cis*-butene-1,4-diol (2.0 g, 22.7 mmol, 1.0 eq) and imidazole (6.18 g, 90.8 mmol, 4.0 eq) in anhydrous CH₂Cl₂ (100 mL) was cooled to 0 °C. A solution of TBSCl (8.2 g, 54.4 mmol, 2.4 eq) and DMAP (1.1 g, 9.0 mmol, 0.4 eq)

in anhydrous CH_2Cl_2 (30 mL) was added slowly and the reaction mixture was allowed to warm to room temperature over 16 h. The reaction was quenched by the addition of H_2O (100 mL), the phases were separated, and the aqueous phase was extracted with CH_2Cl_2 (3×30 mL). The combined organic phases were dried over MgSO_4 , filtered and the solvent was removed under reduced pressure. The crude residue was purified by Biotage® Isolera™ 4 [SNAP Ultra 50 g, 75 mL min⁻¹, petrol : Et₂O (100:0 2CV, 100:0 to 93:7 10 CV, 93:7 4 CV)] to yield the title compound as a colourless oil (6.99 g, 97%).

¹H NMR (400 MHz, CDCl₃) δ_H: 0.07 (12H, s, 2 × Si(CH₃)₂), 0.90 (18H, s, 2 × Si-C(CH₃)₃), 4.19 – 4.27 (4H, m, C(1,4)H₂), 5.50 – 5.60 (2H, m, C(2,3)H).

Data in accordance with literature.⁹⁵ (LB ref: JB-120)

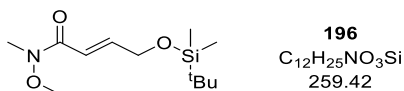
2-[(*t*-Butyl)dimethylsiloxy]acetaldehyde (**195**)



A solution of compound **194** (2.5 g, 7.9 mmol, 1.0 eq) in anhydrous CH_2Cl_2 (45 mL) was cooled to -78 °C. O_3 was bubbled through the solution until a colour change to pale blue was observed (ca. 15 min). Subsequently, the solution was purged with air until it was again colourless. PPh_3 (2.48 g, 9.4 mmol, 1.2 eq) was added in one portion at -78 °C and the reaction mixture was allowed to warm to room temperature and stir until TLC indicated complete conversion. The solvent was removed under reduced pressure and the crude product was purified by Biotage® Isolera™ 4 [SNAP Ultra 50 g, 75 mL min⁻¹, petrol : Et₂O (100:0 4 CV, 100:0 to 90:10 15 CV, 90:10 5 CV)] to yield the title compound as a colourless liquid (2.14 g, 78%).

¹H NMR (400 MHz, CDCl₃) δ_H: 0.13 (6H, s, Si(CH₃)₂), 0.95 (9H, s, C(CH₃)₃), 4.24 (2H, d, *J* 0.8, CHO-CH₂), 9.73 (1H, t, *J* 0.8, CHO).

Data in accordance with literature.¹⁶¹ (LB ref: JB-111, JB-131)

(E)-4-[[[(1,1-Dimethylethyl)dimethylsilyl]oxy]-N-methoxy-N-methyl-2-butenamide**(196)**

Following the procedure reported by Smith and co-workers,¹⁶² to a stirred solution of aldehyde **195** (250 mg, 1.43 mmol, 1.0 eq) in MeCN (5 mL) were added phosphonate **191** (412 mg, 1.72 mmol, 1.2 eq), LiCl (407 mg, 9.6 mmol, 6.7 eq) and *i*-Pr₂NEt (0.27 mL, 1.57 mmol, 1.1 eq) and the reaction mixture was stirred for 48 h at room temperature. The resulting white suspension was diluted with H₂O (5 mL), the phases were separated and the aqueous phase was extracted with EtOAc (3 × 5 mL). The combined organic phases were dried over MgSO₄, filtered and the solvent was removed under reduced pressure. The crude product was purified by silica column chromatography (petrol : EtOAc 2:1, R_f 0.32) to yield the title compound as a colourless oil (198 mg, 53%).

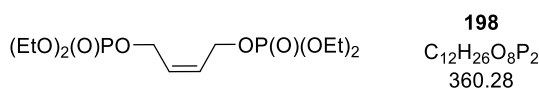
¹H NMR (500 MHz, CDCl₃) δ_H: 0.07 (6H, s, Si(CH₃)₂), 0.91 (9H, s, C(CH₃)₃), 3.23 (3H, s, N-CH₃), 3.68 (3H, s, O-CH₃), 4.36 (2H, dd, *J* 3.2, 2.3, C(4)H₂), 6.68 (1H, d, *J* 15.3, C(2)H), 6.99 (1H, dt, *J* 15.3, 3.3, C(3)H).

¹³C{¹H} NMR (126 MHz, CDCl₃) δ_C: -5.4 (Si(CH₃)₂), 18.3 (C(CH₃)₃), 25.7 (C(CH₃)₃), 32.3 (N-CH₃), 61.6 (O-CH₃), 62.5 (C(4)H₂), 117.0 (C(2)H), 145.9 (C(3)H), 166.8 (C=O).

HRMS (NSI⁺): C₁₂H₂₆NO₃Si [M+H]⁺ found 260.1678, requires 260.1676 (+0.6 ppm).

ν_{max} (CHCl₃, cm⁻¹): 2956 (C-H), 2931, 2858, 1664 (C=O), 1627 (C=C), 1471, 1444, 1417, 1386, 1373, 1253 (Si-C), 1134 (Si-O), 1010, 906.

(LB ref: JB-135, JB-136)

(Z)-But-2-ene-1,4-diyl tetraethyl bis(phosphate) (198)

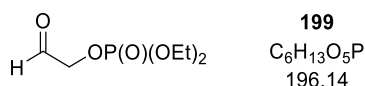
Following **General Procedure A**, *cis*-butene-1,4-diol (2.0 g, 22.7 mmol, 1.0 eq), diethyl chlorophosphate (8.2 mL, 56.7 mmol, 2.5 eq), Et₃N (7.9 mL, 56.7 mmol, 2.5 eq) and DMAP (693 mg, 5.6 mmol, 0.25 eq) in anhydrous CH₂Cl₂ (200 mL) gave the title compound after purification by silica column chromatography (0 to 20% acetone in EtOAc, R_f 0.32 in EtOAc : acetone 4:1) as colourless oil (7.0 g, 86%).

$^1\text{H NMR}$ (400 MHz, CDCl_3) δ_{H} : 1.29 – 1.36 (12H, m, 4 \times OCH_2CH_3), 4.05 – 4.16 (8H, m, 4 \times OCH_2CH_3), 4.58 – 4.65 (4H, m, C(1) H_2 , C(4) H_2), 5.75 – 5.85 (2H, m, C(2) H , C(3) H).

$^{31}\text{P}\{^1\text{H}\}$ NMR (162 MHz, CDCl_3) δ_{P} : -0.8 ($\text{OP}(\text{O})(\text{OEt})_2$).

Data in accordance with literature.¹⁶³ (LB ref: JB-114)

(2-Oxoethyl)phosphoric acid, diethyl ester (199)



A solution of compound **198** (2.0 g, 5.5 mmol, 1.0 eq) in anhydrous CH_2Cl_2 (30 mL) was cooled to -78°C . O_3 was bubbled through the solution until a colour change to pale blue/grey was observed (ca. 15 min). Subsequently, the solution was purged with air until it was again colourless. PPh_3 (1.75 g, 6.6 mmol, 1.2 eq) was added in one portion at -78°C and the reaction mixture allowed to warm to room temperature overnight. The solvent was removed under reduced pressure. The resulting white solid was washed with cold Et_2O (20 mL) and filtered. The filtrate was concentrated under reduced pressure and purified by silica column chromatography (EtOAc : petrol 5:1 to EtOAc : Acetone 9:1, R_f 0.17 in EtOAc , Vanillin stain) to yield the title compound as a pale yellow oil (1.0 g, 46%).

$^1\text{H NMR}$ (500 MHz, CDCl_3) δ_{H} : 1.34 – 1.38 (6H, m, 2 \times OCH_2CH_3), 4.15 – 4.22 (4H, m, 2 \times OCH_2CH_3), 4.58 (2H, d, $^3J_{\text{HP}}$ 9.9, CH_2), 9.69 (1H, s, CHO).

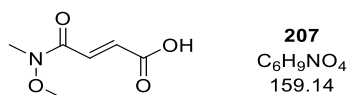
$^{13}\text{C}\{^1\text{H}\}$ NMR (126 MHz, CDCl_3) δ_{C} : 16.24 (d, $^3J_{\text{CP}}$ 6.7, 2 \times OCH_2CH_3), 64.6 (d, $^2J_{\text{CP}}$ 5.5, 2 \times OCH_2CH_3), 70.9 (d, $^2J_{\text{CP}}$ 5.7, CH_2), 196.71 (d, $^3J_{\text{CP}}$ 6.6, $\text{C}=\text{O}$).

$^{31}\text{P}\{^1\text{H}\}$ NMR (162 MHz, CDCl_3) δ_{P} : -0.9 ($\text{OP}(\text{O})(\text{OEt})_2$).

HRMS (NSI $^+$): $\text{C}_6\text{H}_{14}\text{O}_5\text{P}$ [$\text{M}+\text{H}$] $^+$ found 197.0573, requires 197.0573 (± 0 ppm).

ν_{max} (CHCl_3 , cm^{-1}): 3338, 2958 (C-H), 2933, 2912, 1739 (C=O), 1479, 1444, 1394, 1369, 1257 (P=O), 1165, 1014, 966.

(LB ref: JB-117, JB-126)

(E)-4-(Methoxymethylamino)-4-oxo-2-butenoic acid (207)

Following the procedure reported by Jacobi and co-workers,⁹⁶ a stirred solution of maleic anhydride (5.07 g, 51.7 mmol, 1.0 eq) and (*N,O*)-dimethylhydroxylamine hydrochloride (5.55 g, 56.8 mmol, 1.1 eq) in CHCl_3 (60 mL) was cooled to 0 °C. Pyridine (9.2 mL, 113 mmol, 2.2 eq) was added slowly and the reaction was allowed to warm to room temperature and stir for 24 h. The solvent was removed under reduced pressure, the residue was diluted with H_2O (20 mL) and brine (20 mL) and extracted with CH_2Cl_2 (4 × 30 mL). The combined extracts were washed with 1 M HCl (40 mL) and brine (40 mL), dried over MgSO_4 , filtered and the solvent was removed under reduced pressure. The crude product was recrystallised from CH_2Cl_2 to afford the title compound as a yellow solid (2.74 g, 33%). **m.p.** (CH_2Cl_2) 129 – 131 °C.

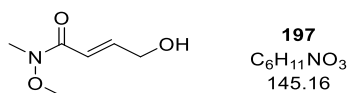
$^1\text{H NMR}$ (500 MHz, CDCl_3) δ_{H} : 3.31 (3H, s, NCH_3), 3.76 (3H, s, OCH_3), 6.91 (1H, d, J 15.6, C(2)*H*), 7.54 (1H, d, J 15.6, C(3)*H*).

$^{13}\text{C}\{^1\text{H}\}$ NMR (126 MHz, CDCl_3) δ_{C} : 32.5 (NCH_3), 62.4 (OCH_3), 131.7 (C(2)*H*), 133.6 (C(3)*H*), 164.5 (C(4)=O), 170.0 (C(1)=O).

HRMS (NSI⁻): $\text{C}_6\text{H}_8\text{NO}_4$ [$\text{M}-\text{H}$]⁻ found 158.0461, requires 158.0459 (+1.4 ppm).

ν_{max} (film, cm^{-1}): 2943 (O-H), 2763, 2630, 2551, 1720 (C=O_{acid}), 1660 (C=O_{amide}), 1602 (C=C), 1481, 1392, 1286, 1247, 1201, 1166, 1114, 995.

(LB ref: JB-142, JB-148, JB-174, JB-226, JB-495, JB-536, JB-544)

(E)-4-Hydroxy-*N*-methoxy-*N*-methyl-2-butenamide (197)

Following **General Procedure D**, acid **207** (3.0 g, 18.8 mmol, 1.0 eq), Et_3N (2.89 mL, 20.7 mmol, 1.1 eq) and ethyl chloroformate (1.98 mL, 20.7 mmol, 1.1 eq) in anhydrous THF (50 mL) followed by NaBH_4 (1.78 g, 47.1 mmol, 2.5 eq) in H_2O (30 mL) gave the title compound after purification by silica column chromatography (EtOAc : Acetone 6:1, R_f 0.31) as pale yellow oil (1.22 g, 45%). (LB ref: JB-145, JB-153, JB-184, JB-244, JB-500)

The title compound was also synthesised starting from silyl protected allylic alcohol **196**:

Following the procedure reported by Houk and co-workers,¹⁶⁴ TBAF (1 M in THF, 6.0 mL, 6.0 mmol, 3.0 eq) was added to a stirred solution of **196** (520 mg, 2.0 mmol, 1.0 eq) in THF (80 mL) at 0 °C. The reaction was allowed to warm to room temperature and stir overnight. To the reaction mixture were added H₂O (20 mL) and Et₂O (50 mL), the phases were separated and the aqueous phase was extracted with Et₂O (2 × 50 mL). The combined organic phases were washed with brine (2 × 50 mL), dried over MgSO₄, filtered and the solvent was removed under reduced pressure. The crude product was purified by silica column chromatography (CH₂Cl₂ : 4% MeOH, R_f 0.46 in CH₂Cl₂ : MeOH 9:1) to yield the title compound as a brown oil (100 mg, 34%). (LB ref: JB-143)

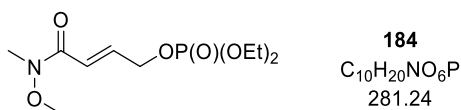
¹H NMR (400 MHz, CDCl₃) δ_H: 3.24 (3H, s, NCH₃), 3.70 (3H, s, OCH₃), 4.36 (2H, dd, *J* 4.0, 2.1, C(4)H₂), 6.67 (1H, br dt, *J* 15.5, C(2)H), 7.03 (1H, dt, *J* 15.5, 4.0, C(3)H).

¹³C{¹H} NMR (126 MHz, CDCl₃) δ_C: 32.3 (NCH₃), 61.8 (OCH₃), 62.2 (C(4)H₂), 117.4 (C(2)H), 145.7 (C(3)H), 166.6 (C=O).

HRMS (NSI⁺): C₆H₁₂NO₃ [M+H]⁺ found 146.0809, requires 146.0812 (−1.8 ppm).

ν_{max} (film, cm⁻¹): 3390 (O-H), 2970, 2937 (C-H), 1774, 1660 (C=O), 1612 (C=C), 1421, 1384, 1178, 1111, 1085, 1002, 958.

(E)-(4-(Methoxy(methyl)amino)-4-oxobut-2-en-1-yl) phosphoric acid, diethyl ester
(184)



Following **General Procedure A**, allylic alcohol **197** (516 mg, 3.55 mmol, 1.0 eq), diethyl chlorophosphate (0.77 mL, 5.33 mmol, 1.5 eq), Et₃N (0.74 mL, 5.33 mmol, 1.5 eq) and DMAP (108 mg, 0.88 mmol, 0.25 eq) in anhydrous CH₂Cl₂ (35 mL) gave the title compound after purification by silica column chromatography (EtOAc : Acetone 4:1, R_f 0.33 in EtOAc : Acetone 2:1) as a pale yellow oil (819 mg, 82 %).

(LB ref: JB-118, JB-144, JB-149, JB-156, JB-192, JB-489, JB-501)

The title compound was also synthesised via Horner-Wadsworth-Emmons reaction:

In a flame dried and argon flushed Schlenk tube, NaH (60 wt% suspension in oil, 133 mg, 3.3 mmol, 1.3 eq) was washed twice with *n*-hexane, dried under reduced pressure and subsequently suspended in anhydrous THF (3 mL). Phosphonate **191** (642 mg, 2.6 mmol

1.05 eq) was added dropwise at 0 °C and stirred at this temperature for 45 min. A solution of aldehyde **199** (500 mg, 2.5 mmol, 1.0 eq) in anhydrous THF (1 mL) was added dropwise and the reaction was allowed to warm to room temperature overnight. The reaction was quenched with sat. aq. NH₄Cl solution (5 mL), the phases were separated, and the aqueous phase was extracted with Et₂O (3 × 5 mL). The combined organic phases were dried over MgSO₄, filtered and the solvent was removed under reduced pressure. The crude product was purified by silica column chromatography (0 to 25% acetone in EtOAc) to give the title compound as a pale yellow oil (100 mg, 15%). (LB ref: JB-129)

¹H NMR (500 MHz, CDCl₃) δ_H: 1.36 (6H, td, *J* 7.1, 0.9, P(OCH₂CH₃)₂), 3.27 (3H, s, NCH₃), 3.72 (3H, s, OCH₃), 4.12 – 4.19 (4H, m, P(OCH₂CH₃)₂), 4.74 (2H, ddd, *J* 7.4, 4.3, 2.0, C(1)H₂), 6.68 – 6.76 (1H, m, C(3)H), 6.96 (1H, dtd, *J* 15.4, 4.3, 1.7, C(2)H).

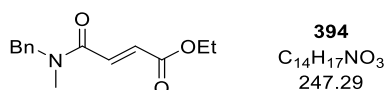
¹³C{¹H} NMR (126 MHz, CDCl₃) δ_C: 16.1 (d, ³*J*_{CP} 6.6, P(OCH₂CH₃)₂), 32.3 (NCH₃), 61.8 (OCH₃), 64.0 (d, ²*J*_{CP} 5.9, P(OCH₂CH₃)₂), 66.0 (d, ²*J*_{CP} 5.2, C(1)H₂), 119.5 (C(3)H), 139.8 (d, ³*J*_{CP} 7.4, C(2)H), 165.7 (C=O).

³¹P{¹H} NMR (162 MHz, CDCl₃) δ_P: -1.07 (OP(O)(OEt)₂).

HRMS (NSI⁺): C₁₀H₂₁NO₆P [M+H]⁺ found 282.1102, requires 282.1101 (+0.4 ppm).

*v*_{max} (CHCl₃, cm⁻¹): 2981 (C-H), 2937, 2910, 1670 (C=O), 1635 (C=C), 1444, 1417, 1386, 1261 (P=O), 1166, 1105, 1018 (P-O), 960.

(E)-4-[Methyl(phenylmethyl)amino]-4-oxo-2-butenoic acid, ethyl ester (**394**)



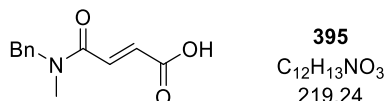
Following **General Procedure B**, monoethyl fumarate (7.5 g, 52.0 mmol, 1.0 eq), *N*-benzylmethylamine (7.4 mL, 57.2 mmol, 1.1 eq), EDCI·HCl (10.9 g, 57.2 mmol, 1.1 eq) and DMAP (636 mg, 5.2 mmol, 0.1 eq) in CH₂Cl₂ (130 mL) gave a rotameric mixture (55:45) of the title compound as yellow oil, (12.7 g, 98%), which was used without further purification.

¹H NMR (400 MHz, CDCl₃) *major rotamer* δ_H: 1.31 (3H, t, *J* 7.1, OCH₂CH₃), 3.02 (3H, s, NCH₃), 4.24 (2H, app. dq, *J* 14.2, 7.1, OCH₂CH₃), 4.66 (2H, s, NCH₂), 6.85 (1H, d, *J* 15.3, C(2)H or C(3)H), 7.14 – 7.19 (1H, m, ArC(4)H), 7.23 – 7.39 (4H, m, ArC(2,3,5,6)H), 7.43 (1H, d, *J* 15.3, C(2)H or C(3)H); *minor rotamer (selected)* δ_H: 1.28 (3H, t, *J* 7.1, OCH₂CH₃), 3.00 (3H,

s, NCH₃), 4.61 (2H, s, NCH₂), 6.85 (1H, d, *J* 15.3, C(2)*H* or C(3)*H*), 7.41 (1H, d, *J* 15.3, C(2)*H* or C(3)*H*).

(LB ref: JB-180)

(E)-4-[Methyl(phenylmethyl)amino]-4-oxo-2-butenic acid (395)

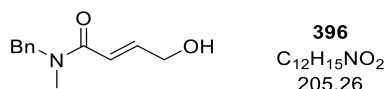


Following **General Procedure C**, ester **394** (12.1 g, 48.9 mmol, 1.0 eq) and LiOH·H₂O (2.3 g, 53.8 mmol, 1.1 eq) in H₂O : THF 1:1 (50 mL) after 16 h gave a rotameric mixture (55:45) of the title compound after extraction with CH₂Cl₂ as a yellow oil (9.9 g, 93%), which was used without further purification.

¹H NMR (400 MHz, MeOH-*d*₄) *major rotamer* δ_H: 3.08 (3H, s, NCH₃), 4.67 (2H, s, NCH₂), 6.71 (1H, d, *J* 15.3, C(2)*H* or C(3)*H*), 7.19 – 7.42 (5H, m, 5 × Ar*H*), 7.49 (1H, dd, *J* 15.4, 13.8 Hz, 1H), 7.51 (1H, d, *J* 15.3, C(2)*H* or C(3)*H*); *minor rotamer (selected)* δ_H: 3.01 (3H, s, NCH₃), 4.72 (2H, s, NCH₂), 6.70 (1H, d, *J* 15.3, C(2)*H* or C(3)*H*), 7.47 (1H, d, *J* 15.3, C(2)*H* or C(3)*H*).

(LB ref: JB-185)

(E)-4-Hydroxy-N-methyl-N-(phenylmethyl)-2-butenamide (396)



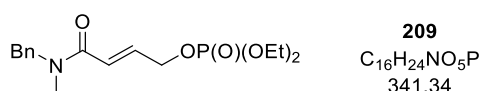
Following **General Procedure D**, acid **395** (9.8 g, 44.8 mmol, 1.0 eq), Et₃N (6.8 mL, 49.2 mmol, 1.1 eq) and ethyl chloroformate (4.7 mL, 49.2 mmol, 1.1 eq) in anhydrous THF (110 mL) followed by NaBH₄ (4.2 g, 112 mmol, 2.5 eq) in H₂O (70 mL) gave the title compound as a rotameric mixture (55:45) after purification by silica column chromatography (petrol : EtOAc 1:1 to EtOAc, R_f 0.20 in EtOAc) as a yellow oil (6.2 g, 67%). Attempts to remove remaining impurities were unsuccessful, so alcohol **396** was used as obtained after silica column chromatography.

¹H NMR (500 MHz, CDCl₃) *major rotamer* δ_H: 2.97 (3H, s, NCH₃), 4.31 – 4.36 (2H, m, C(4)*H*₂), 4.62 (2H, s, NCH₂), 6.52 – 6.63 (1H, m, C(2)*H* or C(3)*H*), 6.96 – 7.04 (1H, m, C(2)*H* or C(3)*H*), 7.12 – 7.18 (1H, m, Ar(4)*H*), 7.19 – 7.39 (4H, m, Ar(2,3,5,6)*H*); *minor rotamer (selected)* δ_H: 2.96 (3H, s, NCH₃), 4.26 – 4.31 (2H, m, C(4)*H*₂), 4.58 (2H, s, NCH₂).

$^{13}\text{C}\{^1\text{H}\}$ NMR (126 MHz, CDCl_3) *major rotamer* δ_{c} : 35.0 (NCH₃), 51.1 (NCH₂), 62.0 (C(4)H₂), 118.8 (C(2)H or C(3)H), 126.5 (ArC(4)H), 128.0 (ArC(2,6)H or ArC(3,5)H), 128.6 (ArC(2,6)H or ArC(3,5)H), 137.1 (ArC(1)), 145.3 (C(2)H or C(3)H), 166.8 (C=O); *minor rotamer (selected)* δ_{c} : 34.0 (NCH₃), 53.4 (NCH₂), 62.0 (C(4)H₂), 136.5 (ArC(1)), 145.2 (C(2)H or C(3)H), 167.3 (C=O).

(LB ref: JB-189)

(E)-(4-(Benzyl(methyl)amino)-4-oxobut-2-en-1-yl) phosphoric acid, diethyl ester (209)



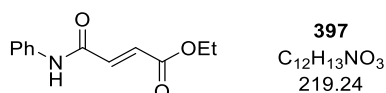
Following **General Procedure A**, allylic alcohol **396** (560 mg, 2.7 mmol, 1.0 eq), diethyl chlorophosphate (0.59 mL, 4.1 mmol, 1.5 eq), Et₃N (0.57 mL, 4.1 mmol, 1.5 eq) and DMAP (83 mg, 0.7 mmol, 0.25 eq) in anhydrous CH_2Cl_2 (30 mL) gave the title compound as a rotameric mixture (55:45) after purification by silica column chromatography (5 to 10% *i*-PrOH in EtOAc) as colourless oil (730 mg, 78%). Attempts to remove remaining impurities were unsuccessful, so phosphate **209** was used as obtained after silica column chromatography (ca. 25% impurities).

^1H NMR (500 MHz, CDCl_3) *major rotamer* δ_{H} : 1.28 – 1.33 (6H, m, $\text{P}(\text{OCH}_2\text{CH}_3)_2$), 2.96 (3H, s, NCH₃), 4.06 – 4.15 (4H, m, $\text{P}(\text{OCH}_2\text{CH}_3)_2$), 4.61 (2H, s, NCH₂), 4.69 (2H, ddd, J 7.5, 4.3, 2.0, C(1)H₂), 6.59 (1H, dt, J 15.0, 2.0, C(3)H), 6.84 – 6.94 (1H, m, C(2)H), 7.11 – 7.16 (1H, m, Ar(4)H), 7.17 – 7.35 (4H, m, Ar(2,3,5,6)H); *minor rotamer (selected)* δ_{H} : 1.20 – 1.25 (6H, m, $\text{P}(\text{OCH}_2\text{CH}_3)_2$), 2.96 (3H, s, NCH₃), 3.97 – 4.03 (4H, m, $\text{P}(\text{OCH}_2\text{CH}_3)_2$), 4.56 (2H, s, NCH₂), 4.63 (2H, ddd, J 7.6, 4.3, 2.0, C(1)H₂), 6.53 (1H, dt, J 15.0, 2.0, C(3)H).

$^{13}\text{C}\{^1\text{H}\}$ NMR (126 MHz, CDCl_3) *major rotamer* δ_{c} : 16.0 (d, $^3J_{\text{CP}}$ 6.8, $\text{P}(\text{OCH}_2\text{CH}_3)_2$), 34.9 (NCH₃), 51.1 (NCH₂), 63.9 – 64.0 (m, $\text{P}(\text{OCH}_2\text{CH}_3)_2$), 66.0 (d, $^2J_{\text{CP}}$ 5.2, C(1)H₂), 121.1 (C(3)H), 126.5 (ArC(4)H), 128.0 (ArC(2,6)H or ArC(3,5)H), 128.9 (ArC(2,6)H or ArC(3,5)H), 137.0 (ArC(1)), 139.0 (C(2)H), 165.7 (C=O); *minor rotamer (selected)* δ_{c} : 16.1 (d, $^3J_{\text{CP}}$ 6.8, $\text{P}(\text{OCH}_2\text{CH}_3)_2$), 34.1 (NCH₃), 53.3 (NCH₂), 65.9 (d, $^2J_{\text{CP}}$ 5.1, C(1)H₂), 121.0 (C(3)H), 136.4 (ArC(1)), 139.0 (C(2)H), 166.2 (C=O).

$^{31}\text{P}\{^1\text{H}\}$ NMR (162 MHz, CDCl_3) *major rotamer* δ_{P} : -1.09 ($\text{OP}(\text{O})(\text{OEt})_2$); *minor rotamer* δ_{P} : -1.15 ($\text{OP}(\text{O})(\text{OEt})_2$).

(LB ref: 202)

(E)-4-Oxo-4-(phenylamino)-2-butenic acid, ethyl ester (397)

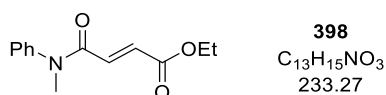
Following **General Procedure B** with modifications, monoethyl fumarate (6.0 g, 41.6 mmol, 1.0 eq), aniline (5.3 mL, 58.2 mmol, 1.4 eq), EDCI·HCl (10.3 g, 54.1 mmol, 1.3 eq) and DMAP (508 mg, 4.2 mmol, 0.1 eq) in CH₂Cl₂ (100 mL) gave the title compound after recrystallisation from Et₂O as an off-white solid (7.4 g, 81 %). **m.p.** (Et₂O) 113 – 116 °C. ¹H NMR (500 MHz, CDCl₃) δ_H: 1.33 (3H, t, *J* 7.1, OCH₂CH₃), 4.27 (2H, q, *J* 7.1, OCH₂CH₃), 6.96 (1H, d, *J* 15.3, C(2)*H*), 7.12 – 7.20 (2H, m, C(3)*H*, ArC(4)*H*), 7.34 (2H, t, *J* 7.9, ArC(3,5)*H*), 7.62 (2H, d, *J* 7.7, ArC(2,6)*H*), 8.15 (1H, br s, NH).

¹³C{¹H} NMR (126 MHz, CDCl₃) δ_C: 14.1 (OCH₂CH₃), 61.5 (OCH₂CH₃), 120.1 (ArC(2,6)*H*), 125.0 (ArC(4)*H*), 129.1 (ArC(3,5)*H*), 131.2 (C(2)*H*), 137.0 (C(3)*H*), 137.4 (ArC(1)), 161.6 (C(4)=O), 165.8 (C(1)=O).

HRMS (NSI⁺): C₁₂H₁₄NO₃ [M+H]⁺ found 220.0964, requires 220.0968 (–1.9 ppm).

ν_{\max} (CHCl₃, cm⁻¹): 3350 (N-H), 2978 (C-H), 1705 (C=O_{ester}), 1678 (C=O_{amide}), 1649 (C=C), 1602, 1544, 1500 (C=C_{Ar}), 1489, 1444, 1371, 1338, 1294, 1201, 1153, 1020, 960.

(LB ref: JB-154, JB-169)

(E)-4-(Methylphenylamino)-4-oxo-2-butenic acid, ethyl ester (398)

Adapting the procedure reported by Snaddon and co-workers,⁶⁴ in a flame dried flask under argon atmosphere, NaH (602 mg, 15.0 mmol, 1.1 eq) was washed twice with *n*-hexane, dried under reduced pressure and subsequently suspended in anhydrous THF (35 mL). Ester **397** (3.0 g, 13.6 mmol, 1.0 eq), dissolved in anhydrous THF (35 mL), was slowly added to the NaH suspension at 0 °C. After gas evolution had ceased, the reaction mixture was allowed to warm to room temperature. MeI (0.93 mL, 15.0 mmol, 1.1 eq) was added, the flask was sealed and heated to 80 °C for 16 h. After cooling to room temperature, the reaction was quenched with sat. aq. NH₄Cl solution (40 mL), the phases were separated and the aqueous phase was extracted with Et₂O (3 × 60 mL). The combined organic phases were dried over MgSO₄, filtered and the solvent was removed under

reduced pressure to afford the crude product as a black oil. Purification by Biotage® Isolera™ 4 [SNAP Ultra 50 g, 100 mL min⁻¹, petrol : EtOAc 4:1 (15 CV), R_f 0.16] afforded the title compound as an off-white solid (1.73 g, 55 %). **m.p.** (petrol) 74 – 77 °C.

¹H NMR (500 MHz, CDCl₃) δ_H: 1.24 (3H, t, *J* 7.1, OCH₂CH₃), 3.38 (3H, s, NCH₃), 4.16 (2H, q, *J* 7.1, OCH₂CH₃), 6.85 (2H, s, C(2)*H*, C(3)*H*), 7.14 – 7.19 (2H, m, ArC(2,6)*H*), 7.34 – 7.38 (1H, m, ArC(4)*H*), 7.40 – 7.46 (2H, m, ArC(3,5)*H*).

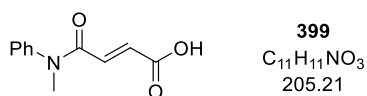
¹³C{¹H} NMR (126 MHz, CDCl₃) δ_C: 14.2 (OCH₂CH₃), 37.8 (NCH₃), 61.1 (OCH₂CH₃), 127.1 (ArC(2,6)*H*), 128.2 (ArC(4)*H*), 130.0 (ArC(3,5)*H*), 131.1 (=CH), 134.3 (=CH), 142.7 (ArC(1)), 164.1 (C(4)=O), 165.8 (C(1)=O).

HRMS (NSI⁺): C₁₃H₁₆NO₃ [M+H]⁺ found 234.1127, requires 234.1125 (+1.0 ppm).

v_{max} (film, cm⁻¹): 3352, 3049 (=C-H), 2991 (C-H), 2939, 1716 (C=O_{ester}), 1660 (C=O_{amide}), 1631 (C=C), 1593 (C=C_{Ar}), 1546, 1492 (C=C_{Ar}), 1419, 1379, 1294, 1280, 1249, 1155, 1020, 966.

(LB ref: JB-164, JB-173)

(*E*)-4-(Methylphenylamino)-4-oxo-2-butenic acid (**399**)

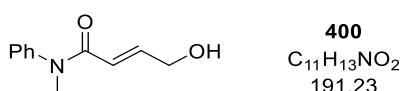


Following **General Procedure C**, ester **398** (1.5 g, 6.4 mmol, 1.0 eq) and LiOH·H₂O (297 mg, 7.0 mmol, 1.1 eq) in H₂O : THF 1:1 (7 mL) after 16 h gave the title compound after extraction with CH₂Cl₂ as an off-white solid (1.28 g, 97%), which was used without further purification.

¹H NMR (500 MHz, DMSO) δ_H: 3.28 (3H, s, NCH₃), 6.55 (1H, d, *J* 15.3, C(2)*H*), 6.64 (1H, d, *J* 15.3, C(3)*H*), 7.31 – 7.36 (2H, m, ArC(2,6)*H*), 7.38 – 7.44 (1H, m, ArC(4)*H*), 7.46 – 7.52 (2H, m, ArC(3,5)*H*).

(LB ref: JB-166, JB-175)

(*E*)-4-Hydroxy-*N*-methyl-*N*-phenyl-2-butenamide (**400**)



Following **General Procedure D**, acid **399** (2.6 g, 13.0 mmol, 1.0 eq), Et₃N (2.0 mL, 14.3 mmol, 1.1 eq) and ethyl chloroformate (1.4 mL, 14.3 mmol, 1.1 eq) in anhydrous THF

(45 mL) followed by NaBH₄ (1.2 g, 32.7 mmol, 2.5 eq) in H₂O (25 mL) gave the title compound after purification by silica column chromatography (CH₂Cl₂ : acetone 7:3, R_f 0.48 in CH₂Cl₂ : acetone 1:1) as a colourless oil (1.7 g, 70%), which solidified slowly.

m.p. (EtOAc) 70 – 73 °C.

¹H NMR (500 MHz, CDCl₃) δ_H: 1.84 (1H, br s, OH), 3.34 (3H, s, NCH₃), 4.19 – 4.24 (2H, m, C(4)H₂), 6.00 (1H, d, *J* 15.1, C(2)H), 6.98 (1H, dt, *J* 15.2, 4.2, C(3)H), 7.15 – 7.19 (2H, m, ArC(2,6)H), 7.30 – 7.35 (1H, m, ArC(4)H), 7.38 – 7.43 (2H, m, ArC(3,5)H).

¹³C{¹H} NMR (126 MHz, CDCl₃) δ_C: 37.5 (NCH₃), 62.1 (C(4)H₂), 120.1 (C(2)H), 127.2 (ArC(2,6)H), 127.6 (ArC(4)H), 129.6 (ArC(3,5)H), 143.4 (ArC(1)), 143.9 (C(3)H), 165.8 (C=O).

HRMS (NSI⁻): C₁₁H₁₂NO₂ [M-H]⁻ found 190.0877, requires 190.0874 (+1.8 ppm).

ν_{max} (film, cm⁻¹): 3385 (O-H), 3053 (Ar-H), 2864 (C-H), 2808, 1654 (C=O), 1600 (C=C), 1589, 1492 (C=C_{Ar}), 1419, 1373, 1274, 1099, 1022, 958.

(LB ref: JB-183)

(*E*)-(4-(Methyl(phenyl)amino)-4-oxobut-2-en-1-yl) phosphoric acid, diethyl ester (210)



Following **General Procedure A**, allylic alcohol **400** (516 mg, 2.7 mmol, 1.0 eq), diethyl chlorophosphate (0.58 mL, 4.0 mmol, 1.5 eq), Et₃N (0.56 mL, 4.0 mmol, 1.5 eq) and DMAP (82 mg, 0.7 mmol, 0.25 eq) in anhydrous CH₂Cl₂ (30 mL) gave the title compound after purification by silica column chromatography (EtOAc : 1% *i*-PrOH to 5% *i*-PrOH, R_f 0.41 in EtOAc : 10% *i*-PrOH) as a pale yellow oil (670 mg, 76%).

¹H NMR (500 MHz, CDCl₃) δ_H: 1.23 (6H, t, *J* 7.1, P(OCH₂CH₃)₂), 3.34 (3H, s, NCH₃), 3.92 – 4.01 (4H, m, P(OCH₂CH₃)₂), 4.53 – 4.62 (2H, m, C(1)H₂), 6.01 (1H, d, *J* 15.1, C(3)H), 6.88 (1H, dtd, *J* 15.1, 4.4, 1.4, C(2)H), 7.14 – 7.19 (2H, m, ArC(2,6)H), 7.30 – 7.35 (1H, ArC(4)H), 7.37 – 7.43 (2H, ArC(3,5)H).

¹³C{¹H} NMR (126 MHz, CDCl₃) δ_C: 16.2 (d, ³*J*_{CP} 6.6, P(OCH₂CH₃)₂), 37.6 (NCH₃), 64.0 (d, ²*J*_{CP} 5.9, P(OCH₂CH₃)₂), 65.8 (d, ²*J*_{CP} 5.0, C(1)H₂), 122.1 (C(3)H), 127.4 (ArC(2,6)H), 127.8 (ArC(4)H), 129.7 (ArC(3,5)H), 138.3 (d, ³*J*_{CP} 7.5, C(2)H), 143.4 (ArC(1)), 165.1 (C=O).

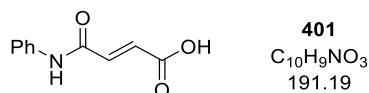
³¹P{¹H} NMR (202 MHz, CDCl₃) δ_P: -1.26 (OP(O)(OEt)₂).

HRMS (NSI⁺): C₁₅H₂₃NO₅P [M+H]⁺ found 328.1310, requires 328.1308 (+0.5 ppm).

ν_{\max} (film, cm^{-1}): 2983 (C-H), 2933, 2910, 1670 (C=O), 1631 (C=C), 1595 (C=C_{Ar}), 1496 (C=C_{Ar}), 1367, 1263 (P=O), 1018, 960.

(LB ref: JB-193)

(E)-4-oxo-4-(phenylamino)-2-butenic acid (401)

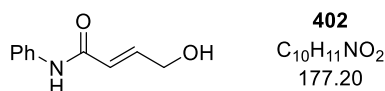


Following **General Procedure C**, ester **397** (2.7 g, 12.3 mmol, 1.0 eq) and LiOH·H₂O (568 mg, 13.5 mmol, 1.1 eq) in H₂O : THF 1:1 (13 mL) for 16 h gave the title compound after extraction with EtOAc as an off-white solid (2.97 g, 99%), which was used without further purification.

¹H NMR (400 MHz, DMSO-*d*₆) δ_{H} : 6.66 (1H, d, *J* 15.4, CH), 7.07 – 7.12 (1H, m, ArC(4)H), 7.15 (1H, d, *J* 15.4, CH), 7.31 – 7.37 (2H, m, ArC(2,6)H), 7.65 – 7.70 (2H, m, ArC(3,5)H), 10.52 (1H, s, C(O)OH).

(LB ref: JB-160)

(E)-4-hydroxy-N-phenyl-2-butenamide (402)

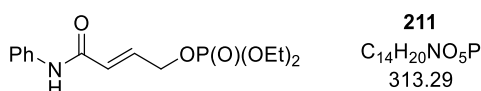


Following **General Procedure D**, acid **401** (2.5 g, 13.0 mmol, 1.0 eq), Et₃N (2.0 mL, 14.3 mmol, 1.1 eq) and ethyl chloroformate (1.4 mL, 14.3 mmol, 1.1 eq) in anhydrous THF (45 mL) followed by NaBH₄ (1.2 g, 32.7 mmol, 2.5 eq) in H₂O (25 mL) gave the title compound after recrystallisation from EtOAc as a colourless solid (636 mg, 28%).

m.p. (EtOAc) 160 – 163 °C.

¹H NMR (500 MHz, MeOH-*d*₄) δ_{H} : 4.29 (2H, dd, *J* 3.9, 2.1, C(4)H₂), 6.37 (1H, dt, *J* 15.3, 2.1, C(2)H), 6.99 (1H, dt, *J* 15.3, 3.9, C(3)H), 7.09 (1H, t, *J* 7.4, ArC(4)H), 7.28 – 7.34 (2H, m, ArC(2,6)H), 7.61 (d, *J* 7.7, ArC(3,5)H).

Data in accordance with literature.¹⁶⁵ (LB ref: JB-161)

(E)-(4-oxo-4-(phenylamino)but-2-en-1-yl) phosphoric acid, diethyl ester (211)

Following **General Procedure A**, allylic alcohol **402** (550 mg, 3.1 mmol, 1.0 eq), diethyl chlorophosphate (0.67 mL, 4.6 mmol, 1.5 eq), Et₃N (0.65 mL, 4.6 mmol, 1.5 eq) and DMAP (95 mg, 0.8 mmol, 0.25 eq) in anhydrous CH₂Cl₂ (30 mL) gave the title compound after purification by Biotage® Isolera™ 4 [SNAP Ultra 25 g, 75 mL min⁻¹, petrol : EtOAc (50:50 5 CV, 50:50 to 0:100 14 CV, 0:100 6 CV), R_f 0.28 in EtOA] as a pale yellow oil, which solidified upon freezing. Recrystallisation from toluene afforded the title compound as a colourless crystalline solid (864 mg, 89%). **m.p.** (EtOAc) 76 – 79 °C.

¹H NMR (500 MHz, CDCl₃) δ_H: 1.33 (6H, t, *J* 7.1, P(OCH₂CH₃)₂), 4.13 (4H, app. p, *J* 7.3, P(OCH₂CH₃)₂), 4.70 (2H, ddd, *J* 7.0, 4.2, 1.9, C(1)H₂), 6.38 (1H, dt, *J* 15.1, 1.8, C(3)H), 6.95 (1H, dtd, *J* 15.2, 4.2, 1.8, C(2)H), 7.09 (1H, t, *J* 7.4, ArC(4)H), 7.30 (2H, t, *J* 7.9, ArC(3,5)H), 7.65 (2H, d, *J* 7.9, ArC(2,6)H), 8.63 (1H, s, NH).

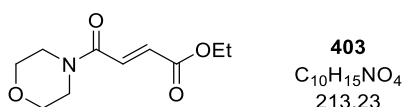
¹³C{¹H} NMR (126 MHz, CDCl₃) δ_C: 16.1 (d, ³J_{CP} 6.6, P(OCH₂CH₃)₂), 64.2 (d, ²J_{CP} 5.9, P(OCH₂CH₃)₂), 65.9 (d, ²J_{CP} 5.4, C(1)H₂), 119.9 (ArC(2,6)H), 124.2 (ArC(4)H), 125.2 (C(3)H), 128.9 (ArC(3,5)H), 137.7 (d, ³J_{CP} 7.5, C(2)H), 138.3 (ArC(1)), 163.2 (C=O).

³¹P{¹H} NMR (121 MHz, CDCl₃) δ_P: -1.74 (OP(O)(OEt)₂).

HRMS (ESI⁺): C₁₄H₂₀NO₅PNa [M+Na]⁺ found 336.0963, requires 336.0971 (-2.4 ppm).

ν_{max} (film, cm⁻¹): 3269 (N-H), 3130 (=C-H), 2991 (C-H), 2904, 1687 (C=O), 1651 (C=C), 1600 (C=C_{Ar}), 1544, 1492 (C=C_{Ar}), 1440, 1392, 1328, 1240 (P=O), 1172, 1018 (P-O), 941.

(LB ref: JB-168)

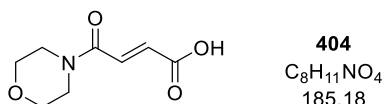
(E)-4-(4-Morpholinyl)-4-oxo-2-butenoic acid, ethyl ester (403)

Following **General Procedure B**, monoethyl fumarate (7.5 g, 52.0 mmol, 1.0 eq), morpholine (5.0 mL, 57.2 mmol, 1.1 eq), EDCI·HCl (10.9 g, 57.2 mmol, 1.1 eq) and DMAP (636 mg, 5.2 mmol, 0.1 eq) in CH₂Cl₂ (130 mL) gave the title compound as an off-white solid (10.6 g, 95 %), which was used without further purification.

$^1\text{H NMR}$ (400 MHz, CDCl_3) δ_{H} : 1.31 (3H, t, J 7.1, OCH_2CH_3), 3.56 – 3.60 (2H, m, $\text{CH}_{2(\text{morph})}$), 3.67 – 3.73 (6H, m, $3 \times \text{CH}_{2(\text{morph})}$), 4.25 (2H, q, J 7.1, OCH_2CH_3), 6.78 (1H, d, J 15.3, CH), 7.35 (1H, d, J 15.3, CH).

(LB ref: JB-181)

(E)-4-(4-Morpholinyl)-4-oxo-2-butenic acid (404)

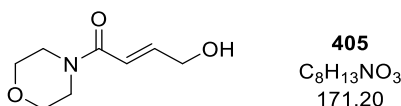


Following **General Procedure C**, ester **403** (9.8 g, 46.3 mmol, 1.0 eq) and $\text{LiOH}\cdot\text{H}_2\text{O}$ (2.1 g, 50.9 mmol, 1.1 eq) in $\text{H}_2\text{O} : \text{THF}$ 1:1 (50 mL) after 16 h gave the title compound as an off-white solid (5.75 g, 67%), which was used without further purification.

$^1\text{H NMR}$ (400 MHz, MeOH-d_4) δ_{H} : 3.62 – 3.72 (8H, m, $4 \times \text{CH}_{2(\text{morph})}$), 6.65 (1H, d, J 15.4, CH), 7.45 (1H, d, J 15.4, CH).

(LB ref: JB-186)

(E)-4-Hydroxy-N-morpholinyl-2-butenamide (405)



Following **General Procedure D**, acid **404** (5.4 g, 29.5 mmol, 1.0 eq), Et_3N (4.5 mL, 32.4 mmol, 1.1 eq) and ethyl chloroformate (3.1 mL, 32.4 mmol, 1.1 eq) in anhydrous THF (74 mL) followed by NaBH_4 (2.8 g, 73.7 mmol, 2.5 eq) in H_2O (46 mL) gave the title compound after purification by silica column chromatography (5 to 15% *i*-PrOH in EtOAc, R_f 0.26 in 15% *i*-PrOH in EtOAc) followed by recrystallisation from toluene as a colourless solid (808 mg, 16%). **m.p.** (toluene) 100 – 102 °C.

$^1\text{H NMR}$ (500 MHz, CDCl_3) δ_{H} : 3.55 – 3.60 (2H, m, $\text{NCH}_{2(\text{morph})}$), 3.64 – 3.71 (6H, m, $2 \times \text{OCH}_{2(\text{morph})}$, $\text{NCH}_{2(\text{morph})}$), 4.34 (2H, dd, J 3.7, 2.2, $\text{C}(4)\text{H}_2$), 6.52 (1H, dt, J 15.1, 2.1, $\text{C}(2)\text{H}$), 6.94 (1H, dt, J 15.2, 3.8, $\text{C}(3)\text{H}$).

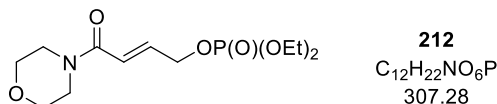
$^{13}\text{C}\{^1\text{H}\}$ NMR (126 MHz, CDCl_3) δ_{C} : 42.3 ($\text{NCH}_{2(\text{morph})}$), 46.2 ($\text{NCH}_{2(\text{morph})}$), 62.0 ($\text{C}(4)\text{H}_2$), 66.7 ($\text{OCH}_{2(\text{morph})}$), 66.8 ($\text{OCH}_{2(\text{morph})}$), 118.1 ($\text{C}(2)\text{H}$), 145.0 ($\text{C}(3)\text{H}$), 165.6 ($\text{C}=\text{O}$).

HRMS (NSI $^-$): $\text{C}_8\text{H}_{12}\text{NO}_3$ [$\text{M}-\text{H}$] $^-$ found 170.0827, requires 170.0823 (+2.5 ppm).

ν_{\max} (film, cm^{-1}): 3412 (O-H), 2980, 2931, 2872 (C-H), 2810, 1666 (C=O), 1643, 1604 (C=C), 1438, 1296, 1267, 1190, 1097, 1043, 952.

(LB ref: JB-190)

(E)-(4-Morpholino-4-oxobut-2-en-1-yl) phosphoric acid, diethyl ester (212)



Following **General Procedure A**, allylic alcohol **405** (417 mg, 2.43 mmol, 1.0 eq), diethyl chlorophosphate (0.53 mL, 3.64 mmol, 1.5 eq), Et₃N (0.51 mL, 3.64 mmol, 1.5 eq) and DMAP (74 mg, 0.6 mmol, 0.25 eq) in anhydrous CH₂Cl₂ (25 mL) gave the title compound after purification by silica column chromatography (2.5% MeOH in CH₂Cl₂, R_f 0.55 in CH₂Cl₂ : MeOH 9:1) as a pale yellow oil (673 mg, 94 %).

¹H NMR (500 MHz, CDCl₃) δ_{H} : 1.30 (6H, td, *J* 7.1, 0.9, P(OCH₂CH₃)₂), 3.49 – 3.55 (2H, m, NCH₂(morph)), 3.60 – 3.68 (6H, m, NCH₂(morph), 2 × OCH₂(morph)), 4.10 (4H, app. p, P(OCH₂CH₃)₂), 4.66 (2H, ddd, *J* 7.5, 4.2, 2.0, C(1)H₂), 6.51 (1H, dt, *J* 15.1, 2.0, C(3)H), 6.82 (1H, dtd, *J* 15.1, 4.2, 1.8, C(2)H).

¹³C{¹H} NMR (126 MHz, CDCl₃) δ_{C} : 16.1 (d, ³J_{CP} 6.6, P(OCH₂CH₃)₂), 42.3 (NCH₂(morph)), 46.2 (NCH₂(morph)), 64.0 (d, ²J_{CP} 5.8, P(OCH₂CH₃)₂), 66.0 (d, ²J_{CP} 5.2, C(1)H₂), 66.8 (2 × OCH₂(morph)), 120.4 (C(3)H), 139.1 (d, ³J_{CP} 7.3, C(2)H), 164.6 (C=O).

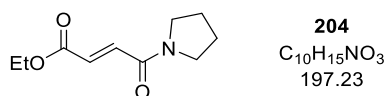
³¹P{¹H} NMR (202 MHz, CDCl₃) δ_{P} : -1.11 (OP(O)(OEt)₂).

HRMS (ESI⁺): C₁₂H₂₂NO₆PNa [M+Na]⁺ found 330.1068, requires 330.1077 (-2.7 ppm).

ν_{\max} (film, cm^{-1}): 2983 (C-H), 2908, 2858, 1668 (C=O), 1620 (C=C), 1433, 1265 (P=O), 1114, 1018 (P-O), 970.

(LB ref: JB-197, JB-201)

(E)-4-Oxo-4-(pyrrolidine-1-yl)-2-butenic acid, ethyl ester (204)



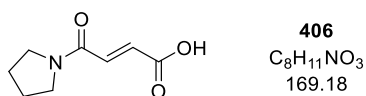
Following **General Procedure B**, monoethyl fumarate (7.5 g, 52.0 mmol, 1.0 eq), pyrrolidine (4.7 mL, 57.2 mmol, 1.1 eq), EDCI·HCl (10.9 g, 57.2 mmol, 1.1 eq) and DMAP

(636 mg, 5.2 mmol, 0.1 eq) in CH_2Cl_2 (130 mL) gave the title compound as a yellow oil (10.2 g, 99%), which was used without further purification.

$^1\text{H NMR}$ (400 MHz, CDCl_3) δ_{H} : 1.29 (3H, t, J 7.1, OCH_2CH_3), 1.84 – 2.02 (4H, m, $2 \times \text{CH}_2(\text{pyrr})$), 3.53 (2H, t, J 6.8, $\text{NCH}_2(\text{pyrr})$), 3.57 (2H, t, J 6.8, $\text{NCH}_2(\text{pyrr})$), 4.23 (2H, q, J 7.1, OCH_2CH_3), 6.82 (1H, d, J 15.3, C(2) H), 7.22 (1H, d, J 15.3, C(3) H).

(LB ref: JB-176)

(*E*)-4-Oxo-4-(1-pyrrolidinyl)-2-butenic acid (406)

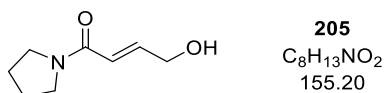


Following **General Procedure C**, ester **204** (1.0 g, 5.0 mmol, 1.0 eq) and $\text{LiOH} \cdot \text{H}_2\text{O}$ (234 mg, 5.5 mmol, 1.1 eq) in $\text{H}_2\text{O} : \text{THF}$ 1:1 (6.0 mL) after 16 h gave the title compound as a yellow solid (848 mg, 98%). **m.p.** 156 – 158 (*dec*).

$^1\text{H NMR}$ (400 MHz, $\text{DMSO}-d_6$) δ_{H} : 1.75 – 1.84 (2H, m, $\text{CH}_2(\text{pyrr})$), 1.85 – 1.94 (2H, m, $\text{CH}_2(\text{pyrr})$), 3.36 (2H, t, J 6.8, $\text{NCH}_2(\text{pyrr})$), 3.57 (2H, t, J 6.8, $\text{NCH}_2(\text{pyrr})$), 6.52 (1H, d, J 15.3, C(2) H or C(3) H), 7.16 (1H, d, J 15.3, C(2) H or C(3) H).

Data in accordance with literature.¹⁴⁶ (LB ref: JB-150, JB-162, JB-179)

(*E*)-4-hydroxy-1-(pyrrolidin-1-yl)but-2-en-1-one (205)



Following **General Procedure D**, acid **406** (6.8 g, 40.2 mmol, 1.0 eq), Et_3N (6.1 mL, 44.2 mmol, 1.1 eq) and ethyl chloroformate (4.2 mL, 44.2 mmol, 1.1 eq) in anhydrous THF (100 mL) followed by NaBH_4 (3.8 g, 100.4 mmol, 2.5 eq) in H_2O (60 mL) gave the title compound after purification by silica column chromatography (CH_2Cl_2 : acetone 1:1 to 3:7, R_f 0.22 in CH_2Cl_2 : acetone 3:7) followed by recrystallisation from toluene as colourless solid (908 mg, 15%). **m.p.** (toluene) 86 – 88 °C.

$^1\text{H NMR}$ (500 MHz, CDCl_3) δ_{H} : 1.86 (2H, p, J 6.8, $\text{CH}_2(\text{pyrr})$), 1.95 (2H, p, J 6.8, $\text{CH}_2(\text{pyrr})$), 2.93 (1H, br s, OH), 3.48 – 3.55 (4H, m, $2 \times \text{NCH}_2(\text{pyrr})$), 4.29 – 4.36 (2H, m, C(4) H_2), 6.39 (1H, dt, J 15.2, 2.0, C(2) H), 6.96 (1H, dt, J 15.2, 3.9, C(3) H).

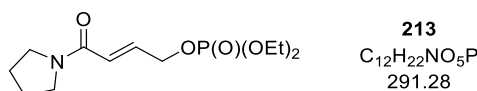
$^{13}\text{C}\{^1\text{H}\}$ NMR (126 MHz, CDCl_3) δ_{C} : 24.4 ($\text{CH}_2(\text{pyrr})$), 26.1 ($\text{CH}_2(\text{pyrr})$), 46.0 ($\text{NCH}_2(\text{pyrr})$), 46.7 ($\text{NCH}_2(\text{pyrr})$), 62.1 ($\text{C}(4)\text{H}_2$), 120.2 ($\text{C}(2)\text{H}$), 144.1 ($\text{C}(3)\text{H}$), 164.8 ($\text{C}=\text{O}$).

HRMS (NSI⁺): $\text{C}_8\text{H}_{14}\text{NO}_2$ [$\text{M}+\text{H}$]⁺ found 156.1016, requires 156.1019 (−2.0 ppm).

ν_{max} (film, cm^{-1}): 3305 (O-H), 2976, 2951, 2872 (C-H), 1662 (C=O), 1639, 1593 (C=C), 1448, 1363, 1192, 1099, 1041, 952.

(LB ref: JB-151, JB-165, JB-182)

(E)-(4-Oxo-4-(pyrrolidin-1-yl)but-2-en-1-yl) phosphoric acid, diethyl ester (213)



Following **General Procedure A**, allylic alcohol **205** (770 mg, 4.96 mmol, 1.0 eq), diethyl chlorophosphate (1.0 mL, 7.44 mmol, 1.5 eq), Et_3N (1.0 mL, 7.44 mmol, 1.5 eq) and DMAP (151 mg, 1.24 mmol, 0.25 eq) in anhydrous CH_2Cl_2 (50 mL) gave the title compound after purification by silica column chromatography (2.5% MeOH in CH_2Cl_2 , R_f 0.43 in CH_2Cl_2 : MeOH 9:1) as pale pink oil (1.3 g, 91 %).

^1H NMR (500 MHz, CDCl_3) δ_{H} : 1.30 (6H, t, J 7.1, $\text{P}(\text{OCH}_2\text{CH}_3)_2$), 1.84 (2H, p, J 6.7, $\text{CH}_2(\text{pyrr})$), 1.93 (2H, p, J 6.7, $\text{CH}_2(\text{pyrr})$), 3.49 (4H, td, J 6.8, 3.8, $\text{NCH}_2(\text{pyrr})$), 4.09 (4H, app. p, J 7.2, $\text{P}(\text{OCH}_2\text{CH}_3)_2$), 4.66 (2H, ddd, J 7.0, 4.3, 1.9, $\text{C}(1)\text{H}_2$), 6.39 (1H, dt, J 15.1, 1.9, $\text{C}(3)\text{H}$), 6.84 (1H, dtd, J 15.1, 4.3, 1.7, $\text{C}(2)\text{H}$).

$^{13}\text{C}\{^1\text{H}\}$ NMR (126 MHz, CDCl_3) δ_{C} : 16.1 (d, $^3J_{\text{CP}}$ 6.7, $\text{P}(\text{OCH}_2\text{CH}_3)_2$), 24.3 ($\text{CH}_2(\text{pyrr})$), 26.1 ($\text{CH}_2(\text{pyrr})$), 45.9 ($\text{NCH}_2(\text{pyrr})$), 46.6 ($\text{NCH}_2(\text{pyrr})$), 64.0 (d, $^2J_{\text{CP}}$ 5.8, $\text{P}(\text{OCH}_2\text{CH}_3)_2$), 66.0 (d, $^2J_{\text{CP}}$ 5.1, $\text{C}(1)\text{H}_2$), 122.4 ($\text{C}(3)\text{H}$), 137.8 (d, $^2J_{\text{CP}}$ 7.5, $\text{C}(2)\text{H}$), 163.7 ($\text{C}(4)=\text{O}$).

$^{31}\text{P}\{^1\text{H}\}$ NMR (202 MHz, CDCl_3) δ_{P} : −1.12 ($\text{OP}(\text{O})(\text{OEt})_2$).

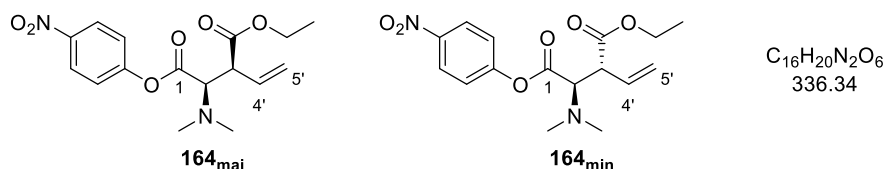
HRMS (ESI⁺): $\text{C}_{12}\text{H}_{22}\text{NO}_5\text{PNa}$ [$\text{M}+\text{Na}$]⁺ found 314.1120, requires 314.1128 (−2.5 ppm).

ν_{max} (film, cm^{-1}): 2978 (C-H), 2873, 1670 (C=O), 1616 (C=C), 1427, 1265 (P=O), 1020 (P-O), 956.

(LB ref: JB-167, JB-196)

5.4.3 Relay Pd and ITU catalysis products

(2*R*,3*S*)-2-(Dimethylamino)-3-vinylbutanedioic acid, 4-ethyl 1-(4-nitrophenyl) ester (164_{maj}) and (2*R*,3*R*)-2-(Dimethylamino)-3-vinylbutanedioic acid, 4-ethyl 1-(4-nitrophenyl) ester (164_{min})



Following **General Procedure E**, PNP ester **159** (65.0 mg, 0.25 mmol, 1.0 eq), PdFurCat **154** (9.3 mg, 12.5 μ mol, 5 mol%), (*S*)-TM·HCl (12.0 mg, 0.05 mmol, 10 mol%), phosphate **160** (83.0 mg, 0.31 mmol, 1.25 eq) and *i*-Pr₂NEt (0.1 mL, 0.6 mmol, 2.4 eq) in MeCN (4.4 mL) gave the title compound after purification by silica column chromatography (petrol : EtOAc 6:1 to 4:1, R_f 0.23 in petrol : EtOAc 6:1) as a yellow oil (60.0 mg, 71%) as an inseparable mixture of diastereomers (60:40 dr). $[\alpha]_D^{20}$ -0.5 (*c* 0.45 in CHCl₃).

HRMS (NSI⁺): C₁₆H₂₁N₂O₆ [M+H]⁺ found 337.1386, requires 337.1394 (-2.4 ppm).

ν_{\max} (film, cm⁻¹): 3084 (C-H), 2981 (C-H), 2939, 2358, 1732 (C=O), 1716 (C=O), 1616, 1591 (C=C_{Ar}), 1523 (N=O), 1489 (C=C_{Ar}), 1446, 1344 (N=O), 1305, 1257, 1203, 1157, 1109, 1026, 929.

Data for major diastereoisomer 164_{maj}

Chiral HPLC analysis, Chiralcel OD-H, (*n*-hexane : *i*-PrOH 99:1, flow rate 0.5 mLmin⁻¹, 254 nm, 30 °C) t_R (2*S*,3*R*): 26.7 min, t_R (2*R*,3*S*): 29.5 min, 10:90 er.

¹H NMR (300 MHz, CDCl₃) δ_H : 1.28 (3H, t, *J* 7.1, OCH₂CH₃), 2.47 (6H, s, N(CH₃)₂), 3.64 – 3.70 (1H, m, C(3)H), 3.85 (1H, d, *J* 11.4, C(2)H), 4.12 - 4.20 (2H, m, OCH₂CH₃), 5.28 – 5.40 (2H, m, C(5')H₂), 5.89 (1H, ddd, *J* 17.1, 10.1, 8.9, C(4')H), 7.21 – 7.26 (2H, m, Ar(2,6)H), 8.23 – 8.30 (2H, m, Ar(3,5)H).

¹³C{¹H} NMR (126 MHz, CDCl₃) δ_C : 14.1 (OCH₂CH₃), 41.8 (N(CH₃)₂), 51.3 (C(3)H), 61.0 (OCH₂CH₃), 69.2 (C(2)H), 120.9 (C(5')H₂), 122.6 (ArC(2,6)H), 125.3 (ArC(3,5)H), 131.8 (C(4')H), 145.5 (ArC(1)), 154.9 (ArC(4)), 166.7 (C(1)=O), 171.0 (C(4)=O).

Data for minor diastereoisomer 164_{min}

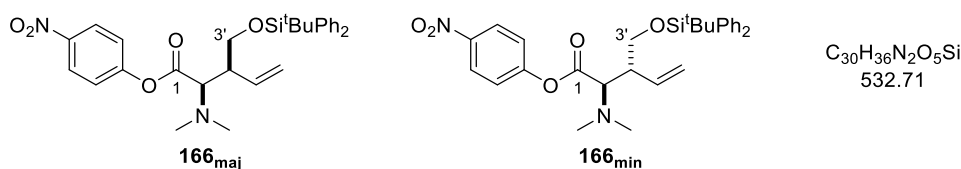
Chiral HPLC analysis, Chiralcel OD-H, (*n*-hexane : *i*-PrOH 99:1, flow rate 0.5 mLmin⁻¹, 254 nm, 30 °C) t_R (2*R*,3*R*): 25.0 min, t_R (2*S*,3*S*): 41.7 min, 70:30 er.

$^1\text{H NMR}$ (300 MHz, CDCl_3) δ_{H} : 1.23 (3H, t, J 7.1, OCH_2CH_3), 2.46 (6H, s, $\text{N}(\text{CH}_3)_2$), 3.60 – 3.68 (1H, m, $\text{C}(3)\text{H}$), 3.88 (1H, d, J 11.4, $\text{C}(2)\text{H}$), 4.16 – 4.26 (2H, m, OCH_2CH_3), 5.25 – 5.34 (2H, m, $\text{C}(5')\text{H}_2$), 5.84 (1H, ddd, J 17.3, 10.0, 8.3, $\text{C}(4')\text{H}$), 7.27 – 7.32 (2H, m, $\text{Ar}(2,6)\text{H}$), 8.23 – 8.30 (2H, m, $\text{Ar}(3,5)\text{H}$).

$^{13}\text{C}\{^1\text{H}\}$ NMR (126 MHz, CDCl_3) δ_{C} : 14.1 (OCH_2CH_3), 41.7 ($\text{N}(\text{CH}_3)_2$), 49.6 ($\text{C}(3)\text{H}$), 61.3 (OCH_2CH_3), 67.8 ($\text{C}(2)\text{H}$), 119.4 ($\text{C}(5')\text{H}_2$), 122.6 ($\text{ArC}(2,6)\text{H}$), 125.3 ($\text{ArC}(3,5)\text{H}$), 132.5 ($\text{C}(4')\text{H}$), 145.5 ($\text{ArC}(1)$), 155.1 ($\text{ArC}(4)$), 168.0 ($\text{C}(1)=\text{O}$), 172.0 ($\text{C}(4)=\text{O}$).

(LB ref: JB-073 (\pm), JB-076, JB-080)

(2*R*,3*S*)-3-(((*t*-Butyldiphenylsilyl)oxy)methyl)-2-(dimethylamino)pent-4-enoic acid, 4-nitrophenyl ester (166_{maj}) and (2*R*,3*R*)-3-(((*t*-butyldiphenylsilyl)oxy) methyl)-2-(dimethylamino)pent-4-enoic acid, 4-nitrophenyl ester (166_{min})



Following **General Procedure E**, PNP ester **159** (65.0 mg, 0.25 mmol, 1.0 eq), PdFurCat **154** (9.3 mg, 12.5 μmol , 5 mol%), (\pm)-TM-HCl (12.0 mg, 0.05 mmol, 20 mol%), phosphate **162** (143 mg, 0.31 mmol, 1.25 eq) and *i*-Pr₂NEt (0.1 mL, 0.6 mmol, 2.4 eq) in MeCN (4.4 mL) gave crude product **166** (55:45 dr), which was purified by silica column chromatography (petrol : EtOAc 6:1 to 4:1) to give:

Major diastereoisomer **166_{maj}** (R_{f} 0.42 in petrol : EtOAc 4:1, 24 mg, 18%) as a colourless solid.

$^1\text{H NMR}$ (500 MHz, CDCl_3) δ_{H} : 1.05 (9H, s, $\text{C}(\text{CH}_3)_3$), 2.45 (6H, s, $\text{N}(\text{CH}_3)_2$), 2.81 – 2.88 (1H, m, $\text{C}(3)\text{H}$), 3.69 – 3.81 (2H, m, $\text{CH}_2\text{-OSi}$), 3.82 (1H, d, J 10.9, $\text{C}(2)\text{H}$), 5.16 – 5.28 (2H, m, $\text{C}(5)\text{H}_2$), 5.99 (1H, dt, J 17.2, 9.8, $\text{C}(4)\text{H}$), 6.99 – 7.05 (2H, m, $\text{Ar}(2,6)\text{H}$), 7.30 – 7.46 (6H, m, 2 \times Ph(2,4,6)H), 7.59 – 7.66 (4H, m, 2 \times Ph(3,5)H), 8.15 – 8.21 (2H, m, $\text{Ar}(3,5)\text{H}$).

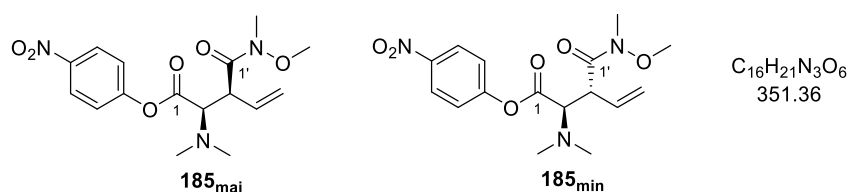
$^{13}\text{C}\{^1\text{H}\}$ NMR (126 MHz, CDCl_3) δ_{C} : 19.3 ($\text{C}(\text{CH}_3)_3$), 26.8 ($\text{C}(\text{CH}_3)_3$), 41.5 ($\text{N}(\text{CH}_3)_2$), 46.3 ($\text{C}(3)\text{H}$), 65.6 ($\text{CH}_2\text{-OSi}$), 67.5 ($\text{C}(2)\text{H}$), 117.2 ($\text{C}(5)\text{H}_2$), 122.6 ($\text{ArC}(2,6)\text{H}$), 125.1 ($\text{ArC}(3,5)\text{H}$), 127.7 (2 \times PhC(2,6)H), 129.8 (2 \times PhC(4)H), 133.2 (PhC(1)), 135.6 (2 \times PhC(3,5)H), 136.9 ($\text{C}(4)\text{H}$), 145.2 ($\text{ArC}(1)$), 155.0 ($\text{ArC}(4)$), 168.1 ($\text{C}=\text{O}$).

Minor diastereoisomer **166_{min}** (R_f 0.59 in petrol : EtOAc 4:1, 23 mg, 17%) as an off-white solid. $^1\text{H NMR}$ (400 MHz, CDCl_3) δ_{H} : 1.09 (9H, s, $\text{C}(\text{CH}_3)_3$), 2.43 (6H, s, $\text{N}(\text{CH}_3)_2$), 2.72 – 2.80 (1H, m, $\text{C}(3)\text{H}$), 3.72 – 3.79 (2H, m, $\text{C}(2)\text{H}$, $\text{CH}^{\text{A}}\text{H}^{\text{B}}\text{-OSi}$), 4.00 (1H, dd, J 9.7, 4.6, $\text{CH}^{\text{A}}\text{H}^{\text{B}}\text{-OSi}$), 5.24 – 5.32 (2H, m, $\text{C}(5)\text{H}_2$), 6.09 (1H, ddd, J 16.7, 10.8, 9.0, $\text{C}(4)\text{H}$), 7.23 – 7.27 (2H, m, $\text{Ar}(2,6)\text{H}$), 7.38 – 7.47 (6H, m, $2 \times \text{Ph}(2,4,6)\text{H}$), 7.70 – 7.79 (3H, m, $2 \times \text{Ph}(3,5)\text{H}$), 8.26 – 8.31 (2H, m, $\text{Ar}(3,5)\text{H}$).

$^{13}\text{C}\{^1\text{H}\}$ NMR (126 MHz, CDCl_3) δ_{C} : 19.3 ($\text{C}(\text{CH}_3)_3$), 26.8 ($\text{C}(\text{CH}_3)_3$), 41.4 ($\text{N}(\text{CH}_3)_2$), 45.4 ($\text{C}(3)\text{H}$), 63.2 ($\text{CH}_2\text{-OSi}$), 67.0 ($\text{C}(2)\text{H}$), 118.7 ($\text{C}(5)\text{H}_2$), 122.7 ($\text{ArC}(2,6)\text{H}$), 125.2 ($\text{ArC}(3,5)\text{H}$), 127.6 ($2 \times \text{PhC}(2,6)\text{H}$), 129.6 ($2 \times \text{PhC}(4)\text{H}$), 133.0 ($\text{PhC}(1)$), 135.6 ($2 \times \text{PhC}(3,5)\text{H}$), 136.4 ($\text{C}(4)\text{H}$), 145.3 ($\text{ArC}(1)$), 155.2 ($\text{ArC}(4)$), 168.5 (C=O).

(LB ref: JB-066)

(2*R*,3*S*)-2-(Dimethylamino)-3-(methoxy(methyl)carbamoyl)pent-4-enoic acid, 4-nitrophenyl ester (185_{maj}) and (2*R*,3*R*)-2-(Dimethylamino)-3-(methoxy(methyl)carbamoyl)pent-4-enoic acid, 4-nitrophenyl ester (185_{min})



Following **General Procedure E**, PNP ester **159** (65.0 mg, 0.25 mmol, 1.0 eq), $\text{Pd}_2\text{dba}_3 \cdot \text{CHCl}_3$ (6.5 mg, 6.25 μmol , 2.5 mol%), $\text{P}(2\text{-furyl})_3$ (5.8 mg, 25 μmol , 10 mol%), (*S*)-**TM**· HCl (12.0 mg, 0.05 mmol, 20 mol%), phosphate **184** (77.4 mg, 0.27 mmol, 1.1 eq) and *i*- Pr_2NEt (0.1 mL, 0.6 mmol, 2.4 eq) in MeCN (4.4 mL) gave the crude product (60:40 dr), which was purified by silica column chromatography (CH_2Cl_2 : Et_2O 15:1 to 4:1) to give:

Major diastereoisomer **185_{maj}** (R_f 0.37 in CH_2Cl_2 : Et_2O 4:1) as a pale yellow glass (30 mg, 34%). $[\alpha]_{\text{D}}^{20} + 0.2$ (c 0.5 in CHCl_3); **Chiral HPLC** analysis, Chiralcel OD-H, (*n*-hexane : *i*- PrOH 95:5, flow rate 1.0 mLmin^{-1} , 211 nm, 40 °C) t_{R} (2*R*,3*S*) 19.5 min, t_{R} (2*S*,3*R*) 14.7 min, 91:9 er. $^1\text{H NMR}$ (500 MHz, CDCl_3) δ_{H} : 2.47 (6H, s, $\text{N}(\text{CH}_3)_2$), 3.25 (3H, s, $\text{C}(\text{O})\text{NCH}_3$), 3.75 (3H, s, OCH_3), 4.01 – 4.07 (m, 1H, $\text{C}(2)\text{H}$), 4.17 – 4.30 (1H, m, $\text{C}(3)\text{H}$), 5.30 (1H, d, J 10.2, $\text{C}(5)\text{H}^{\text{A}}\text{H}^{\text{B}}$), 5.36 (1H, d, J 17.2, $\text{C}(5)\text{H}^{\text{A}}\text{H}^{\text{B}}$), 5.87 – 5.96 (1H, m, $\text{C}(4)\text{H}$), 7.23 – 7.26 (2H, m, $\text{Ar}(2,6)\text{H}$), 8.24 – 8.29 (2H, m, $\text{Ar}(3,5)\text{H}$).

$^{13}\text{C}\{^1\text{H}\}$ NMR (126 MHz, CDCl_3) δ_{C} : 32.4 (C(O)NCH₃), 42.2 (N(CH₃)₂), 46.1 (C(3)H), 61.9 (OCH₃), 69.0 (C(2)H), 120.7 (C(5)H₂), 122.8 (ArC(2,6)H), 125.3 (ArC(3,5)H), 133.3 (C(4)H), 145.5 (ArC(1)), 155.1 (ArC(4)), 167.5 (C(1)=O), 171.6 (C(1')=O).

HRMS (NSI⁺): C₁₆H₂₂N₃O₆ [M+H]⁺ found 352.1506, requires 352.1503 (+0.8 ppm).

ν_{max} (CDCl_3 , cm^{-1}): 2941 (C-H), 2837, 2791, 1755 (C=O), 1654 (C=O), 1635, 1616, 1593 (C=C_{Ar}), 1525 (N=O), 1489 (C=C_{Ar}), 1346 (N=O), 1205, 1161, 1111, 908.

Minor diastereoisomer **185_{min}** (R_f 0.61 in CH_2Cl_2 : Et₂O 4:1) as a pale yellow glass (20 mg, 23%). $[\alpha]_{\text{D}}^{20}$ +15.8 (c 0.25 in CHCl_3); **Chiral HPLC** analysis, Chiralcel OD-H, (*n*-hexane : *i*-PrOH 95:5, flow rate 1.0 mLmin⁻¹, 211 nm, 40 °C) t_{R} (2*R*,3*R*): 10.1 min, t_{R} (2*S*,3*S*): 13.3 min, 83:17 er.

^1H NMR (500 MHz, CDCl_3) δ_{H} : 2.50 (6H, s, N(CH₃)₂), 3.18 (3H, s, C(O)NCH₃), 3.75 (3H, s, OCH₃), 3.99 – 4.04 (1H, m, C(2)H), 4.04 – 4.12 (1H, m, C(3)H), 5.24 – 5.34 (2H, m, C(5)H₂), 5.83 – 5.93 (1H, m, C(4)H), 7.26 – 7.31 (2H, m, Ar(2,6)H), 8.23 – 8.28 (2H, m, Ar(3,5)H).

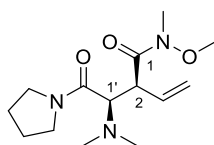
$^{13}\text{C}\{^1\text{H}\}$ NMR (126 MHz, CDCl_3) δ_{C} : 32.3 (C(O)NCH₃), 42.1 (N(CH₃)₂), 45.8 (C(3)H), 61.3 (OCH₃), 68.3 (C(2)H), 118.9 (C(5)H₂), 122.8 (ArC(2,6)H), 125.3 (ArC(3,5)H), 133.5 (C(4)H), 145.5 (ArC(1)), 155.3 (ArC(4)), 168.8 (C(1)=O), 172.3 (C(1')=O).

HRMS (NSI⁺): C₁₆H₂₂N₃O₆ [M+H]⁺ found 352.1505, requires 352.1503 (+0.5 ppm).

ν_{max} (CHCl_3 , cm^{-1}): 2978, 2941 (C-H), 2837, 2791, 1749 (C=O), 1651 (C=O), 1633, 1616, 1593 (C=C_{Ar}), 1525 (N=O), 1489 (C=C_{Ar}), 1346 (N=O), 1205, 1141, 1112, 908.

(LB ref: JB-140 (±), JB-146, JB-507)

(S)-2-((R)-1-(dimethylamino)-2-oxo-2-(pyrrolidin-1-yl)ethyl)-N-methoxy-N-methylbut-3-enamide (186_{maj})



186_{maj}
C₁₄H₂₅N₃O₃
283.37

A solution of PNP ester **185_{maj}** (57.0 mg, 0.17 mmol, 1.0 eq) and pyrrolidine (43 μL , 0.51 mmol, 3.0 eq) in CH_2Cl_2 (3.5 mL) was stirred at room temperature overnight. The reaction was quenched by the addition of 1 M NaOH (3 mL), the phases were separated and the aqueous phase was extracted with CH_2Cl_2 (3 \times 3 mL). The combined organic phases were washed with 1 M NaOH (2 \times 5 mL), H₂O (5 mL) and brine (5 mL), dried over

MgSO₄, filtered and the solvent was removed under reduced pressure. The crude product was purified by silica column chromatography (2 to 4% MeOH in CH₂Cl₂, R_f 0.47 in CH₂Cl₂ : MeOH 9:1) to yield the title compound **186_{maj}** as a white solid (13 mg, 27%).

m.p. (CH₂Cl₂) 115 – 118 °C.

$[\alpha]_D^{20}$ -7.0 (*c* 0.3 in CHCl₃); **Chiral HPLC** analysis, Chiralpak ID, (*n*-hexane : *i*-PrOH 88:12, flow rate 1.5 mLmin⁻¹, 211 nm, 40 °C) t_R (2*S*,1'*R*): 20.0 min, t_R (2*R*,1'*S*) 13.9 min, 90:10 er.

¹H NMR (500 MHz, CDCl₃) δ_H: 1.76 – 1.86 (2H, m, CH₂(pyrr)), 1.86 – 1.97 (2H, m, CH₂(pyrr)), 2.37 (6H, s, N(CH₃)₂), 3.22 (3H, s, C(O)NCH₃), 3.45 (2H, td, *J* 7.0, 2.7, NCH₂(pyrr)), 3.52 (2H, td, *J* 6.8, 1.8, NCH₂(pyrr)), 3.71 (3H, s, OCH₃), 3.96 (1H, d, *J* 10.9, C(1'*H*)), 4.18 – 4.32 (1H, m, C(2'*H*)), 5.12 (1H, dd, *J* 10.3, 1.1, C(4)*H*^A*H*^B), 5.22 – 5.29 (1H, m, C(4)*H*^A*H*^B), 5.70 – 5.80 (1H, m, C(3'*H*)).

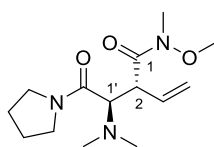
¹³C{¹H} NMR (126 MHz, CDCl₃) δ_C: 24.4 (CH₂(pyrr)), 26.3 (CH₂(pyrr)), 32.4 (C(O)NCH₃), 42.2 (N(CH₃)₂), 45.2 (NCH₂(pyrr)), 45.6 (C(2'*H*)), 47.1 (NCH₂(pyrr)), 61.9 (OCH₃), 66.1 (C(1'*H*)), 119.5 (C(4)*H*₂), 133.7 (C(3'*H*)), 168.1 (C(2')=O), 173.0 (C(1)=O).

HRMS (NSI⁺): C₁₄H₂₆N₃O₃ [M+H]⁺ found 284.1971, requires 284.1969 (+0.8 ppm).

ν_{\max} (CHCl₃, cm⁻¹): 2972 (C-H), 2875 (C-H), 2831, 1625 (C=O), 1429, 1384, 1340, 1174, 997.

(LB ref: JB-140 (±), JB-146, JB-157)

(*R*)-2-((*R*)-1-(Dimethylamino)-2-oxo-2-(pyrrolidin-1-yl)ethyl)-*N*-methoxy-*N*-methylbut-3-enamide (186_{min}**)**



186_{min}
C₁₄H₂₆N₃O₃
283.37

A solution of PNP ester **186_{min}** (57.0 mg, 0.17 mmol, 1.0 eq) and pyrrolidine (43 μL, 0.51 mmol, 3.0 eq) in CH₂Cl₂ (3.5 mL) was stirred at room temperature overnight. The reaction was quenched by the addition of 1 M NaOH (3 mL), the phases were separated and the aqueous phase was extracted with CH₂Cl₂ (3 × 3 mL). The combined organic phases were washed with 1 M NaOH (2 × 5 mL), H₂O (5 mL) and brine (5 mL), dried over MgSO₄, filtered and the solvent was removed under reduced pressure. The crude product was purified by silica column chromatography (2 to 4% MeOH in CH₂Cl₂, R_f 0.55 in CH₂Cl₂ : MeOH 9:1) to yield the title compound **186_{min}** as a colourless glass (13 mg, 27%).

$[\alpha]_D^{20} + 9.8$ (*c* 0.2 in CHCl_3); **Chiral HPLC** analysis, Chiralpak ID, (*n*-hexane : *i*-PrOH 88:12, flow rate 1.5 mLmin⁻¹, 211 nm, 40 °C) *t_R* (major) 12.5 min, *t_R* (minor) 6.2 min, 84:16 er.

¹H NMR (400 MHz, CDCl_3) δ_{H} : 1.75 – 1.88 (2H, m, $\text{CH}_2(\text{pyrr})$), 1.88 – 1.96 (2H, m, $\text{CH}_2(\text{pyrr})$), 2.42 (6H, s, $\text{N}(\text{CH}_3)_2$), 3.15 (3H, s, $\text{C}(\text{O})\text{NCH}_3$), 3.36 – 3.48 (2H, m, $\text{NCH}_2(\text{pyrr})$), 3.55 (1H, dt, *J* 10.0, 7.0, $\text{N}(\text{CH}^{\text{A}}\text{H}^{\text{B}})_{(\text{pyrr})}$), 3.74 (1H, dt, *J* 10.0, 6.6, $\text{N}(\text{CH}^{\text{A}}\text{H}^{\text{B}})_{(\text{pyrr})}$), 3.81 (3H, s, OCH_3), 3.94 (1H, d, *J* 10.8, $\text{C}(1')\text{H}$), 4.21 – 4.35 (1H, m, $\text{C}(2)\text{H}$), 5.23 (1H, dd, *J* 10.2, 1.2, $\text{C}(4)\text{H}^{\text{A}}\text{H}^{\text{B}}$), 5.29 (1H, d, *J* 17.3, $\text{C}(4)\text{H}^{\text{A}}\text{H}^{\text{B}}$), 5.89 (1H, ddd, *J* 17.2, 10.2, 8.8, $\text{C}(3)\text{H}$).

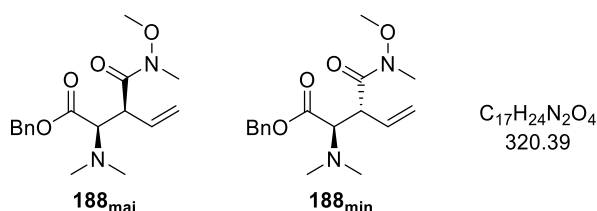
¹³C{¹H} NMR (126 MHz, CDCl_3) δ_{C} : 24.4 ($\text{CH}_2(\text{pyrr})$), 26.2 ($\text{CH}_2(\text{pyrr})$), 32.2 ($\text{C}(\text{O})\text{NCH}_3$), 41.9 ($\text{N}(\text{CH}_3)_2$), 45.5 ($\text{NCH}_2(\text{pyrr})$), 45.9 ($\text{C}(2)\text{H}$), 46.8 ($\text{NCH}_2(\text{pyrr})$), 61.5 (OCH_3), 65.6 ($\text{C}(1')\text{H}$), 118.6 ($\text{C}(4)\text{H}_2$), 135.1 ($\text{C}(3)\text{H}$), 168.7 ($\text{C}(2')=\text{O}$), 172.6 ($\text{C}(1)=\text{O}$).

HRMS (NSI⁺): $\text{C}_{14}\text{H}_{26}\text{N}_3\text{O}_3$ [$\text{M}+\text{H}$]⁺ found 284.1972, requires 284.1969 (+1.2 ppm).

ν_{max} (film, cm^{-1}): 2976 (C-H), 2877, 2791, 1647 (C=O), 1629 (C=O), 1440, 1386, 1338, 1170, 906.

(LB ref: JB-140 (\pm), JB-146, JB-157)

(2*R*,3*S*)-2-(Dimethylamino)-3-(methoxy(methyl)carbamoyl)pent-4-enoic acid, benzyl ester (188_{maj}) and (2*R*,3*R*)-2-(Dimethylamino)-3-(methoxy(methyl) carbamoyl)pent-4-enoic acid, benzyl ester (188_{min})



Following **General Procedure E**, PNP ester **159** (78.2 mg, 0.30 mmol, 1.0 eq), $\text{Pd}_2\text{dba}_3 \cdot \text{CHCl}_3$ (7.7 mg, 7.5 μmol , 2.5 mol%), $\text{P}(2\text{-furyl})_3$ (6.9 mg, 0.03 mmol, 10 mol%), (*S*)-TM-HCl (14.4 mg, 0.06 mmol, 20 mol%), phosphate **184** (105 mg, 0.37 mmol, 1.25 eq) and *i*-Pr₂NEt (125 μL , 0.7 mmol, 2.4 eq) in MeCN (5.0 mL) gave the crude product (63:37 dr), which was used directly for derivatisation with NaOBn (0.45 mL, 0.45 mmol, 1.5 eq) in THF (6.0 mL). Subsequent purification of the crude derivatised product via silica column chromatography (petrol : EtOAc 4:1 to EtOAc) gave:

Major diastereoisomer **188_{maj}** (*R_f* 0.12 in petrol : EtOAc 1:1) as a yellow oil (33 mg, 34%).

$[\alpha]_D^{20} -1.6$ (*c* 0.9 in CHCl_3); **chiral HPLC analysis**, Chiralcel OD-H (95:5 hexane : *i*-PrOH, flow rate 1 mLmin⁻¹, 211 nm, 40 °C) *t_R*(2*R*,3*S*): 8.3 min, *t_R*(2*S*,3*R*): 9.8 min, 87:13 er.

¹H NMR (500 MHz, CDCl₃) δ_H: 2.31 (6H, s, N(CH₃)₂), 3.20 (3H, s, C(O)NCH₃), 3.70 (3H, s, OCH₃), 3.80 (1H, d, *J* 11.4, C(2)H), 4.10 – 4.19 (1H, m, C(3)H), 5.10 (1H, dd, *J* 10.1, 1.3, C(5)H^AH^B), 5.10 (1H, d, *J* 12.2, OCH^AH^B), 5.14 (1H, d, *J* 12.2, OCH^AH^B), 5.21 (1H, dt, *J* 17.2, 0.8, C(5)H^AH^B), 5.76 (1H, ddd, *J* 17.2, 10.2, 8.8, C(4)H), 7.29 – 7.37 (5H, m, 5 × ArH).

¹³C{¹H} NMR (126 MHz, CDCl₃) δ_C: 32.2 (C(O)NCH₃), 42.0 (N(CH₃)₂), 45.9 (C(3)H), 61.7 (OCH₃), 65.8 (OCH₂), 68.9 (C(2)H), 119.9 (C(5)H₂), 128.2 (ArCH), 128.5 (ArCH), 128.5 (ArCH), 133.3 (C(4)H), 135.8 (ArC), 169.4 (C(1)=O), 172.1 (C(3)=O).

HRMS (ESI⁺): C₁₇H₂₅N₂O₄ [M+H]⁺ found 321.1805 requires 321.1809 (−1.2 ppm).

v_{max} (CHCl₃, cm^{−1}): 3008 (=CH), 2943 (C-H), 2835, 2792 (N(C-H)), 1724 (C=O_{ester}), 1654 (C=O_{amide}), 1635 (C=C), 1454, 1384, 1257, 1215, 1149, 995.

Minor diastereoisomer 188_{min} (R_f 0.33 in petrol : EtOAc 1:1) as a colourless glass (21 mg, 22%).

[α]_D²⁰ +8.5 (*c* 1.4 in CHCl₃); **chiral HPLC analysis**, Chiralcel OD-H (99:1 hexane : *i*-PrOH, flow rate 1 mlmin^{−1}, 211 nm, 40 °C) t_R(2*R*,3*R*): 16.3 min, t_R(2*S*,3*S*): 19.0 min, 77:23 er.

¹H NMR (500 MHz, CDCl₃) δ_H: 2.33 (6H, s, N(CH₃)₂), 3.12 (3H, s, C(O)NCH₃), 3.69 (3H, s, OCH₃), 3.83 (1H, d, *J* 11.3, C(2)H), 3.98 – 4.07 (1H, m, C(3)H), 5.05 (1H, d, *J* 12.3, OCH^AH^B), 5.20 – 5.26 (3H, m, OCH^AH^B, C(5)H₂), 5.82 (1H, ddd, *J* 17.0, 10.5, 8.4, C(4)H), 7.28 – 7.38 (5H, m, 5 × ArH).

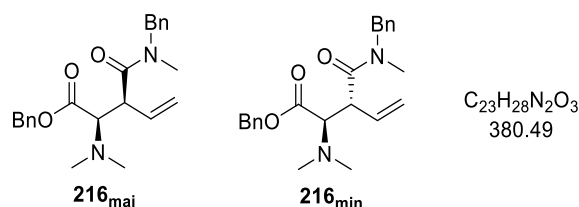
¹³C{¹H} NMR (126 MHz, CDCl₃) δ_C: 32.1 (C(O)NCH₃), 41.9 (N(CH₃)₂), 45.6 (C(3)H), 61.0 (OCH₃), 66.1 (OCH), 68.0 (C(2)H), 118.2 (C(5)H₂), 128.2 (ArCH), 128.4 (ArCH), 128.5 (ArCH), 134.1 (C(4)H), 135.9 (ArC), 170.5 (C=O_{ester}), 172.4 (C=O_{amide}).

HRMS (ESI⁺): C₁₇H₂₄N₂O₄Na [M+Na]⁺ found 343.1616, requires 343.1628 (−3.6 ppm).

v_{max} (CHCl₃, cm^{−1}): 3016 (C=CH), 2943 (C-H), 2835, 2789 (N(C-H)), 1720 (C=O_{ester}), 1651 (C=O_{amide}), 1631 (C=C), 1454, 1384, 1338, 1215, 1165, 995.

(LB ref: JB-195 (±), JB-212)

(2*R*,3*S*)-3-(Benzyl(methyl)carbamoyl)-2-(dimethylamino)pent-4-enoic acid, benzyl ester (216_{maj}) and (2*R*,3*R*)-3-(Benzyl(methyl)carbamoyl)-2-(dimethylamino)pent-4-enoic acid, benzyl ester (216_{min})



Following **General Procedure E**, PNP ester **159** (78.2 mg, 0.30 mmol, 1.0 eq), Pd₂dba₃·CHCl₃ (7.7 mg, 7.5 μmol, 2.5 mol%), P(2-furyl)₃ (6.9 mg, 0.03 mmol, 10 mol%), (*S*)-TM·HCl (14.4 mg, 0.06 mmol, 20 mol%), phosphate **209** (205 mg, 0.6 mmol, 2.0 eq) and *i*-Pr₂NEt (125 μL, 0.7 mmol, 2.4 eq) in MeCN (5.0 mL) gave the crude product (54:46 dr), which was used directly for derivatisation with NaOBn (0.45 mL, 0.45 mmol, 1.5 eq) in THF (6.0 mL). Subsequent purification of the crude derivatised product via silica column chromatography (petrol : EtOAc 3:1 to 1:1) gave:

Major diastereoisomer 216_{maj} (R_f 0.18 in petrol : EtOAc 1:1) as a yellow oil (36 mg, 32%) as a rotameric mixture (3:2).

[α]_D²⁰ -0.8 (c 0.5 in CHCl₃); **chiral HPLC** analysis, Chiralcel OD-H (98:2 hexane : *i*-PrOH, flow rate 1 mlmin⁻¹, 211 nm, 40 °C) t_R(2*R*,3*S*): 22.4 min, t_R(2*S*,3*R*): 29.9 min, 71:29 er.

¹H NMR (500 MHz, CDCl₃) *major rotamer* δ_H: 2.35 (6H, s, N(CH₃)₂), 2.97 (3H, s, C(O)NCH₃), 3.89 (1H, dd, *J* 10.9, 8.5, C(3)H), 3.95 (1H, d, *J* 11.0, C(2)H), 4.54 (1H, d, *J* 14.9, NCH^AH^B), 4.75 (d, *J* 14.9, NCH^AH^B), 5.09 – 5.15 (2H, m, OCH^AH^B, C(5)H^AH^B), 5.17 (1H, d, *J* 12.3, OCH^AH^B), 5.22 (1H, d, *J* 17.2, C(5)H^AH^B), 5.78 (1H, ddd, *J* 17.3, 10.2, 8.5, C(4)H), 7.18 – 7.26 (3H, m, 3 × NCH₂ArH), 7.27 – 7.39 (7H, m, 2 × NCH₂ArH, 5 × OCH₂ArH); *minor rotamer (selected)* δ_H: 2.23 (6H, s, N(CH₃)₂), 3.75 (1H, dd, *J* 10.8, 8.6, C(3)H), 3.96 (1H, d, *J* 10.9, C(2)H), 4.49 (1H, d, *J* 16.8, NCH^AH^B), 4.68 (1H, d, *J* 16.8, NCH^AH^B), 5.07 (1H, d, *J* 12.3, OCH^AH^B), 5.76 (1H, ddd, *J* 17.3, 10.3, 8.6, C(4)H).

¹³C{¹H} NMR (126 MHz, CDCl₃) *major rotamer* δ_C: 34.8 (C(O)NCH₃), 42.2 (N(CH₃)₂), 46.9 (C(3)H), 51.1 (NCH₂), 65.9 (OCH₂), 69.2 (C(2)H), 119.9 (C(5)H₂), 127.2 (NCH₂ArCH), 127.7 (NCH₂ArCH), 128.2 (OCH₂ArCH), 128.2 (OCH₂ArCH), 128.5 (OCH₂ArCH), 128.8 (OCH₂ArCH), 133.0 (C(4)H), 135.8 (OCH₂ArC(1)), 137.2 (NCH₂ArC(1)), 169.7 (C(1)=O), 171.6 (C(3')=O); *minor rotamer (selected)* δ_C: 34.5 (C(O)NCH₃), 42.4 (N(CH₃)₂), 46.7 (C(3)H),

53.0 (NCH₂), 65.8 (OCH₂), 119.9 (C(5)H₂), 126.5 (NCH₂ArCH), 127.6 (NCH₂ArCH), 133.3 (C(4)H), 136.6 (NCH₂ArC(1)), 169.4 (C(1)=O), 171.4 (C(3')=O).

HRMS (ESI⁺): C₂₃H₂₉N₂O₃ [M+H]⁺ found 381.2165, requires 381.2173 (-2.0 ppm).

v_{max} (CHCl₃, cm⁻¹): 3012 (=CH), 2943 (C-H), 2835, 2789 (N(C-H)), 1724 (C=O_{ester}), 1643 (C=O_{amide}), 1631 (C=C), 1454, 1404, 1261, 1215, 1153, 1118, 991.

Minor diastereoisomer 216_{min} (R_f 0.32 in petrol : EtOAc 1:1) as a yellow oil (30 mg, 26%) as a rotameric mixture (2:1).

[α]_D²⁰ +0.7 (c 0.8 in CHCl₃); **chiral HPLC** analysis, Chiralcel OD-H (98:2 hexane : *i*-PrOH, flow rate 1 mlmin⁻¹, 211 nm, 40 °C) t_R(2*R*,3*R*): 13.4 min, t_R(2*S*,3*S*): 20.8 min, 53:47 er.

¹H NMR (500 MHz, CDCl₃) *major rotamer* δ _H: 2.36 (6H, s, N(CH₃)₂), 2.99 (3H, s, C(O)NCH₃), 3.81 – 3.88 (1H, m, C(3)H), 3.95 (1H, d, *J* 10.8, C(2)H), 4.57 (2H, s, NCH₂), 5.15 (1H, app. t, *J* 12.3, OCH^AH^B), 5.18 – 5.31 (3H, m, OCH^AH^B, C(5)H₂), 5.87 – 5.97 (1H, m, C(4)H), 7.20 (1H, d, *J* 7.5, ArCH), 7.24 – 7.29 (1H, m, ArCH), 7.29 – 7.44 (8H, m, ArCH). *minor rotamer (selected)* δ _H: 2.32 (6H, s, N(CH₃)₂), 2.82 (3H, s, C(O)NCH₃), 3.92 (1H, d, *J* 10.8, C(2)H), 4.48 (1H, d, *J* 16.4, NCH^AH^B), 4.65 (1H, d, *J* 16.4, NCH^AH^B), 5.07 (1H, d, *J* 17.4, C(5)H^AH^B), 5.15 (1H, app. t, *J* 12.3, OCH^AH^B).

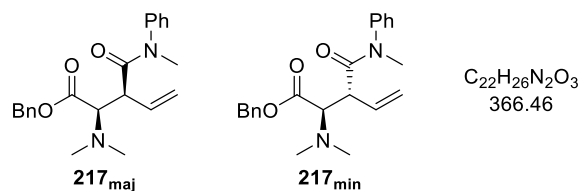
¹³C{¹H} NMR (126 MHz, CDCl₃) *major rotamer* δ _C: 34.7 (C(O)NCH₃), 42.0 (N(CH₃)₂), 46.6 (C(3)H), 50.9 (NCH₂), 66.1 (OCH₂), 68.8 (C(2)H), 118.1 (C(5)H₂), 127.1 (ArCH), 127.2 (ArCH), 127.5 (ArCH), 127.8 (ArCH), 128.1 (ArCH), 128.4 (ArCH), 128.4 (ArCH), 128.5 (ArCH), 128.5 (ArCH), 128.7 (ArCH), 134.1 (C(4)H), 136.0 (OCH₂ArC(1)), 137.2 (NCH₂ArC(1)), 170.6 (C(1)=O), 171.6 (C(3')=O); *minor rotamer (selected)* δ _C: 33.5 (C(O)NCH₃), 42.0 (N(CH₃)₂), 46.5 (C(3)H), 53.2 (NCH₂), 66.0 (OCH₂), 69.0 (C(2)H), 118.1 (C(5)H₂), 134.6 (C(4)H), 136.1 (OCH₂ArC(1)), 136.5 (NCH₂ArC(1)), 170.3 (C(1)=O), 171.7 (C(3')=O).

HRMS (ESI⁺): C₂₃H₂₉N₂O₃ [M+H]⁺ found 381.2160, requires 381.2173 (-3.3 ppm).

v_{max} (CHCl₃, cm⁻¹): 3016 (=CH), 2943 (C-H), 2870, 2792 (N(C-H)), 1720 (C=O_{ester}), 1627 (C=C), 1593 (C=C_{Ar}), 1496, 1454, 1338, 1215, 1165, 1029.

(LB ref: JB-207 (\pm), JB-214)

(2R,3S)-2-(Dimethylamino)-3-(methyl(phenyl)carbamoyl)pent-4-enoic acid, benzyl ester (217_{maj}) and (2R,3R)-2-(Dimethylamino)-3-(methyl(phenyl)carbamoyl)pent-4-enoic acid, benzyl ester (217_{min})



Following **General Procedure E**, PNP ester **159** (78.2 mg, 0.30 mmol, 1.0 eq), Pd₂dba₃·CHCl₃ (7.7 mg, 7.5 μmol, 2.5 mol%), P(2-furyl)₃ (6.9 mg, 0.03 mmol, 10 mol%), (S)-TM·HCl (14.4 mg, 0.06 mmol, 20 mol%), phosphate **210** (122 mg, 0.37 mmol, 1.25 eq) and *i*-Pr₂NEt (125 μL, 0.7 mmol, 2.4 eq) in MeCN (5.0 mL) gave the crude product (57:43 dr), which was used directly for derivatisation with NaOBn (0.45 mL, 0.45 mmol, 1.5 eq) in THF (6.0 mL). Subsequent purification of the crude derivatised product via silica column chromatography (CH₂Cl₂ : Et₂O 9:1 to 4:1) gave:

Major diastereoisomer 217_{maj} (R_f 0.28 in CH₂Cl₂ : Et₂O 4:1) as a yellow glass (19 mg, 17%).

[α]_D²⁰ +1.8 (c 0.85 in CHCl₃); **chiral HPLC** analysis, Chiralpak AD-H (98.2:1.8 hexane : *i*-PrOH, flow rate 1 mlmin⁻¹, 211 nm, 30 °C) t_R(2R,3S): 26.8 min, t_R(2S,3R): 31.4 min, 66:34 er. ¹H NMR (500 MHz, CDCl₃) δ_H: 2.19 (6H, s, N(CH₃)₂), 3.27 (3H, s, C(O)NCH₃), 3.40 (1H, dd, *J* 11.1, 8.8, C(3)H), 3.86 (1H, d, *J* 11.2, C(2)H), 4.94 (1H, d, *J* 17.2, C(5)H^AH^B), 5.00 (1H, d, *J* 12.4, OCH^AH^B), 5.03 – 5.08 (2H, m, OCH^AH^B, C(5)H^AH^B), 5.69 (1H, ddd, *J* 17.3, 10.2, 8.9, C(4)H), 7.16 – 7.21 (2H, m, 2 × NArH), 7.26 – 7.38 (6H, m, NArH, 5 × OCH₂ArH), 7.38 – 7.43 (2H, m, 2 × NArH).

¹³C{¹H} NMR (126 MHz, CDCl₃) δ_C: 37.7 (C(O)NCH₃), 42.3 (N(CH₃)₂), 47.8 (C(3)H), 65.6 (OCH₂), 69.4 (C(2)H), 119.8 (C(5)H₂), 127.7 (NArCH), 128.0 (ArCH), 128.1 (ArCH), 128.3 (ArCH), 128.4 (ArCH), 129.5 (NArCH), 133.5 (C(4)H), 135.9 (OArC(1)), 143.4 (NArC(1)), 169.2 (C(1)=O), 170.8 (C(3')=O).

HRMS (ESI⁺): C₂₂H₂₆N₂O₃Na [M+Na]⁺ found 389.1825, requires 389.1836 (−2.7 ppm).

ν_{\max} (CHCl₃, cm⁻¹): 3012 (=CH), 2943 (C-H), 2835, 2789 (N(C-H)), 1728 (C=O_{ester}), 1651 (C=O_{amide}), 1635 (C=C), 1597 (C=C_{Ar}), 1496 (C=C_{Ar}), 1454, 1384, 1215, 1149, 1118.

Minor diastereoisomer 217_{min} (R_f 0.42 in CH₂Cl₂ : Et₂O 4:1) as a yellow glass (18 mg, 17%).

[α]_D²⁰ +6.9 (c 0.6 in CHCl₃); **chiral HPLC** analysis, Chiralcel OD-H (99.5:0.5 hexane : *i*-PrOH, flow rate 1 mlmin⁻¹, 211 nm, 30 °C) t_R(2R,3R): 33.1 min, t_R(2S,3S): 38.4 min, 67:33 er.

$^1\text{H NMR}$ (500 MHz, CDCl_3) δ_{H} : 2.18 (6H, s, $\text{N}(\text{CH}_3)_2$), 3.18 (3H, s, $\text{C}(\text{O})\text{NCH}_3$), 3.51 (1H, dd, J 10.9, 8.7, $\text{C}(3)\text{H}$), 3.85 (1H, d, J 10.9, $\text{C}(2)\text{H}$), 4.64 (1H, dt, J 17.2, 0.9, $\text{C}(5)\text{H}^{\text{A}}\text{H}^{\text{B}}$), 5.06 (1H, dd, J 10.2, 1.1, $\text{C}(5)\text{H}^{\text{A}}\text{H}^{\text{B}}$), 5.13 (1H, d, J 12.3, $\text{OCH}^{\text{A}}\text{H}^{\text{B}}$), 5.25 (1H, d, J 12.3, $\text{OCH}^{\text{A}}\text{H}^{\text{B}}$), 5.66 (1H, ddd, J 17.3, 10.1, 8.8), 7.18 – 7.23 (2H, m, $2 \times \text{NArH}$), 7.30 – 7.43 (8H, m, $3 \times \text{NArH}$, $5 \times \text{OCH}_2\text{ArH}$).

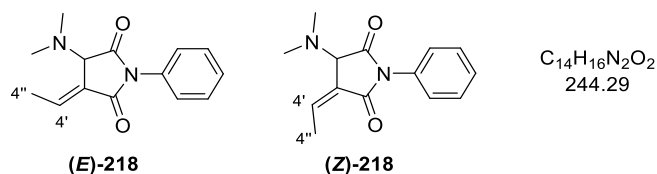
$^{13}\text{C}\{^1\text{H}\}$ NMR (126 MHz, CDCl_3) δ_{C} : 37.5 ($\text{C}(\text{O})\text{NCH}_3$), 41.9 ($\text{N}(\text{CH}_3)_2$), 47.2 ($\text{C}(3)\text{H}$), 66.1 (OCH_2), 68.8 ($\text{C}(2)\text{H}$), 118.2 ($\text{C}(5)\text{H}_2$), 127.8 (ArCH), 128.1 (ArCH), 128.2 (ArCH), 128.5 (ArCH), 128.5 (ArCH), 129.3 (ArCH), 134.3 ($\text{C}(4)\text{H}$), 136.0 ($\text{OArC}(1)$), 143.4 ($\text{NArC}(1)$), 170.4 ($\text{C}(1)=\text{O}$), 171.1 ($\text{C}(3')=\text{O}$).

HRMS (ESI $^+$): $\text{C}_{22}\text{H}_{26}\text{N}_2\text{O}_3\text{Na}$ [$\text{M}+\text{Na}$] $^+$ found 389.1822, requires 389.1836 (–3.5 ppm).

ν_{max} (CHCl_3 , cm^{-1}): 3012 (=CH), 2943 (C-H), 2835, 2789 (N(C-H)), 1724 ($\text{C}=\text{O}_{\text{ester}}$), 1647 ($\text{C}=\text{O}_{\text{amide}}$), 1631 (C=C), 1593 ($\text{C}=\text{C}_{\text{Ar}}$), 1496 ($\text{C}=\text{C}_{\text{Ar}}$), 1454, 1388, 1215, 1165, 1122, 1029.

(LB ref: JB-198 (\pm), JB-213)

(E)-3-(Dimethylamino)-4-ethylidene-1-phenylpyrrolidine-2,5-dione ((E)-218) and (Z)-3-(Dimethylamino)-4-ethylidene-1-phenylpyrrolidine-2,5-dione ((Z)-218)



Following **General Procedure E**, PNP ester **159** (78.2 mg, 0.30 mmol, 1.0 eq), $\text{Pd}_2\text{dba}_3 \cdot \text{CHCl}_3$ (7.7 mg, 7.5 μmol , 2.5 mol%), $\text{P}(2\text{-furyl})_3$ (6.9 mg, 0.03 mmol, 10 mol%), (S)-TM-HCl (14.4 mg, 0.06 mmol, 20 mol%), phosphate **211** (118 mg, 0.37 mmol, 1.25 eq) and *i*-Pr $_2\text{NEt}$ (125 μL , 0.7 mmol, 2.4 eq) in MeCN (5.0 mL) gave the crude product (80:20 (E):(Z)). Purification via silica column chromatography (pentane : EtOAc 4:1 to 1:1) gave: **(E)-218** (R_f 0.36 in pentane : EtOAc 2:1) as a colourless solid (23 mg, 32%).

$[\alpha]_{\text{D}}^{20}$ +1.7 (*c* 1.15 in CHCl_3); **chiral HPLC analysis**, Chiralcel OD-H (98:2 hexane : *i*-PrOH, flow rate 1 mlmin $^{-1}$, 254 nm, 30 $^\circ\text{C}$) t_{R} (minor): 18.0 min, t_{R} (major): 21.0 min, 45:55 er.

$^1\text{H NMR}$ (500 MHz, CDCl_3) δ_{H} : 2.07 (3H, dd, J 7.3, 1.4, $\text{C}(4'')\text{H}_3$), 2.52 (6H, s, $\text{N}(\text{CH}_3)_2$), 4.22 – 4.26 (1H, m, $\text{C}(3)\text{H}$), 7.21 (1H, qd, J 7.3, 2.2, $\text{C}(4')\text{H}$), 7.28 – 7.32 (2H, m, $\text{Ar}(2,6)\text{H}$), 7.36 – 7.40 (1H, m, $\text{Ar}(4)\text{H}$), 7.44 – 7.49 (2H, m, $\text{Ar}(3,5)\text{H}$).

$^{13}\text{C}\{^1\text{H}\}$ NMR (126 MHz, CDCl_3) δ_{C} : 14.9 ($\text{C}(4'')\text{H}_3$), 40.9 ($\text{N}(\text{CH}_3)_2$), 63.2 ($\text{C}(3)\text{H}$), 126.5 ($\text{ArC}(2,6)\text{H}$), 128.1 ($\text{C}(4)$), 128.5 ($\text{ArC}(4)\text{H}$), 129.0 ($\text{ArC}(3,5)\text{H}$), 131.6 ($\text{ArC}(1)$), 140.4 ($\text{C}(4')\text{H}$), 168.0 ($\text{C}(5)=\text{O}$), 174.1 ($\text{C}(2)=\text{O}$).

HRMS (ESI $^+$): $\text{C}_{14}\text{H}_{17}\text{N}_2\text{O}_2$ [$\text{M}+\text{H}$] $^+$ found 245.1276, requires 245.1284 (-3.4 ppm).

ν_{max} (CHCl_3 , cm^{-1}): 3018, 2939 (C-H), 2878, 2779, 1770, 1707 (C=O), 1674, 1597 ($\text{C}=\text{C}_{\text{Ar}}$), 1494 ($\text{C}=\text{C}_{\text{Ar}}$), 1454, 1367, 1234, 1203, 1145, 1041, 947.

(**Z**)-**218** (R_f 0.26 in pentane : EtOAc 1:1) as a colourless oil (3 mg, 4%).

$[\alpha]_{\text{D}}^{20}$ -0.6 (c 0.15 in CHCl_3); **chiral HPLC analysis**, Chiralcel OD-H (99:1 hexane : *i*-PrOH, flow rate 1 ml min^{-1} , 254 nm, 30 $^{\circ}\text{C}$) $t_{\text{R},1}$: 20.1 min, $t_{\text{R},2}$: 23.5 min, 50:50 er.

^1H NMR (500 MHz, CDCl_3) δ_{H} : 2.38 (3H, dd, J 7.5, 1.9, $\text{C}(4'')\text{H}_3$), 2.54 (6H, s, $\text{N}(\text{CH}_3)_2$), 4.10 – 4.13 (1H, m, $\text{C}(3)\text{H}$), 6.64 (1H, qd, J 7.4, 1.9, $\text{C}(4')\text{H}$), 7.27 – 7.31 (2H, m, $\text{Ar}(2,6)\text{H}$), 7.36 – 7.41 (1H, m, $\text{Ar}(4)\text{H}$), 7.45 – 7.49 (2H, m, $\text{Ar}(3,5)\text{H}$).

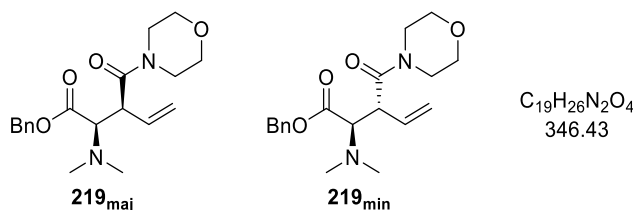
$^{13}\text{C}\{^1\text{H}\}$ NMR (126 MHz, CDCl_3) δ_{C} : 15.1 ($\text{C}(4'')\text{H}_3$), 41.1 ($\text{N}(\text{CH}_3)_2$), 65.3 ($\text{C}(3)\text{H}$), 126.6 ($\text{C}(4)$), 126.6 ($\text{ArC}(2,6)\text{H}$), 128.5 ($\text{ArC}(4)\text{H}$), 129.0 ($\text{ArC}(3,5)\text{H}$), 131.5 ($\text{ArC}(1)$), 142.8 ($\text{C}(4')\text{H}$), 167.7 ($\text{C}(5)=\text{O}$), 173.8 ($\text{C}(2)=\text{O}$).

HRMS (ESI $^+$): $\text{C}_{14}\text{H}_{17}\text{N}_2\text{O}_2$ [$\text{M}+\text{H}$] $^+$ found 245.1277, requires 245.1284 (-3.1 ppm).

ν_{max} (CHCl_3 , cm^{-1}): 2937 (C-H), 2870, 2781, 1766, 1705 (C=O), 1674, 1597 ($\text{C}=\text{C}_{\text{Ar}}$), 1496 ($\text{C}=\text{C}_{\text{Ar}}$), 1454, 1369, 1201, 1143, 1016.

(LB ref: JB-178 (\pm), JB-512)

(2R,3S)-2-(Dimethylamino)-3-(morpholine-4-carbonyl)pent-4-enoic acid, benzyl ester (219_{maj}) and (2R,3R)-2-(Dimethylamino)-3-(morpholine-4-carbonyl)pent-4-enoic acid, benzyl ester (219_{min})



Following **General Procedure E**, PNP ester **159** (78.2 mg, 0.30 mmol, 1.0 eq), $\text{Pd}_2\text{dba}_3 \cdot \text{CHCl}_3$ (7.7 mg, 7.5 μmol , 2.5 mol%), $\text{P}(2\text{-furyl})_3$ (6.9 mg, 0.03 mmol, 10 mol%), (*S*)-TM $\cdot\text{HCl}$ (14.4 mg, 0.06 mmol, 20 mol%), phosphate **212** (115 mg, 0.37 mmol, 1.25 eq) and *i*-Pr $_2\text{NEt}$ (125 μL , 0.7 mmol, 2.4 eq) in MeCN (5.0 mL) gave the crude product

(64:36 dr), which was used directly for derivatisation with NaOBn (0.45 mL, 0.45 mmol, 1.5 eq) in THF (6.0 mL). Subsequent purification of the crude derivatised product via silica column chromatography (petrol : EtOAc 1:2 to EtOAc : 15% *i*-PrOH) gave:

Major diastereoisomer 219_{maj} (R_f 0.14 in EtOAc) as a yellow glass (22 mg, 21%).

$[\alpha]_D^{20}$ -0.5 (*c* 1.1 in CHCl₃). **chiral HPLC** analysis, Chiralcel OD-H (95:5 hexane : *i*-PrOH, flow rate 1 mlmin⁻¹, 211 nm, 40 °C) t_R (2*R*,3*S*): 15.4 min, t_R (2*S*,3*R*): 18.7 min, 75:25 er.

¹H NMR (500 MHz, CDCl₃) δ_H : 2.30 (6H, s, N(CH₃)₂), 3.50 – 3.74 (8H, m, 4 × CH_{2(morph)}), 3.77 (1H, dd, *J* 10.9, 8.6, C(3)*H*), 3.90 (1H, d, *J* 10.9, C(2)*H*), 5.09 (1H, d, *J* 12.3, OCH^AH^B), 5.11 (1H, dd, *J* 10.2, 0.8, C(5)*H*^AH^B), 5.14 (1H, d, *J* 12.3, OCH^AH^B), 5.15 (1H, br d, *J* 17.2, C(5)*H*^AH^B), 5.72 (1H, ddd, *J* 17.3, 10.2, 8.5, C(4)*H*), 7.29 – 7.37 (5H, m, 5 × Ar*H*).

¹³C{¹H} NMR (126 MHz, CDCl₃) δ_C : 42.1 (N(CH₃)₂), 42.6 (NCH_{2(morph)}), 46.1 (C(3)*H*), 46.2 (NCH_{2(morph)}), 66.0 (OCH₂), 66.7 (OCH_{2(morph)}), 67.0 (OCH_{2(morph)}), 69.0 (C(2)*H*), 120.0 (C(5)*H*₂), 128.3 (ArCH), 128.6 (ArCH), 128.6 (ArCH), 133.1 (C(4)*H*), 135.8 (ArC), 169.5 (C(3')=O), 169.6 (C(1)=O).

HRMS (ESI⁺): C₁₉H₂₇N₂O₄ [M+H]⁺ found 347.1959, requires 347.1966 (-1.8 ppm).

ν_{max} (CHCl₃, cm⁻¹): 3012 (=CH), 2862 (C-H), 2789 (N(C-H)), 1724 (C=O_{ester}), 1643 (C=O_{amide}), 1631 (C=C), 1435, 1284, 1261, 1215, 1149, 1114, 1029, 960.

Minor diastereoisomer 219_{min} (R_f 0.42 in EtOAc) as a yellow glass (12 mg, 11%).

$[\alpha]_D^{20}$ +1.6 (*c* 0.35 in CHCl₃). **chiral HPLC** analysis, Chiralcel OD-H (97:3 hexane : *i*-PrOH, flow rate 1 mlmin⁻¹, 211 nm, 40 °C) t_R (2*S*,3*S*): 14.0 min, t_R (2*R*,3*R*): 15.9 min, 44:56 er.

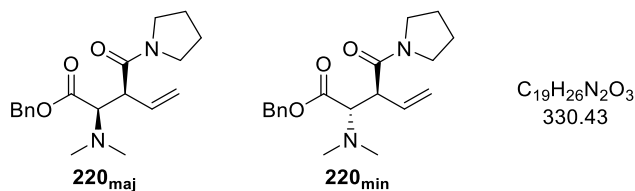
¹H NMR (500 MHz, CDCl₃) δ_H : 2.31 (6H, s, N(CH₃)₂), 3.46 – 3.52 (3H, m, NCH_{2(morph)}, NCH^AH^{B(morph)}), 3.55 – 3.66 (5H, m, 2 × OCH_{2(morph)}, NCH^AH^{B(morph)}), 3.74 (1H, dd, *J* 10.8, 8.3, C(3)*H*), 3.86 (1H, d, *J* 10.8, C(2)*H*), 5.06 (1H, d, *J* 12.3, OCH^AH^B), 5.14 (1H, dt, *J* 17.3, 0.9, C(5)*H*^AH^B), 5.23 (1H, d, *J* 12.3, OCH^AH^B), 5.24 (1H, d, *J* 10.3, C(5)*H*^AH^B), 5.85 (1H, ddd, *J* 17.4, 10.3, 8.3, C(4)*H*), 7.29 – 7.38 (5H, m, 5 × Ar*H*).

¹³C{¹H} NMR (126 MHz, CDCl₃) δ_C : 42.0 (N(CH₃)₂), 42.1 (NCH_{2(morph)}), 45.8 (C(3)*H*), 46.0 (NCH_{2(morph)}), 66.1 (OCH₂), 66.4 (OCH_{2(morph)}), 66.8 (OCH_{2(morph)}), 68.6 (C(2)*H*), 118.0 (C(5)*H*₂), 128.2 (ArCH), 128.4 (ArCH), 128.5 (ArCH), 134.3 (C(4)*H*), 135.9 (ArC), 170.0 (C(3')=O), 170.3 (C(1)=O).

HRMS (ESI⁺) C₁₉H₂₆N₂O₄Na [M+Na]⁺ found 369.1772, requires 369.1785 (-3.4 ppm).

ν_{max} (CHCl₃, cm⁻¹) 3012 (=CH), 2974 (C-H), 2862, 2792 (N(C-H)), 1720 (C=O_{ester}), 1627 (C=C), 1454, 1438, 1215, 1165, 1114, 1029. (LB ref: JB-200 (±), JB-211)

(2R,3S)-2-(Dimethylamino)-3-(pyrrolidine-1-carbonyl)pent-4-enoic acid, benzyl ester (220_{maj}) and (2S,3S)-2-(Dimethylamino)-3-(pyrrolidine-1-carbonyl)pent-4-enoic acid, benzyl ester (220_{min})



Following **General Procedure E**, PNP ester **159** (78.2 mg, 0.30 mmol, 1.0 eq), Pd₂dba₃·CHCl₃ (7.7 mg, 7.5 μmol, 2.5 mol%), P(2-furyl)₃ (6.9 mg, 0.03 mmol, 10 mol%), (S)-TM·HCl (14.4 mg, 0.06 mmol, 20 mol%), phosphate **213** (109 mg, 0.37 mmol, 1.25 eq) and *i*-Pr₂NEt (125 μL, 0.7 mmol, 2.4 eq) in MeCN (5.0 mL) gave the crude product (61:39 dr), which was used directly for derivatisation with NaOBn (0.45 mL, 0.45 mmol, 1.5 eq) in THF (6.0 mL). Subsequent purification of the crude derivatised product via silica column chromatography (petrol : EtOAc 1:2 to EtOAc : 15% *i*-PrOH) gave:

Major diastereoisomer 220_{maj} (*R_f* 0.09 in EtOAc) as a yellow solid (28 mg, 28%).

m.p. (EtOAc) 58 – 60 °C. $[\alpha]_D^{20}$ -0.9 (*c* 0.9 in CHCl₃).

chiral HPLC analysis, Chiralcel OD-H (95:5 hexane : *i*-PrOH, flow rate 1 mlmin⁻¹, 211 nm, 40 °C) *t_R* (2R,3S): 12.4 min, *t_R* (2S,3R): 19.0 min, 71:29 er.

¹H NMR (500 MHz, CDCl₃) δ_H: 1.78 – 2.01 (4H, m, 2 × CH₂(pyrr)), 2.31 (6H, s, N(CH₃)₂), 3.40 – 3.56 (4H, m, 2 × NCH₂(pyrr)), 3.60 (1H, dd, *J* 11.0, 8.8, C(3)H), 3.90 (1H, d, *J* 11.0, C(2)H), 5.07 (1H, dd, *J* 10.1, 1.1, C(5)H^AH^B), 5.09 (1H, d, *J* 12.3, OCH^AH^B), 5.13 (1H, d, *J* 12.3, OCH^AH^B), 5.17 (1H, d, *J* 17.2, C(5)H^AH^B), 5.71 (1H, ddd, *J* 17.3, 10.1, 8.9 Hz, C(4)H), 7.29 – 7.37 (5H, m, 5 × ArH).

¹³C{¹H} NMR (126 MHz, CDCl₃) δ_C: 24.3 (CH₂(pyrr)), 26.1 (CH₂(pyrr)), 42.2 (N(CH₃)₂), 46.0 (NCH₂(pyrr)), 46.3 (NCH₂(pyrr)), 49.4 (C(3)H), 65.8 (OCH₂), 68.9 (C(2)H), 119.6 (C(5)H₂), 128.3 (ArC(4)H), 128.5 (ArC(2,3,5,6)H), 133.2 (C(4)H), 135.9 (ArC), 169.1 (C(3')=O), 169.8 (C(1)=O).

HRMS (ESI⁺): C₁₉H₂₆N₂O₃Na [M+Na]⁺ found 353.1826, requires 353.1836 (-2.7 ppm).

v_{max} (CHCl₃, cm⁻¹): 2981 (C-H), 2877, 2789 (N(C-H)), 1724 (C=O_{ester}), 1627 (C=O_{amide}), 1435, 1338, 1257, 1215, 1149, 1114, 1029, 995.

Minor diastereoisomer **220_{min}** (R_f 0.37 in EtOAc) as a yellow solid (30 mg, 30%).

m.p. (EtOAc) 97 – 99 °C. $[\alpha]_D^{20}$ +4.8 (c 0.45 in CHCl_3).

chiral HPLC analysis, Chiralcel OD-H (95:5 hexane : *i*-PrOH, flow rate 1 mlmin⁻¹, 211 nm, 40 °C) t_R (2*S*,3*S*): 7.9 min, t_R (2*R*,3*R*): 8.8 min, 66:34 er.

¹H NMR (500 MHz, CDCl_3) δ_H : 1.71 – 1.92 (4H, m, 2 × $\text{CH}_2(\text{pyrr})$), 2.32 (6H, s, $\text{N}(\text{CH}_3)_2$), 3.33 – 3.43 (2H, m, $\text{NCH}_2(\text{pyrr})$), 3.45 – 3.55 (2H, m, $\text{NCH}_2(\text{pyrr})$), 3.57 – 3.64 (1H, m, C(3)*H*), 3.89 (1H, d, J 10.9, C(2)*H*), 5.04 (1H, d, J 12.3, OCH^AH^B), 5.16 (1H, d, J 17.3, C(5)*H*^A*H*^B), 5.21 (1H, d, J 10.1, C(5)*H*^A*H*^B), 5.22 (1H, d, J 12.3, OCH^AH^B), 5.82 (1H, dt, J 17.3, 9.4, C(4)*H*), 7.28 – 7.38 (5H, m, 5 × Ar*H*).

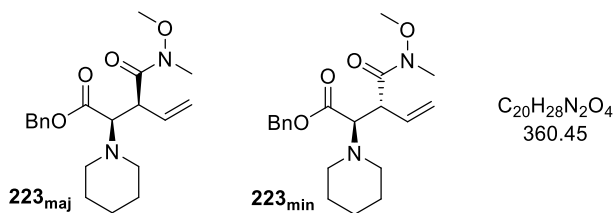
¹³C{¹H} NMR (126 MHz, CDCl_3) δ_C : 24.2 ($\text{CH}_2(\text{pyrr})$), 25.9 ($\text{CH}_2(\text{pyrr})$), 41.9 ($\text{N}(\text{CH}_3)_2$), 45.8 ($\text{NCH}_2(\text{pyrr})$), 46.1 ($\text{NCH}_2(\text{pyrr})$), 49.0 (C(3)*H*), 66.1 (OCH_2), 68.2 (C(2)*H*), 117.7 (C(5)*H*₂), 128.1 (ArCH), 128.4 (ArCH), 128.4 (ArCH), 134.4 (C(4)*H*), 136.0 (ArC), 169.6 (C(3')=O), 170.4 (C(1)=O).

HRMS (ESI⁺): $\text{C}_{19}\text{H}_{26}\text{N}_2\text{O}_3\text{Na}$ [$\text{M}+\text{Na}$]⁺ found 353.1823, requires 353.1836 (–3.6 ppm).

ν_{max} (CHCl_3 , cm^{-1}): 3066, 2974 (C–H), 2873, 2789 (N(C–H)), 1720 (C=O_{ester}), 1627 (C=O_{amide}), 1496 (C=C_{Ar}), 1435, 1338, 1249, 1215, 1161, 1029, 987.

(LB ref: JB-199 (±), JB-210)

(2*R*,3*S*)-3-(Methoxy(methyl)carbamoyl)-2-(piperidin-1-yl)pent-4-enoic acid, benzyl ester (223_{maj}) and (2*R*,3*R*)-3-(methoxy(methyl)carbamoyl)-2-(piperidin-1-yl)pent-4-enoic acid, benzyl ester (223_{min})



Following **General Procedure E**, PNP ester **221** (90.2 mg, 0.30 mmol, 1.0 eq), $\text{Pd}_2\text{dba}_3\cdot\text{CHCl}_3$ (7.7 mg, 7.5 μmol , 2.5 mol%), $\text{P}(\text{2-furyl})_3$ (6.9 mg, 0.03 mmol, 10 mol%), (*S*)-TM·HCl (14.4 mg, 0.06 mmol, 20 mol%), phosphate **184** (105 mg, 0.37 mmol, 1.25 eq) and *i*-Pr₂NEt (125 μL , 0.7 mmol, 2.4 eq) in MeCN (5.0 mL) after 84 h gave the crude product (61:39 dr), which was used directly for derivatisation with NaOBn (0.45 mL, 0.45 mmol, 1.5 eq) in THF (6.0 mL). Subsequent purification of the crude derivatised product via silica column chromatography (CH_2Cl_2 to CH_2Cl_2 :Et₂O 95:5, R_f 0.32 in

CH₂Cl₂:Et₂O 95:5) gave the title compound as an inseparable mixture of diastereoisomers (61:39 dr) as a colourless glass (31 mg, 29%). The enantiomeric ratios for the major and minor diastereoisomer could not be determined. $[\alpha]_D^{20} +2.1$ (*c* 1.3 in CHCl₃).

HRMS (ESI⁺): C₂₀H₂₉N₂O₄ [M+H]⁺ found 361.2109, requires 361.2122 (-3.5 ppm).

v_{max} (CHCl₃, cm⁻¹): 3032, 2933 (C-H), 2852, 2810, 1726 (C=O_{ester}), 1658 (C=O_{amide}), 1635 (C=C), 1498 (C=C_{Ar}), 1454, 1382, 1336, 1251, 1213, 1165, 1130, 1103, 995.

Data for major diastereoisomer 223_{maj}:

¹H NMR (500 MHz, CDCl₃) δ_H: 1.29 – 1.55 (6H, m, 3 × CH₂(pip)), 2.29 – 2.39 (2H, m, NCH₂), 2.66 – 2.75 (2H, m, NCH₂), 3.20 (3H, s, NCH₃), 3.68 (3H, s, OCH₃), 3.71 (1H, d, *J* 11.4, C(2)H), 4.14 – 4.26 (1H, m, C(3)H), 5.01 – 5.24 (4H, m, C(5)H₂, OCH₂), 5.79 (1H, ddd, *J* 17.2, 10.2, 8.7, C(4)H), 7.28 – 7.39 (5H, m, 5 × ArH).

¹³C{¹H} NMR (126 MHz, CDCl₃) δ_C: 24.5 (C(4)H₂(pip)), 26.7 (C(3,5)H₂(pip)), 32.4 (NCH₃), 45.7 (C(3)H), 51.2 (NCH₂), 61.8 (OCH₃), 65.8 (OCH₂), 70.2 (C(2)H), 119.6 (C(5)H₂), 128.2 (ArC(4)H), 128.4 (ArC(2,6)H and ArC(3,5)H), 133.5 (C(4)H), 135.9 (ArC(1)), 169.4 (C(1)=O), 173.0 (C(3')=O)*.

Data for minor diastereoisomer 223_{min}:

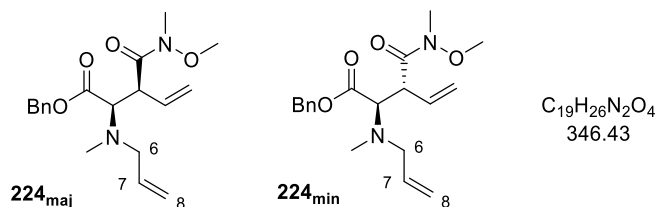
¹H NMR (500 MHz, CDCl₃) (*selected*) δ_H: 3.12 (3H, s, NCH₃), 3.73 (1H, d, *J* 11.2, C(2)H), 3.98 – 4.08 (1H, C(3)H), 5.85 (1H, ddd, *J* 17.3, 10.3, 7.7, C(4)H).

¹³C{¹H} NMR (126 MHz, CDCl₃) (*selected*) δ_C: 24.5 (C(4)H₂(pip)), 26.5 (C(3,5)H₂(pip)), 32.0 (NCH₃), 44.8 (C(3)H), 51.5 (NCH₂), 61.1 (OCH₃), 66.0 (OCH₂), 68.8 (C(2)H), 117.3 (C(5)H₂), 128.1 (ArC(4)H), 128.4 (ArC(2,3,5,6)H), 134.6 (C(4)H), 136.0 (ArC(1)), 170.9 (C(1)=O), 172.7 (C(3')=O)*.

* peak not visible in 1D ¹³C NMR, but inferred from cross peaks in the HMBC spectrum.

(LB ref: JB-510)

(2*R*,3*S*)-2-(Allyl(methyl)amino)-3-(methoxy(methyl)carbamoyl)pent-4-enoic acid, benzyl ester (224_{maj}) and (2*R*,3*R*)-2-(allyl(methyl)amino)-3-(methoxy(methyl)carbamoyl)pent-4-enoic acid, benzyl ester (224_{min})



Following **General Procedure E**, PNP ester **222** (86.0 mg, 0.30 mmol, 1.0 eq), Pd₂dba₃·CHCl₃ (7.7 mg, 7.5 μmol, 2.5 mol%), P(2-furyl)₃ (6.9 mg, 0.03 mmol, 10 mol%), (*S*)-TM·HCl (14.4 mg, 0.06 mmol, 20 mol%), phosphate **184** (105 mg, 0.37 mmol, 1.25 eq) and *i*-Pr₂NEt (125 μL, 0.7 mmol, 2.4 eq) in MeCN (5.0 mL) gave the crude product (56:44 dr), which was used directly for derivatisation with NaOBn (0.45 mL, 0.45 mmol, 1.5 eq) in THF (6.0 mL). Subsequent purification of the crude derivatised product via silica column chromatography (CH₂Cl₂ to CH₂Cl₂:Et₂O 95:5) gave:

Major diastereoisomer 224_{maj} (R_f 0.22 in CH₂Cl₂ : Et₂O 95:5) as a colourless oil (11 mg, 11%). [α]_D²⁰ -0.4 (c 0.45 in CHCl₃). **chiral HPLC** analysis, Chiralcel OD-H (99:1 hexane : *i*-PrOH, flow rate 1 mlmin⁻¹, 211 nm, 30 °C) t_R(2*R*,3*S*): 17.1 min, t_R(2*S*,3*R*): 22.7 min, 85:15 er.

¹H NMR (500 MHz, CDCl₃) δ_H: 2.27 (3H, s, NCH₃), 2.88 (1H, dd, *J* 13.9, 7.2, C(6)H^AH^B), 3.19 (3H, s, CONCH₃), 3.31 (1H, dd, *J* 14.0, 5.2, C(6)H^AH^B), 3.69 (3H, s, OCH₃), 3.87 (1H, d, *J* 11.5, C(2)H), 4.13 – 4.23 (1H, m, C(3)H), 5.03 – 5.12 (4H, m, OCH^AH^B, C(5)H^AH^B, C(8)H₂), 5.16 (1H, d, *J* 12.3, OCH^AH^B), 5.21 (1H, ddd, *J* 17.1, 1.3, 0.7, C(5)H^AH^B), 5.69 (1H, dddd, *J* 17.3, 10.1, 7.2, 5.2, C(7)H), 5.78 (1H, ddd, *J* 17.2, 10.2, 8.7, C(4)H), 7.30 – 7.38 (5H, m, 5 × ArH).

¹³C{¹H} NMR (126 MHz, CDCl₃) δ_C: 32.2 (CONCH₃), 38.8 (NCH₃), 46.0 (C(3)H), 57.3 (C(6)H₂), 61.8 (OCH₃), 65.9 (OCH₂), 67.7 (C(2)H), 116.8 (C(8)H₂), 119.8 (C(5)H₂), 128.2 (ArC(4)H), 128.5 (ArC(2,6)H, ArC(3,5)H), 133.4 (C(4)H), 135.8 (ArC(1)), 136.2 (C(7)H), 169.7 (C(1)=O), 172.3 (C(3')=O)*.

* peak not visible in 1D ¹³C NMR, but inferred from cross peaks in the HMBC spectrum.

HRMS (ESI⁺): C₁₉H₂₇N₂O₄ [M+H]⁺ found 347.1954, requires 347.1965 (-3.3 ppm).

v_{max} (CHCl₃, cm⁻¹): 3080, 2939 (C-H), 2804, 1728 (C=O_{ester}), 1660 (C=O_{amide}), 1637 (C=C), 1519, 1496 (C=C_{Ar}), 1454, 1417, 1382, 1255, 1149, 995.

Minor diastereoisomer **224**_{min} (*R*_f 0.30 in CH₂Cl₂ : Et₂O 95:5) as a colourless oil (5 mg, 5%).

$[\alpha]_D^{20}$ +9.5 (*c* 0.2 in CHCl₃). (Enantiomeric ratio could not be determined.)

¹H NMR (500 MHz, CDCl₃) δ_H: 2.24 (3H, s, NCH₃), 3.05 – 3.11 (1H, m, C(6)H^AH^B), 3.13 (3H, s, CONCH₃), 3.22 (1H, ddt, *J* 13.9, 5.6, 1.6, C(6)H^AH^B), 3.70 (3H, s, OCH₃), 3.94 (1H, d, *J* 11.2, C(2)H), 3.99 – 4.09 (1H, m, C(3)H), 5.05 (1H, d, *J* 12.3, OCH^AH^B), 5.07 – 5.10 (1H, m, C(8)H^AH^B), 5.13 (1H, dq, *J* 17.2, 1.7, C(8)H^AH^B), 5.16 – 5.21 (2H, m, C(5)H₂), 5.24 (1H, d, *J* 12.3, OCH^AH^B), 5.72 (1H, dddd, *J* 17.2, 10.1, 7.1, 5.6, C(7)H), 5.82 (1H, ddd, *J* 17.1, 10.3, 8.1, C(4)H), 7.29 – 7.39 (5H, m, 5 × ArH).

¹³C{¹H} NMR (126 MHz, CDCl₃) δ_C: 32.1 (CONCH₃), 38.1 (NCH₃), 45.5 (C(3)H), 58.0 (C(6)H₂), 61.0 (OCH₃), 66.2 (OCH₂), 66.3 (C(2)H), 117.4 (C(8)H₂), 117.9 (C(5)H₂), 128.2 (ArC(4)H), 128.4 (ArC(2,6 or 3,5)H), 128.5 (ArC(2,6 or 3,5)H), 134.4 (C(4)H), 135.9 (C(7)H), 135.9 (ArC(1)), 171.1 (C(1)=O). C(3')=O not visible.

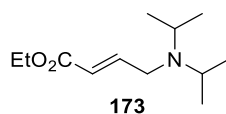
HRMS (ESI⁺): C₁₉H₂₇N₂O₄ [M+H]⁺ found 347.1956, requires 347.1965 (−2.6 ppm).

*v*_{max} (CHCl₃, cm^{−1}): 3080, 2978 (C-H), 2947, 2796, 1722 (C=O_{ester}), 1654 (C=O_{amide}), 1635 (C=C), 1519, 1498 (C=C_{Ar}), 1450, 1384, 1342, 1246, 1176, 1157, 995.

(LB ref: JB-511)

5.4.4 Identified side-products

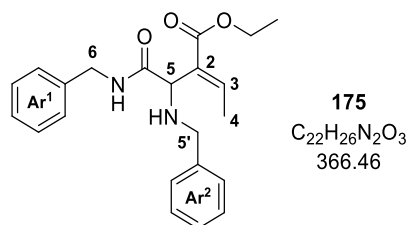
(E)-4-(Diisopropylamino)but-2-enoic acid, ethyl ester (173)



$^1\text{H NMR}$ (400 MHz, CDCl_3) δ_{H} : 0.99 (12H, d, J 6.6, $2 \times \text{CH}(\text{CH}_3)_2$), 1.28 (3H, t, J 7.1, OCH_2CH_3), 3.02 (2H, hept, J 6.6, $2 \times \text{CH}(\text{CH}_3)_2$), 3.23 (2H, dd, J 5.2, 1.9, $\text{C}(4)\text{H}_2$), 4.18 (2H, q, J 7.1, OCH_2CH_3), 6.04 (1H, dt, J 15.5, 1.9, $\text{C}(2)\text{H}$), 6.98 (1H, dt, J 15.5, 5.2, $\text{C}(3)\text{H}$).

(LB ref: JB-019)

(E)-2-(1,2-Bis(benzylamino)-2-oxoethyl)but-2-enoic acid, ethyl ester (175)



PNP ester **164** (30.0 mg, 0.09 mmol, 1.0 eq) was dissolved in 2.0 mL CH_2Cl_2 , benzylamine (48 μL , 0.45 mmol, 5.0 eq) added and the reaction mixture was stirred at room temperature overnight. The reaction was quenched by the addition of 1 M NaOH, diluted with CH_2Cl_2 and the phases separated. The aqueous phase was extracted with CH_2Cl_2 (3×5 mL). The combined organic phases were washed with 1 M NaOH (2×5 mL), and brine (5 mL), dried over MgSO_4 , filtered and the solvent was removed under reduced pressure. The crude product was purified by silica column chromatography (CH_2Cl_2 : Et_2O 9:1 to 4:1) to give the title compound as a yellow glass (10 mg, 30%) as a rotameric mixture (6:1). $^1\text{H NMR}$ (500 MHz, CDCl_3) *major rotamer* δ_{H} : 1.26 (3H, t, J 7.1, OCH_2CH_3), 1.83 (3H, d, J 7.2, $\text{C}(4)\text{H}_3$), 3.61 (1H, d, J 13.2, $\text{C}(5')\text{H}^{\text{A}}\text{H}^{\text{B}}$), 3.86 (1H, d, J 13.2, $\text{C}(5')\text{H}^{\text{A}}\text{H}^{\text{B}}$), 4.11 (1H, s, $\text{C}(5)\text{H}$), 4.18 (2H, qd, J 7.1, 1.2, OCH_2CH_3), 4.49 (2H, d, J 6.0, $\text{C}(6)\text{H}_2$), 7.21 – 7.25 (1H, q, J 7.2, $\text{C}(3)\text{H}$), 7.26 – 7.37 (10H, m, $10 \times \text{ArH}$), 7.96 (1H, t, J 5.5, $\text{C}(\text{O})\text{NH}$); *minor rotamer (selected)* δ_{H} : 2.13 (3H, d, J 7.2, $\text{C}(4)\text{H}_3$), 3.68 (1H, s, $\text{C}(5)\text{H}$), 4.47 (2H, d, J 6.0, $\text{C}(6)\text{H}_2$), 6.20 (1H, q, J 7.2, $\text{C}(3)\text{H}$), 7.79 (1H, br s, $\text{C}(\text{O})\text{NH}$).

$^{13}\text{C}\{^1\text{H}\}$ NMR (126 MHz, CDCl_3) *major rotamer* δ_{C} : 14.1 (OCH_2CH_3), 14.6 ($\text{C}(4)\text{H}_3$), 43.1 ($\text{C}(6)\text{H}_2$), 51.3 ($\text{C}(5')\text{H}_2$), 57.6 ($\text{C}(5)\text{H}$), 60.7 (OCH_2CH_3), 127.2 ($\text{Ar}^1\text{C}(4)\text{H}$), 127.3 ($\text{Ar}^2\text{C}(4)\text{H}$), 127.6 ($\text{Ar}^1\text{C}(2,6)\text{H}$), 128.1 ($\text{Ar}^2\text{C}(2,6)\text{H}$), 128.5 ($\text{Ar}^1\text{C}(3,5)\text{H}$), 128.6 ($\text{Ar}^2\text{C}(3,5)\text{H}$), 130.0 ($\text{C}(2)$),

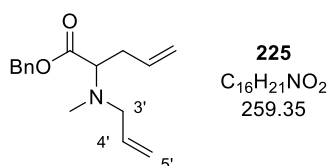
138.7 (Ar¹C(1)), 139.2 (Ar²C(1)), 142.2 (C(3)H), 166.5 (C=O_{amide}), 171.7 (C(1)=O); *minor rotamer (selected)* δ_c: 16.0 (C(4)H₃), 66.2 (C(2)H), 143.0 (C(3)H).

HRMS (ESI⁺): C₂₂H₂₇N₂O₃ [M+H]⁺ found 367.2007, requires 367.2016 (-2.5 ppm).

v_{max} (CHCl₃, cm⁻¹): 3367 (N-H), 3028 (=C-H), 2980 (C-H), 2927, 2841, 2358, 1699 (C=O_{ester}), 1674 (C=O_{amide}), 1516, 1496 (C=C_{Ar}), 1454, 1292, 1255, 1141, 1028.

(LB ref: JB-023)

2-(Allyl(methyl)amino)pent-4-enoic acid, benzyl ester (225)



Following **General Procedure E**, PNP ester **222** (86.0 mg, 0.30 mmol, 1.0 eq), Pd₂dba₃·CHCl₃ (7.7 mg, 7.5 μmol, 2.5 mol%), P(2-furyl)₃ (6.9 mg, 0.03 mmol, 10 mol%), (S)-TM·HCl (14.4 mg, 0.06 mmol, 20 mol%), phosphate **184** (105 mg, 0.37 mmol, 1.25 eq) and *i*-Pr₂NEt (125 μL, 0.7 mmol, 2.4 eq) in MeCN (5.0 mL) gave the crude product, which was used directly for derivatisation with NaOBn (0.45 mL, 0.45 mmol, 1.5 eq) in THF (6.0 mL). Subsequent purification of the crude derivatised product via silica column chromatography (CH₂Cl₂ to CH₂Cl₂:Et₂O 95:5, R_f 0.44 in CH₂Cl₂:Et₂O 95:5) afforded the title compound as yellow glass (10 mg, 13%).

¹H NMR (500 MHz, CDCl₃) δ_H: 2.31 (3H, s, NCH₃), 2.41 (1H, dtt, *J* 14.1, 6.9, 1.4, C(3)H^AH^B), 2.53 (1H, dddt, *J* 14.2, 8.3, 7.1, 1.3, C(3)H^AH^B), 3.10 (1H, ddt, *J* 13.8, 6.9, 1.2, C(3')H^AH^B), 3.22 (1H, ddt, *J* 13.8, 5.9, 1.5, C(3')H^AH^B), 3.43 (1H, dd, *J* 8.1, 7.0, C(2)H), 5.00 – 5.18 (6H, m, OCH₂, C(5)H₂, C(5')H₂), 5.72 – 5.84 (2H, m, C(4)H, C(4')H), 7.29 – 7.38 (5H, m, 5 × ArH).

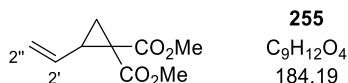
¹³C{¹H} NMR (126 MHz, CDCl₃) δ_c: 34.1 (C(3)H₂), 37.8 (NCH₃), 57.5 (C(3')H₂), 65.4 (C(2)H), 65.9 (OCH₂), 117.1 (C(5)H₂), 117.4 (C(5')H₂), 128.2 (ArC(4)H), 128.4 (ArC(2,6)H), 128.5 (ArC(3,5)H), 134.5 (C(4)H), 135.9 (C(4')H, ArC(1)), 171.8 (C=O).

(LB ref: JB-511)

5.5 Experimental details for Chapter 3

5.5.1 Preparation of vinylcyclopropanes

2-Vinylcyclopropane-1,1-dicarboxylic acid, dimethyl ester (255)

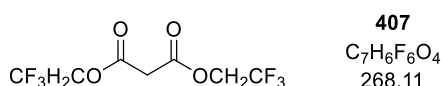


Following **General Procedure F**, dimethyl malonate (1.14 mL, 10.0 mmol, 1.0 eq), 1,4-dibromobut-2-ene (2.14 g, 10.0 mmol, 1.0 eq) and Cs_2CO_3 (8.1 g, 25.0 mmol, 2.5 eq) in THF (50 mL) at reflux for 16 h gave the title compound after purification by Biotage® Isolera™ 4 [SNAP KP-Sil 50 g, 100 mL min⁻¹, petrol : Et₂O (90:10 15 CV), R_f 0.16] as a colourless oil (1.37 g, 74%).

¹H NMR (400 MHz, CDCl₃) δ_H : 1.59 (1H, dd, J 9.0, 5.0, C(3)H^AH^B), 1.72 (1H, dd, J 7.6, 4.9, C(3)H^AH^B), 2.58 (1H, app. q, J 8.3, C(2)H), 3.74 (6H, s, 2 × OCH₃), 5.14 (1H, ddd, J 10.0, 1.6, 0.6, C(2'')H^AH^B), 5.29 (1H, ddd, J 17.0, 1.7, 0.6, C(2'')H^AH^B), 5.43 (1H, ddd, J 17.0, 10.1, 8.2, C(2')H).

Spectroscopic data in accordance with literature.¹⁴¹ (LB ref: JB-441)

Bis(2,2,2-trifluoroethyl) malonate (407)

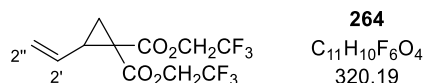


Following the procedure reported by Waser and co-workers¹⁶⁶, conc. H₂SO₄ (0.47 mL, 8.75 mmol, 0.25 eq) was added to a solution of malonic acid (3.64 g, 35.0 mmol, 1.0 eq) and trifluoroethanol (10.2 mL, 140 mmol, 4.0 eq) in toluene (20 mL) and heated to reflux for 8 h. The reaction mixture was allowed to cool to room temperature and diluted with CH₂Cl₂ (20 mL). The organic phase was washed with 1 M NaOH (1 × 40 mL), H₂O (1 × 40 mL) and brine (1 × 40 mL), dried over MgSO₄, filtered and the solvent was removed under reduced pressure to yield the title compound as a colourless oil (1.88 g, 20%), which was used without further purification.

¹H NMR (400 MHz, CDCl₃) δ_H : 3.61 (2H, s, CH₂), 4.55 (4H, q, J 8.2, 2 × OCH₂).

¹⁹F{¹H} NMR (376 MHz, CDCl₃) δ_F : -73.8 (6F, s, 2 × CF₃).

Spectroscopic data in accordance with literature.¹⁶⁷ (LB ref: JB-686)

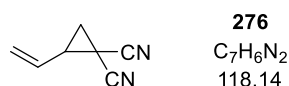
2-Vinylcyclopropane-1,1-dicarboxylic acid, bis(2,2,2-trifluoroethyl) ester (264)

Following **General Procedure F**, bis(2,2,2-trifluoroethyl)malonate **407** (1.8 g, 6.7 mmol, 1.0 eq), 1,4-dibromobut-2-ene (1.44 g, 6.7 mmol, 1.0 eq) and K₂CO₃ (2.32 g, 16.7 mmol, 2.5 eq) in THF (33 mL) at reflux for 24 h gave the title compound after purification by Biotage® Select™ [Sfär 50 g, 120 mL min⁻¹, Et₂O in hexane (2% to 20%, 10 CV), R_f 0.32 in 10% Et₂O in hexane] as a colourless oil (1.71 g, 80%).

¹H NMR (400 MHz, CDCl₃) δ_H: 1.72 (1H, dd, *J* 9.1, 5.2, C(3)H^AH^B), 1.89 (1H, dd, *J* 8.0, 5.2, C(3)H^AH^B), 2.68 – 2.79 (1H, m, C(2)H), 4.41 – 4.65 (4H, m, 2 × CH₂), 5.21 (1H, ddd, *J* 10.0, 1.6, 0.7, C(2'')H^AH^B), 5.34 (1H, ddd, *J* 17.0, 1.6, 0.7, C(2'')H^AH^B), 5.46 (1H, ddd, *J* 17.0, 10.0, 7.8, C(2')H).

¹⁹F{¹H} NMR (376 MHz, CDCl₃) δ_F: -74.0 (3F, m, CF₃), -73.8 (3F, m, CF₃).

Spectroscopic data in accordance with literature.¹¹⁷ (LB ref: JB-689)

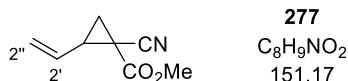
2-Vinylcyclopropane-1,1-dicarbonitrile (276)

Following **General Procedure F**, malononitrile (1.98 g, 30.0 mmol, 1.0 eq), 1,4-dibromobut-2-ene (6.42 g, 30.0 mmol, 1.0 eq) and K₂CO₃ (10.4 g, 75.0 mmol, 2.5 eq) in THF (150 mL) at reflux for 24 h gave the title compound after purification by silica column chromatography (petrol : EtOAc 5:1, R_f 0.19) as a colourless oil (2.39 g, 67%).

¹H NMR (400 MHz, CDCl₃) δ_H: 1.81 (1H, dd, *J* 8.3, 6.2, C(3)H^AH^B), 2.04 (1H, dd, *J* 9.1, 6.2, C(3)H^AH^B), 2.62 – 2.72 (1H, m, C(2)H), 5.45 – 5.65 (3H, m, CH=CH₂).

Spectroscopic data in accordance with literature.¹⁴¹

(LB ref.: JB-409, JB433, JB-460, JB499, JB-579, JB-581, JB669, JB-756)

1-Cyano-2-vinylcyclopropane-1-carboxylic acid, methyl ester (277)

Following **General Procedure F**, methyl cyanoacetate (0.88 mL, 10.0 mmol, 1.0 eq), 1,4-dibromobut-2-ene (2.14 g, 10.0 mmol, 1.0 eq) and K_2CO_3 (3.4 g, 25.0 mmol, 2.5 eq) in THF (50 mL) at reflux for 24 h gave the title compound after purification by silica column chromatography (petrol : EtOAc 9:1 to 6:1) as a colourless oil (1.18 g, 78%) as a partially separable mixture of diastereoisomers (2:1 dr).

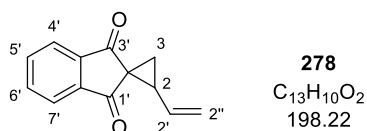
Data for major diastereoisomer (R_f 0.38 in petrol : EtOAc 6:1)

1H NMR (400 MHz, $CDCl_3$) δ_H : 1.63 (1H, dd, J 7.9, 5.1, C(3) $H^A H^B$), 1.94 (1H, dd, J 9.0, 5.1, C(3) $H^A H^B$), 2.48 – 2.56 (1H, m, C(2) H), 3.78 (3H, s, OCH_3), 5.33 (1H, ddd, J 10.2, 1.2, 0.6, C(2'') $H^A H^B$), 5.36 – 5.44 (1H, m, C(2'') $H^A H^B$), 5.53 – 5.68 (1H, m, C(2') H).

Data for minor diastereoisomer (R_f 0.33 in petrol : EtOAc 6:1)

1H NMR (400 MHz, $CDCl_3$) (selected) δ_H : 1.85 – 1.92 (2H, m, C(3) H_2), 2.54 – 2.63 (1H, m, C(2) H), 3.76 (3H, s, OCH_3), 5.23 (1H, ddd, J 10.3, 1.4, 0.6, C(2'') $H^A H^B$).

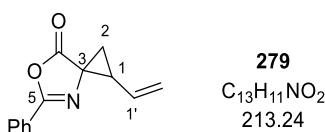
Spectroscopic data in accordance with literature.¹⁴¹ (LB ref: JB-467, JB-763)

2-Vinylspiro[cyclopropane-1,2'-indene]-1',3'-dione (278)

Following **General Procedure F**, 1,3-indanedione (731 mg, 5.0 mmol, 1.0 eq), 1,4-dibromobut-2-ene (1.07 g, 5.0 mmol, 1.0 eq) and K_2CO_3 (1.73 g, 12.5 mmol, 2.5 eq) in THF (25 mL) at reflux for 16 h gave the title compound after purification by silica column chromatography (petrol : EtOAc 9:1 to 6:1, R_f 0.33 in petrol : EtOAc 6:1) as a yellow solid (244 mg, 25%). **m.p.** (EtOAc) 126 – 128 °C {Lit.¹⁶⁸ 128 – 130 °C (EtOAc)}.

1H NMR (300 MHz, $CDCl_3$) δ_H : 1.98 (1H, dd, J 8.1, 4.0, C(3) $H^A H^B$), 2.13 (1H, dd, J 8.7, 4.0, C(3) $H^A H^B$), 2.81 (1H, app. q, J 8.7, C(2) H), 5.14 (1H, dd, J 10.3, 1.5, C(2'') $H^A H^B$), 5.28 (1H, dd, J 17.1, 1.5, C(2'') $H^A H^B$), 6.02 (1H, app. dt, J 17.1, 9.9, C(2') H), 7.72 – 7.86 (2H, m, ArC(5',6') H), 7.88 – 8.00 (2H, m, ArC(4',7') H).

Spectroscopic data in accordance with literature.¹⁶⁸ (LB ref: JB-682, JB-774)

5-Phenyl-1-vinyl-6-oxa-4-azaspiro[2.4]hept-4-en-7-one (279)

Following **General Procedure F**, 2-phenyloxazol-5(4*H*)-one (806 mg, 5.0 mmol, 1.0 eq), 1,4-dibromobut-2-ene (1.07 g, 5.0 mmol, 1.0 eq) and K_2CO_3 (1.73 g, 12.5 mmol, 2.5 eq) in THF (25 mL) at reflux for 16 h gave the title compound after purification by Biotage® Select™ [Sfär 25 g, 80 mL min⁻¹, Et₂O in petrol (0% to 20%, 20 CV), *R_f* 0.23 in 10% Et₂O in petrol] as a white solid (251 mg, 24%) as an inseparable mixture of diastereoisomers (3:2 dr). **m.p.** (EtOAc) 126 – 128 °C {Lit.¹⁶⁸ 128 – 130 °C (EtOAc)}

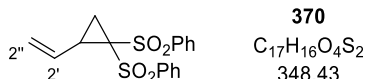
Data for major diastereoisomer

¹H NMR (400 MHz, CDCl₃) δ_H: 1.98 (1H, dd, *J* 8.1, 5.2, C(2)*H^AH^B*), 2.07 (1H, dd, *J* 9.3, 5.2, C(2)*H^AH^B*), 2.69 (1H, td, *J* 9.3, 8.1, C(1)*H*), 5.21 (1H, dd, *J* 10.4, 1.2, C(1'')*H^AH^B*), 5.33 (1H, dd, *J* 17.2, 1.2, C(1'')*H^AH^B*), 5.80 (1H, ddd, *J* 17.2, 10.4, 9.1, C(1')*H*), 7.41 – 7.48 (2H, m, Ar(3,5)*H*), 7.48 – 7.56 (1H, m, Ar(4)*H*), 7.91 – 8.01 (2H, m, Ar(2,6)*H*).

Data for minor diastereoisomer

¹H NMR (400 MHz, CDCl₃) δ_H: 1.91 (1H, dd, *J* 8.5, 5.3, C(2)*H^AH^B*), 2.21 (1H, dd, *J* 9.2, 5.3, C(2)*H^AH^B*), 2.86 (1H, td, *J* 9.2, 8.5, C(1)*H*), 5.22 (1H, dd, *J* 10.3, 1.3, C(1'')*H^AH^B*), 5.35 (1H, dd, *J* 17.0, 1.3, C(1'')*H^AH^B*), 5.94 (1H, ddd, *J* 17.0, 10.3, 9.2, C(1')*H*), 7.41 – 7.48 (2H, m, Ar(3,5)*H*), 7.48 – 7.56 (1H, m, Ar(4)*H*), 7.91 – 8.01 (2H, m, Ar(2,6)*H*).

Spectroscopic data in accordance with literature.¹²³ (LB ref: JB-650, JB-657, JB-746)

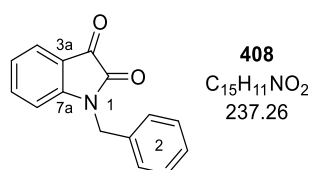
1,1-Bis(phenylsulfonyl)-2-vinylcyclopropane (370)

Following **General Procedure F**, bis(phenylsulfonyl)methane (500 mg, 1.69 mmol, 1.0 eq), 1,4-dibromobut-2-ene (361 mg, 1.69 mmol, 1.0 eq) and Cs_2CO_3 (1.38 g, 4.23 mmol, 2.5 eq) in THF (10 mL) at reflux for 16 h gave the title compound after purification by Biotage® Isolera™ 4 [SNAP KP-Sil 25 g, 100 mL min⁻¹, petrol : EtOAc (80:20 15 CV), *R_f* 0.31] as an off-white solid (403 mg, 68%). **m.p.** (EtOAc) 111 – 113 °C {Lit.¹⁶⁹ 107.5 – 108 °C (EtOH)}.

$^1\text{H NMR}$ (400 MHz, CDCl_3) δ_{H} : 1.59 (1H, dd, J 9.0, 5.0, $\text{C}(3)\text{H}^{\text{A}}\text{H}^{\text{B}}$), 1.72 (1H, dd, J 7.6, 4.9, $\text{C}(3)\text{H}^{\text{A}}\text{H}^{\text{B}}$), 2.58 (1H, app. q, J 8.3, $\text{C}(2)\text{H}$), 3.74 (6H, s, $2 \times \text{OCH}_3$), 5.14 (1H, ddd, J 10.0, 1.6, 0.6, $\text{C}(2'')\text{H}^{\text{A}}\text{H}^{\text{B}}$), 5.29 (1H, ddd, J 17.0, 1.7, 0.6, $\text{C}(2'')\text{H}^{\text{A}}\text{H}^{\text{B}}$), 5.43 (1H, ddd, J 17.0, 10.1, 8.2, $\text{C}(2')\text{H}$).

Spectroscopic data in accordance with literature.¹⁴¹ (LB ref: JB-442)

1-Benzylindoline-2,3-dione (408)

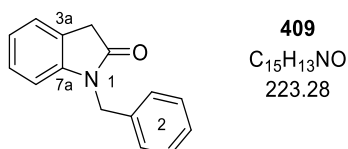


Following the procedure reported by Bower and co-workers¹⁷⁰, to a solution of isatin (1.47 g, 10.0 mmol, 1.0 eq) in MeCN (100 mL) were added K_2CO_3 (4.15 g, 30.0 mmol, 3.0 eq) and benzyl bromide (1.78 mL, 15.0 mmol, 1.5 eq). The mixture was heated at reflux for 18 h, allowed to cool to room temperature and filtered over Celite with EtOAc. The combined organic filtrates were concentrated under reduced pressure and the crude product was recrystallised from toluene (20 mL) to afford the title compound as an orange, crystalline solid (1.9 g, 80%). **m.p.** (toluene) 128 – 131 °C {Lit.¹⁷⁰ 129 – 131 °C (EtOH)}.

$^1\text{H NMR}$ (500 MHz, CDCl_3) δ_{H} : 4.94 (2H, s, NCH_2), 6.77 (1H, d, J 7.9, $\text{ArC}(7)\text{H}$), 7.09 (1H, td, J 7.6, 0.8, $\text{ArC}(5)\text{H}$), 7.28 – 7.39 (5H, m, $5 \times \text{Ar}^2\text{H}$), 7.48 (1H, td, J 7.8, 1.4, $\text{ArC}(6)\text{H}$), 7.62 (1H, dd, J 7.4, 1.3, $\text{ArC}(4)\text{H}$).

Spectroscopic data in accordance with literature.¹⁷⁰ (LB ref: JB-694)

1-Benzylindolin-2-one (409)



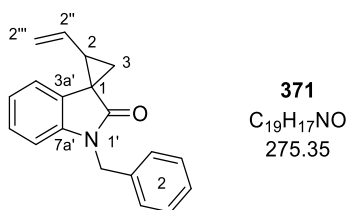
Adapting a procedure reported by Overman and co-workers¹⁷¹, a suspension of *N*-benzyl isatin **408** (428 mg, 1.8 mmol, 1.0 eq) and hydrazine hydrate (65% solution, 5 mL) was heated at reflux for 24 h. The reaction mixture was cooled to room temperature, diluted with H_2O (10 mL) and extracted with EtOAc (3×10 mL). The combined organic phases were dried over MgSO_4 , filtered and the solvent was removed under reduced pressure.

The crude product was purified by silica column chromatography (*n*-hexane : EtOAc 3:1, R_f 0.20) to yield the title compound as a viscous, orange oil (372 mg, 92%).

$^1\text{H NMR}$ (400 MHz, CDCl_3) δ_{H} : 3.65 (2H, s, C(3) H_2), 4.95 (2H, s, NCH $_2$), 6.75 (1H, d, J 7.8, ArC(7) H), 7.03 (1H, td, J 7.5, 1.0, ArC(5) H), 7.15 – 7.23 (1H, m, ArC(6) H), 7.24 – 7.38 (6H, m, ArC(4) H , 5 \times Ar 2H).

Spectroscopic data in accordance with literature.¹⁷¹ (LB ref: JB-719, JB-735)

1'-Benzyl-2-vinylspiro[cyclopropane-1,3'-indolin]-2'-one (371)



Following **General Procedure F**, 1-benzylindolin-2-one **409** (344 mg, 1.54 mmol, 1.0 eq), 1,4-dibromobut-2-ene (330 g, 1.54 mmol, 1.0 eq) and K_2CO_3 (532 g, 3.85 mmol, 2.5 eq) in THF (8 mL) at reflux for 48 h gave the crude product (73:27 dr). Purification by silica column chromatography (5 to 10% Et $_2$ O in *n*-hexane) allowed partial separation of the diastereoisomers to give **371**_{maj} (R_f 0.25) as a red solid (>99:1 dr, 103 mg, 24%).

m.p. (Et $_2$ O) 93 – 96 °C {Lit.¹⁴² 97 – 99 °C (EtOAc)}.

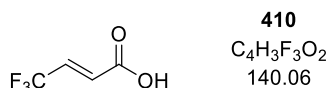
$^1\text{H NMR}$ (400 MHz, CDCl_3) δ_{H} : 1.98 (1H, dd, J 8.7, 4.7, C(3) $H^A H^B$), 2.05 (1H, dd, J 7.8, 4.7, C(3) $H^A H^B$), 2.47 – 2.60 (1H, m, C(2) H), 4.95 (1H, d, J 15.7, NCH $^A H^B$), 5.00 (1H, d, J 15.7, NCH $^A H^B$), 5.15 (1H, dd, J 10.3, 1.7, C(2'') $H^A H^B$), 5.27 (1H, dd, J 17.2, 1.7, C(2'') $H^A H^B$), 6.29 (1H, ddd, J 17.2, 10.3, 9.4, C(2') H), 6.77 (1H, d, J 7.7, ArC(4 or 7) H), 6.85 (1H, ddd, J 7.4, 1.3, 0.6, ArC(4 or 7) H), 7.00 (1H, td, J 7.5, 1.0, ArC(5 or 6) H), 7.13 (1H, td, J 7.7, 1.3, ArC(5 or 6) H), 7.22 – 7.37 (5H, m, 5 \times Ar 2H).

The minor diastereoisomer was not isolated. Spectroscopic data in accordance with literature.¹⁴² (LB ref: JB-702, JB-726, JB-742)

5.5.2 Preparation of Michael acceptors

The following PNP ester starting materials were prepared by colleagues according to literature procedures: **339**, **341** and **356** were prepared by Anastassia Matviitsuk,¹⁴⁶ **316** and **358** were prepared by Jiufeng Wu.¹⁷²

(*E*)-4,4,4-Trifluorobut-2-enoic acid (**410**)



Following the procedure reported by Smith and co-workers¹⁴⁸, (*E*)-4,4,4-trifluorobut-2-enoic acid, ethyl ester (8.9 mL, 59 mmol, 1.0 eq) was dissolved in THF (100 mL) and NaOH (1 M, 65 mL, 65 mmol, 1.1 eq) was added. The reaction mixture was stirred at room temperature for 4 h and subsequently acidified with HCl (1 M) to pH 2. Excess THF was removed under reduced pressure, the remaining aqueous phase diluted with brine and extracted with Et₂O (3 × 50 mL). The combined organic phases were dried over MgSO₄, filtered and the solvent was removed under reduced pressure to yield the title compound as a colourless solid (7.1 g, 86%), which was used without further purification. (Note: product slowly sublimates if left for a prolonged time under reduced pressure)

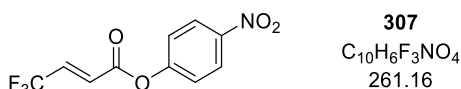
m.p. (Et₂O) 52 – 55 °C {Lit.¹⁷³ 54-55 °C (pentane)}.

¹H NMR (400 MHz, CDCl₃) δ_H: 6.52 (1H, dq, *J* 15.8, 1.9, C(2)H), 6.90 (1H, dq, *J* 15.8, 6.4, C(3)H), 12.14 (1H, br s, OH).

¹⁹F{¹H} NMR (376 MHz, CDCl₃) δ_F: -66.0 (3F, s, CF₃)

Spectroscopic data in accordance with literature.¹⁷⁴ (LB ref: JB-351, JB-485)

(*E*)-4,4,4-Trifluorobut-2-enoic acid, 4-nitrophenyl ester (**307**)



Following **General Procedure G**, (*E*)-4,4,4-trifluorobut-2-enoic acid **410** (2.98 g, 21.3 mmol, 1.0 eq), oxalyl chloride (1.89 mL, 22.4 mmol, 1.05 eq) and DMF (3 drops) in anhydrous CH₂Cl₂ (65 mL) followed by 4-nitrophenol (2.96 g, 21.3 mmol, 1.0 eq) and *i*-Pr₂NEt (7.4 mL, 42.6 mmol, 2.0 eq) in anhydrous CH₂Cl₂ (65 mL) gave a brown solid, which was triturated with Et₂O. The colourless solid (*i*-Pr₂NEt·HCl) was filtered and washed with Et₂O. The

combined filtrates were concentrated to give a light brown solid, which was recrystallised from hexane (80 mL). The hot solution was decanted from insoluble residues to yield the title compound as an off-white crystalline solid (4.3 g, 77%).

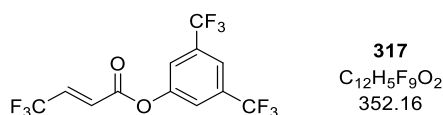
m.p. (hexane) 100 – 103 °C {Lit.¹⁴⁸ 93 – 95 °C (hexane)}.

¹H NMR (400 MHz, CDCl₃) δ_H: 6.72 (1H, dq, *J*_{HF} 15.8, 1.9, C(2)*H*), 7.02 (1H, dq, *J*_{HF} 15.8, 6.4, C(3)*H*), 7.33 – 7.41 (2H, m, Ar(2,6)*H*), 8.26 – 8.35 (2H, m, Ar(3,5)*H*).

¹⁹F{¹H} NMR (377 MHz, CDCl₃) δ_F: –65.7 (3F, s, CF₃).

Spectroscopic data in accordance with literature.¹⁴⁸ (LB ref: JB-352, JB-496, JB-580, JB-772)

(*E*)-4,4,4-Trifluorobut-2-enoic acid, 3,5-bis(trifluoromethyl)phenyl ester (317)

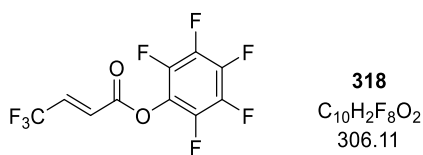


Following **General Procedure G**, (*E*)-4,4,4-trifluorobut-2-enoic acid **410** (1.1 g, 8.0 mmol, 1.0 eq), oxalyl chloride (0.71 mL, 8.4 mmol, 1.05 eq) and DMF (2 drops) in anhydrous CH₂Cl₂ (24 mL) followed by 3,5-bis(trifluoromethyl)phenol (1.21 mL, 8.0 mmol, 1.0 eq) and *i*-Pr₂NEt (2.7 mL, 16.0 mmol, 2.0 eq) in anhydrous CH₂Cl₂ (24 mL) gave a yellow solid, which was triturated with Et₂O. The colourless solid (*i*-Pr₂NEt·HCl) was filtered, washed with Et₂O and the filtrate was concentrated under reduced pressure. The crude oil was purified by Biotage® Isolera™ 4 [SNAP KP-Sil 50 g, 100 mL min⁻¹, petrol : Et₂O (100:0 2 CV, 100:0 to 90:10 10 CV, 90:10 2 CV), R_f 0.17 in petrol] to afford the title compound as a colourless, volatile oil (2.05 g, 73%).

¹H NMR (400 MHz, CDCl₃) δ_H: 6.73 (1H, dq, *J*_{HF} 15.8, 1.9, C(2)*H*), 7.03 (1H, dq, *J*_{HF} 15.8, 6.3, C(3)*H*), 7.65 – 7.70 (2H, m, Ar(2,6)*H*), 7.80 – 7.85 (1H, m, Ar(4)*H*).

¹⁹F{¹H} NMR (376 MHz, CDCl₃) δ_F: –66.0 (3F, s, C(4)F₃), –63.2 (6F, s, 2 × ArCF₃).

Spectroscopic data in accordance with literature.¹⁴⁸ (LB ref: JB-487)

(E)-4,4,4-Trifluorobut-2-enoic acid, pentafluorophenyl ester (318)

Following **General Procedure G**, (*E*)-4,4,4-trifluorobut-2-enoic acid **410** (1.1 g, 8.0 mmol, 1.0 eq), oxalyl chloride (0.71 mL, 8.4 mmol, 1.05 eq) and DMF (2 drops) in anhydrous CH₂Cl₂ (24 mL) followed by pentafluorophenol (1.47 g, 8.0 mmol, 1.0 eq) and *i*-Pr₂NEt (2.7 mL, 16.0 mmol, 2.0 eq) in anhydrous CH₂Cl₂ (24 mL) gave a brown solid, which was triturated with Et₂O. The colourless solid (*i*-Pr₂NEt·HCl) was filtered, washed with Et₂O and the combined filtrates were concentrated under reduced pressure. The crude oil was purified by Biotage® Isolera™ 4 [SNAP KP-Sil 50 g, 100 mL min⁻¹, petrol : Et₂O (100:0 5 CV, 100:0 to 95:5 5 CV, 95:5 5 CV), R_f 0.27 in petrol] to afford the title compound as a colourless, volatile oil (1.56 g, 64%).

¹H NMR (500 MHz, CDCl₃) δ_H: 6.76 (1H, dq, *J* 15.8, 1.9, C(2)H), 7.06 (1H, dq, *J* 15.9, 6.3, C(3)H).

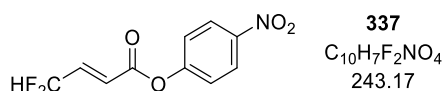
¹³C{¹H} NMR (126 MHz, CDCl₃) δ_C: 121.3 (q, ¹J_{CF} 270, CF₃), 125.5 (q, ³J_{CF} 6.2, C(2)H), 124.3 (t, ²J_{CF} 14.4, ArC(1)), 135.3 (q, ²J_{CF} 36.3, C(3)H), 136.8 – 137.1 (m, ArC), 138.7 – 139.2 (m, ArC), 140.0 (dq, *J*_{CF} 12.2, 3.9, ArC), 140.9 (tt, *J*_{CF} 13.6, 3.8, ArC), 142.0 (dq, *J*_{CF} 12.2, 3.9, ArC), 159.7 (C=O).

¹⁹F{¹H} NMR (376 MHz, CDCl₃) δ_F: -161.8 – -161.6 (m, ArC(4)F), -156.7 (t, 21.7, ArC(3,5)F), -152.4 (d, 16.7, ArC(2,6)F), -66.1 (s, CF₃).

HRMS (EI⁺) C₁₀H₂F₈O₂ [M]⁺ found 305.9934, requires 305.9927 (+2.3 ppm).

ν_{max} (film, cm⁻¹) 1778 (C=O), 1517, 1300, 1120, 995.

(LB ref: JB-488)

(E)-4,4-Difluorobut-2-enoic acid, 2-fluoro-4-nitrophenyl ester (337)

Following **General Procedure G**, (*E*)-4,4-difluorobut-2-enoic acid (387 mg, 3.17 mmol, 1.0 eq), oxalyl chloride (0.29 mL, 3.33 mmol, 1.05 eq) and DMF (1 drops) in anhydrous CH₂Cl₂ (10 mL) followed by 4-nitrophenol (441 mg, 3.17 mmol, 1.0 eq) and *i*-Pr₂NEt (1.1 mL, 6.3 mmol, 2.0 eq) in anhydrous CH₂Cl₂ (10 mL) gave an orange solid, which was

trituated with Et₂O. The colourless solid (*i*-Pr₂NEt·HCl) was filtered, washed with Et₂O and the filtrate concentrated under reduced pressure. The crude solid was purified by silica column chromatography (20% to 25% Et₂O in hexane, R_f 0.29 in 25% Et₂O in hexane) to afford the title compound as a yellow solid (649 mg, 84%). **m.p.** (hexane) 68 – 70 °C.

¹H NMR (300 MHz, CDCl₃) δ_H: 6.33 (1H, tdd, *J* 54.5, 3.8, 0.8, C(4)*H*) 6.51 (1H, dtd, *J* 15.9, 2.8, 0.8, C(2)*H*), 7.05 (1H, dtd, *J* 15.9, 10.3, 3.8, C(3)*H*), 7.29 – 7.42 (2H, m, Ar(2,6)*H*), 8.24 – 8.39 (2H, m, Ar(3,5)*H*).

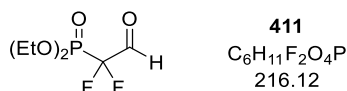
¹⁹F{¹H} NMR (282 MHz, CDCl₃) δ_F: -116.9 (s, C(4)*F*₂).

HRMS (EI⁺) C₁₀H₇F₂NO₄ [M]⁺ found 243.0333, requires 243.0337 (-0.4 ppm).

ν_{\max} (film, cm⁻¹) 3118, 3082, 1735 (C=O), 1699, 1678, 1620, 1591, 1531 (NO₂), 1487, 1390, 1344 (NO₂), 1307, 1257, 1197, 1172, 1037, 1012, 979, 964, 952.

Spectroscopic data in accordance with literature.¹⁷⁵ (LB ref: JB-683)

Diethyl (1,1-difluoro-2-oxoethyl)phosphonate (411)



Note: strict exclusion of moisture must be assured. Once CeCl₃·7H₂O has been dehydrated it must not be exposed to air at any point.

Adapting the procedure from Pajkert and Röschenthaler,¹⁷⁶ CeCl₃·7H₂O (2.93 g, 7.8 mmol, 1.05 eq) was placed into a flame-dried 2-necked round bottom flask, heated to 200 °C at 0.1 mbar over to 2 h and kept at this temperature for 18 h. After cooling to room temperature, anhydrous THF (dried over CaH₂, 0.33 M, 23 mL) was added under N₂ to the dried CeCl₃ and the suspension cooled to -78 °C. LDA (1.4 M solution in THF, 5.65 mL, 8.25 mmol, 1.1 eq) was added dropwise and the suspension was stirred vigorously for 20 min, followed by the dropwise addition of diethyl (difluoromethyl)phosphonate (1.18 mL, 7.5 mmol, 1.0 eq). After 1 h at -78 °C, anhydrous DMF (0.64 mL, 8.25 mmol, 1.1 eq) was added, the reaction warmed to room temperature and quenched by the addition of 3 M HCl (15 mL). After the complete dissolution of all cerium salts (ca. 30 min), the phases were separated and the aqueous phase was extracted with CH₂Cl₂ (3 × 20 mL). The combined organic phases were washed with brine (1 × 30 mL), dried over MgSO₄, filtered and the solvent was removed under reduced pressure. The crude residue was

purified by distillation over P₂O₅ to yield the title compound as a colourless oil (835 mg, 51%). **b.p.** 45 – 47 °C (0.1 mbar) {Lit.¹⁷⁶ 74 – 77 °C (0.1 mmHg)}

¹H NMR (400 MHz, CDCl₃) δ_H: 1.40 (6H, td, *J* 7.1, 0.7, 2 × OCH₂CH₃), 4.33 (4H, dq, *J* 8.2, 7.1, 2 × OCH₂CH₃), 9.60 (1H, app. q, *J* 3.4, CHO).

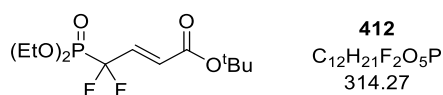
¹⁹F{¹H} NMR (377 MHz, CDCl₃) δ_F: -123.5 (d, ²*J*_{FP} 96.6, CF₂).

³¹P{¹H} NMR (162 MHz, CDCl₃) δ_P: 2.5 (t, ²*J*_{PF} 96.6, P(O)(OEt)₂).

Spectroscopic data in accordance with literature.¹⁷⁶

(LB ref: JB-596, JB-608, JB-614, JB-617, JB-627, JB-651, JB-655)

(*E*)-4-(Diethoxyphosphoryl)-4,4-difluorobut-2-enoic acid, *t*-butyl ester (412)



t-Butyl diethylphosphonoacetate (0.46 mL, 1.97 mmol, 1.1 eq), LiCl (84 mg, 1.97 mmol, 1.1 eq) and *i*-Pr₂NEt (0.34 mL, 1.97 mmol, 1.1 eq) were stirred in anhydrous MeCN (6.5 mL) for 30 min at room temperature. A solution of aldehyde **411*** (386 mg, 1.79 mmol, 1.0 eq) in anhydrous MeCN (6.5 mL) was added slowly and the reaction mixture allowed to stir overnight. The resulting white suspension was diluted with H₂O (10 mL) and extracted with EtOAc (3 × 10 mL). The combined organic phases were washed with brine, dried over MgSO₄, filtered and concentrated under reduced pressure. The crude product was purified by silica column chromatography (5% Et₂O in CH₂Cl₂, R_f 0.45) to afford the title compound as a colourless oil (484 mg, 86%).

¹H NMR (500 MHz, CDCl₃) δ_H: 1.37 (6H, td, *J* 7.1, 0.7, 2 × OCH₂CH₃), 1.48 (9H, s, C(CH₃)₃), 4.23 – 4.32 (4H, m, 2 × OCH₂CH₃), 6.32 (1H, app. dq, *J* 15.8, 2.7, C(2)H), 6.77 (1H, dtd, *J* 15.8, 12.8, 2.2, C(3)H).

¹³C{¹H} NMR (126 MHz, CDCl₃) δ_C: 16.3 (d, ³*J*_{CP} 5.4, 2 × OCH₂CH₃) 27.9 (C(CH₃)₃), 65.0 (d, ²*J*_{CP} 6.6, 2 × OCH₂CH₃), 81.9 (C(CH₃)₃), 116.3 (td, ¹*J*_{CF} 260, ¹*J*_{CP} 217, C(4)), 129.8 (td, ³*J*_{CF} 9.4, ³*J*_{CP} 5.5, C(2)H), 134.1 (td, ²*J*_{CF} 21.9, ²*J*_{CP} 13.0, C(3)H), 163.5 (C=O).

¹⁹F{¹H} NMR (376 MHz, CDCl₃) δ_F: -111.2 (d, ²*J*_{FP} 108, C(4)F₂).

³¹P{¹H} NMR (162 MHz, CDCl₃) δ_P: 5.1 (t, ²*J*_{PF} 108, C(4)P(O)(OEt)₂).

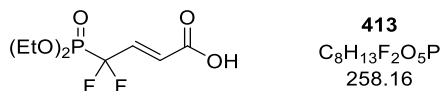
HRMS (ESI⁺) C₁₂H₂₁F₂O₅PNa [M+Na]⁺ found 337.0973, requires 337.0987 (-4.1 ppm).

v_{max} (film, cm⁻¹) 2981, 2935 (C-H), 2875, 1718 (C=O), 1664, 1654, 1479, 1394 (C(CH₃)₃), 1369 (C(CH₃)₃), 1319, 1273 (P=O), 1153, 1101, 1012, 970.

* Alternatively, the corresponding crude acetal prior to distillation over P_2O_5 can also be used.

(LB ref: JB-658, JB-661, JB-672)

(E)-4-(Diethoxyphosphoryl)-4,4-difluorobut-2-enoic acid (413)



Following **General Procedure H**, ester **412** (454 mg, 1.44 mmol, 1.0 eq) in TFA : CH₂Cl₂ 1:2 (2.1 mL) after 16 h gave the title compound as an off-white solid (358 mg, 96%), which was used without further purification. **m.p.** (MeOH) 65 – 68 °C.

¹H NMR (500 MHz, CDCl₃) δ_H: 1.39 (6H, t, *J* 7.1, 2 × OCH₂CH₃), 4.23 – 4.38 (4H, m, 2 × OCH₂CH₃), 6.40 (1H, app. dq, *J* 15.8, 2.6, C(2)H), 6.94 (1H, dtd, *J* 15.8, 12.6, 1.7, C(3)H), 9.63 (1H, s, OH).

¹³C{¹H} NMR (126 MHz, CDCl₃) δ_C: 16.3 (d, ³J_{CP} 5.4, 2 × OCH₂CH₃), 65.5 (d, ²J_{CP} 6.8, 2 × OCH₂CH₃), 116.0 (td, ¹J_{CF} 260, ¹J_{CP} 217, C(4)), 127.7 (td, ³J_{CF} 9.4, ³J_{CP} 5.6, C(2)H), 136.5 (td, ²J_{CF} 21.9, ²J_{CP} 13.1, C(3)H), 167.7 (C=O).

¹⁹F{¹H} NMR (376 MHz, CDCl₃) δ_F: -112.2 (d, ²J_{FP} 108, C(4)F₂).

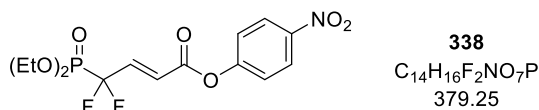
³¹P{¹H} NMR (202 MHz, CDCl₃) δ_P: 4.9 (t, ²J_{PF} 108, C(4)P(O)(OEt)₂).

HRMS (ESI⁺) C₈H₁₃F₂O₅PNa [M+Na]⁺ found 281.0351, requires 281.0361 (-3.5 ppm).

ν_{\max} (film, cm⁻¹) 2991 (O-H), 2659, 2559, 1720 (C=O), 1668, 1481, 1446, 1390, 1251 (P=O), 1174, 1056, 1022 (P-OEt), 989, 966.

(LB ref: JB-660, JB-665, JB-675)

(E)-4-(Diethoxyphosphoryl)-4,4-difluorobut-2-enoic acid, 4-nitrophenol ester (338)



Following **General Procedure G**, acid **413** (430 mg, 1.66 mmol, 1.0 eq), oxalyl chloride (0.15 mL, 1.75 mmol, 1.05 eq) and DMF (1 drop) in anhydrous CH₂Cl₂ (5.0 mL) followed by 4-nitrophenol (232 mg, 1.66 mmol, 1.0 eq) and *i*-Pr₂NEt (0.57 mL, 3.33 mmol, 2.0 eq) in anhydrous CH₂Cl₂ (5.0 mL) gave an orange solid, which was triturated with Et₂O. The colourless solid (*i*-Pr₂NEt·HCl) was filtered, washed with Et₂O and the filtrate was concentrated under reduced pressure. The resulting crude oil was purified by silica

column chromatography (5% Et₂O in CH₂Cl₂, R_f 0.32) to afford the title compound as a colourless oil (572 mg, 90%).

¹H NMR (500 MHz, CDCl₃) δ_H: 1.42 (6H, t, *J* 7.1, 2 × OCH₂CH₃), 4.27 – 4.39 (4H, m, 2 × OCH₂CH₃), 6.63 (1H, app. dq, *J* 15.9, 2.6, C(2)*H*), 7.13 (1H, dtd, *J* 15.9, 12.4, 2.1, C(3)*H*), 7.32 – 7.39 (2H, m, Ar(2,6)*H*), 8.27 – 8.34 (2H, m, Ar(3,5)*H*).

¹³C{¹H} NMR (126 MHz, CDCl₃) δ_C: 16.4 (d, ³*J*_{CP} 5.3, 2 × OCH₂CH₃), 65.3 (d, ²*J*_{CP} 6.9, 2 × OCH₂CH₃), 115.9 (td, ¹*J*_{CF} 260, ¹*J*_{CP} 217, C(4)), 122.3 (ArC(2,6)*H*), 125.3 (ArC(3,5)*H*), 126.4 (td, ³*J*_{CF} 9.6, ³*J*_{CP} 5.4, C(2)*H*), 138.4 (td, ²*J*_{CF} 22.2, ²*J*_{CP} 13.1, C(3)*H*), 145.6 (ArC(4)), 154.8 (ArC(1)), 161.8 (C=O).

¹⁹F{¹H} NMR (376 MHz, CDCl₃) δ_F: -112.0 (d, ²*J*_{FP} 106, C(4)*F*₂).

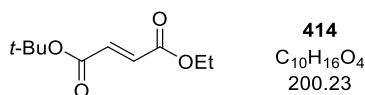
³¹P{¹H} NMR (202 MHz, CDCl₃) δ_P: 4.5 (t, ²*J*_{PF} 106, C(4)*P*(O)(OEt)₂).

HRMS (ESI⁺) C₁₄H₁₆F₂NO₇PNa [M+Na]⁺ found 402.0518, requires 402.0525 (-1.6 ppm).

v_{max} (film, cm⁻¹) 3116, 3084, 2987, 2870, 1749 (C=O), 1662, 1616 (C=C), 1593, 1523 (NO₂), 1490 (C=C_{Ar}), 1346 (NO₂), 1271 (P=O), 1207, 1182, 1161, 1143, 1097, 1008, 968, 948.

(LB ref: JB-668, JB-680)

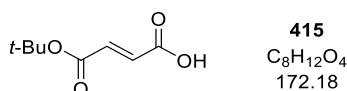
t-Butyl ethyl fumarate (414)



Adapting the procedure reported by Smith and co-workers¹⁴⁶, di-*t*-butyl dicarbonate (5.4 g, 25.0 mmol, 1.25 eq) and DMAP (489 mg, 4.0 mmol, 0.2 eq) were added to a stirred solution of monoethyl fumarate (2.8 g, 20.0 mmol, 1.0 eq) in THF (30 mL) at 0 °C. The reaction mixture was stirred at room temperature for 16 h, diluted with EtOAc (30 mL) and washed sequentially with 10% sulfuric acid (50 mL), 1 M NaOH (50 mL) and brine (50 mL). The organic phase was dried over MgSO₄, filtered and the solvent was removed under reduced pressure. The crude product was purified by silica column chromatography (petrol : EtOAc 5:1, R_f 0.61) to afford the title compound as a colourless oil (1.9 g, 48%).

¹H NMR (400 MHz, CDCl₃) δ_H: 1.31 (3H, t, *J* 7.1, OCH₂CH₃), 1.50 (9H, s, C(CH₃)₃), 4.24 (2H, q, *J* 7.1, OCH₂CH₃), 6.73 (1H, d, *J* 15.7, C(2)*H* or C(3)*H*), 6.77 (1H, d, *J* 15.7, C(2)*H* or C(3)*H*).

Spectroscopic data in accordance with literature.¹⁷⁷ (LB ref: JB-513, JB-754)

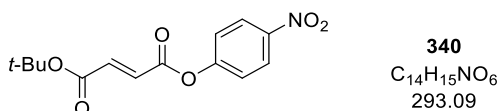
(E)-4-(*t*-Butoxy)-4-oxobut-2-enoic acid (415)

Following **General Procedure C**, *t*-butyl ethyl fumarate **414** (1.9 g, 9.5 mmol, 1.0 eq) and LiOH·H₂O (438 mg, 10.4 mmol, 1.1 eq) in H₂O : THF 1:1 (10 mL) after 6 h gave the title compound as a white solid (1.49 g, 86%), which was used without further purification.

m.p. (CH₂Cl₂) 61 – 64 °C {Lit.¹⁷⁸ 65 – 68 °C(EtOAc)}.

¹H NMR (400 MHz, CDCl₃) δ_H: 1.51 (9H, s, C(CH₃)₃), 6.74 (1H, d, *J* 15.7, C(2)*H* or C(3)*H*), 6.86 (1H, d, *J* 15.7, C(2)*H* or C(3)*H*).

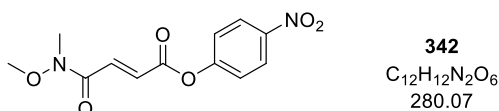
Spectroscopic data in accordance with literature.¹⁷⁸ (LB ref: JB-515, JB-757)

***t*-Butyl (4-nitrophenyl) fumarate (340)**

Following **General Procedure G**, acid **415** (1.2 g, 7.0 mmol, 1.0 eq), oxalyl chloride (0.62 mL, 7.3 mmol, 1.05 eq) and DMF (1 drop) in anhydrous CH₂Cl₂ (21 mL) followed by 4-nitrophenol (974 mg, 7.0 mmol, 1.0 eq) and *i*-Pr₂NEt (2.4 mL, 14.0 mmol, 2.0 eq) in anhydrous CH₂Cl₂ (21 mL) gave a brown solid, which was triturated with Et₂O. The colourless solid (*i*-Pr₂NEt·HCl) was filtered, washed with Et₂O and the filtrate was concentrated under reduced pressure. The crude solid was recrystallised from hexane (30 mL) and the hot solution decanted to separate from insoluble residue to afford the title compound as an off-white, crystalline solid (1.56 g, 76%). **m.p.** (hexane) 72 – 74 °C.

¹H NMR (400 MHz, CDCl₃) δ_H: 1.54 (9H, s, C(CH₃)₃), 6.94 (1H, d, *J* 15.8, C(2)*H* or C(3)*H*), 7.01 (1H, d, *J* 15.7, C(2)*H* or C(3)*H*), 7.31 – 7.38 (2H, m, Ar(2,6)*H*), 8.27 – 8.33 (2H, m, Ar(3,5)*H*).

Spectroscopic data in accordance with literature.¹⁷⁹ (LB ref: JB-523, JB-533, JB-762)

(E)-4-(Methoxy(methyl)amino)-4-oxobut-2-enoic acid, 4-nitrophenol ester (342)

Following **General Procedure G**, acid **207** (1.35 g, 8.4 mmol, 1.0 eq), oxalyl chloride (0.75 mL, 8.9 mmol, 1.05 eq) and DMF (3 drops) in anhydrous CH₂Cl₂ (25 mL) followed by 4-nitrophenol (1.17 g, 8.4 mmol, 1.0 eq) and *i*-Pr₂NEt (2.9 mL, 16.8 mmol, 2.0 eq) in anhydrous CH₂Cl₂ (25 mL) gave a brown solid, which was triturated with Et₂O. The colourless solid (*i*-Pr₂NEt·HCl) was filtered, washed with Et₂O and the filtrate was concentrated under reduced pressure. The crude solid was purified by silica column chromatography (petrol : EtOAc 1:1, R_f 0.24) to afford the title compound as a white solid (674 mg, 29%). **m.p.** (EtOAc) 93 – 95 °C.

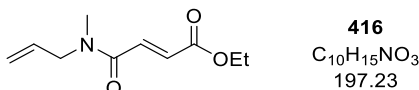
¹H NMR (500 MHz, CDCl₃) δ_H: 3.33 (3H, s, NCH₃), 3.78 (3H, s, OCH₃), 7.09 (1H, d, *J* 15.5, C(2)*H* or C(3)*H*), 7.34 – 7.38 (2H, m, Ar(2,6)*H*), 7.67 (1H, d, *J* 15.5, C(2)*H* or C(3)*H*), 8.28 – 8.32 (2H, m, Ar(3,5)*H*).

¹³C{¹H} NMR (126 MHz, CDCl₃) δ_C: 32.4 (NCH₃), 62.4 (OCH₃), 122.3 (ArC(2,6)*H*), 125.3 (ArC(3,5)*H*), 130.5 (C(2)*H* or C(3)*H*), 134.6 (C(2)*H* or C(3)*H*), 145.5 (ArC(4)), 155.0 (ArC(1)), 163.1 (C(1)=O), 163.9 (C(4)=O).

HRMS (ESI⁺) C₁₂H₁₃N₂O₆ [M+H]⁺ found 281.0764, requires 281.0768 (–1.4 ppm).

ν_{\max} (film, cm⁻¹) 3115, 2953 (C–H), 1741 (C=O_{ester}), 1660 (C=O_{amide}), 1635 (C=C), 1631, 1614, 1591 (C=C_{Ar}), 1517 (NO₂), 1469, 1390, 1346 (NO₂), 1294, 1261, 1211, 1103.

(LB ref: JB-559)

(E)-4-(Allyl(methyl)amino)-4-oxobut-2-enoic acid, ethyl ester (416)

Adapting the procedure reported by Snaddon and co-workers⁶⁴, monoethyl fumarate (1.0 g, 7.0 mmol, 1.0 eq) and methyl allyl amine (0.74 mL, 7.7 mmol, 1.1 eq) were dissolved in CH₂Cl₂ (20 mL), followed by the addition of EDCI·HCl (1.48 g, 7.7 mmol, 1.1 eq) and DMAP (85 g, 0.7 mmol, 0.1 eq) at 0 °C. The reaction mixture was allowed to warm to room temperature overnight and subsequently washed with 1 M HCl (2 × 20 mL) and brine (2 × 20 mL). The organic phase was dried over MgSO₄, filtered and the solvent was removed

under reduced pressure to afford the crude product as a dark red oil. Filtration over a short plug of silica with petrol : EtOAc 3:1 afforded a rotameric mixture (4:3) of the title compound as a pale yellow oil (1.1 g, 82%), which was used without further purification.

$^1\text{H NMR}$ (400 MHz, CDCl_3) *major rotamer* δ_{H} : 1.27 – 1.34 (3H, m, OCH_2CH_3), 3.01 (3H, s, NCH_3), 4.00 (2H, dt, J 4.9, 1.8, NCH_2), 4.20 – 4.29 (2H, m, OCH_2CH_3), 5.14 – 5.28 (2H, m, $\text{CH}=\text{CH}_2$), 5.71 – 5.85 (1H, m, $\text{CH}=\text{CH}_2$), 6.79 (1H, d, J 15.3, $\text{C}(2)\text{H}$ or $\text{C}(3)\text{H}$), 7.29 (1H, d, J 15.3, $\text{C}(2)\text{H}$ or $\text{C}(3)\text{H}$).

minor rotamer (selected) δ_{H} : 3.06 (3H, s, NCH_3), 4.07 (2H, dt, J 6.0, 1.5, NCH_2), 6.80 (1H, d, J 15.3, $\text{C}(2)\text{H}$ or $\text{C}(3)\text{H}$), 7.40 (1H, d, J 15.3, $\text{C}(2)\text{H}$ or $\text{C}(3)\text{H}$).

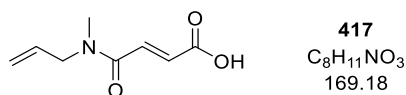
$^{13}\text{C}\{^1\text{H}\}$ NMR (126 MHz, CDCl_3) *major rotamer* δ_{C} : 14.1 (OCH_2CH_3), 34.0 (NCH_3), 52.3 (NCH_2), 61.1 (OCH_2CH_3), 117.3 ($\text{CH}=\text{CH}_2$), 131.3 ($\text{C}(2)\text{H}$ or $\text{C}(3)\text{H}$), 132.1 ($\text{CH}=\text{CH}_2$), 133.7 ($\text{C}(2)\text{H}$ or $\text{C}(3)\text{H}$), 165.1 ($\text{C}(4)=\text{O}$), 165.7 ($\text{C}(1)=\text{O}$). *minor rotamer (selected)* δ_{C} : 34.9 (NCH_3), 50.4 (NCH_2), 117.9 ($\text{CH}=\text{CH}_2$), 131.5 ($\text{C}(2)\text{H}$ or $\text{C}(3)\text{H}$), 164.4 ($\text{C}(4)=\text{O}$).

HRMS (ESI $^+$) $\text{C}_{10}\text{H}_{15}\text{NO}_3\text{Na}$ $[\text{M}+\text{Na}]^+$ found 220.0941, requires 220.0944 (–1.3 ppm).

ν_{max} (film, cm^{-1}) 3080 (=C-H), 2983 (C-H), 2877, 1720 ($\text{C}=\text{O}_{\text{ester}}$), 1653 ($\text{C}=\text{O}_{\text{amide}}$), 1625 (C=C), 1402, 1284, 1176, 1031, 974.

(LB ref: JB-514)

(E)-4-(Allyl(methyl)amino)-4-oxobut-2-enoic acid (417)



Following **General Procedure C**, ethyl ester **416** (1.1 g, 5.7 mmol, 1.0 eq) and $\text{LiOH}\cdot\text{H}_2\text{O}$ (264 mg, 6.3 mmol, 1.1 eq) in H_2O : THF 1:1 (6 mL) after 8 h gave a rotameric mixture (4:3) of the title compound as an off-white solid (722 mg, 75%), which was used without further purification.

$^1\text{H NMR}$ (500 MHz, CDCl_3) *major rotamer* δ_{H} : 3.04 (3H, s, NCH_3), 3.98 – 4.03 (2H, m, NCH_2), 5.15 – 5.30 (2H, m, $\text{CH}=\text{CH}_2$), 5.71 – 5.85 (1H, m, $\text{CH}=\text{CH}_2$), 6.80 (1H, d, J 15.3, $\text{C}(2)\text{H}$ or $\text{C}(3)\text{H}$), 7.35 (1H, d, J 15.3, $\text{C}(2)\text{H}$ or $\text{C}(3)\text{H}$), 11.02 (1H, br s, OH). *minor rotamer (selected)* δ_{H} : 3.07 (3H, s, NCH_3), 4.08 (2H, d, J 6.0, NCH_2), 6.81 (1H, d, J 15.3, $\text{C}(2)\text{H}$ or $\text{C}(3)\text{H}$), 7.46 (1H, d, J 15.3, $\text{C}(2)\text{H}$ or $\text{C}(3)\text{H}$).

$^{13}\text{C}\{^1\text{H}\}$ NMR (126 MHz, CDCl_3) *major rotamer* δ_{c} : 34.2 (NCH₃), 52.5 (NCH₂), 117.5 (CH=CH₂), 130.7 (C(2)H or C(3)H), 131.9 (CH=CH₂), 135.3 (C(2)H or C(3)H), 165.1 (C(4)=O), 169.6 (C(1)=O).

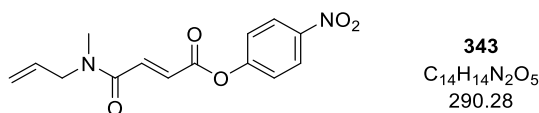
minor rotamer (selected) δ_{c} : 35.0 (NCH₃), 50.5 (NCH₂), 118.25 (CH=CH₂), 130.9 (C(2)H or C(3)H), 164.5 (C(4)=O), 169.6 (C(1)=O).

HRMS (ESI⁻) C₈H₁₀NO₃ [M-H]⁻ found 168.0660, requires 168.0666 (-3.6 ppm).

ν_{max} (film, cm⁻¹) 2933 (O-H), 2756 (NC-H), 1712 (C=O_{ester}), 1658 (C=O_{amide}), 1600 (C=C), 1408, 1168.

(LB ref: JB-516)

(E)-4-(Allyl(methyl)amino)-4-oxobut-2-enoic acid, 4-nitrophenol ester (343)



Adapting the procedure reported by Smith and co-workers¹⁸⁰, acid **417** (677 mg, 4.0 mmol, 1.0 eq) and EDCI·HCl (997 mg, 5.2 mmol, 1.3 eq) were dissolved in anhydrous CH₂Cl₂ (7 mL) and stirred for 10 min at room temperature. 4-Nitrophenol (835 mg, 6.0 mmol, 1.5 eq) was added, the reaction mixture stirred for 16 h and quenched by the addition of H₂O (7 mL). The phases were separated and the aqueous phase was extracted with CH₂Cl₂ (3 × 10 mL). The combined organic phases were dried over MgSO₄, filtered and the solvent was removed under reduced pressure. The crude product was purified by silica column chromatography (5 to 10% Et₂O in CH₂Cl₂, R_f 0.22 in 5% Et₂O in CH₂Cl₂) to afford a rotameric mixture (4:3) of the title compound as a colourless oil (583 mg, 50%).

^1H NMR (500 MHz, CDCl_3) *major rotamer* δ_{H} : 3.04 (3H, s, NCH₃), 4.03 (2H, dt, J 4.8, 1.8, NCH₂), 5.15 – 5.30 (2H, m, CH=CH₂), 5.71 – 5.87 (1H, m, CH=CH₂), 6.97 (1H, d, J 15.3, C(3)H), 7.29 – 7.36 (2H, m, Ar(2,6)H), 7.48 (1H, d, J 15.3, C(2)H), 8.23 – 8.30 (2H, m, Ar(3,5)H). *minor rotamer (selected)* δ_{H} : 3.09 (3H, s, NCH₃), 4.09 (2H, dt, J 6.0, 1.5, NCH₂), 6.98 (1H, d, J 15.3, C(3)H), 7.61 (1H, d, J 15.3, C(2)H).

$^{13}\text{C}\{^1\text{H}\}$ NMR (126 MHz, CDCl_3) *major rotamer* δ_{c} : 34.2 (NCH₃), 52.4 (NCH₂), 117.4 (CH=CH₂), 122.3 (ArC(2,6)H), 125.2 (ArC(3,5)H), 129.4 (C(3)H), 132.0 (CH=CH₂), 136.8 (C(2)H), 145.5 (ArC(4)), 155 (ArC(1)), 163.2 (C(1)=O), 164.3 (C(4)=O). *minor rotamer (selected)*

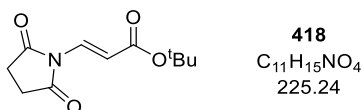
δ_{C} : 35.0 (NCH₃), 50.4 (NCH₂), 118.2 (CH=CH₂), 125.3 (ArC(3,5)H), 129.5 (C(3)H), 131.8 (CH=CH₂), 136.8 (C(2)H), 163.6 (C(4)=O).

HRMS (ESI⁺) C₁₄H₁₅N₂O₅ [M+H]⁺ found 291.0973, requires 291.0975 (−0.8 ppm).

ν_{max} (film, cm^{−1}) 3082 (=CH₂), 2931 (C-H), 1741 (C=O_{ester}), 1654 (C=O_{amide}), 1616 (C=C), 1591(C=C_{Ar}), 1519 (C-NO₂), 1489 (C=C_{Ar}), 1344 (C-NO₂), 1199, 1124.

(LB ref: JB-524)

(E)-3-(2,5-Dioxopyrrolidin-1-yl)prop-2-enoic acid, *t*-butyl ester (418)



Adapting the procedure of Mola et. al¹⁸¹, succinimide (495 mg, 5.0 mmol, 1.0 eq) and DABCO (112 mg, 1.0 mmol, 0.2 eq) were dissolved in MeCN (50 mL). *t*-Butyl propiolate (0.82 mL, 6.0 mmol, 1.2 eq) was added dropwise and the reaction mixture stirred at room temperature until TLC (petrol : EtOAc 4:1) indicated full conversion (ca. 2 h). The solvent was removed under reduced pressure and the crude product was purified by silica column chromatography (2% Et₂O in CH₂Cl₂, R_f 0.26) to afford the title compound as a pale yellow solid (987 mg, 87%). **m.p.** (CH₂Cl₂) 99 – 102 °C.

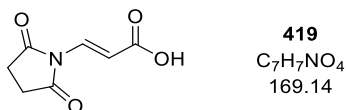
¹H NMR (500 MHz, CDCl₃) δ_{H} : 1.49 (9H, s, C(CH₃)₃), 2.81 (4H, s, 2 × CH₂), 6.89 (1H, d, *J* 14.8, C(2)H), 7.64 (1H, d, *J* 14.8, C(3)H).

¹³C{¹H} NMR (126 MHz, CDCl₃) δ_{C} : 27.7 (2 × CH₂), 28.1 (C(CH₃)₃), 81.0 (C(CH₃)₃), 112.8 (C(2)H), 130.0 (C(3)H), 165.9 (C(1)=O), 174.4 (2 × C=O_{pyrr}).

HRMS (ESI⁺) C₁₁H₁₅NO₄Na [M+Na]⁺ found 248.0888, requires 248.0893 (−2.0 ppm).

ν_{max} (film, cm^{−1}) 3107, 3076, 2980, 2933 (C-H), 1789 (C=O_{imide}), 1714 (C=O_{ester}), 1693, 1639 (C=C), 1477, 1454, 1369, 1290, 1255, 1151, 1107, 987.

(LB ref: JB-594, JB-704)

(E)-3-(2,5-Dioxopyrrolidin-1-yl)prop-2-enoic acid (419)

Following **General Procedure H**, ester **418** (922 mg, 4.0 mmol, 1.0 eq) in TFA : CH₂Cl₂ 1:2 (5 mL) after 4 h gave the title compound as a pale yellow solid (683 mg, 98%), which was used without further purification. **m.p.** (CH₂Cl₂) 224 – 226 °C.

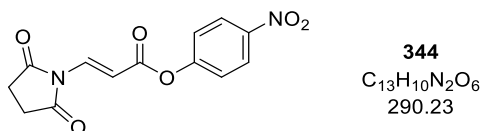
¹H NMR (500 MHz, DMSO-*d*₆) δ_H: 2.72 (4H, s, 2 × CH₂), 6.71 (1H, d, *J* 14.8, C(2)H), 7.50 (1H, d, *J* 14.8, C(3)H), 12.56 (1H, br s, OH).

¹³C{¹H} NMR (126 MHz, DMSO-*d*₆) δ_C: 28.4 (2 × CH₂), 109.3 (C(2)H), 131.6 (C(3)H), 168.1 (C(1)=O), 176.5 (2 × NC=O).

HRMS (ESI) C₇H₆NO₄ [M-H]⁻ found 168.0296, requires 168.0302 (-3.9 ppm).

ν_{max} (film, cm⁻¹) 3111, 2954 (O-H), 2650, 2590, 2474, 1772 (C=O_{imide}), 1732 (C=O_{acid}), 1678, 1597, 1429, 1365, 1234, 1161, 1111, 985 (=C-H), 898, 779.

(LB ref: JB-597, JB-709)

(E)-3-(2,5-Dioxopyrrolidin-1-yl)prop-2-enoic acid, 4-nitrophenol ester (344)

Following **General Procedure G**, acid **419** (665 mg, 3.9 mmol, 1.0 eq), oxalyl chloride (0.35 mL, 4.1 mmol, 1.05 eq) and DMF (1 drop) in anhydrous CH₂Cl₂ (12 mL) followed by 4-nitrophenol (542 mg, 3.9 mmol, 1.0 eq) and *i*-Pr₂NEt (1.3 mL, 7.8 mmol, 2.0 eq) in anhydrous CH₂Cl₂ (12 mL) gave a brown solid, which was purified by silica column chromatography (5% Et₂O in CH₂Cl₂, R_f 0.43) to afford an off-white solid. Trituration with Et₂O removed remaining 4-nitrophenol impurities to afford the title compound as a white crystallin solid (860 mg, 76%). **m.p.** (Et₂O) 184 – 187 °C.

¹H NMR (500 MHz, CDCl₃) δ_H: 2.89 (4H, s, 2 × CH₂), 7.22 (1H, d, *J* 14.8, C(2)H), 7.32 – 7.39 (2H, m, Ar(2,6)H), 7.95 (1H, d, *J* 14.8, C(3)H), 8.26 – 8.33 (2H, m, Ar(3,5)H).

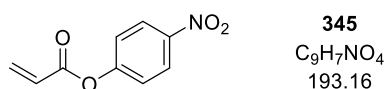
¹³C{¹H} NMR (126 MHz, CDCl₃) δ_C: 27.8 (2 × CH₂), 108.8 (C(2)H), 122.4 (ArC(2,6)H), 125.2 (ArC(3,5)H), 133.2 (C(3)H), 145.3 (ArC(4)), 155.3 (ArC(1)), 164.3 (C(1)=O), 174.1 (2 × C=O_{imide}).

HRMS (ESI⁺) C₁₄H₁₄N₂O₇Na [M+MeOH+Na]⁺ found 345.0690, requires 345.0693 (−0.8 ppm).

ν_{\max} (film, cm^{−1}) 3134, 3109, 3008 (=C-H), 2947 (C-H), 2866 (C-H), 1784 (C=O_{imide}), 1739, 1726 (C=O_{ester}), 1716, 1627, 1618, 1591, 1519 (NO₂), 1490, 1425, 1379, 1350, 1205, 1093, 850.

(LB ref: JB-600, JB-714)

Propenoic acid, 4-nitrophenyl ester (345)



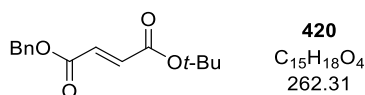
Following **General Procedure G**, acrylic acid (0.69 mL, 10.0 mmol, 1.0 eq), oxalyl chloride (0.89 mL, 10.5 mmol, 1.05 eq) and DMF (2 drops) in anhydrous CH₂Cl₂ (30 mL) followed by 4-nitrophenol (1.39 g, 10.0 mmol, 1.0 eq) and *i*-Pr₂NEt (3.5 mL, 20.0 mmol, 2.0 eq) in anhydrous CH₂Cl₂ (30 mL) gave a brown solid. Purification by silica column chromatography (petrol : CH₂Cl₂ 2:3, R_f 0.44) afforded the title compound as a white solid (1.19 g, 62%). **m.p.** (hexane) 69 – 72 °C {Lit.¹⁸² 63 – 65 °C (EtOAc)}.

¹H NMR (400 MHz, CDCl₃) δ_{H} : 6.11 (1H, dd, *J* 10.5, 1.1, CH^AH^B), 6.34 (1H, dd, *J* 17.3, 10.5, C(2)*H*), 6.67 (1H, dd, *J* 17.3, 1.1, CH^AH^B), 7.31 – 7.38 (2H, m, Ar(2,6)*H*), 8.27 – 8.33 (2H, m, Ar(3,5)*H*).

ν_{\max} (film, cm^{−1}) 3116, 3089 (=CH₂), 2848, 1741 (C=O), 1631, 1614, 1593 (C=C), 1514 (NO₂), 1487, 1406, 1346 (NO₂), 1290, 1209, 1155, 1105, 977.

Spectroscopic data in accordance with literature.¹⁸³ The title compound was prepared by Calum McLaughlin (LB ref: CM-858)

Benzyl *t*-butyl fumarate (420)



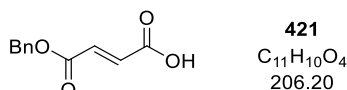
Adapting the procedure reported by Smith and co-workers¹⁴⁶, acid **415** (700 mg, 4.0 mmol, 1.0 eq), DCC (923 mg, 4.4 mmol, 1.1 eq) and DMAP (99 mg, 0.8 mmol, 0.2 eq) were dissolved in CH₂Cl₂ (4 mL) and cooled to 0 °C. BnOH (0.43 mL, 4.1 mmol, 1.02 eq) was added dropwise and the reaction mixture allowed to warm to room temperature overnight. The mixture was filtered to remove the by-product dicyclohexylurea, the solid was washed with CH₂Cl₂ and the combined filtrates concentrated. The crude product was

purified by silica column chromatography (petrol : EtOAc 9:1, R_f 0.43) to afford the title compound as an off-white solid (758 mg, 71%). **m.p.** (EtOAc) 85 – 88 °C.

$^1\text{H NMR}$ (400 MHz, CDCl_3) δ_{H} : 1.49 (9H, s, $\text{C}(\text{CH}_3)_3$), 5.23 (2H, s, OCH_2), 6.78 (1H, d, J 15.8, $\text{C}(2)\text{H}$ or $\text{C}(3)\text{H}$), 6.82 (1H, d, J 15.8, $\text{C}(2)\text{H}$ or $\text{C}(3)\text{H}$), 7.33 – 7.40 (5H, m, $5 \times \text{ArH}$).

Spectroscopic data in accordance with literature.¹⁴⁶ (LB ref: JB-519)

(*E*)-4-(Benzyloxy)-4-oxobut-2-enoic acid (**421**)

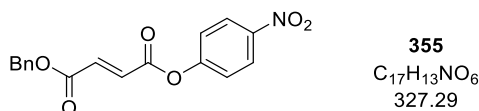


Following **General Procedure H**, benzyl *t*-butyl fumarate **420** (758 mg, 2.8 mmol, 1.0 eq) in TFA : CH_2Cl_2 1:2 (4 mL) after 4 h gave the title compound as an off-white solid (600 mg, >99%), which was used without further purification.

$^1\text{H NMR}$ (400 MHz, $\text{DMSO-}d_6$) δ_{H} : 5.23 (2H, s, OCH_2), 6.74 (2H, s, $\text{CH}=\text{CH}$), 7.32 – 7.44 (5H, m, $5 \times \text{ArH}$).

Spectroscopic data in accordance with literature.¹⁸⁴ (LB ref: JB-522)

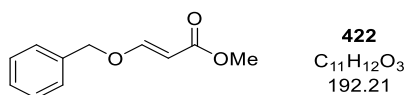
Benzyl (4-nitrophenyl) fumarate (**355**)



Adapting the procedure reported by Smith and co-workers¹⁸⁰, acid **421** (594 mg, 2.8 mmol, 1.0 eq) and EDCI·HCl (718 mg, 3.7 mmol, 1.3 eq) were dissolved in anhydrous CH_2Cl_2 (5 mL) and stirred for 10 min at room temperature. 4-Nitrophenol (600 mg, 4.3 mmol, 1.5 eq) was added, the reaction mixture stirred for 16 h and quenched by the addition of H_2O (5 mL). The phases were separated, and the aqueous phase was extracted with CH_2Cl_2 (3×5 mL). The combined organic phases were dried over MgSO_4 , filtered and the solvent was removed under reduced pressure. The crude product was purified by silica column chromatography (petrol : EtOAc 6:1, R_f 0.26) to afford the title compound as a white solid (370 mg, 39%). **m.p.** (EtOAc) 75 – 78 °C {Lit.¹⁴⁶ 74 – 76 °C (EtOAc)}.

$^1\text{H NMR}$ (400 MHz, CDCl_3) δ_{H} : 5.29 (2H, s, OCH_2), 7.07 (1H, d, J 15.8, $\text{C}(2)\text{H}$ or $\text{C}(3)\text{H}$), 7.13 (1H, d, J 15.8, $\text{C}(2)\text{H}$ or $\text{C}(3)\text{H}$), 7.32 – 7.43 (7H, m, $5 \times \text{ArH}_{\text{Bn}}$, $\text{Ar}(2,6)\text{H}$), 8.27 – 8.33 (2H, m, $\text{Ar}(3,5)\text{H}$).

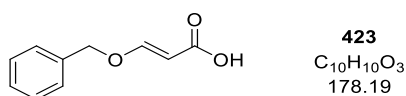
Spectroscopic data in accordance with literature.¹⁴⁶ (LB ref: JB-526)

(E)-3-(Phenylmethoxy)-2-propenoic acid, methyl ester (422)

Adopting the procedure reported by García-Tellado and co-workers,¹⁸⁵ to a stirred solution of methyl propiolate (0.26 mL, 2.9 mmol, 1.0 eq) and BnOH (0.34 mL, 3.2 mmol, 1.1 eq) in anhydrous CH₂Cl₂ (10 mL) was added DABCO (33.0 mg, 0.29 mmol, 0.1 eq) and the reaction was stirred at room temperature until TLC (Petrol : EtOAc 4:1) indicated complete conversion (ca. 2 h). The reaction mixture was concentrated under reduced pressure and purified by silica column chromatography (Petrol : EtOAc 9:1 to 4:1, R_f 0.49 in Petrol : EtOAc 4:1) to give the title compound as a colourless liquid (568 mg, 99%).

¹H NMR (400 MHz, CDCl₃) δ_H: 3.73 (3H, s, CO₂CH₃), 4.93 (2H, s, CH₂-O), 5.35 (1H, d, *J* 12.6, C(2)*H*), 7.34 – 7.45 (5H, m, Ar-*H*₅), 7.71 (1H, d, *J* 12.6, C(3)*H*).

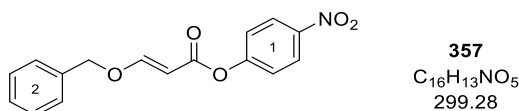
Spectroscopic data in accordance with literature.¹⁸⁶ (LB ref: JB-012, JB-017, JB-585)

(E)-3-(Benzyloxy)prop-2-enoic acid (423)

Methyl ester **422** (569 mg, 2.96 mmol, 1.0 eq) was stirred in a mixture of NaOH (1 M, 3.3 mL, 1.1 eq) and 1,4-dioxane (3.3 mL) at room temperature until TLC (petrol : EtOAc 4:1) indicated complete conversion (ca. 48 h). The reaction mixture was acidified with 2 M HCl to pH 1 and extracted with CH₂Cl₂ (3 × 10 mL). The combined organic extracts were dried over MgSO₄, filtered and concentrated under reduced pressure to yield the title compound as a white solid (500 mg, 94%), which was used without further purification.

¹H NMR (400 MHz, DMSO-*d*₆) δ_H: 4.99 (2H, s, OCH₂), 5.25 (1H, d, *J* 12.4, C(2)*H*), 7.27 – 7.44 (5H, m, 5 × Ar*H*), 7.61 (1H, d, *J* 12.4, C(3)*H*).

Spectroscopic data in accordance with literature.¹⁸⁷ (LB ref: JB-626)

(E)-3-(Benzyloxy)prop-2-enoic acid, 4-nitrophenol ester (357)

Following **General Procedure G**, acid **423** (500 mg, 2.8 mmol, 1.0 eq), oxalyl chloride (0.25 mL, 2.9 mmol, 1.05 eq) and DMF (1 drop) in anhydrous CH₂Cl₂ (8.5 mL) followed by 4-nitrophenol (390 mg, 2.8 mmol, 1.0 eq) and *i*-Pr₂NEt (0.98 mL, 5.6 mmol, 2.0 eq) in anhydrous CH₂Cl₂ (8.5 mL) gave a brown solid, which was triturated with Et₂O. The colourless solid (*i*-Pr₂NEt·HCl) was filtered, washed with Et₂O and the filtrate was concentrated under reduced pressure. The crude solid was purified by Biotage® Isolera™ 4 [SNAP KP-Sil 50 g, 100 mL min⁻¹, petrol : EtOAc 90:10 to 75:25 (10 CV), R_f 0.45 in petrol : EtOAc 4:1] followed by recrystallisation from Et₂O to afford the title compound as a white crystalline solid (265 mg, 31%). **m.p.** (Et₂O) 106 – 109 °C.

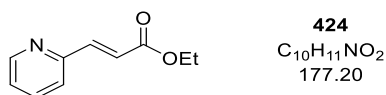
¹H NMR (500 MHz, CDCl₃) δ_H: 5.02 (2H, s, OCH₂), 5.51 (1H, d, *J* 12.5, C(2)*H*), 7.27 – 7.34 (2H, m, Ar¹(2,6)*H*), 7.35 – 7.46 (5H, m, 5 × Ar²*H*), 7.88 (1H, d, *J* 12.5, C(3)*H*), 8.23 – 8.31 (2H, m, Ar¹(3,5)*H*).

¹³C{¹H} NMR (126 MHz, CDCl₃) δ_C: 73.6 (OCH₂), 96.0 (C(2)*H*), 122.5 (Ar¹C(2,6)*H*), 125.1 (Ar¹C(3,5)*H*), 127.8 (Ar²C(3,5)*H*), 128.9 (Ar²C(2,4,6)*H*), 134.6 (Ar²C(1)), 145.0 (Ar¹C(4)), 155.6 (Ar¹C(1)), 164.7 (C(3)*H*), 165.0 (C(1)=O).

HRMS (ESI⁺) C₁₆H₁₃NO₅Na [M+Na]⁺ found 322.0683, requires 322.0685 (−0.8 ppm).

v_{max} (film, cm⁻¹) 3120, 3101, 3086, 2845 (C-H), 1718 (C=O), 1685, 1614, 1589 (C=C_{Ar}), 1514 (NO₂), 1489 (C=C_{Ar}), 1334 (NO₂), 1236, 1205, 1165, 1105, 985, 974.

(LB ref: JB-630)

(E)-3-(Pyridin-2-yl)-2-propenoic acid, ethyl ester (424)

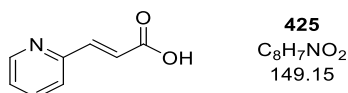
Triethylphosphonoacetate (2.2 mL, 11.0 mmol, 1.1 eq), LiCl (466 mg, 11.0 mmol, 1.1 eq) and *i*-Pr₂NEt (1.9 mL, 11.0 mmol, 1.1 eq) were stirred in anhydrous MeCN (33 mL) for 30 min at room temperature. A solution of 2-pyridinecarboxaldehyde (0.95 mL, 10.0 mmol, 1.0 eq) in anhydrous MeCN (33 mL) was added slowly and the reaction mixture allowed to stir overnight. The resulting orange suspension was diluted with H₂O (40 mL) and

extracted with EtOAc (3 × 30 mL). The combined organic phases were washed with brine, dried over MgSO₄, filtered and concentrated under reduced pressure. The crude product was purified by Biotage® Select™ [Sfär 50 g, 120 mL min⁻¹, EtOAc in petrol (12% to 100%, 20 CV), R_f 0.5 in petrol : EtOAc 1:1] to afford the title compound as a yellow oil (1.34 g, 75%).

¹H NMR (500 MHz, CDCl₃) δ_H: 1.33 (3H, t, *J* 7.1, OCH₂CH₃), 4.27 (2H, q, *J* 7.1, OCH₂CH₃), 6.92 (1H, d, *J* 15.8, C(2)*H*), 7.26 – 7.30 (1H, m, Ar(5)*H*), 7.43 (1H, d, *J* 7.7, Ar(3)*H*), 7.68 (1H, d, *J* 15.8, C(3)*H*), 7.70 – 7.75 (1H, m, Ar(4)*H*), 8.62 – 8.69 (1H, m, Ar(6)*H*).

Spectroscopic data in accordance with literature.¹⁸⁸ (LB ref: JB-687, JB-693)

(*E*)-3-(Pyridin-2-yl)-2-propenoic acid (425)

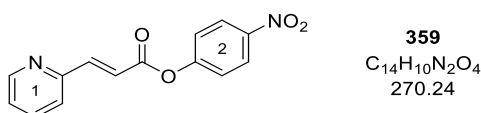


Following **General Procedure C**, ethyl ester **424** (976 mg, 5.5 mmol, 1.0 eq) and LiOH·H₂O (254 mg, 6.1 mmol, 1.1 eq) in H₂O : THF 1:1 (5 mL) were stirred for 2 h and the reaction mixture acidified with 2 M HCl to pH 2. The formed precipitate was filtered, washed with H₂O and Et₂O and dried under reduced pressure to afford the title compound as a white solid (585 mg, 71%). **m.p.** 160 °C (dec).

¹H NMR (500 MHz, DMSO *d*₆) δ_H: 6.82 (1H, d, *J* 15.7, C(2)*H*), 7.39 (1H, ddd, *J* 7.6, 4.8, 1.2, Ar(5)*H*), 7.59 (1H, d, *J* 15.7, C(3)*H*), 7.71 (1H, d, *J* 7.8, Ar(3)*H*), 7.85 (1H, app. td, *J* 7.7, 1.8, Ar(4)*H*), 8.63 (1H, d, *J* 4.8, Ar(6)*H*), 12.62 (1H, br s, OH).

Spectroscopic data in accordance with literature.¹⁸⁹ (LB ref: JB-690, JB-697)

(*E*)-3-(Pyridin-2-yl)-2-propenoic acid, 4-nitrophenol ester (359)



Following **General Procedure G**, acid **425** (559 g, 3.74 mmol, 1.0 eq), oxalyl chloride (0.34 mL, 3.93 mmol, 1.05 eq) and DMF (1 drops) in anhydrous CH₂Cl₂ (12 mL) followed by 4-nitrophenol (520 mg, 3.74 mmol, 1.0 eq) and *i*-Pr₂NEt (1.29 mL, 7.48 mmol, 2.0 eq) in anhydrous CH₂Cl₂ (12 mL) gave a black solid, which was purified by Biotage® Select™ [Sfär 50 g, 120 mL min⁻¹, EtOAc in petrol (15% to 100%, 20 CV), R_f 0.47 in petrol : EtOAc

1:1] to give a pale yellow solid. Trituration with Et₂O removed remaining *p*-nitrophenol impurities to afford the title compound as a beige solid (326 mg, 32%).

m.p. (Et₂O) 190 – 192 °C.

¹H NMR (500 MHz, CDCl₃) δ_H: 7.18 (1H, d, *J* 15.6, C(2)H), 7.33 – 7.43 (3H, m, Ar¹(5)H, Ar²(2,6)H), 7.50 (1H, d, *J* 7.7, Ar¹(3)H), 7.79 (1H, app. td, *J* 7.7, 1.8, Ar¹(4)H), 7.90 (1H, d, *J* 15.6, C(3)H), 8.28 – 8.35 (2H, m, Ar²(3,5)H), 8.71 (1H, d, *J* 4.6, Ar(6)H).

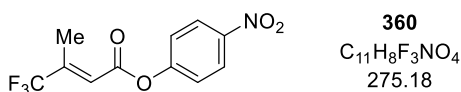
¹³C{¹H} NMR (126 MHz, CDCl₃) δ_C: 120.6 (C(2)H), 122.4 (Ar²C(2,6)H), 125.0 (Ar¹C(3,5)H), 125.2 (Ar²C(3,5)H), 137.1 (Ar¹C(4)H), 145.3 (Ar²C(4)), 146.1 (C(3)H), 150.2 (Ar¹C(6)H), 152.0 (Ar¹C(2)), 155.5 (Ar²C(1)), 164.1 (C=O).

HRMS (ESI⁺) C₁₄H₁₁N₂O₄ [M+H]⁺ found 271.0704, requires 271.0713 (–3.6 ppm).

ν_{max} (film, cm⁻¹) 3113, 3066, 1764, 1728 (C=O), 1637, 1577 (C=C_{Ar}), 1512 (NO₂), 1433, 1344 (NO₂), 1321, 1219, 1130, 985.

(LB ref: JB-698)

(E)-4,4,4-Trifluoro-3-methylbut-2-enoic acid, 4-nitrophenol ester (360)



Following **General Procedure G**, (*E*)-4,4,4-trifluoro-3-methylbut-2-enoic acid* (1.37 g, 10.0 mmol, 1.0 eq), oxalyl chloride (0.92 mL, 10.5 mmol, 1.05 eq) and DMF (3 drops) in anhydrous CH₂Cl₂ (30 mL) followed by 4-nitrophenol (1.39 g, 10.0 mmol, 1.0 eq) and *i*-Pr₂NEt (3.5 mL, 20.0 mmol, 2.0 eq) in anhydrous CH₂Cl₂ (30 mL) gave a brown oil, which was triturated with Et₂O. The colourless solid (*i*-Pr₂NEt·HCl) was filtered, washed with Et₂O and the filtrate was concentrated under reduced pressure. The resulting crude oil was purified by silica column chromatography (8% Et₂O in *n*-hexane, R_f 0.34) to afford the title compound as a pale yellow oil, which solidifies upon cooling (1.26 g, 46%).

m.p. (Et₂O) 32 – 34 °C.

¹H NMR (500 MHz, CDCl₃) δ_H: 2.34 (3H, d, *J* 1.6, CH₃), 6.56 (1H, app. p, *J* 1.4, C(2)H), 7.31 – 7.38 (2H, m, Ar(2,6)H), 8.26 – 8.33 (2H, m, Ar(3,5)H).

¹³C{¹H} NMR (126 MHz, CDCl₃) δ_C: 12.8 (CH₃), 119.8 (q, ³J_{CF} 5.8, C(2)H), 122.3 (ArC(2,6)H), 122.7 (q, ¹J_{CF} 274, CF₃), 125.3 (ArC(3,5)H), 145.6 (ArC(4)), 146.2 (q, ²J_{CF} 30.8, C(3)), 154.6 (ArC(1)), 162.1 (C=O).

¹⁹F{¹H} NMR (376 MHz, CDCl₃) δ_F: –71.4 (CF₃).

HRMS (EI⁺) C₁₁H₈F₃NO₄ [M]⁺ found 275.0406, requires 275.0399 (+0.6 ppm).

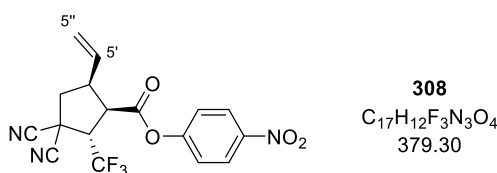
ν_{\max} (film, cm⁻¹) 3116, 3095, 2860 (C-H), 1755 (C=O), 1676, 1618 (C=C), 1591 (C=C_{Ar}), 1521 (NO₂), 1489, 1346 (NO₂), 1294, 1176, 1136, 1095, 1004, 925, 891, 856.

(LB ref: JB-790)

*(*E*)-4,4,4-Trifluoro-3-methylbut-2-enoic acid was prepared by Claire M. Young according to the published procedure.¹⁷²

5.5.3 Cooperative Pd and ITU catalysis products

(1*R*,2*S*,5*S*)-3,3-Dicyano-2-(trifluoromethyl)-5-vinylcyclopentane-1-carboxylic acid, 4-nitrophenyl ester (308)



Following **General Procedure J**, PNP ester **307** (261 mg, 1.0 mmol, 1.0 eq), Pd(PPh₃)₄ (57.8 mg, 0.05 mmol, 5 mol%), (*R*)-BTM (50.5 mg, 0.2 mmol, 20 mol%), LiCl (0.5 M in THF, 0.6 mL, 0.3 mmol, 30 mol%) and VCP **276** (118 mg, 1.0 mmol, 1.0 eq) in THF : EtOAc 3:2 (5 mL) for 24 h gave the crude product (95:5 dr). Purification by silica column chromatography (*n*-hexane : EtOAc 4:1, R_f 0.23) gave a pale yellow oil, which was triturated with Et₂O to afford the title compound as an inseparable mixture of diastereomers (95:5 dr) as an off-white solid (97 mg, 51%). **m.p.** (Et₂O) 96 – 99 °C.

$[\alpha]_D^{20}$ +43.7 (*c* 1.1 in CHCl₃).

HRMS (ESI⁻) C₁₇H₁₁F₃N₃O₄ [M-H]⁻ found 378.0699, requires 378.0707 (-2.1 ppm).

ν_{\max} (CHCl₃, cm⁻¹) 3086 (=C-H), 2951 (C-H), 2258 (C≡N), 1762 (C=O), 1618, 1593 (C=C_{Ar}), 1525 (C-NO₂), 1489 (C=C_{Ar}), 1346 (C-NO₂), 1271, 1201, 1128.

Data for major diastereoisomer 308_{maj}

chiral HPLC analysis Chiralcel OD-H (hexane : *i*-PrOH 97:3, flow rate 1.0 mlmin⁻¹, 254 nm, 40 °C) *tr* (1*S*,2*R*,5*R*): 30.1 min, *tr* (1*R*,2*S*,5*S*): 32.3 min, 7:93 er.

¹H NMR (500 MHz, CDCl₃) δ_H : 2.58 (1H, dd, *J* 13.2, 12.0, C(4)*H*^AH^B), 2.90 (1H, dd, *J* 13.2, 6.0, C(4)*H*^AH^B), 3.61 – 3.70 (1H, m, C(5)*H*), 3.74 (1H, dd, *J* 10.8, 8.4, C(1)*H*), 3.85 – 3.98 (1H, m, C(2)*H*), 5.41 – 5.47 (2H, m, C(5'')*H*₂), 5.82 (1H, ddd, *J* 17.1, 10.2, 7.9, C(5')*H*), 7.25 – 7.31 (2H, m, Ar(2,6)*H*), 8.28 – 8.34 (2H, m, Ar(3,5)*H*).

$^{13}\text{C}\{^1\text{H}\}$ NMR (126 MHz, CDCl_3) δ_{C} : 34.3 (C(3)), 43.5 (C(4) H_2), 44.1 (C(5)H), 45.7 (C(1)H), 55.0 (q, $^2J_{\text{CF}}$ 29.8, C(2)H), 111.9 (CN), 112.9 (CN), 121.4 (C(5'') H_2), 122.2 (ArC(2,6)H), 123.6 (q, $^1J_{\text{CF}}$ 280, CF_3), 125.4 (ArC(3,5)H), 131.7 (C(5')H), 145.9 (ArC(4)), 154.3 (ArC(1)), 168.2 (C=O).

$^{19}\text{F}\{^1\text{H}\}$ NMR (376 MHz, CDCl_3) δ_{F} : -67.3 (s, CF_3).

Data for minor diastereoisomer **308**_{min}

chiral HPLC analysis Chiralcel OD-H (hexane : *i*-PrOH 97:3, flow rate 1.0 mlmin⁻¹, 254 nm, 40 °C) t_{R} (1*S*,2*R*,5*S*): 40.4 min, t_{R} (1*R*,2*S*,5*R*): 45.2 min, <5:95 er.

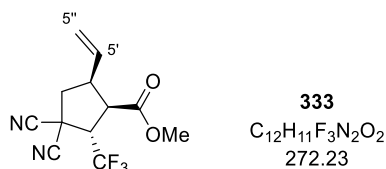
^1H NMR (500 MHz, CDCl_3) (*selected*) δ_{H} : 3.00 (1H, dd, *J* 13.7, 6.8, C(4) $\text{H}^{\text{A}}\text{H}^{\text{B}}$), 3.30 – 3.38 (2H, m, C(1)H and C(5)H), 5.37 – 5.41 (2H, m, C(5'') H_2), 5.92 (1H, ddd, *J* 16.9, 10.2, 7.5, C(5')H).

$^{13}\text{C}\{^1\text{H}\}$ NMR (126 MHz, CDCl_3) (*selected*) δ_{C} : 44.6 (C(4) H_2), 47.1 (C(5)H), 49.7 (C(1)H), 120.2 (C(5'') H_2), 134.0 (C(5')H), 167.9 (C=O).

$^{19}\text{F}\{^1\text{H}\}$ NMR (376 MHz, CDCl_3) δ_{F} : -67.0 (s, CF_3).

(LB ref: JB-417 (\pm), JB-421, JB-541, JB-752, JB-793, JB-801, JB-811)

(1*R*,2*S*,5*S*)-3,3-Dicyano-2-(trifluoromethyl)-5-vinylcyclopentane-1-carboxylic acid, methyl ester (333)



Following **General Procedure J**, PNP ester **307** (261 mg, 1.0 mmol, 1.0 eq), Pd(PPh₃)₄ (57.8 mg, 0.05 mmol, 5 mol%), (*R*)-BTM (50.5 mg, 0.2 mmol, 20 mol%), LiCl (0.5 M in THF, 0.6 mL, 0.3 mmol, 30 mol%) and VCP **276** (118 mg, 1.0 mmol, 1.0 eq) in THF : EtOAc 3:2 (5 mL) for 24 h followed by MeOH (1.0 mL) and DMAP (24.4 mg, 0.2 mmol, 20 mol%) for 24 h gave the crude product (95:5 dr). Purification by silica column chromatography (*n*-hexane : EtOAc 4:1 to 3:1, R_{f} 0.42 in *n*-hexane : EtOAc 3:1) gave the title compound as an inseparable mixture of diastereomers (95:5 dr) as a pale yellow oil (205 mg, 75%), which slowly solidifies at ca. -18 °C.

333 was also synthesised starting from isolated cyclopentane PNP ester **308**:

To a solution of PNP ester **308** (379 mg, 1.0 mmol, 1.0 eq, 95:5 dr) in EtOAc (4.0 mL) were added anhydrous MeOH (1.0 mL, 25.0 mmol, 25.0 eq) and DMAP (24 mg, 0.2 mmol, 0.2 eq) and the reaction mixture was stirred at room temperature for 24 h. The reaction mixture was diluted with EtOAc (10 mL), washed with 1 M NaOH (2 × 10 mL) and brine (10 mL), dried over MgSO₄, filtered and the solvent was removed under reduced pressure. The crude product was purified by silica column chromatography (*n*-hexane : EtOAc 4:1, R_f 0.35) to afford the title compound as an inseparable mixture of diastereoisomers (95:5 dr) as a colourless oil (247 mg, 90%), which slowly solidifies at ca. -18 °C.

m.p. (EtOAc) 69 – 70 °C. $[\alpha]_D^{20}$ +30.6 (*c* 1.31 in CHCl₃).

HRMS (ESI) C₁₂H₁₀F₃N₂O₂ [M-H]⁻ found 271.0698, requires 271.0699 (-0.6 ppm).

v_{max} (film, cm⁻¹) 3088 (C=CH₂), 2956 (C-H), 1724 (C=O), 1643 (C=C), 1444, 1408, 1369, 1271, 1247, 1224, 1168, 1132, 935.

Data for major diastereoisomer 333_{maj}

Chiral GC analysis, Restek Rt-βDEXcst (length: 30 m, thickness: 0.25 mm, film thickness: 0.25 μm, carrier gas: He, linear velocity: 28 cmsec⁻¹, temperature: 120 °C (60 min), 120 to 140 °C (20 min)) t_R (1R,2S,5S): 64.5 min, t_R (1S,2R,5R): 65.5 min, 93:7 er.

¹H NMR (500 MHz, CDCl₃) δ_H: 2.45 – 2.55 (1H, m, C(4)H^AH^B), 2.74 (1H, dd, *J* 11.8, 4.3, C(4)H^AH^B), 3.36 – 3.46 (2H, m, C(1)H, C(5)H), 3.74 (3H, s, OCH₃), 3.87 (1H, p, *J* 7.7, C(2)H), 5.21 – 5.28 (2H, m, C(5'')H₂), 5.56 – 5.65 (1H, m, C(5')H).

¹³C{¹H} NMR (126 MHz, CDCl₃) δ_C: 34.3 (C(3)), 43.4 (C(4)H₂), 44.2 (C(5)H), 45.9 (C(1)H), 52.9 (OCH₃), 55.1 (q, ²J_{CF} 29.7, C(2)H), 112.2 (CN), 113.3 (CN), 120.2 (C(5'')H₂), 123.8 (q, ¹J_{CF} 279, CF₃), 131.8 (C(5')H), 170 (C=O).

¹⁹F{¹H} NMR (377 MHz, CDCl₃) δ_F: -67.5 (CF₃).

Data for minor diastereoisomer 333_{min} (selected)

chiral GC analysis, Restek Rt-βDEXcst (length: 30 m, thickness: 0.25 mm, film thickness: 0.25 μm, carrier gas: He, linear velocity: 28 cmsec⁻¹, temperature: 120 °C (60 min), 120 to 140 °C (20 min)) t_R (1R,2S,5R): 69.8 min, t_R (1S,2R,5S): 72.7 min, >99:1 er.

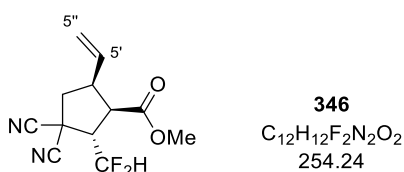
¹H NMR (500 MHz, CDCl₃) δ_H: 2.86 (1 H, dd, *J* 13.7, 7.6, C(4)H^AH^B), 3.02 (1H, t, *J* 9.7, C(1)H), 3.78 (3H, s, OCH₃), 5.79 (1H, ddd, *J* 17.5, 10.1, 7.6, C(5')H).

$^{13}\text{C}\{^1\text{H}\}$ NMR (126 MHz, CDCl_3) δ_{C} : 44.5 (C(4) H_2), 46.5 (C(5) H), 49.6 (C(1) H), 53.2 (OCH_3), 119.3 (C(5'') H_2), 134.4 (C(5') H).

$^{19}\text{F}\{^1\text{H}\}$ NMR (377 MHz, CDCl_3) δ_{F} : -67.3 (CF_3).

(LB ref: JB-476, JB-481A(\pm), JB-528, JB-582, JB-760, JB-786, JB-804)

(1R,2S,5S)-3,3-Dicyano-2-(difluoromethyl)-5-vinylcyclopentane-1-carboxylic acid, methyl ester (346)



Following **General Procedure J**, PNP ester **337** (243 mg, 1.0 mmol, 1.0 eq), $\text{Pd}(\text{PPh}_3)_4$ (57.8 mg, 0.05 mmol, 5 mol%), (*R*)-BTM (50.5 mg, 0.2 mmol, 20 mol%), LiCl (0.5 M in THF, 0.6 mL, 0.3 mmol, 30 mol%) and VCP **276** (118 mg, 1.0 mmol, 1.0 eq) in THF : EtOAc 3:2 (5 mL) for 24 h followed by MeOH (1.0 mL) and DMAP (24.4 mg, 0.2 mmol, 20 mol%) for 24 h gave the crude product (95:5dr). Purification by silica column chromatography (*n*-hexane : EtOAc 4:1, R_{f} 0.26) gave the title compound as an inseparable mixture of diastereomers (95:5 dr) as an off-white solid (187 mg, 74%). **m.p.** (EtOAc) 43 – 46 °C.

$[\alpha]_{\text{D}}^{20}$ +33.1 (*c* 1.19 in CHCl_3).

HRMS (ESI): $\text{C}_{12}\text{H}_{11}\text{F}_2\text{N}_2\text{O}_2$ $[\text{M}-\text{H}]^-$ found 253.0757, requires 253.0794 (-3.7 ppm).

ν_{max} (film, cm^{-1}): 3088 (C-H), 2989, 2956 (C-H), 2256 ($\text{C}\equiv\text{N}$), 1732 (C=O), 1643 (C=C), 1438, 1240, 1207, 1178, 1087, 1055, 929.

Data for major diastereoisomer 346_{maj}

Chiral GC analysis Restek Rt- β DEXcst (length: 30 m, thickness: 0.25 mm, film thickness: 0.25 μm , carrier gas: He, linear velocity: 28 cmsec^{-1} , temperature: 90 to 135 °C (45 min), 135 °C (40 min), 135 to 170 °C (35 min)) t_{R} (1R,2S,5S): 97.2 min, t_{R} (1S,2R,5R): 98.1 min, 90:10 er.

^1H NMR (500 MHz, CDCl_3) δ_{H} : 2.48 (1H, dd, *J* 13.1, 11.4, C(4) $\text{H}^{\text{A}}\text{H}^{\text{B}}$), 2.71 (1H, ddd, *J* 13.1, 6.1, 1.8 Hz, C(4) $\text{H}^{\text{A}}\text{H}^{\text{B}}$), 3.26 (1H, dd, *J* 10.4, 8.0, C(1) H), 3.29 – 3.39 (1H, m, C(5) H), 3.51 – 3.60 (1H, m, C(2) H), 3.71 (3H, s, OCH_3), 5.18 – 5.25 (2H, m, C(5'') H_2), 5.61 (1H, ddd, *J* 17.6, 10.1, 7.8, C(5') H), 6.06 (1H, td, *J* 54.6, 5.6, CF_2H).

$^{13}\text{C}\{^1\text{H}\}$ NMR (126 MHz, CDCl_3) δ_{C} : 34.2 (dd, $^3J_{\text{CF}}$ 5.7, 1.5 C(3)), 43.0 (C(4) H_2), 44.0 (C(5)H), 46.1 (d, $^3J_{\text{CF}}$ 4.2, C(1)H), 52.6 (OCH₃), 54.4 (t, $^2J_{\text{CF}}$ 22.7, C(2)H), 112.9 (CN), 113.8 (CN), 114.4 (t, $^1J_{\text{CF}}$ 244, CF₂H), 119.8 (C(5'')H₂), 132.4 (C(5')H), 170.7 (C=O).

$^{19}\text{F}\{^1\text{H}\}$ NMR (377 MHz, CDCl_3) δ_{F} : -121.1 (1F, d, $^2J_{\text{FF}}$ 297, CF^AF^B), -117.8 (1F, d, $^2J_{\text{FF}}$ 297, CF^AF^B).

Data for minor diastereoisomer **346**_{min} (selected)

Chiral GC analysis Restek Rt- β DEXcst (length: 30 m, thickness: 0.25 mm, film thickness: 0.25 μm , carrier gas: He, linear velocity: 28 cmsec^{-1} , temperature: 90 to 135 $^{\circ}\text{C}$ (45 min), 135 $^{\circ}\text{C}$ (40 min), 135 to 170 $^{\circ}\text{C}$ (35 min)) t_{R} (1*R*,2*S*,5*R*): 100.1 min, t_{R} (1*S*,2*R*,5*S*): 102.9 min, 88:12 er.

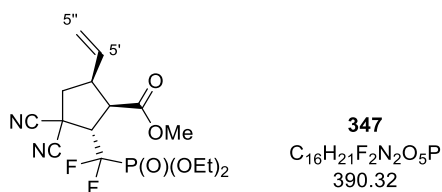
^1H NMR (500 MHz, CDCl_3) δ_{H} : 2.39 (1H, dd, J 13.4, 10.1, C(4) $\text{H}^{\text{A}}\text{H}^{\text{B}}$), 3.76 (3H, s, OCH₃), 5.78 (1H, ddd, J 17.0, 10.2, 7.6, C(5')H).

$^{13}\text{C}\{^1\text{H}\}$ NMR (126 MHz, CDCl_3) δ_{C} : 43.9 (C(4) H_2), 52.9 (OCH₃), 134.9 (C(5')H).

$^{19}\text{F}\{^1\text{H}\}$ NMR (377 MHz, CDCl_3) δ_{F} : -122.3 (1F, d, $^2J_{\text{FF}}$ 296, CF^AF^B), -119.8 (1F, d, $^2J_{\text{FF}}$ 296, CF^AF^B).

(LB ref: JB-575(\pm), JB-700, JB-761)

(1*R*,2*S*,5*S*)-3,3-Dicyano-2-((diethoxyphosphoryl)difluoromethyl)-5-vinylcyclopentane-1-carboxylic acid, methyl ester (347)



Following **General Procedure J**, PNP ester **338** (379 mg, 1.0 mmol, 1.0 eq), Pd(PPh₃)₄ (57.8 mg, 0.05 mmol, 5 mol%), (*R*)-BTM (50.5 mg, 0.2 mmol, 20 mol%), LiCl (0.5 M in THF, 0.6 mL, 0.3 mmol, 30 mol%) and VCP **276** (118 mg, 1.0 mmol, 1.0 eq) in THF : EtOAc 3:2 (5 mL) for 24 h followed by MeOH (1.0 mL) and DMAP (122 mg, 1.0 mmol, 1.0 eq) for 96 h gave the crude product (dr n.d.). Purification by silica column chromatography (*n*-hexane : EtOAc 2:1 to 1:1, R_{f} 0.23 in *n*-hexane : EtOAc 1:1) gave the title compound as a single diastereoisomer (>95:5 dr) as a white solid (73 mg, 19%). **m.p.** (CHCl_3) 59 – 61 $^{\circ}\text{C}$. $[\alpha]_{\text{D}}^{20}$ +9.4 (c 1.06 in CH_2Cl_2).

Chiral HPLC analysis, Chiralpak AD-H, (*n*-hexane : *i*-PrOH 96:4, flow rate 1.5 mLmin⁻¹, 254 nm, 40 °C) *t_R* (1*R*,2*S*,5*S*): 26.8 min, *t_R* (1*S*,2*R*,5*R*): 30.9 min, 81:19 er. (determined from PNP ester from crude reaction mixture (0.2 mL aliquot, filtered over silica) before addition of MeOH)

¹H NMR (500 MHz, CDCl₃) δ_H: 1.38 (6H, t, *J* 7.1, 2 × OCH₂CH₃), 2.44 (1H, app. t, *J* 12.9, C(4)*H^AH^B*), 2.63 (1H, dd, *J* 12.7, 5.3, C(4)*H^AH^B*), 3.29 – 3.39 (1H, m, C(5)*H*), 3.41 – 3.48 (1H, m, C(1)*H*), 3.69 (3H, s, OCH₃), 3.90 (1H, dddd, *J* 25.0, 6.9, 5.1, 3.2, C(2)*H*), 4.21 – 4.36 (4H, m, 2 × OCH₂CH₃), 5.14 – 5.24 (2H, m, C(5'')*H*₂), 5.59 (1H, ddd, *J* 16.8, 10.6, 7.4, C(5')*H*).

¹³C{¹H} NMR (126 MHz, CDCl₃) δ_C: 16.3 (t, ³*J*_{CP} 4.6, 2 × OCH₂CH₃), 34.0 – 34.2 (m, C(3)), 42.9 (C(4)*H*₂), 45.0 (C(5)*H*), 46.3 – 46.5 (m, C(1)*H*), 52.5 (OCH₃), 55.2 (dt, ²*J*_{CP} 21, ²*J*_{CF} 18, C(2)*H*), 65.4 (d, ²*J*_{CP} 6.9, OCH₂CH₃), 65.7 (d, ²*J*_{CP} 6.9, OCH₂CH₃), 113.4 (CN), 114.4 (CN), 117.8 (td, ¹*J*_{CF} 266, ¹*J*_{CP} 215, CF₂P), 119.3 (C(5'')*H*₂), 132.2 (C(5')*H*), 171.7 (C=O).

¹⁹F{¹H} NMR (377 MHz, CDCl₃) δ_F: -118.2 (1F, dd, ²*J*_{FF} 307, ²*J*_{FP} 104, CF^AFB), -111.5 (1F, dd, ²*J*_{FF} 307, ²*J*_{FP} 94, CF^AFB).

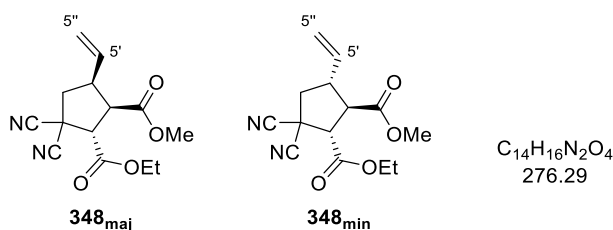
³¹P{¹H} NMR (202 MHz, CDCl₃) δ_P: 3.36 (1P, dd, ²*J*_{PF} 104, 94).

HRMS (ESI⁺): C₁₆H₂₁F₂N₂O₅PNa [M+Na]⁺ found 413.1038, requires 413.1048 (-2.5 ppm).

ν_{max} (film, cm⁻¹): 2991 (C-H), 2958, 1728 (C=O), 1689, 1643 (C=C), 1438, 1371, 1280 (P=O), 1215 1178, 1051 (P-O), 1020, 966.

(LB ref: JB-674 (±), JB-768)

(1*R*,2*S*,5*S*)-3,3-Dicyano-5-vinylcyclopentane-1,2-dicarboxylic acid, 2-ethyl 1-methyl diester (348_{maj}) and (1*R*,2*S*,5*R*)-3,3-Dicyano-5-vinylcyclopentane-1,2-dicarboxylic acid, 2-ethyl 1-methyl diester (348_{min})



Following **General Procedure J**, PNP ester **339** (265 mg, 1.0 mmol, 1.0 eq), Pd(PPh₃)₄ (57.8 mg, 0.05 mmol, 5 mol%), (*R*)-BTM (50.5 mg, 0.2 mmol, 20 mol%), LiCl (0.5 M in THF, 0.6 mL, 0.3 mmol, 30 mol%) and VCP **276** (118 mg, 1.0 mmol, 1.0 eq) in THF : EtOAc 3:2 (5 mL) for 39 h followed by MeOH (1.0 mL) and DMAP (24.4 mg, 0.2 mmol, 20 mol%) for

24 h gave the crude product (88:7:5 dr). Purification by silica column chromatography (*n*-hexane : EtOAc 5:1 to 4:1, R_f 0.25 in *n*-hexane : EtOAc 4:1) gave the title compound as an inseparable mixture of diastereomers (91:1 dr) as a colourless oil (173 mg, 63%).

$[\alpha]_D^{20}$ +30.8 (*c* 1.03 in CHCl_3).

HRMS (ESI⁺): $\text{C}_{14}\text{H}_{16}\text{N}_2\text{O}_4\text{Na}$ $[\text{M}+\text{Na}]^+$ found 299.0991, requires 299.1002 (−3.8 ppm).

ν_{max} (film, cm^{-1}): 3086 (C-H), 2985 (C-H), 2956, 2916, 2254 (C≡N), 1732 (C=O), 1643 (C=C), 1438, 1232, 1193, 1176, 1014, 931.

Data for major diastereoisomer 348_{maj}

Chiral HPLC analysis, Chiralpak AD-H, (*n*-hexane : *i*-PrOH 95:5, flow rate 1.0 mLmin^{−1}, 254 nm, 40 °C) t_R (1*S*,2*R*,5*R*): 27.9 min, t_R (1*R*,2*S*,5*S*): 36.8 min, 5:95 er. (determined from PNP ester from crude reaction mixture (0.2 mL aliquot, filtered over silica) before addition of MeOH)

¹H NMR (500 MHz, CDCl_3) δ_H : 1.33 (3H, t, *J* 7.2, OCH_2CH_3), 2.41 (1H, dd, *J* 13.3, 11.0, C(4)*H^AH^B*), 2.71 (1H, dd, *J* 13.3, 6.5, C(4)*H^AH^B*), 3.28 – 3.38 (1H, m, C(5)*H*), 3.56 (1H, dd, *J* 10.6, 9.1, C(1)*H*), 3.69 (3H, s, OCH_3), 3.99 (1H, d, *J* 9.1, C(2)*H*), 4.23 – 4.37 (2H, m, OCH_2CH_3), 5.14 – 5.22 (2H, m, C(5'')*H*₂), 5.60 (1H, ddd, *J* 17.0, 10.2, 8.1, C(5')*H*).

¹³C{¹H} NMR (126 MHz, CDCl_3) δ_C : 13.9 (OCH_2CH_3), 36.4 (C(3)), 43.0 (C(4)*H*₂), 43.3 (C(5)*H*), 47.8 (C(1)*H*), 52.5 (OCH_3), 55.7 (C(2)*H*), 62.9 (OCH_2CH_3), 113.9 (CN), 114.4 (CN), 119.3 (C(5'')*H*₂), 133.2 (C(5')*H*), 167.1 (C(2')=O), 171.2 (C(1')=O).

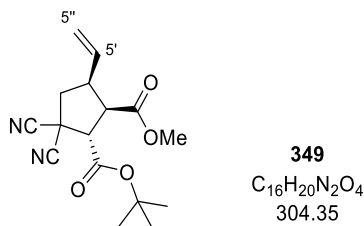
Data for minor diastereoisomer 348_{min} (selected)

Chiral HPLC analysis, Chiralpak AD-H, (*n*-hexane : *i*-PrOH 95:5, flow rate 1.0 mLmin^{−1}, 254 nm, 40 °C) t_R (1*S*,2*R*,5*S*): 27.9 min, t_R (1*R*,2*S*,5*R*): 36.8 min, 25:75 er. (determined from PNP ester from crude reaction mixture (0.2 mL aliquot, filtered over silica) before addition of MeOH)

¹H NMR (500 MHz, CDCl_3) δ_H : 2.50 (1H, dd, *J* 14.0, 8.0, C(4)*H^AH^B*), 2.81 (1H, dd, *J* 14.0, 9.0, C(4)*H^AH^B*), 3.02 – 3.10 (1H, m, C(5)*H*), 3.17 (1H, app. t, *J* 10.1, C(1)*H*), 3.74 (3H, s, OCH_3), 3.83 (1H, d, *J* 10.5, C(2)*H*), 5.81 (1H, ddd, *J* 17.0, 10.3, 7.8, C(5')*H*).

¹³C{¹H} NMR (126 MHz, CDCl_3) δ_C : 35.4 (C(3)), 43.5 (C(4)*H*₂), 45.7 (C(5)*H*), 50.8 (C(1)*H*), 52.7 (OCH_3), 56.1 (C(2)*H*), 114.1 (CN), 114.8 (CN), 118.2 (C(5'')*H*₂), 135.9 (C(5')*H*), 171.4 (C(1')=O).

(LB ref: JB-565 (±), JB-648 (±), JB-758)

(1R,2S,5S)-3,3-Dicyano-5-vinylcyclopentane-1,2-dicarboxylic acid, 2-(*t*-butyl) 1-methyl diester (349)

Following **General Procedure J**, PNP ester **340** (293 mg, 1.0 mmol, 1.0 eq), Pd(PPh₃)₄ (57.8 mg, 0.05 mmol, 5 mol%), (*R*)-BTM (50.5 mg, 0.2 mmol, 20 mol%), LiCl (0.5 M in THF, 0.6 mL, 0.3 mmol, 30 mol%) and VCP **276** (118 mg, 1.0 mmol, 1.0 eq) in THF : EtOAc 3:2 (5 mL) for 24 h followed by MeOH (1.0 mL) and DMAP (24.4 mg, 0.2 mmol, 20 mol%) for 24 h gave the crude product (88:12 dr). Purification by silica column chromatography (*n*-hexane : EtOAc 6:1, R_f 0.24) gave the title compound as a single diastereoisomer (>95:5 dr) as a white solid (169 mg, 56%). **m.p.** (EtOAc) 70 – 72 °C. [α]_D²⁰ +37.9 (*c* 1.07 in CHCl₃). **Chiral HPLC** analysis, Chiralcel OD-H, (*n*-hexane : *i*-PrOH 96:4, flow rate 1.0 mLmin⁻¹, 254 nm, 40 °C) t_R (1*S*,2*R*,5*R*): 17.4 min, t_R (1*R*,2*S*,5*S*): 34.1 min, 8:92 er. (determined from PNP ester from crude reaction mixture (0.2 mL aliquot, filtered over silica) before addition of MeOH)

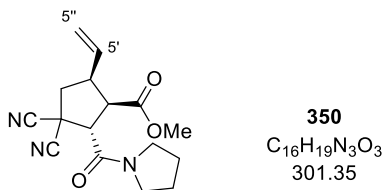
¹H NMR (500 MHz, CDCl₃) δ_H: 1.54 (9H, s, OC(CH₃)₃), 2.39 (1H, dd, *J* 13.2, 11.2, C(4)H^AH^B), 2.70 (1H, dd, *J* 13.2, 6.5, C(4)H^AH^B), 3.27 – 3.37 (1H, m, C(5)H), 3.54 (1H, dd, *J* 10.8, 9.0, C(1)H), 3.71 (3H, s, OCH₃), 3.93 (1H, d, *J* 9.0, C(2)H), 5.15 – 5.21 (2H, m, C(5'')H₂), 5.60 (1H, ddd, *J* 17.1, 10.1, 8.1, C(5')H).

¹³C{¹H} NMR (126 MHz, CDCl₃) δ_C: 27.8 (OC(CH₃)₃), 36.7 (C(3)), 43.1 (C(4)H₂), 43.2 (C(5)H), 47.5 (C(1)H), 52.5 (OCH₃), 56.4 (C(2)H), 84.8 (OC(CH₃)₃), 114.1 (CN), 114.6 (CN), 119.2 (C(5'')H₂), 133.4 (C(5')H), 166.0 (C(2')=O), 171.4 (C(1')=O).

HRMS (ESI⁺): C₁₆H₂₀N₂O₄Na [M+Na]⁺ found 327.1305, requires 327.1315 (–3.1 ppm).

ν_{\max} (film, cm⁻¹): 3003, 2987 (C-H), 2924, 1730 (C=O), 1641 (C=C), 1440 (C-H), 1381, 1369 (C-(CH₃)₃), 1251, 1232, 1174, 1155.

(LB ref: JB-577(±), JB-649 (±), JB-699, JB-766)

(1R,2S,5S)-3,3-Dicyano-2-(pyrrolidine-1-carbonyl)-5-vinylcyclopentane-1-carboxylic acid, methyl ester (350)

Following **General Procedure J**, PNP ester **341** (290 mg, 1.0 mmol, 1.0 eq), Pd(PPh₃)₄ (57.8 mg, 0.05 mmol, 5 mol%), (*R*)-BTM (50.5 mg, 0.2 mmol, 20 mol%), LiCl (0.5 M in THF, 0.6 mL, 0.3 mmol, 30 mol%) and VCP **276** (118 mg, 1.0 mmol, 1.0 eq) in THF : EtOAc 3:2 (5 mL) for 39 h followed by MeOH (1.0 mL) and DMAP (24.4 mg, 0.2 mmol, 20 mol%) for 24 h gave the crude product (79:21 dr). Purification by silica column chromatography (5 to 10% Et₂O in CH₂Cl₂, R_f 0.20 in 5% Et₂O in CH₂Cl₂) gave the title compound as a single diastereoisomer (>95:5 dr) as an off-white solid (192 mg, 64%). **m.p.** (Et₂O) 86 – 88 °C.

[α]_D²⁰ +13.2 (c 1.02 in CHCl₃).

Chiral HPLC analysis, Chiralpak IA, (*n*-hexane : *i*-PrOH 95:5, flow rate 1.0 mLmin⁻¹, 211 nm, 30 °C) tr (1*S*,2*R*,5*R*): 30.7 min, tr (1*R*,2*S*,5*S*): 39.4 min, 9:91 er.

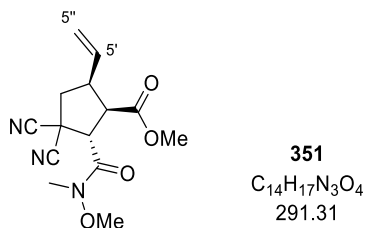
¹H NMR (500 MHz, CDCl₃) δ_H: 1.85 – 2.10 (4H, m, 2 × CH₂), 2.52 (1H, dd, *J* 13.4, 8.1, C(4)*H*^A*H*^B), 2.78 (1H, dd, *J* 13.4, 6.8, C(4)*H*^A*H*^B), 3.42 (1H, app. dtd, *J* 9.4, 8.1, 6.8, C(5)*H*), 3.48 – 3.59 (2H, m, NCH₂), 3.65 (3H, s, OCH₃), 3.67 – 3.72 (2H, m, NCH₂), 3.80 (1H, app. t, *J* 9.0 C(1)*H*), 3.99 (1H, d, *J* 8.8, C(2)*H*), 5.15 – 5.22 (2H, m, C(5'')*H*₂), 5.67 (1H, ddd, *J* 17.0, 10.2, 8.3, C(5')*H*).

¹³C{¹H} NMR (126 MHz, CDCl₃) δ_C: 24.2 (CH₂(pyrr)), 26.0 (CH₂(pyrr)), 36.2 (C(3)), 44.2 (C(5)*H*), 44.3 (C(4)*H*₂), 46.7 (NCH₂), 47.2 (NCH₂), 50.8 (C(1)*H*), 52.3 (OCH₃), 53.3 (C(2)*H*), 113.8 (CN), 115.7 (CN), 119.1 (C(5'')*H*₂), 133.8 (C(5')*H*), 164.7 (C(2')=O), 171.3 (C(1')=O).

HRMS (ESI⁺): C₁₆H₂₀N₃O₃ [M+H]⁺ found 302.1490, requires 302.1499 (–3.0 ppm).

v_{max} (film, cm⁻¹): 2985 (C-H), 2953, 2889, 1737 (C=O_{ester}), 1637 (C=O_{amide}), 1446 (C-H), 1313, 1247, 1207, 1082, 1026, 987, 935.

(LB ref: JB-530A, JB-564(±), JB-759)

(1*R*,2*S*,5*S*)-3,3-Dicyano-2-(methoxy(methyl)carbamoyl)-5-vinyl cyclopentane-1-carboxylic acid, methyl ester (351)

Following **General Procedure J**, PNP ester **342** (280 mg, 1.0 mmol, 1.0 eq), Pd(PPh₃)₄ (57.8 mg, 0.05 mmol, 5 mol%), (*R*)-BTM (50.5 mg, 0.2 mmol, 20 mol%), LiCl (0.5 M in THF, 0.6 mL, 0.3 mmol, 30 mol%) and VCP **276** (118 mg, 1.0 mmol, 1.0 eq) in THF : EtOAc 3:2 (5 mL) for 24 h followed by MeOH (1.0 mL) and DMAP (24.4 mg, 0.2 mmol, 20 mol%) for 24 h gave the crude product (>95:5 dr). Purification by silica column chromatography (0 to 5% Et₂O in CH₂Cl₂, R_f 0.37 in 5% Et₂O in CH₂Cl₂) gave the title compound as a single diastereoisomer (>95:5 dr) as a pale yellow solid (212 mg, 73%). **m.p.** (Et₂O) 72 – 75 °C. $[\alpha]_D^{20}$ +5.0 (*c* 1.14 in CHCl₃).

Chiral HPLC analysis, Chiralpak AD-H, (*n*-hexane : *i*-PrOH 95:5, flow rate 1.0 mLmin⁻¹, 211 nm, 40 °C) t_R (1*S*,2*R*,5*R*): 15.5 min, t_R (1*R*,2*S*,5*S*): 18.9 min, 8:92 er.

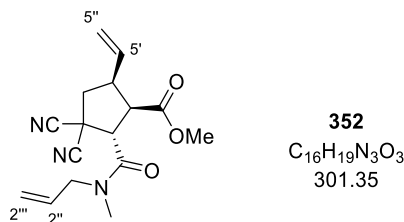
¹H NMR (500 MHz, CDCl₃) δ_H: 2.62 – 2.72 (2H, m, C(4)H₂), 3.27 – 3.37 (1H, m, C(5)H), 3.30 (3H, s, NCH₃), 3.69 (3H, s, OCH₃), 3.75 (1H, app. t, *J* 8.1, C(1)H), 3.83 (3H, s, N-OCH₃), 4.13 (1H, d, *J* 8.0, C(2)H), 5.18 – 5.25 (2H, m, C(5'')H₂), 5.75 (1H, ddd, *J* 17.0, 10.4, 8.0, C(5')H).

¹³C{¹H} NMR (126 MHz, CDCl₃) δ_C: 33.0 (NCH₃), 35.9 (C(3)), 43.8 (C(4)H₂), 45.1 (C(5)H), 49.7 (C(1)H), 52.3 (OCH₃), 53.5 (C(2)H), 61.3 (N-OCH₃), 114.6 (CN), 116.3 (CN), 119.2 (C(5'')H₂), 133.2 (C(5')H), 167.4 (C(2')=O), 171.4 (C(1')=O).

HRMS (ESI⁺): C₁₄H₁₇N₃O₄Na [M+Na]⁺ found 314.1104, requires 314.1111 (-2.3 ppm).

ν_{max} (film, cm⁻¹): 3088, 2985 (C-H), 2953, 2252 (C≡N), 1730 (C=O_{ester}), 1662 (C=O_{amide}), 1593, 1435, 1371, 1246, 1195, 1172, 991, 927.

(LB ref: JB-576(±), JB-613, JB-767)

(1R,2S,5S)-2-(Allyl(methyl)carbamoyl)-3,3-dicyano-5-vinylcyclopentane-1-carboxylic acid, methyl ester (352)

Following **General Procedure J**, PNP ester **343** (290 mg, 1.0 mmol, 1.0 eq), Pd(PPh₃)₄ (57.8 mg, 0.05 mmol, 5 mol%), (*R*)-BTM (50.5 mg, 0.2 mmol, 20 mol%), LiCl (0.5 M in THF, 0.6 mL, 0.3 mmol, 30 mol%) and VCP **276** (118 mg, 1.0 mmol, 1.0 eq) in THF : EtOAc 3:2 (5 mL) for 39 h followed by MeOH (1.0 mL) and DMAP (24.4 mg, 0.2 mmol, 20 mol%) for 24 h gave the crude product (93:7 dr). Purification by silica column chromatography (4 to 6% Et₂O in CH₂Cl₂, R_f 0.32 in 4% Et₂O in CH₂Cl₂) gave the title compound as a single diastereoisomer (>95:5 dr) as a colourless oil (226 mg, 75%) as a rotameric mixture (5:4). $[\alpha]_D^{20}$ +14.4 (*c* 1.12 in CHCl₃).

Chiral HPLC analysis, Chiralpak IA, (*n*-hexane : *i*-PrOH 96:4, flow rate 1.0 mLmin⁻¹, 211 nm, 40 °C) *tr* (1*S*,2*R*,5*R*): 17.8 min, *tr* (1*R*,2*S*,5*S*): 25.9 min, 7:93 er.

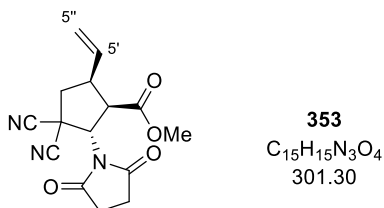
¹H NMR (500 MHz, CDCl₃) *major rotamer* δ_H: 2.49 – 2.58 (1H, m, C(4)*H*^A*H*^B), 2.73 – 2.81 (1H, m, C(4)*H*^A*H*^B), 3.15 (3H, s, NCH₃), 3.35 – 3.45 (1H, m, C(5)*H*), 3.63 (3H, s, OCH₃), 3.79 (1H, app. t, *J* 9.0, C(1)*H*), 3.98 (1H, ddt, *J* 15.1, 6.1, 1.5, NCH^A*H*^B), 4.02 – 4.18 (2H, m, C(2)*H*, NCH^A*H*^B), 5.11 – 5.25 (4H, m, C(2'')*H*₂, C(5'')*H*₂), 5.60 – 5.77 (2H, m, C(2')*H*, C(5')*H*). *minor rotamer* δ_H: 2.98 (3H, s, NCH₃), 3.62 (3H, s, OCH₃), 3.74 (1H, app. t, *J* 8.9, C(1)*H*), 5.27 (1H, dq, *J* 10.3, 1.3, C(2'')*H*^A*H*^B), 5.83 (1H, ddt, *J* 16.9, 10.3, 5.2, C(2')*H*).

¹³C{¹H} NMR (126 MHz, CDCl₃) *major rotamer* δ_C: 35.3 (NCH₃), 36.2 (C(3)), 44.0 (C(5)*H*), 44.2 (C(4)*H*₂), 51.0 (NCH₂), 51.0 (C(2)*H*), 51.3 C(1)*H*, 52.3 (OCH₃), 113.7 (CN), 115.6 (CN), 118.0 (C(2'')*H*₂), 119.1 (C(5'')*H*₂), 131.8 (C(2')*H*), 133.8 (C(5')*H*), 166.4 (C(2')=O), 171.2 (C(1')=O). *minor rotamer* δ_C: 34.6 (NCH₃), 36.8 (C(3)), 44.3 (C(4)*H*₂), 44.4 (C(5)*H*), 50.9 (C(2)*H*), 51.5 (C(1)*H*), 52.3 (OCH₃), 52.6 (NCH₂), 113.9 (CN), 115.6 (CN), 118.1 (C(2'')*H*₂), 119.2 (C(5'')*H*₂), 132.0 (C(2')*H*), 133.7 (C(5')*H*), 167.0 (C(2')=O), 171.1 (C(1')=O).

HRMS (ESI⁺): C₁₆H₁₉N₃O₃Na [M+Na]⁺ found 324.1309, requires 324.1319 (−2.9 ppm).

v_{max} (film, cm⁻¹): 3084, 2985 (C-H), 2953, 2858, 2249 (C≡N), 1730 (C=O_{ester}), 1651 (C=O_{amide}), 1641, 1436, 1371, 1265, 1197, 1176, 991, 925.

(LB ref: JB-592(±), JB-778)

(1R,2S,5S)-3,3-Dicyano-2-(2,5-dioxopyrrolidin-1-yl)-5-vinylcyclopentane-1-carboxylic acid, methyl ester (353)

Following **General Procedure J**, PNP ester **344** (290 mg, 1.0 mmol, 1.0 eq), Pd(PPh₃)₄ (57.8 mg, 0.05 mmol, 5 mol%), (*R*)-BTM (101 mg, 0.4 mmol, 40 mol%), LiCl (0.5 M in THF, 0.6 mL, 0.3 mmol, 30 mol%) and VCP **276** (207 mg, 1.75 mmol, 1.75 eq) in THF : EtOAc 3:2 (5 mL) for 66 h followed by MeOH (1.0 mL) and DMAP (24.4 mg, 0.2 mmol, 20 mol%) for 24 h gave the crude product (68:32 dr). Purification by silica column chromatography (2 to 6% Et₂O in CH₂Cl₂, R_f 0.29 in 4% Et₂O in CH₂Cl₂) gave a yellow solid. Further purification by silica column chromatography (*n*-hexane : EtOAc 2:1 to 1:1, R_f 0.27 in *n*-hexane : EtOAc 1:1) gave the title compound as a single diastereoisomer (>95:5 dr) as a white solid (60 mg, 20%). **m.p.** (EtOAc) 150 – 153 °C. [α]_D²⁰ +39.3 (*c* 1.01 in CHCl₃).

¹⁹F{¹H} NMR (377 MHz, CDCl₃) δ_F (1*R*,2*S*,5*S*): -113.1, δ_F (1*S*,2*R*,5*R*): -113.3, 96:4 er.*

¹H NMR (500 MHz, CDCl₃) δ_H : 2.64 (1H, dd, *J* 13.6, 7.4, C(4)*H*^A*H*^B), 2.83 (4H, s, 2 × CH₂(*imide*)), 2.86 (1H, dd, *J* 13.6, 6.5, C(4)*H*^A*H*^B), 3.60 (1H, app. p, *J* 7.7, C(5)*H*), 3.68 (3H, s, OCH₃), 4.34 (1H, app. t, *J* 8.1, C(1)*H*), 5.20 – 5.27 (2H, m, C(5′)*H*₂), 5.48 (1H, d, *J* 7.8, C(2)*H*), 5.77 (1H, ddd, *J* 17.0, 10.3, 8.1, C(5′)*H*).

¹³C{¹H} NMR (126 MHz, CDCl₃) δ_C : 28.0 (2 × CH₂(*imide*)), 38.4 (C(3)), 42.2 (C(4)*H*₂), 44.4 (C(5)*H*), 47.4 (C(1)*H*), 52.5 (OCH₃), 59.6 (C(2)*H*), 113.6 (CN), 114.8 (CN), 119.6 (C(5′)*H*₂), 132.9 (C(5′)*H*), 170.6 (C(1′)=O), 176.1 (2 × NC=O).

HRMS (ESI⁺): C₁₅H₁₅N₃O₄Na [M+Na]⁺ found 324.0949, requires 324.0955 (-1.7 ppm).

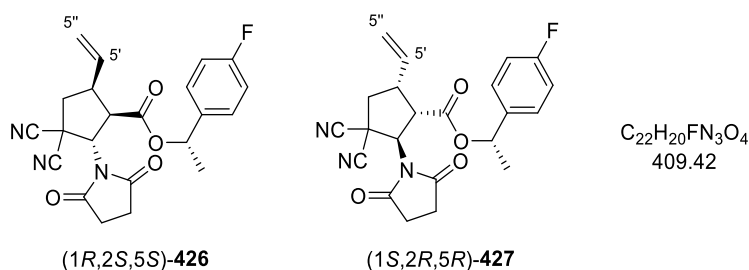
ν_{max} (film, cm⁻¹): 2999, 2962 (C-H), 1780 (C=O_{imide}), 1728 (C=O_{ester}), 1708 (C=O_{imide}), 1645 (C=C), 1435, 1375, 1361, 1213, 1161, 1089, 956, 941.

* The enantiomeric ratio was determined by derivatisation with (1*S*)-1-(4-fluorophenyl)ethan-1-ol: An aliquot (0.2 mL) of the crude reaction mixture after 66 h was concentrated under reduced pressure and dissolved in 0.5 mL CH₂Cl₂. (1*S*)-1-(4-Fluorophenyl)ethan-1-ol (15 μ L, 120 μ mol, 3.0 eq) and DMAP (1.0 mg, 8.0 μ mol, 0.2 eq) were added and the reaction mixture stirred at room temperature until ¹H NMR analysis

indicated full conversion of the intermediate PNP ester (ca. 48 h). The er was determined directly from the crude mixture by $^{19}\text{F}\{^1\text{H}\}$ NMR analysis.

(LB ref: JB-606(\pm), JB-663, JB-695, JB-769, JB-775, JB-779, JB-784)

(1R,2S,5S)-3,3-Dicyano-2-(2,5-dioxopyrrolidin-1-yl)-5-vinylcyclopentane-1-carboxylic acid, (S)-1-(4-fluorophenyl)ethyl ester (426) and **(1S,2R,5R)-3,3-Dicyano-2-(2,5-dioxopyrrolidin-1-yl)-5-vinylcyclopentane-1-carboxylic acid, (S)-1-(4-fluorophenyl)ethyl ester (427)**



Following **General Procedure J**, PNP ester **344** (145 mg, 0.5 mmol, 1.0 eq), $\text{Pd}(\text{PPh}_3)_4$ (28.9 mg, 0.025 mmol, 5 mol%), (\pm)-TM \cdot HCl (30.0 mg, 0.12 mmol, 25 mol%), *i*-Pr $_2$ NEt (25.7 μL , 0.12 mmol, 25 mol%) and VCP **276** (118 mg, 1.0 mmol, 2.0 eq) in acetone (2.5 mL) for 84 h gave the crude product. Purification by silica column chromatography (1 to 5% Et $_2$ O in CH $_2$ Cl $_2$, R_f 0.37 in 5% Et $_2$ O in CH $_2$ Cl $_2$) gave a yellow gum, which was triturated with Et $_2$ O to give the PNP ester product as an off-white solid (60 mg, 15%). The PNP ester was derivatised with (1S)-1-(4-fluorophenyl)ethan-1-ol (33.6 mg, 0.24 mmol, 1.7 eq) and DMAP (3.4 mg, 0.03 mmol, 0.2 eq) in CH $_2$ Cl $_2$ (1.0 mL) and the conversion monitored by ^1H NMR analysis. After full consumption of PNP ester was observed (ca. 36 h), the reaction mixture was diluted with CH $_2$ Cl $_2$ (5 mL) and washed with 1 M NaOH (2 \times 5 mL) and brine (5 mL). The organic phase was dried over MgSO $_4$, filtered and the solvent was removed under reduces pressure. Purification of the crude product by silica column chromatography (*n*-hexane : EtOAc 4:1 to 1:1) gave the title compound as a 1:1 mixture of diastereoisomers as a colourless glass (26 mg, 46%).

HRMS (ESI $^+$): $\text{C}_{22}\text{H}_{20}\text{FN}_3\text{O}_4\text{Na}$ [$\text{M}+\text{Na}$] $^+$ found 432.1323, requires 432.1330 (−1.6 ppm).

ν_{max} (CHCl $_3$, cm $^{-1}$): 3084, 2985, 2939 (C-H), 2254 (C \equiv N), 1784 (C=O $_{\text{imide}}$), 1720 (C=O $_{\text{ester}}$), 1645 (C=C), 1606, 1512 (C=C $_{\text{Ar}}$), 1373, 1219, 1159, 1056, 906.

Data for (1R,2S,5S)-426:

$^1\text{H NMR}$ (500 MHz, CDCl_3) δ_{H} : 1.49 (3H, d, J 6.6, CH_3), 2.60 (1H, dd, J 13.6, 7.1, $\text{C}(4)\text{H}^{\text{A}}\text{H}^{\text{B}}$), 2.79 (4H, s, $2 \times \text{CH}_{2(\text{imide})}$), 2.81 – 2.84 (1H, m, $\text{C}(4)\text{H}^{\text{A}}\text{H}^{\text{B}}$), 3.51 – 3.60 (1H, m, $\text{C}(5)\text{H}$), 4.30 (1H, app. t, J 8.0, $\text{C}(1)\text{H}$), 4.94 (1H, d, J 10.3, $\text{C}(5'')\text{H}^{\text{A}}\text{H}^{\text{B}}$), 5.04 (1H, d, J 17.0, $\text{C}(5'')\text{H}^{\text{A}}\text{H}^{\text{B}}$), 5.44 (1H, d, J 7.9, $\text{C}(2)\text{H}$), 5.51 (1H, ddd, J 17.0, 10.3, 7.0, $\text{C}(5')\text{H}$), 5.84 (1H, q, J 6.6, OCH), 6.99 – 7.07 (2H, m, Ar(3,5)H), 7.30 (2H, ddd, J 8.9, 5.3, 2.5, Ar(2,6)H).

$^{13}\text{C}\{^1\text{H}\}$ NMR (126 MHz, CDCl_3) δ_{C} : 22.0 (CH_3), 27.9 ($2 \times \text{CH}_{2(\text{imide})}$), 38.2 ($\text{C}(3)$), 42.3 ($\text{C}(4)\text{H}_2$), 44.6 ($\text{C}(5)\text{H}$), 47.4 ($\text{C}(1)\text{H}$), 59.6 ($\text{C}(2)\text{H}$), 73.5 (OCH), 113.5 (CN), 114.9 (CN), 115.5 (d, $^2J_{\text{CF}}$), 19.1, ArC(3,5)H), 119.6 ($\text{C}(5'')\text{H}_2$), 128.7 (d, $^3J_{\text{CF}}$, 8.3, ArC(2,6)H), 132.4 ($\text{C}(5')\text{H}$), 136.3 (d, $^4J_{\text{CF}}$, 3.2, ArC(1)), 162.6 (d, $^1J_{\text{CF}}$, 247, ArC(4)), 169.3 ($\text{C}=\text{O}$), 176.0 ($2 \times \text{NC}=\text{O}$).

$^{19}\text{F}\{^1\text{H}\}$ NMR (377 MHz, CDCl_3) δ_{F} : -113.1 (ArC(4)F).

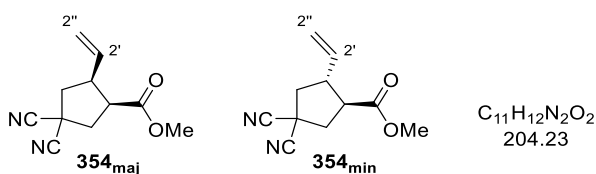
Data for (1S,2R,5R)-427:

$^1\text{H NMR}$ (500 MHz, CDCl_3) δ_{H} : 1.53 (3H, d, J 6.7, CH_3), 2.64 (1H, dd, J 13.5, 7.3, $\text{C}(4)\text{H}^{\text{A}}\text{H}^{\text{B}}$), 2.79 (4H, s, $2 \times \text{CH}_{2(\text{imide})}$), 2.87 (1H, dd, J 13.5, 6.5, $\text{C}(4)\text{H}^{\text{A}}\text{H}^{\text{B}}$), 3.61 – 3.68 (1H, m, $\text{C}(5)\text{H}$), 4.31 (1H, app. t, J 8.0, $\text{C}(1)\text{H}$), 5.19 – 5.27 (2H, m, $\text{C}(5'')\text{H}_2$), 5.47 (1H, d, J 7.8, $\text{C}(2)\text{H}$), 5.78 (1H, ddd, J 17.0, 10.4, 8.1, $\text{C}(5')\text{H}$), 5.84 (1H, q, J 6.7, OCH), 6.99 – 7.07 (2H, m, Ar(3,5)H), 7.30 (2H, ddd, J 8.9, 5.3, 2.5, Ar(2,6)H).

$^{13}\text{C}\{^1\text{H}\}$ NMR (126 MHz, CDCl_3) δ_{C} : 21.6 (CH_3), 27.9 ($2 \times \text{CH}_{2(\text{imide})}$), 38.3 ($\text{C}(3)$), 42.4 ($\text{C}(4)\text{H}_2$), 44.6 ($\text{C}(5)\text{H}$), 47.4 ($\text{C}(1)\text{H}$), 59.6 ($\text{C}(2)\text{H}$), 73.5 (OCH), 113.5 (CN), 114.9 (CN), 115.4 (d, $^2J_{\text{CF}}$), 19.1, ArC(3,5)H), 119.6 ($\text{C}(5'')\text{H}_2$), 128.2 (d, $^3J_{\text{CF}}$, 8.2, ArC(2,6)H), 132.9 ($\text{C}(5')\text{H}$), 136.0 (d, $^4J_{\text{CF}}$, 3.1, ArC(1)), 162.5 (d, $^1J_{\text{CF}}$, 247, ArC(4)), 169.3 ($\text{C}=\text{O}$), 176.0 ($2 \times \text{NC}=\text{O}$).

$^{19}\text{F}\{^1\text{H}\}$ NMR (377 MHz, CDCl_3) δ_{F} : -113.3 (ArC(4)F).

(LB ref: [JB-718](#) (\pm), JB-730)

(1S,2S)-4,4-Dicyano-2-vinylcyclopentane-1-carboxylic acid, methyl ester (354_{maj}) and**(1S,2R)-4,4-Dicyano-2-vinylcyclopentane-1-carboxylic acid, methyl ester (354_{min})**

Following **General Procedure J**, PNP ester **345** (193 mg, 1.0 mmol, 1.0 eq), $\text{Pd}(\text{PPh}_3)_4$ (57.8 mg, 0.05 mmol, 5 mol%), (*R*)-BTM (50.5 mg, 0.2 mmol, 20 mol%), LiCl (0.5 M in THF,

0.6 mL, 0.3 mmol, 30 mol%) and VCP **276** (118 mg, 1.0 mmol, 1.0 eq) in THF : EtOAc 3:2 (5 mL) for 48 h followed by MeOH (1.0 mL) and DMAP (24.4 mg, 0.2 mmol, 20 mol%) for 24 h gave the crude product. Purification by silica column chromatography (*n*-hexane : EtOAc 5:1, R_f 0.18) gave the title compound as an inseparable mixture of diastereomers (79:21 dr) as a colourless oil (51 mg, 25%). $[\alpha]_D^{20} +7.9$ (c 1.07 in CHCl_3).

HRMS (ESI⁺): $\text{C}_{11}\text{H}_{12}\text{N}_2\text{O}_2\text{Na}$ $[\text{M}+\text{Na}]^+$ found 227.0785, requires 227.0790 (-2.6 ppm).

ν_{max} (film, cm^{-1}): 3084 (C-H), 2954 (C-H), 2924, 2852, 2250 ($\text{C}\equiv\text{N}$), 1728 (C=O), 1643 (C=C), 1436, 1373, 1205, 1172, 993, 927.

Data for major diastereoisomer 354_{maj}

Chiral GC analysis Restek Rt- β DEXcst (length: 30 m, thickness: 0.25 mm, film thickness: 0.25 μm , carrier gas: He, linear velocity: 28 cmsec^{-1} , temperature: 100 to 145 °C (45 min), 145 °C (20 min), 145 to 165 °C (20 min)) t_R (1*R*,2*R*): 71.8 min, t_R (1*S*,2*S*): 73.0 min, 33:67 er.

¹H NMR (500 MHz, CDCl_3) δ_{H} : 2.48 (1H, dd, J 13.3, 10.3, C(3) $H^A H^B$), 2.64 (1H, dd, J 13.3, 6.6, C(3) $H^A H^B$), 2.70 – 2.81 (1H, m, C(5) $H^A H^B$), 2.83 (1H, dd, J 14.3, 6.6, C(5) $H^A H^B$), 3.18 – 3.31 (2H, m, C(1)*H*, C(2)*H*), 3.68 (3H, s, OCH_3), 5.14 – 5.22 (2H, m, C(2'')*H*₂), 5.66 (1H, ddd, J 17.4, 10.1, 7.5, C(2')*H*).

¹³C{¹H} NMR (126 MHz, CDCl_3) δ_{C} : 32.6 (C(4)), 40.6 (C(5)*H*₂), 42.6 (C(3)*H*₂), 45.4 (C(2)*H*), 46.7 (C(1)*H*), 52.2 (OCH_3), 115.6 (CN), 116.6 (CN), 118.8 (C(2'')*H*₂), 133.4 (C(2')*H*), 172.0 (C=O).

Data for minor diastereoisomer 354_{min} (selected)

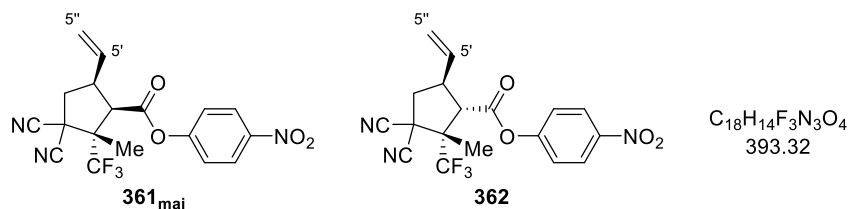
Chiral GC analysis Restek Rt- β DEXcst (length: 30 m, thickness: 0.25 mm, film thickness: 0.25 μm , carrier gas: He, linear velocity: 28 cmsec^{-1} , temperature: 100 to 145 °C (45 min), 145 °C (20 min), 145 to 165 °C (20 min)) t_R (1*S*,2*R*): 70.4 min, t_R (1*R*,2*S*): 73.9 min, 67:33 er.

¹H NMR (500 MHz, CDCl_3) δ_{H} : 2.30 (1H, dd, J 13.6, 10.0, C(3) $H^A H^B$), 2.91 (1H, app. q, J 9.0, C(1)*H*), 3.09 – 3.18 (1H, m, C(2)*H*), 3.73 (3H, s, OCH_3), 5.78 (1H, ddd, J 17.4, 10.3, 7.4 Hz, C(2')*H*).

¹³C{¹H} NMR (126 MHz, CDCl_3) δ_{C} : 32.4 (C(4)), 41.1 (C(5)*H*₂), 44.0 (C(3)*H*₂), 46.6 (C(2)*H*), 48.4 (C(1)*H*), 52.5 (OCH_3), 115.8 (CN), 116.0 (CN), 117.9 (C(2'')*H*₂), 135.9 (C(2')*H*), 172.0 (C=O).

(LB ref: JB-643(±), JB-696, JB-773)

(1R,2S,5S)-3,3-Dicyano-2-methyl-2-(trifluoromethyl)-5-vinylcyclopentane-1-carboxylic acid, 4-nitrophenyl ester (361_{maj}) and (1S,2S,5S)-3,3-Dicyano-2-methyl-2-(trifluoromethyl)-5-vinylcyclopentane-1-carboxylic acid, 4-nitrophenyl ester (362)



Following **General Procedure J**, PNP ester **360** (275 mg, 1.0 mmol, 1.0 eq), Pd(PPh₃)₄ (57.8 mg, 0.05 mmol, 5 mol%), (*R*)-BTM (50.5 mg, 0.2 mmol, 20 mol%), LiCl (0.5 M in THF, 0.6 mL, 0.3 mmol, 30 mol%) and VCP **276** (118 mg, 1.0 mmol, 1.0 eq) in THF : EtOAc 3:2 (5 mL) for 24 h gave the crude product (75:17:8 dr). Purification by silica column chromatography (*n*-hexane : EtOAc 5:1 to 4:1) resulted in partial separation of the diastereoisomers to give:

361 (*R_f* 0.29 in *n*-hexane : EtOAc 4:1) as an inseparable mixture of diastereomers (93:7 dr) as a red oil (94 mg, 24%). [α]_D²⁰ +41.6 (*c* 1.18 in CHCl₃).

HRMS (ESI⁻): C₁₈H₁₄F₃N₃O₄Cl [M+Cl]⁻ found 428.0618, requires 428.0630 (-1.2 ppm).

ν_{\max} (film, cm⁻¹): 3120, 3086 (C-H), 2931 (C-H), 2862, 1766 (C=O), 1643 (C=C), 1618, 1593 (C=C_{Ar}), 1525 (NO₂), 1489, 1346 (NO₂), 1201, 1145 (C-F), 1072, 860.

Data for major diastereoisomer 361_{maj}

Chiral HPLC analysis, Chiralcel OD-H, (*n*-hexane : *i*-PrOH 98:2, flow rate 1.0 mLmin⁻¹, 254 nm, 40 °C) *t_R* (1S,2R,5R): 35.1 min, *t_R* (1R,2S,5S): 39.0 min, 6:94 er.

¹H NMR (500 MHz, CDCl₃) δ_{H} : 1.76 (3H, s, CH₃), 2.75 (1H, dd, *J* 13.7, 11.0, C(4)H^AH^B), 2.96 (1H, dd, *J* 13.7, 7.3, C(4)H^AH^B), 3.55 – 3.65 (1H, m, C(5)H), 3.87 (1H, d, *J* 10.1, C(1)H), 5.31 – 5.41 (2H, m, C(5'')H₂), 5.85 (1H, ddd, *J* 16.9, 10.1, 8.4, C(5')H), 7.19 – 7.25 (2H, m, Ar(2,6)H), 8.23 – 8.32 (2H, m, Ar(3,5)H).

¹³C{¹H} NMR (126 MHz, CDCl₃) δ_{C} : 16.2 (CH₃), 40.6 (C(3)), 42.9 (C(4)H₂), 43.4 (C(5)H), 49.9 (C(1)H), 58.0 (q, ²*J*_{CF} 26.6, C(2)), 112.1 (CN), 113.2 (CN), 121.0 (C(5'')H₂), 122.3 (ArC(2,6)H), 125.4 (q, ¹*J*_{CF} 281, CF₃), 125.4 (ArC(3,5)H), 133.6 (C(5')H), 145.8 (ArC(4)), 154.2 (ArC(1)), 165.9 (C=O).

¹⁹F{¹H} NMR (377 MHz, CDCl₃) δ_{F} : -71.8 (CF₃).

Data for minor diastereoisomer **361_{min}** (selected)

¹H NMR (500 MHz, CDCl₃) δ_H: 1.66 (3H, s, CH₃), 2.59 – 2.65 (1H, m, C(4)H^AH^B), 3.46 – 3.54 (2H, m, C(1)H, C(5)H), 5.22 – 5.31 (2H, m, C(5'')H₂).

¹³C{¹H} NMR (126 MHz, CDCl₃) δ_C: 15.0 (CH₃), 42.2 (C(4)H₂), 43.7 (C(5)H), 52.3 (C(1)H), 119.5 (C(5'')H₂).

¹⁹F{¹H} NMR (377 MHz, CDCl₃) δ_F: -71.2 (CF₃).

362 after further purification by silica column chromatography (CH₂Cl₂ : *n*-hexane 2:1, R_f 0.33) as a mixture of diastereomers (362 : 361_{maj} 90:10 dr) as a pale yellow oil (15 mg, 4%).
[α]_D²⁰ +22.8 (*c* 0.75 in CHCl₃).

Chiral HPLC analysis, Chiralpak AS-H, (*n*-hexane : *i*-PrOH 97:3, flow rate 1.0 mLmin⁻¹, 254 nm, 40 °C) t_R (1*R*,2*R*,5*R*): 19.9 min, t_R (1*S*,2*S*,5*S*): 27.4 min, 6:94 er.

¹H NMR (500 MHz, CDCl₃) δ_H: 1.96 (3H, s, CH₃), 2.59 (1H, dd, *J* 14.1, 7.1, C(4)H^AH^B), 3.07 (1H, dd, *J* 14.1, 10.1, C(4)H^AH^B), 3.15 (1H, d, *J* 10.9, C(1)H), 3.68 – 3.80 (1H, m, C(5)H), 5.27 (1H, d, *J* 10.1, C(5'')H^AH^B), 5.33 (1H, d, *J* 16.9, C(5'')H^AH^B), 5.81 (1H, ddd, *J* 16.9, 10.1, 8.1, C(5'')H), 7.27 – 7.33 (2H, m, Ar(2,6)H), 8.30 – 8.35 (2H, m, Ar(3,5)H).

¹³C{¹H} NMR (126 MHz, CDCl₃) δ_C: 20.2 (CH₃), 41.8 (C(4)H₂), 41.9 (C(3)), 42.9 (C(5)H), 56.5 (C(1)H), 59.2 (q, ²*J*_{CF} 26.1, C(2)), 111.7 (CN), 113.5 (CN), 119.3 (C(5'')H₂), 122.1 (ArC(2,6)H), 125.3 (q, ¹*J*_{CF} 285, CF₃), 125.4 (ArC(3,5)H), 136.0 (C(5')H), 145.8 (ArC(4)), 154.4 (ArC(1)), 165.4 (C=O).

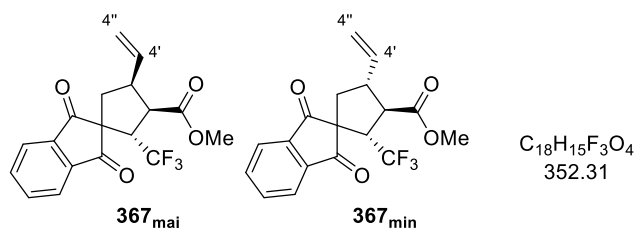
¹⁹F{¹H} NMR (377 MHz, CDCl₃) δ_F: -67.0 (CF₃).

HRMS (ESI⁺): C₁₈H₁₄F₃N₃O₄Na [M+Na]⁺ found 416.0830, requires 416.0828 (+0.1 ppm).

v_{max} (film, cm⁻¹): 3120, 3086 (C-H), 3003, 1766 (C=O), 1645 (C=C), 1618, 1593 (C=C_{Ar}), 1527 (NO₂), 1490, 1348 (NO₂), 1182 (C-F), 860.

(LB ref: JB-792(±), JB-814)

(2*S*,3*R*,4*S*)-1',3'-Dioxo-2-(trifluoromethyl)-4-vinyl-1',3'-dihydrospiro [cyclopentane-1,2'-indene]-3-carboxylic acid, methyl ester (367_{maj}) and (2*S*,3*R*,4*R*)-1',3'-Dioxo-2-(trifluoro-methyl)-4-vinyl-1',3'-dihydrospiro [cyclopentane-1,2'-indene]-3-carboxylic acid, methyl ester (367_{min})



Following **General Procedure J**, PNP ester **307** (261 mg, 1.0 mmol, 1.0 eq), Pd(PPh₃)₄ (57.8 mg, 0.05 mmol, 5 mol%), (*R*)-BTM (50.5 mg, 0.2 mmol, 20 mol%), LiCl (0.5 M in THF, 0.6 mL, 0.3 mmol, 30 mol%) and VCP **278** (198 mg, 1.0 mmol, 1.0 eq) in THF : EtOAc 3:2 (5 mL) for 48 h followed by MeOH (1.0 mL) and DMAP (48.8 mg, 0.4 mmol, 40 mol%) for 72 h gave the crude product (68:32 dr). Purification by silica column chromatography (*n*-hexane : EtOAc 5:1, R_f 0.25) gave the title compound as an inseparable mixture of diastereomers (68:32 dr) as an off-white solid (142 mg, 40%). **m.p.** (EtOAc) 79 – 82 °C. $[\alpha]_D^{20} +34.9$ (*c* 1.21 in CHCl₃).

HRMS (ESI⁺): C₁₈H₁₅F₃O₄Na [M+Na]⁺ found 375.0806, requires 375.0815 (−2.3 ppm).

ν_{\max} (film, cm^{−1}): 3082 (=C-H), 2956 (C-H), 2854, 1741 (C=O_{ester}), 1732 (C=O_{ester}), 1705 (C=O_{ketone}), 1641 (C=C), 1591 (C=C_{Ar}), 1438, 1400, 1350, 1271, 1215, 1157, 1116, 927.

Data for major diastereoisomer 367_{maj}

Chiral HPLC analysis, Chiralpak AD-H, (*n*-hexane : *i*-PrOH 99:1, flow rate 1.0 mLmin^{−1}, 211 nm, 30 °C) t_r (2*S*,3*R*,4*S*): 26.3 min, Chiralpak AD-H, (*n*-hexane : *i*-PrOH 94:6, flow rate 1.0 mLmin^{−1}, 211 nm, 30 °C) t_r (2*R*,3*S*,4*R*): 14.4 min, 89:11 er.

¹H NMR (500 MHz, CDCl₃) δ_H: 2.00 – 2.06 (1H, m, C(5)H^AH^B), 2.10 – 2.17 (1H, m, C(5)H^AH^B), 3.72 (3H, s, OCH₃), 3.70 – 3.81 (2H, m, C(4)H, C(3)H), 3.97 (1H, app. p, *J* 9.2, C(2)H), 5.04 – 5.19 (2H, m, C(4'')H₂), 5.69 (1H, ddd, *J* 16.9, 10.1, 8.3, C(4')H), 7.85 – 7.93 (2H, m, Ar(4',7')H), 7.98 – 8.04 (2H, m, Ar(5',6')H).

¹³C{¹H} NMR (126 MHz, CDCl₃) δ_C: 40.8 (C(5)H₂), 44.1 (C(4)H), 52.1 (OCH₃), 52.2 (q, ²J_{CF} 28.5, C(2)H), 52.3 (C(3)H) 58.9 (C(1)), 118.1 (C(4'')H₂), 123.8 (ArC(4',7')H), 125.3 (q, ¹J_{CF} 280, CF₃), 135.8 (C(4')H), 136.2 (ArC(5',6')H), 140.8 (ArC(4a' or 7a')), 140.9 (ArC(4a' or 7a')), 171.8 (CO₂CH₃), 199.0 (C(1' or 3')=O), 199.6 (C(1' or 3')=O).

$^{19}\text{F}\{^1\text{H}\}$ NMR (377 MHz, CDCl_3) δ_{F} : -65.5 (CF_3).

Data for minor diastereoisomer **367**_{min} (selected)

Chiral HPLC analysis, Chiralpak AD-H, (*n*-hexane : *i*-PrOH 99:1, flow rate 1.0 mLmin⁻¹, 211 nm, 30 °C) *t*_R (2*S*,3*R*,4*R*): 28.4 min, Chiralpak AD-H, (*n*-hexane : *i*-PrOH 94:6, flow rate 1.0 mLmin⁻¹, 211 nm, 30 °C) *t*_R (2*R*,3*S*,4*S*): 15.5 min, 98:2 er.

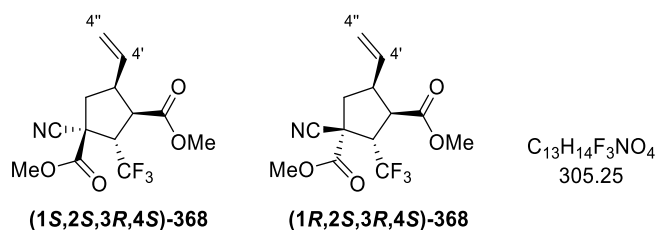
^1H NMR (500 MHz, CDCl_3) δ_{H} : 1.98 (1H, dd, *J* 13.7, 8.9, C(5)*H*^A*H*^B), 2.30 (1H, dd, *J* 13.7, 9.1, C(5)*H*^A*H*^B), 3.21 (1H, app. p, *J* 9.1, C(4)*H*), 3.37 (1H, dd, *J* 11.9, 10.6, C(3)*H*), 3.63 – 3.70 (1H, m, C(2)*H*), 3.74 (3H, s, OCH_3), 5.85 (1H, ddd, *J* 17.0, 10.2, 8.3, C(4')*H*).

$^{13}\text{C}\{^1\text{H}\}$ NMR (126 MHz, CDCl_3) δ_{C} : 40.1 (C(5)*H*₂), 47.1 (OCH_3), 47.8 (C(4)*H*), 50.7 (C(3)*H*), 53.8 (q, $^2J_{\text{CF}}$ 28.6, C(2)*H*), 57.6 (C(1)), 117.3 (C(4'')*H*₂), 123.7 (ArC(4,7)*H*), 125.0 (q, $^1J_{\text{CF}}$ 279, CF_3), 136.3 (ArC(5,6)*H*), 137.1 (C(4')*H*), 140.7 (ArC(4a or 7a)), 141.4 (ArC(4a or 7a)), 172.0 (CO_2CH_3), 199.8 (C(1' or 3')=O), 200.6 (C(1' or 3')=O).

$^{19}\text{F}\{^1\text{H}\}$ NMR (377 MHz, CDCl_3) δ_{F} : -64.2 (CF_3).

(LB ref: JB-732(±), JB-781)

(1*S*,2*S*,3*R*,4*S*)-1-Cyano-2-(trifluoromethyl)-4-vinylcyclopentane-1,3-dicarboxylic acid, dimethyl ester (**368**) and (1*R*,2*S*,3*R*,4*S*)-1-Cyano-2-(trifluoromethyl)-4-vinylcyclopentane-1,3-dicarboxylic acid, dimethyl ester (**368**)*



Following **General Procedure J**, PNP ester **307** (261 mg, 1.0 mmol, 1.0 eq), $\text{Pd}(\text{PPh}_3)_4$ (57.8 mg, 0.05 mmol, 5 mol%), (*R*)-BTM (50.5 mg, 0.2 mmol, 20 mol%), LiCl (0.5 M in THF, 0.6 mL, 0.3 mmol, 30 mol%) and VCP **277** (151 mg, 1.0 mmol, 1.0 eq) in THF : EtOAc 3:2 (5 mL) for 48 h followed by MeOH (1.0 mL) and DMAP (24.4 mg, 0.2 mmol, 20 mol%) for 30 h gave the crude product (49:41:6:4 dr). Purification by silica column chromatography (*n*-hexane : EtOAc 5:1) allowed partial separation of the diastereoisomers to give: **368-A** (*R*_f 0.28) as an inseparable mixture of diastereoisomers (92:8 dr) as a colourless oil (60 mg, 20%). $[\alpha]_{\text{D}}^{20}$ +29.0 (*c* 1.24 in CHCl_3). The er could not be determined.

HRMS (ESI⁺) $\text{C}_{13}\text{H}_{15}\text{F}_3\text{NO}_4$ [*M*+*H*]⁺ found 306.0943, requires 306.0947 (-0.5 ppm).

ν_{\max} (film, cm^{-1}) 3020 (C=CH₂), 2962 (C-H), 2848, 1735 (C=O), 1645 (C=C), 1442, 1398, 1338, 1280, 1238, 1215, 1166, 1124, 1066, 1001, 974, 945.

Data for major diastereoisomer 368-A_{maj}

¹H NMR (500 MHz, CDCl₃) δ_{H} : 2.22 (1H, dd, *J* 13.6, 10.4, C(5)H^AH^B), 2.63 (1H, dd, *J* 13.6, 7.5, C(5)H^AH^B), 3.48 (1H, app. t, *J* 10.8, C(3)H), 3.62 – 3.72 (1H, m, C(4)H), 3.68 (3H, s, C(3')OCH₃), 3.84 (3H, s, C(1')OCH₃), 3.82 – 3.91 (1H, m, C(2)H), 5.08 – 5.19 (2H, m, C(4'')H₂), 5.58 (1H, ddd, *J* 16.9, 10.1, 8.9, C(4')H).

¹³C{¹H} NMR (126 MHz, CDCl₃) δ_{C} : 42.8 (C(5)H₂), 43.8 (C(4)H), 46.9 (C(3)H), 47.1 (C(1)), 52.4 (C(3')OCH₃), 54.1 (C(1')OCH₃), 54.9 (q, ²*J*_{CF} 28.9, C(2)H), 117.4 (CN), 119.0 (C(4'')H₂), 124.4 (q, ¹*J*_{CF} 279, CF₃), 135.0 (C(4')H), 166.6 (C(1')=O), 170.9 (C(3')=O).

¹⁹F{¹H} NMR (377 MHz, CDCl₃) δ_{F} : -67.2 (CF₃).

Data for minor diastereoisomer 368-A_{min} (selected)

¹H NMR (500 MHz, CDCl₃) δ_{H} : 2.50 (1H, dd, *J* 14.0, 9.6, C(5)H^AH^B), 3.05 (1H, app. t, *J* 10.3, C(3)H), 3.07 – 3.16 (1H, m, C(4)H), 3.73 (3H, s, C(3')OCH₃), 5.82 (1H, ddd, *J* 17.0, 10.2, 7.8, C(4')H).

¹³C{¹H} NMR (126 MHz, CDCl₃) δ_{C} : 41.6 (C(5)H₂), 46.8 (C(4)H), 49.6 (C(3)H), 52.7 (C(3')OCH₃), 54.3 (C(1')OCH₃), 55.7 (q, ²*J*_{CF} 29.0, C(2)H), 118.0 (C(4'')H₂), 118.2 (CN), 124.2 (q, ¹*J*_{CF} 280, CF₃), 136.0 (C(4')H), 166.5 (C(1')=O), 171.3 (C(3')=O).

¹⁹F{¹H} NMR (377 MHz, CDCl₃) δ_{F} : -66.8 (CF₃).

368-B (*R_f* 0.22) as an inseparable mixture of diastereoisomers (84:11:5 dr) as a colourless oil (74 mg, 24%). [α]_D²⁰ +30.5 (*c* 1.06 in CHCl₃).

HRMS (ESI⁺) C₁₃H₁₄F₃NO₄Na [M+Na]⁺ found 328.0766, requires 328.0767 (-0.1 ppm).

ν_{\max} (film, cm^{-1}) 3086 (C=CH₂), 2958 (C-H), 2852, 2249 (C≡N), 1743 (C=O), 1643 (C=C), 1438, 1402, 1359, 1224, 1166, 1126, 1082, 972, 929.

Data for major diastereoisomer 368-B_{maj}

Chiral HPLC analysis, Chiralpak AD-H, (*n*-hexane : *i*-PrOH 95:5, flow rate 1.0 mLmin⁻¹, 254 nm, 40 °C) *t_R* (2*S*,3*R*,4*S*): 15.5 min, *t_R* (2*R*,3*S*,4*R*): 25.7 min, 97:3 er. (determined from PNP ester from crude reaction mixture (0.2 mL aliquot, filtered over silica) before addition of MeOH)

$^1\text{H NMR}$ (500 MHz, CDCl_3) δ_{H} : 2.29 – 2.37 (1H, m, C(5) $H^A H^B$), 2.46 – 2.53 (1H, m, C(5) $H^A H^B$), 3.36 – 3.51 (2H, m, C(3) H , C(4) H), 3.70 (3H, s, C(3') OCH_3), 3.90 (3H, s, C(1') OCH_3), 4.05 (1H, app. p, J 8.2, C(2) H), 5.10 – 5.22 (2H, m, C(4'') H_2), 5.57 – 5.66 (1H, m, C(4') H).

$^{13}\text{C}\{^1\text{H}\}$ NMR (126 MHz, CDCl_3) δ_{C} : 43.2 (C(5) H_2), 44.6 (C(4) H), 46.3 (C(3) H), 48.7 (C(1)), 52.4 (C(3') OCH_3), 53.4 (q, $^2J_{\text{CF}}$ 28.9, C(2) H), 54.5 (C(1') OCH_3), 115.9 (CN), 119.2 (C(4'') H_2), 124.6 (q, $^1J_{\text{CF}}$ 279, CF_3), 133.3 (C(4') H), 166.7 (C(1')=O), 171.1 (C(3')=O).

$^{19}\text{F}\{^1\text{H}\}$ NMR (377 MHz, CDCl_3) δ_{F} : -67.5 (CF_3).

Data for minor diastereoisomer 368-B_{min} (selected)

$^1\text{H NMR}$ (500 MHz, CDCl_3) δ_{H} : 2.67 – 2.74 (1H, m, C(5) $H^A H^B$), 2.96 – 3.03 (2H, m, C(3) H , C(4) H), 3.74 (3H, s, C(3') OCH_3), 5.77 (1H, ddd, J 17.8, 10.3, 5.4, C(4') H).

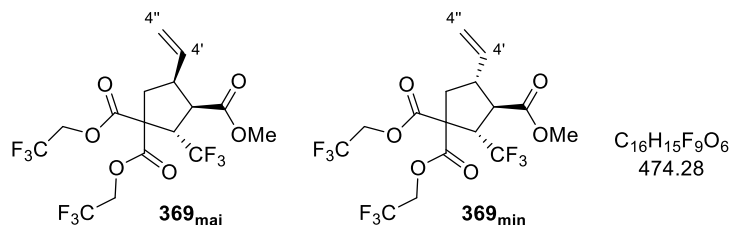
$^{13}\text{C}\{^1\text{H}\}$ NMR (126 MHz, CDCl_3) δ_{C} : 43.5 (C(5) H_2), 46.5 (C(4) H), 50.1 (C(3) H), 52.7 (C(3') OCH_3), 53.5 (q, $^2J_{\text{CF}}$ 28.1, C(2) H), 54.7 (C(1') OCH_3), 116.1 (CN), 118.1 (C(4'') H_2), 124.5 (q, $^1J_{\text{CF}}$ 279, CF_3), 135.8 (C(4') H), 167.5 (C(1')=O), 171.2 (C(3')=O).

$^{19}\text{F}\{^1\text{H}\}$ NMR (377 MHz, CDCl_3) δ_{F} : -67.0 (CF_3).

**The unambiguous assignment of the C(1) centre was not possible with the configuration for the isolated diastereoisomers A and B at C(1) remaining unknown.*

(LB ref: JB-771 (\pm), JB-780, JB-812 (\pm), PNP ester), JB-819)

(2S,3R,4S)-2-(Trifluoromethyl)-4-vinylcyclopentane-1,1,3-tricarboxylic acid, 3-methyl 1,1-bis(2,2,2-trifluoroethyl) ester (369_{maj}) and (2S,3R,4R)-2-(Trifluoromethyl)-4-vinylcyclopentane-1,1,3-tricarboxylic acid, 3-methyl 1,1-bis(2,2,2-trifluoroethyl) ester (369_{min})



Following **General Procedure J**, PNP ester **307** (261 mg, 1.0 mmol, 1.0 eq), $\text{Pd}(\text{PPh}_3)_4$ (57.8 mg, 0.05 mmol, 5 mol%), (*R*)-BTM (50.5 mg, 0.2 mmol, 20 mol%), LiCl (0.5 M in THF, 0.6 mL, 0.3 mmol, 30 mol%) and VCP **264** (320 mg, 1.0 mmol, 1.0 eq) in THF : EtOAc 3:2 (5 mL) for 96 h followed by MeOH (1.0 mL) and DMAP (24.4 mg, 0.2 mmol, 20 mol%) for 24 h gave the crude product (75:19:6 dr). Purification by silica column chromatography

(15% Et₂O in *n*-hexane, R_f 0.27) gave the title compound as an inseparable mixture of diastereomers (80:15:5 dr) as a pale yellow oil (240 mg, 51%). [α]_D²⁰ +39.4 (*c* 1.23 in CHCl₃).

HRMS (ESI⁺): C₁₆H₁₅F₉O₆Na [M+Na]⁺ found 497.0606, requires 497.0617 (-2.2 ppm).

ν_{\max} (film, cm⁻¹): 29800 (C-H), 2960, 1755 (C=O_{ester}), 1643 (C=C), 1440, 1413, 1278, 1220, 1159 (C-F), 1122, 983, 974, 964.

Data for major diastereoisomer 369_{maj}

Chiral GC analysis Restek Rt- β DEXcst (length: 30 m, thickness: 0.25 mm, film thickness: 0.25 μ m, carrier gas: He, linear velocity: 28 cmsec⁻¹, temperature: 110 °C (95 min)) t_R (2R,3S,4R): 85.4 min, t_R (2S,3R,4S): 88.3 min, 3:97 er.

¹H NMR (500 MHz, CDCl₃) δ_{H} : 2.07 (1H, dd, *J* 13.4, 10.6, C(5)H^AH^B), 2.68 (1H, dd, *J* 13.3, 6.7, C(5)H^AH^B), 3.33 (1H, dd, *J* 10.3, 8.2, C(3)H), 3.50 – 3.62 (1H, m, C(4)H), 3.68 (3H, s, OCH₃), 4.27 (1H, app. p, *J* 8.9, C(2)H), 4.37 (1H, dq, *J* 12.5, 8.2, C(1'a)OCH^AH^B), 4.49 (1H, dq, *J* 12.6, 8.2, C(1'b)OCH^AH^B), 4.57 – 4.69 (2H, m, C(1'a)OCH^AH^B, C(1'b)OCH^AH^B), 5.10 (1H, d, *J* 10.2, C(4'')H^AH^B), 5.14 (1H, d, *J* 17.0, C(4'')H^AH^B), 5.57 (1H, ddd, *J* 17.0, 10.2, 8.3, C(4')H).

¹³C{¹H} NMR (126 MHz, CDCl₃) δ_{C} : 41.2 (C(5)H₂), 44.4 (C(4)H), 48.0 (C(3)H), 51.7 (q, ²J_{CF} 28.9, C(2)H), 52.2 (OCH₃), 59.8 (C(1)), 61.6 (q, ²J_{CF} 37.4, C(1'a)OCH₂), 61.6 (q, ²J_{CF} 37.4, C(1'b)OCH₂), 118.3 (C(4'')H₂), 122.3 (q, ¹J_{CF} 278, CH₂CF₃), 122.3 (q, ¹J_{CF} 278, CH₂CF₃), 125.1 (q, ¹J_{CF} 279, C(2')F₃), 134.8 (C(4')H), 167.1 (C(1'b)=O), 167.4 (C(1'a)=O), 171.6 (C(3')=O).

¹⁹F{¹H} NMR (377 MHz, CDCl₃) δ_{F} : -73.9 (CH₂CF₃), -73.7 (CH₂CF₃), -66.8 (C(2')F₃).

Data for minor diastereoisomer 369_{min} (selected)

Chiral GC analysis Restek Rt- β DEXcst (length: 30 m, thickness: 0.25 mm, film thickness: 0.25 μ m, carrier gas: He, linear velocity: 28 cmsec⁻¹, temperature: 110 °C (95 min)) t_R (2R,3S,4S): 79.2 min, t_R (2S,3R,4R): 81.9 min, 2:98 er.

¹H NMR (500 MHz, CDCl₃) δ_{H} : 2.45 (1H, dd, *J* 13.8, 7.2, C(5)H^AH^B), 2.60 – 2.64 (1H, m, C(5)H^AH^B), 2.73 – 2.82 (1H, m, C(4)H), 2.89 (1H, dd, *J* 10.1, 8.6, C(3)H), 3.73 (3H, s, OCH₃), 4.14 (1H, app. p, *J* 9.2, C(2)H), 5.77 (1H, ddd, *J* 17.4, 10.2, 7.5, C(5')H).

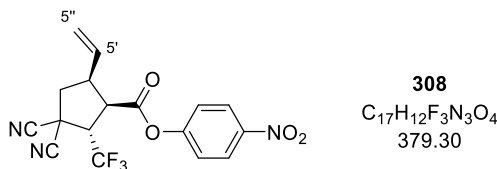
¹³C{¹H} NMR (126 MHz, CDCl₃) δ_{C} : 40.1 (C(5)H₂), 44.9 (C(4)H), 50.2 (C(3)H), 52.5 (OCH₃), 117.5 (C(4'')H₂), 136.3 (C(4')H), 166.0 (C(1')=O), 167.9 (C(1')=O), 171.5 (C(3')=O).

¹⁹F{¹H} NMR (377 MHz, CDCl₃) δ_{F} : -73.8 (CH₂CF₃), -73.7 (CH₂CF₃), -66.9 (C(2')F₃).

(LB ref: JB-740(\pm), JB-785)

5.5.4 Gram scale catalytic reaction

(1*R*,2*S*,5*S*)-3,3-Dicyano-2-(trifluoromethyl)-5-vinylcyclopentane-1-carboxylic acid, 4-nitrophenyl ester (**308**_{maj})

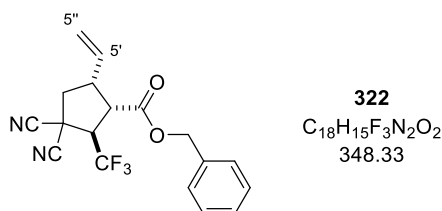


Following **General Procedure J**, PNP ester **307** (1.31 g, 5.0 mmol, 1.0 eq), Pd(PPh₃)₄ (289 mg, 0.25 mmol, 5 mol%), (*R*)-BTM (252 mg, 1.0 mmol, 20 mol%), LiCl (0.5 M in THF, 3.0 mL, 1.5 mmol, 30 mol%) and VCP **276** (591 mg, 5.0 mmol, 1.0 eq) in THF : EtOAc 3:2 (25 mL) for 24 h gave the crude product (95:5 dr). Purification by silica column chromatography (*n*-hexane : EtOAc 4:1, R_f 0.23) gave a pale yellow oil, which was triturated with Et₂O to afford the title compound as an inseparable mixture of diastereomers (95:5 dr) as an off-white solid (1.49 g, 78%).

chiral HPLC analysis Chiralcel OD-H (hexane : *i*-PrOH 97:3, flow rate 1.0 mlmin⁻¹, 254 nm, 40 °C) *major diastereoisomer*: t_R (1*S*,2*R*,5*R*): 30.1 min, t_R (1*R*,2*S*,5*S*): 32.3 min, 7:93 er. *minor diastereoisomer*: t_R (1*S*,2*R*,5*S*): 40.4 min, t_R (1*R*,2*S*,5*R*): 45.2 min, 5:95 er.

5.5.5 Product Derivatisations

rel-(1*S*,2*R*,5*R*)-3,3-Dicyano-2-(trifluoromethyl)-5-vinylcyclopentane-1-carboxylic acid, benzyl ester (**322**)



Following **General Procedure J**, PNP ester **307** (65.3 mg, 0.25 mmol, 1.0 eq), Pd(PPh₃)₄ (14.4 mg, 0.013 mmol, 5 mol%), (±)-TM·HCl (6.0 mg, 0.025 mmol, 10 mol%), *i*-Pr₂NEt (4.3 μL, 0.025 mmol, 10 mol%) and VCP **276** (29.5 mg, 0.25 mmol, 1.0 eq) in acetone (1.3 mL) for 24 h followed by BnOH (0.13, 1.25 mmol, 5.0 eq) and DMAP (6.1 mg, 0.05 mmol, 20 mol%) for 24 h gave the crude product (95:5 dr). Purification by silica column chromatography (petrol : EtOAc 6:1, R_f 0.29) gave the title compound as an inseparable mixture of diastereoisomers (95:5 dr) as a white solid (49 mg, 56%).

m.p. (*n*-hexane) 59 – 61 °C

HRMS (ESI) C₁₈H₁₄F₃N₂O₂ [M-H]⁻ found 347.1010, requires 347.1012 (-0.8 ppm).

v_{max} (film, cm⁻¹) 3035 (=CH₂), 2956 (C-H), 1724 (C=O), 1647 (C=C), 1500 (C=C_{Ar}), 1456, 1402, 1265, 1170 (C-F), 1128, 937.

Data for major diastereoisomer 322_{maj}

¹H NMR (500 MHz, CDCl₃) δ_H: 2.48 (1H, app. t, *J* 12.3, C(4)*H^AH^B*), 2.72 (1H, dd, *J* 13.1, 5.1, C(4)*H^AH^B*), 3.35 – 3.47 (2H, m, C(1)*H*, C(5)*H*), 3.89 (1H, app. p, *J* 7.6, C(2)*H*), 5.09 (1H, d, *J* 10.3, C(5'')*H^AH^B*), 5.13 (1H, d, *J* 12.0, OCH^AH^B), 5.15 – 5.21 (2H, m, C(5'')*H^AH^B*, OCH^AH^B), 5.50 (1H, ddd, *J* 17.2, 10.2, 7.3, C(5')*H*), 7.30 – 7.41 (5H, m, 5 × Ar*H*).

¹³C{¹H} NMR (126 MHz, CDCl₃) δ_C: 34.3 (C(3)), 43.4 (C(4)H₂), 44.4 (C(5)H), 45.8 (C(1)H), 55.1 (q, ²*J*_{CF} 29.6, C(2)H), 68.1 (OCH₂), 112.2 (CN), 113.3 (CN), 120.3 (C(5'')H₂), 123.8 (q, ¹*J*_{CF} 280, CF₃), 128.7 (ArC(3,5)H), 128.8 (ArC(2,6)H), 128.9 (ArC(4)H), 131.8 (C(5')H), 134.4 (ArC(1)), 170.1 (C=O).

¹⁹F{¹H} NMR (377 MHz, CDCl₃) δ_F: -67.5 (CF₃).

Data for minor diastereoisomer 322_{min} (selected)

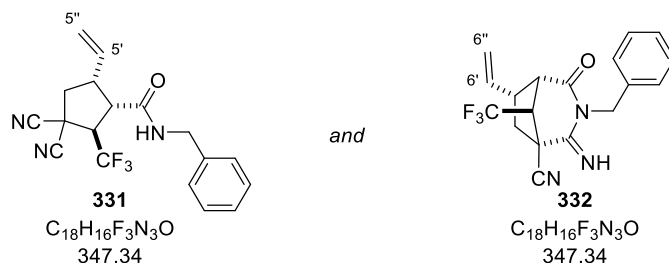
¹H NMR (500 MHz, CDCl₃) δ_H: 2.85 (1H, dd, *J* 13.7, 7.4, C(4)*H^AH^B*), 3.05 (1H, app. t, *J* 9.6, C(1)*H*), 3.08 – 3.15 (1H, m, C(5)*H*), 3.79 (1H, app. p, *J* 8.3, C(2)*H*), 5.76 (1H, ddd, *J* 17.4, 10.3, 7.6, C(5')*H*).

¹³C{¹H} NMR (126 MHz, CDCl₃) δ_C: 44.5 (C(4)H₂), 46.6 (C(5)H), 49.7 (C(1)H), 119.4 (C(5'')H₂), 134.2 (C(5')H).

¹⁹F{¹H} NMR (377 MHz, CDCl₃) δ_F: -67.2 (CF₃).

(LB ref: JB-481B)

rel-(1*S*,2*R*,5*R*)-*N*-Benzyl-3,3-dicyano-2-(trifluoromethyl)-5-vinylcyclopentane-1-carboxamide (**331**) and *rel*-(1*R*,5*S*,6*R*,8*S*)-3-Benzyl-2-imino-4-oxo-8-(trifluoromethyl)-6-vinyl-3-azabicyclo[3.2.1]octane-1-carbonitrile (**332**)



Following **General Procedure J**, PNP ester **307** (65.3 mg, 0.25 mmol, 1.0 eq), Pd(PPh₃)₄ (14.4 mg, 0.013 mmol, 5 mol%), (±)-TM·HCl (6.0 mg, 0.025 mmol, 10 mol%), *i*-Pr₂NEt (4.3 μL, 0.025 mmol, 10 mol%) and VCP **276** (29.5 mg, 0.25 mmol, 1.0 eq) in acetone (1.3 mL) for 24 h followed by BnNH₂ (0.13, 1.25 mmol, 5.0 eq) for 4 h gave the crude product as a mixture of 3 isomers (**331** : **332**_{maj} : **332**_{min} 67:30:3). Purification by silica column chromatography (*n*-hexane : EtOAc 4:1) gave:

331 (*R*_f 0.22) as a single diastereoisomer as a colourless oil (43 mg, 49%).

¹H NMR (500 MHz, CDCl₃) δ_H: 2.51 – 2.61 (1H, m, C(4)*H*^A*H*^B), 2.66 (1H, dd, *J* 12.8, 5.8, C(4)*H*^A*H*^B), 3.03 (1H, dd, *J* 10.3, 7.4, C(1)*H*), 3.24 – 3.35 (1H, m, C(5)*H*), 4.08 (1H, app. p, *J* 7.9, C(2)*H*), 4.37 – 4.50 (2H, m, NCH₂), 5.17 (1H, d, *J* 10.1, C(5'')*H*^A*H*^B), 5.24 (1H, d, *J* 17.1, C(5'')*H*^A*H*^B), 5.59 (1H, ddd, *J* 17.1, 10.1, 8.7, C(5')*H*), 5.80 – 5.96 (1H, m, NH), 7.21 – 7.26 (2H, m, Ar(2,6)*H*), 7.28 – 7.38 (3H, m, Ar(3,4,5)*H*).

¹³C{¹H} NMR (126 MHz, CDCl₃) δ_C: 34.4 (C(3)), 44.1 (C(4)H₂), 44.3 (NCH₂), 45.3 (C(5)H), 47.2 (C(1)H), 55.1 (q, ²*J*_{CF} 29.4, C(2)H), 112.6 (CN), 113.3 (CN), 120.6 (C(5'')H₂), 124.1 (q, ¹*J*_{CF} 279, CF₃), 127.9 (ArC(2,6)H), 128.0 (ArC(4)H), 128.8 (ArC(3,5)H), 132.7 (C(5')H), 136.9 (ArC(1)), 168.3 (C=O).

¹⁹F{¹H} NMR (377 MHz, CDCl₃) δ_F: -67.3 (CF₃).

HRMS (ESI⁺) C₁₈H₁₆F₃N₃ONa [M+Na]⁺ found 370.1126, requires 370.1138 (-3.1 ppm).

*v*_{max} (film, cm⁻¹) 3304 (N-H), 3088, 3024 (C=CH), 2943 (C-H), 1651 (C=O), 1608, 1541 (C=O), 1454, 1400, 1269, 1174 (C-F), 1128, 1029, 933.

332 (*R*_f 0.42) as an inseparable mixture of diastereoisomers (92:8 dr) as a white solid (21 mg, 24%). **m.p.** (CHCl₃) 111 – 114 °C.

HRMS (ESI⁺) C₁₈H₁₇F₃N₃O [M+H]⁺ found 348.1308, requires 348.1318 (-2.8 ppm).

ν_{\max} (film, cm^{-1}) 3302 (N-H), 3068 (C=CH), 2985 (C-H), 2850, 2256 (C \equiv N), 1695 (C=N), 1622 (C=O), 1581, 1494 (C=C_{Ar}), 1438, 1386, 1280, 1261, 1170, 1126, 1080, 935, 925, 900.

Data for major diastereoisomer **332**_{maj}

¹H NMR (500 MHz, CDCl₃) δ_{H} : 2.09 (1H, dd, *J* 14.4, 6.4, C(7)H^AH^B), 2.88 (1H, dd, *J* 14.4, 10.9, C(7)H^AH^B), 3.17 (1H, q, *J* 9.0, C(8)H), 3.32 – 3.41 (1H, m, C(6)H), 3.42 – 3.47 (1H, m, C(5)H), 5.04 – 5.16 (4H, m, NCH₂, C(6'')H₂), 5.41 (1H, ddd, *J* 17.4, 10.3, 7.5, C(6')H), 7.26 – 7.32 (3H, m, Ar(3,4,5)H), 7.37 – 7.44 (2H, m, Ar(2,6)H), 8.71 (1H, s, NH).

¹³C{¹H} NMR (126 MHz, CDCl₃) δ_{C} : 39.1 (C(7)), 42.7 (C(6)H), 44.5 (NCH₂), 48.0 (C(1)), 49.2 (q, ²*J*_{CF} 29.9, C(8)H), 50.3 (C(5)H), 115.1 (CN), 119.2 (C(6'')H₂), 123.9 (q, ¹*J*_{CF} 280, CF₃), 127.8 (ArC(4)H), 128.4 (ArC(3,5)H), 129.1 (ArC(2,6)H), 133.5 (C(6')H), 136.5 (ArC(1)), 159.2 (C=N), 168.2 (C=O).

¹⁹F{¹H} NMR (377 MHz, CDCl₃) δ_{F} : -65.9 (CF₃).

Data for minor diastereoisomer **332**_{min} (selected)

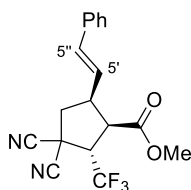
¹H NMR (500 MHz, CDCl₃) δ_{H} : 2.26 (1H, dd, *J* 14.4, 6.4, C(7)H^AH^B), 2.96 – 3.04 (1H, m, C(7)H^AH^B), 3.26 (1H, q, *J* 9.2, C(8)H), 3.54 – 3.59 (1H, m, C(5)H), 4.83 (1H, d, *J* 15.8, NCH^AH^B), 4.95 (1H, d, *J* 15.8, NCH^AH^B), 5.04 – 5.16 (2H, m, C(6'')H₂), 5.64 (1H, ddd, *J* 17.2, 10.3, 6.8, C(6')H), 7.90 (1H, s, NH).

¹³C{¹H} NMR (126 MHz, CDCl₃) δ_{C} : 42.4, 44.1 (NCH₂), 126.9, 128.5, 129.3.

¹⁹F{¹H} NMR (377 MHz, CDCl₃) δ_{F} : -65.6 (CF₃).

(LB ref: JB-605, JB-821)

(1R,2S,5S)-3,3-Dicyano-5-((E)-styryl)-2-(trifluoromethyl)cyclopentane-1-carboxylic acid, methyl ester (372)



372
C₁₈H₁₅F₃N₂O₂
348.33

Following the procedure reported by Yao and co-workers,¹⁹⁰ a pressure tube was charged with methyl ester **333** (136 mg, 0.5 mmol, 1.0 eq), Pd(OAc)₂ (5.6 mg, 0.025 mmol, 5 mol%) and K₂CO₃ (104 mg, 0.75 mmol, 1.5 eq) and evacuated and flushed with N₂ three times. Acetone (5.0 mL, purged with Ar for 30 min) and iodobenzene (0.08 mL, 0.75 mmol, 1.5 eq) were added, the tube was sealed and the reaction mixture was stirred at 100 °C for 220 |

24 h. The reaction was allowed to cool to room temperature, diluted with EtOAc and filtered over Celite with EtOAc. The combined filtrates were concentrated under reduced pressure and the crude product was purified by silica column chromatography (15 to 20% Et₂O in *n*-hexane, R_f 0.22 in 20% Et₂O in *n*-hexane) to give the title compound as a single diastereoisomer (>99:1 dr) as a yellow oil (81 mg, 46%). $[\alpha]_D^{20} +54.1$ (*c* 1.08 in CHCl₃).

chiral HPLC analysis Chiralpak AD-H (hexane : *i*-PrOH 93:7, flow rate 1.0 mlmin⁻¹, 254 nm, 40 °C) t_R (1*R*,2*S*,5*S*): 10.4 min, t_R (1*S*,2*R*,5*R*): 22.7 min, 93:7 er.

¹H NMR (500 MHz, CDCl₃) δ_H: 2.58 (1H, app. t, *J* 12.7, C(4)*H*^A*H*^B), 2.82 (1H, dd, *J* 13.0, 6.0, C(4)*H*^A*H*^B), 3.48 (1H, dd, *J* 10.7, 8.1, C(1)*H*), 3.56 – 3.65 (1H, m, C(5)*H*), 3.69 (3H, s, OCH₃), 3.95 (1H, app. p, *J* 7.5, C(2)*H*), 5.91 (1H, dd, *J* 15.8, 8.4, C(5')*H*), 6.57 (1H, d, *J* 15.8, C(5'')*H*), 7.27 – 7.38 (5H, m, 5 × Ar*H*).

¹³C{¹H} NMR (126 MHz, CDCl₃) δ_C: 34.4 (C(3)), 43.7 (C(5)*H*), 43.9 (C(4)*H*₂), 46.2 (C(1)*H*), 53.0 (OCH₃), 55.0 (q, ²*J*_{CF} 29.6, C(2)*H*), 112.3 (CN), 113.3 (CN), 122.6 (C(5')*H*), 123.9 (q, ¹*J*_{CF} 279, CF₃), 126.4 (ArC(2,6)*H*), 128.5 (ArC(4)*H*), 128.8 (ArC(3,5)*H*), 135.2 (C(5'')*H*), 135.5 (ArC(1)), 170.7 (C=O).

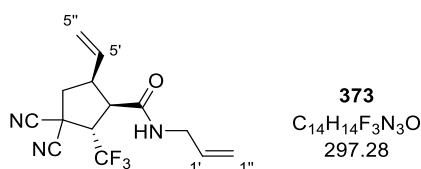
¹⁹F{¹H} NMR (377 MHz, CDCl₃) δ_F: -67.4 (CF₃).

HRMS (ESI⁺) C₁₈H₁₆F₃N₂O₂ [M+H]⁺ found 349.1149, requires 349.1158 (-2.6 ppm).

ν_{\max} (film, cm⁻¹) 3026 (=CH), 2954 (C-H), 1735 (C=O), 1494 (C=C_{Ar}), 1438, 1398, 1271, 1217, 1172, 1134, 968.

(LB ref: JB-795 (±), JB-809)

(1*R*,2*S*,5*S*)-*N*-Allyl-3,3-dicyano-2-(trifluoromethyl)-5-vinylcyclopentane-1-carboxamide (373)



To a solution of PNP ester **308** (379 mg, 1.0 mmol, 1.0 eq) in EtOAc (5.0 mL) was added allyl amine (0.15 mL, 2.0 mmol, 2.0 eq) and the reaction mixture was stirred at room temperature until TLC indicated full conversion (ca. 5 h). The mixture was diluted with EtOAc (10 mL) and washed with 1 M NaOH (2 × 10 mL) and brine (10 mL). The organic phase was dried over MgSO₄, filtered and concentrated under reduced pressure. The

crude product was purified by silica column chromatography (*n*-hexane : EtOAc 3:1, R_f 0.24) to give the title compound as a single diastereoisomer (>99:1 dr) as a white solid (233 mg, 78%). **m.p.** (EtOAc) 127 – 130 °C. $[\alpha]_D^{20} +21.8$ (*c* 1.12 in CHCl₃).

chiral HPLC analysis Chiralpak IA, (*n*-hexane : *i*-PrOH 97:3, flow rate 1.0 mLmin⁻¹, 211 nm, 40 °C) t_R (1*R*,2*S*,5*S*): 13.8 min, t_R (1*S*,2*R*,5*R*): 23.3 min, 92:8 er.

¹H NMR (500 MHz, CDCl₃) δ_H: 2.55 (1H, app. t, *J* 12.8, C(4)*H*^A*H*^B), 2.66 (1H, dd, *J* 12.8, 5.9, C(4)*H*^A*H*^B), 3.06 (1H, dd, *J* 10.3, 7.4, C(1)*H*), 3.25 – 3.36 (1H, m, C(5)*H*), 3.81 – 3.95 (2H, m, NCH₂), 4.03 (1H, app. p, *J* 7.9, C(2)*H*), 5.14 – 5.22 (2H, m, C(1'')*H*₂), 5.22 – 5.32 (2H, m, C(5'')*H*₂), 5.62 (1H, ddd, *J* 17.0, 10.1, 8.7, C(5')*H*), 5.78 (1H, ddt, *J* 17.2, 10.2, 5.7, C(1')*H*), 5.83 (1H, br t, *J* 5.8, NH).

¹³C{¹H} NMR (126 MHz, CDCl₃) δ_C: 34.4 (C(3)), 42.4 (NCH₂), 44.1 (C(4)*H*₂), 45.3 (C(5)*H*), 47.1 (C(1)*H*), 55.1 (q, ²*J*_{CF} 29.3, C(2)*H*), 112.6 (CN), 113.3 (CN), 117.3 (C(1'')*H*₂), 120.6 (C(5'')*H*₂), 124.1 (q, ¹*J*_{CF} 279, CF₃), 132.6 (C(5')*H*), 133.0 (C(1')*H*), 168.4 (C=O).

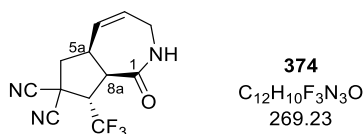
¹⁹F{¹H} NMR (377 MHz, CDCl₃) δ_F: -67.3 (CF₃).

HRMS (ESI⁺) C₁₄H₁₅F₃N₃O [M+H]⁺ found 298.1157, requires 298.1161 (-1.5 ppm).

ν_{max} (film, cm⁻¹) 3288 (N-H), 3115, 2945 (C-H), 2850, 1681(C=C), 1653 (C=C), 1639 (C=O), 1575 (C=O), 1433, 1371, 1271, 1170, 1134, 1031, 993, 941, 923.

(LB ref: JB-787 (±), JB-805)

(5*aS*,8*S*,8*aR*)-1-Oxo-8-(trifluoromethyl)-2,3,5*a*,6,8,8*a*-hexahydrocyclopent[c]azepine-7,7(2*H*)-dicarbonitrile (374)



Amide **373** (148 mg, 0.5 mmol, 1.0 eq) and *p*-TsOH·H₂O (129 mg, 0.75 mmol, 1.5 eq) were placed in a flame-dried round bottom flask under a N₂ atmosphere. Toluene (50 mL, degassed with Ar for 30 min) was added, followed by HG-II catalyst (16 mg, 0.025 mmol, 5 mol%) and the reaction mixture was heated to 80 °C. After 24 h, additional 5 mol% HG-II catalyst were added and stirring at 80 °C continued for another 24 h. The reaction mixture was allowed to cool to room temperature and the solvent was removed under reduced pressure. The crude residue was dissolved in CH₂Cl₂ (50 mL) and washed with 1 M NaOH (50 mL). The aqueous phase was extracted with CH₂Cl₂ (3 × 15 mL), the

combined organic phases were dried over MgSO_4 , filtered and the solvent was removed under reduced pressure. The crude product was purified by silica column chromatography (10 to 20% Et_2O in CH_2Cl_2 , R_f 0.33 in 20% Et_2O in CH_2Cl_2) to afford the title compound as a single diastereoisomer (>99:1 dr) as a white solid (28 mg, 20%).

m.p. (CHCl_3) 123 – 125 °C. $[\alpha]_D^{20} +7.7$ (c 1.30 in CHCl_3).

chiral HPLC analysis Chiralpak AD-H (hexane : *i*-PrOH 92:8, flow rate 1.0 mlmin^{-1} , 211 nm, 40 °C) t_R (5aS,8S,8aR): 14.3 min, t_R (5aR,8R,8aS): 23.2 min, 94:6 er.

$^1\text{H NMR}$ (500 MHz, CDCl_3) δ_H : 2.18 (1H, dd, J 14.4, 12.7, C(6) $H^A H^B$), 2.76 (1H, dd, J 12.7, 4.8, C(6) $H^A H^B$), 3.22 – 3.33 (1H, m, C(5a) H), 3.43 (1H, app. dt, J 16.6, 7.6, C(3) $H^A H^B$), 3.69 (1H, dd, J 9.0, 3.7, C(8a) H), 3.99 – 4.10 (1H, m, C(3) $H^A H^B$), 4.74 (1H, qd, J 9.4, 3.7, C(8) H), 5.71 (1H, dt, J 10.9, 2.7, C(5) H), 6.08 – 6.18 (1H, m, C(4) H), 7.03 – 7.16 (1H, m, NH).

$^{13}\text{C}\{^1\text{H}\}$ NMR (126 MHz, CDCl_3) δ_C : 32.8 (C(7)), 37.5 (C(3) H_2), 40.8 (C(5a) H), 44.1 (C(8a) H), 44.2 (C(6) H_2), 53.1 (q, $^2J_{CF}$ 29.4, C(8) H), 113.1 (CN), 114.0 (CN), 124.6 (q, $^1J_{CF}$ 279, CF_3), 129.0 (C(5) H), 129.6 (C(4) H), 169.4 (C=O).

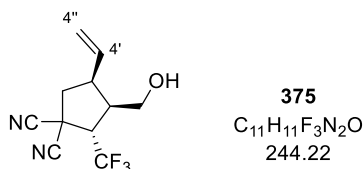
$^{19}\text{F}\{^1\text{H}\}$ NMR (377 MHz, CDCl_3) δ_F : -67.2 (CF_3).

HRMS (ESI $^+$) $\text{C}_{12}\text{H}_{10}\text{F}_3\text{N}_3\text{ONa}$ $[\text{M}+\text{Na}]^+$ found 292.0660, requires 292.0668 (-2.8 ppm).

ν_{max} (film, cm^{-1}) 3261 (N-H), 3088, 2960 (C-H), 2256 ($\text{C}\equiv\text{N}$), 1672 (C=O), 1475, 1381, 1305, 1274, 1201, 1159, 1132, 1103, 900.

(LB ref: JB-794 (\pm), JB-808)

(2S,3R,4S)-3-(Hydroxymethyl)-2-(trifluoromethyl)-4-vinylcyclopentane-1,1-dicarbonitrile (375)



To a solution of PNP ester **308** (379 mg, 1.0 mmol, 1.0 eq) in MeOH (4.7 mL) and DME (0.3 mL) was added NaBH_4 (76 mg, 2.0 mmol, 2.0 eq) in portions at 0 °C. After complete addition, the reaction mixture was allowed to warm to room temperature and the reaction progress monitored by TLC. After full consumption of starting material (ca. 1h), the reaction was quenched by the addition of sat. aq. NH_4Cl (20 mL). The aqueous phase was extracted with EtOAc (3 \times 20 mL) and the combined organic phases were washed with

1 M NaOH (2 × 20 mL) and brine (20 mL). The organic phase was dried over MgSO₄, filtered and the solvent was removed under reduced pressure. The crude product was purified by silica column chromatography (*n*-hexane : EtOAc 4:1, R_f 0.21) to give the title compound as a single diastereoisomer (>99:1 dr) as a pale yellow oil (90 mg, 36%).

$[\alpha]_D^{20} +2.8$ (*c* 1.29 in CHCl₃).

Chiral GC analysis Restek Rt-βDEXcst (length: 30 m, thickness: 0.25 mm, film thickness: 0.25 μm, carrier gas: He, linear velocity: 28 cmsec⁻¹, temperature: 60 to 190 °C (43 min), 190 °C (15 min)) t_R (2*S*,3*R*,4*S*): 51.1 min, t_R (2*R*,3*S*,4*R*): 51.6 min, 93:7 er.

¹H NMR (500 MHz, CDCl₃) δ_H: 1.71 (1H, br s, OH), 2.51 (1H, app. t, *J* 12.7, C(5)*H*^A*H*^B), 2.55 – 2.62 (1H, m, C(3)*H*), 2.64 (1H, dd, *J* 12.6, 6.1, C(5)*H*^A*H*^B), 3.16 – 3.27 (1H, m, C(4)*H*), 3.62 (1H, app. p, *J* 8.2, C(2)*H*), 3.67 (1H, dd, *J* 10.9, 3.3, OCH^A*H*^B), 3.87 (1H, d, *J* 10.9, OCH^A*H*^B), 5.22 – 5.31 (2H, m, C(4'')*H*₂), 5.94 (1H, ddd, *J* 17.0, 10.3, 8.1, C(4')*H*).

¹³C{¹H} NMR (126 MHz, CDCl₃) δ_C: 34.2 (C(1)), 41.8 (C(3)*H*), 44.5 (C(5)*H*₂), 44.6 (C(4)*H*), 53.1 (q, ²*J*_{CF} 28.5, C(2)*H*), 60.2 (OCH₂), 113.0 (CN), 114.3 (CN), 119.7 (C(4'')*H*₂), 124.8 (q, ¹*J*_{CF} 279, CF₃), 133.9 (C(4')*H*).

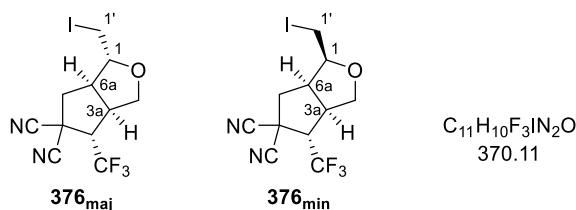
¹⁹F{¹H} NMR (377 MHz, CDCl₃) δ_F: -67.0 (CF₃).

HRMS (ESI⁺) C₁₁H₁₂F₃N₂O [M+H]⁺ found 245.0896, requires 245.0896 (±0.0 ppm).

*v*_{max} (film, cm⁻¹) 3549 (O-H), 3086 (=CH₂), 2953 (C-H), 2893, 2258 (C≡N), 1643 (C=C), 1384, 1267, 1165, 1126, 999, 929.

(LB ref: JB-788, JB-793, JB-797(±), JB-799, JB-806, JB-807, JB-810, JB-815, JB-816, JB-817, JB-818)

(1*R*,3*aR*,4*S*,6*aR*)-1-(Iodomethyl)-4-(trifluoromethyl)tetrahydro-1*H*-cyclopenta[*c*]furan-5,5(3*H*)-dicyanonitrile (376_{maj}) and (1*S*,3*aR*,4*S*,6*aR*)-1-(Iodomethyl)-4-(trifluoromethyl)tetrahydro-1*H*-cyclopenta[*c*]furan-5,5(3*H*)-dicyanonitrile (376_{min})



Following the procedure reported by Jørgensen and co-workers¹¹⁹, alcohol **375** (76 mg, 0.3 mmol, 1.0 eq) was dissolved in THF : sat. aq. NaHCO₃ 3:1 (2.4 mL) and cooled to 0 °C. Iodine (237 mg, 0.93 mmol, 3.0 eq) was added in portions over 5 h and the reaction mixture

stirred for another 16 h at 0 °C. The reaction was quenched by the addition of brine (20 mL) and the aqueous phase was extracted with EtOAc (3 × 20 mL). The combined organic phases were washed with sat. aq. Na₂S₂O₃ (20 mL), H₂O (20 mL) and brine (20 mL), dried over MgSO₄, filtered and the solvent was removed under reduced pressure. The crude product was purified by silica column chromatography (*n*-hexane : EtOAc 5:1 to 4:1) to give:

376_{maj} (R_f 0.34 in *n*-hexane : EtOAc 4:1) as an off-white solid (66 mg, 58%). **m.p.** (EtOAc) 54 – 57 °C. $[\alpha]_D^{20}$ –10.0 (*c* 1.02 in CHCl₃). The enantiomeric ratio could not be determined.

¹H NMR (500 MHz, CDCl₃) δ_H: 2.29 (1H, dd, *J* 13.3, 9.3, C(6)*H^AH^B*), 2.99 (1H, dq, *J* 9.8, 7.1, C(4)*H*), 3.03 – 3.29 (5H, m, C(1')*H*₂, C(3a)*H*, C(6)*H^AH^B*, C(6a)*H*), 3.90 (1H, dd, *J* 10.3, 2.5, C(3)*H^AH^B*), 4.07 (1H, dd, *J* 10.3, 6.5, C(3)*H^AH^B*), 4.11 (1H, td, *J* 5.6, 2.7, C(1)*H*).

¹³C{¹H} NMR (126 MHz, CDCl₃) δ_C: 5.4 (C(1')*H*₂), 36.8 (C(5)), 44.2 (C(3a)*H*), 44.5 (C(6)*H*₂), 47.5 (C(6a)*H*), 56.8 (q, ²*J*_{CF} 28.6, C(4)*H*), 70.5 (C(3)*H*₂), 84.9 (C(1)*H*), 112.0 (CN), 112.9 (CN), 123.9 (q, ¹*J*_{CF} 280, CF₃).

¹⁹F{¹H} NMR (377 MHz, CDCl₃) δ_F: –66.9 (CF₃).

HRMS (ESI[–]) C₁₁H₁₀F₃IN₂OCl [M+Cl][–] found 404.9458, requires 404.9484 (–2.6 ppm).

ν_{max} (CHCl₃, cm^{–1}) 3020 (CH₂-I), 2956 (C-H), 2887, 2258 (C≡N), 1392, 1271, 1176, 1132, 1070, 916.

376_{min} (R_f 0.39 in *n*-hexane : EtOAc 4:1) as a white solid (24 mg, 21%). **m.p.** (EtOAc) 121 – 124 °C. $[\alpha]_D^{20}$ –70.1 (*c* 1.15 in CHCl₃). The enantiomeric ratio could not be determined.

¹H NMR (500 MHz, CDCl₃) δ_H: 2.18 (1H, dd, *J* 12.9, 11.1, C(6)*H^AH^B*), 2.81 – 2.92 (2H, m, C(4)*H*, C(6)*H^AH^B*), 3.01 (1H, dd, *J* 10.4, 9.3, C(1')*H^AH^B*), 3.19 (1H, td, *J* 9.7, 6.5, C(3a)*H*), 3.30 – 3.39 (2H, m, C(1')*H^AH^B*, C(6a)*H*), 3.79 (1H, dd, *J* 10.2, 6.5, C(3)*H^AH^B*), 3.94 – 4.02 (2H, m, C(1)*H*, C(3)*H^AH^B*).

¹³C{¹H} NMR (126 MHz, CDCl₃) δ_C: –2.1 (C(1')*H*₂), 35.7 (C(5)), 38.5 (C(6)*H*₂), 43.7 (C(3a)*H*), 45.1 (C(6a)*H*), 58.0 (q, ²*J*_{CF} 28.5, C(4)*H*), 72.2 (C(3)*H*₂), 81.3 (C(1)*H*), 111.9 (CN), 112.7 (CN), 124.0 (q, ¹*J*_{CF} 278, CF₃).

¹⁹F{¹H} NMR (377 MHz, CDCl₃) δ_F: –67.2 (CF₃).

HRMS (ESI[–]) C₁₁H₁₀F₃IN₂OCl [M+Cl][–] found 404.9475, requires 404.9484 (–0.9 ppm).

ν_{max} (film, cm^{–1}) 2958 (C-H), 2875, 2854, 2260 (C≡N), 1390, 1271, 1259, 1168, 1136, 1026, 950. (LB ref: JB-802(±), JB-820)

5.6 NOE Experiment

Experiments were performed on a 400 MHz spectrometer. For each experiment, a ^1H NMR spectrum was measured and a NOE was obtained on the same NMR spectrometer with a selective pulse at the required chemical shift measured to 4 decimal places in MestreNova 9.1 without referencing to solvent.

Determination of alkene configuration for **175**:

Amide **175** (approx. 10 mg) was dissolved in CDCl_3 (approx. 0.6 mL) and a ^1H NMR spectrum was obtained. The chemical shift of the alkene CH_3 signal (C(4) H_3 , δ_{H} 1.8570 ppm, uncorrected) was determined and subsequently irradiated on the same NMR spectrometer (Figure S18). The resulting spectrum showed significant radiation transfer to protons with chemical shifts of 4.13 ppm (s, C(5) H) and 7.20–7.31 ppm (m, C(3) H). Then, the chemical shift of the C(5) H signal (C(5) H , δ_{H} 4.1359 ppm, uncorrected) was determined and irradiated on the same NMR spectrometer (Figure S19). The resulting spectrum showed significant radiation transfer to protons with chemical shifts of 1.86 (d, J 7.2 Hz, C(4) H_3) and 3.64 (d, J 13.2 Hz, C(5') H_2).

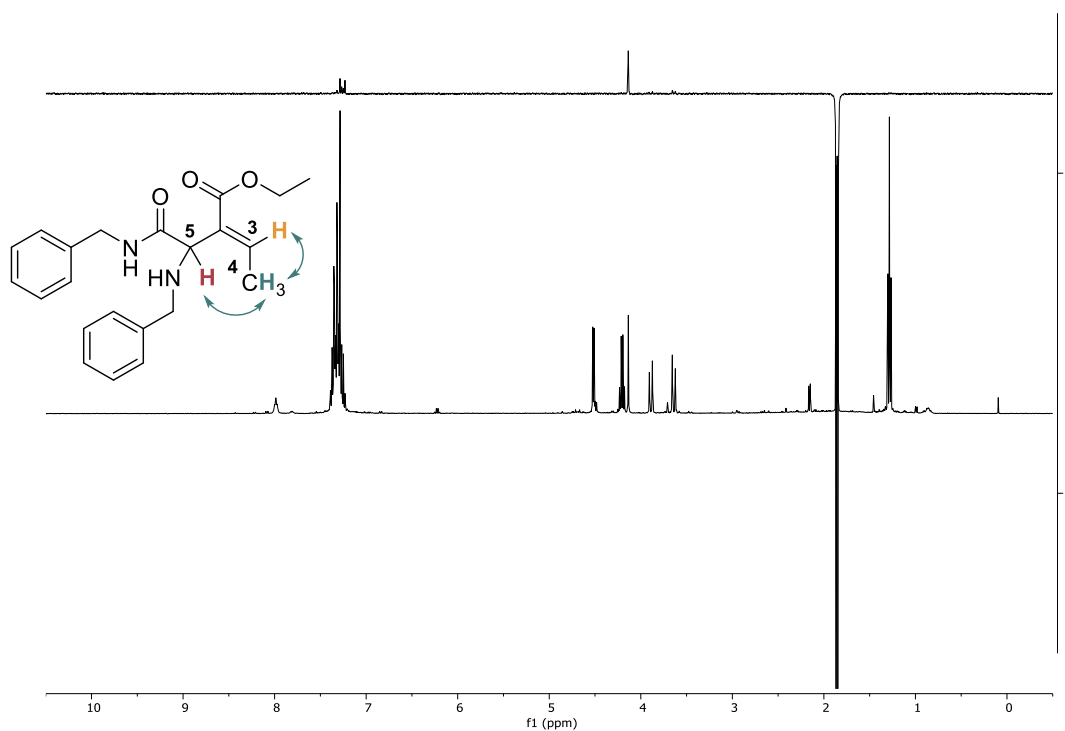


Figure S18 NOE spectra for **175**. ^1H NMR, CDCl_3 , 400 MHz, irradiation at δ_{H} 1.8570 ppm.

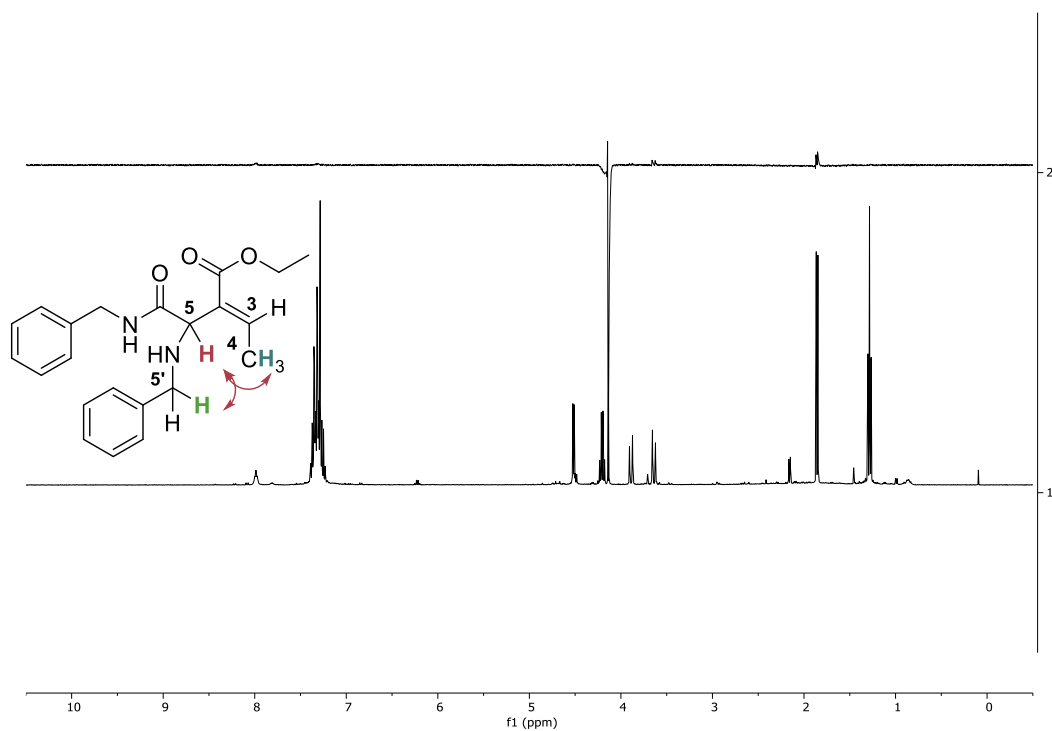


Figure S19: NOE spectra for **175**. ^1H NMR, CDCl_3 , 400 MHz, irradiation at δ_{H} 4.1359 ppm.

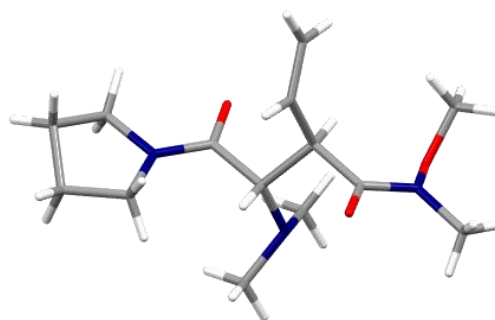
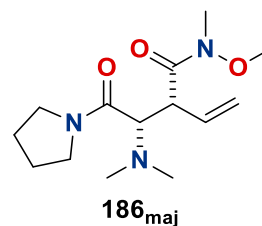
5.7 Single crystal X-ray diffraction analysis

Data were collected using CrystalClear¹ and processed (including correction for Lorentz, polarization and absorption) using CrysAlisPro.² Structures were solved by dual-space (SHELXT¹⁹¹), direct (SIR2011¹⁹²) or charge-flipping (Superflip¹⁹³) methods and refined by full-matrix least-squares against F^2 (SHELXL-2018/3¹⁹⁴). Non-hydrogen atoms were refined anisotropically, and all hydrogen atoms were refined using a riding model. All calculations were performed using the CrystalStructure³ interface.

Data for **186_{maj}**

X-ray diffraction data were collected at 125 K on a Rigaku XtaLAB P200 diffractometer using multi-layer mirror monochromated Cu-K α radiation ($\lambda = 1.54187 \text{ \AA}$).

186_{maj}	
CCDC	2000698
empirical formula	C ₁₄ H ₂₅ N ₃ O ₃
fw	283.37
crystal description	colourless, plate
crystal size [mm]	0.100 × 0.050 × 0.020
space group	C2/c (#15)
<i>a</i> [Å]	20.9650(8)
<i>b</i> [Å]	6.25949(18)
<i>c</i> [Å]	23.5608(11)
vol [Å] ³	3022.0(2)
β [°]	102.201(4)
<i>Z</i>	8
ρ (calc) [g/cm ³]	1.246
μ [mm ⁻¹]	0.718
F(000)	1232.00
reflections collected	16059
independent reflections (R_{int})	3076 (0.0711)
data/parameters	3076/181
GOF on F^2	1.035
R_1 [$I > 2\sigma(I)$]	0.0951
wR_2 (all data)	0.2765
largest diff. peak/hole [e/Å ³]	0.84, -0.50



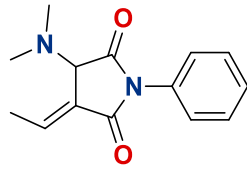
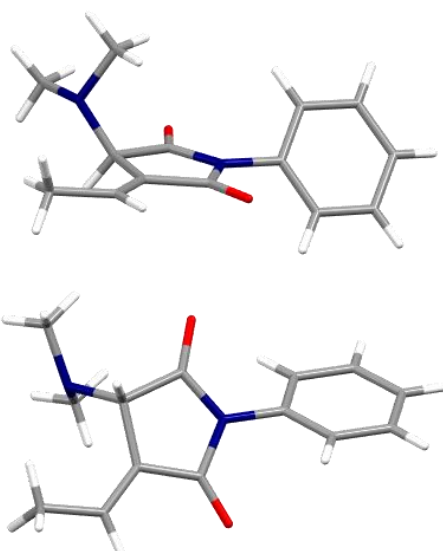
¹ CrystalClear-SM Expert v2.1. Rigaku Americas, The Woodlands, Texas, USA, and Rigaku Corporation, Tokyo, Japan, 2015

² CrysAlisPro v1.171.38.46. Rigaku Oxford Diffraction, Rigaku Corporation, Oxford, U.K. 2015

³ CrystalStructure v4.3.0. Rigaku Americas, The Woodlands, Texas, USA, and Rigaku Corporation, Tokyo, Japan, 2018.

Data for (*E*)-218 (JB-512)

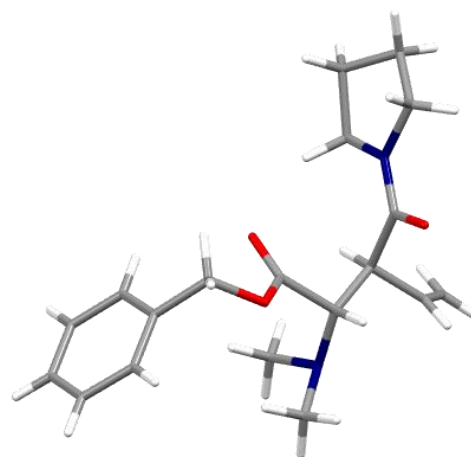
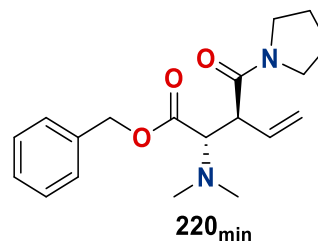
X-ray diffraction data were collected at 125 K on a Rigaku XtaLAB P200 diffractometer using multi-layer mirror monochromated Cu-K α radiation ($\lambda = 1.54187 \text{ \AA}$).

		(<i>E</i>)-218	
CCDC		2000699	 <p style="text-align: center;">(<i>E</i>)-218</p> 
empirical formula		C ₁₄ H ₁₆ N ₂ O ₂	
fw		244.29	
crystal description		colourless, prism	
crystal size [mm]		0.200 × 0.100 × 0.050	
space group		P-1(#2)	
<i>a</i> [Å]		8.1528(2)	
<i>b</i> [Å]		9.51231(16)	
<i>c</i> [Å]		16.9230(4)	
vol [Å] ³		1256.30(5)	
α [°]		101.2680(17)	
β [°]		92.223(2)	
γ [°]		101.6720(18)	
<i>Z</i>		4	
ρ (calc) [g/cm ³]		1.291	
μ [mm ⁻¹]		0.709	
F(000)		520.00	
reflections collected		13192	
independent reflections (<i>R</i> _{int})		4892 (0.0154)	
data/parameters		4892/332	
GOF on <i>F</i> ²		1.064	
<i>R</i> ₁ [<i>I</i> > 2 σ (<i>I</i>)]		0.0415	
<i>wR</i> ₂ (all data)		0.1093	
largest diff. peak/hole [e/Å ³]		0.25, -0.27	

Data for **220_{min}** (**JB-210**)

X-ray diffraction data were collected at 125 K on a Rigaku XtaLAB P200 diffractometer using multi-layer mirror monochromated Cu-K α radiation ($\lambda = 1.54187 \text{ \AA}$).

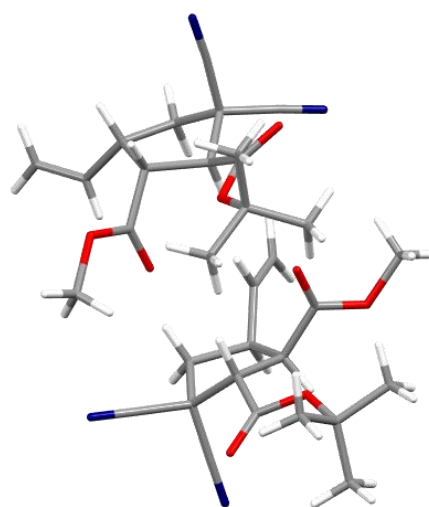
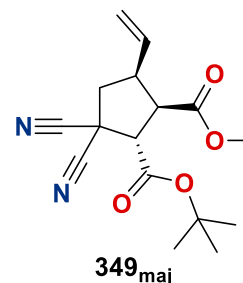
	220_{min} (2S,3S)
CCDC	2000700
empirical formula	C ₁₉ H ₂₆ N ₂ O ₃
fw	330.42
crystal description	colourless, prism
crystal size [mm]	0.110 × 0.090 × 0.080
space group	P1(#1)
<i>a</i> [Å]	5.95743(14)
<i>b</i> [Å]	7.72174(8)
<i>c</i> [Å]	10.83510(9)
vol [Å] ³	445.939(13)
α [°]	101.1780(7)
β [°]	97.4202(15)
γ [°]	110.9130(17)
<i>Z</i>	1
ρ (calc) [g/cm ³]	1.230
μ [mm ⁻¹]	0.670
F(000)	178.00
reflections collected	11042
independent reflections (<i>R</i> _{int})	3250 (0.0232)
data/parameters	3250/237
GOF on <i>F</i> ²	1.071
<i>R</i> ₁ [<i>I</i> > 2 σ (<i>I</i>)]	0.0315
<i>wR</i> ₂ (all data)	0.0855
largest diff. peak/hole [e/Å ³]	0.15, -0.15
Flack parameter	0.08(9)



Data for **349_{maj}** (**JB-766**)

X-ray diffraction data were collected at 173 K on a Rigaku XtaLAB P100 diffractometer using multi-layer mirror monochromated Cu-K α radiation ($\lambda = 1.54187 \text{ \AA}$).

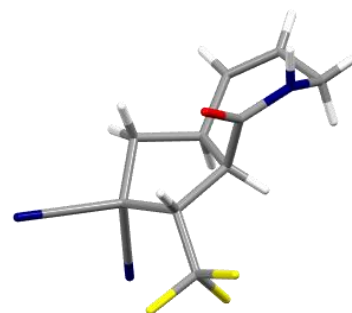
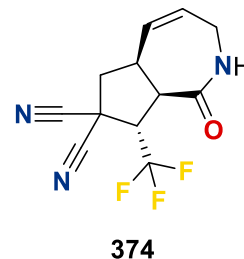
349_{maj} (1 <i>R</i> ,2 <i>S</i> ,5 <i>S</i>)	
empirical formula	C ₁₆ H ₂₀ N ₂ O ₄
fw	304.34
crystal description	colourless, prism
crystal size [mm]	0.200 × 0.100 × 0.100
space group	P2 ₁ (#4)
<i>a</i> [Å]	9.560(3)
<i>b</i> [Å]	15.563(4)
<i>c</i> [Å]	11.591(4)
vol [Å ³]	1724.5(9)
β [°]	90.427(6)
<i>Z</i>	4
ρ (calc) [g/cm ³]	1.172
μ [mm ⁻¹]	0.700
F(000)	648.00
reflections collected	18151
independent reflections (<i>R</i> _{int})	5516 (0.0520)
data/parameters	5516/406
GOF on <i>F</i> ²	1.052
<i>R</i> ₁ [<i>I</i> > 2 σ (<i>I</i>)]	0.0556
<i>wR</i> ₂ (all data)	0.1343
largest diff. peak/hole [e/Å ³]	0.62, -0.63
Flack parameter	0.04(6)



Data for **374 (JB-808)**

X-ray diffraction data were collected at 173 K on a Rigaku XtaLAB P200 diffractometer using multi-layer mirror monochromated Mo-K α radiation ($\lambda = 0.71075 \text{ \AA}$).

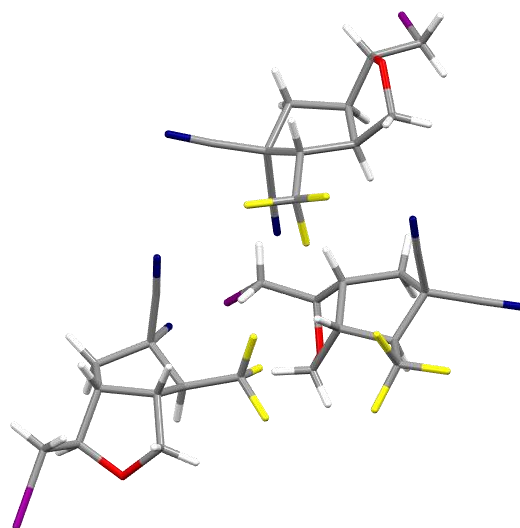
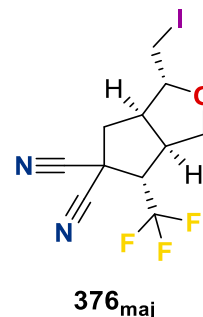
374 (5aS,8S,8aR)	
empirical formula	C ₁₂ H ₁₀ F ₃ N ₃ O
fw	269.23
crystal description	colourless, platelet
crystal size [mm]	0.100 × 0.100 × 0.010
space group	P4 ₃ 2 ₁ 2 (#96)
<i>a</i> [Å]	7.5386(8)
<i>c</i> [Å]	42.598(5)
vol [Å] ³	2420.9(5)
<i>Z</i>	8
ρ (calc) [g/cm ³]	1.477
μ [mm ⁻¹]	0.288
F(000)	1104.00
reflections collected	18286
independent reflections (<i>R</i> _{int})	2212 (0.0418)
data/parameters	2212/176
GOF on <i>F</i> ²	1.140
<i>R</i> ₁ [<i>I</i> > 2 σ (<i>I</i>)]	0.0509
<i>wR</i> ₂ (all data)	0.1324
largest diff. peak/hole [e/Å ³]	0.23, -0.16



Data for **376_{maj}** (**JB-820-3**)

X-ray diffraction data were collected at 173 K on a Rigaku SCX mini diffractometer using graphite monochromated Mo-K α radiation ($\lambda = 0.71075 \text{ \AA}$).

376_{maj} (1 <i>R</i> ,3 <i>aR</i> ,4 <i>S</i> ,6 <i>aR</i>)	
empirical formula	C ₁₁ H ₁₀ F ₃ IN ₂ O
fw	370.11
crystal description	colourless, prism
crystal size [mm]	0.340 × 0.190 × 0.170
space group	P1 (#1)
<i>a</i> [Å]	7.6910(5)
<i>b</i> [Å]	11.5327(8)
<i>c</i> [Å]	11.9797(8)
vol [Å ³]	991.04(12)
α [°]	79.079(6)
β [°]	79.774(6)
γ [°]	73.365(5)
<i>Z</i>	3
ρ (calc) [g/cm ³]	1.860
μ [mm ⁻¹]	2.4495
F(000)	534.00
reflections collected	9863
independent reflections (<i>R</i> _{int})	8424 (0.0252)
data/parameters	8424/487
GOF on <i>F</i> ²	1.046
<i>R</i> ₁ [<i>I</i> > 2 σ (<i>I</i>)]	0.0340
<i>wR</i> ₂ (all data)	0.0886
largest diff. peak/hole [e/ Å ³]	0.70, -1.03
Flack parameter	0.025(11)



References

- 1 H. C. Erythropel, J. B. Zimmerman, T. M. de Winter, L. Petitjean, F. Melnikov, C. H. Lam, A. W. Lounsbury, K. E. Mellor, N. Z. Janković, Q. Tu, L. N. Pincus, M. M. Falinski, W. Shi, P. Coish, D. L. Plata and P. T. Anastas, *Green Chem.*, 2018, **20**, 1929–1961.
- 2 R. A. Sheldon, *Green Chem.*, 2016, **18**, 3180–3183.
- 3 J. Singh and T. J. Hagen, in *Burger's Medicinal Chemistry and Drug Discovery*, Wiley, 2010, pp. 127–166.
- 4 P. Jeschke, *Pest Manag. Sci.*, 2018, **74**, 2389–2404.
- 5 E. Brenna, C. Fuganti and S. Serra, *Tetrahedron: Asymmetry*, 2003, **14**, 1–42.
- 6 L. Friedman and J. G. Miller, *Science*, 1971, **172**, 1044–1046.
- 7 L. A. Nguyen, H. He and C. Pham-Huy, *Int. J. Biomed. Sci.*, 2006, **2**, 85–100.
- 8 S.-M. Paek, M. Jeong, J. Jo, Y. Heo, Y. Han and H. Yun, *Molecules*, 2016, **21**, 951.
- 9 Z. G. Brill, M. L. Condakes, C. P. Ting and T. J. Maimone, *Chem. Rev.*, 2017, **117**, 11753–11795.
- 10 H. Fujiwara, T. Kurogi, S. Okaya, K. Okano and H. Tokuyama, *Angew. Chem. Int. Ed.*, 2012, **51**, 13062–13065.
- 11 G. Diaz-Muñoz, I. L. Miranda, S. K. Sartori, D. C. Rezende and M. Alves Nogueira Diaz, *Chirality*, 2019, **31**, 776–812.
- 12 D. Enders and L. Reichenbach, *Synthesis*, 2013, **45**, 959–965.
- 13 W. S. Knowles, M. J. Sabacky, B. D. Vineyard and D. J. Weinkauff, *J. Am. Chem. Soc.*, 1975, **97**, 2567–2568.
- 14 R. Gawley and J. Aubé, *Principles of Asymmetric Synthesis*, Elsevier, 2012.
- 15 D. L. Boger, R. M. Garbaccio and S. L. Castle, *Modern Organic Synthesis: Lecture Notes*, TSRI press, La Jolla, 1st ed., 1999.
- 16 K.-J. Haack, S. Hashiguchi, A. Fujii, T. Ikariya and R. Noyori, *Angew. Chem. Int. Ed.*, 1997, **36**, 285–288.
- 17 K. A. Ahrendt, C. J. Borths and D. W. C. MacMillan, *J. Am. Chem. Soc.*, 2000, **122**, 4243–4244.
- 18 PDB 3bl7 structure summary < Protein Data Bank in Europe (PDBe) < EMBL-EBI,

- <https://www.ebi.ac.uk/pdbe/entry/pdb/3bl7>, (accessed 20 July 2021).
- 19 V. B. Birman and X. Li, *Org. Lett.*, 2006, **8**, 1351–1354.
- 20 C. A. Leverett, V. C. Purohit and D. Romo, *Angew. Chem. Int. Ed.*, 2010, **49**, 9479–9483.
- 21 E. R. T. Robinson, C. Fallan, C. Simal, A. M. Z. Slawin and A. D. Smith, *Chem. Sci.*, 2013, **4**, 2193–2200.
- 22 M. Kobayashi and S. Okamoto, *Tetrahedron Lett.*, 2006, **47**, 4347–4350.
- 23 V. B. Birman and X. Li, *Org. Lett.*, 2008, **10**, 1115–1118.
- 24 I. Shiina, K. Nakata, K. Ono, Y. Onda and M. Itagaki, *J. Am. Chem. Soc.*, 2010, **132**, 11629–11641.
- 25 D. Belmessieri, C. Joannesse, P. A. Woods, C. MacGregor, C. Jones, C. D. Campbell, C. P. Johnston, N. Duguet, C. Concellón, R. A. Bragg and A. D. Smith, *Org. Biomol. Chem.*, 2011, **9**, 559–570.
- 26 J. Merad, J.-M. Pons, O. Chuzel and C. Bressy, *Eur. J. Org. Chem.*, 2016, **2016**, 5589–5610.
- 27 C. McLaughlin and A. D. Smith, *Chem. – A Eur. J.*, 2021, **27**, 1533–1555.
- 28 J. Bitai, M. T. Westwood and A. D. Smith, *Org. Biomol. Chem.*, 2021, **19**, 2366–2384.
- 29 D. J. Pascoe, K. B. Ling and S. L. Cockroft, *J. Am. Chem. Soc.*, 2017, **139**, 15160–15167.
- 30 C. M. Young, A. Elmi, D. J. Pascoe, R. K. Morris, C. McLaughlin, A. M. Woods, A. B. Frost, A. de la Houpliere, K. B. Ling, T. K. Smith, A. M. Z. Slawin, P. H. Willoughby, S. L. Cockroft and A. D. Smith, *Angew. Chem. Int. Ed.*, 2020, **59**, 3705–3710.
- 31 P. Liu, X. Yang, V. B. Birman and K. N. Houk, *Org. Lett.*, 2012, **14**, 3288–3291.
- 32 M. E. Abbasov, B. M. Hudson, D. J. Tantillo and D. Romo, *J. Am. Chem. Soc.*, 2014, **136**, 4492–4495.
- 33 E. R. T. Robinson, D. M. Walden, C. Fallan, M. D. Greenhalgh, P. H. Y. Cheong and A. D. Smith, *Chem. Sci.*, 2016, **7**, 6919–6927.
- 34 E. M. Phillips, M. Wadamoto, H. S. Roth, A. W. Ott and K. A. Scheidt, *Org. Lett.*, 2009, **11**, 105–108.
- 35 Y. Kawanaka, E. M. Phillips and K. A. Scheidt, *J. Am. Chem. Soc.*, 2009, **131**, 18028–18029.
- 36 B. M. Trost and M. L. Crawley, *Chem. Rev.*, 2003, **103**, 2921–2944.

- 37 V. Andrushko and N. Andrushko, Eds., *Stereoselective Synthesis of Drugs and Natural Products*, John Wiley & Sons, Inc., Hoboken, NJ, USA, 2013.
- 38 O. Pàmies, J. Margalef, S. Cañellas, J. James, E. Judge, P. J. Guiry, C. Moberg, J.-E. Bäckvall, A. Pfaltz, M. A. Pericàs and M. Diéguez, *Chem. Rev.*, 2021, **121**, 4373–4505.
- 39 J. Qu and G. Helmchen, *Acc. Chem. Res.*, 2017, **50**, 2539–2555.
- 40 M. Beller, *Transition Metal Catalyzed Enantioselective Allylic Substitution in Organic Synthesis*, Springer Berlin Heidelberg, Berlin, Heidelberg, 2012, vol. 38.
- 41 L. A. Evans, N. Fey, J. N. Harvey, D. Hose, G. C. Lloyd-Jones, P. Murray, A. G. Orpen, R. Osborne, G. J. J. Owen-Smith and M. Purdie, *J. Am. Chem. Soc.*, 2008, **130**, 14471–14473.
- 42 S. T. Madrahimov, Q. Li, A. Sharma and J. F. Hartwig, *J. Am. Chem. Soc.*, 2015, **137**, 14968–14981.
- 43 B. M. Trost and D. L. Van Vranken, *Chem. Rev.*, 1996, **96**, 395–422.
- 44 J. Tsuji, H. Takahashi and M. Morikawa, *Tetrahedron Lett.*, 1965, **6**, 4387–4388.
- 45 B. M. Trost and T. J. Fullerton, *J. Am. Chem. Soc.*, 1973, **95**, 292–294.
- 46 B. M. Trost, T. Zhang and J. D. Sieber, *Chem. Sci.*, 2010, **1**, 427–440.
- 47 S. Martínez, L. Veth, B. Lainer and P. Dydio, *ACS Catal.*, 2021, **11**, 3891–3915.
- 48 H. Pellissier, *Adv. Synth. Catal.*, 2020, **362**, 2289–2325.
- 49 Z. Du and Z. Shao, *Chem. Soc. Rev.*, 2013, **42**, 1337–1378.
- 50 D.-F. Chen, Z.-Y. Han, X.-L. Zhou and L.-Z. Gong, *Acc. Chem. Res.*, 2014, **47**, 2365–2377.
- 51 S. Afewerki and A. Córdova, *Chem. Rev.*, 2016, **116**, 13512–13570.
- 52 Z. Shao and Y.-H. Deng, in *Dual Catalysis in Organic Synthesis 2*, Georg Thieme Verlag, Stuttgart, 2020, pp. 1–58.
- 53 A. E. Allen and D. W. C. MacMillan, *Chem. Sci.*, 2012, **3**, 633.
- 54 B. Montaignac, M. R. Vitale, V. Ratovelomanana-Vidal and V. Michelet, *Eur. J. Org. Chem.*, 2011, **2011**, 3723–3727.
- 55 B. Montaignac, V. Östlund, M. R. Vitale, V. Ratovelomanana-Vidal and V. Michelet, *Org. Biomol. Chem.*, 2012, **10**, 2300–2306.
- 56 B. Montaignac, C. Praveen, M. R. Vitale, V. Michelet and V. Ratovelomanana-Vidal, *Chem. Commun.*, 2012, **48**, 6559–6561.
- 57 S. Singha, E. Serrano, S. Mondal, C. G. Daniliuc and F. Glorius, *Nat. Catal.*, 2020, **3**,

- 48–54.
- 58 Z.-Y. Han, H. Xiao, X.-H. Chen and L.-Z. Gong, *J. Am. Chem. Soc.*, 2009, **131**, 9182–9183.
- 59 K. J. Schwarz, J. L. Amos, J. C. Klein, D. T. Do and T. N. Snaddon, *J. Am. Chem. Soc.*, 2016, **138**, 5214–5217.
- 60 K. J. Schwarz, C. M. Pearson, G. A. Cintron-Rosado, P. Liu and T. N. Snaddon, *Angew. Chem. Int. Ed.*, 2018, **57**, 7800–7803.
- 61 K. J. Schwarz, C. Yang, J. W. B. Fyfe and T. N. Snaddon, *Angew. Chem. Int. Ed.*, 2018, **57**, 12102–12105.
- 62 W. R. Scaggs and T. N. Snaddon, *Chem. Eur. J.*, 2018, **24**, 14378–14381.
- 63 J. W. B. Fyfe, O. M. Kabia, C. M. Pearson and T. N. Snaddon, *Tetrahedron*, 2018, **74**, 5383–5391.
- 64 L. Hutchings-Goetz, C. Yang and T. N. Snaddon, *ACS Catal.*, 2018, **8**, 10537–10544.
- 65 S. S. M. Spoehrle, T. H. West, J. E. Taylor, A. M. Z. Slawin and A. D. Smith, *J. Am. Chem. Soc.*, 2017, **139**, 11895–11902.
- 66 L. Li, D. Ding, J. Song, Z. Han and L. Gong, *Angew. Chem.*, 2019, **131**, 7729–7733.
- 67 J. Song, Z.-J. Zhang and L.-Z. Gong, *Angew. Chem. Int. Ed.*, 2017, **56**, 5212–5216.
- 68 X. Lu, L. Ge, C. Cheng, J. Chen, W. Cao and X. Wu, *Chem. Eur. J.*, 2017, **23**, 7689–7693.
- 69 J. Song, Z.-J. Zhang, S.-S. Chen, T. Fan and L.-Z. Gong, *J. Am. Chem. Soc.*, 2018, **140**, 3177–3180.
- 70 X. Jiang, J. J. Beiger and J. F. Hartwig, *J. Am. Chem. Soc.*, 2017, **139**, 87–90.
- 71 A. Kinens, S. Balkaitis, O. K. Ahmad, D. W. Piotrowski and E. Suna, *J. Org. Chem.*, 2021, **86**, 7189–7202.
- 72 D. Gasperini, M. D. Greenhalgh, R. Imad, S. Siddiqui, A. Malik, F. Arshad, M. I. Choudhary, A. M. Al-Majid, D. B. Cordes, A. M. Z. Slawin, S. P. Nolan and A. D. Smith, *Chem. Eur. J.*, 2019, **25**, 1064–1075.
- 73 O. Diels and K. Alder, *Liebigs Ann.*, 1928, **460**, 98–122.
- 74 R. Hoffmann and R. B. Woodward, *Acc. Chem. Res.*, 1968, **1**, 17–22.
- 75 R. B. Woodward and R. Hoffmann, *J. Am. Chem. Soc.*, 1965, **87**, 395–397.
- 76 R. Hoffmann and R. B. Woodward, *J. Am. Chem. Soc.*, 1965, **87**, 2046–2048.
- 77 R. B. Woodward and R. Hoffmann, *J. Am. Chem. Soc.*, 1965, **87**, 2511–2513.

- 78 N. Shirai and Y. Sato, *J. Org. Chem.*, 1988, **53**, 194–196.
- 79 R. Tang and K. Mislow, *J. Am. Chem. Soc.*, 1970, **92**, 2100–2104.
- 80 D. A. Evans, G. C. Andrews and C. L. Sims, *J. Am. Chem. Soc.*, 1971, **93**, 4956–4957.
- 81 T. Nakai and K. Mikami, *Chem. Rev.*, 1986, **86**, 885–902.
- 82 R. W. Hoffmann, *Angew. Chem. Int. Ed.*, 1979, **18**, 563–572.
- 83 Y. D. Wu, K. N. Houk and J. A. Marshall, *J. Org. Chem.*, 1990, **55**, 1421–1423.
- 84 C. Nájera and J. M. Sansano, *Chem. Rev.*, 2007, **107**, 4584–4671.
- 85 T. H. West, S. S. M. Spoehrle, K. Kasten, J. E. Taylor and A. D. Smith, *ACS Catal.*, 2015, **5**, 7446–7479.
- 86 J. B. Sweeney, *Chem. Soc. Rev.*, 2009, **38**, 1027.
- 87 A. Soheili and U. K. Tambar, *J. Am. Chem. Soc.*, 2011, **133**, 12956–12959.
- 88 P. A. van der Schaaf, J.-P. Sutter, M. Grellier, G. P. M. van Mier, A. L. Spek, G. van Koten and M. Pfeffer, *J. Am. Chem. Soc.*, 1994, **116**, 5134–5144.
- 89 J. A. Workman, N. P. Garrido, J. Sançon, E. Roberts, H. P. Wessel and J. B. Sweeney, *J. Am. Chem. Soc.*, 2005, **127**, 1066–1067.
- 90 J. Blid, O. Panknin and P. Somfai, *J. Am. Chem. Soc.*, 2005, **127**, 9352–9353.
- 91 T. H. West, D. S. B. Daniels, A. M. Z. Slawin and A. D. Smith, *J. Am. Chem. Soc.*, 2014, **136**, 4476–4479.
- 92 L. Zhang, Z.-J. Zhang, J.-Y. Xiao and J. Song, *Org. Lett.*, 2018, **20**, 5519–5522.
- 93 T. H. West, D. M. Walden, J. E. Taylor, A. C. Brueckner, R. C. Johnston, P. H. Y. Cheong, G. C. Lloyd-Jones and A. D. Smith, *J. Am. Chem. Soc.*, 2017, **139**, 4366–4375.
- 94 S. Drissi-Amraoui, M. S. T. Morin, C. Crévisy, O. Baslé, R. Marcia de Figueiredo, M. Mauduit and J.-M. Campagne, *Angew. Chem. Int. Ed.*, 2015, **54**, 11830–11834.
- 95 S. F. Vanier, G. Larouche, R. P. Wurz and A. B. Charette, *Org. Lett.*, 2010, **12**, 672–675.
- 96 P. A. Jacobi, C. A. Blum, R. W. DeSimone and U. E. S. Udodong, *Tetrahedron Lett.*, 1989, **30**, 7173–7176.
- 97 D. H. Ripin and D. A. Evans, Evans pKa table, http://ccc.chem.pitt.edu/wipf/MechOMs/evans_pKa_table.pdf, (accessed 3 August 2021).
- 98 T. H. West, S. S. M. Spoehrle and A. D. Smith, *Tetrahedron*, 2017, **73**, 4138–4149.
- 99 K. Kasten, A. M. Z. Slawin and A. D. Smith, *Org. Lett.*, 2017, **19**, 5182–5185.

- 100 A. Soheili and U. K. Tambar, *Org. Lett.*, 2013, **15**, 5138–5141.
- 101 M. D. Greenhalgh, S. M. Smith, D. M. Walden, J. E. Taylor, Z. Brice, E. R. T. Robinson, C. Fallan, D. B. Cordes, A. M. Z. Slawin, H. C. Richardson, M. A. Grove, P. H.-Y. Cheong and A. D. Smith, *Angew. Chem. Int. Ed.*, 2018, **57**, 3200–3206.
- 102 I. Shiina, K. Nakata, K. Ono, M. Sugimoto and A. Sekiguchi, *Chem. Eur. J.*, 2010, **16**, 167–172.
- 103 K. Nakata, K. Gotoh, K. Ono, K. Futami and I. Shiina, *Org. Lett.*, 2013, **15**, 1170–1173.
- 104 A. J. Ferreira and C. M. Beaudry, *Tetrahedron*, 2017, **73**, 965–1084.
- 105 B. Heasley, *Curr. Org. Chem.*, 2014, **18**, 641–686.
- 106 Z. Yang, *Acc. Chem. Res.*, 2021, **54**, 556–568.
- 107 V. Pirenne, B. Muriel and J. Waser, *Chem. Rev.*, 2021, **121**, 227–263.
- 108 M. A. Cavitt, L. H. Phun and S. France, *Chem. Soc. Rev.*, 2014, **43**, 804–818.
- 109 Y. Xia, X. Liu and X. Feng, *Angew. Chem. Int. Ed.*, 2021, **60**, 9192–9204.
- 110 M. Meazza, H. Guo and R. Rios, *Org. Biomol. Chem.*, 2017, **15**, 2479–2490.
- 111 J. Wang, S. A. Blaszczyk, X. Li and W. Tang, *Chem. Rev.*, 2021, **121**, 110–139.
- 112 J. Caillé and R. Robiette, *Org. Biomol. Chem.*, 2021, **19**, 5702–5724.
- 113 I. Shimizu, Y. Ohashi and J. Tsuji, *Tetrahedron Lett.*, 1985, **26**, 3825–3828.
- 114 K. Yamamoto, T. Ishida and J. Tsuji, *Chem. Lett.*, 1987, **16**, 1157–1158.
- 115 A. F. G. Goldberg and B. M. Stoltz, *Org. Lett.*, 2011, **13**, 4474–4476.
- 116 B. M. Trost and P. J. Morris, *Angew. Chem. Int. Ed.*, 2011, **50**, 6167–6170.
- 117 B. M. Trost, P. J. Morris and S. J. Sprague, *J. Am. Chem. Soc.*, 2012, **134**, 17823–17831.
- 118 M. Laugeois, S. Ponra, V. Ratovelomanana-Vidal, V. Michelet and M. R. Vitale, *Chem. Commun.*, 2016, **52**, 5332–5335.
- 119 K. S. Halskov, L. Næsborg, F. Tur and K. A. Jørgensen, *Org. Lett.*, 2016, **18**, 2220–2223.
- 120 H. Zhu, P. Du, J. Li, Z. Liao, G. Liu, H. Li and W. Wang, *Beilstein J. Org. Chem.*, 2016, **12**, 1340–1347.
- 121 M. Meazza and R. Rios, *Chem. Eur. J.*, 2016, **22**, 9923–9928.
- 122 K. Zhang, M. Meazza, A. Izaga, C. Contamine, M. Gimeno, R. Herrera and R. Rios, *Synthesis*, 2016, **49**, 167–174.
- 123 M. Kamlar, M. Franc, I. Čísařová, R. Gyepes and J. Veselý, *Chem. Commun.*, 2019, **55**, 3829–3832.

- 124 M. Meazza, M. Kamlar, L. Jašíková, B. Formánek, A. Mazzanti, J. Roithová, J. Veselý and R. Rios, *Chem. Sci.*, 2018, **9**, 6368–6373.
- 125 M. Franc, I. Císařová and J. Veselý, *Adv. Synth. Catal.*, 2021, adsc.202100571.
- 126 S. Pandiancherri, S. J. Ryan and D. W. Lupton, *Org. Biomol. Chem.*, 2012, **10**, 7903.
- 127 G. Liu, M. E. Shirley, K. N. Van, R. L. McFarlin and D. Romo, *Nat. Chem.*, 2013, **5**, 1049–1057.
- 128 E. Robinson, A. Frost, P. Elías-Rodríguez and A. Smith, *Synthesis*, 2016, **49**, 409–423.
- 129 S. Vellalath, K. N. Van and D. Romo, *Tetrahedron Lett.*, 2015, **56**, 3647–3652.
- 130 S. Vellalath and D. Romo, *Angew. Chem. Int. Ed.*, 2016, **55**, 13934–13943.
- 131 N. Moszner, F. Zeuner, T. Völkel and V. Rheinberger, *Macromol. Chem. Phys.*, 1999, **200**, 2173–2187.
- 132 N. Nomura, K. Tsurugi, N. Yoshida and M. Okada, *Curr. Org. Synth.*, 2005, **2**, 21–38.
- 133 K. Alfonsi, J. Colberg, P. J. Dunn, T. Fevig, S. Jennings, T. A. Johnson, H. P. Kleine, C. Knight, M. A. Nagy, D. A. Perry and M. Stefaniak, *Green Chem.*, 2008, **10**, 31–36.
- 134 Y. S. Gee, D. J. Rivinoja, S. M. Wales, M. G. Gardiner, J. H. Ryan and C. J. T. Hyland, *J. Org. Chem.*, 2017, **82**, 13517–13529.
- 135 K. Fagnou and M. Lautens, *Angew. Chem. Int. Ed.*, 2002, **41**, 26–47.
- 136 B. M. Trost and F. D. Toste, *J. Am. Chem. Soc.*, 1999, **121**, 4545–4554.
- 137 P. Fristrup, T. Jensen, J. Hoppe and P.-O. Norrby, *Chem. Eur. J.*, 2006, **12**, 5352–5360.
- 138 N. Solin and K. J. Szabó, *Organometallics*, 2001, **20**, 5464–5471.
- 139 P. Fristrup, M. Ahlquist, D. Tanner and P.-O. Norrby, *J. Phys. Chem. A*, 2008, **112**, 12862–12867.
- 140 M. Shevchuk, Q. Wang, R. Pajkert, J. Xu, H. Mei, G. Rösenthaller and J. Han, *Adv. Synth. Catal.*, 2021, **363**, 2912–2968.
- 141 A. P. Dieskau, M. S. Holzwarth and B. Plietker, *J. Am. Chem. Soc.*, 2012, **134**, 5048–5051.
- 142 J.-A. Xiao, X.-L. Cheng, Y.-C. Li, Y.-M. He, J.-L. Li, Z.-P. Liu, P.-J. Xia, W. Su and H. Yang, *Org. Biomol. Chem.*, 2019, **17**, 103–107.
- 143 T. Sarkar, K. Talukdar, B. K. Das, T. A. Shah, B. Debnath and T. Punniyamurthy, *Org. Biomol. Chem.*, 2021, **19**, 3776–3790.
- 144 N. A. Ahlemeyer, E. V. Streff, P. Muthupandi and V. B. Birman, *Org. Lett.*, 2017, **19**,

- 6486–6489.
- 145 S. S. Zaleskiy and V. P. Ananikov, *Organometallics*, 2012, **31**, 2302–2309.
- 146 A. Matviitsuk, M. D. Greenhalgh, D.-J. B. Antúnez, A. M. Z. Slawin and A. D. Smith, *Angew. Chem. Int. Ed.*, 2017, **56**, 12282–12287.
- 147 P. A. Jacobi, C. A. Blum, R. W. DeSimone and U. E. S. Udodong, *J. Am. Chem. Soc.*, 1991, **113**, 5384–5392.
- 148 M. D. Greenhalgh, S. Qu, A. M. Z. Slawin and A. D. Smith, *Chem. Sci.*, 2018, **9**, 4909–4918.
- 149 D. Daniels, S. Smith, T. Lebl, P. Shapland and A. Smith, *Synthesis*, 2014, **47**, 34–41.
- 150 N. R. Guha, R. M. Neyyappadath, M. D. Greenhalgh, R. Chisholm, S. M. Smith, M. L. McEvoy, C. M. Young, C. Rodríguez-Esrich, M. A. Pericàs, G. Hähner and A. D. Smith, *Green Chem.*, 2018, **20**, 4537–4546.
- 151 T. O. Ronson, J. R. Carney, A. C. Whitwood, R. J. K. Taylor and I. J. S. Fairlamb, *Chem. Commun.*, 2015, **51**, 3466–3469.
- 152 E. Abraham, J. W. B. Cooke, S. G. Davies, A. Naylor, R. L. Nicholson, P. D. Price and A. D. Smith, *Tetrahedron*, 2007, **63**, 5855–5872.
- 153 G.-Q. Tian, J. Yang and K. Rosa-Perez, *Org. Lett.*, 2010, **12**, 5072–5074.
- 154 M. A. Kacprzyński, S. A. Kazane, T. L. May and A. H. Hoveyda, *Org. Lett.*, 2007, **9**, 3187–3190.
- 155 Q. Yang, J. T. Njardarson, C. Draghici and F. Li, *Angew. Chem. Int. Ed.*, 2013, **52**, 8648–8651.
- 156 J. R. Hwu and P. S. Furth, *J. Am. Chem. Soc.*, 1989, **111**, 8834–8841.
- 157 R. Shintani, K. Takatsu, M. Takeda and T. Hayashi, *Angew. Chem. Int. Ed.*, 2011, **50**, 8656–8659.
- 158 Y. Yoshimura, Y. Yamazaki, M. Kawahata, K. Yamaguchi and H. Takahata, *Tetrahedron Lett.*, 2007, **48**, 4519–4522.
- 159 M. Mailig, A. Hazra, M. K. Armstrong and G. Lalic, *J. Am. Chem. Soc.*, 2017, **139**, 6969–6977.
- 160 D. Brandt, A. Dittoo, V. Bellosta and J. Cossy, *Org. Lett.*, 2015, **17**, 816–819.
- 161 I. Paterson, O. Delgado, G. J. Florence, I. Lyothier, M. O'Brien, J. P. Scott and N. Sereinig, *J. Org. Chem.*, 2005, **70**, 150–160.
- 162 E. Abraham, S. G. Davies, N. L. Millican, R. L. Nicholson, P. M. Roberts and A. D.

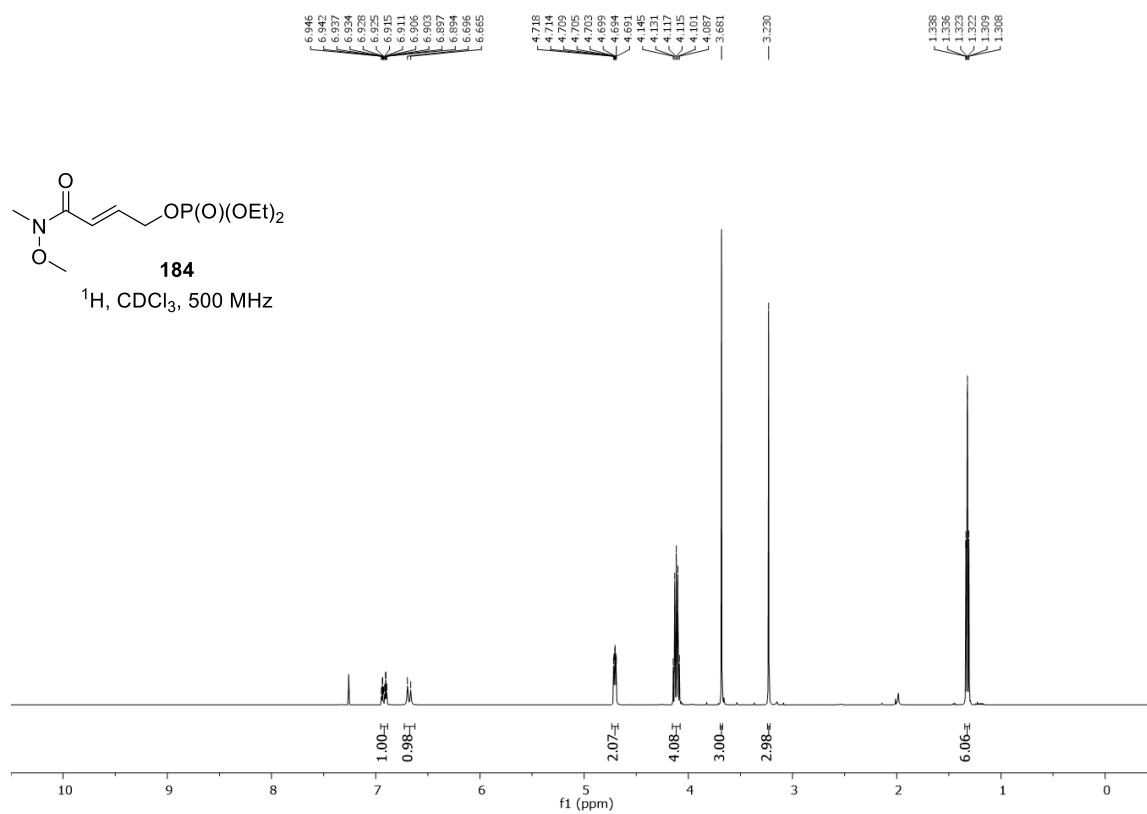
- Smith, *Org. Biomol. Chem.*, 2008, **6**, 1655.
- 163 J. L. Markley and P. R. Hanson, *Org. Lett.*, 2017, **19**, 2552–2555.
- 164 J. F. Hooper, N. C. James, E. Bozkurt, V. Aviyente, J. M. White, M. C. Holland, R. Gilmour, A. B. Holmes and K. N. Houk, *J. Org. Chem.*, 2015, **80**, 12058–12075.
- 165 A. M. Abdou, S. Botros, R. A. Hassan, M. M. Kamel, D. F. Taber and A. T. Taher, *Tetrahedron*, 2015, **71**, 139–146.
- 166 J. Preindl, S. Chakrabarty and J. Waser, *Chem. Sci.*, 2017, **8**, 7112–7118.
- 167 J. M. Takacs, Z. Xu, X. Jiang, A. P. Leonov and G. C. Theriot, *Org. Lett.*, 2002, **4**, 3843–3845.
- 168 F. Wei, C.-L. Ren, D. Wang and L. Liu, *Chem. Eur. J.*, 2015, **21**, 2335–2338.
- 169 K. Burgess, *J. Org. Chem.*, 1987, **52**, 2046–2051.
- 170 C. S. Buxton, D. C. Blakemore and J. F. Bower, *Angew. Chem. Int. Ed.*, 2017, **56**, 13824–13828.
- 171 J. M. Ellis, L. E. Overman, H. R. Tanner and J. Wang, *J. Org. Chem.*, 2008, **73**, 9151–9154.
- 172 J. Wu, C. M. Young and A. D. Smith, *Tetrahedron*, 2021, **78**, 131758.
- 173 H. M. Walborsky and M. Schwarz, *J. Am. Chem. Soc.*, 1953, **75**, 3241–3243.
- 174 H. Plenkiewicz, W. Dmowski and M. Lipinski, *J. Fluor. Chem.*, 2001, **111**, 227–232.
- 175 C. Shu, H. Liu, A. M. Z. Slawin, C. Carpenter-Warren and A. D. Smith, *Chem. Sci.*, 2020, **11**, 241–247.
- 176 R. Pajkert and G.-V. Röschenhaler, *J. Org. Chem.*, 2013, **78**, 3697–3708.
- 177 P. Zaderenko, M. C. López and P. Ballesteros, *J. Org. Chem.*, 1996, **61**, 6825–6828.
- 178 A. El-Batta, C. Jiang, W. Zhao, R. Anness, A. L. Cooksy and M. Bergdahl, *J. Org. Chem.*, 2007, **72**, 5244–5259.
- 179 N. Kaur, B. Zhou, F. Breitbeil, K. Hardy, K. S. Kraft, I. Trantcheva and O. Phanstiel IV, *Mol. Pharm.*, 2008, **5**, 294–315.
- 180 C. McLaughlin, A. M. Z. Slawin and A. D. Smith, *Angew. Chem. Int. Ed.*, 2019, **58**, 15111–15119.
- 181 L. Mola, J. Font, L. Bosch, J. Caner, A. M. Costa, G. Etxebarria-Jardí, O. Pineda, D. de Vicente and J. Vilarrasa, *J. Org. Chem.*, 2013, **78**, 5832–5842.
- 182 L. Barr, S. F. Lincoln and C. J. Easton, *Chem. Eur. J.*, 2006, **12**, 8571–8580.
- 183 Y. Monguchi, K. Kunishima, T. Hattori, T. Takahashi, Y. Shishido, Y. Sawama and

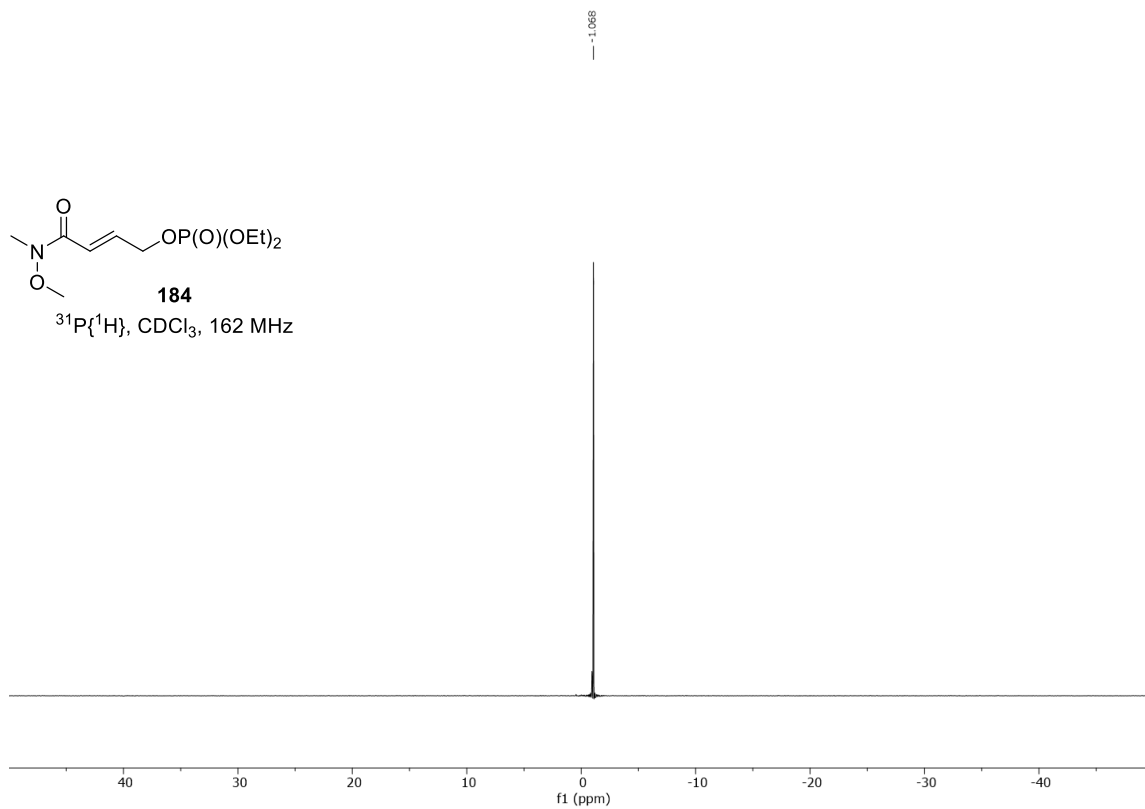
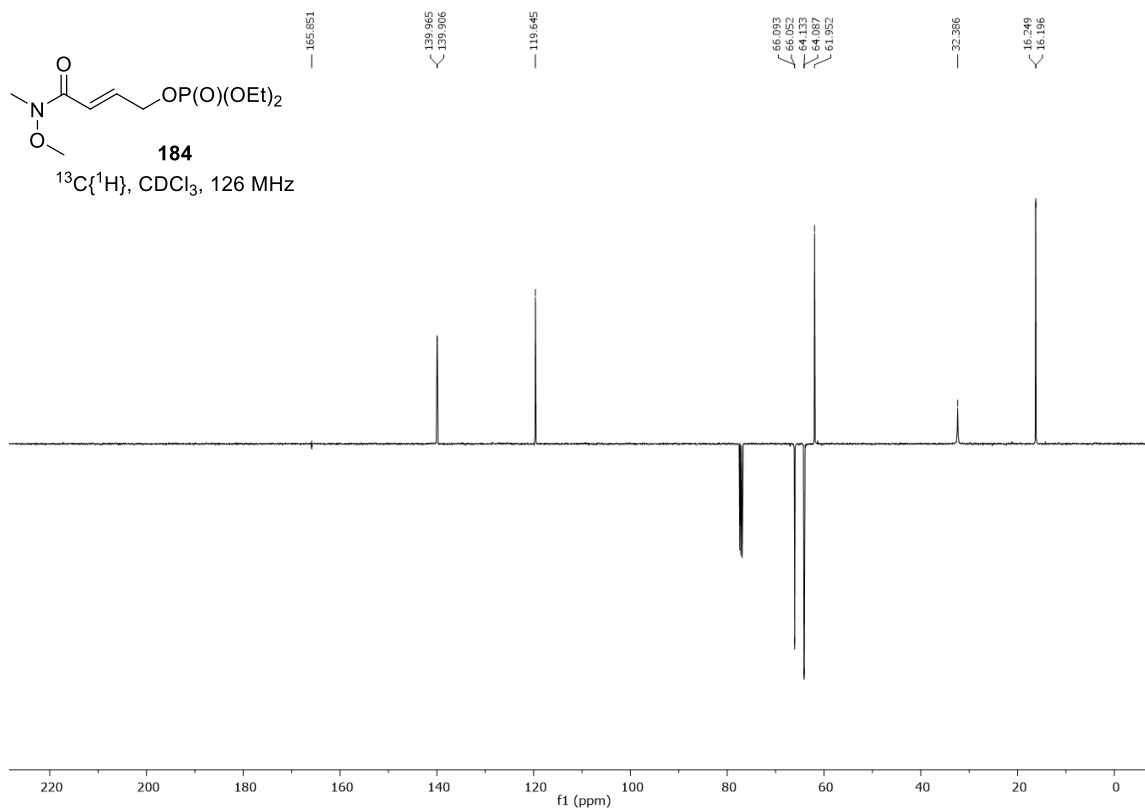
- H. Sajiki, *ACS Catal.*, 2016, **6**, 3994–3997.
- 184 A. Ovat, F. Muindi, C. Fagan, M. Brouner, E. Hansell, J. Dvořák, D. Sojka, P. Kopáček, J. H. McKerrow, C. R. Caffrey and J. C. Powers, *J. Med. Chem.*, 2009, **52**, 7192–7210.
- 185 D. Tejedor, S. J. Álvarez-Méndez, J. M. López-Soria, V. S. Martín and F. García-Tellado, *Eur. J. Org. Chem.*, 2014, **2014**, 198–205.
- 186 M. Wende and J. A. Gladysz, *J. Am. Chem. Soc.*, 2003, **125**, 5861–5872.
- 187 S. Karlsson and H.-E. Högberg, *Org. Lett.*, 1999, **1**, 1667–1669.
- 188 H. Lebel and M. Davi, *Adv. Synth. Catal.*, 2008, **350**, 2352–2358.
- 189 X. Lu, W. Wang, Q. Dong, X. Bao, X. Lin, W. Zhang, X. Dong and W. Zhao, *Chem. Commun.*, 2015, **51**, 1498–1501.
- 190 Z. Yuan, W. Wei, A. Lin and H. Yao, *Org. Lett.*, 2016, **18**, 3370–3373.
- 191 G. M. Sheldrick, *Acta Crystallogr., Sect. A*, 2015, **71**, 3–8.
- 192 M. C. Burla, R. Caliendo, M. Camalli, B. Carrozzini, G. L. Casciarano, C. Giacovazzo, M. Mallamo, A. Mazzone, G. Polidori and R. Spagna, *J. Appl. Crystallogr.*, 2012, **45**, 357–361.
- 193 L. Palatinus and G. Chapuis, *J. Appl. Crystallogr.*, 2007, **40**, 786–790.
- 194 G. M. Sheldrick, *Acta Crystallogr., Sect. C*, 2015, **71**, 3–8.

Appendix I: Example NMR spectra

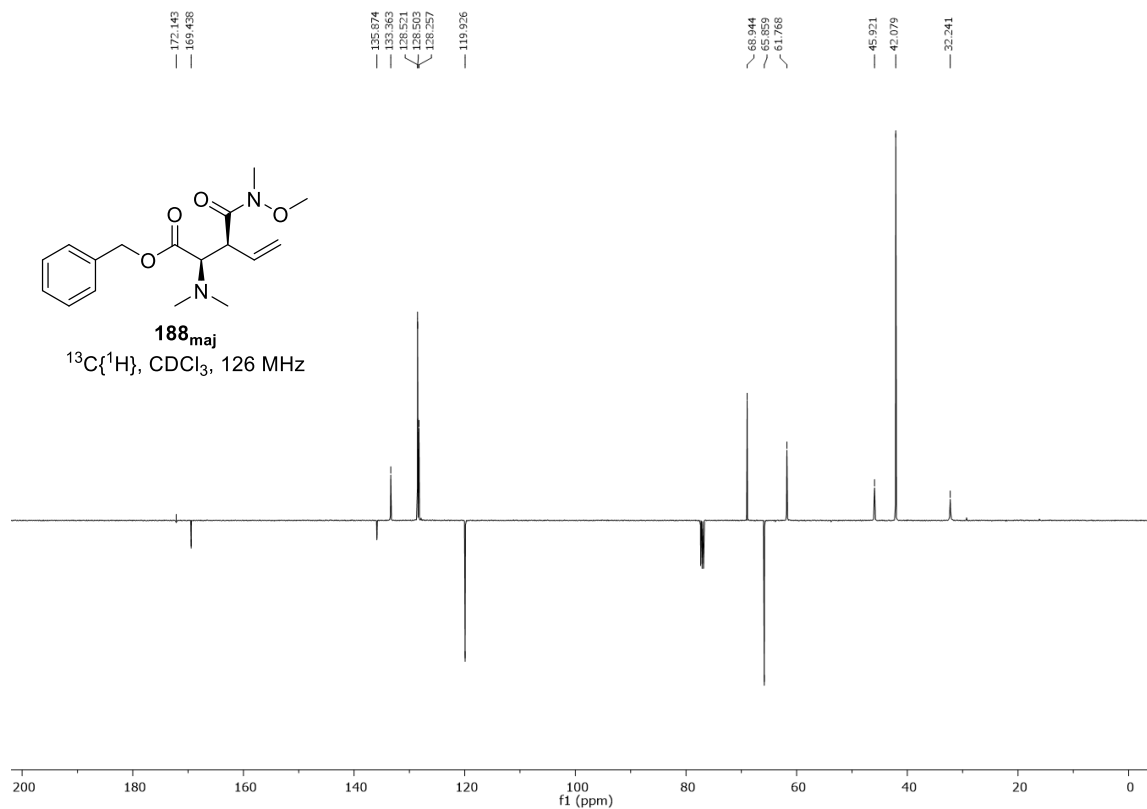
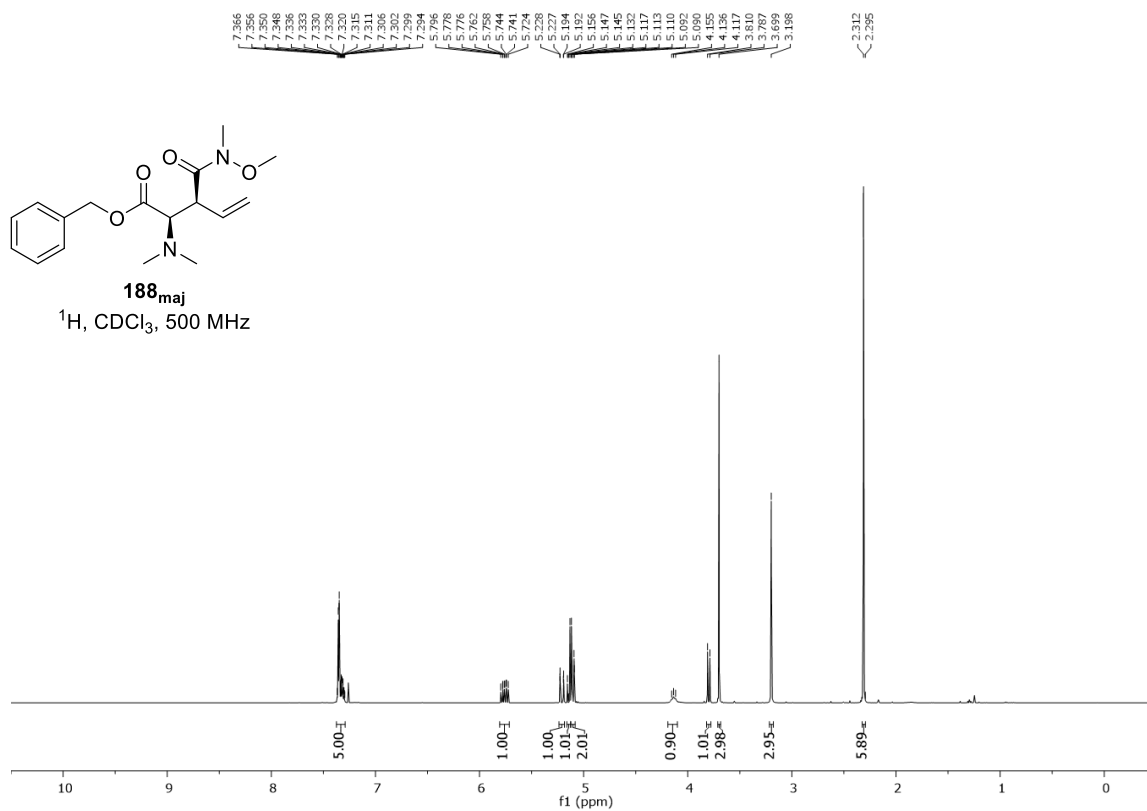
Example spectra from Chapter 2

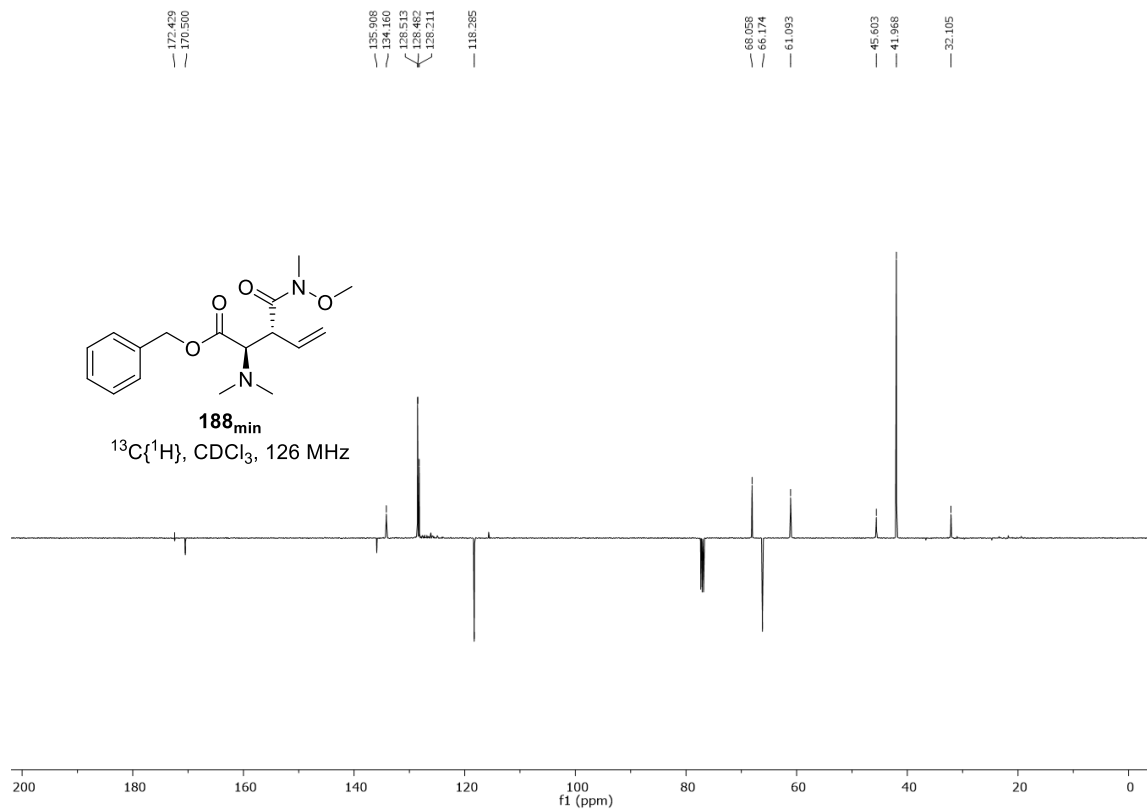
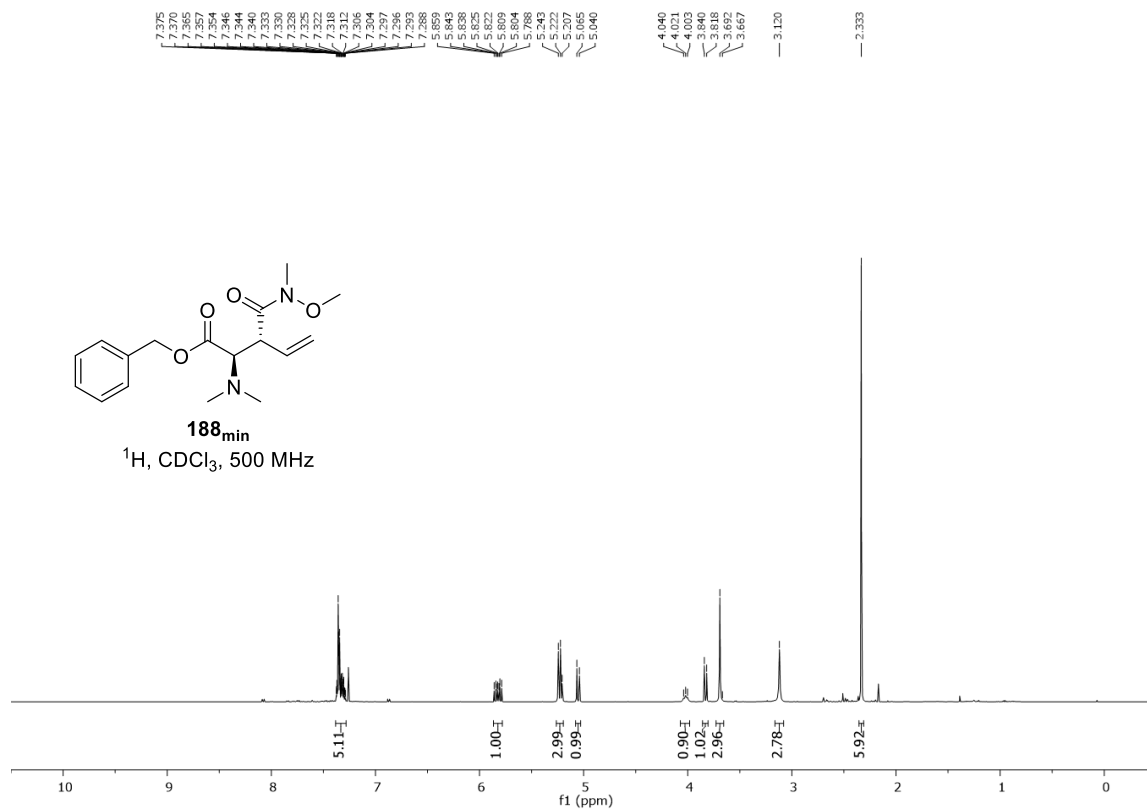
^1H , $^{13}\text{C}\{^1\text{H}\}$ and $^{31}\text{P}\{^1\text{H}\}$ spectra of compound 184





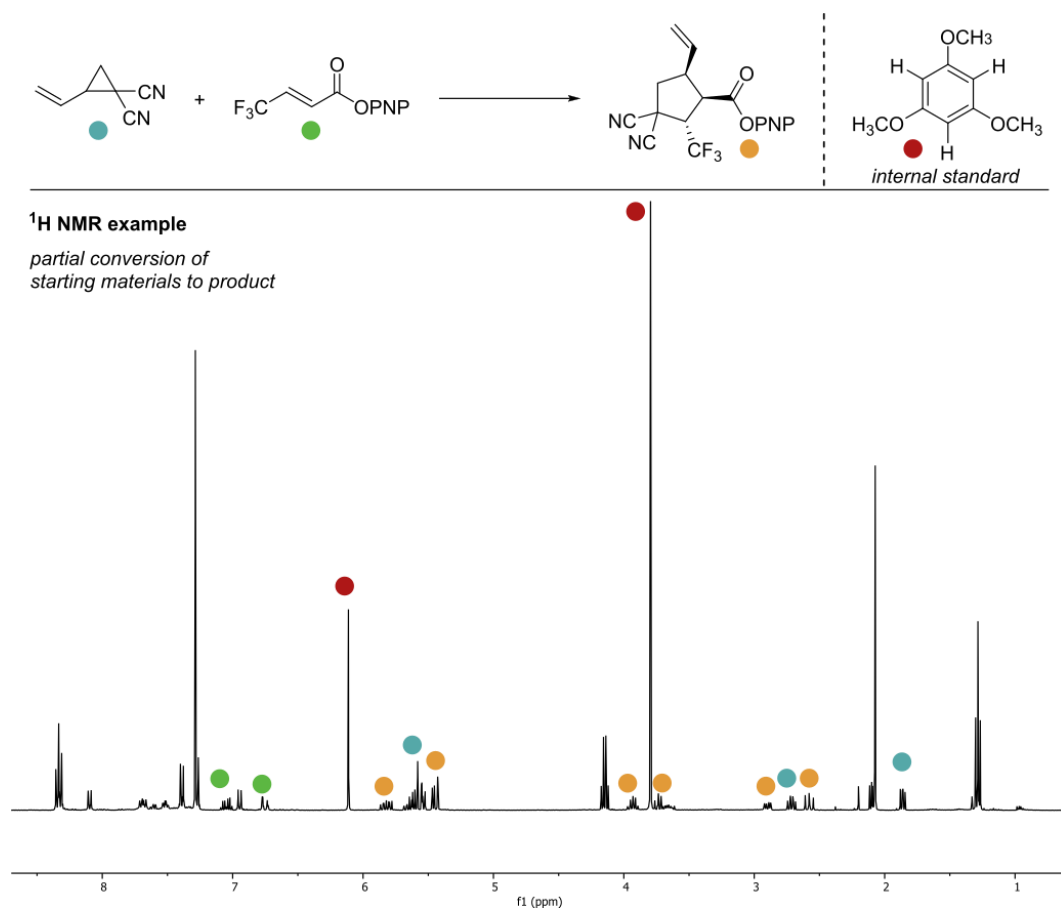
^1H , and $^{13}\text{C}\{^1\text{H}\}$ spectra of compound **188**

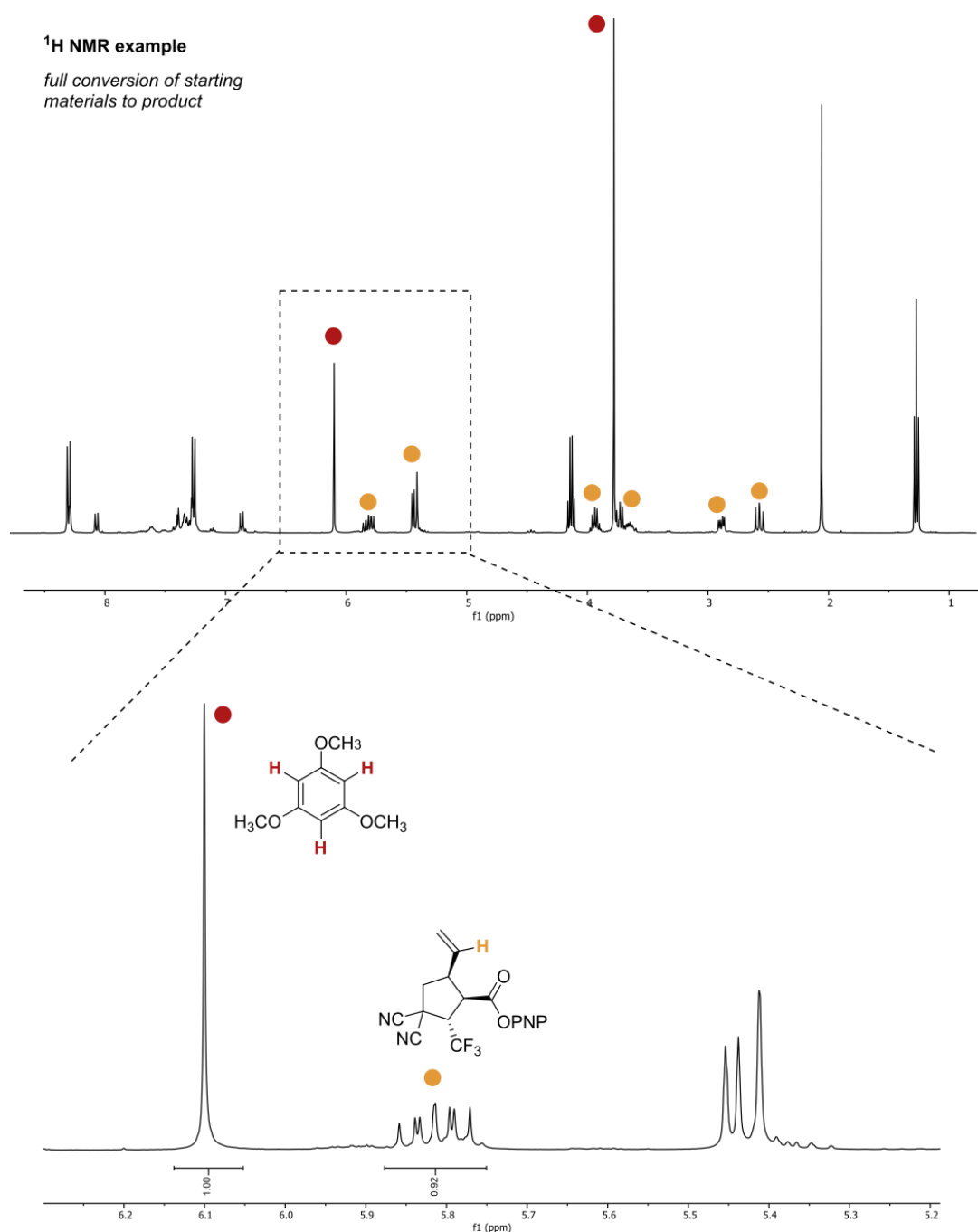




Calculation of ^1H NMR yield and dr for Chapter 3

As an example, ^1H NMR spectra from a typical reaction from the optimisation process have been chosen and the majority of peaks assigned to the corresponding compounds. The first example depicts a reaction with partial conversion to product and remaining, unreacted starting materials. This example highlights that the chosen internal standard, which shows a singlet at 6.10 ppm, does not overlap with any other signals. In addition, the conversion of starting materials can also be assessed, if required, by integrating the signals at 6.75 ppm (dq, green dot) and at 1.86 ppm (dd, blue dot). The second example depicts the more usual case with full conversion of starting materials, which will be used to demonstrate how the ^1H NMR yield was derived during the optimisation process.



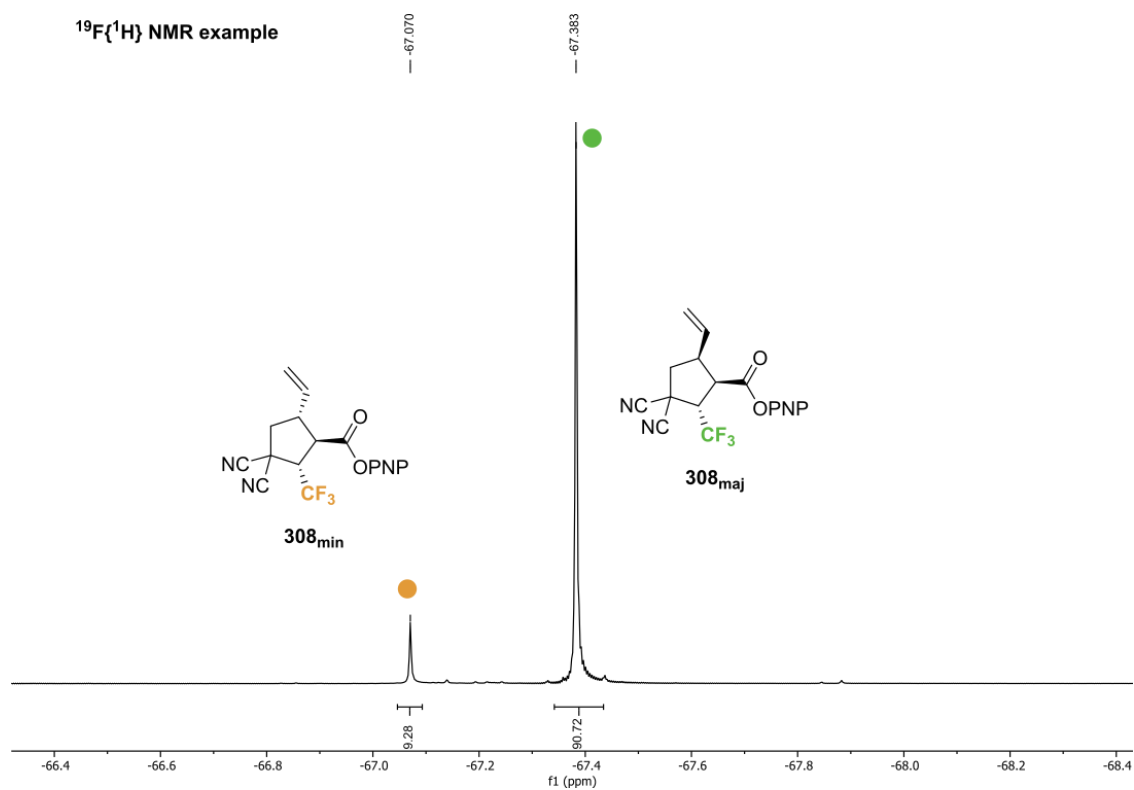


Determination of ^1H NMR yield:

The peak corresponding to the aromatic protons of the internal standard (highlighted in red) and the multiplet corresponding to the vinylic proton of the product (highlighted in yellow) were chosen as reference signals to determine the ^1H NMR yield (see figure above). As the internal standard peak corresponds to 3 protons, but the multiplet (ddd) of the product only to 1 proton, only 0.33 eq of internal standard are used to allow a direct comparison of the integrals. The integral of the internal standard peak is set to 1.0. Integration of the product multiplet (0.92) and multiplication by 100 gives the corresponding ^1H NMR yield (92%).

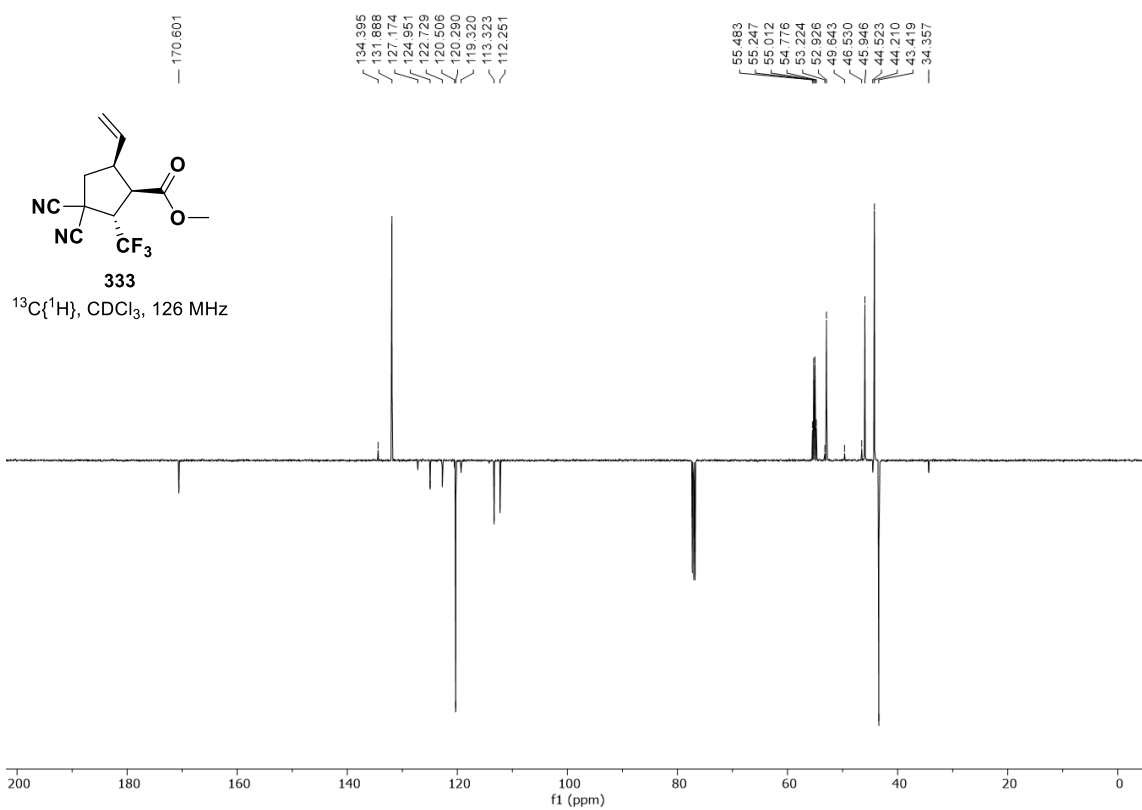
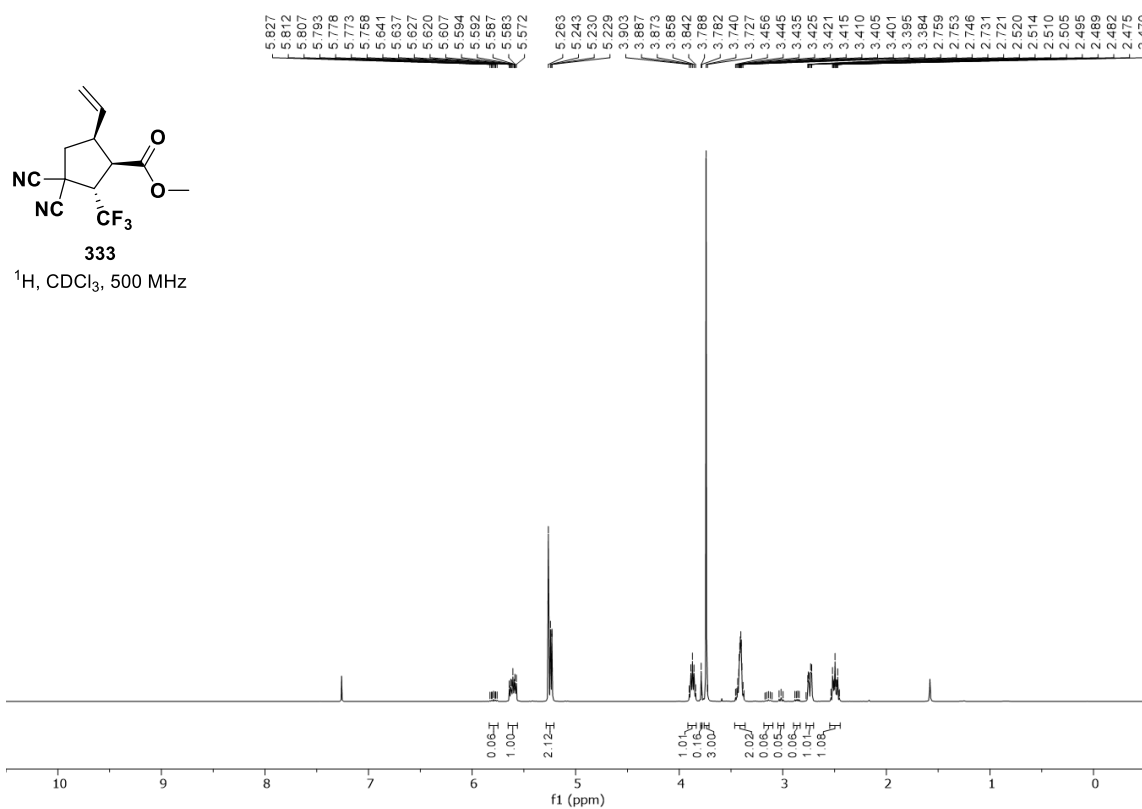
Determination of dr by $^{19}\text{F}\{^1\text{H}\}$ NMR analysis:

The dr is determined by $^{19}\text{F}\{^1\text{H}\}$ NMR analysis of the crude reaction mixture. The singlets corresponding to the CF_3 group of the two major diastereoisomers at -67.0 ppm and -67.3 ppm are integrated and the sum of the two integrals set to 100. The resulting value for the integrals, rounded to the nearest integer corresponds to the diastereomeric ratio of the product (9:91 dr in this example).

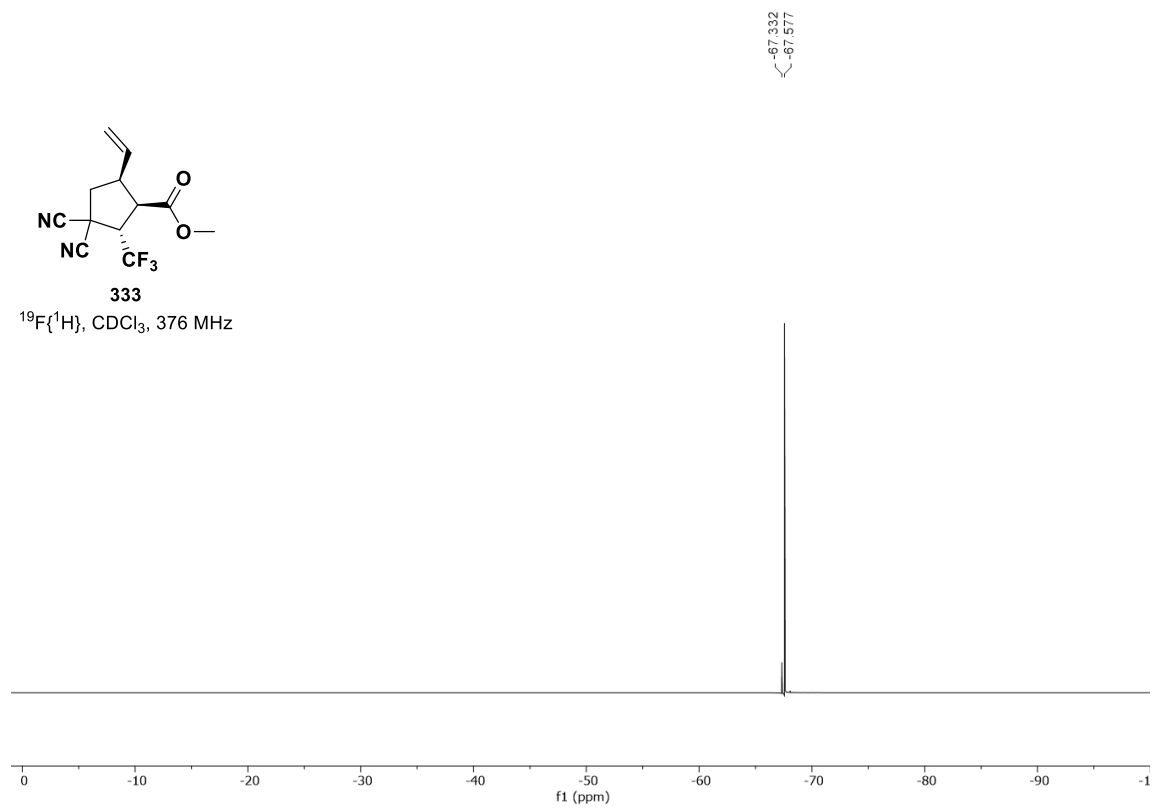


Example spectra from Chapter 3

^1H , $^{13}\text{C}\{^1\text{H}\}$ and $^{19}\text{F}\{^1\text{H}\}$ spectra of compound 333



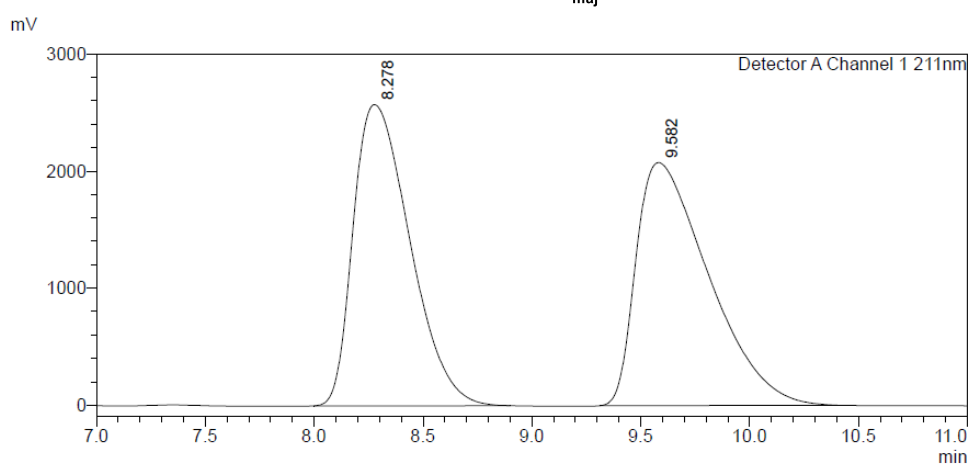
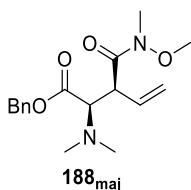
Appendix I: Example NMR spectra |



Appendix II: Example HPLC and GC traces

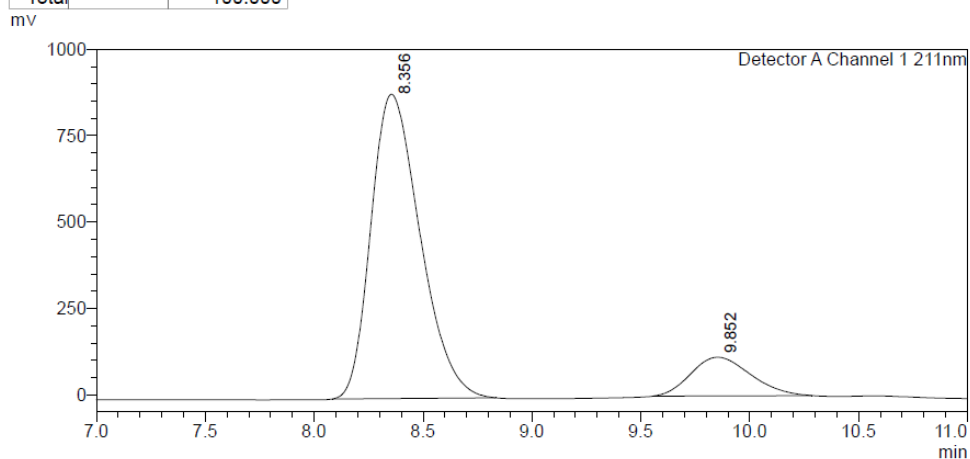
Example HPLC traces from Chapter 2

HPLC Data for **188_{maj}**: Chiralcel OD-H (95:5 hexane : *i*-PrOH, flow rate 1.0 mlmin⁻¹, 211 nm, 40 °C) t_R (2*R*,3*S*): 8.3 min, t_R (2*S*,3*R*): 9.8 min, 87:13 er.



<Peak Table>

Detector A Channel 1 211nm		
Peak#	Ret. Time	Area%
1	8.278	49.210
2	9.582	50.790
Total		100.000

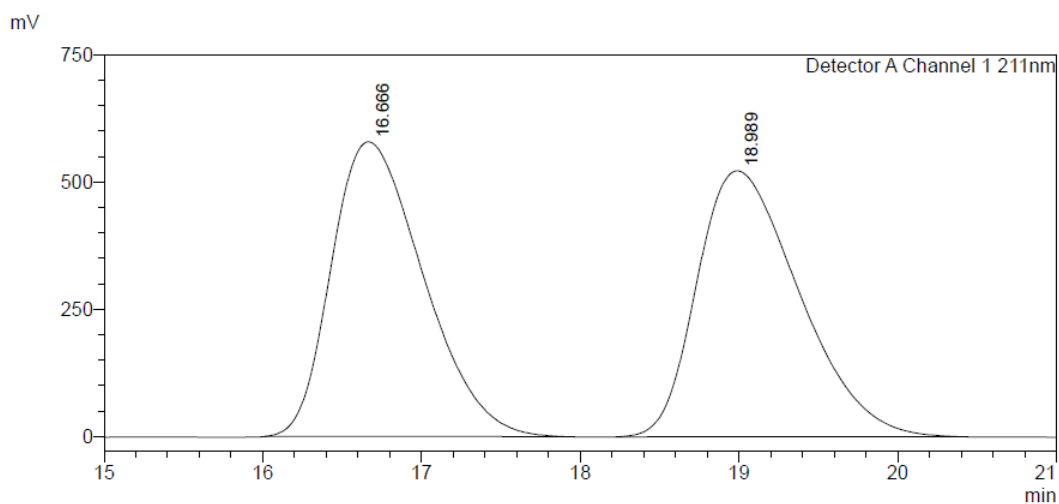
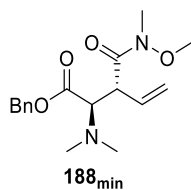


<Peak Table>

Detector A Channel 1 211nm		
Peak#	Ret. Time	Area%
1	8.356	86.597
2	9.852	13.403
Total		100.000

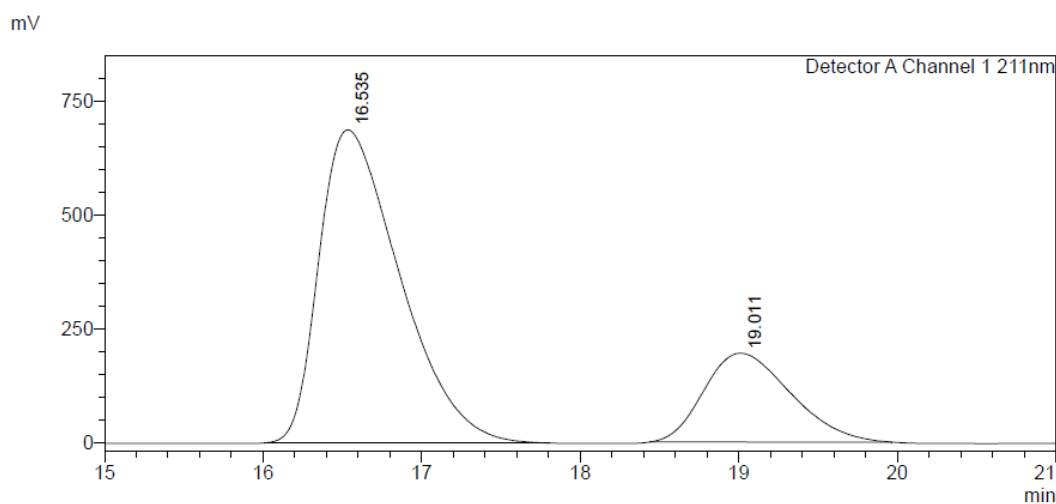
Appendix II: Example HPLC and GC traces |

HPLC Data for **188_{min}**: Chiralcel OD-H (99:1 hexane : *i*-PrOH, flow rate 1.0 mlmin⁻¹, 211 nm, 40 °C) *t_R* (2*R*,3*R*): 16.3 min, *t_R* (2*S*,3*S*): 19.0 min, 77:23 er.



<Peak Table>

Detector A Channel 1 211nm		
Peak#	Ret. Time	Area%
1	16.666	49.940
2	18.989	50.060
Total		100.000

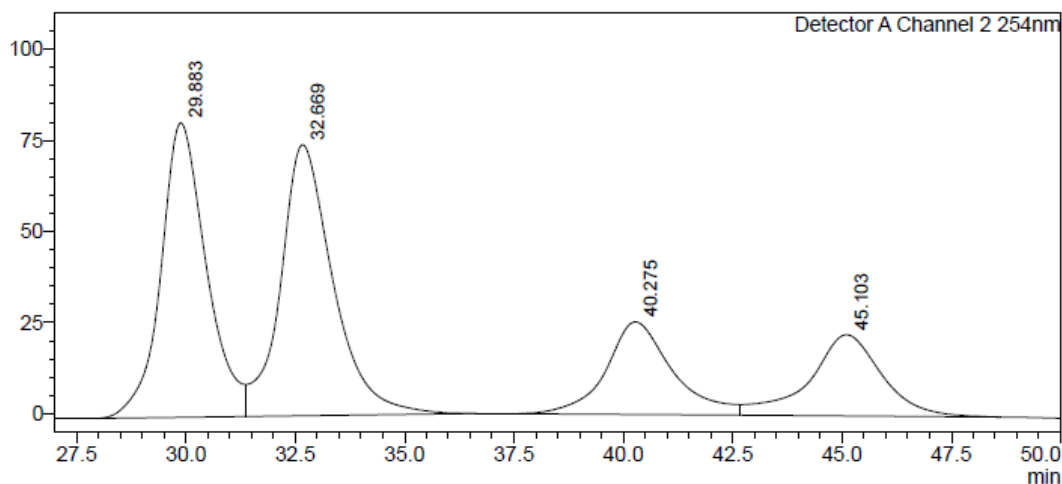
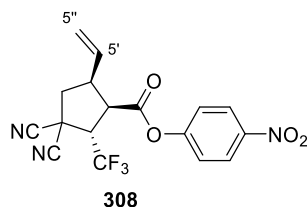


<Peak Table>

Detector A Channel 1 211nm		
Peak#	Ret. Time	Area%
1	16.535	76.652
2	19.011	23.348
Total		100.000

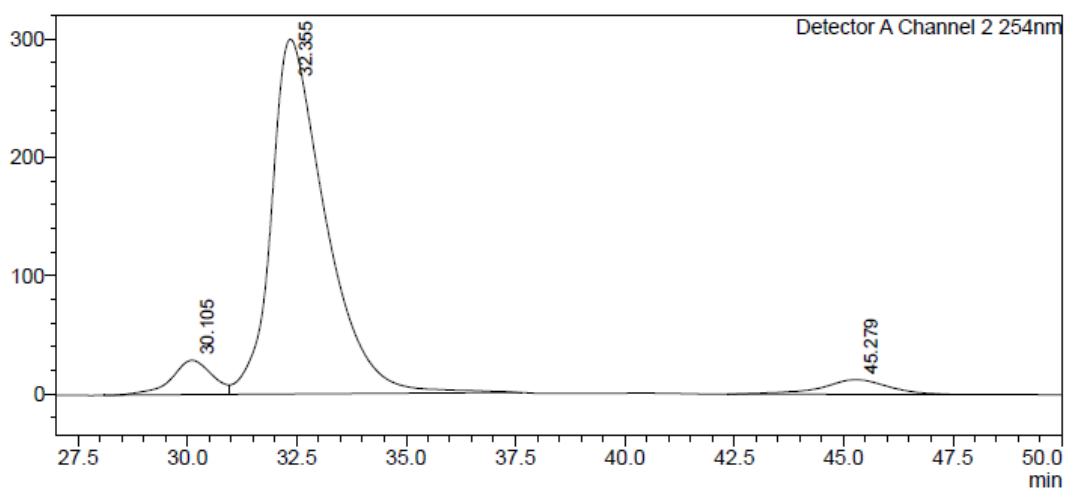
Example HPLC and GC traces from Chapter 3

HPLC Data for **308**: Chiralcel OD-H (hexane : *i*-PrOH 97:3, flow rate 1.0 mlmin⁻¹, 254 nm, 40 °C) *major diastereoisomer*: *t_r* (1*S*,2*R*,5*R*): 30.1 min, *t_r* (1*R*,2*S*,5*S*): 32.3 min, 7:93 er. *minor diastereoisomer*: *t_r* (1*S*,2*R*,5*S*): 40.4 min, *t_r* (1*R*,2*S*,5*R*): 45.2 min, <5:95 er.



Detector A Channel 2 254nm

Peak#	Ret. Time	Area%
1	29.883	33.698
2	32.669	35.969
3	40.275	15.536
4	45.103	14.798
Total		100.000

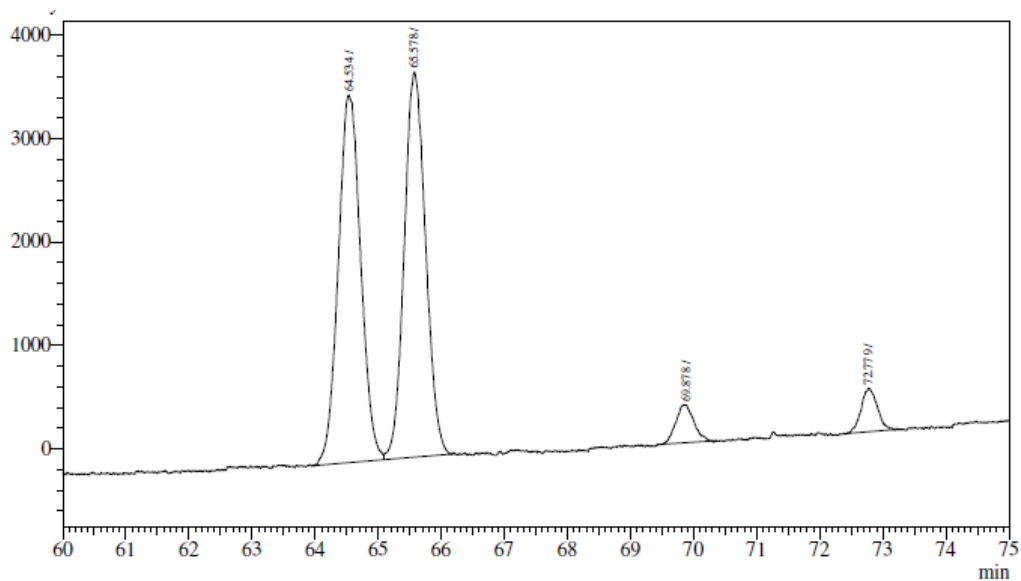
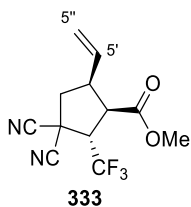


Detector A Channel 2 254nm

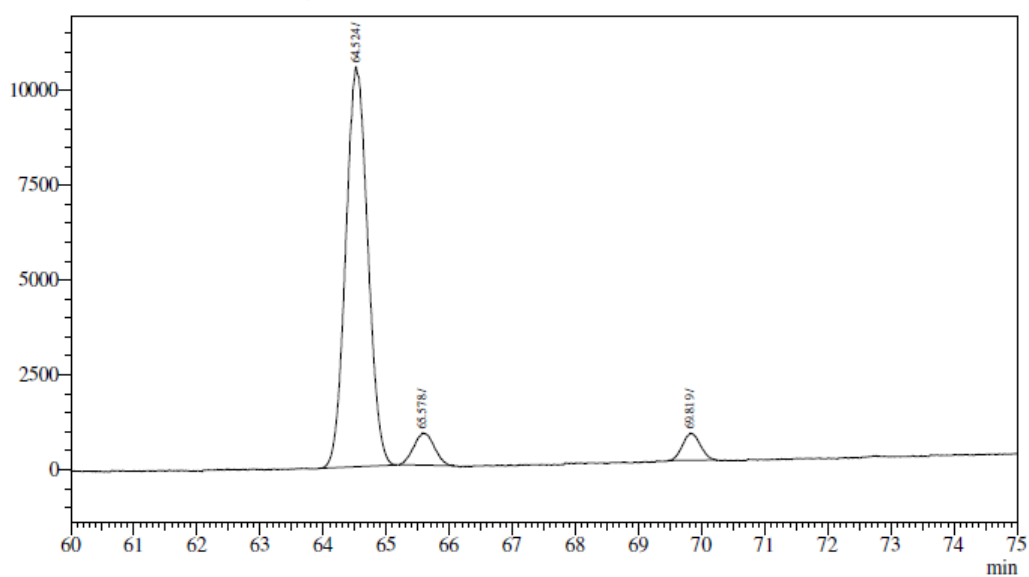
Peak#	Ret. Time	Area%
1	30.105	6.491
2	32.355	88.957
3	45.279	4.551
Total		100.000

Appendix II: Example HPLC and GC traces |

GC Data for **333**: Restek Rt- β DEXcst (length: 30 m, thickness: 0.25 mm, film thickness: 0.25 μ m, carrier gas: He, linear velocity: 28 cmsec⁻¹, temperature: 120 °C (60 min), 120 to 140 °C (20 min)) *major diastereoisomer*: t_R (1*R*,2*S*,5*S*): 64.5 min, t_R (1*S*,2*R*,5*R*): 65.5 min, 93:7 er. *minor diastereoisomer*: $t_{R,1}$: 69.8 min, $t_{R,2}$: 72.7 min, >99:1 er.



Peak#	Ret.Time	Area	Height	Conc.	Unit Mark	ID#	Cmpd Name
1	64.534	87915	3558	46.141			
2	65.578	87883	3726	46.124	V		
3	69.878	7272	367	3.817			
4	72.779	7467	420	3.919			
Total		190537	8071				



Peak#	Ret.Time	Area	Height	Conc.	Unit Mark	ID#	Cmpd Name
1	64.524	256193	10551	88.576			
2	65.578	19181	848	6.632			
3	69.819	13861	719	4.792			
Total		289235	12118				